Vol. 123, January 1, 1981
Complete in one issue

ISSN 0003-2670

ANALYTICA CHIMICA ACTA

International journal devoted to all branches of analytical chemistry

ELSEVIER SCIENTIFIC PUBLISHING COMPANY

ANALYTICA CHIMICA ACTA

International journal devoted to all branches of analytical chemistry
Revue internationale consacrée à tous les domaines de la chimie analytique
Internationale Zeitschrift für alle Gebiete der analytischen Chemie

PUBLICATION SCHEDULE FOR 1981 (incorporating the section on Computer Techniques and Optimization).

	J	F	M	A	M	J	J	A	S	O	N	D
Analytica Chimica Acta	123	124/1	124/2	125	126	127	128	129	130/1	130/2	131	132
Section on Computer Techniques and Optimization		133/1			133/2			133/3			133/4	

Scope. *Analytica Chimica Acta* publishes original papers, short communications, and reviews dealing with every aspect of modern chemical analysis, both fundamental and applied. The section on *Computer Techniques and Optimization* is devoted to new developments in chemical analysis by the application of computer techniques and by interdisciplinary approaches, including statistics, systems theory and operation research. The section deals with the following topics: Computerized acquisition, processing and evaluation of data. Computerized methods for the interpretation of analytical data including chemometrics, cluster analysis, and pattern recognition. Storage and retrieval systems. Optimization procedures and their application. Automated analysis for industrial processes and quality control. Organizational problems.

Submission of Papers. Manuscripts (three copies) should be submitted as designated below for rapid and efficient handling:

Papers from the Americas to: Professor Harry L. Pardue, Department of Chemistry, Purdue University, West Lafayette, IN 47907, U.S.A.

Papers from all other countries to: Dr. A. M. G. Macdonald, Department of Chemistry, The University, P.O. Box 363, Birmingham B15 2TT, England.

For the section on *Computer Techniques and Optimization:* Dr. J. T. Clerc, Universität Bern, Pharmazeutisches Institut, Sahlistrasse 10, CH-3012 Bern, Switzerland.

American authors are recommended to send manuscripts and proofs by INTERNATIONAL AIRMAIL.

Information for Authors. Papers in English, French and German are published. There are no page charges. Manuscripts should conform in layout and style to the papers published in this Volume. Authors should consult Vol. 121, p. 353 for detailed information. Reprints of this information are available from the Editors or from: Elsevier Editorial Services Ltd., Mayfield House, 256 Banbury Road, Oxford OX2 7DE (Great Britain).

Reprints. Fifty reprints will be supplied free of charge. Additional reprints (minimum 100) can be ordered. An order form containing price quotations will be sent to the authors together with the proofs of their article.

Advertisements. Advertisement rates are available from the publisher.

Subscriptions. Subscriptions should be sent to: Elsevier Scientific Publishing Company, P.O. Box 211, 1000 AE Amsterdam, The Netherlands. The section on *Computer Techniques and Optimization* can be subscribed to separately.

Publication. *Analytica Chimica Acta* (including the section on *Computer Techniques and Optimization*) appears in 11 volumes in 1981. The subscription for 1981 (Vols. 123–133) is Dfl. 1639.00 plus Dfl. 198.00 (postage) (total approx. U.S. $942.00). The subscription for the *Computer Techniques and Optimization* section only (Vol. 133) is Dfl. 149.00 plus Dfl. 18.00 (postage) (total approx. U.S. $86.00). Journals are sent automatically by airmail to the U.S.A. and Canada at no extra cost and to Japan, Australia and New Zealand for a small additional postal charge. All earlier volumes (Vols. 1–121) except Vols. 23 and 28 are available at Dfl. 164.00 (U.S. $84.00), plus Dfl. 13.00 (U.S. $6.50) postage and handling, per volume.

Claims for issues not received should be made within three months of publication of the issue, otherwise they cannot be honoured free of charge.

Customers in the U.S.A. and Canada who wish to obtain additional bibliographic information on this and other Elsevier journals should contact Elsevier/North Holland Inc., Journal Information Center, 52 Vanderbilt Avenue, New York, NY 10017. Tel: (212) 867-9040.

ANALYTICA CHIMICA ACTA
VOL. 123 (1981)

ANALYTICA CHIMICA ACTA

International journal devoted to all branches of analytical chemistry

ELSEVIER SCIENTIFIC PUBLISHING COMPANY

Anal. Chim. Acta, Vol. 123 (1981)

Printed in The Netherlands.

Analytica Chimica Acta, 123 (1981) 1—8

THE SEPARATION OF PLATINUM AND IRIDIUM BY ION FLOTATION

EUGENE W. BERG* and DANIEL M. DOWNEY

Department of Chemistry, Louisiana State University, Baton Rouge, LA 70803 (U.S.A.)

(Received 17th June 1980)

SUMMARY

The anionic chlorocomplexes of platinum(IV) and iridium(III) are separated by ion flotation from acidic, aqueous solutions with cationic surfactants of the type $C_{16}H_{33}NR'_3Br$, where R' is methyl, ethyl, n-propyl, or n-butyl. The $PtCl_6^{2-}$, which forms readily floatable salts with each of the surfactants, is selectively floated from the $IrCl_6^{3-}$ and recovered after flotation in n-butyl acetate. The efficiency of the separation increases as the R' chain length increases and a quantitative separation is obtained with hexadecyltributylammonium bromide (HTBAB) in 0.1 M HCl solutions. Since the flotation properties of Ir(IV) are similar to those of Pt(IV), hydroxylamine hydrochloride is used to reduce Ir(IV) to Ir(III) selectively in the presence of Pt(IV).

A previous paper by Berg and Downey [1] presented an experimental study of the ion flotation properties of $PtCl_6^{2-}$, $PdCl_4^{2-}$, $IrCl_6^{2-}$, $IrCl_6^{3-}$, $AuCl_4^-$ and $RhCl_6^{3-}$. Significant differences in the flotation of the Ir(IV) and Rh(III) complex ions with cationic surfactants of the quaternary ammonium type were found. These observations led to the development of a novel ion flotation separation procedure for iridium and rhodium reported earlier [2].

The present paper presents a novel ion flotation separation procedure for platinum and iridium. The separation is also based on observations made during the initial study [1] in which it was found that there were significant differences in the amount of the Pt(IV) and Ir(III) chlorocomplex ions which were floated from aqueous hydrochloric acid and saline (NaCl) solutions under identical experimental conditions.

The separation involves the selective flotation of $PtCl_6^{2-}$ from $IrCl_6^{3-}$ with either hexadecyltrimethylammonium bromide (HTMAB), hexadecyltriethylammonium bromide (HTEAB), hexadecyltripropylammonium bromide (HTPAB) or hexadecyltributylammonium bromide (HTBAB). The floated metal—surfactant salts or sublates are recovered by the addition of n-butyl acetate after the flotation of platinum reaches steady state.

It would be useful to separate the metals as Pt(IV) and Ir(IV) since these are the oxidation states obtained from the direct oxidation of the metals. However, the flotation properties of Ir(IV) are similar to those of Pt(IV) and ion flotation is not useful for their separation. Thus a reducing agent, hydroxylamine, is used in these studies to reduce the Ir(IV) to Ir(III) selectively, in the presence of Pt(IV).

Ion flotation separations of platinum and iridium presented in this paper are rapid, simple and efficient. The method offers an alternative to ion exchange and extraction methods [3—6] and may be useful for both laboratory and industrial separations of these metals.

EXPERIMENTAL

Reagents

Hexachloroplatinate(IV) stock solutions were prepared by dissolving the high purity platinum metal (A. D. Mackay, Inc.) in aqua regia. The solution was fumed to dryness twice with hydrochloric acid and the residue was finally dissolved in 2 M HCl.

High-purity sodium hexachloroiridate(IV) (Alfa-Ventron Chemical Co.) was activated for one month with neutrons from ^{252}Cf to produce radioactive iridium. The major isotope produced was ^{192}Ir (74.2 days). The salt was allowed to decay for four days before use to eliminate activity due to ^{24}Na (15 h). A stock radioactive Ir(IV) solution was prepared by dissolving the salt in 6 M HCl and slowly passing chlorine gas through the solution for 2 h. After again boiling to dryness, the final Ir(IV) solution was made up in 2 M HCl.

Hexachloroiridite(III) solutions were prepared by heating aliquots of the Ir(IV) stock solution with 0.25-ml aliquots of a 10% hydroxylammonium-chloride solution.

Four cationic surfactants of the quaternary ammonium type were used for flotation. The preparation of stock solutions was described in the previous paper [1]. The surfactants were HTMAB, HTEAB, HTPAB and HTBAB.

A 10% hydroxylammonium chloride (J. T. Baker Chemical Co.) solution was prepared by dissolving 10 g of the salt in 90 g of distilled and deionized water.

All other chemicals used in these studies were also of analytical reagent grade.

Apparatus

The flotation cell was made by lengthening an ordinary 60-ml glass Buchner funnel to 30 cm. The Buchner funnel contained a fine sintered (4—5.5 μm) glass frit through which nitrogen gas was purged into the sample solutions. A port was drilled 1 cm above the frit and fitted with a rubber septum for sample removal. The entire flotation system was of the same design as that of Rubin and Johnson [7].

A TMC 401A multichannel analyser coupled with a 2 × 2-in. NaI(Tl) well crystal detector was used for determining the activity of radioactive solutions. Absorbance measurements were made with a Beckman DB spectrophotometer and matched quartz cuvettes.

General flotation procedure

Sample solutions were prepared for flotation by the following general procedure. Aliquots of the Pt(IV) and radioactive Ir(IV) stock solutions

were heated for 5 min with 0.25 ml of 10% hydroxylammoniumchloride. Since the aliquots of Pt(IV) and Ir(III) stock solution contained 2 M HCl, the mixture with the reducing agent remained approximately 2 M in HCl. After cooling, the mixture was transferred to a 200-ml volumetric flask that contained a known amount of surfactant which was added in 2 ml of absolute ethanol. After dilution to 200 ml, the mixture was slowly stirred for 10 min. Exactly 100 ml of the sample solution was then pipetted into the cell for flotation.

In addition to the above procedure, certain sample solutions were prepared with aliquots of stock solutions of HCl or NaCl to give final sample solutions ranging from 0.01 M to 3.0 M HCl or 0.1 M to 3.0 M NaCl.

After the sample solutions were transferred to the flotation cell, nitrogen that had been filtered and saturated with water vapor was passed through the solution with a controlled flow rate of 10 cm^3 min^{-1}. Sublate was observed on the surface of the foam within the first five minutes.

After the maximum amount of metal was floated, the nitrogen flow was shut off and 25 ml of n-butyl acetate was added to the top of the flotation sample solution, which caused the foam to collapse. Most of the floated metal-surfactant salt or sublate was immediately dissolved in the organic solvent as the foam collapsed. However some of the sublate was redispersed into the bulk solution, thus nitrogen was again passed through the solution for an additional 10 min in order to float all the redispersed sublate into the organic layer.

The organic and aqueous layers were then separated and analysed for platinum and iridium. The sublate was recovered from the organic solvent by rotary evaporation. The floated initial chlorocomplex was recovered from the sublate by wet ashing with H_2SO_4, HNO_3, or H_2O_2 and fuming to dryness with HCl. The unfloated metal chlorocomplex was recovered from the bulk aqueous solution by heating to dryness on a hot plate.

Analytical techniques

The progress of each flotation experiment was followed by the analysis of 1—5-ml aliquots of the flotation sample solution, which were removed from the flotation cell at appropriate intervals. The concentration of iridium remaining in the solution was calculated from the measured radioactivity of the iridium tracer. The concentration of platinum was determined spectrophotometrically by the tin(II) chloride method of Sandell [8]. Since Ir(III) has a significant molar absorptivity at the working wavelength of 400 nm, suitable reagent blanks containing Ir(III) were used to compensate for the absorbance of iridium.

Rate of removal curves were obtained by dividing the concentration, C_t, of solute remaining in the solution at any time by the original concentration, C_0, and plotting versus flotation time. In addition, the percentage of metal floated at any time may be calculated as $\%F_t = (1 - C_t/C_0)\,(100)$.

RESULTS AND DISCUSSION

For the separation of platinum and iridium by ion flotation, it was necessary to prepare the hexachlorocomplexes of Pt(IV) and Ir(III) simultaneously in aqueous solutions. A selective reductant for reducing Ir(IV) to Ir(III) in the presence of Pt(IV) was needed since the oxidation and dissolution of mixtures of platinum and iridium by common means produce Pt(IV) and Ir(IV) complexes. Hydroxylamine as the water-soluble hydrochloride form was chosen as the reductant. In solutions of 2 to 3 M HCl and with heating for 3 to 5 min in a boiling water bath, the hydroxylamine completely reduced Ir(IV) to Ir(III) while Pt(IV) was unaffected [3]. In solutions of greater acidity, the Ir(IV) was only partially reduced. Furthermore, longer heating intervals resulted in partial reduction of the Pt(IV) to Pt(II).

The initial solutions prepared for flotation were 5×10^{-5} M in both Ir(III) and Pt(IV) and 2×10^{-4} M in either HTMAB, HTEAB, HTPAB or HTBAB. These concentration levels were chosen so that the sample solutions contained less than 10 ppm of each metal and more than a stoichiometric excess of surfactant. The rate of removal curves for the flotation of Pt(IV) and Ir(III) mixtures with these surfactants are shown in Fig. 1.

The percentage of Pt(IV) floated increases as the quaternary ammonium substituent chain increases from methyl to n-butyl. However, the amount of Ir(III) floated decreases as the chain length increases. The reduction in the flotation of Ir(III) is apparently due to the steric problem of crowding three bulky ammonium groups around each $IrCl_6^{3-}$ ion, which is required for its flotation. The crowding increases with increasing chain length; thus flotation decreases. The information in Fig. 1 therefore suggest that at least a partial separation of platinum and iridium is possible by ion flotation.

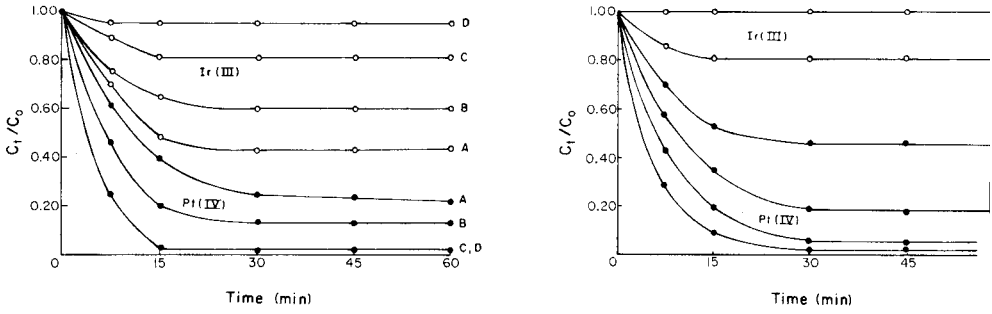

Fig. 1. Flotation of mixtures of Ir(III) and Pt(IV) with various surfactants. Initial conditions: [Ir(III)] = [Pt(IV)] = 5×10^{-5} M, [Surfactant] = 2×10^{-4} M, pH = 2, N_2 flow rate = 10 cm^3 min^{-1}. (○) Ir(III); (●) Pt(IV); (A) HTMAB; (B) HTEAB; (C) HTPAB; (D) HTBAB.

Fig. 2. Flotation of mixtures of Ir(III) and Pt(IV) with HTPAB from solutions of various HCl concentrations. Initial conditions: [Ir(III)] = [Pt(IV)] = 5×10^{-5} M, [HTPAB] = 2×10^{-4} M, N_2 flow rate = 10 cm^3 min^{-1}. (○) Ir(III); (●) Pt(IV); (A) 0.01 M HCl; (B) 0.5 M HCl; (C) 2.0 M HCl; (D) 3.0 M HCl.

TABLE 1

Recovery data for the separation of Pt(IV) and Ir(III) from solutions of various hydrochloric acid concentrations
(Initial separation conditions: [Pt(IV)] = [Ir(III)] = 5×10^{-5} M, [Surfactant] = 2×10^{-4} M, 100-ml sample solutions. Flotation time, 1 h. Recovery: Pt(IV) in n-butyl acetate, Ir(III) from residual aqueous solution. 0.25 ml of 10% $NH_3OH \cdot HCl$ solution added to reduce Ir(IV) ro Ir(III).)

Surfactant	HCl (M)	Ir recovered[a] (mg)	Ir recovered (%)	Pt recovered[b] (mg)	Pt recovered (%)
HTMAB	0.01	0.412	43	0.759	78
	0.10	0.566	59	0.740	76
	0.50	0.884	92	0.724	74
	1.00	0.960	100	0.634	65
	2.00	0.943	98	0.568	58
	3.00	0.971	101	0.486	50
HTEAB	0.01	0.578	60	0.801	82
HTPAB	0.01	0.807	84	0.952	99
	0.10	0.932	97	0.966	99
	0.50	0.961	100	0.924	95
	1.00	0.953	99	0.816	84
	2.00	0.960	100	0.850	77
	3.00	0.970	101	0.640	66
HTBAB	0.01	0.896	93	0.947	97
	0.10	0.962	100	0.975	100
	1.00	0.978	102	0.960	98
	2.00	0.961	100	0.910	93
	3.00	0.969	101	0.822	84

[a]Ir added = 0.961 mg. [b]Pt added = 0.975 mg.

Ion-exchange studies [4—6] of the separation of the platinum metals indicated that variations in the HCl or NaCl concentrations resulted in significant changes in the elution characteristics of the chlorocomplex anions. The rate of removal curves for the flotation of mixtures of Ir(III) and Pt(IV) from solutions of various initial hydrochloric acid concentrations with the surfactant HTPAB are shown in Fig. 2. Both the percentages of Ir(III) and Pt(IV) floated decrease as the hydrochloric acid concentration increases. Significantly, the amount of Ir(III) floated decreases to zero in solutions of greater than 0.5 M HCl. From the same solutions, the percentage of Pt(IV) floated, although less than 100%, remains high. Although a quantitative separation is not indicated, the platinum is floated free of iridium.

Solvent sublation [9] has been used for the recovery of floated materials without contamination from unfloated materials entrained in the foam liquid. However, solvent sublation has been shown to be inefficient for the quantitative recovery of certain sublates and a modified solvent sublation procedure was developed [2]. This method involves the simple addition of

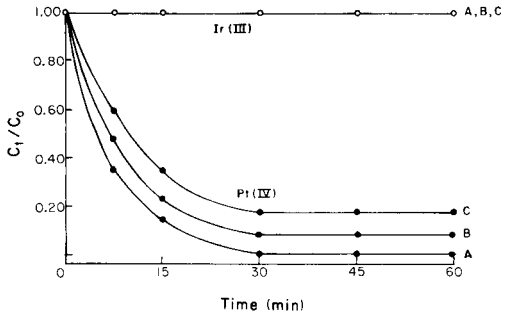

Fig. 3. Flotation of mixtures of Ir(III) and Pt(IV) with HTPAB from solutions of various NaCl concentrations. Initial conditions: [Ir(III)] = [Pt(IV)] = 5×10^{-5} M; [HTPAB] = 2×10^{-4} M, pH = 2, N_2 flow rate = 10 cm^3 min^{-1}. (○) Ir(III); (●) Pt(IV); (A) 0.5 M NaCl; (B) 1.0 M NaCl; (C) 3.0 M NaCl.

an organic solvent to a flotation experiment that has reached steady state. That it is termed sublation at all is due to the continuation of flotation after the solvent has been added.

A modified solvent sublation procedure using n-butyl acetate as the solvent was used in these studies to recover the floated Pt(IV) sublates from the

TABLE 2

Recovery data for the separation of Pt(IV) and Ir(III) from solutions of various sodium chloride concentrations
(Conditions as in Table 1, except pH = 2)

Surfactant	NaCl (M)	Ir recovered[a] (mg)	Ir recovered (%)	Pt recovered[b] (mg)	Pt recovered (%)
HTMAB	—	0.412	43	0.759	78
	0.10	0.529	55	0.595	61
	0.50	0.907	94	0.741	76
	1.00	0.942	98	0.693	71
	2.00	0.962	100	0.635	65
	3.00	0.955	99	0.598	61
HTEAB	—	0.578	60	0.800	82
HTPAB	—	0.807	84	0.952	99
	0.10	0.934	97	0.760	78
	0.50	0.971	101	0.960	98
	1.00	0.959	100	0.898	92
	2.00	0.951	99	0.845	87
	3.00	0.963	100	0.805	83
HTBAB	—	0.896	93	0.965	99
	0.10	0.943	98	0.806	83
	1.00	0.962	100	0.936	96
	2.00	0.970	101	0.918	94
	3.00	0.963	100	0.915	94

[a]Ir added = 0.961 mg. [b]Pt added = 0.975 mg.

TABLE 3

Recovery data for the separation of various concentrations of Pt(IV) and Ir(III) with HTBAB
(Initial separation conditions: flotation time, 1 h, 100-ml sample solutions, 0.1 M HCl. Recovery: Pt(IV) in n-butyl acetate, Ir(III) from residual aqueous solution. Hydroxylammoniumchloride added to reduce Ir(IV) to Ir(III).)

Ir(III) ($\times 10^{-5}$ M)	Pt(IV) ($\times 10^{-5}$ M)	HTBAB ($\times 10^{-5}$ M)	Ir recovered (%)	Pt recovered (%)
5.0	5.0	20.0	100	100
5.0	0.5	5.0	100	98
5.0	40.0	100.0	98	99
0.5	5.0	20.0	98	100
40.0	5.0	100.0	95	98

foam. Data are given in Table 1 for the separation and recovery of Pt(IV) and Ir(III) with each of the surfactants from solutions of various hydrochloric acid concentrations. Excellent separations were found for several solutions, particularly with the surfactant, HTBAB, in 0.1 M HCl in which a quantitative separation was obtained.

The separation of Pt(IV) and Ir(III) was also investigated with respect to sodium chloride concentration in the solution. The rate of removal curves for the flotation of Pt(IV) and Ir(III) with HTPAB from solutions of various sodium chloride concentrations are shown in Fig. 3. The data for the flotation, separation and recovery of the metals with each surfactant, from solutions of various sodium chloride concentrations, are given in Table 2. The floated platinum was again recovered with n-butyl acetate.

The percentage of Pt(IV) floated decreases as the sodium chloride concentration increases, although the degree of reduction is not as great as found for the hydrochloric acid variation. The percentage of Ir(III) floated decreases to zero as the sodium chloride concentration increases, thus conditions for separation were again found. It is important to note that a large reduction in the flotation of Pt(IV) is found in 0.1 M NaCl solutions. This reduction in flotation was noted in a previous study [1] and similar behavior for the flotation of Pd(II) has been discussed by Walkowiak and Bartecki [10].

Finally, the significance of the solution metal ion concentration on separations was investigated by varying the mole ratios of Pt(IV) and Ir(III) in the initial solutions. The surfactant HTBAB was used for flotation from 0.1 M HCl solutions and its concentration was maintained at levels in excess of the stoichiometric amount required for flotation. The data given in Table 3 indicate that the initial concentrations of Pt(IV) and Ir(III) are not important in achieving quantitative separations.

REFERENCES

1 E. W. Berg and D. M. Downey, Anal. Chim. Acta, 120 (1980) 237.
2 E. W. Berg and D. M. Downey, Anal. Chim. Acta, 121 (1980) 239.
3 D. D. Busch, J. M. Prospero and R. A. Naumann, Anal. Chem., 31 (1959) 884.
4 K. A. Kraus, F. Nelson and G. Smith, J. Phys. Chem., 58 (1954) 11.
5 S. S. Berman and W. A. E. McBryde, Can. J. Chem., 36 (1958) 835.
6 J. Korkisch, Modern Methods for the Separation of Rarer Metal Ions, Pergamon Press, New York, 1969, p. 526.
7 A. J. Rubin and D. J. Johnson, Anal. Chem., 39 (1967) 298.
8 E. B. Sandell, Colorimetric Determination of Traces of Metals (3rd edn.), Interscience, New York, 1959, p. 726.
9 B. L. Karger, in R. Lemlich (Ed.), Adsorptive Bubble Separation Techniques, Academic Press, New York, 1972, p. 145.
10 W. Walkowiak and A. Bartecki, Nucleonika, 18 (1973) 133.

Analytica Chimica Acta, 123 (1981) 9—17

ENRICHMENT OF TRACE ANIONS FROM WATER WITH 2,2′-DIAMINODIETHYLAMINE CELLULOSE FILTERS

J. SMITS and R. VAN GRIEKEN*

Department of Chemistry, University of Antwerp (U.I.A.), Universiteitsplein 1, B-2610 Wilrijk (Belgium)

(Received 25th July 1980)

SUMMARY

Cellulose filters with immobilized 2,2′-diaminodiethylamine (DEN) functional groups are studied for trace anion preconcentration from aqueous solution, with subsequent x-ray fluorescence measurements. For most oxoanions with a central metal atom, nearly quantitative collection can be achieved by 10-cm² DEN filters under the following optimized conditions: pH 3—6, filtration rate up to 0.5 ml cm^{-2} min^{-1}, and sample volume up to 100 ml cm^{-2}. The collection yield is independent of the trace oxoanion concentration up to at least 1.5 μmol cm^{-2}. Although the DEN filter exhibits some selectivity towards oxoanions with a central metal atom, ionic strength affects the results; the collection efficiency is strongly depressed with salt (e.g. NaCl) concentrations above 0.01 M. The applicability of the DEN filter in anion collection is therefore limited to dilute solutions.

Ion-collecting filters can be used advantageously for preconcentrations from aqueous solutions: the enrichment is accomplished by a simple filtration step, preferably at the natural pH, and the loaded filter is ideal for direct x-ray fluorescence analysis. A chelating cellulose filter with immobilized 2,2′-diaminodiethylamine (diethylenetriamine, DEN) molecules as the functional groups has recently been described [1]. These filters were shown to preconcentrate trace cations at a pH above 5—6, with satisfactory efficiency and capacity, independent of the usually abundant alkali and alkaline earth ions in solution. Leyden et al. [2—4] have observed that ethylenediamine functional groups immobilized on silica gel also collect oxoanions with a central metal ion selectively with respect to, for example, the halides. This functional group is very similar to the DEN which can be considered as the dimer. The collecting properties to the DEN filter for oxoanions with a central metal atom were therefore also studied.

EXPERIMENTAL

Synthesis of DEN filters

The optimization of the synthesis procedure has been described in detail elsewhere [5]. The synthesis starts from Whatman-41 cellulose filters (5.5 cm

diameter; 0.2 g weight) which are preswollen in dried *N,N*-dimethylformamide, and then transformed to chlorodeoxycellulose filters by treatment with $POCl_3$ at 90°C. After washing, these filters are heated in purified DEN at 130°C for 2 h. The final filters contained about 10 μmol DEN cm^{-2} (1.1 mol g^{-1} cellulose), of which 2.4 μmol cm^{-2} can easily be reached in filtration, as was determined for cations [1].

Apparatus

The material collected on the DEN filter was determined by energy-dispersive x-ray fluorescence (x.r.f.), with molybdenum as the secondary fluorescer (or tin whenever molybdenum had to be measured). The x.r.f. spectra were stored on magnetic tape and evaluated off-line using a non-linear least-squares fitting computer routine [6]. For calibration a series of commercial thin-film standards was available.

The filtration unit was a home-made unit with a straightforward cylindrical shape, which yielded a more homogeneous flow through the filter than commercial funnels with a conical bottom part. The active filtration area was 10 cm^2.

Procedures

Working solutions, containing 25 or 50 μg of each element, were prepared from 100-ppm stock solutions. These were made by dissolving in 0.1 M NaOH the appropriate amounts of analytical-grade NH_4VO_3, K_2CrO_4, As_2O_3, $As_2O_5 \cdot 5H_2O$, H_2SeO_3, H_2SeO_4, $Na_2MoO_4 \cdot 2H_2O$, $SnCl_4$, $Na_2WO_4 \cdot 2H_2O$ or NaBr.

To determine the influence of the filtration rate, 250-ml portions at pH 3 were filtered. To evaluate the influence of the ionic strength, 250-ml portions of pH 4.5 and with increasing NaCl concentrations were filtered at a rate of 0.5 ml min^{-1} cm^{-2}. The influence of the volume was studied on solutions containing 25 μg of each element in 75, 250, 500, 1000 or 2000 ml, which were filtered at a pH of 4.5 and a filtration rate of 0.5 ml min^{-1} cm^{-2}. The study of the influence of the trace anion concentration made use of 100 or 200-ml solutions with 0.5, 1.0, 2.5, 5.0, 10, 25, 50, 100, 200, 500 and 1000 μg of the metals as anions, at pH 4.5; these were also filtered at 0.5 ml min^{-1} cm^{-2}. For the determination of the influence of the pH the filters were soaked for at least three days in twice-distilled water of the appropriate pH, with regular pH readjustments with 0.1 M HCl or NaOH. The final pH, after filtration, was taken as the pH at which the collection occurred. The filtration rate was again 0.5 ml min^{-1} cm^{-2}.

Since none of the ions was precipitated to any extent at the trace concentrations and pH levels studied, previous filtration through a Nuclepore 0.4-μm pore-size membrane was not necessary.

RESULTS AND DISCUSSION

Influence of the filtration rate

The influence of the filtration rate on the collection efficiency of the DEN filter is shown for some typical anions in Fig. 1. Good collection of most trace oxoanions was obtained up to a rate of 0.7 ml min^{-1} cm^{-2}; other anions gave similar patterns. The reason why the arsenite is not collected by the DEN filter will be explained below. The collection of bromide is not as complete as for the other ions. This indicates some selectivity for the DEN filter, an observation in good agreement with the selectivity for anions with a central metal atom reported by Leyden et al. [4] for ethylenediamine groups immobilized on silica gel or glass beads by a silylation reaction.

According to Fig. 1, within an hour, a sample volume of 450 ml may be filtered through the typical filtration area of 10 cm^2 with efficient collection of most trace oxoanions.

Influence of pH

In order to comprehend the influence of the pH on the collection efficiency of DEN for the various anions, knowledge of the ionic distribution is desirable. The following formulae [7] were used to calculate the ionic distribution curves:

$$\alpha_N = \left[1 + \frac{K_{a1}}{[H^+]} + \frac{K_{a1}K_{a2}}{[H^+]^2} + \cdots \frac{K_{a1}K_{a2}\cdots K_{aN}}{[H^+]^N}\right]^{-1} \quad (1)$$

$$\alpha_{N-i} = \alpha_N \, (K_{a1} \cdots K_{ai})/[H^+]^i \quad (2)$$

$$\alpha_0 = \alpha_N \, (K_{a1}K_{a2} \cdots K_{aN})/[H^+]^N \quad (3)$$

As acid dissociation constants the following values were selected from the literature [8, 9]: for DEN, pK_1 4.42, pK_2 9.21 and pK_3 10.02; for chromate, pK_1 0.74 and pK_2 6.94; for arsenite, pK_1 9.38 and for arsenate, pK_1 2.19,

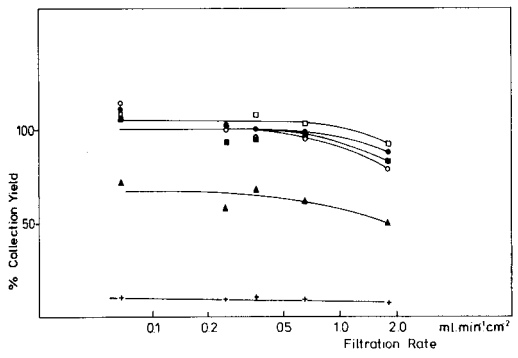

Fig. 1. Influence of the filtration rate on the DEN filter collection efficiency for vanadate (○), arsenite (+), selenate (●), bromide (▲), molybdate (■) and tungstate (□).

pK_2 6.94 and pK_3 11.50; for selenite, pK_1 2.75 and pK_2 0.50 and for selenate, pK_2 1.66. For the other substances, quantitative data could not be found, and qualitative information from other sources [10, 11] was used.

The ionic distribution of the DEN functional group is shown in Fig. 2. The functional groups are positively charged over practically the whole pH range. As stated earlier [1], the collection of trace cations occurs at pH values above 5.5 and is accompanied by loss of protons [12]. Mainly because of these positive charges, the DEN filter could, in principle, act as an anion collector by simple ion-pair formation.

Figure 3 shows the influence of the pH on the collection efficiency of the DEN filter for various anions. For those anions where it was possible to calculate the ionic distribution curves, the predominant species is also indicated in Fig. 3. Table 1 summarizes the pH ranges within which collection occurs and the average collection yield together with the percent standard deviation for the collected anions. This standard deviation includes uncertainties in the x.r.f. analysis (spectrum fitting, analysis geometry, x-ray absorption correction) and uncertainties arising from heterogeneity of the filter loading (only the central cm^2 of the filter is measured by x.r.f.).

At acidic pH, the collection is mainly limited by protonation of the anions to give neutral species, as is clearly the case for arsenate and selenite. Arsenite is not collected at any pH because it is not charged over the whole pH range examined. This indicates that the collection is based primarily on charge attraction. For vanadate, molybdate, stannate and tungstate also, the depression of the collection efficiency seems to be caused by a change in the charge of the ionic species. Although quantitative data could not be found for these ions in the literature, and although their chemistry is complicated

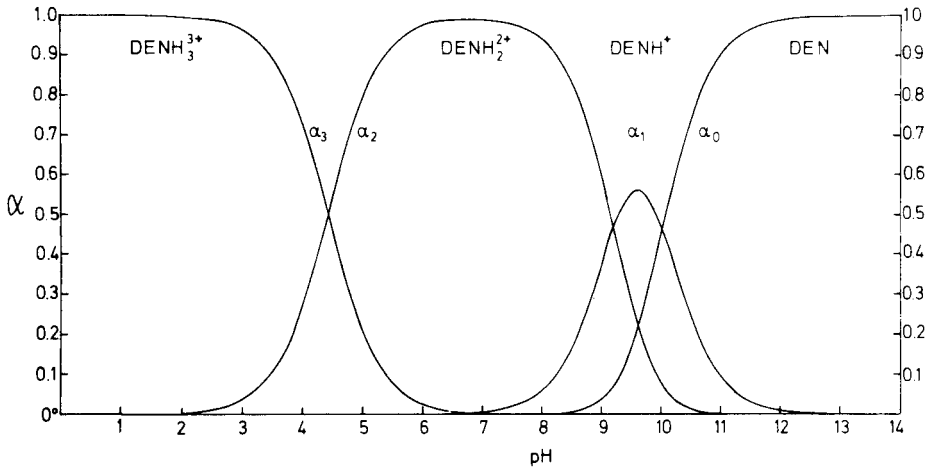

Fig. 2. Ionic distribution of the 2,2'-diaminodiethylamine functional group as a function of the pH.

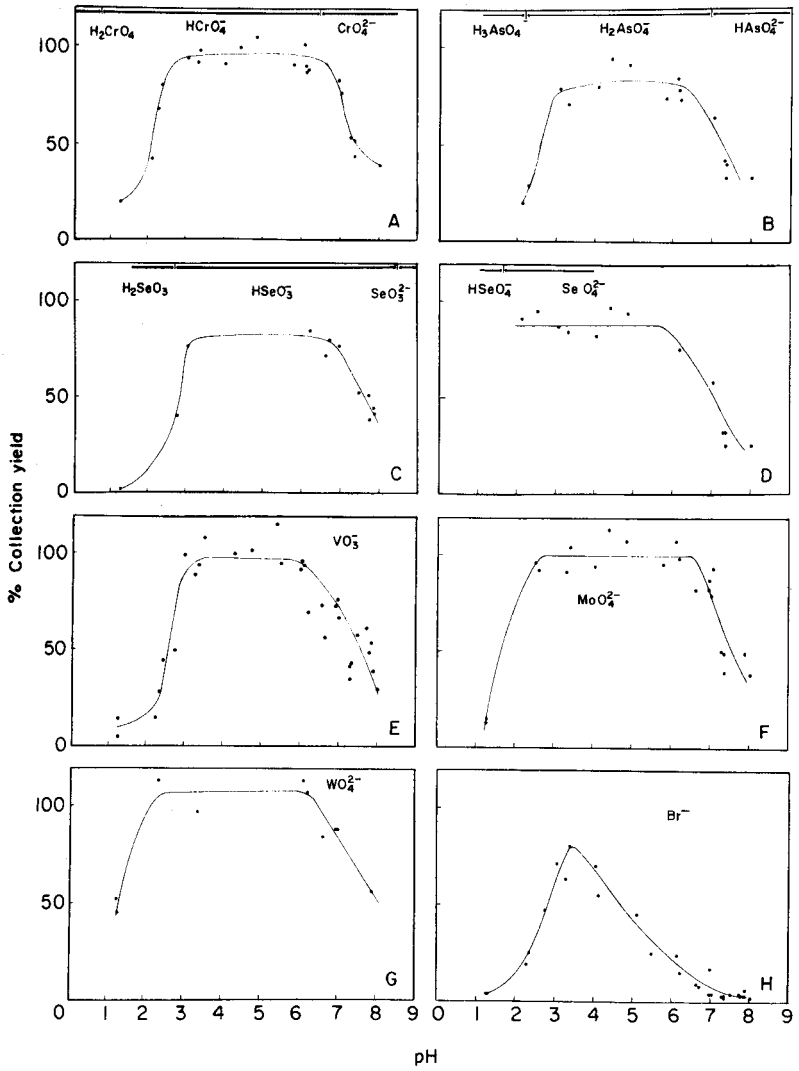

Fig. 3. Influence of the pH on the collection efficiency of the DEN filter (and on the ionic distribution) for (A) chromate, (B) arsenate, (C) selenite, (D) selenate, (E) vanadate, (F) molybdate, (G) tungstate, and (H) bromide.

by oxidation–reduction aspects and polynuclear ion formation, those elements can form neutral or even positively charged species at acidic pH levels [10, 11]. For chromate, the drop in collection efficiency at decreasing pH does not clearly match the formation of uncharged species, but the uncertainty in the literature pK_1 values (ranging from −0.83 to 4.15) and the occurrence of polynuclear forms must be considered.

Another fact that may play an important role is the occurrence, at acidic

TABLE 1

Useful pH range, average collection efficiency and reproducibility for various anions

Anion	Optimal pH range	Collection efficiency[a] (%)	Anion	Optimal pH range	Collection efficiency[a] (%)
VO_3^-	3—6	101 ± 9 (11)	MoO_4^{2-}	2.5—6.5	99 ± 7 (11)
CrO_4^{2-}	3—6.5	93 ± 7 (12)	$Sn(OH)_6^{2-}$	3—6.5	83 ± 15 (4)
AsO_4^{3-}	3—6.5	83 ± 11 (9)	WO_4^{2-}	2—6.5	107 ± 7 (4)
SeO_3^{2-}	3—7	81 ± 6 (5)	$Sb(OH)_6^-$	—	84 (1)
SeO_4^{2-}	2—6.5	88 ± 9 (7)	AsO_3^{3-}	—	2 ± 1 (7)

[a] Average collection efficiency with standard deviation per measurement (%) and, in parentheses, the number of experiments involved.

pH, of the excess of halide ions introduced as the counter ion during pH regulation, as the DEN filter is not very selective against such ions (see below). Selenate is collected quantitatively even at pH 2 because it remains doubly charged at that pH. At the higher pH end, there is a sharp decrease in collection efficiency for all oxoanions at pH 6—7.

Figure 3 also shows the collection efficiency for bromide, the halide that is readily measured by x.r.f., as a function of pH. The halide seems to be collected only by the triprotonated DEN form, down to a pH where the excess of competing chloride ions begins to depress the collection yield again.

Influence of the ionic strength

The results in Table 2 show that, up to a chloride concentration of 0.01 M (350 ppm Cl^-) the collection of the oxoanions remains satisfactory. At higher ionic strengths the collection efficiencies drop sharply. Tungstate

TABLE 2

Influence of the ionic strength (in NaCl solutions at pH 4.5) on the collection yield

Ionic strength (mol l^{-1})	Collection efficiency (%) for						
	VO_3^-	CrO_4^{2-}	AsO_4^{3-}	SeO_4^{2-}	MoO_4^{2-}	WO_4^{2-}	Br^-
0.00025	96	91	85	86	94	93	66
0.0005	98	99	100	102	105	110	41
0.001	83	91	78	82	95	99	6
0.01	86	93	76	81	93	96	5
0.05	26	17	11	9	22	59	2
0.1	18	6	5	5	10	42	2
0.5	13	9	1	1	5	20	2
1.0	13	2		1	4	8	2
5.0	9	5	1	1		11	1

seems to be influenced to a lesser extent than the other anions. The bromide collection is reduced even at a very low ionic strength.

Increasing total anion concentrations in solution cause an increasing pH rise during the filtration. It appeared that, on average, the pH changes from the original level of 4.5 to 5.3 for an ionic strength I of 0.001 mol l^{-1}, to 6.4 for I = 0.005, to 7.1 for I = 0.01, to 8.6 for I = 0.1 and to 9.2 for I = 1. This pH change results from the simultaneous retention of protons together with the anions in the filter. Clearly, even for 0.01 M NaCl, the pH after filtration is beyond the optimal range for anion collection, and this could have been the reason for the strong effect of ionic strength. In attempts to overcome these effects, repeated filtrations and stringent pH control were examined. The same trace anion solutions, with 0.5 M NaCl, were filtered up to six times through the same DEN filter, and the pH of the effluent was repeatedly adjusted to 4.5. Except for tungstate, however, the improvement was not significant. Also, previous saturation of the DEN filters with chloride gave poor results; although the pH after the trace anion solution filtration was only 5.5, the collection efficiency was below 28% for all oxoanions. Experiments with sodium bromide, iodide and sulphate showed that the influence of ionic strength is independent of the salt.

This significant ionic strength effect greatly limits the applicability of the DEN filter for anion preconcentrations. In drinking and surface water, the total anion concentration is typically 0.007 mol l^{-1}, which corresponds roughly to the maximum tolerable level for quantitative enrichments.

Influence of the volume of the solution filtered

To study the effect of volume on unwanted elution of the collected material, water samples of 75—2000 ml, containing 25 μg of six oxoanions, were filtered through a 10-cm^2 DEN filter. The results showed that chromate, selenate, molybdate, vanadate and tungstate can be collected quantitatively from a volume of 200 ml cm^{-2}, whereas for arsenate some suppression of collection efficiency occurs above 100 ml cm^{-2}. For bromide unwanted elution occurs earlier.

An optimized general preconcentration procedure for trace oxoanions would consist of filtering solutions at pH 4.5 with volumes not greater than 100 ml cm^{-2}, at a rate not above 0.5 ml cm^{-2} min^{-1}.

Influence of the oxoanion concentration

Figure 4 shows the concentration ranges for which the x.r.f. responses on the loaded filter are linear with the concentration for solutions containing simultaneously vanadate, chromate, arsenate, selenate, molybdate, tungstate and bromide. The curves do not deviate from linearity at the lowest concentrations, which indicates the absence of significant contamination and blank problems for these elements. At the highest concentrations, the deviations are due to exceeding the collection capacity of the filter. The concentration level at which this occurs is different for each element. Bromide is not

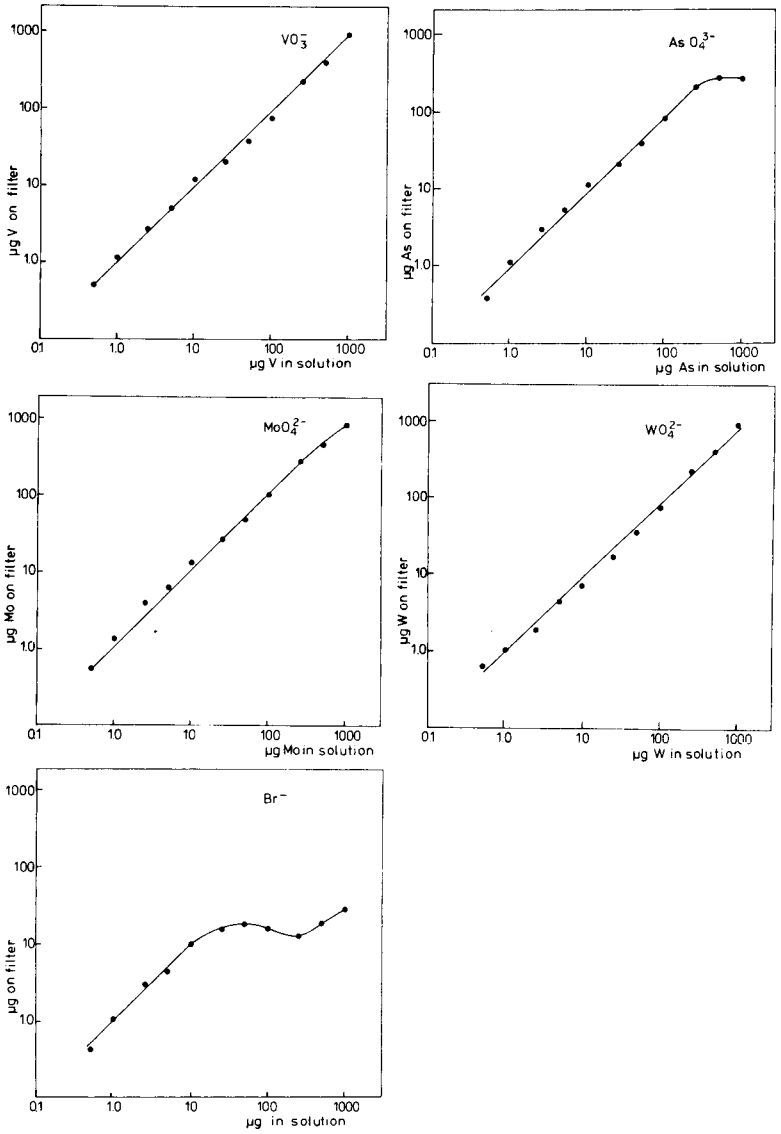

Fig. 4. Influence of the trace anion concentrations on their collection from a multi-element solution by the DEN filter. The curves for selenate and chromate are similar to those for arsenate and molybdate, respectively.

quantitatively collected above a total load of 0.06 μmol cm^{-2}. Arsenate and selenate are increasingly less efficiently collected above a total load of 1.5 μmol cm^{-2}, molybdate and chromate above 2.9 μmol cm^{-2}, whereas vanadate and tungstate are still collected quantitatively at a load of 5.5 μmol cm^{-2}. This experiment indicates the order of selectivity for the different ions.
Linear regression analyses were carried out for the results up to 250 μg of

each metal. The calculated correlation coefficients were 0.9970, 0.9984, 0.9997, 0.9997, 0.9989, 0.9983 for vanadate, chromate, arsenate, selenate, molybdate and tungstate, respectively, while the 99.9% probability level for a linear correlation would yield a 0.898 coefficient. These results prove that, up to 1.5 μmol cm^{-2} or more, the collection efficiency is not influenced by the oxoanion concentration.

In view of the linear response, favourable detection limits and precision, direct x.r.f. determinations seem to be well suited for combination with DEN filter preconcentration.

Selectivity of the DEN filter

The above results indicate the approximate selectivity order of the DEN filter: $WO_4^{2-} > VO_3^- \geqslant MoO_4^{2-} \geqslant CrO_4^{2-} > SeO_4^{2-} \geqslant AsO_4^{3-} \gg Br^-$. However, the affinity of the DEN filter for oxoanions with a central metal atom is insufficient relative to the halides for selective preconcentration of these oxoanions, except from solutions of low salinity.

Leyden et al. [4, 13] have reported a selective preconcentration of molybdate and tungstate from brines by ethylenediamine immobilized on silica gel. Their finding that this substrate collects only oxoanions with a central metal atom does not agree with the present findings. It is not clear whether this is due to the slightly different functional group, the different substrate, or the use of a column rather than a filter technique. The nature of the actual interaction between the protonated amine and the anions still remains to be elucidated.

J. Smits acknowledges financial support from the Belgian I.W.O.N.L.

REFERENCES

1 J. A. Smits and R. E. van Grieken, Anal. Chem., 52 (1980) 1479.
2 D. E. Leyden, W. K. Nonidez and P. W. Carr, Anal. Chem., 47 (1975) 1449.
3 D. E. Leyden, G. H. Luttrell, A. E. Sloan and N. J. De Angelis, Anal. Chim. Acta, 84 (1976) 97.
4 D. E. Leyden, M. L. Steele, B. B. Jablonski and R. B. Somoano, Anal. Chim. Acta, 100 (1978) 545.
5 J. Smits and R. van Grieken, Angew. Makromol. Chem., 88 (1978) 105.
6 P. van Espen, H. Nullens and F. Adams, Nucl. Instrum. Methods, 142 (1977) 243.
7 J. N. Butler, Ionic Equilibria, A Mathematical Approach, Addison—Wesley, Reading, Massachusetts, 1964.
8 L. G. Sillen and A. E. Martell, Stability Constants, Special Publication No. 17, The Chemical Society, London, 1964.
9 L. S. Sillen and A. E. Martell, Stability Constants, Suppl. No. 1, Special Publication No. 25, The Chemical Society, London, 1971.
10 I. M. Kolthoff, P. J. Elving and E. B. Sandell, Treatise on Analytical Chemistry, Part II, Interscience, New York/London, 1961—1978.
11 F. A. Cotton and G. Wilkinson, Advanced Inorganic Chemistry, A Comprehensive Text, Interscience, New York/London, 1972.
12 J. E. Prue and G. Schwarzenbach, Helv. Chim. Acta, 33 (1950) 985.
13 D. E. Leyden, G. H. Luttrell, W. K. Nonidez and D. B. Werho, Anal. Chem., 48 (1976) 67.

Analytica Chimica Acta, 123 (1981) 19—24

PRECONCENTRATION OF TRACE METAL IONS BY COMBINED COMPLEXATION-ANION EXCHANGE
Part 2. Cobalt, Zinc, Cadmium and Lead With 8-Hydroxyquinoline-5-Sulfonic Acid [1]

DOUGLAS G. BERGE*

Department of Chemistry, University of Wisconsin—Oshkosh, Oshkosh, WI 54901 (U.S.A.)

JOHN E. GOING

Midwest Research Institute, 425 Volker Boulevard, Kansas City, MO 64110 (U.S.A.)

(Received 7th July 1980)

SUMMARY

The ligand, 8-hydroxyquinoline-5-sulfonic acid, forms anionic complexes with cobalt(II), zinc(II), cadmium(II), and lead(II), each resulting complex showing a high affinity for anion-exchange resins. The effect of pH, ligand/metal ratio, volume, and concentration on percent retention of the anionic complexes by an anion-exchange resin are reported. At optimum conditions, all four metals are quantitatively retained by the column. Zinc, cadmium and lead(II) ions are completely eluted with 11 ml or less of 2 M HNO_3; cobalt(II) is totally removed by 12 M HCl and 2 M HNO_3. Concentration enhancements of 100-fold are easily achieved. All four anionic complexes can be left on the column for 7 days and still be quantitatively (99%) recovered. A ligand-loaded resin column can also remove all four metals quantitatively. Distribution coefficients for the metal complexes and their ligand/metal ratios were determined by using batch methods that may also serve as the isolation procedure.

With the current interest in environmental pollution, there is a continual need for trace metal determinations. In many situations involving the use of multi-element techniques [1—5], the preconcentration of trace metals is often a critical step [6]. Many methods for preconcentration are available. Of particular interest has been the chemical bonding of a ligand to ion-exchange resins for the purpose of metal ion removal by chelate formation [7—13]. Several recent studies [14—16] have employed a variety of techniques for preconcentration.

Going et al. [1] proposed a complexation—ion exchange technique utilizing conventional anion-exchange resins. In that study, a metal—ligand complex using the ligand 2-(3′-sulfobenzoyl)-pyridine-2-pyridylhydrazone (BPPH-S) was formed in which the resulting complex has a net charge of −2 in basic solution. When the complex was passed through an anion-exchange resin, the resin was found to have a very high affinity for the negatively charged metal complex. Their study showed the feasibility of this approach for the separation and preconcentration of Co(II), Zn(II), and Cd(II).

This approach has been extended to the commercially available ligand, 8-hydroxyquinoline-5-sulfonic acid (HOx-S). This compound is different from the BPPH-S in that the latter has a periferally located ionizable proton, whereas HOx-S has the ionizable proton on the complexing group. The parent compound, 8-hydroxyquinoline, is one of the ligands in which much interest has been shown in chemically bonding to ion-exchange resins to form chelate-type ion-affinity resins [13, 17, 18]. Studies of the isolation of Co(II), Cd(II), Pb(II), and Zn(II) complexes of HOx-S by conventional anion-exchange resins are reported herein.

This study involves experiments in which metal ions are complexed with HOx-S prior to addition to the resin in its OH^- form and experiments in which uncomplexed metal ions are added to resin to which the HOx-S ligand has been attached. These approaches are identified as "precomplexation" and "ligand-loaded resins" below.

EXPERIMENTAL

Reagents

The 8-hydroxyquinoline-5-sulfonic acid (Aldrich Chemical Company) was recrystallized from water (m.p. 322°C, literature value 322—3°C). A 2.00×10^{-3} M stock solution was prepared, using a minimum amount of sodium hydroxide to solubilize the compound.

Stock 0.1 M metal ion solutions were prepared from cobalt(II) and zinc(II) perchlorates, lead(II) nitrate, and cadmium metal dissolved in a minimum volume of concentrated hydrochloric acid and then diluted to volume with deionized water. The stock cobalt(II) solution was standardized by an electrodeposition method [19]. The Zn(II), Pb(II), and Cd(II) solutions were standardized by EDTA titration procedures [20]. The stock solutions were then diluted appropriately with deionized water to give the desired concentrations.

A pH 8 buffer was prepared by mixing 50 ml of 0.1 M Tris with 29 ml of 0.1 M HCl and diluting the mixture to 100 ml [21].

The anion-exchange resin (Bio-Rad 140-1242 AG1-X2; 100—200 mesh) was used in two forms, namely the OH^- form and complexed with HOx-S. To prepare the OH^- form, fines were removed and the resin was treated with several additions of 1 M HCl followed by several additions of 1 M NaOH and rinsed with deionized water. To prepare the complexed form, desired amounts of the dry resin and HOx-S were stirred in a buffer solution at pH 8.

Equipment and techniques

Distribution of Zn(II), Co(II), and Cd(II) were monitored by radioactivity counting of ^{65}Zn, ^{60}Co, and ^{109}Cd added as tracers to the solutions; lead(II) was monitored by atomic absorption spectrometry. Radioactivity measurements of γ-emission were made using a 3 × 3-in. well NaI (Tl) crystal scintillation detector in conjunction with a single-channel analyzer, linear amplifier

(Hewlett-Packard 5582A), and an electronic scaler (Canberra Model 895). Atomic absorption measurements were done with a Perkin-Elmer Model 360 atomic absorption spectrometer and a Perkin-Elmer HGA-2100 graphite furnace.

An all-glass column similar to the design of Pankow and Janauer [22] was used for the column experiments. The system was modified by attaching the column to a 3-way stopcock by a 5/20 ground-glass joint shortened to 5/12. The column was 1 × 6 cm and was generally filled with 3 ml of wet resin in the desired form. The 3-way stopcock allowed the sample to be loaded onto the bottom of the column by ascending flow. For elution studies, descending flow was used to elute the metal ions through the bottom of the column; this approach served to minimize the elution volume.

Percentage recoveries were determined by comparing radioactive counts or concentrations before and after passage through the columns.

Distribution coefficients were determined by a batch technique. Weighed amounts (1.0 g) of resin were added to known volumes of the sample and gently stirred until equilibrium was attained. Concentrations before and after equilibrium were determined by radioactive counting for Co(II), Zn(II), and Cd(II) and by atomic absorption spectrometry for Pb(II). The D value for each ion was computed from the formula

$$D = (C_i - C_f)\, V/C_f m$$

where C_i and C_f are the initial and final tracer concentrations for Cd(II), Zn(II), and Co(II), and the total concentration for Pb(II), V is the volume of the solution (in ml) and m is the mass of the resin (in g). Averages of 2—4 measurements were generally used.

The time required to reach equilibrium was determined by withdrawing small aliquots periodically and determining the ion concentration in solution.

Procedures

The pre-complexation column procedure is applicable to up to 1 l of sample containing up to 2×10^{-6} M heavy metal ions. For each 100 ml of sample, add 5 ml of HOx-S solution and 25 ml of pH 8 Tris-HCl buffer (check final pH), and pass the solution through the column at a flow rate of 10 ml min^{-1} using diluted (1 part buffer:4 parts water) pH 8 buffer to wash the final amounts of the sample onto the column. Elute Zn(II), Cd(II), and Pb(II) with 2 M HNO_3; elute Co(II) by adding 3 ml of 12 M HCl followed by sufficient 2 M HNO_3 to complete the elution.

For the ligand-loaded resin experiments, 100-ml volumes of ions in pH 8 buffer were passed through the column and eluted as described above.

RESULTS AND DISCUSSION

Batch studies

The initial step in the batch studies was to determine the time required for the various metal ions to reach equilibrium. Figure 1 shows the results for

Cd(II) and Pb(II). Results were similar for the other two ions. Equilibrium was reached in 20 min for Cd(II), Co(II), and Pb(II), with 30 min necessary for Zn(II).

Solution pH determines the percentage of metal ion retained by the resin. Figure 2 shows the effect of pH on the distribution coefficients for the metals. At pH 8, log D values greater than 4 were achieved for all the metal ions, representing removal of more than 99% of each ion. For small volumes of solution, the batch procedure can be experimentally simpler to perform and is commonly used [7, 12, 23].

Ligand—metal studies were carried out using the batch technique. A 20-fold excess of the ligand gave a quantitative uptake of the metal by the resin. A typical plot of such a study, that for Cd(II), is shown in Fig. 3. Identical ligand—metal results were observed, when the column procedure was used. A 100:1 ratio of ligand to metal was normally used in all subsequent studies.

Column experiments using pre-complexation method

Guided by earlier experiences [1, 24], various strong acids were tested as eluents by descending flow. Results for Cd(II), Co(II), and Pb(II) using the eluting procedures described above are presented in Fig. 4; results for Zn(II) are similar to those for Cd(II). Cd(II) and Zn(II) were quantitatively removed from the column by no more than 10 ml of either 2 M HNO_3 or 2 M H_2SO_4, and Pb(II) was quantitatively removed by no more than 11 ml of 2 M HNO_3.

The cobalt complex was not completely removed by nitric or sulfuric acid. The addition of 3 ml of 12 M HCl to the column destroyed the complex, and the Co(II) could then be eluted with no more than 4 ml of 2 M HNO_3.

A stability study was carried out with each of the ions. Columns were loaded with the metal complexes having a 100:1 ligand/metal ratio, and a pH of 8. The metals were then allowed to remain in the column for seven

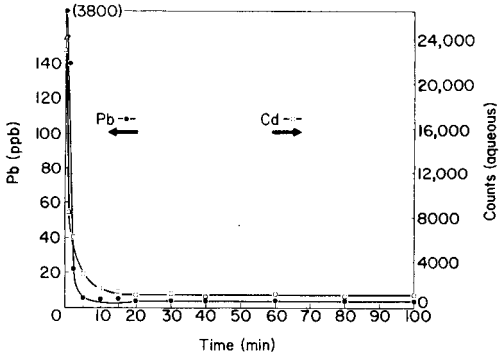

Fig. 1. Rate of removal of lead and cadmium by batch procedure using 4% ligand-loaded resin at pH 8.

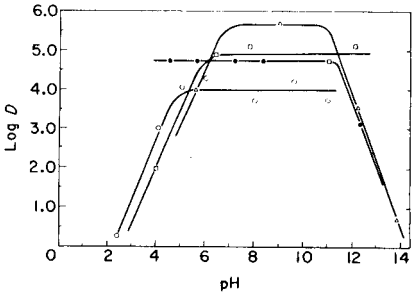

Fig. 2. Effect of pH on distribution coefficients for cobalt (○), zinc (△), cadmium (□) and lead (●) ions.

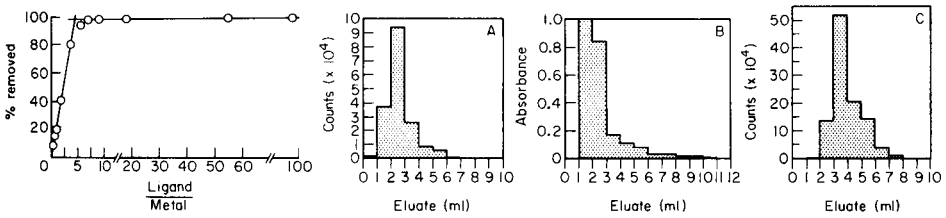

Fig. 3. Ligand/metal study for removal of cadmium using the precomplexation—ion-exchange batch technique at pH 8.

Fig. 4. Elution profiles: (A) for cobalt with 3 ml of 12 M HCl, then 2 M HNO_3 as eluent; (B) for lead with 2 M HNO_3 as eluent; (C) for cadmium with 2 M HNO_3 as eluent.

days, whereupon elution was carried out for each metal. Recovery was 99% or greater for all four metals. Thus, it is apparent that samples can be placed in the column and still be quantitatively eluted days later, which is valuable for field work.

Studies were conducted for the purpose of concentrating the metal ions, while maintaining quantitative recovery. When 0.1—1 μmol of each ion, a 100:1 ligand-to-metal ion ratio, and sample volumes of 250 ml and 1 l were used, recoveries of greater than 99% for all four metal ions were obtained in 11 ml or less final volume. The concentration factors were 25X and 100X for the 250-ml and the 1-l volumes respectively.

Percentage recoveries were determined with decreasing metal concentrations at a constant sample volume of 250 ml and ligand concentration of 0.1 mM. Recoveries of over 99% were attained for Co(II) from 0.24 to 24 ppb, for Cd(II) from 0.45 to 40 ppb, for Zn(II) from 0.26 to 30 ppb, and for Pb(II) at 40 ppb.

Column experiments with ligand-loaded resins

The ligand-loaded resin was evaluated for 100-ml volumes of sample containing 0.1 μmol Cd(II), Co(II), or Zn(II), or 0.4 μmol of Pb(II) at pH 8. Recoveries of greater than 99% were obtained for Cd(II) and Zn(II) at both 4% and 10% ligand-loaded resin and for Pb(II) at 10% ligand-loaded resin. Recoveries of 98% were obtained for Pb(II) at 4% ligand-loaded resin and for Co(II) at both loadings.

CONCLUSIONS AND APPLICATIONS

This procedure for the preconcentration of trace metal ions is superior to the BPPH-S system [1] in terms of the log D and percent removal of the cobalt ion, when the batch technique is employed. The log D for Co(II) with BPPH-S is 3.5 (better than 97% removal), whereas with the HOx-S system the log D is greater than 4 (more than 99% removal). Also, with the batch technique, equilibrium removal of Co(II) required 20 min with HOx-S, but 30 min with BPPH-S. It was shown in the current study that the metal

ions could be left on the column for at least seven days before elution with recoveries of 99%, or greater, for the four metal ions. In the BPPH-S study, a 48 h and 96 h stability study was reported. A greater than 99% recovery for Zn(II) was observed for both times, while Cd(II) showed a 99% recovery at 48 h and a 98% recovery at 96 h, with Co(II) only a 94% recovery at 48 h.

The technique described is well suited to on-site sampling and field work. Samples can be collected and concentrated and the loaded resins stored for a week before elution and measurement. The use of ligand-loaded resins, over pre-complexation, appears to be the preferable technique for field studies.

Gratitude is herewith expressed for financial support by the James F. Duncan Fund and the UW-O Faculty Development Program.

REFERENCES

1 J. E. Going, G. Wesenberg and G. Andrejat, Anal. Chim. Acta, 81 (1976) 349 (Part 1).
2 D. E. Leyden, Am. Lab., Nov. (1974) 24.
3 P. J. Clark, G. F. Neal and R. O. Allen, Anal. Chem., 47 (1975) 650.
4 C. H. Lochmuller, J. Galbraith, R. Walter and J. Joyce, Anal. Lett., 5 (1972) 943.
5 V. A. Fassel and R. N. Kniseley, Anal. Chem., 46 (1974) 1110A.
6 M. J. Fishman and D. E. Erdmann, Anal. Chem., 51 (1979) 317R.
7 C. W. Blout, D. E. Leyden, T. L. Thomas and S. M. Guill, Anal. Chem., 45 (1973) 1045.
8 J. F. Dingman, K. M. Gloss, E. A. Milano and S. Siggia, Anal. Chem., 46 (1974) 774.
9 D. M. Hercules, L. E. Cox, S. Onisick, G. D. Nichols and J. C. Carver, Anal. Chem., 45 (1973) 1973.
10 D. E. Leyden, T. A. Patterson and J. J. Alberts, Anal. Chem., 47 (1975) 733.
11 J. P. Riley and D. Taylor, Anal. Chim. Acta, 40 (1968) 479.
12 R. G. Smith, Jr., Anal. Chem., 46 (1974) 607.
13 K. F. Sugawara, H. H. Weetall and G. D. Schucker, Anal. Chem., 46 (1974) 489.
14 G. daMota, M. M. Roemer and F. G. Griepink, Fresenius Z. Anal. Chem., 287 (1977) 19.
15 K. V. Krishnamurty and M. M. Reddy, Anal. Chem., 49 (1977) 222.
16 M. I. Abdullah, O. A. El-Rayis and J. P. Riley, Anal. Chim. Acta, 84 (1976) 363.
17 J. R. Parrish and R. Stevenson, Anal. Chim. Acta, 70 (1974) 189.
18 J. A. Buono, J. C. Buono and J. L. Fasching, Anal. Chem., 47 (1975) 1926.
19 N. H. Furman (Ed.), Scott's Standard Methods of Chemical Analysis, Vol. I, D. Van Nostrand, New York, 1962, p. 385.
20 H. A. Flaschka, EDTA Titrations, 2nd edn., Pergamon Press, New York, 1964, pp. 80, 87.
21 I. M. Kolthoff, E. B. Sandell, E. J. Meehan, and S. Bruckenstein, Quantitative Chemical Analysis, 4th edn., Macmillan, New York, 1969, p. 1163.
22 J. F. Pankow and J. E. Janauer, Anal. Chim. Acta, 69 (1974) 97.
23 D. E. Leyden, G. H. Lattrell and W. K. Nonidex, Pittsburgh Conference on Analytical Chemistry and Applied Spectroscopy, 1974, paper 61.
24 J. E. Going and C. Sykora, Anal. Chim. Acta, 70 (1974) 127.

Analytica Chimica Acta, 123 (1981) 25—31

RECOVERY EFFICIENCY OF 2,3,7,8-TETRACHLORODIBENZO-*p*-DIOXIN FROM ACTIVE CARBON AND OTHER PARTICULATES

S. S. CUTIÉ

Analytical Laboratories, Dow Chemicals U.S.A., Midland, MI 48640 (U.S.A.)

(Received 22nd February 1980)

SUMMARY

The use of Amoco active carbon (grade PX-21) as a cleanup step for the determination of 2,3,7,8-tetrachlorodibenzo-*p*-dioxin (TCDD) in environmental samples was investigated. Benzene/toluene (1:1) removed 95% TCDD from Amoco active carbon dispersed in silica gel. Other solvents, including benzene, carbon disulfide, dichloromethane, acetone, hexane, acetone/hexane (1:1), and diethyl ether, did not remove TCDD from Amoco active carbon. *o*-Dichlorobenzene is needed to remove TCDD from Pittsburgh active carbon completely. Hot benzene with Soxhlet extraction is adequate for TCDD removal from soil and fly ash particulates. The results derived from this study are consistent with past and present analytical practice for isolating TCDD from different matrices.

The search for dioxins in fly ash from municipal and chemical refuse incinerators and powerhouses has been the object of recent publications. Dow studies [1] have shown that some refuse incinerators and fossil-fueled powerhouses are sources of both airborne and waterborne particulates which contain chlorinated dioxins. Olie et al. [2] found dioxins in emissions from the incineration of garbage in The Netherlands. Buser and Bosshardt [3] reported polychlorinated dibenzo-*p*-dioxins in fly ash and flue gas from a municipal incinerator and an industrial heating facility in Switzerland. Kimble and Gross [4] reported no TCDD in a fraction of fly ash collected downstream from the electrostatic precipitator in a coal-fired powerhouse.

During the course of the Dow investigation to identify the potential sources of chlorinated dioxins and their routes to the environment, the use of Amoco active carbon, recommended by Huckins et al. [5] as a cleanup step for the isolation of 2,3,7,8-TCDD in Herbicide Orange, was evaluated to determine the possibility of incorporating it into the analytical methodology already in use for environmental samples. For samples containing less than 1 μg of TCDD, Huckins et al. recommended the suspension of Amoco active carbon on polyurethane foam, elution of the TCDD with benzene/toluene (1:1), and an additional cleanup on activated alumina. Gas chromatography with an electron capture detector (g.c.—e.c.) was used for the determination. In order to retain the high sensitivity of g.c.—e.c. and the simplicity of these adsorbent cleanup steps, an investigation of the use of activated carbon dispersed on silica gel was made. In addition to the determination of TCDD,

several other common environmental contaminants were also investigated for their recovery from activated carbon. The proposal of Huckins et al. for the use of active carbon was evaluated and the production of dioxins in combustion was investigated.

EXPERIMENTAL

Instrumentation and reagents

TCDD was determined by low-resolution gas chromatography with mass spectrometry (g.c.—m.s.), by gas chromatography with electron capture detection, and by radiotracer counting of ^{14}C-TCDD. A low-resolution Hewlett-Packard 5992 g.c.—m.s. was tuned to monitor ions at *m/z* 320, 322, 324, for native TCDD and 332 for ^{13}C-2,3,7,8-TCDD. The glass g.c. column was 210 cm long (2 mm i.d.), and packed with 0.6% OV-17—0.4% Poly S-179 on a specially deactivated 80—100 mesh Chromosorb W-AW support (prepared by T. Nestrick, Analytical Laboratory, Dow Chemical Co. and now available from HNU Systems Inc.). For the g.c. separation, a Varian 3700 gas chromatograph with e.c. detection was used. The glass column was 7 ft. long (2 mm i.d.), and packed with 3% SP-2401 on 100/120 Supelcoport (Supelco Inc.). The radiotracer measurements were done with a Packard Tri-Carb liquid scintillation spectrometer, model 3380.

All solvents were of distilled-in-glass quality (Burdick and Jackson). The ^{13}C- and ^{14}C-labeled TCDD used were prepared as described earlier [6]. Other materials used were lindane and 2,2-bis-(*p*-chlorophenyl)-1,1-dichloroethylene (*p,p'*-DDE) (both from Supelco), hexachlorobenzene (Aldrich Chemical Company), di-n-octyl phthalate (RFR Corp.), Amoco active carbon (Amoco Research Corporation), and Pittsburgh active carbon (Pittsburgh Activated Carbon Company). The silica gel was chromatographic-grade silicic acid (100—120 mesh Bio-Sil A; Bio-Rad Laboratories).

Determination of extraction efficiency of the solvents investigated

Synthetic samples were prepared that contained 100 ppb of lindane, hexachlorobenzene, 2,3,7,8-TCDD, di-n-octyl phthalate, and *p,p'*-DDE in benzene, carbon disulfide, dichloromethane, acetone, hexane, acetone/hexane, or diethyl ether. To 1- and 5-ml volumes of these samples, 100 mg of Amoco activated carbon (20—30 μm) was added and the solutions were gently shaken for 4 h in a mechanical shaker. Each solution was then filtered through a Millipore teflon filter (type LS, 5 μm) into a Reacti-vial and separated and quantified by g.c.—e.c. Dichloromethane and carbon disulfide were blown down to dryness and the residue was redissolved in the same volume of benzene. New synthetic samples were prepared with the solvents that showed poorer extraction power (dichloromethane and hexane) and the equilibration was performed at 75°C. Then the solution was filtered as before and the components were determined by g.c.—e.c.

Procedure for isolation of TCDD from Amoco active carbon

One part Amoco active carbon (20—30 μm) was mixed with 25 parts (w/w) of silica gel. This mixture was Soxhlet-extracted with benzene/toluene (1:1) for 24 h, and placed in a desiccator under vacuum until used. A 10 cm × 7 mm glass disposable transfer pipet was packed with 0.5 g of the active carbon/silica gel mixture. The sample containing TCDD and other common environmental contaminants dissolved in hexane was added to the column. The column was eluted with 20 ml of benzene/toluene to remove interferences, and then the TCDD was eluted with 40 ml of benzene/toluene at 95°C. The benzene/toluene was evaporated to dryness and an appropriate volume of hexane was added for separation and quantification by g.c.—e.c.

Recovery of TCDD from different matrices

Fly ash particles from incinerator and particulates. The fly ash for the present study was collected in incinerators and powerhouses by use of a sampling train as described in Environmental Protection Agency (EPA) Method 5 [7]. Particulate matter was collected in fireplaces and a private house electrostatic precipitator. The fly ash and particulates were composed of carbonaceous material. The fly ash particles were first separated from water by filtering through a 47-mm diameter glass fiber filter with a pore size range of 0.2—10 μm. Then the particles were Soxhlet-extracted with hot benzene for 16 h. The extract was subjected to either a cleanup procedure and determination as described earlier [1] or by using the procedure described above with Amoco active carbon dispersed in silica gel.

Pittsburgh active carbon. About 10 g of carbon was placed in a modified Soxhlet extractor and refluxed with *o*-dichlorobenzene for 8 h (cf. Fig. 1). The *o*-dichlorobenzene was removed by adding 2 ml of hexadecane and distillation at reduced pressure. The solution was diluted to 100 ml with hexane, then submitted to a cleanup to remove interferences and separated and quantified by low-resolution g.c.—m.s.

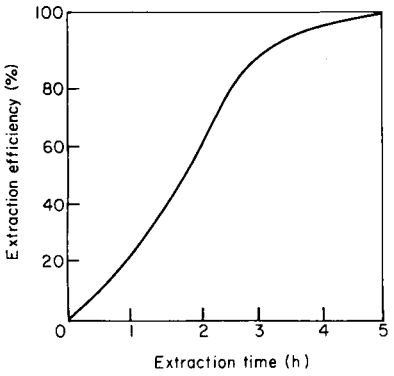

Fig. 1. Extraction efficiency of TCDD from Pittsburgh active carbon using *o*-dichlorobenzene as solvent.

Soil samples. Samples of 2—10 g may be extracted, cleaned, and processed by using the procedure described earlier [1], or by using the procedure described in this paper with Amoco active carbon dispersed in silica gel.

RESULTS AND DISCUSSION

It was found that none of the solvents included in Table 1 would successfully remove TCDD from Amoco active carbon; therefore another approach was taken. The carbon was dispersed on silica gel, and the dispersion was Soxhlet-extracted before use. Silica gel was chosen because it is relatively free of interferences when properly extracted. Under these conditions, benzene/toluene at 95°C extracted more than 95% of the TCDD at amounts ranging from 5 ng to 1 μg total. The TCDD was successfully determined by g.c.—e.c. but the high background with g.c.—m.s. (see Fig. 2) made the determination of TCDD impossible with this latter approach. The high background may have been due to the adsorption of organic materials from air during the loading of the cleanup columns or from "unextractable" hydrocarbons. The identification of the high background was not pursued because by that time a multistep cleanup procedure had been developed [1]. This procedure proved to be specific for the different TCDD isomers, and showed

TABLE 1

Extraction efficiency from Amoco active carbon

Solvent	Volume (ml)	Amount remaining in solution[a] (%)				
		C_6Cl_6	Lindane	*p,p'*-DDE	2,3,7,8-TCDD	Dioctyl phthalate
Benzene	1	50	37	60	0	56
	5	28	55	74	17	77
CS_2	1	0	50	81	0	30
	5	16	51	66	18	75
Dichloromethane	1	10	47	84	0	50
	5	6	40	46	0	35
		6[b]	100	100	0	88
Acetone	1	0	7	5	0	0
	5	3	59	57	15	45
Hexane	1	0	0	0	0	0
	5	2	15	23	8	10
		5[b]	29	36	0	<10
Acetone/hexane	1	0	0	0	0	0
	5	4	57	54	0	60
Diethyl ether	1	0	0	20	0	0
	5	4	44	50	0	45

[a]Represents the amount of component left in the solvent after equilibrium with carbon at 25°C except as noted.
[b]75°C.

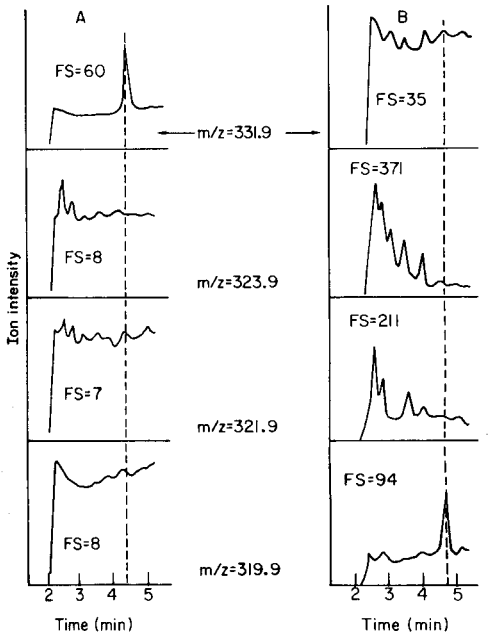

Fig. 2. G.c.—m.s. traces of a ^{13}C-2,3,7,8-TCDD standard and of solvent used to elute an Amoco active carbon column. Also shown are the full-scale (FS) intensities (computer-controlled to keep the largest peak on-scale) of the g.c.—m.s. The peak height multiplied by the full-scale factor corresponds to the total intensity of that ion. (A) Trace of ^{13}C-2,3,7,8-TCDD (500 ng ml^{-1}); dashed line corresponds to TCDD retention time. (B) Trace of a sample fortified with 2,3,7,8-TCDD after activated carbon clean-up; dashed line corresponds to TCDD retention time.

good precision. It also reduced background contamination at these high sensitivity levels. Huckins et al. [5] also suggested an additional cleanup step using alumina for very sensitive (less than 1 μg) TCDD determinations.

Benzene and carbon disulfide (Table 1) proved to be the best solvents for removing hexachlorobenzene, lindane, *p,p'*-DDE and dioctyl phthalate from active carbon. The performance of acetone/hexane in removing lindane and dioctyl phthalate is similar to that of benzene and carbon disulfide. Warm dichloromethane is a better solvent for lindane, *p,p'*-DDE and dioctyl phthalate. There is a discrepancy for dichloromethane between the 1- and 5-ml portions when the results are compared to those of the other solvents. This could be due to losses during the evaporation step when dichloromethane was removed prior to electron capture detection.

Table 2 lists the efficiencies of various solvents and procedures used to extract TCDD from different matrices, as explained in the experimental section.

The use of Amoco active carbon dispersed on silica gel as a cleanup step for the isolation of 2,3,7,8-TCDD in environmental samples shows good results when the species is separated and quantified by gas chromatography

TABLE 2

Removal of 2,3,7,8-TCDD from different matrices

Extraction mode	Solvent	Recovery(%)
Incinerator fly ash particles fortified at 30 × 10^{-6} ppm		
Soxhlet	Benzene	60
Pittsburgh active carbon fortified at 0.5 ppm		
Modified Soxhlet[a]	Acetone/hexane	none
Modified Soxhlet	Formic acid/benzene	none
Modified Soxhlet	Acetonitrile/benzene	none
Modified Soxhlet	Carbon tetrachloride/methylethylketone	none
Modified Soxhlet	Benzene	30
Modified Soxhlet	Benzene/toluene	30
Modified Soxhlet	*o*-Dichlorobenzene	> 95
Soil fortified at 10 × 10^{-6} ppm		
Soxhlet	Benzene	99

[a]Device and procedure as described earlier [12].

with electron capture detection. Its use is limited for g.c.—m.s. analysis because of the excessive background present, even when the carbon and silica gels were Soxhlet-extracted overnight with benzene/toluene. The recovery of dioxin can be affected by the amount of carbon used [8].

Conclusions

These results are consistent with previous experience which indicates that successful extraction and isolation of TCDD from environmental samples depends mostly on the matrix activity toward dioxins. When the structure of the matrix resembles the graphite structure, which shows strong adsorption characteristics for planar molecules such as TCDD, best results are obtained when aromatic solvents [5, 9] and exhaustive Soxhlet extraction for extended periods of time are employed. Successful extraction of TCDD from Pittsburgh activated carbon has been achieved with *o*-dichlorobenzene for 8 h in a modified Soxhlet extractor. In contrast, Lamparski et al. [10] needed only hexane after a potassium hydroxide digestion to extract chlorodioxins completely from fish tissue. These very efficient extractions of dissimilar matrices with solvents of different polarity point out the value of properly matching the sample and the solvent. These findings indicate that the feasibility of using active carbon as packing for high-performance liquid chromatography cleanups should be evaluated. Results reported here may have important implications for studies with other types of samples [11].

The author thanks R. Stehl, W. Crummett and D. Armentrout for their help and suggestions during the course of this investigation.

REFERENCES

1 The Trace Chemistries of Fire—A Source of Chlorinated Dioxins, Dow Chemical Company, Nov. 1978.
2 K. Olie, P. L. Vermeulen and O. Hutzinger, Chemosphere, 8 (1977) 455.
3 H. R. Buser and H. P. Bosshardt, Chemosphere, 2 (1978) 165.
4 B. J. Kimble and M. L. Gross, Science, 207 (1980) 59.
5 J. N. Huckins, D. L. Stalling and W. A. Smith, J. Assoc. Off. Anal. Chem., 61 (1978) 32.
6 A. S. Kende and J. J. Wade, Environ. Health Persp., 5 (1973) 49.
7 Environmental Protection Agency Methods 1, 2, 3 and 5 Federal Register 42 (No. 160) 41754-41789 (August 18, 1977).
8 K. Grob, J. Chromatogr., 84 (1973) 255.
9 L. R. Snyder, Principles of Adsorption Chromatography, M. Dekker, New York, 1968, pp. 62, 169 and 198.
10 L. L. Lamparski, T. J. Nestrick and R. H. Stehl, Anal. Chem., 51 (1979) 1453.
11 G. L. Fisher, Environ. Sci. Technol., 12 (1978) 447.
12 D. L. Stalling, J. Johnson and J. N. Huckins, in F. Coulston (Ed.), Environmental Quality and Safety, Supplement Volume III, G. Thieme Verlag, Stuttgart, 1975, p. 14.

Analytica Chimica Acta, 123 (1981) 33—40

HIGH-PERFORMANCE LIQUID CHROMATOGRAPHIC PROFILES OF LOW-MOLECULAR-WEIGHT, U.V.-ABSORBING COMPOUNDS IN THE SERA OF BEAGLES EXPOSED TO CIGARETTE SMOKE

SEBASTIAN P. ASSENZA and PHYLLIS R. BROWN*

Department of Chemistry, University of Rhode Island, Kingston, RI 02881 (U.S.A.)

(Received 29th April 1980)

SUMMARY

High-performance liquid chromatography with a nonpolar stationary phase was used to determine the low-molecular-weight, u.v.-absorbing compounds in the sera of male beagles exposed to cigarette smoke. The sera from three groups of tracheostomized beagles were processed. The chromatographic profiles of the beagles exposed to the smoke of low-nicotine cigarettes for 610—750 days were not significantly different from the profiles of beagles identically exposed to the smoke of high-nicotine cigarettes. However, several important differences were determined between the profiles of sham controls and the dogs exposed to cigarette smoke. Most notably, a two-fold elevation of serum inosine was found in all beagles exposed to cigarette smoke.

Epidemiological evidence has emphasized the correlation between cigarette smoking and the increased incidence of disease and premature death [1, 2]. Although tobacco smoke has been found to contain many toxic compounds and produce some physiological disorders [8—11], the mechanisms by which smoking causes disease are not known. Furthermore, only a few biochemical alterations have been identified which could be used as "markers" to detect the onset of disease or to recognize smokers at greater risk of disease [12, 13].

Lack of progress in the area of smoke-related biochemical alterations may be partly due to inadequate methods for monitoring subtle and complex biochemical changes. However, with the recent development of microparticle, chemically-bonded, nonpolar packings (so-called reversed phase) for high-performance liquid chromatography (h.p.l.c.), a wide variety of compounds in physiological samples can be determined accurately and rapidly [14—17].

In this laboratory, large numbers of serum samples from subjects with no known disease and patients with various diseases are routinely analyzed by h.p.l.c. The serum metabolic profiles of most subjects with no known disease have been found to be very similar [16, 17]; however, the profiles of several subjects with lung cancer and some heavy smokers were found to be different from normal. Therefore, an investigation of the effects of cigarette smoking on the h.p.l.c. profiles of low-molecular-weight, u.v.-

absorbing serum constituents was conducted using an animal model, the beagle dog, to control carefully experimental parameters such as age, sex, diet, medications, and inhalation routine.

EXPERIMENTAL

Instrumentation

An ALC 204 liquid chromatograph (Waters Associates, Inc., Milford, MA) equipped with a Model 660 solvent programmer, a Model 440 dual-wavelength detector, a Model U6K injector, and Model 6000A solvent delivery system was used. A dual-channel Omniscribe recorder (Houston Instrument, Austin, TX) was used to record the 280 nm and 254 nm detector signals. Retention times and peak areas were obtained on a HP 3380A electronic integrator (Hewlett-Packard, Avondale, PA) fed by the 254 nm channel.

Columns and chromatographic conditions

A μBondapak—C_{18} (Waters Associates) chemically-bonded, 10 μm, nonpolar column (3.9 × 300 mm) was used. A pre-column (4.6 × 50 mm) tap-packed with pellicular, 25 μm, nonpolar material (Whatman Inc., Clifton, NJ) was used to guard and prolong the life of the main column.

The initial eluant was 20 mM KH_2PO_4, prepared by dissolving the anhydrous buffer in double-distilled, deionized water and adjusting the pH to 5.7 with dilute potassium hydroxide solution. The final eluant (specific gravity, 0.904) was a mixture of 60% methanol (Burdick and Jackson, Muskegon, MI) and 40% water (by volume). Each eluant was degassed prior to use in a turbulent stream of helium for 30 s. A linear gradient from 0 to 40% of the final eluant in 35 min was used. The flow-rate was set at 1.5 ml min^{-1} and the determinations were at ambient temperature.

Chemicals

All standard reference compounds were purchased from Sigma Chemical Corp. (St. Louis, MO) and stock solutions were prepared to 100 μM concentrations. Enzymes for peak identification were of the highest purity available from Sigma. Compounds for qualitative tests were purchased from Amend Drug and Chemical Co. (New York, NY) and Pfaltz and Bauer Inc. (Stamford, CT).

Inhalation program

Healthy male beagles from the same blood line, similar in age, weight, and size, were maintained at the Borriston Research Laboratories (Temple Hills, MD) under strict experimental control. One hundred and forty-seven dogs were trained to breathe through a tracheostoma and divided into three groups. A group of 49 dogs received 12 high-nicotine cigarettes per day; a group of 48 dogs received 12 low-nicotine cigarettes per day; and a group of 50 dogs was chosen as the sham control. The low-nicotine cigarettes

used in this study were NCI Series IV, Code 13. Series SEB IV cigarettes, Codes 04, 14, 29, and 32 were used interchangeably as the high-nicotine cigarette. Smoke was administered through a cuffed tracheostomy tube by an ADL II smoking machine (Arthur D. Little, Inc., Cambridge, MA). Dosage consisted of one puff of smoke every 30 s, until a 23-mm butt length was reached. The low- and high-nicotine cigarettes offered the beagles 0.24 and 2.29 mg of nicotine per cigarette, respectively. After the dogs had been exposed regularly to the cigarette smoke for 610—750 days, blood samples were drawn. Control samples were drawn after 620 days. Samples were typically taken before feeding and 18 hours after the smoking sessions.

Sample preparation

Blood from each dog was drawn into evacuated tubes and allowed to clot while standing for 15 min at ambient temperature. The tubes were centrifuged at 1145 relative centrifugal force (RCF) for approximately 10 min. The supernatant fluid was collected, coded, and shipped to us frozen in carbon dioxide.

The coded samples were allowed to sit at room temperature for 3 h [16] before processing. To remove protein with nominal molecular weights greater than 25000 daltons, the sera were ultrafiltered through membrane cones (Amicon Inc., Lexington, MA) at 690 RCF for 20 min. An internal standard, tubercidin, was added to a representative group of samples prior to processing to monitor recovery.

The protein-free filtrates were processed in duplicate and stored at −20°C.

Peak identification

Standards having retention times and absorbance ratios ($Area_{280}/Area_{254}$) similar to those of the serum peaks were co-chromatographed with the canine sera. The complete co-elution of the standard and the serum peak with no change in absorbance ratio provided the basis for tentative identifications. Peak identities were confirmed with on-line fluorescence detection (FS 970 L. C. Fluorometer, Schoeffel Instrument Division, KRATOS, Inc., Westwood, NJ), stopped-flow u.v.-spectra (SF 770 Spectroflow Monitor, Schoeffel Instrument Division), and qualitative chemical tests using enzyme-catalyzed reactions and reactions with functional-group-specific reagents, such as hydrochloric acid, nitrous acid and sodium periodate [15—17].

RESULTS

Recovery studies

A detailed comparison of methods used to process serum prior to chromatographic separation was performed [18] and ultrafiltration was the method chosen for the present study. An internal standard, tubercidin, was added to a number of canine serum samples and processed at physiological pH. There was excellent recovery of a majority of the constituents,

including 98% recovery of the internal standard; however, at physiological pH only 12% of total tryptophan is recovered because of its characteristic binding to protein.

Chromatographic results

The peaks present in the profiles of all the canine sera were labeled A—M. Visually, the coded profiles could be divided into two groups according to the intensity of peak J. Figure 1 shows the representative chromatograms from the two groups of profiles. Computer-assisted grouping revealed that the profiles of the first group (Fig. 1A) have higher levels of peaks F, H, I, J, and K, and lower levels of peak G, than the second group of profiles (Fig. 1B).

When the codes were broken, the first group were found to be comprised of the serum profiles from all the dogs chronically exposed to cigarette smoke. The profiles of the second group were the serum samples taken from the sham controls.

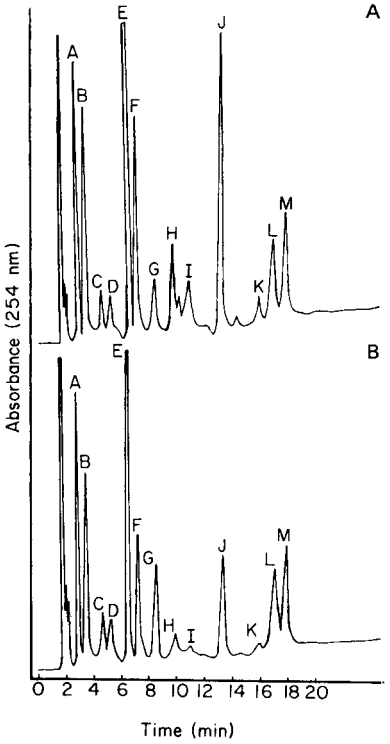

Fig. 1. Chromatograms from the two determined groups of canine sera. The upper chromatogram represents the profiles obtained from all beagles exposed to cigarette smoke. The lower chromatogram is a serum profile obtained from the sham controls. Note the greatly increased level of inosine (J) in the upper chromatogram. Injection volume 40 μl; detector range 0.02 absorbance units. Other conditions in text.

Identity of peaks

Based on the accumulated evidence from retention data, co-chromatography, absorbance ratios, u.v.-spectra, fluorescence, enzymatic reactions, and reactions with functional-group-specific reagents, the peaks of the h.p.l.c. serum profiles (Fig. 1) were identified as creatinine (A), uric acid (B), tyrosine (C), cytidine (D), hypoxanthine (F), xanthine (G), inosine (J), and tryptophan (L). Based on more limited data, peaks H, I, and K were identified as kynurenine, 5-methylcytidine, and inosine 3′,5′-cyclic phosphate (cIMP), respectively. Peak E is believed to be riboflavin and peak M remains unknown.

Quantification

The identified compounds were quantified by an external standard method. An accurately determined concentration of standard compounds in a reference solution was chromatographed to obtain relative molar responses. The response values were determined linear over the range of concentrations found.

Within a group of profiles, mean peak values obtained from the duplicate assays were pooled and frequency distributions plotted. The frequency distributions of the arithmetic values were compared to those of the logarithmic transformations, and judged as to which representation better fit the theoretical curve. Where frequency distributions appear normal, all calculations were done with the arithmetic means. Where log-normal distributions were apparent, logarithmically transformed values were used in all calculations.

Table 1 lists the concentrations of some of the compounds determined in the sera of the sham controls and the dogs exposed to the low- and high-

TABLE 1

Concentrations of some serum compounds in the profiles of tracheostomized beagles

Compound	Concentration (μmol l^{-1})		
	Low nicotine	High nicotine	Control
Creatinine	90.0 (21.2)[a]	88.7 (22.6)	93.5 (24.3)
Tyrosine	42.2 (20.3)	38.7 (14.9)	40.1 (17.5)
Cytidine	1.55 (1.02)	1.66 (1.00)	1.61 (1.00)
Hypoxanthine	11.1 (3.62)	11.7 (3.47)	7.75 (2.93)
Xanthine	7.92 (2.37)	7.51 (1.29)	9.72 (2.11)
Kynurenine	143 (31.0)	147 (43.4)	115 (22.7)
5-Methylcytidine	3.29 (.976)	3.27 (.738)	1.69 (.436)
Inosine	10.9 (3.51)	11.3 (3.52)	5.04 (1.29)
c-IMP	2.31 (1.27)	2.75 (1.03)	0.648 (.213)
Tryptophan	58.8 (12.7)	49.8 (11.2)	52.6 (13.5)

[a]Standard deviations are given in parentheses.

nicotine cigarettes. Corrections have been made for losses of serum components through the filtration process. Tryptophan concentrations are reported as their free levels.

Statistical analysis

A two-group comparison test for paired data was performed to determine the differences between the groups of profiles. The comparisons were based on the values obtained above. All differences were determined at the 98% confidence limit of the Student's *t*.

No significant differences were determined between the profiles of dogs which had been exposed to the smoke of low-nicotine cigarettes and dogs which had been exposed to the smoke of high-nicotine cigarettes. However, all of the dogs exposed to cigarette smoke were found to have higher levels of hypoxanthine, kynurenine, 5-methylcytidine, inosine, and c-IMP, and lower levels of xanthine than the sham controls. Interestingly, inosine levels were at least twice the control values in the dogs which had been exposed to cigarette smoke.

DISCUSSION

An animal model, the beagle dog, was used for this investigation because many important experimental parameters could be maintained constant throughout the study. The reproducibility of the peak patterns observed within a group of profiles is believed to reflect this strict control. Unlike smoke exposure studies using human subjects [19] which preclude the maintenance of all controls, the data obtained from the canine serum profiles can be subjected to statistical analyses with a greater likelihood of observing differences caused by smoke exposure, not the inherent subject-to-subject variability.

The data from this study imply that cigarette smoking alters the metabolism of some compounds in the purine metabolic pathway. The two-fold elevation of serum inosine in the beagles exposed to cigarette smoke is a potentially important finding. Increased levels of inosine arising from purine nucleoside phosphorylase deficiencies have been associated with severe immunodeficiency [20–22]. In addition, high levels of several nucleosides and bases in biological matrices are known to be toxic [23, 24]; an increased level of inosine is believed to be toxic because it inhibits indirectly the activity of adenosine deaminase [25]. Furthermore, the elevation of the compound (peak K) with the spectral, retention, and chemical characteristics of c-IMP is intriguing, since c-IMP has not been implicated in previous smoking studies and its role in purine metabolism is unknown. Although peak identification data to date imply that peak K is c-IMP, further work is proceeding to identify this compound unequivocally.

With the separation and identification techniques used, many of the low-molecular-weight, u.v.-absorbing serum constituents were determined.

Although the identification scheme is time-consuming, the use of on-line, rapid-scan, multi-component detectors [26, 27] would greatly facilitate peak identifications. Thus, the profiles of serum compounds could serve as an even more rapid and efficient tool for the identification of metabolic changes in the studies of disease processes.

We thank Dr. Richard Hartwick, Dr. Raymond Panzica, Mr. Hubert Scoble, and Mr. Malcolm McKeag for their comments and assistance. Appreciation is also extended to Dr. Thomas Nightingale and Dr. Winifred Palmer of Enviro Control, Inc. Support for this work was provided in part by United States Public Health Grant 5 RO1 CA17603-4, Enviro Control Contract NO1 CP55666, and a research fellowship provided by the Personal Care Division, The Gillette Company, Boston, Massachusetts.

REFERENCES

1 U.S. Department of Health, Education, and Welfare, The Health Consequences of Smoking, U.S. Govt. Print. Off., 1974.
2 E. L. Wynder, L. S. Covey and K. Mabuchi, Am. J. Epidemiol., 100 (1974) 168.
3 S. S. Hecht, C. B. Chen, N. Hirota, R. M. Ornaf, T. C. Tso and D. Hoffman, J. Natl. Cancer Inst., 60 (1978) 819.
4 S. S. Hecht, R. Thorne, R. R. Maronpot and D. Hoffmann, J. Natl. Cancer Inst., 55 (1975) 1329.
5 M. R. Guerin, G. Olerich and A. D. Horton, J. Chromatogr. Sci., 12 (1974) 385.
6 S. G. Zeldes and A. D. Horton, Anal. Chem., 50 (1978) 779.
7 Y. Y. Lui, I. Schmeltz and D. Hoffman, Anal. Chem., 46 (1974) 885.
8 N. Kobayashi, D. Hoffmann and E. L. Wynder, J. Natl. Cancer Inst., 53 (1974) 1085.
9 S. S. Park, Y. Kikkawa, I. P. Goldring, M. M. Daly, M. Zelefsky, C. Shin, M. Spierer and T. Morita, Am. Rev. Respir. Dis., 115 (1977) 971.
10 O. Auerbach, E. C. Hammond, D. Kirman and L. Garfinkel, J. Am. Med. Assoc., 199 (1967) 241.
11 O. Auerbach, E. C. Hammond, D. Kirman, L. Garfinkel and A. P. Stout, Cancer, 20 (1967) 2055.
12 M. Marco, B. Mass, D. R. Meranze, G. Weinbaum and P. Kimbel, Am. Rev. Respir. Dis., 104 (1971) 595.
13 A. Janoff, B. Sloan, G. Weinbaum, V. Damiano, R. A. Sandhaus, J. Elias and P. Kimbel, Am. Rev. Respir. Dis., 115 (1977) 461.
14 C. W. Gehrke, K. C. Kuo, G. E. Davis, R. D. Suits, T. P. Waalkes and E. Borek, J. Chromatogr., 150 (1978) 455.
15 R. A. Hartwick, S. P. Assenza and P. R. Brown, J. Chromatogr., 186 (1979) 647.
16 R. A. Hartwick, A. M. Krstulovic and P. R. Brown, J. Chromatogr., 186 (1979) 659.
17 S. P. Assenza and P. R. Brown, J. Chromatogr., 181 (1980) 169.
18 R. A. Hartwick, D. van Haverbeke, M. McKeag and P. R. Brown, J. Liq. Chromatogr., 2(5) (1979) 725.
19 K. Takahashi, H. Takao, T. Takai, K. Gotch, S. Matsukura and H. Imura, Life Sci., 21 (1977) 803.
20 E. R. Giblett, A. J. Amman, D. W. Wara, R. Sandman and L. K. Diamond, Lancet, 1 (1975) 1010.
21 J. E. Seegmiller, T. Watanabe, M. H. Schreier and T. A. Waldmann, in M. M. Maller, E. Karser and J. E. Seegmiller (Eds.), Purine Metabolism in Man II, Plenum Press, New York, 1977, 412.

22 S. K. Wadman, P. D. de Bree, H. H. van Gennip, J. W. Stoop, B. J. M. Zegers, G. E. J. Stool, and L. H. Sigenbeck van Heuklom, in M. M. Maller, et al. (Eds.), Purine Metabolism in Man II, Plenum Press, New York, 1977, 471.
23 R. Parkman, E. W. Gelfand, F. S. Rosen, A. Sanderson and R. Herschhorn, N. Eng. J. Med., 292 (1975) 714.
24 F. L. Meyskens and H. E. Williams, Biochim. Biophys. Acta, 249 (1971) 170.
25 R. P. Agarwal, G. W. Crabtree, R. E. Parks, Jr., R. P. Nelson, R. Keightley, R. Parkman, F. S. Rosen, R. C. Stern and S. H. Polmar, J. Clin. Invest., 57 (1976) 1025.
26 A. McDowell and H. L. Pardue, Anal. Chem., 48 (1976) 1815.
27 I. M. Warner, J. B. Challis, E. R. Davidson and G. D. Christian, Clin. Chem., 22 (1976) 1483.

Analytica Chimica Acta, 123 (1981) 41—44

LIQUID CHROMATOGRAPHIC SEPARATION OF FATTY ACID METHYL ESTERS AND PHOSPHATIDIC ACID DIMETHYL ESTERS WITH SILVER NITRATE-IMPREGNATED SILICA GEL COLUMNS

JOHN Y.-K. HSIEH*, DAVID K. WELCH and JOSEPH G. TURCOTTE

Department of Medicinal Chemistry, University of Rhode Island, Kingston, RI 02881 (U.S.A.)

(Received 31st March 1980)

SUMMARY

Standard fatty acid methyl esters were separated by high-performance liquid chromatography with a silver nitrate-impregnated silica gel column with benzene as eluent and a differential refractometer as the detector. The separation, based on the number of double bonds, was greatly improved when the benzene was dried over calcium chloride for two days. Phosphatidic acid dimethyl esters derived from egg phosphatidylcholines were also resolved into three major fractions on the basis of the degree of unsaturation on a silver(I)-loaded resin column with diethyl ether as eluent and detected with a flame ionization monitor.

Silver nitrate has been used in gas—liquid [1], thin-layer [2], and conventional liquid [3, 4] chromatography for separations of lipids based on the number, position, and geometry of the unsaturated centers. Some existing problems with silver nitrate as a separating medium are sample volatility, thermal instability, low resolution, poor reproducibility, and long separation time. Developments in column theory and instrumentation of modern liquid chromatography indicated that high-performance liquid chromatography (h.p.l.c.) could overcome many of those problems.

Several methods have been reported in which h.p.l.c. on silver(I)-impregnated columns has been used for separations of alken-1-ol acetates [5—8] and fatty acid methyl esters [9—11]. During recent h.p.l.c. studies of molecular species of phosphoglycerides [12], it was found that many phosphoglyceride molecules to be separated differed only by the degree of unsaturation of the two fatty acid moieties. This prompted an investigation of the possibilities of applying silver(I)-treated columns. Here, an h.p.l.c. method is described for the separation of fatty acid methyl esters using a silver(I)-impregnated silica gel column. Resolution of molecular species of phosphoglycerides employing a silver(I)-loaded resin column is reported.

*Present address for correspondence: Psychiatry Service, Bronx Veterans Administration Hospital, Bronx, NY 10468, U.S.A.

EXPERIMENT

Chemicals

Fatty acid methyl ester standards were obtained from Supelco (Bellefonte, PA), NuChek Prep. (Elysian, MN), and Sigma Chemical Co. (St. Louis, MO). Egg phosphatidic acid dimethyl esters were prepared as described previously [12]. Reagent-grade silver nitrate and solvents were used. Benzene and toluene were dried over $CaCl_2$ for two days, filtered with Millipore filters, and then degassed before use. Tetrachloroethane and stabilizer-free dioxane were separately passed through an open silica gel column to remove any impurities which might irreversibly adhere to the adsorbent used to pack the h.p.l.c. columns. The dioxane also was passed through an open alumina column to remove peroxides.

Apparatus

A high-performance liquid chromatograph equipped with a M6000 solvent delivery pump, a U6K injector, and a R401 differential refractometer (ALC/GPC 202, Waters Associates, Milford, MA) was used; in one case a moving wire detector (Pye LCM2, Phillips Electronics Inst., Mt. Vernon, MA) was employed. When specified, the column was heated to 40 ± 1°C in a temperature-controlled block (Waters Associates) by using an external circulating water bath.

Column preparation

Columns with zero dead-volume fittings were made from 4.6 mm i.d. stainless steel tubing. Before use, each tube was successively washed with hexane, dichloromethane, acetone, and methanol.

LiChrosorb SI 100 (EM Laboratories, Inc., Elmsford, NY) was dried overnight at 160°C under 2 torr pressure. Silver nitrate (0.078 g) was dissolved in 4 ml of anhydrous methanol and placed in a 100-ml indented flask wrapped with aluminum foil to exclude light. To this was added 3.8 g of the adsorbent suspended in 25 ml of acetonitrile. The solvents were then evaporated on a rotary evaporator at 50°C under reduced pressure using a water aspirator.

The silver nitrate-coated silica gel, suspended in a solvent mixture of tetrachloroethane and dioxane, was packed into the columns in a manner similar to that described by Heath et al. [8].

A silver(I)-loaded resin column was prepared by passing 300 ml of 1 M $NaNO_3$ solution and then 400 ml of 1 M $AgNO_3$ solution through a Partisil-10 SCX column (Whatman Inc., Clifton, NJ), followed by 300 ml of deionized water until no silver(I) ions were present. Before being used with non-polar solvents such as benzene, diethyl ether, and toluene, the column was flushed with 100 ml of methanol.

RESULTS AND DISCUSSION

Five columns differing in both column length (10, 20, and 30 cm) and silver percentage (0.5, 2, 5, and 20%) were tested for separations of a standard fatty acid methyl ester mixture containing 0—4 double bonds: 18:0 methyl stearate, 18:1 methyl oleate, 18:2 methyl linoleate, 18:3 methyl linolenate, and 20:4 methyl arachidonate (where 18:n means 18 carbon atoms and *n* double bonds). Under the chromatographic conditions employed, a 30-cm column with 2—5% silver loading gave reasonable resolution of the mixture.

Figure 1A shows that the elution order is consistent with the number of double bonds in the olefin. A silica gel column without silver loading yielded no separation under the same chromatographic conditions. Scholfield [11] has recently reported that methyl linolenate (18:3) was not eluted from a 61 cm × 2 mm i.d. silicic acid column impregnated with 16% silver loading using regular benzene. No difficulty was experienced in eluting 18:3 and 20:4 fatty acid methyl ester from a 20-cm 5% $AgNO_3$—silica gel column whereas some 18:3 and 20:4 fatty acid methyl ester was retained on a 30-cm 5% $AgNO_3$—silica gel column.

When dry benzene was used as eluent, a base-line separation was achieved as shown in Fig. 1B. Benzene containing a trace of water could dissociate the Ag—olefin$^+$ complexes more easily than dry benzene and give a poorer separation. A change in temperature from 25°C to 40°C resulted in a shorter retention time for each fatty acid methyl ester, but did not affect the resolution of the standard mixture when the same column and dry benzene were

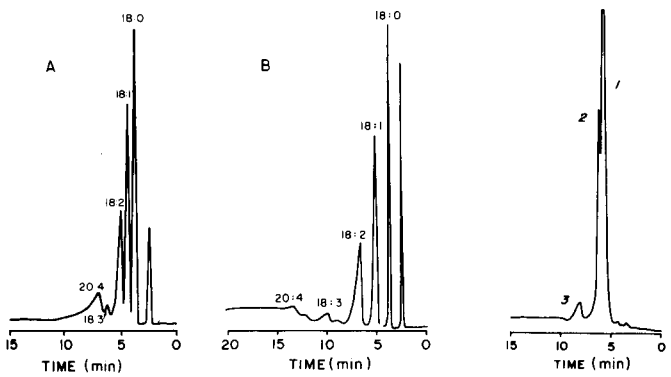

Fig. 1. H.p.l.c. separation of standard fatty acid methyl esters on a 30-cm 5% $AgNO_3$—silica gel column with benzene at 2 ml min^{-1}: (A) regular benzene; (B) dry benzene. Detection refractive index × 16.

Fig. 2. H.p.l.c. separation of phosphatidyl acid dimethyl esters derived from egg phosphatidylcholines on a 25-cm, silver(I)-loaded resin column with diethyl ether at 1 ml min^{-1}. Detection flame ionization × 16. Peaks 1, 2, and 3 are for molecules having 1, 2, and 3 or more double bonds.

used. To avoid the toxic properties of benzene, both wet and dry toluene were evaluated and each yielded resolution similar to the other.

The silver(I)-impregnated silica gel columns were found to be reasonably stable as reported by Heath et al. [6]. Over 100 separations were performed with a single column without any significant deterioration of the column.

When polar solvents are needed in the mobile phase, it is preferable to use a silver(I)-loaded resin column because silver(I) ions tend to be eluted from silica gel columns by polar solvents [13]. A silver(I)-loaded resin column was prepared and tested by injecting a fatty acid methyl ester mixture using benzene as eluent; some degree of resolution among the 18:0, 18:1, and 18:2 methyl esters was obtained but at the sacrifice of no separation between the 18:3 and 20:4 methyl esters.

A number of pure and mixed solvents were tried with no success in resolving phosphoglycerides into molecular species based on the degree of unsaturation using both 2 and 5% $AgNO_3$—silica gel columns. However, egg phosphatidyl acid dimethyl esters were separated on a silver(I)-loaded resin column using diethyl ether as eluent as shown in Fig. 2. Molecular species having one double bond (peak 1) were not well separated from those with two double bonds (peak 2), but both of them were base-line separated from those having three or more double bonds (peak 3).

The silver(I)-loaded resin column, although unsuitable for the separation of fatty acid methyl ester, needs to be investigated further for separations of complex lipids since it is quite stable, readily available, and easily regenerated.

REFERENCES

1 D. M. Ottenstein, D. A. Bartley and W. R. Supina, J. Chromatogr., 119 (1976) 401.
2 A. Kuksis, in A. Kuksis (Ed.), Handbook of Lipid Research, Fatty Acids and Glycerides, Plenum, New York, 1978, p. 1.
3 W. W. Christie, Lipid Analysis, Pergamon, Oxford, 1977, pp. 103, 152.
4 C. R. Schofield and T. L. Mounts, J. Am. Oil Chem. Soc., 54 (1977) 319.
5 N. W. H. Houx, S. Voerman and W. M. F. Jongen, J. Chromatogr., 96 (1974) 25.
6 R. R. Heath, J. H. Tumlinson, R. E. Doolittle and A. T. Proveaux, J. Chromatogr. Sci., 13 (1975) 380.
7 J. D. Warthen, Jr., J. Chromatogr. Sci., 14 (1976) 513.
8 R. R. Heath, J. H. Tumlinson, R. E. Doolittle and J. H. Duncan, J. Chromatogr. Sci., 15 (1977) 10.
9 F. Mikeš, V. Schurig and E. Gil-Av, J. Chromatogr., 83 (1973) 91.
10 N. H. W. Houx and S. Voerman, J. Chromatogr., 129 (1976) 456.
11 C. R. Scholfield, J. Am. Oil Chem. Soc., 56 (1979) 510.
12 J. Y-K. Hsieh, Ph.D. Dissertation, University of Rhode Island, Kingston (1979).
13 B. de Vries, J. Am. Oil Chem. Soc., 40 (1963) 184.

Analytica Chimica Acta, 123 (1981) 45—56

A RAPID AND SIMPLE METHOD FOR THE DETERMINATION OF TRACE METALS IN HAIR SAMPLES BY ATOMIC ABSORPTION SPECTROMETRY

G. BAGLIANO

International Atomic Energy Agency, Safeguards Analytical Laboratory, A-2444 Seibersdorf (Austria)

F. BENISCHEK and I. HUBER*

Österreichisches Forschungszentrum Seibersdorf GmbH, A-2444 Seibersdorf (Austria)

(Received 19th August 1980)

SUMMARY

Acid digestion procedures are described for the dissolution of human head hair in routine determinations of cadmium, chromium, mercury, lead and zinc in the same sample solution by means of atomic absorption spectrometry. The techniques employed are atomization in a Massman graphite furnace or in an air—acetylene flame; the cold-vapor cell is used for mercury. The entire analytical procedure is tested with powdered homogenized head hair samples, previously analyzed by other analytical techniques. Comparison of the results demonstrates that the proposed technique is at least as precise and accurate as the other procedures used.

The application of atomic absorption spectrometry (a.a.s.) to the determination of heavy metal traces in head hair samples has been extensively described. Flame atomization [1—9] and electrothermal atomization as well as cold-vapor techniques [10—14] have been applied. No attempts, however, have so far been reported to determine Cd, Cr, Hg, Pb and Zn in the same hair solution routinely by these techniques. Instrumental neutron activation analysis (i.n.a.a.) is the most frequently used technique for determining trace elements in hair, but it is worthwhile to set up a quick and inexpensive method for the determination of elements such as Cd, Cr and Pb which are rather difficult to measure by i.n.a.a. because of their unfavorable nuclear properties [15—18]. Furthermore, laboratories which do not have easy access to a reactor for irradiation of the samples may need to determine quickly some of the most relevant toxic elements together with at least one essential element. The content of an essential element must be known in order to evaluate the significance of the distribution of the toxic elements along the hair [19]. Thus it is necessary to include in the list of the elements of interest both mercury and zinc; the first is a representative and important pollutant while zinc is frequently used as the essential element of reference because its distribution is well known to be uniform along the hair shaft.

Finally, widely different techniques are useful and necessary in detecting systematic errors and in characterizing intercomparison samples and standard reference materials.

EXPERIMENTAL

Equipment

A Perkin-Elmer (PE) model 305 atomic absorption spectrometer equipped with Intensitron hollow-cathode lamps and deuterium arc lamp, on line with a PE recorder model 56 was the basic instrumentation used. A PE mercury analysis system, an HGA-76 graphite furnace equipped with an AS-1 automatic sampler, and a burner with a 4-in. single-slot head, were assembled in turn with the spectrometer. A micro ball mill (model II, Braun Melsungen equipped with a cylindrical teflon vessel tightly closed with a teflon lid and containing a teflon-coated steel ball, was used to pulverize and homogenize the hair samples. A digestion bomb (PE autoclave-1) heated on a thermostatically controlled ceramic hot plate was used for the preliminary tests to establish the optimal conditions for the dissolution of the hair samples. Home-made screw-capped teflon beakers (50 mm external diameter, 60 mm height) heated in a conventional oven were later used routinely for the decomposition of the samples.

Two resin exchangers (a Seradest Seral in line with an Elgastat) were used to prepare very pure double-deionized water. All glassware was stored in a dithizone solution in carbon tetrachloride; before use it was rinsed thoroughly with the deionized water and drained until dry at room temperature. The digested hair samples were diluted with the deionized water and stored in polyethylene volumetric flasks. Eppendorf pipettes were used to prepare the standard solutions, which were also stored in polyethylene bottles.

Reagents and standard solutions

The above double-deionized water was used for all solutions and dilutions.

Stock solutions (1000 μg ml^{-1}) for cadmium, chromium, lead and zinc were prepared by diluting the content of Titrisol ampoules (Merck) to 1 l with water. A Fixanal ampoule (Riedel de Haen) was used to prepare a 100 μg Hg ml^{-1} stock solution. Two sets of standard solutions were prepared by diluting the stock solutions with two different acid mixtures: a sulfuric (39.4 g l^{-1})/nitric (12 g l^{-1}) acid mixture and a perchloric (8.4 g l^{-1})/nitric (35 g l^{-1}) acid mixture. The concentrated acids used to prepare the mixtures were of Suprapur quality (Merck).

All the reagents used to determine mercury by the Hatch and Ott procedure [20] were of guaranteed low mercury content (PE mercury reagent kit). During the preliminary tests, lead was extracted with a (2% w/v) solution of ammonium pyrrolidinecarbodithioate (Merck-Schuchart) in methyl isobutyl ketone (Merck). Analytical-grade acetone (Merck) was used for washing the hair. Welding-grade acetylene (Messer-Griesheim) was used as

the fuel gas for zinc determinations, and argon (99.99%; Messer-Griesheim) was used as the purge gas with the graphite furnace.

Preparation of hair samples

Sampling was done by the procedure recommended by the IAEA [18]. The samples were cleaned before analysis, as recommended by an IAEA advisory group [18] as well as in other work [3, 21]. Triplicate subsamples of about 100 mg of hair were placed in teflon beakers and stirred magnetically for 10-min periods successively with acetone, three portions of water, and again with acetone; in each wash, 125 ml of solvent was used and decanted off. The hair sample was then wrapped in a sheet of blue-band filter paper and air-dried at room temperature in a clean dust-free room for one day. The wrapped sample was transferred to a closed balance room and left overnight to equilibrate with atmospheric moisture. Two subsamples were then weighed to a tenth of a milligram; the third subsample was dried at 110°C for 2 h. The weight loss, measured to a tenth of a milligram, was used to refer all concentrations to a dried sample basis.

Three large samples each containing about 5 g of hair bundles collected from three different donors, were selected to prepare larger homogeneous batches for test purposes. A tantalum knife was used to cut the bundles into lengths of 2—3 mm, which were then washed and dried as described above. This cleaned hair was pulverized by the brittle fracture technique [22] in fractions of 1 g. For this purpose, the teflon vessel, tightly capped and containing about 1 g of hair strips and a teflon-coated ball, was cooled in liquid nitrogen for a few minutes and vibrated for 1—2 min with the micro ball mill. A fine powder was obtained by repeating the grinding two to three times. This whole procedure was repeated for each fraction as often as needed to pulverize all the available hair material. The fractions of powder from the same donor were collected together and sieved through a 125-μm nylon sieve to provide three batches of homogeneous powders: these are identified below as reference samples 1, 2 and 3.

Procedure

This applies to samples in bundle or powder form. After pretreatment, weigh about 100 mg of hair sample into the dissolution beaker. Add 3 ml of a mixture (5 + 1, v/v) of nitric acid (d = 1.40) and perchloric acid (d = 1.67). Screw the cap on tightly and heat at 110°C for 45 min in a drying oven. Cool to room temperature in a clean, dust-free room and transfer the digestion solution to a 100-ml polyethylene volumetric flask. Dilute to the mark with the double-deionized water. Prepare a blank in parallel. Pipet an aliquot of the solution, containing no more than 0.25 μg of mercury, and transfer it to the aeration flask of the mercury analysis system, previously assembled and aligned with the spectrometer. Select the 253.7-nm wavelength and a 0.7-nm bandpass. Dilute the aliquot with 100 ml of the deionized water and follow the method recommended by the manufacturer. Follow the same

procedure with aliquots of mercury standard solutions. Empty and rinse the aeration flask carefully between measurements. Perform duplicate measurements on each solution and run one standard aliquot every 10 measurements. Measure the height of the peaks recorded. Remove the mercury absorption cell.

Mount the HGA-76 graphite furnace within the burner compartment of the spectrometer. Inject 20-μl aliquots of sample or standard solutions into the carbon tube atomizer and determine Cd, Cr and Pb following the operating conditions given in Table 1; use a pyrolyzed tube atomizer for lead. Inject at least three aliquots of each solution and calculate the mean peak height in each instance.

Replace the graphite furnace with the slot burner, and spray the sample or standard solutions into an air—acetylene (lean) flame; measure the peak height for zinc at the 213.9-nm wavelength using a 0.7-nm bandpass. Carry out two determinations for each solution.

Determine the amount of each element by comparing the peak height of the samples with a linear regression calibration curve obtained from the standard solutions. Determine the content of the five elements in a blank prepared for each daily set of digested samples.

RESULTS AND DISCUSSION

Digestion step

Acid digestion in a closed pressurized vessel has several advantages over other wet ashing methods: losses of volatile elements are reduced, and only a few millilitres of acids are needed [23, 24], with resulting lower blanks. The efficiency of the procedure was initially tested with the Perkin-Elmer autoclave-1 for various acid mixtures at different temperatures. Clear solutions were obtained after 45 min of digestion at 80°C with 3 ml of a mixture (5 + 2 v/v) of sulfuric acid (d = 1.84) and nitric acid (d = 1.40). Simple

TABLE 1

Instrumental conditions used
(Argon was used as purge gas with a flow rate of 145 ml min^{-1}; in all cases, the bandpass was 0.7 nm)

Element	Wavelength (nm)	Background correction	Drying[a]		Charring[b]		Atomization[c]		Clear
			Temp. (°C)	Time (s)	Temp. (°C)	Time (s)	Temp. (°C)	Time (s)	Temp (°C)
Hg	253.7	No	N.A.[d]		N.A.		N.A.		N
Cd	228.8	Yes	300	20	500	20	1900	5	2500
Cr	357.9	No	300	20	900	20	2600	6	2700
Pb	283.3	Yes	300	10	700	20	1950	5	2700
Zn	213.9	Yes	N.A.		N.A.		N.A.		N

[a]Ramp heating rate 3. [b]Ramp heating rate 2. [c]Gas stop for 5 s. [d]Not applicable.

teflon screw-capped beakers were then custom-made and were used successfully instead of the PE autoclave. The specially-made vessels are preferable for routine operation because they are much cheaper, the risk of cross-contamination is reduced, and 20—30 samples can be digested simultaneously in one drying oven. The concentrations of all the five investigated elements in the diluted digestion solution were found to be constant after storage for four weeks in polyethylene flasks.

Attempts were made to estimate the efficiency of the procedures by measuring the mercury recovery. This element is the best indicator because it is so strongly bound in the hair shaft [25], yet is the most volatile analyte. Five replicate digestions of reference sample 1 were done as described above at 80°C, and mercury was determined by the cold-vapor method (see below). The mean result, 0.45 ppm, was significantly lower than the average of 1.23 ppm from 5 independent measurements by i.n.a.a. Incomplete decomposition of the mercury bonding to the abundant disulphide group of the follicular proteins was then suspected. When the digestion temperature of sample 1 was increased stepwise up to 140°C, it was found that the mercury concentration increased from 0.45 ppm at 80°C to 0.96 ppm at 110°C; above 110°C the results remained constant but still significantly lower than the i.n.a.a. results (Table 2). The results obtained by the method of Nord et al. [13] however, agreed very well with those from the proposed method, provided that digestion was done at temperatures between 110 and 140°C (Table 2).

Low mercury recoveries may be caused by volatilization during the digestion step as well as by the strong binding to the disulphide groups of the follicular proteins. The first hypothesis was tested by an addition technique: spikes were added in the form of $HgCl_2$ or CH_3HgCl solution before

TABLE 2

Mercury content of hair sample 1 ($\mu g\ g^{-1}$) by different procedures

Subsample	I.n.a.a.[a]	A.a.s. H_2SO_4/HNO_3 (5 + 2, v/v) digestion at 110°C[b]	A.a.s. Reference digestion procedure[c] [13]
1	1.26	0.93	1.06
2	1.18	1.03	1.07
3	1.17	0.96	0.92
4	1.24	0.95	0.81
5	1.23	0.95	0.81
Confidence interval at 0.95 confidence level	1.22 ± 0.09	0.96 ± 0.09	0.95 ± 0.12

[a]Each analyzed sample weighed 50 mg. [b]Each analyzed sample weighed 100 mg. [c]Each analyzed sample weighed 30 mg.

the digestion; the results reported in Table 3 showed that no mercury losses could be detected for either the inorganic or the organic form which could be present in the human hair shaft [26]. The deviations initially observed with i.n.a.a. were later attributed to calibration errors. The HNO_3/H_2SO_4 acid mixture was therefore considered to provide an efficient and complete recovery after digestion at 110°C.

Unfortunately, this acid mixture gave poor precisions in the measurement of lead A (5 + 1, v/v) mixture of nitric acid (d = 1.40) and perchloric acid (d = 1.67) was considered more suitable in this case. Digestion for 45 min at 110°C with this mixture was found to be as efficient for mercury recovery as the previously tested mixture (Table 4).

TABLE 3

Recovery of mercury on digestion at different temperatures with H_2SO_4/HNO_3 (5 + 2, v/v)

Powdered sample	Temp. (°C)	Hg present[a] (ng)	100 ng Hg added as	ng Hg found	Recovery (%)
1	110	96	CH_3HgCl	194	99.0
1	110	96	CH_3HgCl	196	100.0
1	120	96	$HgCl_2$	195	99.5
1	140	96	$HgCl_2$	196	99.5
2	110	20	$HgCl_2$	118	98.3
2	110	20	$HgCl_2$	116	96.7
2	110	20	CH_3HgCl	121	100.8
2	110	20	CH_3HgCl	119	99.2

[a]The whole 100-ml sample solutions were used.

TABLE 4

Determination of mercury in powdered hair sample 3 by the cold-vapor technique, after the $HNO_3/HClO_4$ (5 + 1, v/v) digestion and the reference digestion [13]

Subsample	$HNO_3/HClO_4$ digestion[a] ($\mu g\ g^{-1}$ hair)	Reference digestion[b] ($\mu g\ g^{-1}$ hair)
1	21.44, 22.9, 22.78, 22.99	21.46, 21.56, 21.96
2	21.78, 22.04, 22.20	22.05, 23.24, 23.03
3	22.12, 21.01, 21.73	22.42, 22.24, 21.46
Confidence interval at 0.95 confidence level	22.11 ± 2.74	22.16 ± 3.24

[a]Each subsample weighed nearly 100 mg. [b]Each subsample weighed nearly 30 mg.

Determination of mercury by the cold-vapor technique

The technique of Hatch and Ott [20] was applied, as recommended for the HGA-76. Calibration curves obtained with pure acid standard solutions were linear between 0.2 and 2.5 ppb Hg. However, low recoveries were observed after additions of known quantities of mercury(II) chloride to solutions of actual samples digested at 80°C with the HNO_3/H_2SO_4 mixture. Similar observations have been reported earlier for blood [27] and hair [26]. The effect may simply be due to the higher viscosity of the sample solutions. In this case, there is a greater spread of the mercury absorption peaks, so that peak heights are no longer comparable. Peak integration could resolve the problem but is not easily done with the equipment used. The standard addition technique was considered inconvenient in routine use because it requires many more measurements than the direct calibration method. Fortunately, the difficulty disappeared when the digestions were done at 110°C rather than 80°C.

A 40-ml aliquot of the digested solution is adequate for samples containing 0.5—5 μg Hg g^{-1} of hair. It was verified that aliquots up to 100 ml may be used without biasing the measurement.

Determination of cadmium and chromium by electrothermal a.a.s.

Precise results were obtained with the HNO_3/H_2SO_4 and $HNO_3/HClO_4$ mixtures when the 20-μl acid aliquot was slowly evaporated by heating up to 300°C at ramp rate 3, as suggested by the manufacturer. Optimal conditions are summarized in Table 1. The cleaning step eliminates memory effects.

The calibration curves were linear over the ranges 0.1—2.5 ppb for cadmium and 0.5—2.5 ppb for chromium. The slopes of the calibration curves were not modified when sample aliquots were used, and were indifferent to the acid mixtures.

Initially, erratic cadmium results were obtained at concentrations below 1 ppb. Contamination of the Eppendorf pipet tips was responsible for the effect, as has been reported earlier [28]. The trouble was eliminated by pickling the tips overnight in HNO_3/H_2SO_4 or $HNO_3/HClO_4$ digestion mixture; the tips were carefully rinsed with the deionized water after pickling and dried in air at room temperature.

Later, the PE autosampler AS-1 was preferred to the Eppendorf pipets because it gives better reproducibility and no contamination with Cd, Cr or Pb is introduced.

The brand dispenser for the automatic dispensing of the digestion acid mixture was found to be a source of chromium contamination. It was replaced by a laboratory-made scoop of teflon mounted on the cap of the reagent flask.

Determination of lead by electrothermal a.a.s.

Best sensitivity and precision were observed for 20-μl aliquots of the HNO_3/H_2SO_4 sample solution when the conditions shown in Table 1 were

modified slightly: the drying time was increased to 20 s, charring was done for 10 s, and atomization at 2000°C. The calibration curve for these conditions was linear between 4 and 60 ppb, but digested samples with known additions showed a definite matrix effect when compared with pure acidic standard solutions. Furthermore, repeated measurements of a sample during the course of a day showed a puzzling time effect with an initial increase of the peak height followed by a slow decrease after about 15 measurements. The latter effect disappeared when standard graphite tubes were replaced by special pyrolyzed graphite tubes.

As the repeatability was still not satisfactory, measurements were made after extraction of lead into solutions of ammonium pyrrolidine carbodithioate (APCD) in methyl isobutyl ketone (MIBK) [29, 30]. The recommended program is then as follows: heating at ramp rate 3 to 100°C and 10-s drying; heating at ramp rate 2 up to 150°C and 5-s charring; 5-s atomization at 2500°C with stopped gas flow. The extraction is maximal between pH 2 and 8 (Table 5); extracts at pH 1 lose 40% lead within 30 min. The efficiency of the extraction was confirmed and approached 100% in a single extraction [30]. This procedure is therefore recommended for the determination of lead in samples that must be digested with HNO_3/H_2SO_4 mixtures.

Digestion with $HNO_3/HClO_4$ mixtures, however, offers a more convenient procedure which is less prone to the hazard of cross-contamination. Lead can be determined directly in these solutions without prior separation. The use of a pyrolyzed graphite tube and the instrumental conditions described in Table 1 are then recommended. The calibration curve is linear between 2 and 40 ppb.

Determination of zinc

Low concentrations of zinc can be determined with the graphite furnace at 213.9 nm (0.7-nm bandpass) with deuterium background correction. The optimal furnace program is as follows: heating to 300°C at ramp rate 3; drying at 300°C for 20 s; heating to 800°C at ramp rate 2 and charring for 20 s; atomization at 2000°C for 5 s with stopped gas flow, followed by maximum power for 3 s. The sensitivity was then 0.4 ng ml^{-1}, and the calibration curve was linear between 2.5 and 20 ppb when pure acidic standard solutions were used. Furthermore, the peak heights found for samples digested in $HNO_3/HClO_4$ and those obtained with the corresponding pure

TABLE 5

Absorbance (in arbitrary units) for 50 ng Pb ml^{-1} solutions as a function of pH and ageing of the organic phase

pH	1	2.3	3.4	4.6	8.2
Fresh extract	44.0	41.2	42.0	42.0	41.0
30 min later	28.0	40.2	41.5	41.2	40.0
2 h later	8.5	40.2	41.5	41.0	40.0

acidic standard solutions were not significantly different. However, the zinc concentration in hair is normally in the range 150—20 $\mu g\ g^{-1}$, thus the acid digests would need to be diluted by a factor of 40 to come within the optimum analytical range. Therefore, it was decided to use flame atomization and to measure zinc directly in the nitric—perchloric sample solutions as described under Experimental.

The appropriate range and the expected performance of the procedure are given in Table 6.

Precision and accuracy

The actual performance of the proposed procedures was examined with respect to precision and accuracy. The precisions achieved with the procedures appear to be equivalent to, or better than, those reported in the literature for various other a.a.s. procedures applied to the analysis of hair (Table 7).

It was considered essential to estimate the accuracy of the proposed procedures. Addition techniques, used in the present work to establish the optimal conditions of recovery of the elements sought, are frequently taken as a test of accuracy. In fact, they cannot provide sufficient evidence, especially when the chemical form of the analyte is not well known and most probably differs from the form in which the spikes are added. This is particularly to be feared in testing methods for the analysis of biological samples. The accuracy of the determinations of mercury and lead was especially in doubt, because of the affinity of these metals for the groups of the follicular proteins.

In the absence of standard reference hair samples, the accuracy of the proposed procedures was examined by comparison with three different analytical methods. A large batch of a homogenized hair powder, donated

TABLE 6

Main characteristics of the proposed analytical procedure

Element	Concentration range,[a] $\mu g\ g^{-1}$ hair or ng ml^{-1} solution	Limit of detection,[b] $\mu g\ g^{-1}$ hair or ng ml^{-1} solution	Recovery[c] (%)	Sensitivity,[d] $\mu g\ g^{-1}$ hair or ng ml^{-1} solution
Hg	0.2—2.5	0.25	98.0 ± 3.7	0.5
Cd	0.1—2.5	0.06	99.5 ± 1.6	0.08
Cr	0.5—2.5	0.25	97.3 ± 1.5	0.9
Pb	2—40	1.0	99.4 ± 1.5	3
Zn	50—300	15.0	N.M.[e]	26

[a] In this concentration range a linear regression can be used. [b] Calculated as the concentration corresponding to twice the signal of the blank. [c] Percentage calculated by comparing the added amount of the analyte in the hair sample before any treatment and the amount found in at least 4 sample solutions. [d] Calculated as the concentration required to cause 1% absorption. [e] Not measured.

TABLE 7

Comparison of the short-term precision of the proposed method with literature data for the analysis of hair by a.a.s.

Element	This work			Literature			
	Concn. level ($\mu g\ g^{-1}$)	N[b]	R.s.d.[a]	Concn. level ($\mu g\ g^{-1}$)	N	R.s.d.	Ref.
Hg	0.56	10	1.9	0.47	3	2.8	[32]
				0.68	3	7.3	[32]
Cd	0.40	25	8.1	0.55	10	12.7	[31]
Cr	0.24[c]	10	11.5	0.40	45	6.2	[12]
Pb	13.2	25	3.8	3.96	10	8.1	[31]
				43.3	10	12.2	[9]
Zn	183.8	25	5.4	190	10	32.7	[9]

[a]The relative standard deviation (r.s.d.) calculated here includes measurement errors and errors in the chemical preparation of the sample. [b]Number of determinations. [c]This concentration is practically equal to the detection limit as defined in Table 6.

by the Life Sciences Division of the IAEA, was divided into 20 samples weighing about 250 mg each and was distributed between four laboratories. The results of the analyses are presented in Table 8. The confidence interval at the 0.95 confidence level include the combined effects of measurement and treatment errors as well as possible heterogeneity of the material. They do not consider systematic or calibration errors. In view of the good agreement observed, the latter errors are probably smaller than the random errors of the comparison techniques.

TABLE 8

Results obtained by analyzing a powdered homogenized head hair sample by instrumental neutron activation analysis (i.n.a.a.), induced photon activation analysis (i.p.a.a.), anodic stripping voltammetry (a.s.v.) and the proposed a.a.s. method

Element	Technique	No. of subsamples analyzed[a]	Replicate measurements	Number of calibration measurements	Mean result and confid interval at 0.95 confide level (ng g^{-1} hair)
Hg	I.n.a.a.	5	1	—	0.60 ± 0.07
	A.a.s.	5	2	8	0.56 ± 0.01
Cd	I.p.a.a.	2	1	—	0.49 ± 0.11
	A.a.s.	5	5	19	0.40 ± 0.03
Cr	I.n.a.a.	5	1	—	⩽0.16 ± 0.04
	A.a.s.	5	5	19	⩽0.24 ± 0.02
Pb	A.s.v.	4	5	—	13.92 ± 2.51
	A.a.s.	5	5	16	13.20 ± 0.22
Zn	I.n.a.a.	5	1	—	180.20 ± 17.72
	A.a.s.	5	5	17	183.77 ± 13.04

[a]In all cases, the size of the subsample was 250 mg.

The results for chromium, which are also in satisfactory agreement, are unfortunately not totally convincing because they are too close to the detection limits of the two procedures utilized. Independent evidence indicates, however, that the proposed atomic absorption method yields accurate analyses of hair actually contaminated with 50—100 ppm chromium [33]. These analyses were performed at the request of the Division of Life Sciences of the IAEA in support of a survey conducted to detect heavy element pollutants in human hair.

The authors gratefully thank Dr. S. Deron for his support and critical revision of the text, and are indebted to all those who participated in testing the accuracy of the procedure: Dr. E. Lanzel and Dr. G. F. Clemente for the i.n.a.a. data, Dr. G. Mastinu for the i.p.a.a. data, Mr. P. Chamard for the a.s.v. data and Dr. S. M'Baku for his graceful donation of the IAEA powdered homogeneous hair sample.

REFERENCES

1 L. M. Klevay, Am. J. Clin. Nutr., 23 (1970) 284.
2 H. G. Petering and D. W. Yeager, Proc. West. Hemisphere Nutr. Congr., II (1969) 38.
3 H. A. Schroeder and A. P. Nason, J. Invest. Dermatol., 53 (1969) 71.
4 J. G. Reinhold, G. A. Kfoury and M. Arslanian, J. Nutr., 96 (1968) 519.
5 U. G. Oleru, Am. Ind. Hyg. Assoc. J., (1975) 229.
6 L. Kopito, R. K. Byers and H. Schwachman, N. Engl. J. Med., 276 (1967) 949.
7 J. P. Creason, T. A. Hinners, J. E. Bumgarner and C. Pinkerton, Clin. Chem., 21 (1975) 603.
8 H. K. Y. Lau and H. Ashmead, Anal. Lett., 8 (1975) 815.
9 J. R. J. Sorenson, E. G. Melby, P. J. Nord and H. G. Petering, Arch. Environ. Health, 27 (1973) 36.
10 H. Hagedorn-Götz, G. Küppers and M. Stoeppler, Arch. Toxicol., 38 (1977) 275.
11 G. D. Renshaw, C. A. Pounds and E. F. Pearson, Nature, 238 (1972) 162; J. Forensic Sci., 18 (1973) 143.
12 J. F. Alder, D. Alger, A. J. Samuel and T. S. West, Anal. Chim. Acta, 87 (1976) 301.
13 P. J. Nord, M. P. Kadaba and J. R. J. Sorenson, Arch. Environ. Health, 27 (1973) 40.
14 Ch. A. Helsby, Anal. Chim. Acta, 82 (1976) 427.
15 V. P. Guinn and J. Hoste, International Symposium on Nuclear Activation Techniques in the Life Sciences, Vienna, May 1978. IAEA-SM-227/102.
16 L. S. Chuang and J. F. Emery, J. Radioanal. Chem., 45 (1978) 169.
17 R. H. Filby, K. R. Shah and A. D. Davis, Radiochem. Lett., 5 (1970) 9.
18 Yu. S. Ryabukhin, Report IAEA/RL/41H, (1977) 8.
19 R. K. Jolly, G. R. Pehrson, S. K. Gupta, O. C. Buckle and H. Aceto, Proc. Third Conference on Application of Small Accelerators, Denton, Texas, Conf. 741-040-P1, (1974) 203.
20 W. R. Hatch and W. L. Ott, Anal. Chem., 40 (1968) 2085.
21 J. Arunachalam, S. Gangadharan and S. Yegnasubramanian, International Symposium on Nuclear Activation Techniques in the Life Sciences, Vienna, May 1978. IAEA-SM-227/24.
22 G. V. Iyengar, Radiochem. Radioanal. Lett., 24 (1976) 35.
23 P. E. Paus, At. Absorpt. Newsl., 11 (1972) 129.
24 B. Welz and M. Melcher, Appl. At. Absorpt. Spectrosc., 9E (1978).

25 Th. A. Hinners, W. J. Terrill and J. L. Kent, Environ. Health Perspectives, 8 (1975) 191.
26 T. Giovanoli-Jakubczak, M. R. Greenwood, J. Crispin-Smith and T. W. Clarkson, Clin. Chem., 20 (1974) 222.
27 L. Magos, J. Assoc. Off. Anal. Chem., 55 (1972) 966.
28 S. Salmela and E. Vuori, Talanta, 26 (1979) 175.
29 C. E. Mulford, At. Absorpt. Newsl., 5 (1966) 88.
30 S. R. Koirtyohann and J. W. Wien, Anal. Chem., 45 (1973) 1986.
31 H. G. Petering, D. W. Yeager and S. O. Witherup, Arch. Environ. Health, 27 (1973) 327.
32 BITC Working party, Anal. Chim. Acta, 84 (1976) 231.
33 M. Ishikawa, private communication, May 1979.

Analytica Chimica Acta, 123 (1981) 57—63

SIMULTANEOUS MULTI-ELEMENT ANALYSIS BY INDUCTIVELY-COUPLED PLASMA EMISSION SPECTROMETRY UTILIZING MICRO-SAMPLING TECHNIQUES WITH INTERNAL STANDARD

HIROSHI UCHIDA[a], YUKIHIRO NOJIRI, HIROKI HARAGUCHI* and KEIICHIRO FUWA

Department of Chemistry, Faculty of Science, University of Tokyo, Bunkyo-ku, Tokyo 113 (Japan)

(Received 29th April 1980)

SUMMARY

A micro-sampling technique, which requires sample volumes of less than 100 μl, is used for multi-element analysis by i.c.p. emission spectrometry. One drop of sample solution in a teflon cup is nebulized through a capillary tube. Internal standardization with yttrium improves the precision of measurement. The method is applied to the analysis of serum and whole blood samples, after dilution or digestion.

In recent years, there has been great demand for the analysis of samples of limited volumes or weights, especially in the geochemical, biological and clinical fields. Microlitre samples have been used in flame atomic absorption spectrometry for the determination of trace elements [1—5]. However, only one element can be determined at a time, and simultaneous multi-element analysis would be preferable, in order to save time and sample consumption. For this purpose, inductively coupled plasma (i.c.p.) emission spectrometry is the most suitable state-of-art technique for liquid samples.

Greenfield and Smith [6] first suggested a micro-sampling technique for the multielement trace analysis of oil and blood, using a 7-MHz i.c.p. as excitation source [6]. A micro-pipet, which contained 25 μl of sample, was connected to a capillary for nebulization into a heated chamber, where the aerosol was evaporated, and then introduced into the plasma. Trace elements in 25 μl of serum and whole blood have also been determined by use of a single-channel i.c.p. spectrometer in conjunction with a device composed of a micro-pipet and pinch clamp [7]. Injection of small volumes with a peristaltic pump for the sequential determination of trace element by i.c.p. emission spectrometry has been recommended in order to reduce physical interference from high viscosity of solutions [8]. A tantalum filament vaporization system has also been examined for determinations at the ng ml^{-1} level [9].

---

[a]On leave from Industrial Research Institute of Kanagawa Prefecture, Isogo-ku, Yokohama 235, Japan.

The present paper deals with a simpler introduction system for the simultaneous multi-element analysis of μl samples by i.c.p. emission spectrometry. No special modifications were made to the instrument. Yttrium was used as internal standard in order to compensate for the variation in the amount of sample introduced into the plasma. The method proposed has been applied successfully to the simultaneous multi-element determination of major and minor elements in 50-μl aliquots of serum and whole blood.

EXPERIMENTAL

Instrumentation and operating parameters

The instrumental components and operating parameters for the measurement are summarized in Table 1. The solution was fed to the nebulizer through a teflon capillary tube (30 cm long, 0.45 mm i.d.). The uptake rate of water through the tube was 0.96 ml min^{-1} at a carrier gas flow rate of 0.66 l min^{-1}. The r.f. power for inorganic acid solutions was usually 1.4 kW while 1.8 kW was used for the analysis of diluted samples of serum and whole blood in order to minimize the interference of concomitant organic compounds [10]. The analytical lines conventionally employed [11] were used (see Tables 2 and 3), and the straight lines joining the points for the blank and a high standard were used as calibration graphs.

Aspiration procedure

A drop of sample solution was transferred with a micro-pipet into a sampling cup. The cup was one of a series of holes (10 mm diam., 6 mm deep), made by drilling the plane surface of a teflon rod [5, 12]. The capillary tube was removed from the blank solution, placed quickly on the drop in the

TABLE 1

Instrumentation and operating parameters

I.c.p. spectrometer	Jarrell-Ash, Plasma Atom Corp., Model 96-984 SP
Output power	1.4 kW and 1.8 kW
Coolant gas	Argon, 18 l min^{-1}
Plasma gas	Argon, 1.0 l min^{-1}
Carrier gas	Argon, 0.66 l min^{-1}
Nebulizer	Cross-flow type
Viewing point	15.0 mm (1.4 kW) and 18.0 mm (1.8 kW) above work coil
Polychromator	Paschen-Runge type (75-cm focal length)
Grating	2400 grooves mm^{-1}
Linear dispersion	0.54 nm mm^{-1} (1st order, at 270 nm)
Entrance slit width	25 μm
Exit slit width	100 μm (Na and K) and 50 μm (others)
Monochromator	Ebert type (50 cm focal length)
Integration time	20 s
Data acquisition system	Digital Equipment Company, Model PDP8 (8K memory)

TABLE 2

Dependence of precision on the sampling volume with and without internal standardization[a]

Sampling volume (μl)	Internal standard	R.s.d. (%)[b]					
		Al	Fe	Na	Ti	V	Zn
5	No	22	8.1	11	8.2	7.7	9.0
	Yes	16	2.1	14	0.4	1.3	2.8
10	No	11	6.7	30	6.3	6.7	5.5
	Yes	7.7	1.9	27	0.4	1.2	1.7
20	No	12	5.9	19	3.7	4.4	4.5
	Yes	6.1	3.7	20	0.6	1.9	2.4
50	No	4.2	4.0	12	3.2	3.3	3.5
	Yes	2.2	0.8	10	0.2	0.4	1.1
100	No	1.8	1.2	5.2	1.2	1.3	1.3
	Yes	1.0	0.5	4.8	0.1	0.3	0.6
Continuous	No	0.5	1.2	1.6	0.5	0.4	1.2
	Yes	0.4	0.9	1.3	0.2	0.2	0.9

[a]The concentration of all elements were 10 $\mu g\ g^{-1}$. The lines used were 308.2 nm (Al), 259.9 nm (Fe), 589.0 nm (Na), 334.9 nm (Ti), 292.4 nm (V), and 213.9 nm (Zn). [b]$n = 8$.

cup, and, whenever the sample had been aspirated, was immediately returned to the blank solution. Transfer of the capillary between the blank and sample solutions must be very quick, because the blank solution must be continuously nebulized between nebulization of the sample solutions to prevent blockage of the nebulizer. When the sample was aspirated into an empty capillary tube, it became scattered in the tube and the nebulization flow ceased.

Chemicals and standard solutions

Commercially available standard solutions (1000 $\mu g\ ml^{-1}$) for atomic absorption spectrometry (Wako Pure Chemical Co.) were used for the stock solutions of aluminum, calcium, copper, iron, lead, potassium silicon, sodium, titanium, vanadium and zinc. A yttrium stock solution (1000 $\mu g\ g^{-1}$) was prepared by dissolving the oxide (Wako Pure Chemical Co., 99%) in nitric acid. Potassium dihydrogenphosphate was dissolved in water for the stock solution of phosphorus. Working standard solutions were prepared by appropriate dilution of these stock solutions. All dilutions and sample preparations were done gravimetrically on a top-pan balance, as this is more accurate than volumetric procedures when small samples are involved.

Application to serum and whole blood

Serum and whole blood were obtained from the hospital in the University of Tokyo. The whole blood sample contained heparin as an anticoagulant. Commercially available control serum (Wako Pure Chemical Co.), prepared

TABLE 3

Analytical results ($\mu g\ g^{-1}$) for serum and whole blood

Sample	Element	Wavelength (nm)	Sample treatment			
			Dilution[a]	Digestion[b]	Digestion[b]	Digestion[c]
			50-μl sample		Continuous	
Serum	Na	589.0	3250	3170	3120	3080
	K	766.5	166	162	167	165
	Ca	317.9	86.2	85.3	83.4	84.8
	Fe	259.9	1.47	1.67	1.33	1.30
	Cu	324.8	1.01	1.07	1.14	1.01
	Mg	279.1	16.2	15.6	16.6	16.7
	Zn	213.9	0.64	0.63	0.67	0.77
	P	214.9	104	106	105	103
Control serum[d]	Na		3240	3190	3220	3220
	K		165	167	161	165
	Ca		78.4	77.6	80.0	73.7
	Fe		1.38	1.63	1.33	1.30
	Cu		1.14	1.18	1.02	1.10
	Mg		18.5	18.3	17.4	17.0
	Zn		0.84	0.86	0.86	0.86
	P		109	109	111	107
Whole blood	Na		1810	1840	1770	1780
	K		1900	1850	1870	1830
	Ca		54.2	56.6	52.8	53.5
	Fe		567	569	551	562
	Cu		—	—	0.25	0.28
	Mg		31.2	30.9	30.3	31.7
	Zn		6.67	7.02	7.11	6.93
	P		375	380	358	360

[a]10-fold dilution. [b]1 g digested in the teflon bomb and diluted to 10 g. [c]10 g digested by conventional method. [d]Na = 3149, K = 160.3, Ca = 96.24, Fe = 0.93, Cu = 1.28 $\mu g\ g^{-1}$.

by lyophilizing serum to a powder, was dissolved in water, and also analysed. Two methods for sample treatment were investigated for nebulization of 50-μl samples. In one, serum and whole blood were diluted 10 times with water. In the other, 1 g of sample was digested in a teflon-lined bomb [13], with 3 ml of concentrated nitric acid and 0.5 ml of concentrated perchloric acid at 120°C for 4 h (serum) or 8 h (whole blood). The contents were transferred to a glass bottle, and diluted with water to 10 g. Yttrium was added as internal standard at a concentration of 10 $\mu g\ g^{-1}$ in both cases. For continuous nebulization, 10 g of the blood sample was digested conventionally with nitric and sulfuric acids, and diluted to 20 g with distilled water. These sample treatments were carried out at the same time to avoid sample heterogeneity.

Two high standards for calibration were prepared. The first contained

10 μg Al g^{-1}, 10 μg Ba g^{-1}, 10 μg Ca g^{-1}, 10 μg Cu g^{-1}, 50 μg Fe g^{-1}, 100 μg K g^{-1}, 10 μg Mg g^{-1}, 300 μg Na g^{-1}, 10 μg Zn g^{-1} and 10 μg Y g^{-1} (Yttrium nitrate in water was used for the dilution of sera and whole blood to prevent their coagulation). The second standard contained 100 μg P g^{-1}, 10 μg Pb g^{-1} and 10 μg Si g^{-1}. Water was used as the blank solution.

RESULTS AND DISCUSSION

Figure 1 shows the yttrium (10 μg g^{-1}) i.c.p. signals obtained for various sample volumes, using the monochromator (Table 1) attached to the spectrometer. The peak height for a 100-μl aliquot is as high as that for continuous nebulization. The relative standard deviation of the peak height recording for 50-μl aliquots of the yttrium solution was 5.3% (n = 8).

For simultaneous multi-element analysis with the polychromator, the emission intensities were integrated for 20 s, and the analytical data were output after data processing. Table 2 shows the repeatability of the simultaneous measurement of 10 μg g^{-1} of aluminum, iron, sodium, titanium, vanadium and zinc, when various sampling volumes were aspirated. Precision became worse as the sample volume decreased. Relative standard deviations of the emission intensities for atomic lines were generally larger than those for ionic lines, especially for the alkali metals.

Internal standardization

Generally, the observed emission intensity includes the net emission intensity of the element and the plasma background (or blank) intensity; it is also influenced by viscosity and surface tension effects. This is usually corrected by internal standardization. In the present work, variations in the amount of sample introduced into the plasma, caused by errors in pipetting and by changes in the nebulization rate, significantly influence the precision. These variations can be seen in Table 2.

For internal standardization, a 10 μg g^{-1} solution of yttrium, whose emission intensity was observed at 371.0 nm, was chosen because of the high sensitivity and stability of the emission signal. In the data treatment for internal

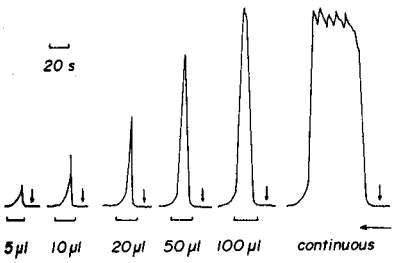

Fig. 1. I.c.p. emission signals of yttrium (10 μg g^{-1}). The arrows indicate the start of aspiration.

standardization, the net intensity should be obtained to correct for the matrix effect and pipetting errors, because the background intensities for some elements are not negligible. For example, the ratio of the net emission intensity to the background intensity at 371.0 nm was 5.85 for a 50-μl aliquot of 10 μg g^{-1} yttrium solution. The data processing facilities of the i.c.p. spectrometer used [11] allow the background intensity at any wavelength, obtained for the blank solution, to be subtracted from the observed emission intensity However, the corrected output is not provided as emission intensity but as the concentration of the element. Therefore, the background-corrected concentration for each element was divided by that for the 10 μg Y g^{-1} internal standard.

The precisions obtained by internal standardization are also summarized in Table 2. With the exception of sodium, the relative standard deviations are much decreased when the internal standard is used, and is less than 2% for titanium and vanadium for as little as a 5-μl aliquot.

A problem with the use of yttrium as internal standard is spectral interference of the yttrium line at 317.942 nm with the calcium line at 317.933 nm. In the present system, the intensity of 10 μg Y g^{-1} at the calcium wavelength (317.933 nm) corresponded to that from 0.6 μg Ca g^{-1}, and this value was subtracted from the measured values for calcium. However, at the concentrations of calcium determined here, the spectral interference of yttrium was insignificant.

Application to blood samples

Analytical results for a serum, control serum and a whole blood sample are summarized in Table 3. Internal standardization was not used in the continuous nebulization experiments. The results obtained by the dilution, teflon bomb digestion and conventional wet digestion methods are consistent. The relative standard deviations calculated from the data for six 50-μl samples were 2—5% for dilution and teflon bomb treatments. The results obtained for the control serum agree well with reported values, except for calcium, for which low values were found. However, in this laboratory, 74 and 80 μg ml^{-1} were obtained for the same sample by atomic absorption (422.7 nm) and single-channel i.c.p. emission (393.4 nm) spectrometry, respectively.

The recovery and precision for the determination of yttrium added as internal standard to diluted whole blood are summarized in Table 4. In continuous nebulization, both the recovery and precision become worse as the dilution is decreased, possibly because of variations in nebulization efficiency with the less diluted viscous blood. The nebulizer sometimes blocked and the background emission intensity increased for these samples.

Good recoveries and precision were obtained with pulse nebulization of 50-μl samples. The aspiration time was only 3 s; for the rest of the time, distilled water was aspirated, cleaning the nebulizer and apparently reducing variations of nebulization efficiency. The increase in the background emission

TABLE 4

Dependence of recovery and precision on the dilution factors in the determination of yttrium (10 $\mu g\ g^{-1}$) added to whole blood

Dilution factor	50 μl nebulization		Continuous nebulization	
	Recovery (%)	R.s.d.[a] (%)	Recovery (%)	R.s.d.[a] (%)
5	93.0	6.0	—	—
10	96.7	3.9	41.8	30
20	101.2	3.2	58.2	20
50	98.9	2.9	75.8	13
100	106.6	3.1	83.6	1.8

[a] $n = 8$.

intensity was also negligible, even when the less diluted whole blood was used. The recovery and precision for whole blood with 5-fold dilution are acceptable (Table 4). Aluminum, silica, lead, copper and barium were determined in 5-fold diluted whole blood, with yttrium as internal standard, and the results were in reasonable agreement with those obtained at greater dilutions.

The method developed is simple and has the advantage of allowing use of a commercially available instrument without modification, provided that internal standardization is used. There is no significant difference in accuracy and precision between nebulization of small volumes and continuous nebulization, and the micro-sampling technique reduces errors from variable nebulization efficiency of viscous samples.

The authors thank Prof. C. Iida for providing the teflon bomb, and the Industrial Research Institute of Kanagawa Prefecture for giving study leave to H.U. This research was supported by Grants-in-Aid for Environmental Science from the Ministry of Education, Science and Culture.

REFERENCES

1 E. Sebastiani, K. Ohls and G. Riemer, Fresenius Z. Anal. Chem., 264 (1973) 105.
2 H. Berndt and E. Jackwerth, Spectrochim. Acta, 30B (1975) 169.
3 E. Jackwerth and H. Berndt, Anal. Chim. Acta, 74 (1975) 299.
4 K. C. Thomson and R. G. Godden, Analyst, 101 (1976) 174.
5 T. Uchida, I. Kojima and C. Iida, Bunseki Kagaku, 27 (1978) T44.
6 S. Greenfield and P. B. Smith, Anal. Chim. Acta, 59 (1972) 341.
7 R. N. Kniseley, V. A. Fassel and C. C. Butler, Clin. Chem., 19 (1973) 807.
8 J. A. C. Broekaert and F. Leis, Anal. Chim. Acta, 109 (1979) 73.
9 D. E. Nixon, V. A. Fassel and R. N. Kniseley, Anal. Chem., 46 (1974) 210.
10 C. W. Mcleod, N. Furuta, H. Haraguchi and K. Fuwa, unpublished data.
11 Jarrell-Ash Division/Fisher Scientific Company, Manual for Model 90-750 Atomcomp, Pub. No. 90-750 (1973).
12 T. Uchida, C. Iida and I. Kojima, Anal. Chim. Acta, 113 (1980) 361.
13 C. Iida, T. Uchida and I. Kojima, Anal. Chim. Acta, 113 (1980) 365.

Analytica Chimica Acta, 123 (1981) 65—74

TRACE ELEMENT DETERMINATIONS IN SHALE OIL PRODUCTS BY NEUTRON ACTIVATION

PETER G. SHAW, DAVID McKOWN[a] and STANLEY E. MANAHAN*

Department of Chemistry, 123 Chemistry Building, University of Missouri, Columbia, MO 65211 (U.S.A.)

(Received 27th May 1980)

SUMMARY

Neutron activation offers some important advantages for the determination of selected trace elements in shale oil products. This paper gives techniques and results of a study of crude shale oil and naphtha, heavy distillate, and wax products of shale oil. The elements determined were Al, As, Au, Br, Ce, Cl, Co, Cr, Fe, Hg, I, K, Mn, Mo, Na, S, Sb, Se, V, and Zn. Some elements (Mn, Na, As) tend to accumulate in heavier fractions, whereas chlorine and iodine are concentrated in the more volatile fractions. The volatility of sulphur compounds in the shale oil products appears to be essentially uniform, with some tendency toward accumulation in distillation residues. The tendency for the trace elements to accumulate in the waxes that precipitated from cooled heavy distillates was very low.

Trace elements, in shale oil and its products, play a strong role in determining the environmental and toxicological effects of shale oil utilization and in determining refining methodologies applicable to shale oil [1, 2]. Therefore, it is necessary to have reliable methods for the determination of low levels of elements in shale oil matrices. Neutron activation (n.a.) is a good method for the determination of many of the important trace elements in shale oil. It has suitable detection limits for a number of elements, it can be essentially non-destructive, and it requires minimal sample handling and preparation, thus minimizing contamination. Particularly because of the ease of sample preparation, n.a. without separations is very well adapted to the determination of trace elements in fossil fuels [3—5]. Despite these advantages, there are a number of pitfalls involved in n.a. of shale oil products, and certain special techniques must be employed. These are discussed in this paper.

EXPERIMENTAL

Samples

The samples used in this study were obtained from the U.S. Department of Energy, Laramie Energy Technology Center (L.E.T.C.), Laramie, WY. One

---

[a]Present address: U.S. Geological Survey, Denver Federal Center, Denver, Colorado 80225, U.S.A.

of these, designated Rock Springs 9, was produced from an in situ shale retort experiment conducted in late 1976. Crude shale oil Sample 10 was obtained from a simulated in situ burn performed at L.E.T.C. in 1973. Trace element levels reported in this study should not be interpreted as being typical of all shale oil samples from all possible sources and processes.

Figure 1 and Table 1 give the identities and processing of the shale oil products. Shale oil obtained from the retort was vacuum-distilled, producing upgraded oil, water, and a residuum. The residuum is designated Residuum A, Samples 5 and 8. Sample 8 is a composite of 16 residua from the upgrading distillation, and Sample 5 is one of the residua. The upgraded oil was immediately fractionated prior to acquisition of the sample and was not available for n.a.

The upgraded oil was subjected to a standard Hempel distillation [6]. This process consists of distillation to 200°C at 760 torr to collect a naphtha fraction, followed by a distillation at 40 torr to 200°C to collect light distillate, and at 50 torr and 300°C (or until cracking occurs) to collect heavy distillate. The residuum from this distillation is designated Residuum B in Fig. 1.

The waxes in this study precipitated when the heavy distillate was cooled from 25°C to −23°C. In this work, Sample 1 refers to the first wax fraction collected at room temperature, Sample 2 refers to the fifth wax fraction collected at 0°C, Sample 3 is a composite of all wax fractions, and Sample 4 is a composite of four wax fractions collected from 2 to 20°C. The liquid from which the wax was precipitated is dewaxed heavy distillate, Sample 11.

One set of samples was prepared for a short-term irradiation and another for a long-term irradiation. For short-term irradiations, approximately 0.5 g of each material was weighed to within 0.1 mg into 2/5 dram high density polyethylene vials (polyvials) precleaned by stepwise washing with acetone, HNO_3, and deionized water. The crude shale oils were sampled using a transfer pipet, and the waxes were sampled by random scoop sampling with

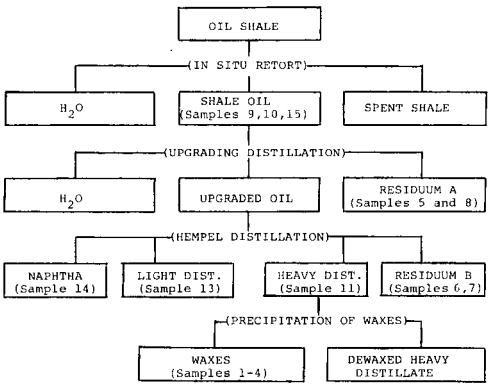

Fig. 1. Flow sheet illustrating the separation scheme of raw crude shale oil from in situ retorting. Details on sample identification are given in Table 1.

TABLE 1

Identification of samples

Sample no.	Sample description
9	Crude shale oil from Rock Springs 9 in situ retorting experiment conducted in 1976, not subjected to upgrading
15	Sample no. 9 subjected to de-watering
8	Composite residuum from upgrading distillation of raw shale oil from Site 9 (Residuum A)
7	Composite residuum from Hempel vacuum distillation of upgraded shale oil (Residuum B)
11	Heavy distillate from Hempel distillation, 200—300°C, 40 torr
13	Light distillate from Hempel distillation, incipient to 200°C, 40 torr
14	Naphtha from Hempel distillation, incipient to 200°C, 40 torr
5	Individual residuum from upgrading distillation (Residuum A)
6	Individual residuum from Hempel distillation (Residuum B)
10	Crude shale oil from 1973 simulated in situ retorting
1	First wax precipitating from heavy distillate at 25°C
2	Fifth wax precipitating from heavy distillate at −2°C
3	Composite of all 10 waxes precipitating from heavy distillate from 25°C to −23°C
4	Composite of the last 3 waxes obtained from cooling heavy distillate
16	NBS Standard heavy fuel oil

a teflon-coated spatula. Because of their viscous nature, it was necessary to freeze the residuum tars in liquid nitrogen, shatter the solid sample, and collect fragments by random scoop sampling with a teflon coated spatula.

For long-term irradiations, approximately 0.5 g of each sample was weighed into silica vials constructed from T-21 Suprasil silica tubing (Amersil, Inc.) using the handling procedures described for the samples subjected to long-term irradiation. The silica vials were cleaned in the same way as the polyethylene vials prior to sample introduction. The silica vials were sealed with a torch while evacuated. Special precautions were taken to avoid overheating the sample during this step.

Standard solutions

Stock aqueous standard solutions were prepared containing 10 mg ml^{-1} of each element to be determined. Most of the stock solutions of metal ions were prepared by dissolving the metal or its oxide in spectro-grade nitric acid; in some cases hydrofluoric acid was employed to aid dissolution. Halogen standards were prepared from their ammonium salts. These stock solutions were quantitatively diluted and mixed to give standards having elemental concentrations similar to those encountered in the samples. This provides similar elemental matrices for both the samples and standards, minimizing potential errors in the γ-ray spectral measurements. For some elements present in the samples at levels approaching the detection limit of the element, slightly larger amounts were added to the standard in order to

obtain satisfactory counting precision for the standard. Separate multi-element irradiation standards were prepared for short-term and long-term irradiations by placing aliquots of the diluted solutions in the polyethylene and quartz vials, respectively.

The selenium standards were prepared to especially exacting standards so that their matrix activities and selenium contents were as close as possible to those of the samples. This minimizes counting interval dead time corrections in the measurement of 17-s ^{77m}Se. Because of the very short decay time prior to counting the ^{77m}Se isotope, ^{19}O activity from water can interfere with the standard spectra. This interference was minimized by placing small amounts of the standard selenium solution on cellulose, followed by drying and irradiating the cellulose to which the standard was sorbed.

Irradiation and counting procedures

The samples were irradiated in the University of Missouri Research Reactor. After investigation of numerous irradiation, decay, and counting schemes, three different irradiation schemes were employed. These are summarized in Table 2. Selenium irradiation was a special case because of the very short half-life of ^{77m}Se. Selenium standards and samples sealed in polyvials were irradiated for 5 s at a thermal neutron flux of 1×10^{14} n cm^{-2} s^{-1}. The returned shuttle rabbit was opened as quickly as possible, and the sample vial transferred to a 45-cm^3 Ge(Li) γ-ray spectrometer detector system. The sample was placed at a distance from the detector that gave less than 10% dead time. All samples were processed by a procedure [7] involving a 5-s irradiation, 15-s decay, and 20-s count.

For the remaining elements giving short-lived radionuclides, the samples previously irradiated for the selenium determination were again irradiated for 1 min at a flux of 1×10^{14} n cm^{-2} s^{-1} using the pneumatic transfer irradiation facility. Each sample was counted in the polyvial for 200 s after a 3-min decay, and again counted for 500 s after a 15-min decay. Blank vials (for background) and multi-element standards were irradiated and counted in the same manner.

TABLE 2

Summary of n.a. conditions for various elements in shale oil products

Irradiation, decay, counting times	Flux (n cm^{-2} s^{-1})	Elements, L_D of <1 ppm	Energy range counted (kEV)	Container
5 s, 15 s, 20 s	1×10^{14}	Se	0—4000	Polyethylene
1 min, 3 min, 200 s	1×10^{14}	V, Al, S[a], I, As	0—4000	Polyethylene
1 min, 12 min, 500 s	1×10^{14}	Br, Mn, Na, Cl	0—4000	Polyethylene
2 h, 30—40 h, 500—1000 s	6×10^{13}	Na, K, Zn, As, Br, Sb, Au, Hg, Zn	0—2000	Silica
2 h, 4—8 day, 1000 s	6×10^{13}	Cr, Co, Ce, Hg, Fe[b], Mo, Zn, I, Se, Sb	0—2000	Silica

[a] L_D (detection limit) of S, 100 ppm. [b] L_D of Fe, 10 ppm.

For the determination of elements giving rise to long-lived isotopes, samples and standards in silica containers were irradiated in groups for 2 h in the reflector of the reactor. Longer irradiations were desired, but a trial irradiation of raw shale oil for 3 h resulted in breakage of the silica vials. Even during the 2-h irradiation, one set of vials containing wax samples broke. The long irradiations were conducted at a flux of 6×10^{13} n cm^{-2} s^{-1}. Each sample was counted twice, generally in the original vial. (In cases where residuum and oil samples were transferred from the original vial to a non-irradiated vial using benzene solvent, no differences were detected in the counts obtained.) The first of the two counts was conducted for 1000 s after a 2-day decay, and the second for 2000 s after a 10-day decay.

Gamma-ray spectra were recorded on computer-compatible magnetic tape to facilitate data reduction. The data were processed on an IBM 370 computer using a modified version of the GAMANL [8] spectrum analysis code. This code measures integrated peak areas after subtraction of the spectral base line contribution within the peak width limits. Peak quality information and an estimate of the statistical error in measuring the base-line-corrected peak areas are also generated. Elemental concentration values were obtained by the direct comparison of the weight-normalized peak areas of the samples to the average peak area per microgram of the standards.

RESULTS AND DISCUSSION

Irradiation conditions

A total of eight different kinds of samples were processed by n.a. These are crude shale oil (Samples 9, 10, and 15), residuum from upgrading distillation (Samples 5 and 8), residuum from Hempel distillation (Samples 6 and 7), heavy distillation (Sample 11), light distillate from Hempel distillation (Sample 13), naphtha from Hempel distillation (Sample 14), waxes (Samples 1–4), and NBS standard heavy fuel oil (Sample 16). All of these samples are described in Table 1. The 20 elements determined were Al, As, Au, Br, Ce, Cl, Co, Cr, Fe, Hg, I, K, Mn, Mo, Na, S, Sb, Se, V, and Zn. Of these, the only elements that it was possible to determine in all of the samples were Al, As, Br, Cl, I, Mn, Na, S, Se, and V, all of which may be determined with a short irradiation.

Long-term irradiations were not attempted for volatile naphtha, light distillate, and heavy distillate because of the danger of vial breakage. Irradiation of raw shale oil resulted in vial breakage after only 3 h, requiring imposition of a 2-h limit for irradiation of all samples.

Unexpectedly, the high molecular weight, non-volatile waxes built up high pressure during 2-h irradiations. This was manifested by rupture of one set of quartz vials containing waxes and strong pressure release from another set when broken after a 2-h irradiation. Tests of the wax samples involving heating them for 2 h at 120°C revealed little weight loss, so heating was not responsible for the pressure buildup. The pressure was almost certainly due

TABLE 3

Distribution of selected elements in Hempel distillation fractions (All concentrations in ppm)

	Shale oil[a]	Distillate			Residuum[e]	Weight av.[f]	Error (%)
		Naphtha[b]	Light[c]	Heavy[d]			
Al	0.61	1.2	0.59	0.52	4.2	0.78	+28
V	0.11	0.19	0.0012	0.001	0.064	0.018	−84
S	6.9×10^3	5.4×10^3	5.9×10^3	5.3×10^3	8.4×10^3	5.8×10^3	−17
Mn	0.08	0.013	0.16	0.11	0.20	0.13	+65
I	0.066	0.25	0.039	0.021	0.0093	0.046	−30
Cl	8.7	48	14	9.1	6.4	14	+64
Br	0.14	0.30	0.12	0.046	0.16	0.11	−21
Na	1.2	0.64	5.1	3.7	44	6.3	+400
As	4.6	—	1.4	4.4	12	3.0	−35
Se	1.1	0.24	0.65	0.61	0.71	0.61	−44

[a]Sample No. 15. [b]Sample No. 14. [c]Sample No. 13. [d]Sample No. 11. [e]Sample No. 7. [f]Weight average based upon 7.2% naphtha, 49.8% light distillate, 37.8% heavy distillate, and 5.2% residuum, assuming all oil goes to these fractions.

to gas resulting from radiation damage in the wax. Rupture of —H bonds could lead to H_2 formation, and rupture of $-CH_3$ bonds could lead to CH_4 formation. The reason that gas formation is more severe in the waxes is that, unlike the other materials, waxes are free of olefinic bonds that scavenge radical species that would otherwise lead to the formation of gases.

A significant aspect of this study is the delineation of the conditions under which long-term irradiations of shale oil may be carried out. The 2-h irradiation at 6×10^{13} n cm^{-2} s^{-1} provides for maximum sensitivity with minimum danger of sample vial breakage. In addition, for reasons discussed

TABLE 4

Trace element concentrations in residuum samples from upgrading distillation of raw shale oil and Hempel vacuum distillation of upgraded shale oil

Element	Concn. in distillation residua (ppm)		Element	Concn. in distillation residua (ppm	
	Sample 8[a]	Sample 7[b]		Sample 8[a]	Sample 7[b]
Al	3.8	4.2	Se	2.1	0.61
Ce	0.1	0.084	Sb	0.52	0.15
S	8.1×10^3	8.4×10^3	Mn	0.14	0.20
As	11	10	Co	3.5	0.60
Br	0.18	0.16	Fe	2.0×10^2	35
Cr	7.1	4.7	Au	0.001	0.00017
Na	1.4×10^2	44	I	0.088	0.0093
K	13	—	Mo	0.90	0.51
V	0.18	0.064	Zn	2.4×10^2	14
Cl	23	6.4			

[a]Composite residuum from upgrading vacuum distillation of raw shale oil (Residuum A).
[b]Composite residuum from Hempel vacuum distillation of upgraded shale oil (Residuum B).

TABLE 5

Comparison of waxed and dewaxed heavy distillate

Element	Elemental concentration (ppm)		
	Composite wax[a]	Heavy distillate[b]	Dewaxed distillate[c]
Al	3.5	0.52	1.1
V	0.0034	0.001	0.0031
S	2.3×10^2	5.3×10^3	5.8×10^3
Mn	0.09	0.11	0.21
I	0.0062	0.021	0.016
Cl	5.9	9.1	5.8
Br	0.044	0.046	0.076
Na	30	3.7	1.2
As	0.084	4.4	5.0
Se	0.031	0.61	0.61

[a]Sample 3. [b]Sample 11. [c]Sample 11 following dewaxing.

in the preceding paragraph, it is worthy to note that hydrocarbon volatility, alone, is not a sufficient indicator of a tendency toward pressure buildup during long irradiations.

TABLE 6

Trace element contents of waxes, heavy distillate, and de-watered crude shale oil[a]

Element	Concentration (ppm)					
	Sample no.					
	1	2	3	4	11	15
Al	3.9	6.2	3.5	2.7	0.52	0.76
V	0.0062	0.0039	0.0034	0.0038	0.001	0.11
S	1.4×10^2	1.0×10^2	2.3×10^2	1.0×10^2	5.3×10^3	6.0×10^3
Mn	0.059	0.072	0.09	0.04	0.11	0.05
I	0.003	0.001	0.005	0.0062	0.021	0.071
Cl	4.1	3.4	5.9	4.7	9.1	12
Br	0.039	0.026	0.042	0.42	0.025	0.10
Na	1.2×10^2	6.3	26	4.5	3.7	1.3
As	0.11	0.24	0.07	0.3	4.4	4.0
Se	0.0041	0.011	0.013	0.031	0.61	1.2
Co	0.012	0.22	0.50	0.17	—	0.7
Mo	—	—	—	—	—	0.73
Fe	—	—	5.3	4.5	—	32
Cr	—	—	0.39	8.8	—	0.13
Au	0.0004	0.001	0.00015	0.00035	—	0.003
K	—	14	3.5	4.3	—	15
Zn	1.1	0.4	0.6	—	—	39
Ce	13	1.5	0.8	0.2	—	0.82
Sb	0.1	0.26	0.12	—	—	0.066

[a]Samples 1—4 are waxes, 11 is a heavy distillate from Hempel distillation, and 15 is de-watered crude shale oil (see Table 1).

TABLE 7

Determination of selected elements in NBS Standard Fuel Oil, SRM 1634

Element	Certified	Method[a]	Elemental content (ppm)	
			Accepted value	This study
S	yes	n.a., titrimetry	$2.14 \pm 0.02 \times 10^4$	$2.24 \pm 0.05 \times 10^4$
V	yes	n.a., a.a.	$3.2 \pm 1.5 \times 10^2$	3×10^2 [b]
Zn	yes	n.a., a.a.	0.23 ± 0.05	<1
Fe	yes	n.a., a.a.	13.5 ± 1.0	13.5 ± 1.2
As	no	n.a.	0.095	0.12
Cr	no	n.a.	0.09	0.08
Hg	no	n.a.	0.0023	<0.01
Mn	no	n.a.	0.12	0.2

[a]The abbreviation, a.a., designates atomic absorption spectrometry. [b]Detector saturation limit exceeded.

Elemental data for different fractions

The elemental determination data for the samples are summarized in Table 3 comparing selected elements in Hempel fractions; Table 4 showing trace element concentrations in residua samples 7 and 8; Table 5 comparing waxed and dewaxed heavy distillate; Table 6 for waxes, heavy distillate and dewatered crude shale oil; and Table 7 for determination of elements in NBS standard fuel oil.

Examination of Table 3 reveals three general trends in the fractionation of trace elements as a function of the distillation temperatures of various Hempel distillation fractions. The most prominent trend is a decrease in concentration of trace elements with decreasing distillation temperature (increasing volatility) of the fraction. Manganese, sodium, arsenic, and possibly sulfur and selenium follow this trend. The second major trend is increasing levels of the element with decreasing distillation cut temperature, i.e., concentration of the element in the more volatile fractions. Chlorine and iodine show this trend in a most pronounced fashion. The third major trend involves accumulation of the elements in both the heavier and lighter fractions, with lower concentrations in the middle fractions. This trend is followed by aluminum and vanadium, both of which have higher concentrations in the residuum and naphtha fractions than they have in the light, and heavier distillate fractions.

The trend toward accumulation of elements in the higher boiling fractions and residuum is to be expected of elements, particularly metals, present in relatively nonvolatile inorganic compounds. Unfortunately, it was not possible to subject the heavy distillate, light distillate, and naphtha fractions to long-term irradiation, so that many of the metals determined by that method were not determined in the lighter fractions. However, the volatilities of many of the metals, particularly the transition metals, may be inferred from an examination of Table 4. In this table, Sample 8 is a residuum from the distillation of raw crude shale oil that had not been subjected to distillation,

except for that occurring in the in situ retorting process. Sample 7 is a residue left from shale oil that had been subjected to a prior upgrading distillation. Therefore, a high concentration of an element in Sample 8 relative to Sample 7 infers relatively low volatility for that element and vice versa. From this argument it is seen that the metals, sodium, cobalt, iron, molybdenum, and zinc are in a relatively nonvolatile category.

The second major trend, which involves accumulation of elements in the more volatile fractions, is illustrated by chlorine and iodine. Examination of Table 3 shows a uniform decrease in the concentrations of these elements in going from naphtha to residuum. Plausibly, bromine belongs in this category also, although its level is elevated in the residuum. These results infer organic binding of the halogens, either as a result of their being bound to kerogen in the original shale, or as a result of chemical reactions occurring during the retorting process. The chlorine levels, particularly, could be of significance because of the corrosive nature of chlorine during petroleum processing.

The third major trend of higher concentration of elements in both higher and lower boiling fractions, with lower levels in the intermediate fractions is shown for aluminum, vanadium, and perhaps bromine. These results may imply the presence of two general classes of compounds of these elements, one volatile and the other nonvolatile. The possibility of contamination by vanadium through contact of shale oil distillates with stainless steel helices in the distillation apparatus exists. Although the vanadium levels are quite low compared to many petroleum crude oils, it is clear that vanadium is present in the lighter fractions. This observation is not surprising in view of the known occurrence of vanadium porphyrin complexes and organometallic compounds in fossil fuels.

The volatility of sulfur compounds in the shale oil products appears to be essentially uniform, with some tendency toward accumulation in the distillation residues. This is seen from examination of Table 3 in which the naphtha, light distillate, and heavy distillate fractions show essentially the same sulfur levels. It is interesting to note that the sulfur levels are essentially the same in Sample 8 (a residue of distillation of a shale oil that had been subjected to prior distillation) as in Sample 7 (a residue from the distillation of shale oil that had been upgraded by a previous distillation), as shown in Table 4. This may indicate that most of the sulfur from shale oil retorted in situ is in a distillable organic form and not present as entrained mineral matter in the raw crude shale oil.

There are no clearly discernible trends in the distribution of the small quantities of selenium present. Examination of the selenium data in Table 3 shows a reasonably uniform distribution of selenium among all the fractions from the Hempel distillation. Table 4 shows a significantly higher concentration of Se in the residuum from the upgrading distillation (Sample 8) compared to the residuum from the Hempel distillation (Sample 7), indicative of an appreciable fraction of nonvolatile selenium in the raw crude shale oil. Table 5 gives data for the short-term irradiations of waxes, the parent heavy distillates from which the waxes were obtained, and the dewaxed heavy

distillates. The most notable feature of the data in this table is the very low tendency of the trace elements determined to accumulate in the waxes. In general, these waxes are solids consisting of paraffinic hydrocarbons, usually C-20 and higher. Apparently they do not bind strongly with elements whose determinations are shown in Table 5. The same general observation may be made for waxes (Samples 1—4) in Table 6, despite some anomalously high individual values, e.g., sodium in Sample 1. The only element that appears to be definitely concentrated in the waxes is aluminum. It is possible that the sodium and aluminum values in the waxes are artifacts of wax handling and purification procedures, and are not inherent to the waxes.

In summary, the use of neutron activation without separation has been demonstrated for the trace element characterization of shale oil and shale oil products. Elements detected by short term irradiations can be determined in even the most volatile fractions. Elements requiring irradiations of more than a few minutes can be determined only in crude shale oil, residua from shale oil distillation, and waxes. Even with these samples, the maximum irradiation time with the neutron flux employed is only approximately two hours. Therefore, a major deterrent to the use of n.a. on shale oil products is the time limit on long-term irradiations of hydrocarbon fractions, thus excluding determination of many of the elements of interest in some of the important fractions. However, the utility of n.a. for certain elements not readily determined by other techniques, lack of need for sample digestion, and generally non-destructive nature of n.a., give it a useful place in the characterization of shale oil and shale oil products.

The provision of samples by Frederic A. Birkholz of the U.S. Department of Energy, L.E.T.C. is gratefully acknowledged. Peter Shaw was provided a summer student traineeship at the L.E.T.C., administered through Associated Western Universities.

REFERENCES

1 A. D. Shendrikar and G. B. Faudel, Environ. Sci. Technol., 12 (1978) 332.
2 J. P. Fox, D. S. Farrier and R. E. Poulson, Chemical Characterization and Analytical Considerations for an In Situ Oil Shale Process Water, LETC/RI-78/7, U.S. Department of Energy, Laramie Energy Technology Center, Laramie, WY, 1978.
3 K. H. Abel and L. A. Rancitelli, Major, Minor, and Trace Element Composition of Coal and Fly Ash as Determined by Instrumental Neutron Activation Analysis, in S. P. Babu (Ed.), Trace Elements in Fuel, Advances in Chemistry Series 141, Ch. 10, American Chemical Society, Washington, DC, 1975.
4 J. S. Fruchter, J. C. Laul, M. R. Peterson and P. W. Ryan, High Precision Trace Element and Organic Constituent Analysis of Oil Shale and Solvent-Refined Coal Materials, Symposium on Analytical Chemistry of Tar Sands and Shale Oil, National Meeting of the American Chemical Society, New Orleans, LA, March, 1977.
5 C. Block and R. Dams, Anal. Chim. Acta, 68 (1973) 11.
6 R. F. Stevens, B. U. Dineen and J. S. Ball, Analysis of Shale Oil, Report of Investigations 4898, U.S.D.I. BuMines, 1952.
7 D. M. McKown and J. S. Morris, J. Radioanal. Chem., 43 (1978) 409.
8 T. Harper, MIT-3944-2/MITNE-97, Department of Nuclear Engineering, Massachusetts Institute of Technology, Cambridge, MA, 1968.

Analytica Chimica Acta, 123 (1981) 75—82

ANALYSIS OF THE ^{13}C-N.M.R. SPECTRA OF MONO- AND DIMETHYLAMPHETAMINES

KEITH BAILEY* and DONALD LEGAULT

Drug Research Laboratories, Health Protection Branch, Tunney's Pasture, Ottawa K1A 0L2 (Canada)

(Received 15th April 1980)

SUMMARY

The ^{13}C-n.m.r. spectra of the three monomethylamphetamines and the six dimethylamphetamines and their hydrochlorides were determined. Spectra were distinctive and suitable for identification and authentication purposes. Signals were assigned by a self-consistent analysis of chemical shift differences between differently-substituted compounds in the series of both the bases and the salts. Determination of the effects of N-protonation on the chemical shifts of aromatic ^{13}C signals was a valuable aid in resolving some ambiguities: C-1 shifted upfield by about 0.9 ppm, and methylated carbons *ortho*, *meta*, and *para* to the isopropylamine side-chain shifted downfield by about 3.3, 3.7, and 4.4 ppm, respectively. The data are useful in the authentication of reference materials employed in forensic analysis.

The mono- and dimethylamphetamines shown in Fig. 1 form a series of closely-related compounds with a structure similar to the corresponding methoxyamphetamines [1], which are notoriously hallucinogenic. Methods for their differentiation and identification have been published [2, 3]. The requirement for the authentication of reference materials has led us to examine the ^{13}C-nuclear magnetic resonance (n.m.r) spectra of the methylamphetamines. The data and their interpretation provide additional valuable reference characteristics which are presented here. This work confirms the conclusions drawn from our previous study of methoxyamphetamines [1] and phencyclidine analogues [4], that ^{13}C-n.m.r. spectroscopy is a powerful tool for discriminating among very similar compounds and at the same time providing fundamental, detailed information about chemical structure.

EXPERIMENTAL

The preparation of the methylamphetamines and their hydrochlorides was described previously [2, 3]. The ^{13}C-n.m.r. spectra were determined at 20.1 MHz on an 8K data-point Bruker WP 80 Fourier Transform spectrometer. Spectra were recorded at ambient temperature using the deuterium resonance of the solvent as the internal lock. Hydrochlorides were examined in D_2O and free bases in $CDCl_3$, containing internal standards of sodium 2,2-dimethyl-

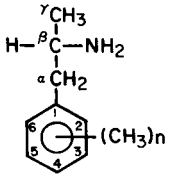

n = 0 : amphetamine (1)
n = 1 : 2-, 3- and 4-methylamphetamine (2, 3, and 4 respectively)
n = 2 : 2,3-, 2,4-, 2,5-, 2,6-, 3,4- and 3,5-dimethylamphetamine (5, 6, 7, 8, 9, and 10 respectively)

Fig. 1. Structure and numbering system for methylamphetamines.

2-silapentane-5-sulphonate (DSS) and tetramethylsilane (TMS), respectively. Solution concentration was usually about 100 mg/1.7 ml solvent in 10-mm tubes. Protons were decoupled by broad-band irradiation (4—5 W at 7.6 ppm in $CDCl_3$ and 5.1 ppm in D_2O) except in single frequency off-resonance decoupling (s.f.o.r.d.) experiments (4 W, at —8.6 ppm in $CDCl_3$ and —11.1 ppm in D_2O [5]. Some 2000 or more interferograms of 5000 Hz sweepwidth were stored for output in 4K data points following transform (address separation 0.06 ppm). Pulse widths were 1.5 μs (19.2° flip angle) with no pulse delay following data acquisition.

Some difficulties were encountered with D_2O solutions of the hydrochlorides: the compounds were not freely soluble, initially forming cloudy solutions which clarified during the time in which the spectra were obtained. The basic DSS seemed to have been extracted into the droplets which had risen to the surface, and it was only detected in the spectra of 1·HCl, 3·HCl, 7·HCl, and 8·HCl. Spectra were therefore obtained on saturated solutions. From our experience with spectra of this type, it is felt that the chemical shifts recorded in Table 1 are within 0.12 ppm (i.e., two addresses) of their correct values. The experimental results support this: with regard to the accurately-measured free bases, C-γ appears at 23.50 ± 0.18 ppm and in the salts, C-γ appears at 20.04 ± 0.12 ppm throughout (except for 8 which is probably a special case caused by steric effects, discussed below). Furthermore, the difference in the sums of the chemical shifts of the aromatic signals resulting from protonation (Δ, Table 1) is remarkably constant (14.97 ± 0.74 ppm).

RESULTS AND DISCUSSION

Data from the spectra, including those from amphetamine which were discussed in connection with the analysis of methoxyamphetamine spectra [1], are presented in Table 1.

The signals from the side-chain were easily identified at chemical shifts similar to those observed in the corresponding methoxy compounds [1], and confirmed for compounds 6, 7, and 8 by s.f.o.r.d. experiments in which C-α, C-β, and C-γ gave triplets, doublets, and quartets, respectively.

Whereas C-γ is at lower field than that of the aromatic CH_3 signals of the bases, it is at higher field in the salts except for 5·HCl in which it is located

TABLE 1

Data from the ^{13}C-n.m.r. spectra of methylamphetamines[a]

Compound		Signal												
		C-1	C-2	C-3	C-4	C-5	C-6	C-α	C-β	C-γ	CH_3[b]	CH_3[b]	ΣAr-C	Δ[c]
Amphetamine	(1)	139.93	129.54	128.75	126.50	128.75	129.54	46.64	48.40	23.38	—	—	783.01	14.39
Amphetamine HCl	(1·HCl)	138.95	132.27	131.85	130.21	131.85	132.27	42.69	51.74	20.04	—	—	797.40	
2-CH_3	(2)	138.28	136.71	130.75[d]	126.63[d]	126.20[d]	130.33[d]	43.90	47.31	23.69	19.62 (2)	—	788.90	15.13
2-CH_3.HCl	(2·HCl)	137.44	140.05	133.67[d]	130.45[d]	129.24[d]	133.18[d]	40.20	50.77	20.16	21.13 (2)	—	804.03	
3-CH_3	(3)	139.80	130.27	138.16	127.17	128.51	126.50	46.58	48.34	23.44	21.38 (3)	—	790.41	14.89
3-CH_3.HCl	(3·HCl)	138.95	132.82	141.93	130.75	131.73	129.12	42.63	51.80	20.04	23.02	—	805.00	
4-CH_3	(4)	136.83	129.42	129.42	136.04	129.42	129.42	46.22	48.40	23.38	21.01 (4)	—	790.55	14.98
4-CH_3.HCl	(4·HCl)	135.86	132.27[d]	132.39[d]	140.35	132.39[d]	132.27[d]	42.33	51.86	20.04	22.77 (4)	—	805.53	
2,3-diCH_3	(5)	137.98[d]	135.19	137.37[d]	128.45	125.59	128.45	44.39	47.49	23.44	15.37 (2)	20.77 (3)	793.03	15.13
2,3-diCH_3.HCl	(5·HCl)	137.25[d]	138.47[d]	140.96	131.79	128.63	131.06	40.81	50.95	20.10	17.18 (2)	22.35 (3)	808.16	
2,4-diCH_3	(6)	135.19	136.46	131.54[d]	136.04	126.81	130.27[d]	43.54	47.37	23.62	19.56 (2)[d]	20.95 (4)[d]	796.31	15.49
2,4-diCH_3.HCl	(6·HCl)	134.22	139.93[d]	134.22[d]	140.53[d]	129.72	133.18[d]	39.84	50.89	20.10	21.07 (2)[d]	22.65 (4)[d]	811.80	
2,5-diCH_3	(7)	138.10	133.55	131.12[d]	127.35	135.49	130.63[d]	43.97	47.31	23.69	19.13 (2)[d]	20.95 (5)[d]	796.24	15.38
2,5-diCH_3.HCl	(7·HCl)	137.31	136.77	133.73	130.94	139.14	133.73	40.14	50.83	20.10	20.58 (2)[d]	22.53 (5)[d]	811.62	
2,6-diCH_3	(8)	137.19	137.19	128.69	126.26	128.69	137.19	39.90	47.37	23.87	20.71 (2)	20.71 (6)	795.21	15.00
2,6-diCH_3.HCl	(8·HCl)	136.16	140.53	131.42	130.15	131.42	140.53	36.20	50.47	19.86	22.11 (2)	22.11 (6)	810.21	
3,4-diCH_3	(9)	137.37[d]	130.94	136.77[d]	134.58	129.97	126.93	46.28	48.40	23.50	19.31 (4)[d]	19.74 (3)[d]	796.56	15.71
3,4-diCH_3.HCl	(9·HCl)	136.52	133.49	140.59	139.01	132.94	129.72	42.33	51.93	20.10	21.07 (4)[d]	21.44 (3)[d]	812.27	
3,5-diCH_3	(10)	139.80	127.35	138.10	128.08	138.10	127.35	46.52	48.34	23.50	21.32 (5)	21.32 (5)	798.78	14.23
3,5-diCH_3.HCl	(10·HCl)	138.89	129.66	141.75	131.30	141.75	129.66	42.45	51.68	19.92	22.77 (3)	22.77 (5)	813.01	

[a]The bases were examined in $CDCl_3$ and the salts in D_2O; see text for method of assignment, chemical shifts in ppm. [b]The numbers in parentheses refer to the position of substitution. [c]Δ = Σ Ar-C salt in D_2O-Σ Ar-C base in $CDCl_3$; Σ Ar-C = sum of aromatic carbon chemical shifts. [d]It is particularly emphasized that these assignments may be interchanged.

between the signals from the 2- and 3-CH_3 substituents. It is not possible to distinguish between C-γ and Ar-CH_3 signals by s.f.o.r.d. experiments, since both then give quartets; reliance has been placed on the consistency of chemical shifts, seen incontravertibly in the methoxyamphetamine series [1]. The C-γ signal appears from about 19.9 to 20.2 ppm for the hydrochlorides and 23.4—23.9 ppm for the bases. A comparison of results from compounds 1 with 2, 3 with 5, 4 with 6, 3 with 7, and 2 with 8, suggests that *ortho* methylation results in a downfield shift of C-γ of up to 0.3 ppm.

The C-β signal appears at about 51.2 ± 0.7 ppm in the salts and 47.9 ± 0.6 ppm for the bases. Inspection of the data reveals that compounds with an *o*-methyl group exhibit the signal at about 1 ppm to high field of the position found in the others. Results with methoxyamphetamines were completely analogous [1].

The chemical shift of the benzylic C-α is very sensitive to the aromatic substitution, as shown by Table 2. The substitution of one *o*-methyl results in upfield shifts of some 2—3 ppm and of a second *o*-methyl in an additional upfield shift of 4 ppm. The effects of a *m*-methyl appear to be generally small and variable, but introduction of a *p*-methyl is associated consistently with an upfield shift of 0.3—0.4 ppm.

The aromatic methyl signals appear at 20.6—22.8 ppm in the salts and 19.1—21.3 ppm in the bases (Table 1) with the exception of 2,3-dimethylamphetamine (5), in which one of them is shifted about 5 ppm upfield. This observation may be contrasted with the exceptionally downfield position noted for the 2-OCH_3 signal in 2,3-dimethoxyamphetamine [1]. It is suggested that the upfield signal arises from the 2-CH_3 group, which is subjected to strong γ-shielding effects from both *ortho* substituents [6]. Assignments in the dimethyl series have been made by consideration of the shifts determined in the monomethyl compounds.

The assignments of aromatic signals are less readily made than those in the comparable methoxyamphetamines because they are spread across a

TABLE 2

Effects of methyl substitution on chemical shifts of C-α of amphetamines[a]

o-Methylation, compounds compared, Δ (ppm)									
2/1	2/1(HCl)	5/3	5/3(HCl)	6/4	6/4(HCl)	7/3	7/3(HCl)	8/2	8/2(HCl)
−2.74	−2.49	−2.19	−1.82	−2.68	−2.49	−2.61	−2.49	−4.00	−4.00
m-Methylation, compounds compared, Δ (ppm)									
3/1	3/1(HCl)	5/2	5/2(HCl)	7/2	7/2(HCl)	9/4	9/4(HCl)	10/3	10/3(HCl
−0.06	−0.06	+0.49	+0.61	+0.07	−0.06	+0.06	0 .00	−0.06	−0.18
p-Methylation, compounds compared, Δ (ppm)									
4/1	4/1(HCl)	6/2	6/2(HCl)	9/3	9/3(HCl)				
−0.42	−0.36	−0.36	−0.36	−0.30	−0.30				

[a]The symbolism 2/1, etc., indicates that the chemical shift of the unsubstituted compound (1) was subtracted from that of the 2-methyl compound (2) and so forth, to give Δ. Positive and negative signs indicate that downfield and upfield shifts, respectively, result from the substitution.

narrower range of chemical shifts. In particular, the position of C-1 is close to those of the carbons to which the CH_3 groups are attached. Both types give singlets on s.f.o.r.d. Under the experimental conditions used, their signals are of comparable, diminished relative intensity compared with those of the proton-bearing carbons. This observation is attributed to the more efficient relaxation of protonated carbons compared with the substituted carbons, for which T_1 is estimated to be several seconds [7]. The distinction between the two substituted types was first accomplished in compounds 8 and **10**, by consideration of the relative intensities of signals: C-1 had half the intensity of the C-2/6 and C-3/5 pairs. The small upfield shifts at C-1 of the two salts in D_2O compared with the bases in $CDCl_3$ and downfield shifts of other aromatic signals, exactly parallel the observations made in amphetamine and the corresponding methoxy compounds.

The remaining signals from 8 and **10** were unambiguously assigned from their relative intensities, and the signals from C-1 and C-3 of **3** and C-2/6 and C-3/5 of **4** were then identified on the basis of effects noted in 8 and **10** as follows: In comparison with the shifts of C-4 and C-1 in amphetamine, the corresponding shifts of 8 and **10** show that two *m*-methyl groups have a very small (<0.5 ppm) shielding effect. Whereas in comparison with the C-1 of amphetamine, the C-1 of compound 8 suggests that two *o*-methyl groups have a small (<3 ppm) shielding effect, the C-4 of compound **10** in comparison with that of amphetamine suggests that they have a small (<2 ppm) deshielding effect. The former result may be a less reliable indicator for subsequent assignments, since it is obtained from a compound in which 1,2,3-type substitution may result in an unusual steric component in the shielding, and the results from **4** also reveal a very small deshielding effect from the *o*-methyl. The signals from C-1 and C-3 of **3** and C-2/6 and C-3/5 of **4** have therefore been assigned (Table 1) in accordance with the foregoing; i.e., minimal effects of a *m*-CH_3 group.

The signals of C-1 and C-2 in **2**·HCl and of C-1 and C-4 in **4**·HCl have been ascribed on the basis of the C-CH_3 signal appearing at lowest field, as in the salts considered thus far; this principle appears to apply for the self-consistent assignment of similar signals throughout the series of salts except for C-2 vs. C-1 of **7**·HCl (Table 1). This exception results from the shielding effect of the *p*-methyl group (at C-5) of ca. 3 ppm, which can be consistently noted from the assignments of Table 1 and is found in *p*-xylene compared with toluene [8].

The quantified effects of protonation of the amino group are given in Table 3 for the substituted aromatic carbon signals; they were useful in resolving some ambiguous assignments. For example, the identification of C-1 at 135.86 ppm in **4**·HCl enables the signal in the base to be identified as that at 136.83 ppm, satisfying the empirical condition (see Table 3) that it be about 0.9 ppm downfield of the position in the salt; indeed, no other assignments of the C-1 and C-4 signals of **4** and **4**·HCl will satisfy this condition. The C-1 and C-2 signals of **2** base were identified similarly (Table 1).

TABLE 3

Effect of protonation on chemical shifts of substituted aromatic carbon signals of methylamphetamines[a]

Compound		C-1 (side-chain)	C-2/6 (*ortho*)	C-3/5 (*meta*)	C-4 (*para*)
Amphetamine[a]	(1)	−0.98	—	—	—
2-CH_3	(2)	−0.84	+3.34	—	—
3-CH_3	(3)	−0.85	—	+3.77	—
4-CH_3	(4)	−0.97	—	—	+4.31
2,3-diCH_3	(5)	−0.73	+3.28	+3.59	—
2,4-diCH_3	(6)	−0.97	+3.47	—	+4.49
2,5-diCH_3	(7)	−0.79	+3.22	+3.65	—
2,6-diCH_3	(8)	−1.03	+3.34	—	—
3,4-diCH_3	(9)	−0.85	—	+3.82	+4.43
3,5-diCH_3	(10)	−0.91	—	+3.65	—

[a]Results in ppm; the chemical shift of the base $CDCl_3$ was subtracted from that of the salt in D_2O. Positive and negative signs indicate that downfield and upfield shifts, respectively, result from protonation.

The signals which remain to be identified in the monomethyl series are the unsubstituted carbons of 2 and 2·HCl and of 3 and 3·HCl. It is possible to predict their approximate positions from those in amphetamine, using the foregoing deshielding parameters (*o*-CH_3, ca. + 0.5—1; *m*-CH_3, ca. 0; *p*-CH_3, ca. −3 ppm). The calculated shifts for 2 are: C-3, 129.2—129.8; C-4, 126.50; C-5, 125.8; C-6, 129.5 ppm and a firm conclusion cannot be drawn, especially between C-3 and C-6. The calculated shifts for 3 are: C-2, 130.0—130.5; C-4, 127.0—127.5; C-5, 128.75; C-6, 126.5; these fit well with the signals observed at 130.27, 127.17, 128.51, and 126.50 and the assignments have been made from this correlation for 3 and 3·HCl (Table 1).

The spectral analysis of the remaining four dimethylamphetamines was started with 7. The chemical shifts of C-3, -4, and -6 should be very close to those of C-3 in 2 and C-4 and C-2 in 3 respectively, differing from them only by *m*-CH_3 effects. An excellent correlation can be made in which a uniformly small (<0.4 ppm) deshielding effect is associated with effects of the *m*-CH_3 group, and which supports the assignments of C-3 and C-6 of 2 (Table 1). The shift of C-1 should be close to that in 2 and is thus uniquely identifiable. The signals of C-2 and C-5 were assigned on the basis that the former should be at higher field, as for C-2 and C-3 of 2 and 3, respectively.

This analytical approach was extended to 9: the shifts of C-2, and -6 should be very close to those of C-2 and -6 in 3 and of C-5 to that of C-5 in 4, respectively. The correlation is again good and shows a small (<0.7 ppm) deshielding effect of the *m*-CH_3 group. The assignments of C-1, -3, and -4 of 9 were provisionally made by the process described for C-1, -2, and -5 of 7. However, the assignments of C-1 and C-3 of 9 were subsequently interchanged

to those shown in Table 1 in order to obey the empirically-observed rule in these compounds, that a methyl-bearing carbon *meta* to the side chain is shifted about 3.7 ppm downfield on protonation but C-1 is shifted upfield by about 0.9 ppm (Table 3, discussed further below).

The same type of analysis was applied to 6, but only five aromatic signals were detected in the salt. It was tentatively concluded that C-1 was coincident with the strong signal ascribed to C-3 (Table 1). The sum of the chemical shifts of the aromatic carbons (Σ Ar-C, Table 1) strongly supported this; other assignments would have given values well outside the usual range. The signals of 5 were assigned in the same way, reliance being placed on the position of C-1 being close to that in 2 and C-2 and -3 appearing in the same relative positions observed in 2 and 3 and in 2,3-dimethoxyamphetamine [1].

Several interesting observations can be made by considering the data in Table 1 as transposed in Tables 2, 3 and 4. These lead to empirical rules, alluded to above, which can prove useful in spectral assignments. In particular, as illustrated in Table 3, the effect of protonation and change in solvent from $CDCl_3$ to D_2O results in remarkably consistent upfield shifts at C-1 of 0.88 ± 0.15 ppm, and downfield shifts at methyl-substituted carbons *ortho*, *meta*, and *para* to the side chain of +3.35 ± 0.12, + 3.71 ± 0.12, and +4.40 ± 0.09 ppm. Table 4 shows the downfield shifts of carbons at positions which are not substituted, that result on protonation. The effects are again greater in the order *ortho* < *meta* < *para*, and of magnitude 2.70 ± 0.40, 2.90 ± 0.30, and 3.56 ± 0.34 ppm with the assignments of Table 1. The results in Table 4 indicate that more self-consistency would be obtained if the assignments of C-3 and C-6 be interchanged in both 6 and 7, but they would not

TABLE 4

Effect of protonation on chemical shifts of unsubstituted aromatic carbon signals of methylamphetamines[a]

Compound		C-2/6 (*ortho*)	C-3/5 (*meta*)	C-4 (*para*)
Amphetamine	(1)	2.73/2.73	3.10/3.10	3.71
2-CH_3	(2)	— /2.85	3.12/3.04	3.82
3-CH_3	(3)	2.55/2.62	— /3.22	3.58
4-CH_3	(4)	2.85/2.85	2.97/2.97	—
2,3-diCH_3	(5)	— /2.61	— /3.04	3.34
2,4-diCH_3	(6)	— /2.91[b]	2.68[b]/2.91	—
2,5-diCH_3	(7)	— /3.10[b]	2.61[b]/—	3.59
2,6-diCH_3	(8)	— /—	2.73/2.73	3.89
3,4-diCH_3	(9)	2.55/2.79	— /2.97	—
3,5-diCH_3	(10)	2.31/2.31	— /—	3.22

[a]These are downfield shifts in ppm which result on subtracting the chemical shift of the base in $CDCl_3$ from that of the salt in D_2O. [b]Comparison with other differences suggests that these assignments are reversed, see text.

then be in keeping with the chemical shift reasoning applied previously. It can also be shown from Table 1, that for the four compounds with one o-CH_3 substituent, protonation results in shifts at C-α, C-β and C-γ of -3.70 ± 0.13 (i.e., upfield) $+3.49 \pm 0.03$ and -3.46 ± 0.13 ppm, respectively; for the five compounds with no o-CH_3 substituent, the shifts are -3.98 ± 0.09, $+3.44 \pm 0.10$ and -3.46 ± 0.12 ppm, respectively. An exactly similar observation of alternating effects was noted for the methoxyamphetamines [1].

Conclusion

Data from the ^{13}C-n.m.r. spectra of mono- and dimethylamphetamines can be interpreted in a self-consistent manner which allows the majority of signals to be confidently assigned, and which confirms the authenticity of structure of the materials. The large data base so generated allows empirical rules to be developed which relate changes in chemical shifts to structural changes in the compounds examined.

The authors are grateful to M. Lebelle for helpful discussions.

REFERENCES

1 K. Bailey and D. Legault, J. Forensic Sci., in press.
2 K. Bailey, H. D. Beckstead, D. Legault and D. Verner, J. Assoc. Off. Anal. Chem., 57 (1974) 1134.
3 K. Bailey, D. Gagné, D. Legault and R. Pike, J. Assoc. Off. Anal. Chem., 60 (1977) 642.
4 K. Bailey and D. Legault, Anal. Chim. Acta, 113 (1980) 375.
5 F. W. Wehrli and T. Wirthlin, Interpretation of Carbon-13 n.m.r. Spectra, Heyden, London, 1976, p. 66.
6 H. Pearson, J. Chem. Soc. Chem. Commun., (1975) 912.
7 G. C. Levy, J. D. Cargioli and F. A. L. Anet, J. Am. Chem. Soc., 95 (1973) 1527.
8 V. Formacek, L. Desnoyer, H. P. Kellerhals, T. Keller, and J. T. Clerc, ^{13}C Data Bank, Vol. 1, Bruker Physik, Zurich, 1976, pp. 80—83.

Analytica Chimica Acta, 123 (1981) 83—95

THE MECHANISM OF THE ELECTROCHEMICAL OXIDATION OF THIOUREA

JITKA KIRCHNEROVÁ and WILLIAM C. PURDY*

Department of Chemistry, McGill University, 801 Sherbrooke St. West, Montreal, Quebec, H3A 2K6 (Canada)

(Received 27th May 1980)

SUMMARY

Cyclic voltammetry and potentiostatic coulometry were used to study the electrochemical oxidation of thiourea in aqueous solutions of nitric acid, nitric acid—ammonium nitrate, and ammonium nitrate—ammonium hydroxide and in acetonitrile. These studies were carried out at glassy carbon and/or platinum working electrodes. In acetonitrile, the cyclic voltammograms show one oxidation peak at +0.6 V and a reduction peak at −0.1 V. In aqueous solutions up to about pH 6, there is a second oxidation peak at 1.3 V which is irreversible and its height is sensitive to acidity. These experiments have confirmed that in acidic and neutral solutions the oxidation of thiourea proceeds via a slow 1-e transfer reaction producing a radical $[(NH_2)_2—C—S^{\cdot}]^+$. Further direct oxidation of this radical takes place only at higher potentials (ca. 1.2 V) and involves hydration and proton-transfer equilibria. Otherwise, C,C′-dithiodiformamidinium ion is formed by a fast dimerization reaction. Coulometric and chronopotentiometric measurements have shown that in strong acid the second oxidation step involves one electron, while at lower acidities the further oxidation involving three (and possibly five) electrons proceeds in two (or three) steps of very similar potential.

The oxidation of thiourea has long been known to yield a variety of products. These range from C,C′-dithiodiformamidinium salts $[(NH_2)_2CSSC(NH_2)_2]^{2+}\cdot 2X^-$ to products of complete oxidation (i.e., NH_4^+, CO_2, and H_2SO_4) and depend on the oxidizing agent and/or conditions [1]. For example, in neutral solution with hydrogen peroxide, thiourea is oxidized to formamidine sulfinic acid, $(NH_2)_2CSO_2$. In contrast, in strongly acidic solutions the two reagents yield C,C′-dithiodiformamidinium salts [2]. The latter product is obtained with several other oxidizing agents.

Nitrous acid is known to react with thiourea by two entirely different reactions [3, 4]. At high acidity the predominant reaction is

$$2H^+ + 2HNO_2 + 2(NH_2)_2CS \rightarrow [(NH_2)_2CSSC(NH_2)_2]^{2+} + 2NO + 2H_2O \quad (1)$$

At low acidities another reaction is favored, namely

$$HNO_2 + (NH_2)_2CS \rightarrow H^+ + SCN^- + N_2 + 2H_2O \quad (2)$$

At pH values between 3 and 5 and for low concentrations of reactants, reaction (2) predominates and has been used for the colorimetric determina-

tion of thiourea or nitrites [5]. However, a recent study [6] has shown that in highly concentrated nitrate solutions, reaction (2) proceeds virtually 100% only under relatively limited conditions. At pH > 4 some other, as yet unidentified reaction yielding sulfur and nitric oxide, takes place in parallel.

The two known reactions (1 and 2) differ in the oxidation site. In reaction (1) it is the thioketone group while in reaction (2) it is the amine group. Elimination of sulfur in the unidentified reaction indicates that the site of oxidation is the thio group; the oxidation requires two electrons.

In an attempt to elucidate the mechanism of this unidentified reaction we have employed three complementary electrochemical methods: cyclic voltammetry, chronopotentiometry, and potentiostatic coulometry. Neither of these methods by itself permitted the mechanistic interpretation of the complex electrochemical reactions of thiourea.

Electrochemical oxidation of thiourea has been studied by several workers, but these studies have been limited to aqueous acid [7—13] or aprotic [14] media. In either medium, the oxidation has been shown to proceed via a one-electron transfer reaction yielding C,C′-dithiodiformamidinium ion (III)

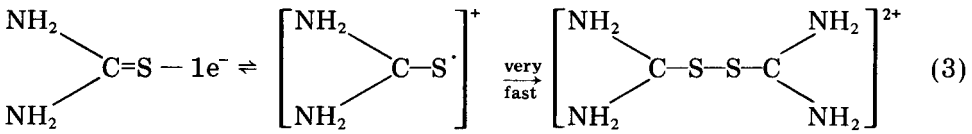

(3)

I II III

Some workers considered this reaction to be reversible [14, 15], with the standard electrochemical potential determined as 0.42 V [15], although the irreversibility of reaction (3) was also reported [10]. While the formation of higher oxidation products has been noted by some workers [11, 12], no detailed study has ever been reported.

In this paper, the results of a systematic study of the electrooxidation of thiourea under a wide range of conditions are presented. From these data a possible mechanism is proposed for the electrochemical oxidation of thiourea.

EXPERIMENTAL

Chemicals

All chemicals in this study were of analytical grade (Fisher Scientific) and were used without further purification. Test solutions were prepared from stock solutions of higher concentration. For thiourea, a 0.1 M or 0.5 M stock solution was employed.

C,C′-Dithiodiformamidinium dichloride was prepared by the method of Preisler and Berger [15] from hydrogen peroxide and thiourea dissolved in 3 M hydrochloric acid. The white crystals which precipitated after cooling were washed with ethanol and ether and were dried (m.p. 173°C).

Formamidine sulfinic acid was prepared by the method of Barnett [16] from hydrogen peroxide and thiourea dissolved in water. Similarly the white

crystals which separated after cooling were washed with ethanol and ether and were dried (m.p. 124.5°C, decomp.). These two compounds were prepared and used for identification of thiourea oxidation products.

Apparatus

Cyclic voltammetry, chronoamperometry, chronopotentiometry, and coulometry were carried out with a PAR (Princeton Applied Research Corp.) Model 175 universal programmer, Model 173 potentiostat/galvanostat, and Model 179 digital coulometer. A commercial PAR cell was used for voltammetric measurements and contained a saturated calomel reference electrode (s.c.e.) and a platinum plate (ca. 2.5 cm^2 area) or platinum spiral counter electrode. A platinum plate (ca. 2.5 cm^2 area) or glassy carbon (g.c.) disc (0.95 cm^2 area) was used as the working electrode. For coulometric measurements, a two-compartment cell was employed. The anode compartment contained an s.c.e. and a cylindrical platinum gauze working electrode; a spiral platinum electrode was placed in the cathode compartment.

The g.c. electrode used for cyclic voltammetry, chronoamperometry, and chronopotentiometry consisted of a 15 × 2 mm g.c. disc mounted in a teflon cylindrical holder; the exposed surface area of the g.c. electrode was 0.95 cm^2. This electrode was described by Hepler et al. [17] but in the present work it was used without wax impregnation. Instead it was resurfaced periodically by polishing to a mirror-like surface on a wet cloth impregnated with very fine alumina.

Voltammograms were recorded on a Houston Omnigraphic Model 2000 XY recorder. Chronoamperograms and chronopotentiograms were recorded on a Heath—Schlumberger Model SR-204 strip-chart recorder.

Procedures

Test solutions for cyclic voltammetry were generally 2 or 5 mM in thiourea when the g.c. electrode was used or 1 mM for the platinum electrode. The aqueous supporting electrolyte solutions were: 0.2 M nitric acid, 2.0 M nitric acid, 0.2—5 M ammonium nitrate with the addition of either nitric acid or ammonium hydroxide to cover the range of pH values from 2 to 8.5, or 0.2 M potassium phosphate buffer. In acetonitrile the supporting electrolyte was 0.1 M lithium perchlorate. Before each run the test solutions were deaerated with a stream of nitrogen. Cyclic voltammograms were taken in quiet solution. In aqueous systems, the voltammetric measurements were carried out mainly at the g.c. electrode since the platinum electrode exhibited high residual currents above 1.1 V.

Chronoamperometric and chronopotentiometric measurements were made in 2 M nitric acid and 0.5 M ammonium nitrate using the same cell and electrode as employed in cyclic voltammetry. In the coulometric studies, 50 ml of 2×10^{-4} to 2×10^{-2} M solutions of thiourea in various electrolytes were used. During electrolysis the solutions were stirred with a magnetic stirring bar. Before each measurement, a blank was run to determine the background current.

RESULTS AND DISCUSSION

Cyclic voltammetry

At both the g.c. and platinum working electrodes, thiourea in acetonitrile medium gives a single one-electron voltammetric oxidation peak and a cathodically shifted reduction peak that is not observed in the absence of prior oxidation. The peak potentials (E_{pa} and E_{pc}) are very sensitive to sweep rate (see Fig. 1 and Table 1). These peaks are apparently due to the oxidation of thiourea to C,C'-dithiodiformamidinium ion (III) and subsequent reduction of the latter to thiourea. However, contrary to an earlier report [14, 15], the electron-transfer process is very slow as indicated by the large ΔE_p ($=E_{pa} - E_{pc}$). Based on the method of Nicholson [18], the estimated rate constant for this electron-transfer reaction is about 10^{-5} cm s^{-1}.

In aqueous solutions the oxidation of thiourea is more complicated. In addition to the oxidation and reduction peaks observed in acetonitrile, a new rather broad peak for an irreversible oxidation step appears at ca. 1.3 V (at a sweep rate of 100 mV s^{-1}). The two oxidation peaks and the reduction peak at −0.15 V are observed in a wide range of acidities going from 2 M HNO_3 up to a pH of about 6 (see Fig. 2).

In acidic solution the anodic portion of the thiourea cyclic voltammogram closely resembles the voltammogram of chlorpromazine [17]. Chlorpromazine and other phenothiazine derivatives were shown to be oxidized in two one-electron transfer steps to give sulfenic acids of these compounds [19].

As shown in Fig. 2, the height of the second anodic peak of thiourea increases strongly with decreasing acidity and at pH ≈ 4 is approximately three times higher than the first peak. Identification of the first anodic peak with oxidation to III is confirmed by the cyclic voltammogram of C,C'-dithiodiformamidium dichloride (Fig. 3) prepared by chemical oxidation. However, while it is evident that the second oxidation peak(s) is due to reactions involving the transfer of hydrogen and hydroxide ions, most likely leading to thiourea oxides, their exact assignment required some additional study.

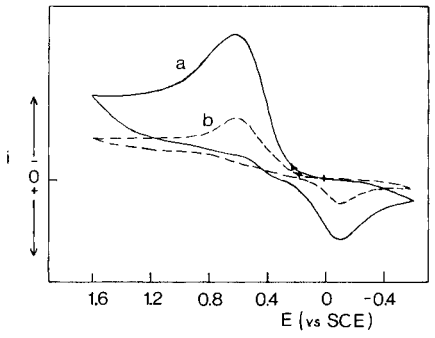

Fig. 1. Cyclic voltammograms of thiourea in acetonitrile. Sweep rate, 100 mV s^{-1}; supporting electrolyte, 0.1 M $LiClO_4$. (a) Pt working electrode; (b) g.c. working electrode.

TABLE 1

E_{p_a} and E_{p_c} values for oxidation of thiourea and its subsequent reduction in acetonitrile[a] at Pt and g.c. electrodes

Sweep rate $V\,s^{-1}$	E_{pa} (V)		E_{pc} (V)	
	Pt electrode	g.c. electrode	Pt electrode	g.c. electrode
1.000	0.71	0.57	−0.075	−0.100
0.500	0.65	0.54	−0.06	−0.085
0.200	0.60	0.515	−0.04	−0.065
0.100	0.55	0.49	−0.02	−0.055
0.050	0.52	0.46	0.00	−0.020
0.020	0.49	0.42	+0.03	0.020
0.010	—	0.39	—	0.045
0.002	—	0.34	—	0.110

[a]Supporting electrolyte was 0.1 M $LiClO_4$.

The appearance of two anodic peaks was reported earlier at platinum and gold electrodes [11] but not at a graphite electrode [12]. Without a detailed study, the second anodic peak was attributed to the secondary oxidation by oxygen adsorbed on platinum [12].

In 2 M HNO_3 and 0.5 M NH_4NO_3, the values of i_{p_1} and i_{p_2} increase faster than would be predicted by the linear relationship between i_p and $v^{1/2}$ indicating a weak adsorption at the electrode. For the first oxidation step, the adsorption of thiourea is evident on both the g.c. and platinum electrodes. This is evident also from curves of i_p vs. C which are linear only above about 2×10^{-3} M; the electrode area in this case is 0.95 cm^2. The low values for the ratio i_{p_c}/i_{p_a} and their insensitivity to scan rates from 1.0 Vs^{-1} to 0.01 Vs^{-1} can be interpreted as an indication of highly different charge-transfer coefficients; this might well be consistent with an $\alpha_a \approx 0.8$ reported in the literature [10]. Because of the very slow charge transfer ($k \sim 10^{-6}$ to 10^{-5} cm s^{-1}), the oxidation of thiourea and the reduction of its product can be treated as independent,

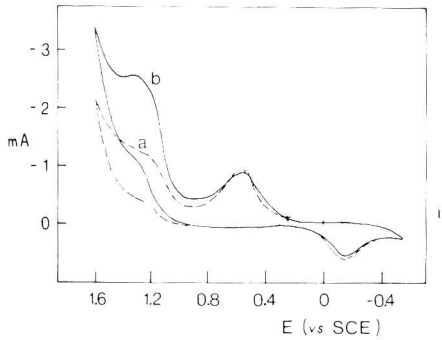

Fig. 2. Cyclic voltammograms of thiourea in aqueous solutions of different acidities. (a) 2 M HNO_3; (b) 0.5 M NH_4NO_3. Sweep rate, 100 mV s^{-1}.

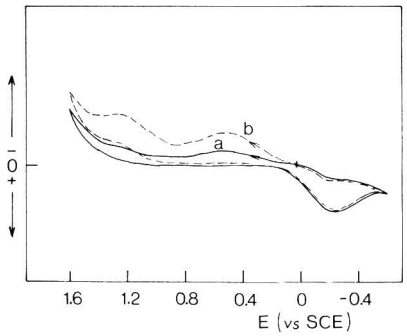

Fig. 3. Cyclic voltammograms of C,C'-dithiodiformamidinium dichloride in aqueous 0.2 M HNO_3. (a) first cycle; (b) second cycle. Sweep rate, 100 mV s^{-1}.

irreversible processes [18, 20]. Expressing i_{p_a} and i_{p_c} as:

$i_{p_a} = 298[(\alpha_a n_a)^{1/2} n A (D_R v)^{1/2} C]$ and $i_{p_c} = 298[(\alpha_c n_c)^{1/2} n A (D_{OX} v)^{1/2} C]$

where a and c indicate the anodic and the cathodic process, n is the theoretical number of electrons involved in the process, v is the sweep rate, and all other terms have their usual meaning [20], the values of α could be evaluated provided the adsorption can be neglected and the values of D are known. The value of D for thiourea is available [21] but only for aqueous solution without electrolyte. An attempt was therefore made to determine it in both 2 M HNO_3 and 0.5 M NH_4NO_3 by a chronoamperometric method. Very good results were obtained (see Table 2). The values of D are 12.1 × 10^{-6} cm^2 s^{-1} and 12.6 × 10^{-6} cm^2 s^{-1} in 2 M HNO_3 and 0.5 M NH_4NO_3, respectively, and these numbers agree well with the literature [21]. To minimize the effect of adsorption the value of $\alpha_a n_a$ was calculated from the slope of the i_{p_a} vs. C curve and was found to be 0.43, while $\alpha_c n_c$ would be 0.18, assuming the same diffusion coefficient.

As mentioned above, the character of cyclic voltammograms of thiourea for solutions of pH 3—6 was very similar. However, in solutions of higher pH, remarkable changes in the voltammograms were observed. The cathodic peak started to diminish while the first oxidation peak shifted to more anodic

TABLE 2

Results of chronoamperometric measurements and the diffusion coefficient for thiourea

Supporting electrolyte	Conc. of thiourea (× 10^{-3} mol l^{-1})	$i\tau^{1/2}$ [a] (mA s^{-1})	D (× 10^{-6} cm^2 s^{-1})
2 M HNO_3	9.09	1.635 ± 0.008	12.10
2 M HNO_3	3.85	0.692 ± 0.003	12.08
0.5 M NH_4NO_3	1.69	0.360 ± 0.004	12.61
0.5 M NH_4NO_3	3.85	0.705 ± 0.005	12.56
0.5 M NH_4NO_3	5.66	1.040 ± 0.008	12.62

[a] $i\tau^{1/2}$ values measured over a period of 2 to 60 s; potential step from 0 to 0.6 V.

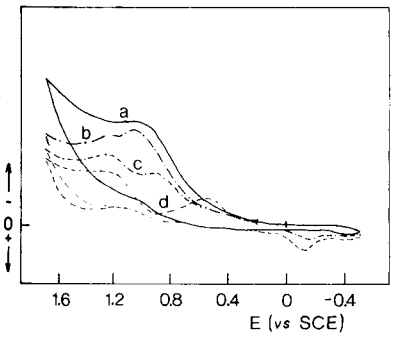

Fig. 4. Cyclic voltammograms of thiourea in aqueous solutions of pH 5—8.5. (a) pH 7.8; (b) pH 7.07; (c) pH 6.39; (d) pH 2.5. Sweep rate, 100 mV s^{-1}.

potentials and increased in height. With increasing pH the cathodic peak disappeared and the anodic peaks merged into a single broad peak with $E_p \approx 1.1$ V (see Fig. 4). The nature of these changes is probably associated with tautomeric changes in the thiourea molecule and will be discussed later.

Chronopotentiometry

Chronopotentiometric measurements were included mainly to provide further information on the second and possibly further oxidation steps. Only a limited number of measurements were made in strong acid and in 0.5 M NH_4NO_3 solution. These chronopotentiograms are shown in Fig. 5. Although not perfectly developed, both chronopotentiograms show two distinct plateaux at $E_{1/4}$ values of about 0.52 and 1.2 V with $\tau_2/\tau_1 \approx 3$ in 2 M HNO_3 and at $E_{1/4}$ values of about 0.52 and 1.16 V with $\tau_2/\tau_1 \approx 15$ in 0.5 M NH_4NO_3. Assuming that the first oxidation step involves one electron, the observed transition time ratios indicate that in 2 M nitric acid the second oxidation step also involves one electron while in 0.5 M ammonium nitrate the second

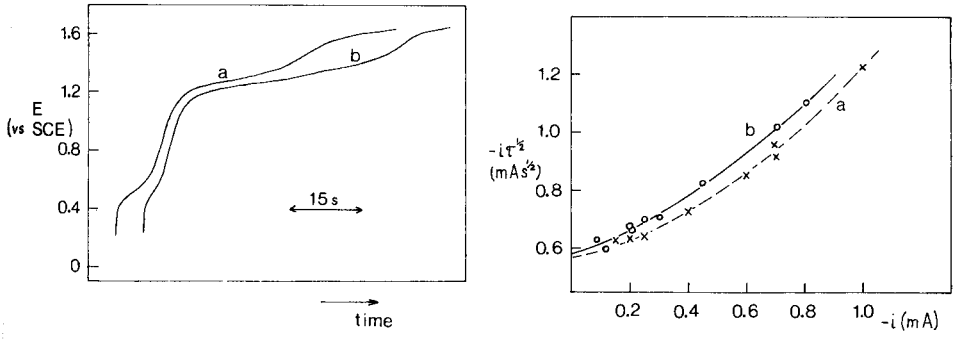

Fig. 5. Chronopotentiograms of 1.96 × 10^{-3} M thiourea in 2 M HNO_3 (a) and 0.5 M NH_4NO_3 (b). Applied current, 1.4 mA.

Fig. 6. $i\tau^{1/2}$ versus i for 1.96 × 10^{-3} M thiourea in 2 M HNO_3 (a), and 0.5 M NH_4NO_3 (b).

TABLE 3

Potentiostatic coulometric data for thiourea in aqueous solutions

Supporting electrolyte	pH	Potential (V)	Thiourea (mmol/50 ml)	Apparent no. of electrons (n°_{app})
2 M HNO_3		0.7	0.01	1.020
		0.7	0.10	1.035
		0.7	1.00	1.04[c]
0.2 M HNO_3		0.7	0.01	1.02, 0.98
		0.7	0.10	1.044
		0.7	1.00	1.22
0.2 M NH_4NO_3	2.4 (2.1)[a]	0.7	0.01	1.06
	5.1	0.7	0.01	1.39
	4.2 (2.1)	0.7	0.20	2.59
	5.28 (2.89)	0.7	0.20	4.51
	2.96 (1.9)	0.7	0.50	1.15
0.1 M phosphate	4.42 (3.3)	0.7	0.20	4.15
2 M HNO_3		1.2	0.01	2.01
		1.3	0.01	2.02
		1.3	0.1	1.49[b]
		1.3	0.2	1.32[b]
		1.3	1.0	1.10[c]
0.2 M HNO_3		1.2	0.01	2.02
		1.3	0.10	1.58[b]
		1.3	0.20	2.50
0.2 M NH_4NO_3	2.4 (1.9)	1.2	0.01	2.39
	4.94 (3.1)	1.2	0.01	3.89
	6.0 (3.6)	1.15	0.01	3.90
0.1 M phosphate	4.42 (3.3)	1.2	0.10	3.91
	8.62 (6.82)	1.0	0.01	4.6

[a]Values in parentheses indicate the pH after the electrolysis. [b]III detected by cyclic voltammetry. [c]White crystals of III dinitrate precipitated.

step involves three electrons. However, in the latter case the three-electron transition is not necessarily a one-step process, but may involve two or three steps of very similar potential. The variation of $i\tau^{1/2}$ with i (Fig. 6) clearly indicates adsorption at the electrode surface. Only as $i \rightarrow 0$ does $i\tau^{1/2}$ approach the value calculated by using D determined by chronoamperometry.

Potentiostatic coulometry

Coulometric measurements were carried out at 0.7 V and 1.2 or 1.3 V in a variety of solutions with acidity ranging from 2 M HNO_3 to pH 8.6 and concentrations of thiourea from 2×10^{-4} to 2×10^{-2} M. The results are summarized in Table 3.

Electrolysis at 0.7 V. In strong acid, the results agree with the literature data. In fact, during the electrolysis of 2×10^{-2} M thiourea in 2 M HNO_3, a white precipitate, identified as C,C'-dithiodiformamidinium dinitrate, was obtained. The coulometric yields are the same in 0.2 M HNO_3 but only for

thiourea concentrations up to 2×10^{-3} M. For a thiourea concentration of 2×10^{-2} M, the coulometric yield is approximately 20% higher than expected. With increasing pH, the number of coulombs necessary for complete oxidation increases and is greater, the higher the buffer capacity; the initial current–time curves are similar, however. Cyclic voltammograms run on solutions of low acidity after extended electrolysis exhibit features similar to those of voltammograms of thiourea, except for peak heights. This could only be explained by some slow secondary reaction producing thiourea and another product oxidizable at 0.7 V. Indeed, III is known to be unstable in solutions of low acidity [2, 15, 22]; it disproportionates to give thiourea, sulfur, and cyanamide. The rate of this reaction

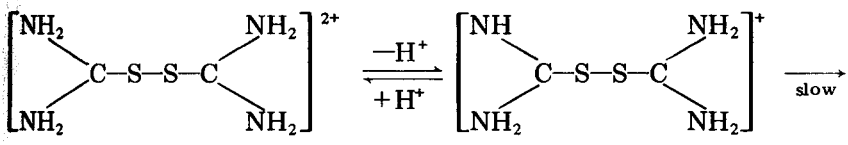

III

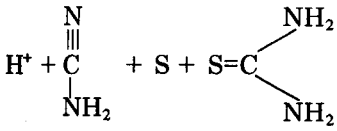

(4)

depends on the pH and is relatively fast at pH 4–5. The pK value of about 2.85 was determined in this laboratory by a potentiometric method and this value agrees well with the observed coulometric data. Because sulfur can be oxidized to sulfite ion at a potential of 0.7 V, it was not observed as a product. However, the presence of sulfite ion was determined qualitatively. The complete oxidation to cyanamide and sulfite, requiring six electrons per mole of thiourea, was not achieved under the conditions employed; during the oxidation, hydrogen ion is released, and the pH of the reaction mixture falls, shifting the equilibrium of the first step of Reaction 4 to the left.

Electrolysis at 1.2 V. In 2 M and 0.2 M HNO_3 the coulometric yields of two electrons, expected from the cyclic voltammetric and chronopotentiometric measurements, were found only for low thiourea concentrations. At higher thiourea concentrations, the coulometric yields were smaller, approaching 1 at a concentration of 2×10^{-2} M. Cyclic voltammograms of the product(s) resulting from electrolysis of 2×10^{-3} M thiourea in 2 M HNO_3 show an anodic peak at about 1.2 V and a cathodic peak at −0.1 V, suggesting the presence of III. In fact, III has been obtained as a precipitate when oxidizing 2×10^{-2} M thiourea in 2 M HNO_3. These results suggest that the product of the oxidation undergoes a coupling reaction with thiourea to give III.

Theoretical aspects of secondary reactions in potentiostatic coulometry have been treated in detail in a review by Bard and Santhanam [23]. For the

case of a coupling reaction of the following type

$$R \underset{p}{\rightarrow} O + ne^-; \quad O + R \underset{k}{\rightarrow} Y$$

(where p is the mass transfer controlled rate constant, k is the rate constant for the coupling reaction, and Y is the product which is not electroactive at the potential used) it was shown that the apparent number of electrons transferred during the electrolysis (n°_{app}) is a function of k, C_0 (the initial concentration of R), and p, where n°_{app} assumes a value between n (when $kC_0p^{-1} \rightarrow 0$) and 0.5 n (when $kC_0p^{-1} \rightarrow \infty$). By comparing the experimental n°_{app} with the theoretical plots of n°_{app} vs. log C_0 for different k/p ratios, the value of k can be deduced.

In view of the results obtained, the second oxidation step for thiourea in strong acid is best described by the following reaction

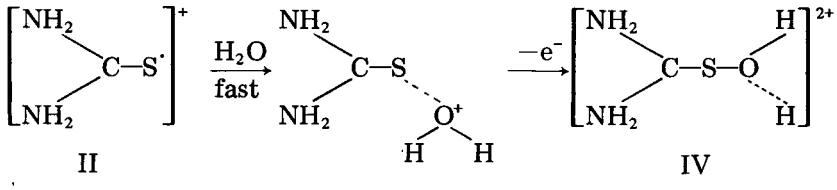

(5)

With a sufficiently high concentration of thiourea, the product of reaction (5), the diprotonated sulfenic acid (IV), apparently undergoes a coupling reaction

$$[(NH_2)_2C{-}S{-}OH_2]^{2+} + (NH_2)_2C{=}S \xrightarrow[H_2O]{k} [(NH_2)_2C{-}S{-}S{-}C(NH_2)_2]^{2+} \qquad (6)$$

IV I III

From the present coulometric data, and from the n°_{app} vs. log C_0 plots reported by Bard and Santhanam [23], the value of the k/p ratio is about 6×10^2 l mol^{-1}. Estimating the value of p to be about 10^{-3} s^{-1}, it follows that k is about 0.6 l mol^{-1} s^{-1}.

In solutions of lower acidity, the species IV apparently undergoes deprotonation to form unstable formamidine sulfenic acid (V), which usually decomposes to cyanamide, sulfur and water [22, 24], or can be oxidized further

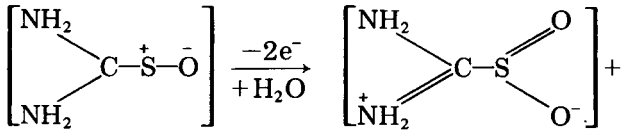

(7)

Species VI, the formamidine sulfinic acid, is a stable, commercially important reducing agent. As mentioned above, it can easily be prepared from thiourea and hydrogen peroxide in water [1, 16]. Cyclic voltammograms for two concentrations of this compound are presented in Fig. 7. The observed peak at 1.3 V is presumably due to the two-electron oxidation of VI to the corresponding sulfonic acid

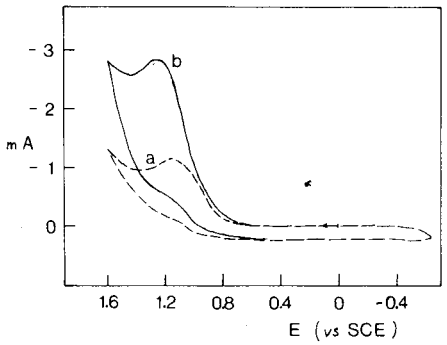

Fig. 7. Cyclic voltammograms of 2×10^{-3} M (a) and 5×10^{-3} M (b) formamidine sulfinic acid in aqueous solution of 0.2 M NH_4NO_3 plus nitric acid (pH 2.8). Sweep rate, 100 mV s^{-1}.

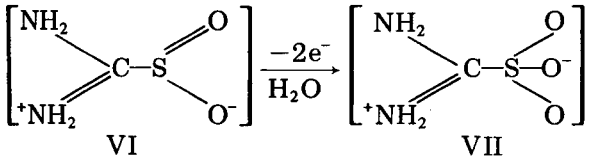

(8)

and is strikingly similar to the second oxidation peak of thiourea.

The present limited coulometric and chronopotentiometric data for the oxidation of thiourea in weakly acid solutions at around 1.2 V suggest a stepwise formation of compound VI provided no other side-reaction interfered. This oxidation would require the transfer of four electrons. The oxidation to compound VII requires a total transfer of six electrons. Evidently this reaction has not been accomplished, probably because of the low oxidation potential employed. Attempts to use oxidation potentials more positive than 1.2 V proved unsuccessful because of the high background currents. For the same reason, coulometric measurements could not be made at potentials more positive than 1.0 V in solutions of pH > 7. Hence only limited coulometric data are available; in the phosphate buffer of pH 8.62 and at a potential of 1.0 V these data suggest that the complete oxidation requires about four electrons. Unfortunately this does not add to the information presented in Fig. 4. However, it is possible to speculate on the following mechanism which involves the zwitter-ionic tautomer of thiourea and two two-electron oxidation steps leading to the formation of compound VI

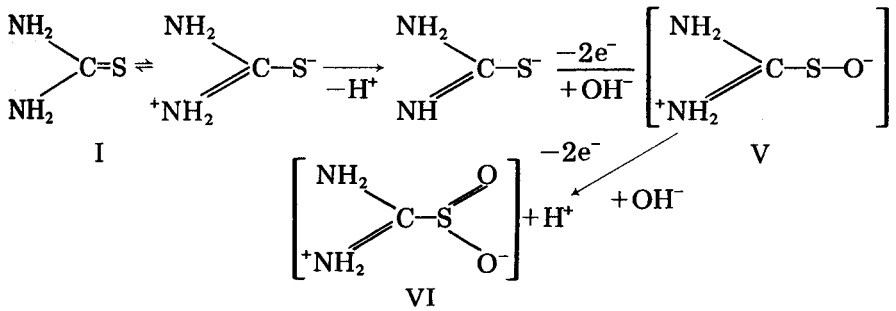

(9)

In solutions of high pH, thiourea has a tendency to form the zwitterionic tautomer [25]. This probably plays a very important role in other thiourea reactions. For example, it now seems clear that the tautomeric equilibria affect the pathways of the reaction between thiourea and nitrous acid. The two known reactions (1 and 2) have been explained by the following mechanism [26]

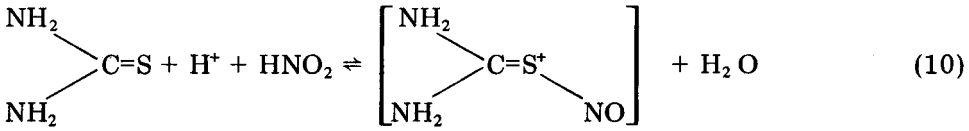

I VIII

In strong acid, two molecules of unstable nitrosothiourea (VIII) react rapidly to form III and two molecules of nitric oxide. At lower acidities, VIII deprotonates and an internal migration of the —NO group takes place.

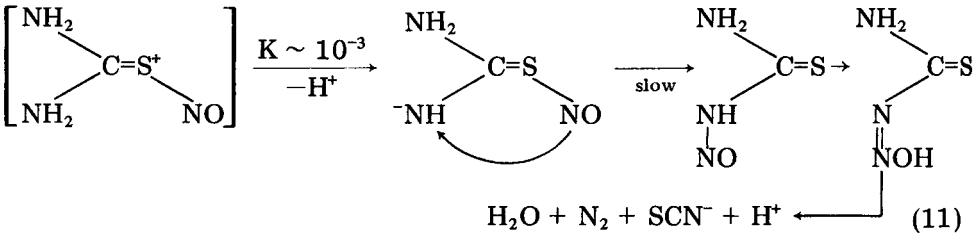

The explanation for the formation of sulfur and nitric oxide from thiourea and nitrite ion could then be found in the following mechanism

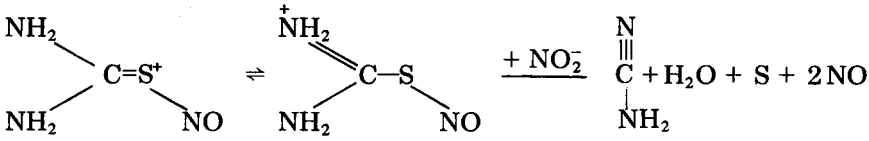

Conclusions

The electrooxidation of thiourea in aqueous solution is a multistep process that is pH-dependent; the oxidation is accomplished by adsorption. In strongly acid solution and in solutions up to pH 6, the first step involves a one-electron transfer taking place at ca. 0.7 V at a platinum and at ca. 0.55 V at a g.c. working electrode. The oxidation product is a short-lived radical ion $[(NH_2)_2—C—S^{\cdot}]^+$ which rapidly dimerizes to C,C'-dithioformamidinium ion (III). Further oxidation steps take place at 1.1—1.4 V and involve, in addition to electron transfer, hydration equilibria and H^+ and OH^- transfer. In strongly acid solution, the product of highest oxidation appears to be the diprotonated sulfonic acid (IV) which reacts with thiourea (when present in sufficient concentration) to give III. The rate constant for this reaction in 2 M HNO_3 was estimated to be 0.6 l mol^{-1}. At low acidity (pH 4—6) the product of oxidation at 1.2 V seems to be formamidine sulfinic acid. Cyclic

voltammetry has shown that the oxidation of this last product at ca. 1.3 V leads to formamidine sulfonic acid. In solutions of higher pH (> 6.5, depending on the ionic concentration), thiourea apparently undergoes tautomeric changes and the oxidation proceeds directly in two-electron steps to higher thiourea oxides.

The authors are grateful to the Natural Sciences and Engineering Research Council for support of this work.

REFERENCES

1 E. E. Reid, Organic Chemistry of Bivalent Sulfur, Vol. 5, Chemical Publishing Co., New York, 1963, pp. 38—40.
2 M. Hoffmann and J. O. Edwards, Inorg. Chem., 16 (1977) 3333.
3 A. E. Werner, J. Chem. Soc., 101 (1912) 2180.
4 M. E. Coade and A. E. Werner, J. Chem. Soc., 103 (1913) 1221.
5 K. Hutchinson and D. F. Boltz, Anal. Chem., 30 (1958) 54.
6 A. Edmons and J. Kirchnerová, unpublished results.
7 F. Fichter and W. Wenk, Ber. Dtsch. Chem. Ges., 45 (1912) 1373.
8 F. Fichter and F. Braun, Ber. Dtsch. Chem. Ges., 47 (1914) 1526.
9 K. S. V. Santhanam and V. R. Krishnan, Z. Phys. Chem., N. F. (Frankfurt), 34 (1962) 312.
10 S. J. J. Reddy and V. R. Krishnan, J. Electroanal. Chem. Interfacial Electrochem., 27 (1970) 473.
11 V. A. Zakharov, I. M. Bessarabova, O. A. Songina and M. A. Timoshkin, Elektrokhimiya, 7 (1971) 1215.
12 V. A. Zakharov, I. M. Bessarabova, V. G. Barikov and T. I. Treshchetkina, Elektrokhimiya, 9 (1973) 58.
13 S. V. Gorbachev, A. G. Atanasyants and Yu. M. Senatorov, Zh. Fiz. Khim., 46 (1972) 2429; 48 (1974) 195; 48 (1974) 3056.
14 A. Astruc, M. Astruc, D. Gonbeau and G. Pfister-Guillouzo, Collect. Czech. Chem. Commun., 41 (1976) 2737.
15 P. W. Preisler and L. Berger, J. Am. Chem. Soc., 69 (1947) 322.
16 E. de B. Barnett, J. Chem. Soc., 97 (1910) 63.
17 B. R. Hepler, S. G. Weber and W. C. Purdy, Anal. Chim. Acta, 102 (1978) 41.
18 R. S. Nicholson, Anal. Chem., 37 (1965) 1351.
19 F. H. Merkle and C. A. Discher, Anal. Chem., 36 (1964) 1639.
20 R. S. Nicholson and I. Shain, Anal. Chem., 36 (1964) 706.
21 D. B. Ludlum, R. C. Warner and H. W. Smith, J. Phys. Chem., 66 (1962) 1540.
22 F. Kurzer and P. M. Sanderson, J. Chem. Soc., (1959) 1058.
23 A. J. Bard and K. S. V. Santhanam, in A. J. Bard (Ed.), Electroanalytical Chemistry, Vol. 4, M. Dekker, New York, 1970, pp. 215—315.
24 W. Walter and G. Randau, Justus Liebigs Ann. Chem., 722 (1969) 52.
25 N. R. Kunchur and M. R. Truter, J. Chem. Soc., (1958) 2551.
26 K. Al-Mallah, P. Colling and G. Stedman, J. Chem. Soc., Dalton Trans., (1974) 2469.

Analytica Chimica Acta, 123 (1981) 97–105

DETERMINATION OF N-NITROSAMINES BY HIGH-PERFORMANCE LIQUID CHROMATOGRAPHIC SEPARATION WITH VOLTAMMETRIC DETECTION†

ROBERT SAMUELSSON‡ and JANET OSTERYOUNG*

Department of Chemistry, State University of New York at Buffalo, Buffalo, New York 14214 (U.S.A.)

(Received 23rd June 1980)

SUMMARY

The highly polar, nonvolatile N-nitrosamines, N-nitrosoproline and N-nitrosodiethanolamine, are determined by high-performance liquid chromatographic separation with electrochemical detection using d.c. voltammetry, normal pulse voltammetry, and differential pulse voltammetry. The influence of flow rate and pulse time are determined, nd detection limits on the order of 10^{-7} M are obtained.

The formation and occurrence of carcinogenic N-nitroso compounds in various environmental systems has been viewed increasingly as a problem during the last ten years. Several investigations of these problems have been reported including the studies of Sen et al. [1], Fazio et al. [2], and Fan et al. [3], but only a few of these are studies on nonvolatile N-nitroso compounds. The reason for that is not that nonvolatile N-nitrosamines are of no interest as hazardous compounds, but rather that suitable analytical methods for these compounds are lacking.

The analytical methods for volatile N-nitrosamines are well developed. Most common are gas chromatographic separation (g.c.) combined with either thermal energy analyzer (t.e.a.) or mass spectrometric (m.s.) detection [4, 5]. These techniques exhibit excellent selectivity which allows applications to very complex samples and have the sensitivity required for determinations at the ppb level.

For nonvolatile N-nitroso compounds, however, no analytical method with sufficient selectivity and sensitivity is now available. High-performance liquid chromatography (h.p.l.c.) has been used successfully for separations of N-nitrosamines [6, 7], but the lack of sensitive detectors has limited the usefulness of this approach. Thermal energy detection has been used with h.p.l.c., but conflicting results on both behavior and sensitivity have been

†This paper was presented at the 10th Northeast Regional ACS Meeting, Potsdam, New York, July, 1980.

‡Present address: Department of Analytical Chemistry, University of Umeå, S-901 87, Umeå, Sweden.

reported [8, 9]. Pulse polarography has been found to be a very sensitive technique for determination of N-nitrosamines [10, 11], but the rather poor selectivity makes determinations in complicated systems impossible without a prior separation step.

Here it is shown that by combining h.p.l.c. with voltammetric detection, a suitable method for determination of non-volatile N-nitroso compounds is obtained. The highly polar N-nitrosodiethanolamine (NDELA) and N-nitrosoproline (NPRO) are chosen as model substances. Behavior of different voltammetric wave-forms will be compared and the optimization of experimental parameters is discussed.

EXPERIMENTAL

Materials

All chemicals used were of analytical grade, except potassium dihydrogenphosphate and acetonitrile, which were of h.p.l.c. grade.

Stock solutions of NDELA and NPRO were prepared from diethanolamine (Eastman Kodak; m.p. 26—28°C), L-(-)-proline (Eastman Kodak; m.p. 200—222°C) and sodium nitrite (Baker Analyzed Reagent) as described earlier [10, 12]. The exact concentration of each of these solutions was measured by determining the amount of unreacted secondary amine with the spectrophotometric method reported by Umbreit [13]. Owing to the high polarity of these secondary amines, the absorbance was measured in the aqueous phase instead of the organic phase.

Presaturated argon gas was used to purge oxygen from the mobile phase and sample solution.

Instrumentation

The instruments used for the voltammetric measurements were a Model 174 Polarographic Analyzer (PARC, Princeton, NJ), an Omnigraph Model 2000 X-Y recorder (Houston Instrument Co., Austin, Texas) and a RAOCHYL 100 PAR conversion module [14]. The working electrode was a Model 303 static mercury drop electrode (s.m.d.e.; PARC, Princeton, NJ). The geometrical drop areas for the s.m.d.e. were: small = 1.1×10^{-2} cm^2; medium = 1.72×10^{-2} cm^2; large = 2.61×10^{-2} cm^2. An Ag/AgCl wire and a platinum wire were used as reference and counter electrodes, respectively. The following instrumental parameters were used, unless otherwise noted: electrode mode = DME; medium drop size; drop time, 1 s; t_{pulse} = 56.7 ms.

The chromatographic system consisted of a pump (Altex model 110A), a homemade pulse dampener, and a sample injector (Rheodyne). A 100-μl sample loop was used unless otherwise noted. The column was a 30.0 cm $\times$ 4.1 mm i.d. Bondapak Phenyl, 10 μm (Alltech Associates), and the detector was a model 310 polarographic detector (PARC, Princeton, NJ). A glass electrode (Orion combination pH 91-05) and an Orion model 601 A/digital ionalyzer were used to measure pH. The temperature during the experiments was 23 $\pm$ 1°C unless otherwise stated.

RESULTS AND DISCUSSION

Voltammetric behavior of NDELA and NPRO

The voltammetric behavior of N-nitrosamines has been studied extensively [12, 15, 16]. The reduction has been shown to be irreversible with pH-dependence and four electrons involved in acidic media. In basic media the reduction is pH-independent and only two electrons participate.

In order to establish the voltammetric behavior of NDELA and NPRO in the electrolytes used in the following chromatographic experiments, normal pulse voltammograms for the nitrosamines were recorded in phosphate buffers of pH 2.5—3.5. Wave analysis of the voltammograms was carried out and diffusion coefficients were calculated from the Cottrell equation for spherical diffusion. The diffusion coefficients were also determined from chronoamperometric experiments. To check the validity of these results, voltammetric data for Cd^{2+} in 0.1 M KCl (pH 2.5) were obtained under the same conditions.

The voltammetric data in the electrolyte most frequently used are summarized in Table 1. The results for both Cd^{2+} and the N-nitrosamines are in good agreement with those of earlier studies [10, 12, 17].

Chromatographic behavior of NDELA and NPRO

Since voltammetric detection requires a highly conductive mobile phase, the chromatographic technique of choice is that involving a mobile aqueous phase. Several reports concerning separation of N-nitrosamines with stationary non-polar phase (so-called reversed phase) chromatography may be found in the literature [6, 7]. The chromatographic parameters for the separation of NDELA and NPRO on a Bondapak Phenyl column were determined with 1% phosphate buffer as mobile phase. The results are shown in Fig. 1 and Table 2.

When phosphate buffer (pH 3.5) is used as a mobile phase, two well separated peaks are observed with k' values of 0.59 and 0.89. These peaks correspond to NDELA and NPRO, respectively. If the pH of the mobile phase is changed to 2.5, a remarkable change in behavior is noticed. A small increase in retention time is observed for NDELA, but the NPRO peak is split into two partly resolved peaks (R_s = 0.8) with k' values of 2.04 and

TABLE 1

Voltammetric characteristics of NDELA and NPRO in 1% (w/v) phosphate buffer (Conditions: [NDELA] = 1.19×10^{-5} M; [NPRO] = 1.31×10^{-5} M; [Cd^{2+}] = 2.76×10^{-3} M; drop size, large; T = 25 ± 0.1°C)

Compound	pH	$E_{1/2}$(n.p.) (V)	Slope E vs. $\log(i_d - i)/i$ (V)	Diff. coeff. ($\times 10^{-5}$ cm^2 s^{-1})
NDELA	3.41	−1.03	−0.065	0.68 ± 0.01
NPRO	3.21	−0.94	−0.059	0.85 ± 0.02
Cd^{2+} in 0.1 M KCl	2.5	−0.59	−0.032	0.780 ± 0.005

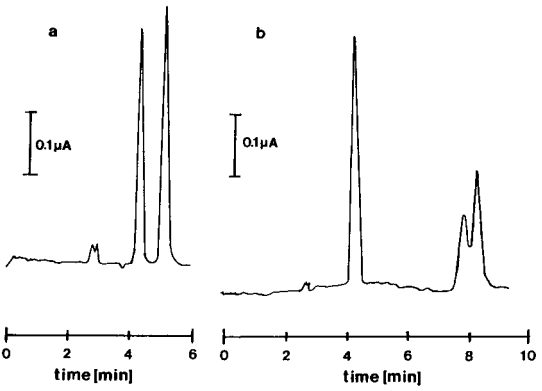

Fig. 1. Chromato-voltammograms of NDELA and NPRO in 1% (w/v) phosphate buffer: (a) pH 3.5; (b) pH 2.5. The baseline current is ca. 0.3 μA in each case. Conditions: see Table 2.

2.19. These latter peaks correspond to the syn- and anti-conformers of NPRO. On addition of 5% acetonitrile to the mobile phase, a decrease in retention time for NDELA and NPRO is observed at both pH values, and the conformers are no longer partially resolved. In addition, 2- and 3-fold increases in column efficiency for NDELA are noticed at pH 3.5 and pH 2.5, respectively.

The large pH dependence of k' for NPRO can be explained by the pK_a value for the amino acid (pK_a = 3.0) as reported by Iwaoka and Tannenbaum [6]. At pH values below pK_a, the dissociation of the carboxylic acid is suppressed, which makes the nitrosamine more retained by the stationary phase, while at higher pH the ionized nitrosamine remains most of the time in the polar mobile phase. However, our results on the separation of the syn- and anti-conformers of NPRO disagree in part with the results of these authors.

To reduce the time of experiments and to obtain chromatograms which were simple and easily evaluated, 1% (w/v) phosphate buffer of pH = 3.5 was used as mobile phase in the following experiments.

TABLE 2

Chromatographic characteristics of NDELA and NPRO in 1% (w/v) phosphate buffer (Conditions: flow rate 1.0 ml min^{-1}; sampled d.c. mode; small drop size; potential −1.1 V (pH 2.5) or −1.2 V (pH 3.5))

pH	NDELA		NPRO	
	k'	N	k'	N
3.5	0.59	3800	0.89	4100
2.5	0.65	3300	2.04, 2.19	~3800

Optimization of parameters for the h.p.l.c. detector

Since 1952, when Kemula introduced polarographic detection in a liquid chromatographic system [18], the combination has been used for the determination of a great number of both inorganic and organic compounds [19, 20] and there have been marked improvements in both the sensitivity and the selectivity of such systems.

The detector used in this paper is based on the design principle of the wall jet and was obtained commercially from PARC; a schematic diagram of the flow cell is shown in Fig. 2. The flow cell is mounted directly on the capillary and is immersed together with reference and counter electrode in a 50 ml vessel which contains supporting electrolyte. The distance between the flow delivery tip and the capillary tip is easily adjustable.

Because the detector is sensitive to oxygen, both the mobile phase and the sample solution have to be deoxygenated carefully before use. It is also necessary to keep an oxygen-free atmosphere over both solutions during the experiments. Stainless steel tubing is preferred for both the inlet and the outlet of the pump to prevent oxygen from diffusing into the mobile phase.

The detector was found to be sensitive to flow pulsations, especially at high flow rates. This means that a good solvent delivery system is needed to minimize the noise level.

In order to examine the dependence and reproducibility of the flow cell installation on detector response, chromato-voltammograms were recorded using different distances between the delivery tip and capillary tip. The installations were repeated several times and it was found that the optimum distance was 1.0 mm. Using this distance, all three drop sizes could be used with high sensitivity and low noise level. Measurements within one installation were repeatable within 2—3%, while the deviation in detector response between different installations was less than 10%.

Because the mass transport to the electrode is controlled by both diffusion and convection, the dependence of detector response on flow rate was studied by pumping a Cd^{2+} solution in 0.1 M KCl (pH 2.5) directly into the flow cell without using the column. Normal pulse voltammograms with different pulse times were recorded for flow rates of 0.1—3.0 ml min^{-1} using the RAOCHYL conversion module. The results shown in Fig. 3 indicate that for low flow rates the limiting current is controlled almost solely by diffusion. At higher flow rates, however, the influence from convection increases, and at flow rates higher than 2.5 ml min^{-1} the response becomes time-independent for pulse times longer than 50 ms. The relationship between current and flow rate for the 100 ms pulse is close to linear in the region 1.0—3.0 ml min^{-1}. Qualitatively, the results are similar to those for pulse voltammetry at a rotating electrode [21]. Further studies are required to describe, even semi-empirically, the time-dependent currents for this very complex convective diffusion case (see Fig. 2).

To find the optimum parameters for the determination of N-nitrosamines, 100-μl samples of nitrosamines were injected at different flow rates. The

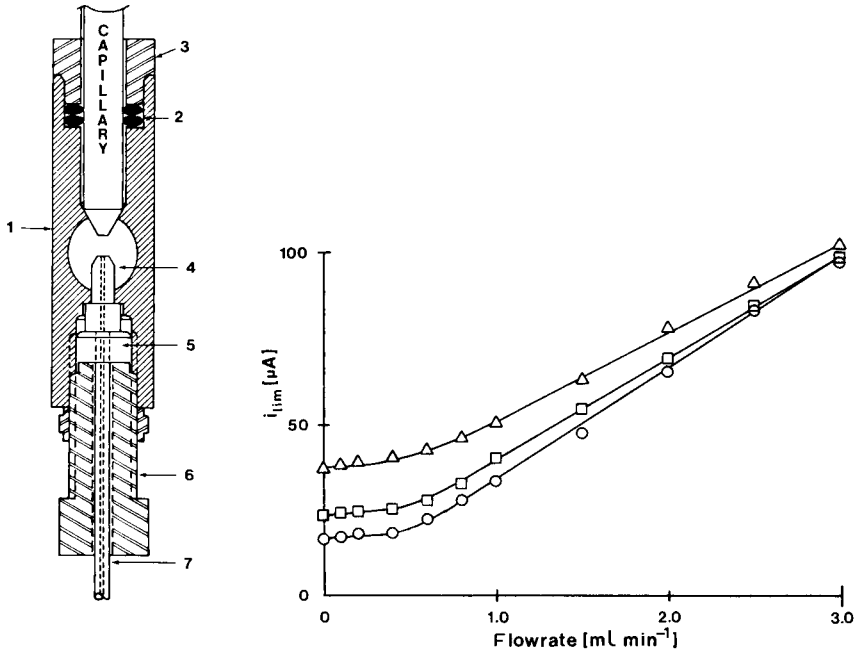

Fig. 2. Schematic diagram of the flow cell. (1) Body; (2) O-ring, viton 8007; (3) plug; (4) flow adapter; (5) grip fitting, 416 HPG; (6) tube-end fitting, 100 HPA; (7) tube, 1/16 in. o.d., 0.012 in. i.d.

Fig. 3. Dependence of limiting current on flow rate for 1.05×10^{-3} M Cd^{2+} in 0.1 M KCl (pH 2.5): (○) t_{pulse} = 100 ms; (□) t_{pulse} = 50 ms; (△) t_{pulse} = 20 ms.

results for NDELA are shown in Fig. 4. The optimum flow rate was found to be 1.5 ml min^{-1}, for which the sensitivity is high and a peak width required for a proper measurement accuracy (as described in the operating manual for the detector) was obtained. The difference between the behavior displayed in Fig. 3 and that in Fig. 4 is due to the difference in dispersion of the sample in the column with different residence times for various flow rates.

Figure 5 shows the detector response for NDELA when different pulse times are applied in the normal pulse mode. As can be seen, at high flow rates, the peak height is almost constant for pulse times longer than 50 ms, while at low flow rates the variation is much greater.

The dependence of peak height on potential in the normal pulse mode is shown for NDELA in Fig. 6. Plots of peak height vs. potential have the shapes of normal pulse voltammograms, and wave analysis gives straight lines for E vs. log $(i_d - i)/i$ with slopes of −0.068 V and −0.078 V for 0.5 ml min^{-1} and 1.5 ml min^{-1}, respectively. The half-wave potential is shifted toward more negative values with increasing flow rate. Thus the electrode reaction appears to be more irreversible with increasing flow rate, as would be expected.

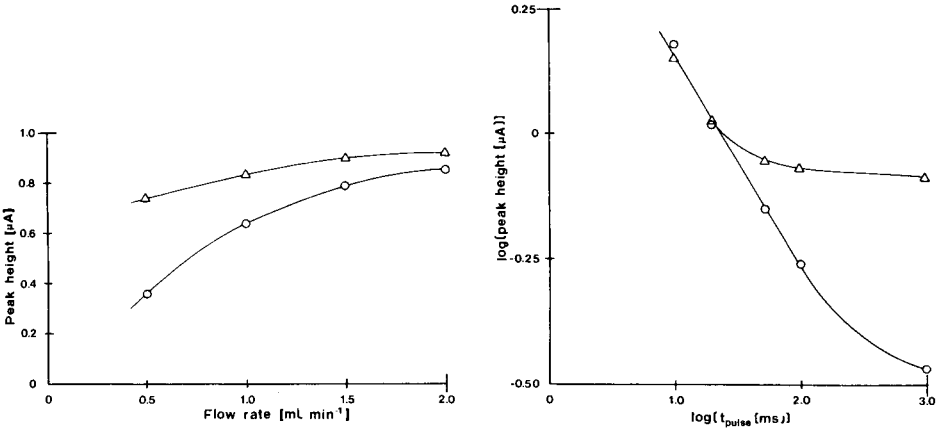

Fig. 4. Dependence of peak height on flow rate for NDELA: (○) sampled d.c.; (△) normal pulse. Conditions: [NDELA] = 2.4×10^{-5} M; mobile phase = 1% (w/v) phosphate buffer, pH 3.5; Potential −1.2 V.

Fig. 5. Dependence of peak height on t_{pulse} for NDELA at different flow rates: (○) 0.5 ml min^{-1}; (△) 1.5 ml min^{-1}. Conditions: see Fig. 4.

Variation of initial potential between −0.3 and −0.8 V for the normal pulse mode did not affect the detector response to any degree.

When the differential pulse (d.p.) mode is applied to the detector, a much greater peak width is required to obtain a proper result. This is due to the rather long measuring time constant (83.3 ms) for the d.p. mode in the unmodified PARC 174. As a result, in the case of the separation of NDELA and NPRO at pH 3.5, broad, tailing, and only partially resolved peaks were observed. However, when the measuring time constant was decreased to 50 ms by using the RAOCHYL conversion module, symmetrical, well-separated peaks were obtained, along with a 30% increase in sensitivity.

The plot of peak height vs. potential for NDELA and NPRO using the d.p. mode is shown in Fig. 7. The shapes of the curves were similar to differential pulse polarograms, with a difference in peak potential between NDELA and NPRO of 50 mV. When the pulse height is changed from −50 mV to −100 mV, a shift in peak potential of 25 mV in the positive direction is observed. This is in agreement with the relationship $E_p = E_{1/2} - \Delta E/2$ expected for d.p. The peak widths of the voltammograms are about 40–60 mV larger than those which would be obtained by direct d.p. This is qualitatively in accord with the increase in irreversibility caused by the high rate of mass transport.

It was found that variation in sample volume between 20 and 100 μl does not affect the peak height, as long as the total amount of nitrosamine is kept constant. This indicates that the maximum sample volume that can be used is determined by the capacity of the column.

Calibration plots were recorded and detection limits were calculated from the standard deviations and the slopes of these plots for sampled d.c., n.p.,

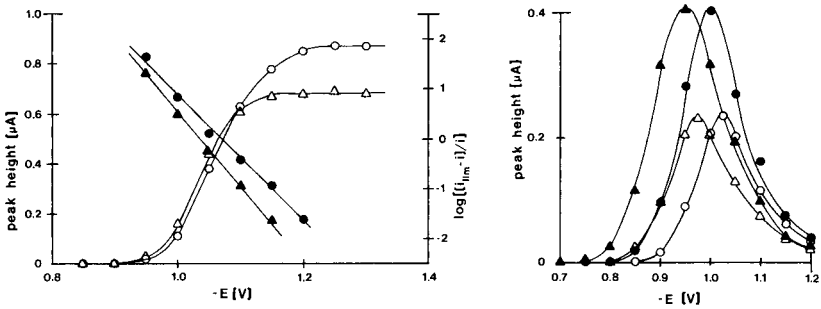

Fig. 6. Plot of peak height vs. potential (open symbols) and log $((i_{lim} - i)/i)$ vs. potential (filled symbols) for NDELA with n.p. mode at different flow rates: (△) 0.5 ml min^{-1}; (○) 1.5 ml min^{-1}. Conditions: see Fig. 4.

Fig. 7. Plot of peak height vs. potential with d.p. mode: (○) NDELA; (△) NPRO. Conditions: modulation amplitude, −50 mV (open symbols) or −100 mV (filled symbols); measuring time constant 50 ms; flow rate 1.5 ml min^{-1}; otherwise see Fig. 4.

and d.p. modes. Both compounds (NDELA and NPRO) were determined simultaneously in the d.p. mode by choosing a potential between the peak potentials for the two nitrosamines that gave approximately an equal peak height. The calibration plots gave straight lines for both nitrosamines; the results for NDELA are summarized in Table 3. Similar results were obtained for NPRO. Detection limits are close to those obtained by polarographic techniques [10—12] without a separation step. Linearity of calibration curves extended beyond an upper concentration limit of 5×10^{-5} M for both NDELA and NPRO. A rather high noise level was observed at high sensitivities, mostly because of pulsations in flow which could not be eliminated completely. However by using a better pump system and by increasing the sample volume, it should be possible to reach a detection limit of the order of 1 ppb.

TABLE 3

Comparison of sensitivities and detection limits of NDELA for different voltammetric modes
(Conditions: mobile phase 1% phosphate buffer (pH 3.5); flow rate 1.5 ml min^{-1}; large drop size; potential (n.p., sampled d.c.) −1.2 V; potential (d.p.) −0.97 V; modulation amplitude (d.p.) −100 mV; measuring time constant (d.p.) 50 ms)

Mode	Slope (nA µM^{-1})	Intercept (nA)	Standard error (nA)	Detection limit[b] (µM)
Sampled d.c.	42 ± 3	−4.4 ± 0.3	2.6	0.18
Normal pulse	50 ± 2	−4.0 ± 0.2	1.9	0.11
Differential pulse[a]	22.9 ± 0.5	0.20 ± 0.04	0.46	0.059

[a]Currents are true d.p. currents, i.e. the PARC 174 currents divided by 10.
[b]Detection limit = ts/m where t is the Student t statistic at 95% confidence, s is the pooled standard deviation of the calibration curve, and m is the slope of the calibration curve.

This work was supported in part by the National Science Foundation under Grant No. CHE-7917543. One of us (RS) wishes to thank the Swedish Work Environment Fund for financial support.

REFERENCES

1 N. P. Sen, B. Donaldson, J. R. Jyengar and T. Panalaks, Nature, 241 (1973) 473.
2 T. Fazio, J. N. Damico, J. W. Howard, R. H. White and J. O. Watts, J. Agric. Food Chem., 19 (1971) 250.
3 T. Y. Fan, J. Morrison, D. P. Rounbehler, R. Ross and D. H. Fine, Science, 196 (1977) 70.
4 D. H. Fine and D. P. Rounbehler, J. Chromatogr., 109 (1975) 271.
5 T. A. Gough, K. S. Webb, M. A. Pringuer and B. J. Wood, J. Agric. Food Chem., 25 (1977) 663.
6 W. Iwaoka and S. R. Tannenbaum, J. Chromatogr., 124 (1976) 105.
7 K. Heyns and H. Röper, J. Chromatogr., 93 (1974) 429.
8 D. H. Fine, D. P. Rounbehler, A. Silvergleid and R. Ross, in B. J. Tinbergen and B. Krol (Eds.), Proceedings of the Second International Symposium of Nitrite in Meat Products, Zeist, The Netherlands, 1977, p. 191.
9 J. K. Baker and Cheng-Yu Ma, in E. A. Walker, M. Categnaro, L. Griciute and R. E. Lyle (Eds.), Environmental Aspects of N-Nitroso Compounds, IARC Scientific Publication No. 19, Lyon, 1978, p. 19.
10 R. Samuelsson, Anal. Chim. Acta, 102 (1978) 133.
11 R. Samuelsson, Anal. Chim. Acta, 108 (1979) 213.
12 K. Hasebe and J. Osteryoung, Anal. Chem., 47 (1975) 2412.
13 G. R. Umbreit, Anal. Chem., 33 (1961) 1572.
14 L. L. Jackson, Ch. Yarnitzky, R. A. Osteryoung and J. Osteryoung, J. Chem. Biomed. Environ. Instrum., 10 (1980) 175.
15 H. Lund, Acta Chem. Scand., 11 (1957) 990.
16 F. Pulidori, G. Borghesani, C. Bighi and R. Pedriali, J. Electroanal. Chem., 27 (1970) 385.
17 M. von Stackelberg, M. Pilgram and W. Toome, Z. Elektrochem., 57 (1953) 342.
18 W. Kemula, Rocz. Chem., 26 (1952) 281.
19 S. Tustanowski, J. Chromatogr., 31 (1967) 266.
20 W. Kemula and D. Sybilska, Nature, 105 (1960) 237.
21 D. J. Myers, R. A. Osteryoung and J. Osteryoung, Anal. Chem., 46 (1974) 2089.

Analytica Chimica Acta, 123 (1981) 107—114

CHARACTERISTICS OF AN AMPEROMETRIC FLOW-THROUGH DETECTOR WITH A RENEWABLE STATIONARY MERCURY ELECTRODE

U. BALTENSPERGER

Institute of Inorganic Chemistry, University of Zürich, CH-8057 Zürich (Switzerland)

R. EGGLI*

Department of Health of the City of Zürich, CH-8035 Zürich (Switzerland)

(Received 8th July 1980)

SUMMARY

The construction of the detector is described and its performance is assessed for 1,4-benzoquinone by flow-injection analysis. The detection limit is 0.5 ng and the relative standard deviation of the peak current is 0.4% for a 102-ng sample. The peak current is highly sensitive to temperature changes of the mercury electrode system. The relative temperature coefficient is 15% K^{-1}, whereas the corresponding value with respect to the mobile phase is 0.6% K^{-1}. The dependence of the peak current on the volume flow rate is described and explained by appropriate models.

Recently, an amperometric flow-through cell with a mercury microelectrode has been used as a detector in an electrochemical double cell arrangement designed for the determination of disulfides and related compounds [1], and has been applied in clinical analysis [2]. Prolonged experience with this device has shown that it is not sufficiently reliable for continuous routine use and that its performance is limited by that of the amperometric detector.

In view of the wide field of applications of a mercury-based electrochemical detector, the main factors affecting the performance of this type of cell, based on a design of Rabenstein and Saetre [3], were evaluated and an improved cell was built. In this paper the construction of this cell and its main operating characteristics, the dependence of the signal on temperature, area of the mercury electrode and flow rate, are described. The results are compared with the appropriate theoretical models.

In these investigations, 1,4-benzoquinine was used as the electroactive species with an aqueous phosphate buffer of pH 6.9 as the mobile phase. In this medium, the reduction of quinone proceeds reversibly with a half-wave potential of +10 mV vs. SCE and no effects due to strong adsorption are known [4]. Thus it was possible to drive the cell under conditions of low background current and to investigate those factors which are related to the construction of the cell, without complications from electrochemical effects.

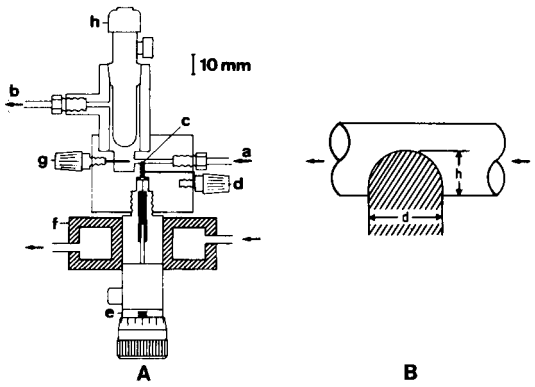

Fig. 1. Amperometric flow-through cell with mercury electrode. (A) Complete cell: (a) inlet and (b) outlet of mobile phase; (c) working electrode with platinum wire electrical contact (d) and feeding system (e), fitted with thermostat mantle (f); (g) counter electrode; (h) reference electrode. (B) Enlarged section of working electrode: h = height, d = diameter of the mercury column.

EXPERIMENTAL

Flow-through cell

Design. The detector cell is shown in Fig. 1. Contained in a rectangular block of plexiglas are the T-shaped working electrode arrangement (vertical bore of smooth inner surface containing the mercury, which protrudes vertically into the horizontal flow path of 0.8 mm diameter) and, 4 mm downstream from the mercury pool, an area of relatively large volume containing the counter electrode (platinum wire, 0.8 mm diameter) and the saturated calomel reference electrode (Philips R-11-NS). Connections for inlet and outlet were made with teflon tubing (0.8 mm inner diameter) using standard Chromatronix fittings. In contrast to earlier designs [1], a thermostatted high-precision system is used to feed the mercury electrode. This system consists of a Kemula-type mercury delivery system (Metrohm E623) which is screwed upside down into the plexiglas block. A tight fit is obtained by an O-Ring (Viton, 3 mm inner diameter), placed between the end of the glass capillary of the Kemula electrode and the entrance to the vertical bore of the plexiglas body. To keep the mercury at constant temperature, a hollow aluminium block, flooded with water from a thermostat, is fitted tightly to the cylindrical body of the Kemula electrode.

Measurement of electrode dimensions. The electroactive part of the mercury electrode is a column with an approximately hemispherical top. A cathetometer (Spindler—Hoyer) was used to determine its overall height h (i.e., the distance between the bottom line of the horizontal flow path and the highest point of the mercury surface) and its diameter d (Fig. 1). From these data, the geometrical area A of the electrode was calculated from $A = \pi dh$ ($h \geqslant d/2$).

Uncompensated resistance. The resistance between the working electrode and the counter electrode, measured with an a.c.-bridge (AMEL 123) at 50 Hz in 0.05 M NaH_2PO_4–0.05 M Na_2HPO_4 was 20 kΩ. When contact to the working electrode was made through the lead of the micrometer feeding system and not with the platinum wire placed directly into the mercury column just below the electroactive surface (d, Fig. 1), considerably larger values were obtained for the uncompensated resistance.

Electronics. The cell was driven by a potentiostat (AMEL 551). An ammeter (AMEL 668/RM), coupled to an XY recorder (Houston 2000), was used to measure the cell currents.

Flow system

The mobile phase was stored in a 1-l glass vessel, deaerated with purified nitrogen and heated to 40 ± 0.1°C to keep the concentration of dissolved gas sufficiently low [5]. A stainless steel capillary (0.8 mm inner diameter), fitted with a filter (Alltech, pore size 2 μm) was used to feed the liquid phase to the pump (Altex 110A). Downstream of the pump, the following components were lined up in series: a stainless steel pulse dampener, a coil of stainless steel tubing (length 1 m, inner diameter 0.5 mm) immersed in a thermostatted water bath (20.0 ± 0.05°C), a stainless steel injection valve (Rheodyne 70-10) and the cell. The pulse dampener was made as described by Ventura and Nikelly [6]: a flexible hose (Swagelok SS-4HO-6-S4) terminating at a pressure gauge (WIKA 232.100) was fitted to a Swagelok T-piece placed between the pump and the thermostatting coil, and a short part of the latter was rolled flat so that, at a flow rate of 0.3 ml min^{-1}, a pressure of about 15 bar was indicated by the gauge. A short piece of teflon tubing (length 5 cm, inner diameter 0.8 mm) was used to connect the cell to the injection valve and the same type of tubing was used to transfer the sample to the injection valve. A stainless steel sample loop of 20 μl was used throughout.

Chemicals

The mobile phase (0.05 M NaH_2PO_4–0.05 M Na_2HPO_4) was prepared from analytical-grade reagents (Merck) and deionized, filtered water (Millipore, Milli-Q). Sample solutions were prepared daily by dissolving the appropriate amount of pure 1,4-benzoquinone (Fluka) in a given volume of mobile phase at ambient temperature. The solutions were then deaerated and stored in darkness. Solutions with concentrations down to 10^{-7} M showed no signs of decomposition after a storage period of 24 h.

Measurement procedure

The flow of the mobile phase was shut off when not required, but the cell potential was kept constant at −300 mV vs. SCE. After activation of the liquid flow, and, if necessary, readjustment of the potential, a new mercury drop was extruded and adjusted to the desired height. Measurements were

then started after a 20-min period required for deaeration and thermostatting of the mobile phase. The mercury electrode was renewed daily or after four hours of continuous measurement.

RESULTS AND DISCUSSION

Mechanical properties of the mercury electrode

Since the electroactive part of the mercury column protrudes vertically into the horizontally flowing stream of the mobile phase, it is subjected to lateral forces which tend to displace it in the flow direction. Thus, for a given height, the mercury column becomes unstable and the whole electroactive column is pushed off when the flow rate exceeds a critical value. With a height of 0.53 mm, which proved to be most suitable for routine measurements, the critical flow rate was 9.9 ml min^{-1}. Up to this rate, no signs of instability were observed as long as the flow rate remained constant. However, the mercury drop was washed away by the pressure jump induced by activation of the injection valve at flow rates above 3.5 ml min^{-1}.

By means of the mercury feeding system and the cathetometer, it was possible to adjust the height of the mercury column with an accuracy of ±0.02 mm. When the height was adjusted without optical control, by advancing the micrometer drive of the Kemula electrode by a given number of turns after the previous mercury drop had been pushed off, the relative precision was about 10%.

Background current

The dependence of the baseline current on the working potential is shown in Fig. 2. With only minor deviations, the resulting curve is similar to that obtained by Rabenstein and Saetre [3] for a similar mobile phase. Small background currents, as shown in Fig. 2, were obtained only when the vertical bore containing the mercury had a smooth surface. With a rough

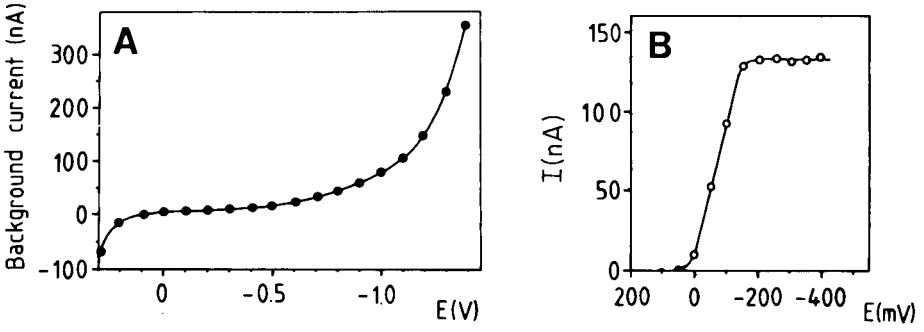

Fig. 2. (A) Background currents (•) and (B) peak currents (○) as a function of working electrode potential. Height of mercury column, 0.53 mm; mobile phase, 0.05 M NaH_2PO_4–0.05 M Na_2HPO_4 pH 6.9 at a flow rate of 0.3 ml min^{-1}; peak currents obtained by injections of 20 μl of 4×10^{-5} M 1,4-benzoquinone.

surface, obtained by drilling too quickly, a thick layer of mobile phase was established between the mercury and the wall of the bore, resulting in cathodic background currents of up to 200 nA at a potential of −300 mV.

Under steady-state conditions at a potential of −300 mV, there was no significant dependence of the background current on the flow rate between 1.0 and 9.9 ml min^{-1}. However, instabilities in the flow rate had a marked influence on the baseline noise: when the outflow of the detector cell was allowed to drop freely, sharp current spikes up to 0.5 nA were observed with the same frequency as the drops. When dropping was prevented by dipping the outflow tube into a pool of liquid, the baseline current had a standard deviation of about 8 pA (determined from 20 current values in the 30-s time interval corresponding to a peak base width; flow rate 0.3 ml min^{-1}; pool height 0.53 mm; potential −300 mV). The average drift was 100 nA h^{-1} under these conditions. After renewal of the electrode, steady-state conditions were usually re-established within 2—3 min. This period was considerably longer after readjustment of the electrode potential.

Analytical performance

A typical peak current—potential curve obtained with 1,4-benzoquinone is shown in Fig. 2 and the analytical results are summarized in Table 1. The calibration curves were completely free of memory effects, i.e., a given signal did not depend on the concentration of the previously injected sample. The practical detection limit of about 0.5 ng was established by the large blank signal, which was caused by dissolved oxygen introduced by diffusion through the short part of teflon tubing used to transfer the sample to the injection valve. By injecting carefully deaerated supporting electrolyte, blank currents of up to 1 nA were obtained, which increased with increasing length of the teflon tubing. Similar effects have been observed, but not explained [7]. According to the standard deviation of the baseline current, the current detection limit is 24 pA corresponding to a theoretical detection

TABLE 1

Characteristics of the mercury drop flow-through cell, determined by injections of 1,4-benzoquinone
(Signals are peak currents from 20-μl injections; mercury electrode at a potential of −300 mV vs. SCE with a height of 0.53 mm and a calculated area of 1.32 mm^2 at a temperature of 20.0 ± 0.05°C; 0.05 M NaH_2PO_4—0.05 M Na_2HPO_4 mobile phase at pH 6.9 and at 20.0 ± 0.1°C; flow rate 0.6 ml min^{-1})

Sensitivity	2.7 nA ng^{-1}
Limit of detection	0.5 ng
Upper limit of linear range	> 260 ng
Linear correlation coefficient	0.999
Relative standard deviation of a single signal (102 ng of 1,4-benzoquinone, 10 measurements)	0.4%
Coulometric yield	⩽1%

limit of 9 pg for quinone [8]. Thus, by optimization of the inlet system with respect to oxygen exclusion, extremely low detection limits should be obtained. For a given concentration, a slight decrease of peak current with time was observed, amounting to about 5% after 4 h. Renewal of the electrode at regular intervals, with appropriate recalibrations, is therefore necessary.

Dependence of the peak current on electrode area

At a constant potential of −300 mV, using a flow rate of 0.1 ml min^{-1} and injections of 20 μl of 5×10^{-5} M quinone, the dependence of the peak current I_p on the height h of the mercury pool was measured. With heights varying between 0.21 and 0.53 mm, corresponding to calculated areas of 0.64 and 1.32 mm^2, respectively, the experimental function $I_p(A)$ was a straight line passing through the origin with a slope of 85 nA mm^{-2}.

Temperature coefficient

The detector signal is very sensitive to variations in temperature. This is due mainly to changes in the volume of the mercury in the feeding system with changing temperature, and, to a minor extent, to the temperature dependence of the mobile phase (Fig. 3). As the volume of mercury stored in the reservoir of the feeding system usually exceeds that of the electroactive part by about two orders of magnitude, even small temperature changes of the mercury reservoir cause considerable variations of the electroactive area of the mercury. Assuming that expansion of the stored mercury of volume V_0 produces a cylindrical electroactive volume element, the relative temperature coefficient of the peak current I_p at a given temperature T is given by

$$(1/I_p)dI_p/dT = (4\alpha/\pi d^2 h)V_0 \quad (h \geqslant d/2) \tag{1}$$

where h and d are the height and the diameter of the mercury pool, respectively, and α denotes the volume expansion coefficient of mercury. This is an approximation to the upper limit of the temperature coefficient, as any change in volume of the cell body has been neglected.

Experimentally (Fig. 3), a linear dependence of the peak current was found between 17 and 21°C, with a relative temperature coefficient of 15% K^{-1}. Using the experimental data of Fig. 3 (V_0 = 330 μl, h = 0.53 mm at 20.5°C, d = 0.8 mm) and a value of 0.000181 K^{-1} for α [9], a temperature coefficient of 22% K^{-1} was calculated from eqn. (1), which is in rough agreement with the experimental value. Thus, from the experimental results, a peak current reproducibility of better than 1% requires that the temperature fluctuations in the mercury reservoir are less than 0.1°C. For practical applications, the amount of mercury in the reservoir should be kept at a maximum of about 100 μl, which is enough to feed the cell for weeks of operation.

At constant temperature of the mercury feeding system, the temperature coefficient caused by temperature variation of the mobile phase was found to be 0.6% K^{-1}.

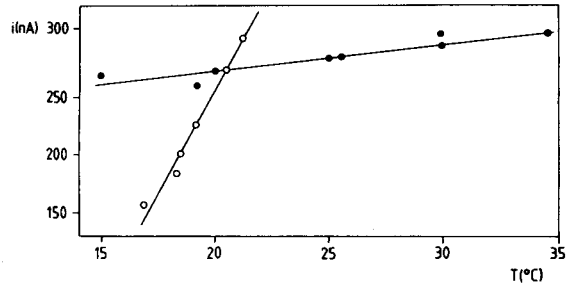

Fig. 3. Dependence of the peak current on the temperature of the mercury reservoir (○) and of the mobile phase (●). Injections of 20 μl of 8×10^{-5} M quinone; detector potential −300 mV vs. SCE; other conditions as noted in Fig. 2.

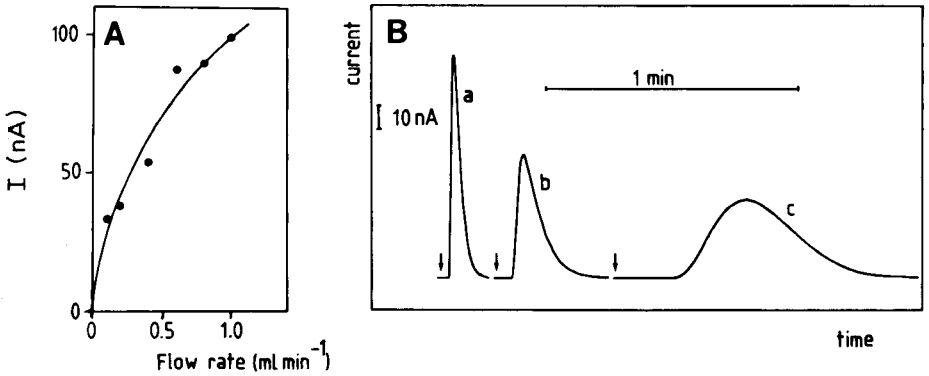

Fig. 4. (A) Dependence of peak current on flow rate. (B) Shapes of current peaks at flow rates of 1.0 (a), 0.4 (b), and 0.1 (c), ml min^{-1}. Injection points are marked by arrows. Injections of 20 μl of 1.6×10^{-5} M quinone; detector potential −300 mV vs. SCE; other conditions as noted in Fig. 2.

Flow-rate dependence of the signal

The dependence of the signal on the volume flow rate F is shown in Fig. 4. From these data, it was found that the peak current was proportional to $F^{0.60}$. Theoretically, the decrease in the peak current with decreasing flow rate can be ascribed to the diminished rate of convective diffusion of the electroactive species to the electrode [10] and to the increased dispersion of the injected sample which results in a decrease of the bulk concentration at the point of detection [11]. The electrode discussed here can be compared roughly with a conical microelectrode. For the latter, the limiting current under steady-state conditions in a laminar flow is proportional to $F^{0.5}$ [12]. Thus, the experimental results indicate that the flow-rate dependence of the peak height is mainly governed by the corresponding variation of the rate of diffusion to the electrode and that the effect of dispersion has only a minor influence.

A more quantitative assessment can be given by application of the tanks-

in-series model, which has already been used to describe sample dispersion in flow systems [13, 14]. According to this model, a dimensionless signal E is given [15] by

$$E = (t/\tau)^{N-1} \cdot \exp[-t/\tau]/(N-1)! \quad (2)$$

where τ and N are system parameters dependent on flow rate and t is the time ($t = 0$ at the point of sample injection). Assuming that E is proportional to the detector current I, the parameters τ and N were determined from six experimental signals at flow rates between 0.1 and 1.0 ml min^{-1} (Fig. 4): τ was calculated from the slope $1/\tau$ of the linear function ln $I(t)$ from the tail of each peak and N was obtained from the maximum condition $t_p = \tau(N-1)$, where t_p is the time at peak maximum.

From the experimentally determined parameter N, the peak signal E_p was calculated from eqn. (2), via the equation for t_p, for each flow rate. The resulting relationship was $E_p \propto F^{0.11}$. Introducing the factor $F^{0.5}$ for the flow-rate dependence of the limiting current at a conical microelectrode, the peak current is thus expected to be proportional to $F^{0.61}$, which is in good accordance with the experimental result.

REFERENCES

1 R. Eggli and R. Asper, Anal. Chim. Acta, 101 (1978) 253.
2 R. Asper, R. Eggli and O. Schmucki, Fortschr. Urol. Nephrol., 11 (1979) 178.
3 D. L. Rabenstein and R. Saetre, Anal. Chem., 49 (1977) 1036.
4 I. M. Kolthoff and J. J. Lingane, Polarography, Interscience, New York, 1952, p. 261.
5 R. Keller, A. Oke, I. Mefford and R. N. Adams, Life Sci., 19 (1976) 995.
6 D. A. Ventura and J. G. Nikelly, Anal. Chem., 50 (1978) 1017.
7 W. Lund, M. Hannisdal and T. Greibrokk, J. Chromatogr., 173 (1979) 249.
8 H. Kaiser, Anal. Chem., 42/4 (1970) 26A.
9 R. C. Weast (Ed.), Handbook of Chemistry and Physics, 55th edn., CRC Press, Cleveland, Ohio, 1974—1975, p. F6.
10 V. G. Levich, Physicochemical Hydrodynamics, Prentice-Hall, Englewood Cliffs, NJ, 1962, p. 19.
11 G. Taylor, Proc. R. Soc. London, Ser. A, 219 (1953) 186.
12 R. N. Adams, Electrochemistry at Solid Electrodes, M. Dekker, New York, 1969, p. 77.
13 J. Růžička and E. H. Hansen, Anal. Chim. Acta, 99 (1978) 37.
14 J. M. Reijn, W. E. van der Linden and H. Poppe, Anal. Chim. Acta, 114 (1980) 105.
15 O. Levenspiel, Chemical Reaction Engineering, 2nd edn., J. Wiley, New York, 1972, p. 291.

Analytica Chimica Acta, 123 (1981) 115—123

FLOW INJECTION DETERMINATION OF ISOSORBIDE DINITRATE WITH POLAROGRAPHIC DETECTION

BJÖRN PERSSON* and LENA ROSÉN

Analytical Chemistry and Biochemistry, AB Hässle S-431 83 Mölndal (Sweden)

(Received 9th June 1980)

SUMMARY

Polarographic determination of isosorbide dinitrate (ISDN) was performed in a flow injection system assembled from commercially available units. The detector could be operated either as a dropping mercury electrode or as a hanging mercury drop electrode. In addition to the influence of injection volume, coil length and pumping rate on sensitivity and peak widths, peak heights also depended on the presence of surfactants in samples and carrier stream. When a pump of high quality was used, the system was equal to a normal polarograph with regard to quality of results and ease of operation. The working range was 0.05—1 mM ISDN and the limit of detection 0.01 mM. The maximum sampling frequency was about 100 samples per hour. No deaeration of samples and carrier stream was required, because the carrier stream contained sodium sulfite in a slightly alkaline medium.

When polarographic procedures do not include time-consuming pretreatment steps, the maximum sampling frequency is determined by the time required for sample exchange, deaeration and recording of the polarographic curve. Mechanization of these three steps considerably improves the sample throughput. Thus, semi-automated polarographic measurements have been performed in air-segmented continuous flow systems (see [1] and references therein). Special attention has been paid to cell design and sample deaeration [2, 3]. Polarographic detection has also been successfully applied in liquid chromatography [4, 5]. The mass transport to the electrode surface in a flow cell is a function of the flow velocity of the mobile phase. Therefore, the detector current will be extremely sensitive to flow variations. Pulsation is generally more troublesome in a gas-segmented liquid stream with its compressible gas bubbles than in an unsegmented carrier stream such as those used in flow injection methods [6] where the flow fluctuations can be minimized without affecting the washout time.

Polarography is very suitable for the determination of isosorbide dinitrate (ISDN) in pharmaceutical formulations [7]. The electrode processs involves 4 electrons per molecule for the reductive cleavage of the two nitrate ester bonds. The half-wave potential is located around —0.4 V vs. SCE and does not depend on pH. A continuous flow system for the assay of ISDN has been reported [8]. The present work describes the development of a flow injection

procedure for routine determinations of the same substance in connection with dissolution tests.

EXPERIMENTAL

Reagents

Standard solutions of ISDN in phosphate buffer pH 6.5 were prepared from a mixture of ISDN and lactose (25:75%, w/w). The specimens contained 0.05—0.7 mM ISDN and 1—5 mM lactose in either 0.1 M HCl or phosphate buffer pH 6.5. Different carrier streams were tried. All contained 0.025 M sodium tetraborate (pH 9.3) and 0.1 M sodium sulfite to which were added different amounts of lactose and polyoxyethylene lauryl ether, which is a nonionic surfactant with the commercial name Brij-35.

Apparatus

Polarographic measurements were made with a PAR 174 polarographic analyzer connected to a PAR 310 polarographic detector, which consisted of a 30-mm long adapter threaded onto the glass capillary of a PAR 303 static mercury drop electrode. The liquid stream was directed towards the mercury drop by the delivery tip of the adapter. The distance between the drop and the delivery tip was about 1 mm. The adapter together with the reference electrode and the counter electrode were placed in a glass cell which was filled with carrier stream to a level somewhat above the electrode tips. A drain for both mercury and mobile phase ensured that the level of the solution was constant during the work. The volume of the solution in the cell under the flow conditions was 50 ml. The reference electrode, to which all potentials are referred, was a silver/silver chloride electrode; its potential with respect to a saturated calomel electrode was −47 mV. All measurements were made at room temperature (22°C).

The following pumps were tested: Altex 100 (dual piston), LDC minipump (single piston), Sage 220 (syringe) and Gilson Minipuls 2 (peristaltic). Samples were injected by a Valco valve provided with a bypass between the inlet and outlet streams. The injection system was connected to the flow cell through 0.5 mm (i.d.) tubing. In the work with the piston pumps, a 20 m × 0.25 mm (i.d.) coiled steel capillary was placed between the pump and the injection valve. Pulses from the low-pressure pumps were damped by a 50 mm × 2 mm (i.d.) tube which was sealed at one end and linked through the other end to the main line with a T-connector.

RESULTS AND DISCUSSION

Removal of oxygen

Sulfite in a borate buffer effectively reduces dissolved oxygen [9], and so bubbling of the carrier stream with inert gas was unnecessary. This is illustrated by the small background current obtained with the piston pumps

(Table 1). The comparatively large baseline currents obtained with the other two pumps were probably caused by diffusion of air through the plastic walls of the pumping tube and transport tubes. The oxygen in the samples was also chemically reduced by the sulfite in the carrier stream. The concentration of oxygen was less than 1% of its original value when the sample plug reached the detector. Consequently, no deaeration of the specimens was considered necessary. The rate of oxygen reduction depended on the sample constituents; about 10% residual oxygen was detected in samples containing 10% (v/v) ethanol.

Performance of the polarographic detector

The flow cell was easily mounted and dismounted. Thus the same electrode assembly could be used for flow injection and for normal polarographic measurements as required. There was a maximum difference in current response of about 5% between measurements made with the same flow cell after successive mounting and dismounting. The reason for this was that it proved impossible to fix the adapter in exactly the same position on the capillary on each occasion. The drift of standard peak heights was normally 1% per hour or less during routine work with the dual-piston pump. The repeatability associated with the different pumps was good enough to make them all useful in polarographic flow systems (Table 1). As expected, the smallest standard deviation from the mean for the peak height of repeated injections was obtained with the dual-piston pump, and this pump was employed in further investigations.

Injection volume, coil length and flow rate

Peak height and peak width in flow systems depend on the dispersion of the sample plug during its passage from injector to detector. Some variables such as injection volume, coil length and flow rate which influence dispersion, were adjusted according to the specific requirements for the present system. The sampled-current mode selected for the present determination of ISDN required a peak width of at least ten drop times according to the

TABLE 1

Comparisons of pumps

Type of pump	Dual piston	Single piston	Syringe	Peristaltic
Repeatability[a] (%)	<1	1	2	2
Baseline current (μA)	0.2	0.2	1.8	1.8
Amplitude of baseline noise (μA)	0.002	0.01	0.02	0.02

[a]Relative standard deviation from the mean for the peak heights of 15 repeated injections of 0.7 mM isosorbide dinitrate.

manufacturer's recommendations; thus 10 s for the drop time of 1 s was used in this work. However, peaks should be as narrow as possible to improve the sample throughput of the system. The question of high sensitivity was not essential here because the samples contained relatively large concentrations of ISDN. A reasonable compromise between these requirements would be a peak about 10 s wide.

During the optimization studies, the detector was used as a hanging mercury drop electrode in the d.c. current mode (Fig. 1, curves a, b). When a stationary electrode is used, it is necessary to be aware of electrode ageing effects. Thus, peak height decreased with time for a carrier stream which did not contain any surface-active substances (Fig. 2). In the presence of surfactants, current response remained constant for at least 20 min during which a standard was injected 26 times.

The peak width was proportional to the injection volume in the range 40—200 μl (Fig. 3). Peak height and thus sensitivity increased with increasing injection volume, whereas they decreased with increasing coil length (Fig. 4). In accordance with a simplified theoretical treatment of dispersion phenomena [6], linear relationships were obtained when the peak width and the inverse peak height were plotted as functions of the square root of the mean residence time for coil lengths up to 2 m. The internal volume in the connectors to the injection valve, by-pass capillary and detector cell was 0.1 ml, as estimated from the time of start of the peak when the injector was connected directly to the detector. Pumping rate affects peak characteristics both by its influence on the thickness of the diffusion layer at the mercury electrode and by the dependence of peak broadening on flow rate. The sum of these two effects resulted in peak heights almost proportional to pumping rate from 0.5 to 3.5 ml min^{-1} (Fig. 5, a). The extrapolated peak width (measured in seconds; Fig. 5, a) and the mean residence time decreased with

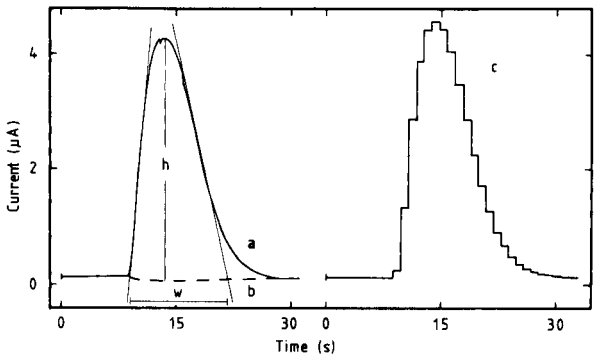

Fig. 1. Current peaks for 0.7 mM isosorbide dinitrate in phosphate buffers (curves a and c), and for the phosphate buffer (curve b). Detection modes were hanging mercury drop and d.c. current for (a) and (b), and dropping mercury electrode and sampled d.c. current for (c). The carrier stream was borate buffer with sodium sulfite, lactose and Brij-35.

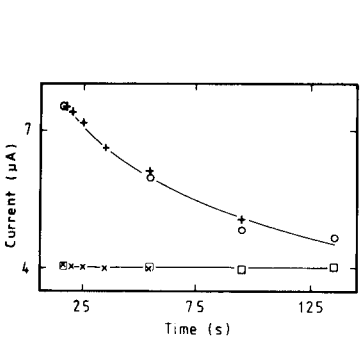

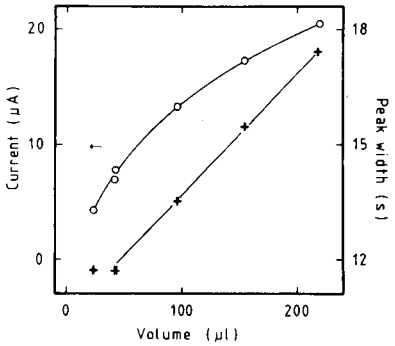

Fig. 2. Dependence of peak current for 0.7 mM isosorbide dinitrate on the life-time of the hanging mercury drop for two different carrier streams: borate buffer and sodium sulfite without (○, +) and with (□, ×) lactose and Brij-35. Different time delays were used before a single injection (+, ×) and subsequent injections at the same mercury drop (○, □).

Fig. 3. Influence of injection volume on peak current (○) and extrapolated peak width (+) for 0.7 mM isosorbide dinitrate. The carrier stream was borate buffer with sodium sulfite at a pumping rate of 2 ml min^{-1}.

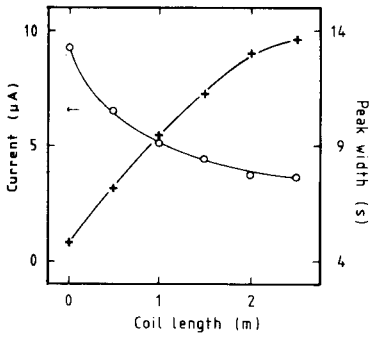

Fig. 4. Dependence of peak current (○) and extrapolated peak width (+) on coil length for 0.7 mM isosorbide dinitrate. The carrier stream was borate buffer with sodium sulfite, lactose and Brij-35. Injection volume 43 μl; pumping rate 2 ml min^{-1}.

increasing flow rate. When these two quantities were expressed in volume units and plotted against flow rate, the slopes at slow and fast flow rates were of different signs (Fig. 5, b).

The combination of an injection volume of 43 μl with a coil length of 1.5 m and a flow rate of 2 ml min^{-1} was considered to be appropriate for routine work. With this system, a time delay of 9 s from the injection to the beginning of the peak (Fig. 1, a) corresponded to a total volume of 0.3 ml between the injector and detector. The mean residence time was 14 s. The sample volume was diluted ten times as estimated from the extrapolated peak width (0.4 ml). Thus, the system should be classified as a medium

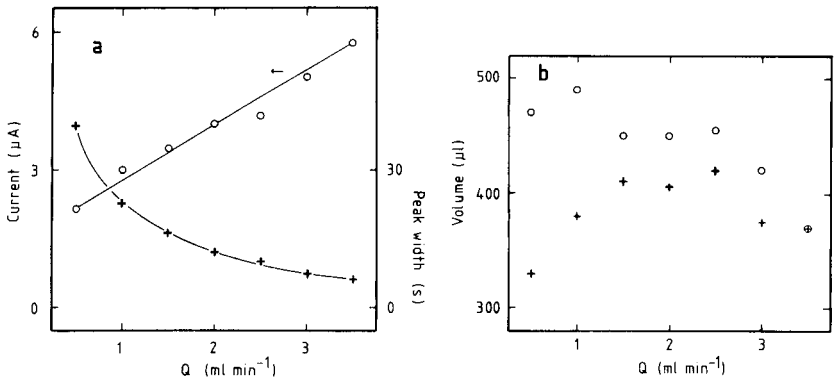

Fig. 5. Influence of pumping rate (Q) on (a) peak current (○) and extrapolated peak width measured in seconds (+), and (b) peak width in μl (+) and elution volume (○). The carrier stream was borate buffer with sodium sulfite, lactose and Brij-35. Samples were 43 μl of 0.7 mM isosorbide dinitrate.

dispersion system [6]. With the dropping electrode in the sampled-current mode, measurements were made six times on the rising part of the peak (Fig. 1, c). The current reached its baseline value about 30 s after an injection, allowing a maximum sampling frequency of about 100 samples per hour.

Carrier stream and detector potential

Adsorption of either the electroactive substance or some other component of the test solution at the electrode surface can affect the polarographic wave with respect to wave height, shape and half-wave potential. Such effects must be taken into account when polarographic analysis is performed in the traditional way. Adsorption phenomena in flow systems should be even more important because the mass transport to the electrode surface takes place over a compressed diffusion layer. The influence of lactose and Brij-35 on the polarographic reduction of ISDN provides an example of such general considerations. In ordinary polarographic measurements, the diffusion current of ISDN was independent of increasing amount of lactose, whereas the difference in half-wave potential between samples containing 1.4 and 12 mM lactose respectively, was 30 mV. Addition of Brij-35 up to 0.001% (v/v) affected neither the diffusion current nor the half-wave potential. A further increase in the concentration of Brij-35 to 0.01% caused a drastic decrease in the slope of the polarographic wave. The half-wave potential was shifted about 400 mV towards more negative potentials, while the wave height decreased by about 5%. With a carrier stream containing borate and sulfite, peak heights in the flow injection system decreased with an increasing amount of lactose in the samples (Table 2). This effect was further demonstrated in the nonlinear calibration curve obtained with the reference substance of ISDN which was a mixture of nitrate ester and sugar. The hydrodynamic polarogram constructed from the peak heights at different potentials

TABLE 2

Dependence of peak current (I_p) for 0.7 mM isosorbide dinitrate on the composition of carrier stream and on the concentration of lactose

Lactose in sample (mM)	I_d[a] (μA)	I_p (μA)			
		Borate/sulfite	Borate/sulfite/ 3 mM lactose	Borate/sulfite/ 0.001% Brij	Borate/sulfite/ 3 mM lactose/ 0.001% Brij
1.4	3.68	8.54	7.49	5.15	5.08
4.2	3.68	8.36	7.44	5.10	5.08
6.9	3.67	8.26	7.41	5.09	5.11
12.5	3.70	7.98	7.29	5.06	5.06

[a]Diffusion current in a stationary solution of equal volumes of sample and 0.1 M KCl in 10% ethanol.

exhibited a current maximum around −1.3 V which made it difficult to select an appropriate detector potential (Fig. 6, curve a). With a mixture of Brij-35 and lactose in the carrier stream, peak heights were reduced by about 40%. The difference in sensitivity between various sample compositions was within the experimental error, indicating that the electrode surface was saturated with adsorbed molecules. The limiting current of the corresponding hydrodynamic polarogram reached a well defined plateau (Fig. 6, curve b). Peak currents were proportional to concentration at a detector potential of −1.4 V. Thus, a carrier stream containing borax, sodium sulfite, 3 mM lactose and 0.001% Brij-35 was selected for routine determinations of ISDN.

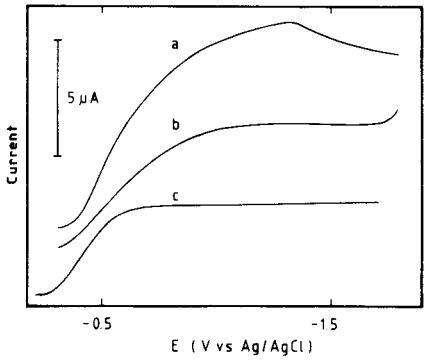

Fig. 6. Hydrodynamic polarograms of 0.7 mM isosorbide dinitrate. The carrier stream was borate buffer and sodium sulfite (a) without and (b) with lactose and Brij-35. (c) Polarogram of 0.4 mM isosorbide dinitrate in a supporting electrolyte of borate, sulfite, lactose and Brij-35.

TABLE 3

Determination of isosorbide dinitrate in connection with dissolution experiments by the normal polarographic method (POL) and the flow injection procedure (f.i.a.)

Batch	Method	Concentration of ISDN (μM) after dissolution time (h) of						
		1	2	3	4	6	8	24
A	POL	196	319	405	481	587	646	717
	F.i.a.	193	325	405	478	590	649	720
B	POL	155	277	362	442	553	622	714
	F.i.a.	155	273	359	437	562	625	716
C	POL	141	224	285	340	440	509	695
	F.i.a.	136	222	283	344	439	510	697

Determination of isosorbide dinitrate

The validity of the flow injection method was established through comparison with a normal polarographic method. The results from the two methods agreed within the experimental errors (Table 3). For the ordinary polarographic analyses the specimens which originated from dissolution tests, were mixed with an equal volume of 0.2 M potassium chloride in 10% ethanol. No chemical treatment of the specimens was needed before the injection into the flow system. One sample was injected every 40 s. Each specimen was measured once. One solution was sufficient for standardization purposes, because the calibration curve was linear and passed through the origin. The injection of the standard was usually repeated between measurements involving a total of ten specimens. Apart from the preparation of the carrier stream which was preferably done a few hours before use, the flow injection system was started up in less than 15 min. This time was long enough to allow exchange of solvent in the pump, assemblage of the flow cell and attainment of a stable baseline. To prevent air from diffusing into the carrier stream, plastic tubing was avoided as far as possible in every part of the system. Thus, the teflon coils utilized during the development work were replaced by steel capillaries.

Limit of detection

The signal from an injected sample depended on several effects such as faradaic processes, pressure variations and changes in viscosity. The most important factor for sample concentrations within the working range (0.05–1 mM ISDN) for which the system was optimized, was the reduction of ISDN. Injection of a blank solution resulted in a current which was slightly smaller than the baseline current (Fig. 1, curve b). Current peaks were badly resolved from the baseline for ISDN concentrations below 0.01 mM, which constituted the limit of detection for the present system. When the injection valve was positioned on the high-pressure side of the steel capillary, a blank injection gave rise to a positive peak. With this alternative experimental set-up, it might be possible to measure ISDN concentrations as low as 1 μM.

REFERENCES

1 P. W. Alexander and M. H. Shah, Talanta, 26 (1979) 97.
2 W. Lund and L.-N. Opheim, Anal. Chim. Acta, 79 (1975) 35.
3 R. J. Rucki, Talanta, 27 (1980) 147.
4 L. Michel and A. Zatka, Anal. Chim. Acta, 105 (1979) 109.
5 H. B. Hanekamp, P. Bos, U. A. Th. Brinkman and R. W. Frei, Fresenius Z. Anal. Chem., 297 (1979) 404.
6 J. Růžička and E. H. Hansen, Anal. Chim. Acta, 99 (1978) 37.
7 W. R. Turner and R. S. Lenkiewicz, J. Pharm. Sci., 65 (1976) 118.
8 S. Silvestri, Pharm. Acta Helv., 50 (1975) 304.
9 I. M. Kolthoff and J. J. Lingane, Polarography, Vol. 1, Interscience, New York, 1952, p. 397.

Analytica Chimica Acta, 123 (1981) 125–133

THE USE OF IMMOBILIZED ALCOHOL OXIDASE IN THE CONTINUOUS FLOW DETERMINATION OF ETHANOL WITH AN OXYGEN ELECTRODE

E. L. GULBERG and G. D. CHRISTIAN*

Department of Chemistry, University of Washington, Seattle, WA 98195 (U.S.A.)

(Received 2nd May 1980)

SUMMARY

Immobilized alcohol oxidase was used in the determination of blood alcohol. The alcohol oxidase catalyzed the aerobic oxidation of ethanol and the oxygen concentration was monitored with an oxygen membrane electrode in a flow cell. The enzyme was immobilized either by covalent attachment via glutaraldehyde to the inside walls of nylon tubing, or by adsorption onto three separate controlled-pore glass support materials: TiO_2, SiO_2, or Al_2O_3. The supports were packed into 10 cm lengths of 3 mm i.d. glass tubing or 30 cm lengths of 5 mm i.d. nylon tubing. The five methods of immobilization were compared for stability and activity toward ethanol. Immobilization on silanized glass beads results in the highest activity and greatest stability of the reactor.

The analytical use of enzymes offers extremely selective and sensitive procedures for determining substrates of interest. For instance, the rate of the aerobic oxidation of ethanol

$$CH_3CH_2OH + O_2 \rightarrow CH_3CHO + H_2O_2 \quad (1)$$

is increased by many orders of magnitude by the presence of alcohol oxidase. With the high cost of some enzymes, the use of immobilized enzymes is desirable. In the enzyme electrode for alcohol employed by Nanjo and Guilbault [1], immobilized alcohol oxidase was sandwiched between a nylon cloth and a platinum cathode which measured the oxygen consumed by electrochemical reduction. Considering the trend toward mechanization and simplification in the determination of blood components, the utilization of immobilized enzymes in a flow system is an attractive possibility. A flow cell incorporating an oxygen membrane electrode that should be suitable as a detector for oxidase enzyme reactions has been developed [2].

Incorporation of immobilized enzymes into a flow system requires their immobilization in a tubular form, allowing relatively free volume flow through the tube. The inside surface of nylon tubing has been treated so as to bind enzymes, including trypsin, uricase, and glucose oxidase [3–6]. Controlled-pore glass particles have also been used as a support for immobilized enzymes and then packed into beds [7, 8].

A new approach for the determination of blood ethanol is described here. The method utilizes immobilized alcohol oxidase in reaction tubes to catalyze reaction (1). Three different methods of enzyme immobilization were evaluated: simple adsorption on untreated SiO_2, TiO_2, or Al_2O_3 beads, covalent bonding via glutaraldehyde to silanized glass beads, and covalent bonding via glutaraldehyde to the inside surface of nylon tubing. The resulting enzyme columns were then inserted into a flow system. The effluent was fed into a flow cell containing an oxygen electrode which amperometrically monitored the oxygen concentration.

EXPERIMENTAL

Apparatus

An oxygen membrane electrode was used to monitor the oxygen concentration in solution. This electrode was housed in a plexiglas flow-cell designed specifically for this electrode for use in continuous flow determination [2].

A Princeton Applied Research Polarographic Analyzer (PAR 174) was used to provide a constant (−0.6 V vs. Ag—AgCl) potential to the oxygen electrode and to monitor the currents produced. A Moseley X-Y recorder was used to record the currents.

The tubing used was Standard Manifold Pumping tubing (Gradko Glass Company) and was fitted to the enzyme columns and the flow-cell via tube-end adapters (Gilson Medical Electronics). All tubing had an inner diameter between 0.25 mm and 1.4 mm. A Gilson Minipuls II pump was used to give flow rates between 50 and 500 μl min^{-1} per inlet tube.

The tubes for the glass-packed enzyme columns were of two types. For the adsorbed enzyme columns, glass tubes 3 mm i.d., 10 cm in length were packed with SiO_2, TiO_2, or Al_2O_3 beads, plugged with glass wool, and the ends drawn out to hold the contents inside, while allowing solution to be pumped through. The flow tubing fit snugly over the ends of these enzyme columns.

In the second type of column, 30 cm lengths of 5 mm i.d. nylon tubing were packed with silanized glass beads, the ends plugged with glass wool, and the contents held in place with tube end adapters to which the tubing was connected.

The nylon tubing used for direct binding of the enzyme to the nylon was type 6 nylon (Nylon 6/6, Universal Plastics, Seattle, WA) with an inner diameter of 1 mm. The lengths employed were from 0.5 to 1.5 cm.

All alcohol assays were done at room temperature, with room temperature controlled to within 1° or better.

Reagents

Phosphate buffer, pH 7.8, 0.1 M, was prepared from potassium hydrogen-phosphate (Baker Reagent Grade) in deionized, distilled water; the pH was adjusted with concentrated HCl or saturated NaOH. Tris buffer, 0.1 M was

TABLE 1

Controlled pore glass beads used for enzyme immobilization

Type of glass	Pore diameter (Å)	Surface area (m^2/g)
Silica (SiO_2)	425	40
Titania (TiO_2)	650	19
Alumina (Al_2O_3)	165	90

prepared from tris(hydroxymethyl)methylamine (Sigma) and adjusted to the desired pH with concentrated HCl or NaOH.

Aqueous ethanol standards were prepared from absolute ethanol (U.S. Industrial Chemicals, New York). All concentrations are expressed as % (v/v).

Alcohol oxidase (from *Candida boidinii*) was obtained from Sigma (Lot 77C-0314). Glutaraldehyde, 2 M in water (Baker) and 3-aminopropyltriethoxysilane (Aldrich) were used.

Immobilization techniques

Inert support for enzyme immobilization. Alcohol oxidase was immobilized on controlled-pore glass beads (45—80 mesh; Corning Glass Works, New York) of three different types (see Table 1).

Immobilization by adsorption. The preparation of alcohol oxidase immobilized on glass beads partly followed the method of Weetall and Messing [9]. Lengths (10 cm) of glass tubing were filled with the three types of controlled pore glass beads, and all three columns were connected in series to 1.4 mm i.d. tygon tubing. Because the surface of silica glass is rather acidic (pH 4) [10] and the pH optimum of alcohol oxidase in solution is 7.8, the surface of the glass beads was preconditioned by perfusing 0.05 M phosphate buffer at pH 7.8 through the columns at ca. 500 μl min^{-1} for 2 h. A solution (2.5 U ml^{-1}) of alcohol oxidase in phosphate buffer was then perfused through the tubes at 100 μl min^{-1} for 3 h, and at about 50 μl min^{-1} for 16 h (overnight). The outlet end of the tubing was fed into the enzyme solution reservoir, forming a closed loop during the loading of the enzyme onto the glass beads.

The enzyme columns were then washed with buffer for 2 h at 500 μl min^{-1} to rid the glass of unadsorbed enzyme. They were stored filled with buffer at 4°C.

Immobilization by covalent attachment to glass beads. The organic silanization method of Weetall [10] was used. The resulting silanized glass beads were mixed 50% with unsilanized silica glass beads and packed into a 30 cm length of 5 mm i.d. nylon tubing. The addition of untreated glass was unnecessary to reduce the pressure drop across the bed of silanized glass in the enzyme column. (The silanization process resulted in glass beads of reduced size, and thus they were more "powdery.") The silanized glass was activated for binding enzyme by perfusing 2.5% glutaraldehyde in phosphate

buffer, pH 7, through the packed column for 90 min at approximately 300 μl min^{-1}. This was followed by washing for 3 h with distilled water at 300 μl min^{-1}.

Alcohol oxidase was loaded onto the column by perfusing a solution (5 U ml^{-1}) solution of the enzyme in pH 7.8 phosphate buffer through the column in a closed loop for 3 h at approximately 100 μl min^{-1}. The column was washed overnight with buffer to remove any unbound and most of the adsorbed enzyme, and stored at 4°C with buffer inside.

Immobilization by covalent attachment to nylon tube. The method of Inman and Hornby [6] was approximately followed here. After hydrolysis and treatment with glutaraldehyde, the 1.5-m nylon tube (1 mm i.d.) was ready to receive the enzyme. A solution (8 U ml^{-1}) of alcohol oxidase in phosphate buffer, pH 7.8, was introduced into the tube, and the tube was sealed and stored at 4°C for three days. On the third day, the tube was removed from the refrigerator and found to be dry. It was washed with 250 ml of 0.1 M phosphate buffer, pH 7.0, which was 0.5 M in NaCl for 2 h before use.

RESULTS AND DISCUSSION

Free enzyme

Standards of ethanol in both phosphate buffer and diluted serum were measured in the flow system using soluble alcohol oxidase for comparison with the enzyme columns. The aqueous measurements showed linearity from 0.5 to 10 mg ethanol per 100 ml ($y = (1.3 \pm 0.06)x + (0.19 \pm 0.03)$, nA, $S_{yx} = 0.052$, $r = 0.993$). Concentrations of ethanol in serum between ca. 50 and 400 mg per 100 ml cover the legally important range and so a 1:100 dilution of blood or serum would provide concentrations in the above range.

Adsorbed alcohol oxidase

Aqueous standards of ethanol in phosphate buffer (1—10 mg/100 ml) were pumped through a single inlet tube (0.03 in. i.d.), through the enzyme column, and then immediately into the oxygen electrode flow cell. The time that a sample spent in the enzyme column was 10—20 s. Some "chromatographing" of the sample in the column was noted. Whereas it would take the solvent 1.5 min to move from the column inlet to the detector, it would take a sample about 2 min to give a signal. (This is not a result of the characteristics of the flow cell or the response time of the electrode [6].) The sample apparently interacted with the glass and the immobilized enzyme in such a way that its progress through the column was impeded.

The titania glass column showed approximately 2.5 times the activity of the silica glass column. The alumina glass column showed only small activity (Fig. 1). A discussion of quantitative column activities follows below. The currents shown on all graphs are the absolute values of the decrease in the current caused by oxygen depletion from the enzymatic reactions (initial current ca. 20 nA).

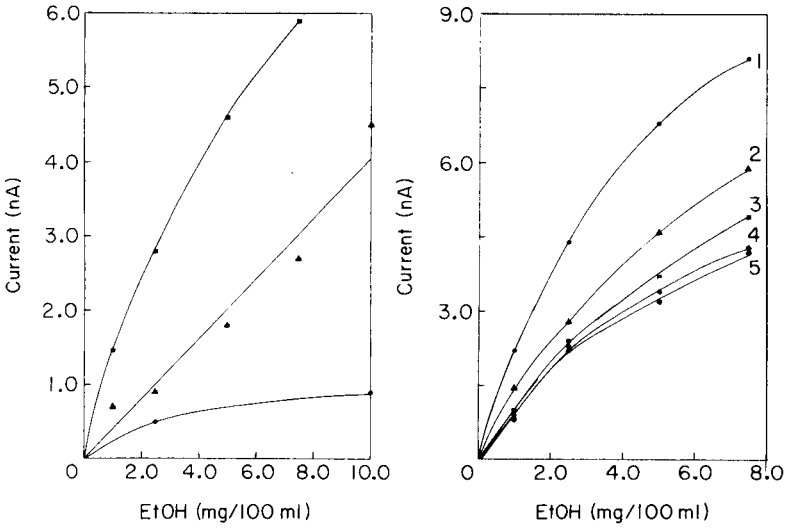

Fig. 1. Current vs. concentration of aqueous ethanol. Enzyme immobilized by adsorption on three different controlled-pore glass supports: (●) TiO_2; (▲) SiO_2; (■) Al_2O_3.

Fig. 2. Current vs. concentration of aqueous ethanol. Enzyme immobilized by adsorption on TiO_2. Ethanol standards run in five consecutive series (about 2 h from the beginning of the first calibration curve to the end of the fifth). Response, thus presumably activity of enzyme column, decreases with each run.

The activities of the enzyme columns correlate with the pore sizes of the glass supports, the titania glass having the largest pore diameter (see Table 1). The alcohol oxidase molecule is evidently excluded from the 165 Å pores of the alumina glass.

The possibility of desorption and washing out of the enzyme from the titania column was investigated (Fig. 2). A fresh enzyme column was prepared and a set of ethanol standards was perfused through (four samples at 5 min/sample) with the intention of ridding the column of any unadsorbed enzyme that the buffer wash had not removed. Then ethanol standards ranging in concentration from 1.0 to 7.5 mg/100 ml were run in five consecutive series, requiring about two hours. The sensitivity of the enzyme column was about four times that for the soluble enzyme, even with a reaction time only 1/4 as long. This sensitivity decreased by a factor of 2 over the five runs. The step size of activity decrease lessened with each set of standards run.

The non-linearity of each run is possibly due to the loss of enzyme from the column as each successive standard goes through. Thus, in determining blood ethanol, it would be necessary to precondition the column by washing until the activity stabilizes. Other causes of non-linearity include the low column activity and the possible presence of catalase, co-immobilized with the alcohol oxidase.

To show the feasibility of serum ethanol determinations, reconstituted serum was diluted 1:10 with phosphate buffer and spiked with ethanol to concentrations from 1.0 to 10.0 mg/100 ml. These samples were run through the column and a calibration curve obtained (Fig. 3) with a regression equation of $y = (0.5 \pm 0.1)x + 1 \pm 1$ ($S_{yx} = 0.3$, $r = 0.999$). In an actual assay, serum should be diluted about 1:50 to achieve an ethanol concentration in the working range of the calibration curve.

Covalently attached alcohol oxidase

Aqueous ethanol standards in phosphate buffer were run through the silanized glass enzyme column and a detection limit of 0.2 mg/100 ml was found [slope = 1 nA/(100 mg/100 ml), linearity to at least 3 mg/100 ml]. This high sensitivity and the linearity demonstrate that the enzyme is not leached from the column, as it was from the adsorbed enzyme columns. This is to be expected because of the stability of the covalent bonds formed between the enzyme and the glutaraldehyde. The enzyme column retained its activity for several weeks. It would have been useful longer had the glass not become so tightly packed as to restrict all flow. Subsequent work with larger size beads is expected to overcome this clogging problem.

An attempt was made to silanize titania glass and covalently attach alcohol oxidase. The resulting column gave an enzyme activity just about equal to that of the titania glass column containing adsorbed enzyme. Presumably no silanization occurred and an adsorbed enzyme column was produced.

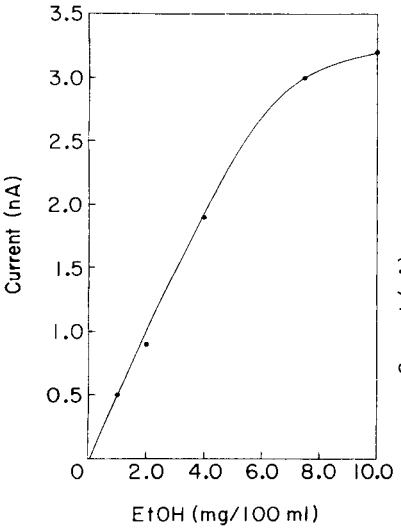

Fig. 3. Current vs. concentration of ethanol in serum diluted 1:10 with buffer. Enzyme immobilized by absorption onto TiO_2.

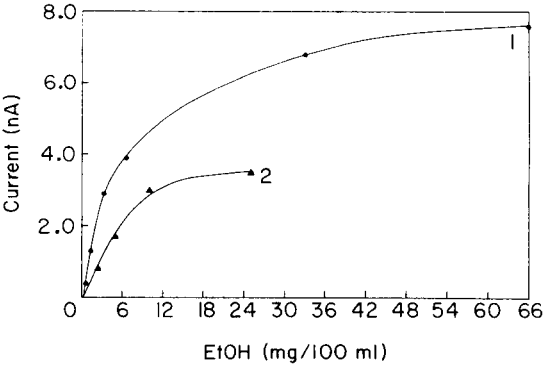

Fig. 4. Current vs. concentration of aqueous ethanol. Enzyme immobilized in nylon tubing by covalent attachment via glutaraldehyde: (1) 2nd day after preparing enzyme column; (2) 10th day.

Nylon tube enzyme column

Aqueous ethanol standards in phosphate buffer were run through a 60-cm nylon enzyme column at a pumping rate of 400 μl min^{-1}; the detection limit found was 0.7 mg/100 ml (Fig. 4). There is undoubtedly less contact between alcohol and enzyme on this column than on the silanized glass column, for there is a leveling in the calibration curve at higher ethanol concentrations, which indicates that not all the ethanol is being oxidized.

The advantage of the nylon tube enzyme column as compared to the bead packed columns is its ability to allow free flow-through. The glass columns impeded the solution flow somewhat, especially the silanized glass column. The pressure drop across the silanized glass column grew to an unacceptable level after several days of work with serum or blood.

The nylon tube enzyme column lost some (ca. 50%) activity over the course of 10 days (Fig. 4). Upon each period of storing (usually overnight) the tube had dried out. The buffer filling apparently evaporated through the walls of the nylon. Possibly the harsh hydrolysis in the original immobilization decomposed too much of the nylon wall. A thicker walled tube might eliminate this problem, as would storing the whole tube immersed in buffer. After two weeks of storage, the column had lost all activity.

Column activity

Freshly prepared alcohol oxidase solution (17 U ml^{-1} in phosphate buffer) was prepared and stirred with aqueous 4×10^{-4} M ethanol. The decrease in the oxygen concentration in the resulting solution caused by reaction (1) was then followed with an oxygen electrode. This current decreased at a rate of 9.4 nA min^{-1} during the first two minutes.

An identical 17 U ml^{-1} alcohol oxidase solution was then perfused through 500 mg of titania glass beads in one column and 25 mg of silanized silica in another column for 3 h. The "spent" enzyme solution was then stirred with aqueous ethanol, as above, and the change in amperometric current caused by the oxygen decrease was found to be 3.6 nA min^{-1}. The loss of activity by the enzyme solution was thus about 60%, or 10 U ml^{-1} (20 U total for the 2 ml of solution). Assuming this 20 U of enzyme activity was now on the immobilized enzyme columns, and finding that the two columns gave approximately the same sensitivity toward ethanol, one can deduce that the titania glass beads removed 10 U/0.5 g or 20 U g^{-1} and the silanized silica removed 10 U/0.04 g or 250 U g^{-1} of alcohol oxidase from the free enzyme solution.

The resulting activities of the enzyme columns were more difficult to ascertain. The binding of the enzyme to the glass beads might well affect the activity, so that one cannot conclude that the activity contained on the silanized glass bead column would be 250 U g^{-1}. Studies were conducted on silanized glass enzyme columns which showed alcohol oxidase activities anywhere from 125 to 200 U g^{-1} of glass. In these studies, an ethanol standard was assayed by perfusion through an enzyme column. The eluent was

collected, aerated briefly, then assayed again. The difference in the amperometric signal was then related to an absolute difference in ethanol concentrations in the two solutions. Of course, this method is only as reliable as the reproducibility of the original oxygen concentration in the eluted solution. In this same manner, a 60 cm long, 1 mm i.d. nylon enzyme column was found to contain ca. 1 U of alcohol oxidase activity (1.7 U m^{-1}).

pH profile

The effect of pH on the activity of the covalently attached alcohol oxidase toward an aqueous ethanol solution of 1 mg/100 ml was determined (Fig. 5). The optimal pH was found to be 8.2 which is slightly higher than the value of 8.0 reported by Nanjo and Guilbault [1]. Both phosphate and Tris buffers were used.

Determinations in blood

Ethanol was determined in whole blood with the immobilized enzyme (silanized glass) flow system and the results were compared with results obtained by gas chromatography. Ten whole blood samples, treated with 1 g each of sodium fluoride and sodium oxalate per liter, were obtained from the Washington State Toxicology Laboratory. The alcohol concentrations ranged from 0.07 to 0.33 g/100 ml (0.7 to 3.3 mg/100 ml after 1:100

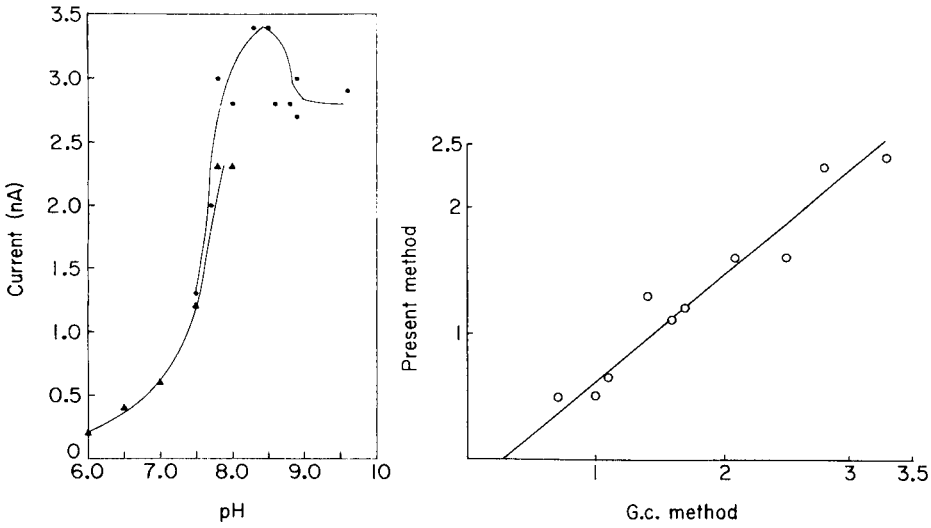

Fig. 5. Current vs. pH of aqueous ethanol solutions using silanized SiO_2 column: (▲) phosphate buffer; (●) Tris buffer.

Fig. 6. Determination of ethanol in samples of whole blood by the present method and by the gas chromatographic method. The equation of the line is y = (0.855 ± 0.077) x − (0.27 ± 0.15); S_{yx} = 0.073; r = 0.963. Results for both methods are expressed as mg/100 ml (i.e., 1:100 dilution of original samples).

dilution). Gas-chromatographic determinations performed between 4 months and 1 year prior to our enzymatic determinations were used for comparisons. The blood was diluted 1:100 with pH 8.2 Tris buffer for this determination. With such dilution, it is assumed that varying initial levels of oxygen in the samples will not affect the accuracy of the determinations.

Results are summarized in Fig. 6. The present method gives consistently low results for blood ethanol concentrations when calibration with aqueous standards is used. Several reasons for the discrepancy are suggested. A small portion of the oxygen content of the diluted samples might be bound to hemoglobin, although 1:100 dilution with aqueous buffer should minimize the effect. The protein present in whole blood, even at 1:100 dilution, might obstruct the surface of the glass beads such that a lower activity of alcohol oxidase is available for reaction with ethanol. Indeed, serum diluted 1:50 was spiked with ethanol, and only 89% recovery was achieved, when aqueous standards were used. Some loss of ethanol occurred in the blood over the time span between gas chromatographic and enzymatic determinations. The results indicate that calibration must be performed using pooled blood samples.

Conclusions

Immobilization of alcohol oxidase on silanized glass beads results in highest activity and greatest stability. Because of pressure buildup, the enzyme column must be changed periodically when blood samples are processed. Use of larger beads may alleviate this requirement. A short column with higher enzyme loading is recommended to minimize pressure drop. Pooled blood samples should be used for calibration.

REFERENCES

1 M. Nanjo and G. G. Guilbault, Anal. Chim. Acta, 75 (1975) 169.
2 E. L. Gulberg and G. D. Christian, Chem., Biomed. Environ. Instrum., 9 (1979) 277.
3 W. E. Hornby and H. Filippusson, Biochim. Biophys. Acta, 220 (1975) 343.
4 J. Campbell, W. E. Hornby and D. L. Morris, Biochim. Biophys. Acta, 384 (1975) 307.
5 C. Horvath and B. A. Solomon, Biotechnol. Bioeng., 14 (1972) 885.
6 D. J. Inman and W. E. Hornby, Biochem. J., 129 (1972) 255.
7 M. K. Weibel, W. Dritshillo, H. J. Bright and S. E. Humphrey, Anal. Biochem., 52 (1973) 402.
8 C. Horvath, Biochim. Biophys. Acta, 358 (1974) 164.
9 H. H. Weetall and R. A. Messing, in M. L. Hair (Ed.), The Chemistry of Biosurfaces, M. Dekker, New York, 1972.
10 H. H. Weetall, in K. Mosbach (Ed.), Methods in Enzymology, Vol. XLIV, Immobilized Enzymes, Academic Press, New York, 1976.

Analytica Chimica Acta, 123 (1981) 135–141

PREPARATION AND PROPERTIES OF AN ANTIBODY-SELECTIVE MEMBRANE ELECTRODE

R. L. SOLSKY** and G. A. RECHNITZ*

Department of Chemistry, University of Delaware, Newark, Delaware 19711 (U.S.A.)

(Received 23rd June 1980)

SUMMARY

A membrane electrode with selective response for the antibodies of the antigenic determinant dinitrophenol (DNP) has been devised by incorporating DNP—ion carrier conjugates in a polyvinyl chloride membrane matrix. Details of the preparative and immobilization procedures are provided along with an evaluation of optimum solution conditions for electrode use. The response mechanism of the antibody electrode is postulated to involve a "selectivity shift" effect.

The use of ion-selective membrane electrodes as components of sensors for biochemical or biological species has emerged as one of the most active research areas of analytical potentiometry [1]. Although most of the attention has been focused on enzyme-based and other biocatalytic sensors, there is now an increasing interest in immunochemical systems [2, 3] with the development of direct antibody-sensing membrane electrodes [4].

In this paper, the preparation and properties of such an immunoelectrode with selective response to antibodies of the antigenic determinant dinitrophenol (DNP) are described. This electrode embodies a new concept in bioselective membrane electrodes in that the antigenic material is covalently coupled to an ion carrier, dibenzo-18-crown-6, and the resulting conjugate is immobilized in a polymeric membrane. It is shown that properly prepared membranes yield electrodes with analytically attractive properties.

EXPERIMENTAL

Apparatus

The electrodes were constructed using the commercially available Orion 92 Series liquid membrane electrode bodies. The only modification to the electrode body was the radial drilling of several holes in the membrane spacer to allow the external reservoir to be filled with the aqueous internal electrolyte solution. The electrode configuration is shown in Fig. 1 and indicates this modification.

**Present address: E. I. DuPont and Co., Wilmington, DE 19898.

The electrode potentials were measured relative to an Orion model 90-01 single-junction reference electrode with a Corning model 12 pH/mV meter and were recorded with a Heath—Schlumberger model 204 strip chart recorder. All measurements were performed at 30.0°C using a Haake model FS circulating temperature bath. Since the electrodes were sensitive to static charge, a Faraday cage was constructed of copper mesh and was attached to the strip chart recorder ground.

Reagents

The membrane matrix was formed of polyvinyl chloride (PVC; Polysciences, Inc., Warrington, Pa.). The plasticizer was dibutyl sebacate (DBS; Eastman Organics, Rochester, N.Y.). The other materials were crown ether dibenzo-18-crown-6 and the activated form of the hapten, fluorodinitrobenzene (both from Aldrich Chemical Co., Milwaukee, Wis.), and the antiserum to dinitrophenol (DNP) and the antiserum to bovine serum albumin (BSA) (both from Miles Laboratories, Elkhart, Ind.). The antisera were obtained as liquid and lyophilized powder, respectively, and were stored either frozen or at 4°C until use.

Preparation of the electrode

The crown ether was activated by the method reported by Feigenbaum and Michel [5]. The dinitrodibenzo-18-crown-6 was first prepared by nitrating the crown in chloroform using a mixture of nitric and acetic acids.

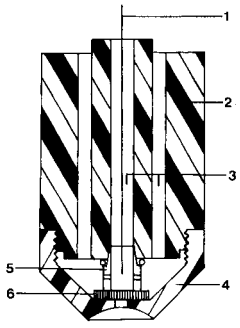

Fig. 1. Schematic diagram of the antibody sensing electrode. (1) Internal Ag/AgCl reference element; (2) electrode body; (3) internal aqueous electrolyte; (4) electrode cap; (5) membrane spacer; (6) sensing membrane.

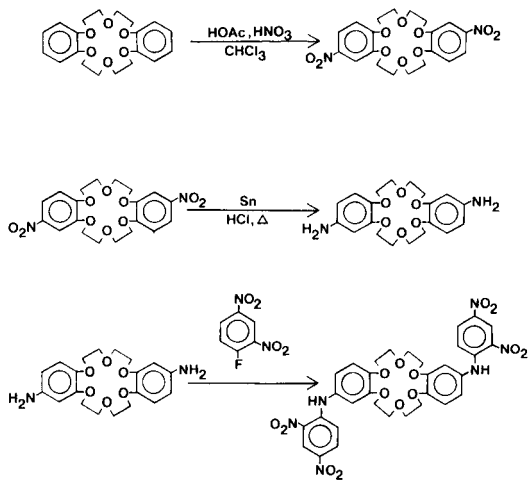

Fig. 2. Synthetic scheme for preparation of the carrier—DNP conjugate (conditions in text).

The nitrating mixture consisting of nitric and acetic acids was dripped into a flask containing the crown ether dissolved in a mixture of chloroform and acetic acid. After refluxing for 3 h, the *trans*-dinitro derivative precipitated out of solution. The precipitate was isolated by gravity filtration while hot; upon cooling of the supernatant solution, the *cis*-dinitro derivative also precipitates out for easy collection. The crude preparations were recrystallized from dimethylformamide using methanol. The *trans*-derivative had a tan color while the *cis*-derivative was yellow; ultraviolet spectra at 338 and 298 nm served to confirm these products.

The *trans*-derivative was chosen for further activation and was reduced to the aryl amine using tin metal and hydrochloric acid. The reduction was carried out by using an equimolar quantity of the tin metal to the dinitro derivative and an excess of hydrochloric acid. After heating at sub-reflux temperature for several hours, the supernatant solution was tested for the presence of the aryl amine with the color-forming reagent, trinitrobenzene sulfonate (picryl sulfonic acid) [6]. This reagent produces an orange color in the presence of the desired product. The contents of the flask were cooled in an ice bath and concentrated sodium hydroxide was added to produce a final pH of about 10—11. This resulted in the formation of a fluffy white precipitate which was immediately filtered under suction and rinsed with dilute sodium hydroxide solution. The precipitate was treated with a dilute hydrochloric acid solution to solubilize the aryl amine and was then precipitated again with sodium hydroxide to purify the product. The spectrum was retaken and peaks at 298 and 231 nm were recorded.

The hapten was coupled to the activated carrier using the classical protein sequencing agent, fluorodinitrobenzene (Sanger's reagent [7]). The coupling proceeds via nucleophilic substitution of the benzene ring at the fluorine site. The diamino-dibenzo-18-crown-6 and fluorodinitrobenzene are added in stoichiometric amounts in an aqueous solution which contains an equimolar amount of triethylamine to complex the released fluoride ion. The mixture was stirred for an hour and the solution turned a heavy orange color. The product was extracted with chloroform and was concentrated by evaporation. Since the fluorodinitrobenzene also reacts with water to form dinitrophenol, the chloroform extract was washed with a saturated sodium hydrogencarbonate solution to remove the weakly acidic phenol side product. The product had the consistency of a heavy, dark reddish oil. The entire synthetic sequence to make the ion carrier—hapten conjugate is shown in Fig. 2.

The electrode membranes were then prepared by incorporating the ion carrier—hapten conjugate in a PVC matrix. Membranes were prepared by dissolving 1.0 mg of the conjugate in 5.0 ml of tetrahydrofuran. Dibutyl sebacate (0.25 ml) was added as the membrane plasticizer. This mixture was poured into a 48-mm diameter Petri dish containing 0.25 g of powdered PVC. After complete dissolution of the PVC, the solvent is permitted to evaporate slowly over a 12-h period. It is important that the Petri dish be protected from dust and mechanical disturbance during this procedure.

When evaporation of the solvent is complete, a coherent smooth membrane remains at the bottom of the dish. This stock membrane is carefully cut to yield 4-mm diameter membrane discs (0.2 mm thick) which are mounted in the plastic electrode body and secured by the electrode cap. A 0.01 M KCl filling solution is then added to charge the electrode internals and the assembled electrode is allowed to soak in 0.1 M KCl solution for some hours before use.

Antibody measurements

There are two principal considerations to be taken into account if analytically useful antibody measurements are to be made.

First, since the electrode membrane contains a cation-selective crown compound as carrier, it is necessary to control the concentrations of ions to which the electrode can respond; only with such control can the net response due to the antibody be isolated. Figure 3 shows the response of the antibody electrode to the several cations of interest in this study. Since K^+ and Na^+ yield the greatest response, salts of either of these cations would be appropriate as electrolytes for antibody measurements. Potassium chloride was selected for this purpose and the effect of varying salt concentrations on antibody response was further evaluated. Figure 4 shows the relative electrode response at a constant (100 μg ml^{-1}) antibody concentration with variation of the KCl concentration. It can be seen that maximum response is obtained in the region of millimolar KCl concentration. For convenience in maintaining ionic strengths and because of the low contribution to the electrode potential by Ca^{2+} (Fig. 3), a solution of 1.0×10^{-3} M KCl and 5.1×10^{-2} M $CaCl_2$ was selected as the working electrolyte.

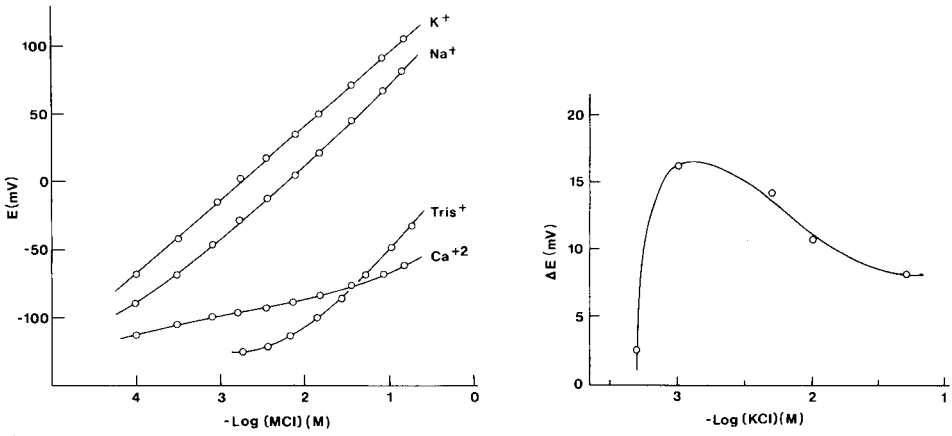

Fig. 3. Potentiometric response of the antibody electrode to selected cations.

Fig. 4. Relative electrode response as a function of KCl concentration in medium of constant 100 μg ml^{-1} ml DNP antibody concentration.

Second, it can be seen from Fig. 5 that the antibody electrode shows a small, but not negligible, sensitivity to pH. In order to simulate physiological conditions, the pH of our working electrolyte was controlled at 7.5 using Tris—HCl buffer. It should be recalled from Fig. 3 that the buffer cation also makes a minor contribution to the overall potential. In view of these considerations, antibody sample solutions were pre-dialyzed and prepared in the same buffered electrolyte for the measurements. The potential measurements taken on the antibody samples are expressed as ΔE values because they represent the difference in electrode potentials observed between values taken in the electrolyte alone and in electrolyte containing various antibody concentrations, respectively.

RESULTS AND DISCUSSION

A typical electrode response plot as a function of DNP antibody concentrations in the pH 7.5 working electrolyte is shown in Fig. 6. Potential readings taken over the 2.8—145.1 μg ml^{-1} concentration range yielded a standard deviation of 4.1% with individual potential readings reproducible to ±0.2 mV. Approximately 6--16 min were required for steady-state potentials to be reached after the addition of antibody-containing aliquots. The response of the electrode was found to be fully reversible.

Also shown in Fig. 6 (lower curve) is the response of the electrode to additions of bovine serum albumin (BSA) antibody. The lack of observed response is an important test of electrode function because the DNP antibodies, which yield the response in the upper curve of Fig. 6, were raised in rabbits using DNP coupled to BSA as stated by the manufacturer. Thus, the selective response of the electrode to the primary species is confirmed. It should also be noted that both curves of Fig. 6 were constructed using

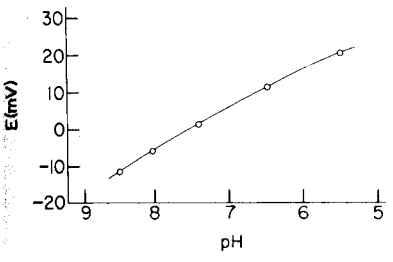

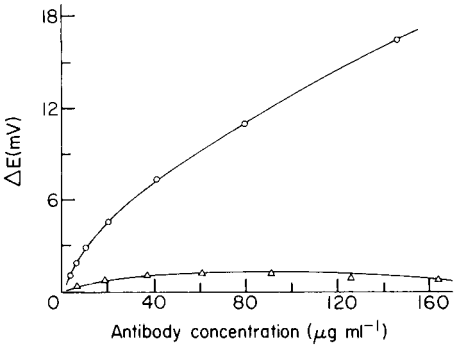

Fig. 5. pH response of the antibody electrode.

Fig. 6. Antibody response of the electrode at pH 7.5; (○) DNP antibodies; (△) BSA antibodies.

antibody sources in whole immune sera (Miles Laboratories) and, therefore, demonstrate the absence of a general serum protein response.

The mechanism by which the observed potential changes arise upon addition of antibody is of particular interest not only from the fundamental point of view but also to provide guidelines for the future design of new electrodes. Separation of the variables is particularly difficult in the case of the DNP antibody electrode because of the broad ion response of the carrier species employed and the need to provide effective buffering of protein-containing solutions.

At the present stage of our admittedly limited knowledge, two seminal experimental results in the mechanistic area can be reported. First, it can be demonstrated that the conjugation of the antigenic determinant (DNP) is necessary within the membrane phase to produce an antibody response. This is clearly shown in Fig. 7, which presents the response of a complete DNP—carrier conjugate membrane electrode to antibody as well as that of another electrode which contains all the membrane components except the DNP under otherwise identical conditions. From these data, it becomes apparent that the properties of the ion carrier alone do not yield an antibody response and that both the antigenic determinant and the carrier act together to mediate a potential change in the presence of the specific antibody.

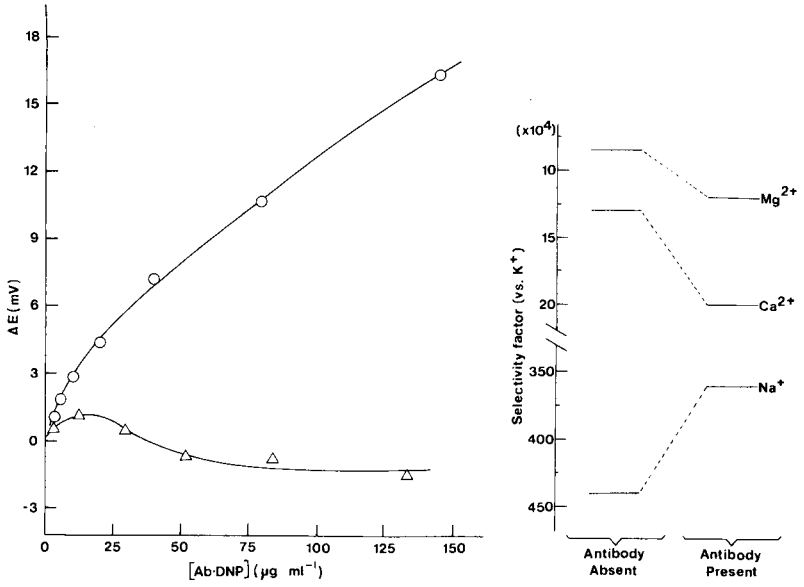

Fig. 7. Antibody response of membrane electrodes containing (○) the DNP—carrier conjugate, and (△) the carrier alone.

Fig. 8. Comparison of electrode selectivity patterns in the presence and absence of DNP antibody.

This point is further clarified in the second key experiment where the effect of specific antibody on the selectivity of the complete electrode is tested. The results (Fig. 8) show that the addition of antibody to DNP produces a shift in the apparent ion selectivity of the membrane electrode containing the complete DNP—carrier conjugate. Although the observed effect cannot be fully quantified from this figure because of the potentiometric contribution of the buffer cation, it is noted that the direction and magnitude of the potential change expected from this selectivity shift are in general accord with the ΔE values found for the antibody measurement. Our preliminary model, therefore, accounts for the potentiometric behavior of the DNP antibody electrode via a perturbation in carrier selectivity arising when the DNP—carrier conjugate contacts the specific antibody at the membrane—solution interface under appropriate solution conditions. Further work is in progress to test this model under more stringently controlled conditions and with more highly selective carrier species to minimize the contribution from mixed potentials.

Although the present model is both preliminary and tentative, one can nevertheless attempt to draw some conclusions concerning the nature of an "ideal" carrier—antigen conjugate. Aside from compatibility with the membrane matrix, such a conjugate should preferably have a simple ion selectivity profile, with dominant selectivity for K^+ and Na^+ in the case of biological fluids. Since the model predicts that the maximum ΔE values in response to antibody additions should be obtained when the contributions from the two ions selected are equal, the selectivity of the "ideal" conjugate should thus be tailored to reflect the approximate Na^+ and K^+ concentration ratio in biological fluid samples. A flat pH response in the physiological range would further serve to simplify analytical measurements.

We gratefully acknowledge the financial support of grant GM 25308 from the National Institutes of Health.

REFERENCES

1 G. Fricke, Anal. Chem., 52 (1980) 259R.
2 M. Aizawa, S. Kato and S. Suzuki, J. Membr. Sci., 2 (1977) 125.
3 N. Yamamoto, Y. Nagasawa, S. Shuto, M. Sawai, T. Sudo and H. Tsubomura, Chem. Lett., (1978) 245.
4 R. L. Solsky and G. A. Rechnitz, Science, 204 (1979) 1308.
5 W. M. Feigenbaum and R. H. Michel, J. Polym. Sci., 9 (1971) 817.
6 J. K. Inman and H. M. Dintzis, Biochemistry, 8 (1969) 4074.
7 F. Sanger, Biochem. J., 39 (1945) 307.

Analytica Chimica Acta, 123 (1981) 143—150

CATALYTIC DETERMINATION OF SELENIUM WITH A PICRATE-SELECTIVE ELECTRODE

E. P. DIAMANDIS and T. P. HADJIIOANNOU*

Laboratory of Analytical Chemistry, University of Athens, Athens (Greece)

(Received 9th July 1980)

SUMMARY

A method is described for the determination of selenium, based on its catalytic effect on the picrate—sulfide reaction. The determination involves a variable-time kinetic procedure using potentiometric monitoring with a picrate-selective electrode and automatic measurement of the time required for the potential to change by a preselected amount (5.0 mV). Selenium in the range 3—30 μg was determined with an average error of about 4% and relative standard deviations of about 2%. The reaction can also be followed spectrophotometrically.

The physiological role of selenium as a trace element is not well established. Selenium has been reported as having carcinogenic properties; other authorities have presented evidence that, at low levels, selenium is an essential element in the diet [1], while at higher concentrations it is toxic. A protective role of selenium against malignant disease has also been reported [2].

The most commonly used methods for the determination of selenium are based on the measurement, spectrophotometric or fluorimetric, of the piazselenols formed when selenium(IV) reacts with aromatic *o*-diamines such as 3,3′-diaminobenzidine or 2,3-diaminonaphthalene [3—6]. These methods are time-consuming and the reagents required are toxic and relatively unstable. The determination of selenium by atomic absorption spectrometry has also been reported [7—9]. The catalytic effect of selenium in redox reactions has been used to determine traces of selenium [10—13].

Recently, a new picrate-selective membrane electrode [14] and its applications to potentiometric titrations [15] and kinetic determinations [16] have been reported. In this paper, an automated kinetic potentiometric method is described for the determination of selenium, based on the catalytic effect of selenium in the reduction of picrate by sodium sulfide in alkaline media. The reaction is monitored with a picrate-selective electrode; the time required for the potential to change by a preselected amount (5.0 mV) is measured automatically with a window comparator [17] and related directly to the selenium concentration. Amounts of selenium in the range 3—30 μg in a sample volume of 15.00 ml can be determined with good accuracy and precision.

EXPERIMENTAL

Instrumentation

Electrodes. The picrate-selective membrane electrode was constructed as previously described [14] but with a teflon membrane [16]. A double-junction silver—silver chloride electrode (Orion model 90-02-00) served as the reference electrode with its outer compartment filled with equitransferent Orion 90-00-01 solution. The electrode potential was measured with an Orion Ionalyzer, Model 801.

Reaction cell. A double-walled 50-ml beaker was used as reaction cell. Water was circulated continuously through the reaction cell jacket with a thermostatted pump. The reaction mixtures were stirred with the aid of a magnetic stirrer.

Recording and measurement system. The recording and measurement system was the same as previously described [17]. The Window Comparator was used for automatic measurement of the time, Δt, required for the recorder pen to cross preselected positions in the chart corresponding to $(E_0 + 2.0)$ mV and $(E_0 + 7.0)$ mV, where E_0 is the initial electrode potential.

Reagents

All solutions were prepared with deionized—distilled water from reagent-grade materials (Merck except where specified).

Sodium picrate solution, 0.0100 M. Neutralize a suitable picric acid solution with sodium hydroxide solution to a pH about 6. No standardization is required. The solution should be kept in an amber bottle. The picric acid used was Fluka purum.

Composite solution A, 5% Na_2EDTA (w/v)—3.0 × 10^{-4} M Fe(III). Dissolve 0.0080 g of $FeCl_3 \cdot 6H_2O$ in about 80 ml of water, add 5.0 g of Na_2EDTA in small portions, adjust the pH to 7.0 with sodium hydroxide and dilute to 100 ml.

Composite buffer solution B, 0.25 M Na_2S—1.00 M $NaHCO_3$, pH 10.8. Dissolve 6.0 g of $Na_2S \cdot 9H_2O$ in about 80 ml of water, add 8.4 g of sodium hydrogencarbonate in small portions, adjust the pH to 10.8 with sodium hydroxide and dilute to 100 ml. The solution is kept in a refrigerator when not in use.

Stock selenium solution, 500 ppm. Dissolve 0.5000 g of pure selenium in a few drops of concentrated nitric acid, boil gently to expel brown fumes and dilute to 1 l with water. Standard working solutions (0.2, 0.5, 1, 2 ppm) were prepared by appropriate dilution.

During measurements all solutions are thermostatted at 60 ± 0.2°C.

Procedure

Transfer 15.00 ml of the selenium standard or sample solution, 3.00 ml of composite solution A and 2.00 ml of composite solution B to the reaction

cell, thermostatted at 60°C (final pH 10.1). Immerse the electrodes in the solution and start stirring at the maximum speed at which air bubbles are not formed. After about 1 min, inject rapidly 1.00 ml of 0.01 M sodium picrate solution, immediately start the recorder and record the potential change for a few minutes. For automatic measurements, after injecting the sodium picrate solution, press the Start button of the Universal Digital Instrument. The analysis is completed automatically and the number on the digital readout (time in hundredths of a second) is recorded. Press the Reset button, empty the cell with suction, rinse the electrodes and the cell with water and dry them with suction. The amount of selenium present is obtained from a calibration curve constructed by plotting Δt^{-1} (s^{-1}) vs. ppm Se.

RESULTS AND DISCUSSION

Effect of pH

The effect of pH on the rate of the selenium-catalyzed picrate–sulfide reaction was studied by carrying out the reaction at various pH values and various selenium concentrations. The composite buffer solution B did not contain hydrogencarbonate, and the pH was adjusted to the desired value with sodium hydroxide or hydrochloric acid. Figure 1 shows calibration curves for selenium at various pH values. The pH chosen, 10.1, is a compromise to ensure small blanks and relatively short measurement times. At lower pH values the blank is smaller but the measurements are less precise.

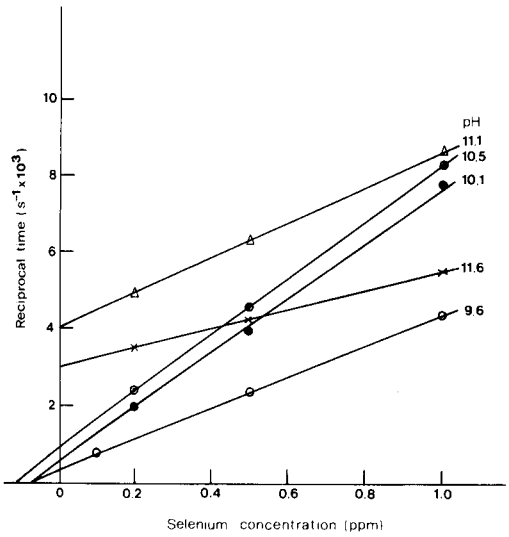

Fig. 1. Calibration curves for selenium at various pH values.

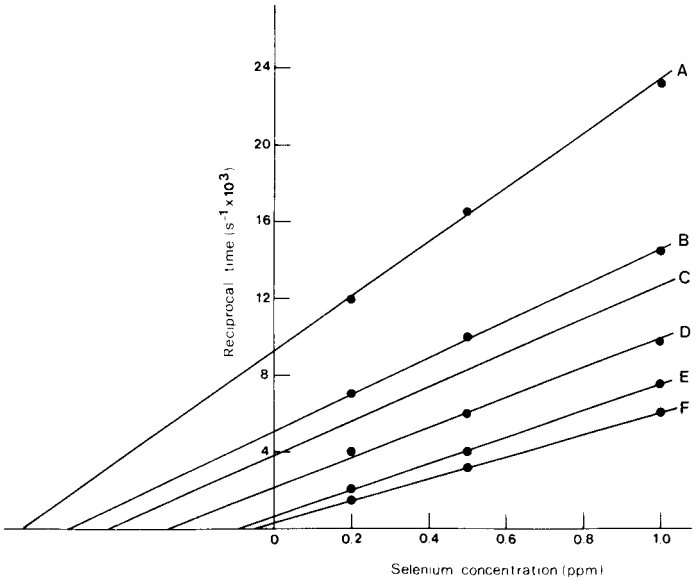

Fig. 2. Calibration curves for selenium at various initial iron concentrations (M): (A) 1.6×10^{-3}; (B) 7.4×10^{-4}; (C) 3.7×10^{-4}; (D) 8.5×10^{-5}; (E) 4.2×10^{-5}; (F) 2.1×10^{-5}. Other conditions as under Procedure.

Effect of iron concentration

It was observed that iron(III) in the presence of EDTA activates strongly the catalytic effect of selenium. This observation parallels earlier observations of West and Ramakrishna with the selenium-catalyzed methylene blue—sodium sulfide reaction [12]. In order to establish the optimum concentration of iron essential to accelerate the reaction, experiments were done as in the recommended procedure but with various concentrations of iron. Figure 2 shows a series of calibration curves obtained with various iron concentrations. As the iron concentration increases, the measurement times decrease but the blank increases. An initial concentration of 4.2×10^{-5} M (curve E) was chosen for the recommended procedure as a compromise between the reaction rate and blank effects.

Effect of picrate and sulfide concentrations

To study the effect of picrate concentration on the selenium-catalyzed picrate—sulfide reaction in the presence of the iron—EDTA complex and a large excess of sulfide [18], the concentration of the picrate solutions used in the recommended procedure was varied in the range 0.01—0.1 M. It was found that the initial rate of potential change is independent of the initial picrate concentration.

The effect of sulfide concentration on the rate of the selenium-catalyzed reaction was studied in the absence of iron for various sulfide and selenium

concentrations. The reaction rate increases with increasing sulfide concentration up to an initial sodium sulfide concentration of about 0.048 M, but remains practically constant at higher concentrations. An initial sulfide concentration of 0.0238 M (0.25 M Na_2S in composite solution B) was chosen to ensure short measurement times and small blanks. Composite buffer solution B is relatively stable when stored in a refrigerator. Over a period of a week the blank increased gradually but the detection limit was unaffected.

Effects of temperature and standing time

The rate of the reaction increases with increasing temperature in the range 30—60°C (Fig. 3). A temperature of 60°C was chosen, to ensure small measurement times without endangering the operation of the electrode. Under these conditions, the electrode response was unaffected for more than two months.

In order to study the effect of standing time, series of solutions containing 0.5 ppm of selenium were treated with all reagents except picrate as described in the recommended procedure. The solutions were allowed to stand for different periods of time (0.5—11 min) before the addition of picrate. It was found that the rate of the reaction is unaffected by standing time.

Interference studies

To investigate the effect of various ions that might interfere in the determination of selenium, measurement times for solutions containing 1 ppm of selenium and 50 ppm of the ion being investigated were compared with

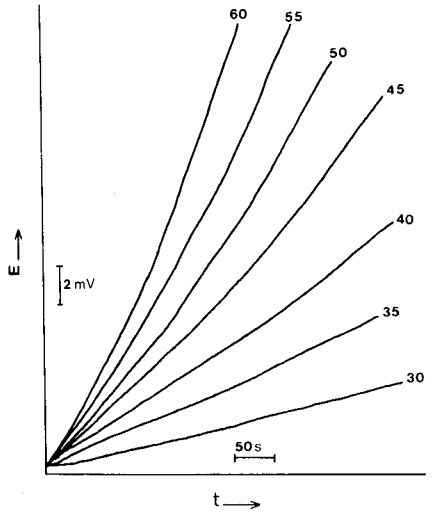

Fig. 3. Recorded curves of the cell voltage vs. time for the picrate—sulfide reaction at various temperatures (°C). Se = 1 ppm, other conditions as under Procedure.

those for a 1 ppm selenium solution (n = 7). The following cations did not interfere: Li^+, K^+, Mg^{2+}, Ca^{2+}, Sr^{2+}, Ba^{2+}, Zn^{2+}, Mn^{2+}, Co^{2+}, Ni^{2+}, Cd^{2+}, Pb^{2+}, Al^{3+}, Cr^{3+}, Zr^{4+} (from the respective chloride or nitrate salts) and Te^{4+} (Na_2TeO_3). Hg^{2+} and Sn^{2+} ions (as their chloride salts) did not interfere at the 10 and 5 ppm level, respectively. Ag^+ ($AgNO_3$) and Cu^{2+} ($CuCl_2 \cdot 2H_2O$) ions interfered even at concentrations below 5 ppm. All interfering ions but Cu^{2+} caused negative errors.

Accuracy and precision

The voltage interval of 5.0 mV was chosen so that the measurement error is small in comparison. Figure 4 shows typical recorded curves and the corresponding calibration curve for the selenium-catalyzed reaction. The accuracy and precision of the method were tested by analyzing solutions containing known amounts of selenium. Results are shown in Table 1.

Spectrophotometric studies

The selenium-catalyzed picrate—sulfide reaction can also be followed by measuring the absorbance of the reaction product at 490 nm. Absorbances were measured with a Heath Model 701 recording spectrophotometer. The cell compartment was modified to accept a 10-ml thermostatted cuvette, with a pathlength of 1.3 cm, and a magnetic stirrer. The following procedure is suitable. An aliquot (5.00 ml) of the selenium standard or sample solution (0.1—1.4 ppm) followed by 1.00 ml of composite solution A and 0.700 ml of composite solution B are transferred to the cuvette and thermostatted at

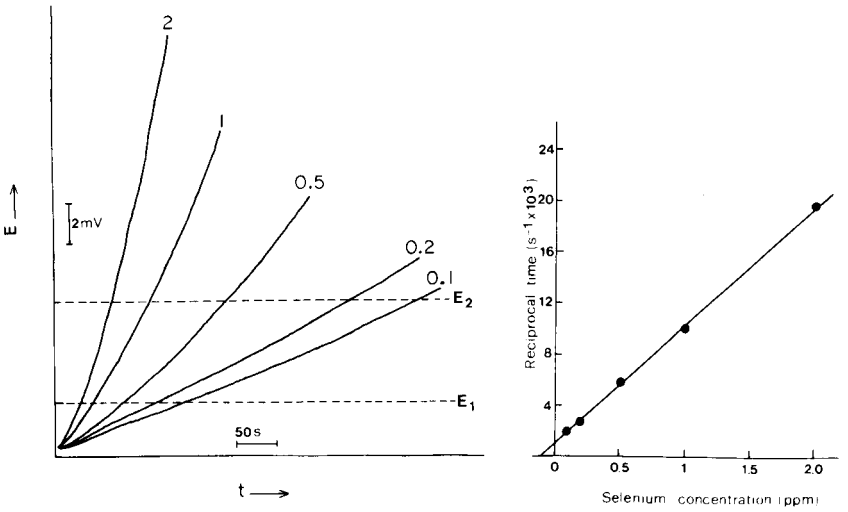

Fig. 4. Recorded curves of the cell voltage vs. time for the picrate—sulfide reaction in the presence of selenium, and the corresponding calibration curve. The numbers on the curves correspond to ppm Se. Other conditions as under Procedure.

TABLE 1

Results for the determination of selenium in aqueous solutions

Taken (ppm)	Found (ppm)[a]	Error (%)	R.s.d. (%)[b]
0.200	0.174	−13	—
0.500	0.479	−4	2.1
1.00	1.02	+2	1.7
2.00	1.99	−0.5	—

[a]Average of two measurements. [b]n = 8.

60°C. The stirrer is started and, after 2 min, 1.00 ml of 3×10^{-3} M sodium picrate solution is added rapidly. Immediately the recorder is started and the absorbance change is measured for about 4 min (at 490 nm). The amount of selenium present is obtained from a calibration curve constructed by plotting ΔA values ($A_{3\ min} - A_{0.5\ min}$) vs. ppm Se (Fig. 5).

The accuracy of the spectrophotometric procedure was checked by analyzing solutions containing known amounts of selenium in the range 0.1—1.4 ppm. The relative error ranged from 0.3 to 6.7% with an average of 3.2%.

In conclusion, the selenium-catalyzed picrate—sulfide reaction can be used

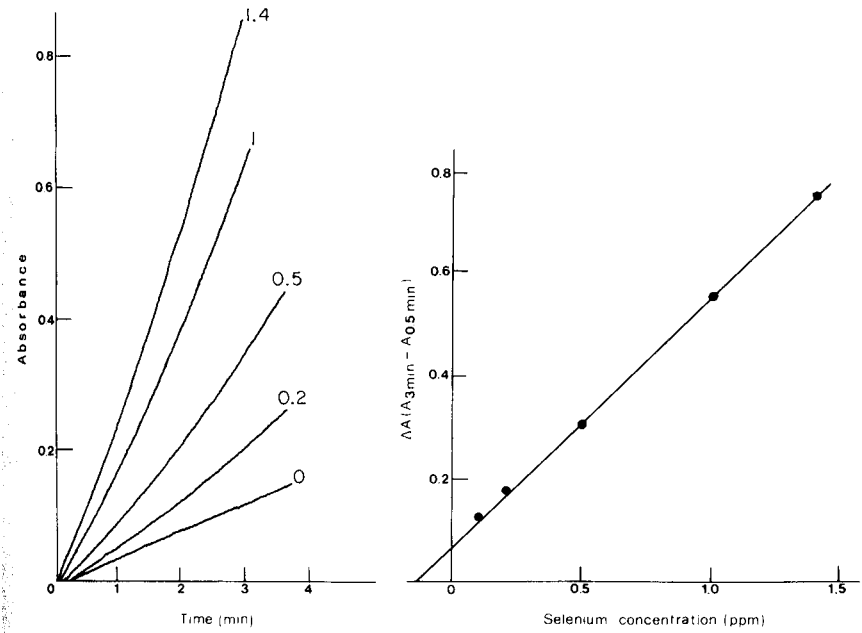

Fig. 5. Recorded curves of the absorbance vs. time for the picrate—sulfide reaction in the presence of selenium, and the corresponding calibration curve. The numbers on the curves correspond to ppm Se. Other conditions as under Procedure.

for analytical purposes to determine selenium in the range 0.1—2 ppm by a potentiometric or spectrophotometric technique.

The authors thank C. E. Efstathiou for stimulating discussions, and C. Athanassopoulou and Z. Nanou for technical assistance.

REFERENCES

1 M. Jacobs, Cancer, 40 (1977) 2557.
2 W. R. Wolf, Anal. Chem., 50 (1978) 190A.
3 R. J. Hall and P. L. Gupta, Analyst, 94 (1969) 292.
4 M. W. Brown and J. H. Watkinson, Anal. Chim. Acta, 89 (1977) 29.
5 N. D. Michie, E. J. Dixon and N. G. Bunton, J. Assoc. Off. Anal. Chem., 61 (1978) 48.
6 Y. Shimoishi and K. Tôei, Anal. Chim. Acta, 100 (1978) 65.
7 K. G. Brodie, Am. Lab., 9 (1977) 73.
8 M. Ihnat and H. J. Miller, J. Assoc. Off. Anal. Chem., 60 (1977) 813.
9 F. D. Pierce and H. R. Brown, Anal. Chem., 49 (1977) 1417.
10 T. Kawashima, S. Kai and S. Takashima, Anal. Chim. Acta, 89 (1977) 65.
11 F. Feigl and P. W. West, Anal. Chem., 19 (1947) 351.
12 P. W. West and T. V. Ramakrishna, Anal. Chem., 40 (1968) 966.
13 J. H. Tzeng and H. Zeitlin, Anal. Chim. Acta, 101 (1978) 71.
14 T. P. Hadjiioannou and E. P. Diamandis, Anal. Chim. Acta, 94 (1977) 443.
15 E. P. Diamandis and T. P. Hadjiioannou, Mikrochim. Acta (Wien), II (1977) 225.
16 E. P. Diamandis, M. A. Koupparis and T. P. Hadjiioannou, Microchem. J., 22 (1977) 498.
17 C. E. Efstathiou and T. P. Hadjiioannou, Anal. Chim. Acta, 89 (1977) 55.
18 T. S. West, Analyst, 17 (1962) 630.

Analytica Chimica Acta, 123 (1981) 151—159

CHLORIDE INTERFERENCE WITH NON-STOICHIOMETRIC COPPER SULPHIDE COPPER(II)-SELECTIVE ELECTRODES
Part 1. Mechanisms

TADEUSZ HEPEL

Institute of Chemistry, Jagiellonian University, 30-060 Kraków (Poland)

(Received 7th February 1980)

SUMMARY

The behaviour of copper(II)-selective electrodes made of non-stoichiometric copper sulphide single crystals is discussed. The mechanism of chloride ion interference with the electrode operation is considered on the basis of potentiometric and dynamic measurements. The occurrence of irreversible processes at the electrode surface is described.

The electrochemical behaviour of solid-state membrane electrodes is of great practical, as well as theoretical interest, and various electrodes have been investigated [1—6], particularly with regard to analytical applications. Several papers have considered the thermodynamics of these electrodes [6—10] and the kinetic parameters of the potential-determining reactions proceeding with participation of the electrode material [11—15]. Such investigations can help to explain the different observations noted by different workers. On the basis of dynamic measurements, some conclusions can be drawn concerning the construction of ion-selective electrodes and the best measuring conditions for ion activities. Various aspects of the mechanism of anodic dissolution of copper sulphide electrodes in aqueous ammonia solutions have been described previously [12]. The establishment of the electrochemical metastable equilibrium

$$CuS(n-s) + Cu(NH_3)_p^{2+} + 2e^- = Cu_2S(n-s) + p\ NH_3(aq) \quad (1)$$

has been proved [10—12], and for this case the Nernst equation has been proposed [10] in the form (for p = 4)

$$E_{n-s}^{(ms)} = E_{n-s}^{0(ms)} + RT(2F)^{-1} \ln [Cu(NH_3)_4^{2+}] - 2RTF^{-1} \ln [NH_3] \quad (2)$$

$$E_{n-s}^{0(ms)} = E^{0(ms)} + RT(2F)^{-1} \ln \{[CuS(n-s)]/[Cu_2S(n-s)]\} \quad (3)$$

In these equations (ms) denotes the metastable equilibrium; $[CuS(n-s)]$ and $[Cu_2S(n-s)]$ are the respective activities of the CuS and Cu_2S components in the non-stoichiometric solid phase (or phases) $Cu_{2-x}S(s)$. Quite a different situation exists in concentrated chloride solutions where the strong influence of chloride ions on the electrode potential has been observed repeatedly

[2, 7, 16—20] for Radiometer Selectrodes as well as for Orion 94-29 copper(II)-selective electrodes. For the latter electrodes, this has been attributed [16] to the reaction

$$Ag_2S(s) + Cu^{2+}(aq) + 2Cl^-(aq) = CuS(s) + 2AgCl(s) \quad (4)$$

(possibly with formation of chlorosilver complexes [7]), or to the complexation of copper(II) [17]

$$Cu^{2+} + p\ Cl^- = CuCl_p^{2-p} \quad (5)$$

The use of an electrode material which does not contain silver sulphide makes it possible to establish whether or not reaction (5) is responsible for the chloride interference with the copper sulphide electrode operation. In this paper, the mechanism of a non-stoichiometric copper sulphide electrode operation in concentrated chloride solutions is discussed; it is shown that non-equilibrium processes occur at the electrode surface.

EXPERIMENTAL

Non-stoichiometric copper sulphide with the composition $Cu_{1.88}S$ was used. This material was made from spectrally pure copper (Johnson Matthey) and elemental sulphur (POCh, Gliwice) in quartz ampoules under vacuum (10^{-5} torr), by heating gradually to melting (1250°C) and then slowly cooling for 3 days to room temperature. The cylindrical samples were cut into wafers about 2 mm thick by means of a tungsten wire saw (for semiconductors; IF-07A, Unipress; 20 μm diameter wire). The wafers were glued with epoxy resin to teflon or plexiglas holders fitted with a spring-loaded silver-gilt electric contact. The electrode surface was polished with alumina of different grain sizes up to 1200. The measurements were done by using the rotating disk electrode technique. The instrumentation used was similar to that described earlier [11]; the measurement error was less than ±0.1%.

The copper sulphide single-crystal electrode potential was measured with respect to a conventional saturated calomel electrode (SCE) using a digital voltmeter (V-529, Meratronik) with an error of 0.05%. In all the equations presented here, the electrode potentials are referred to the normal hydrogen electrode (NHE); the potential of the SCE was assumed to be 243.8 mV at 25°C and 247.1 mV at 20°C vs. NHE [21]. The liquid junction potential was neglected; it was presumably less than 1 mV in the case of NH_4Cl/KCl junction (the transport numbers and the limiting equivalent conductivities for NH_4^+ and K^+ are almost equal [22]).

Solutions were prepared from triply-distilled water and analytical reagent-grade chemicals which were always recrystallized twice at least. Before measurement the solutions were deoxygenated by passing purified argon (saturated with water vapour) through them.

RESULTS AND DISCUSSION

Before the actual experiments, the copper-sulphide electrodes were tested in copper(II) nitrate solutions acidified to a pH value of 3. A typical dependence of the electrode potential on the activity of copper(II) ions in solutions with compositions of (0.1 − 3x) M KNO_3 + x M $Cu(NO_3)_2$ and (0.1 − 3x) M NH_4ClO_4 + x M $Cu(NO_3)_2$, is presented in Fig. 1. The slopes obtained, $\partial E_{n-s}^{(ms)}/\partial$ log [Cu(II)], which are 29.5 mV/decade, agree very well with the Nernst equation at 25°C for a two-electron reaction: $Cu^{2+}(aq) + CuS(n - s) + 2e^- = Cu_2S(n - s)$. The activity coefficients for copper(II) ions were calculated from the Davies equation (using the value 78.30 for the dielectric constant of water, and the value 0.5115 for the limiting Debye-Hückel slope A [22]). The influence of nitrate and perchlorate on the electrode potential at higher concentrations of copper(II) ions is clearly not greater than the effect of ionic strength changed up to 5 M. There was a small shift of the electrode potential towards more negative values in ammonium sulphate solutions, and this can be explained by formation of the $CuSO_4(aq)$ ion pair in concentrated solutions [10].

A much stronger effect was noted in chloride solutions. The results of experiments carried out in aqueous ammonium chloride solutions containing 10^{-4} M $Cu(NO_3)_2$ at a pH of about 3 are shown in Fig. 2. Pronounced chloride interference starts from $[Cl^-] \cong 5 \times 10^{-2}$ M, with a shift in the electrode potential of about −10 mV. According to Orion Research [16], the interference for the Orion 94-29 copper(II) ion electrode depends on the level of chloride ion relative to the level of copper(II) ion in the solution and occurs if 2 log $[Cl^-]$ + log $[Cu^{2+}] > -5.80$. However, Crombie et al. [18] stated that the Orion electrode responds to the chloride concentration when the experimental relation is 2.8 log $[Cl^-]$ − log $[Cu^{2+}] > -2.7$. The latter

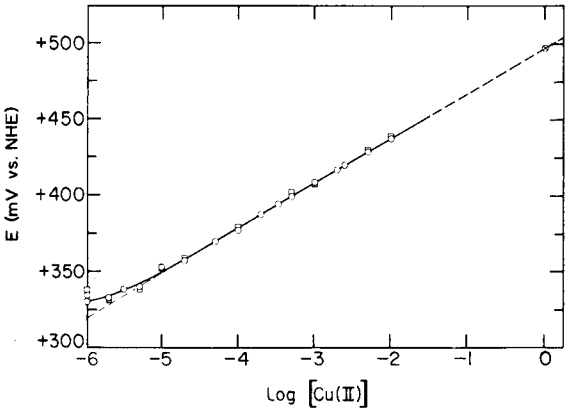

Fig. 1. Calibration curve for the non-stoichiometric copper sulphide electrode in: (○) (0.1−3x) M KNO_3 + xM $Cu(NO_3)_2$; (□) (0.1−3x)M NH_4ClO_4 + xM $Cu(NO_3)_2$; 25°C, pH 3. $E_{n-s}^{o(ms)}$ = 497 mV vs. NHE. Copper concentrations in molarity.

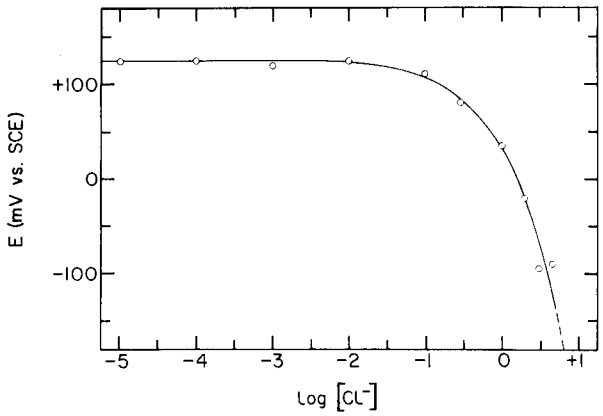

Fig. 2. Effect of chloride ion molarity on the copper sulphide electrode potential at a constant initial Cu(II) concentration of 10^{-4} M at pH 3 and 20°C.

expression gives a value of about 4×10^{-3} M for the critical chloride concentration for 10^{-4} M $[Cu^{2+}]$. The non-stoichiometric copper sulphide single-crystal electrodes synthesized in the present work are then less sensitive to the chloride level in the solution.

Considering the ionic equilibria in the solutions in question, the following set of expressions was constructed for the copper(II) ion-copper sulphide electrode potential in concentrated chloride solutions

$$E_{n-s}^{(ms)} = E_p^{0(ms)} + RT(2F)^{-1} \ln \{[CuS(n-s)]/[Cu_2S(n-s)]\} +$$

$$RT(2F)_X^{-1} \ln [CuCl_p^{2-p}] - pRT(2F)^{-1} \ln [Cl^-] \quad (6)$$

where p is the number of ligands in the p-chlorocopper(II) complexes. The standard electrode potentials calculated for the possible reactions:

$$CuCl_p^{2-p} + CuS(n-s) + 2e = Cu_2S(n-s) + pCl^- \quad (7)$$

corresponding to eqn. (6) are presented in Table 1. Other data concerning particular copper(II) complexes are also given in Table 1.

TABLE 1

Formal standard electrode potentials for reaction (7) with activity coefficients for the respective chloro complexes of copper(II) at ionic strength 5 M and 25°C, calculated from recent data [23]

Species	Cu^{2+}	$CuCl^+$	$CuCl_2$	$CuCl_3^-$	$CuCl_4^{2-}$
$E_f^{0\,ms}$ (V)	+0.571	+0.564	+0.573	+0.597	+0.638
$\log \beta_{1,p}$	—	+0.176	−0.201	−1.05	−2.50
$[Cl^-]$ (M)[a]		0.667	2.38	(7.14)	(27.8)

[a]Concentration of chloride ions at the boundary of the domains of the relative predominance of particular Cu(II) species at an ionic strength of 5 M.

It follows from Table 1 and eqn. (6) that at the boundary of two domains of relative predominance of $Cu^{2+}(aq)$ and $CuCl^{+}$ ions, i.e. at a chloride ion concentration of 0.67 M (at μ = 5 M), the shift of the copper sulphide electrode potential should be −8.9 mV. Such a deviation was obtained experimentally even at a chloride ion level of 4.8×10^{-2} M, and therefore it cannot be explained by any complex formation in the copper(II)—chloride ion system. The remaining complexes, $CuCl_2$, $CuCl_3^-$ and $CuCl_4^{2-}$, are of no importance because they exist in relative predominance only at higher chloride ion concentrations. Suggestions that the formation of chloro—copper(II) complexes are responsible for the chloride ion interference do not then explain the electrode behaviour in chloride media, and reaction (7) cannot be considered as potential-determining.

As the occurrence of some irreversible reactions at the copper sulphide electrodes is expected, polarization measurements were studied. Investigations were done with the rotating disk electrode technique [24] by using stationary current—voltage characteristics. The anodic currents flowing through the electrode at linear potential sweep are presented in Fig. 3. Measurements were done for 4.5 M NH_4NO_3 and 4.5 M NH_4Cl solutions without addition of Cu(II) and Cu(I) ions. On the basis of this plot and additional detailed investigations concerning the effect of the chloride ion on the rate of the electrode process, it is notable that anodic dissolution of the electrode material in concentrated chloride solutions requires participation of chloride ion as reagent. At the same time, Cu(I) ions pass from the electrode material into the solution. In this connection, the overall reaction taking place under these conditions can be written as

$$Cu_{2-x}S(s) + \delta\, pCl^- - \delta\, e^- = Cu_{2-x-\delta}S(s) + \delta\, CuCl_p^{1-p} \qquad (8)$$

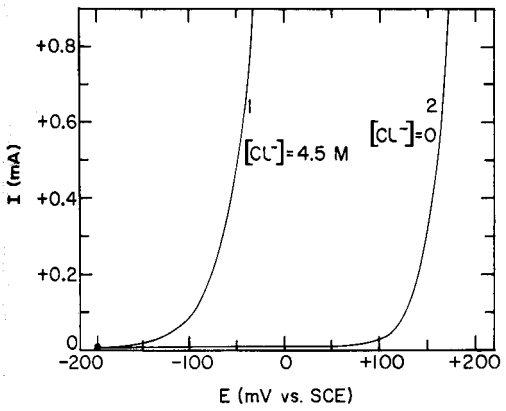

Fig. 3. Anodic current—voltage characteristics for the non-stoichiometric copper sulphide single crystal electrode in 4.5 M NH_4Cl (curve 1) and 4.5 M NH_4NO_3 (curve 2) in the absence of Cu(II) ions at pH 2.5. Rotation speed of the $Cu_{2-x}S$-disk electrode, 3400 rpm; potential sweep, 15 mV s^{-1}.

$$\text{or } Cu_2S(n-s) + pCl^- - e^- = CuS(n-s) + CuCl_p^{1-p} \quad (9)$$

The current efficiency of this reaction with respect to copper(I) ions was found to be 100.6 ± 0.2% (n = 1).

To check whether the reverse rate of reaction (8, 9) is sufficiently large, and so whether or not this reaction can be potential-determining for these copper sulphide electrodes in chloride-containing solutions, a series of measurements was done in 4.5 M NH_4Cl solution containing various amounts of copper(I) chloride, because some chlorocopper(I) complexes are substrates of this reaction. The cathodic wave of the copper(I) reduction in a solution of 2×10^{-4} M $CuCl_3^{2-}$ at an angular velocity of the rotating disk of 356 rad s^{-1} (3400 rpm) is shown in Fig. 4. (curve 1). It can be concluded from the shape of this curve (and also from the analysis of other data for other Cu(I) concentrations) that the reaction under consideration is very fast. Since copper(I) complexes can be reduced to form copper metal, similar experiments were made on a rotating copper-disk electrode (curve 2). It can be concluded from Fig. 4 (curves 1 and 2) that the chlorocopper(I) complexes are reduced at the copper sulphide electrode without volume-phase deposition of copper metal when the electrode potential does not attain a value of about −370 mV vs. SCE (i.e., about −126 mV vs. NHE, neglecting the liquid junction potential). At higher electrode potentials, no copper grains or films can exist at the copper sulphide membrane surface, but must be oxidized and pass into the solution or be incorporated into the copper sulphide crystal lattice as Cu^+ ions ($Cu_2S_{(n-s)}$). In this way, the occurrence of reaction (9) is proved to be not only fast but reversible. At extremely low copper(II) ion concentrations, the copper sulphide electrode potential in concentrated chloride solutions containing copper(I) ions ought then to fulfil a Nernst

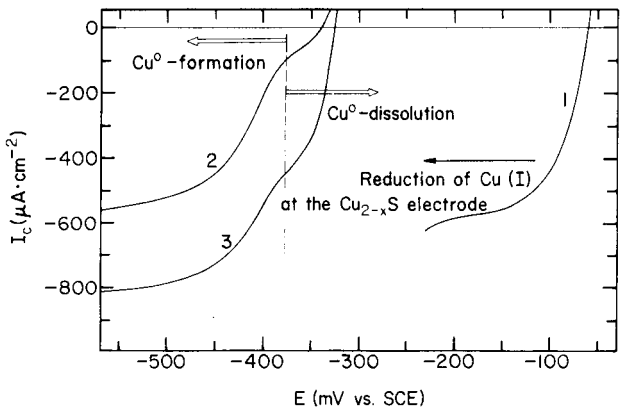

Fig. 4. Cathodic polarization waves for the reduction of Cu(I) ions at the copper sulphide disk electrode (curve 1) and copper metal disk electrode (curve 2) in 4.5 M NH_4Cl + 2×10^{-4} M Cu(I). Curve 3 corresponds to consecutive reduction of Cu(II) ions at the copper disk electrode in 4.5 M NH_4Cl + 10^{-4} M Cu(II). Rotation speed, 3400 rpm; potential sweep rate, 15 mV s^{-1}.

equation of the type

$$E^{(ms)} = E^{0(ms)}_{n-s} + RTF^{-1} \ln [CuCl_p^{1-p}] - pRTF^{-1} \ln [Cl^-] \quad (10)$$

which in the domain of relative predominance of $CuCl_3^{2-}$ complexes (i.e., at free chloride ion concentrations greater than about 1 M [25]) may be rewritten in the form (for 25°C)

$$E^{(ms)} = E^{0(ms)}_{n-s} + 0.05916 \log [CuCl_3^{2-}] - 0.17748 \log [Cl^-] \quad (11)$$

It follows from thermodynamic calculations that the formal standard electrode potential for reaction (9) with p = 3 equals 0.597 V vs. NHE.

For confirmation of the dependence of the copper sulphide electrode potential on the $CuCl_3^{2-}$ ion concentration, potentiometric measurements were carried out in ammonium chloride solutions of composition 4.5 M NH_4Cl + 10^{-3} M HCl + x M Cu(I); the results obtained are plotted in Fig. 5 (curve 3). The measurements were made by using the rotating copper sulphide disk electrode and each point on this curve is the mean of 5—9 measurements at various rotation speeds of the electrode. No systematic changes of the electrode potential with the angular velocity of the disk were observed. The linear relation obtained has a slope ($\partial E^{(ms)}/\partial \log [CuCl_3^{2-}]$) equal to 55.0 mV/decade change in the $CuCl_3^{2-}$ concentration; this agrees reasonably well with the theoretical expectation (of 58.1 mV/decade at 20°C) (see below). These investigations (cf. [26]) thus do not confirm the results obtained by Vencatachalam and Mallikarjunan [27] who found that the copper sulphide single crystal electrode potential did not depend on the copper(I) ion concentration in chloride solutions.

The reactions that occur at the copper sulphide all-solid-state membrane electrode when it is immersed in concentrated chloride solution containing

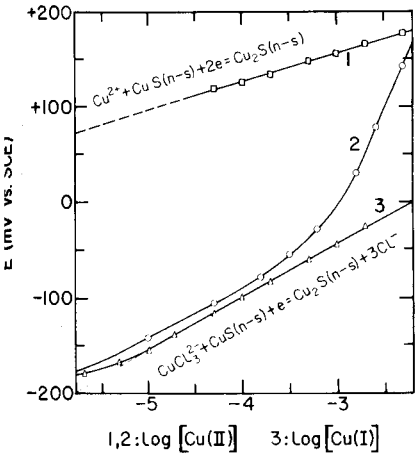

Fig. 5. Dependence of the non-stoichiometric copper sulphide electrode potential on the Cu(II) ion concentration (curves 1, 2) and Cu(I) ion concentration (curve 3) in solutions which contained (1) 4.5 NH_4NO_3; (2, 3) 4.5 M NH_4Cl, at pH 3, and 20°C.

copper(II) ions may be considered as follows. The potentiometric measurements for such a case are shown in Fig. 5, curve 2. In the copper(II) ion concentration range up to about 4×10^{-4} M, the course of the E vs. log [Cu(II)] relationship indicates that neither the redox reaction

$$CuCl_p^{2-p} + (q - p)\,Cl^- + e^- = CuCl_q^{1-q} \qquad (12)$$

for which the equilibrium potential measured at the platinum indicator electrode is very high, nor the reaction

$$CuCl_p^{2-p} + CuS(n - s) + 2e = Cu_2S(n - s) + pCl^- \qquad (13)$$

can control the electrode potential. The slope ($\partial E/\partial$ log [Cu(II)]) of 55 mV suggests that the potential-determining reaction occurs with transfer of one electron. The assumption that the reaction

$$CuCl_3^{2-} + CuS(n - s) + e^- = Cu_2S(n - s) + 3Cl^- \qquad (14)$$

is potential-determining, is the most probable explanation for this phenomenon. Indeed, the copper(I) complexes can form at the electrode surface even at quite small anodic polarization, because of the high exchange current density j_0 of reaction (14). Anodic polarization in this case is due to the reduction of copper(II) via eqns. (12) and (13).

Because the non-equilibrium potential (the so-called mixed potential) of the copper sulphide electrode lies near the metastable equilibrium of reaction (14), reactions (12) and (13), which presumably proceed in the diffusion kinetics region, may be characterized by the limiting diffusion current density j_d^I, which is much smaller than the exchange current density for reaction (14): $j_d^I/j_0^{II} \approx 0$. However with increasing copper(II) ion concentrations in the solution, j_d^I increases in direct proportion to copper(II) concentration, whereas the rate of the exchange reaction (14) increases only by the power $\alpha \cong 0.5$ (where α is the charge-transfer coefficient for the cathodic direction of reaction 14). Accordingly, the higher the copper(II) concentration in the solution, the greater the deviations of the observed non-equilibrium electrode potential from the equilibrium value characteristic for reaction (14). The experimental results presented in Fig. 5 show such a situation.

REFERENCES

1 See, e.g. H. Frieser (Ed.), Ion-selective Electrodes in Analytical Chemistry, Plenum, New York, 1979.
2 R. P. Buck, Anal. Chem., 48 (1976) 23 R; Ion Enzyme Electrodes Biol. Med., Int. Workshop, 1976, 38.
3 G. J. M. Heijne, W. E. van der Linden and G. den Boef, Anal. Chim. Acta, 89 (1977) 287; 93 (1977) 99; 96 (1978) 13; 98 (1978) 221.
4 W. G. Morf, G. Kahr and W. Simon, Anal. Chem., 46 (1974) 1538.
5 M. Koebel, Anal. Chem., 46 (1974) 1559.
6 E. H. Hansen, C. G. Lamm and J. Růžička, Anal. Chim. Acta, 59 (1972) 403.
7 P. Lanza, Anal. Chim. Acta, 105 (1979) 53.
8 M. Sato, Electrochim. Acta, 11 (1966) 361.

9 H. J. Mathieu and H. Rickert, Z. Phys. Chem. N.F., 79 (1972) 315.
10 T. Hepel and M. Hepel, Electrochim. Acta, 22 (1977) 295.
11 M. Hepel, J. Electroanal. Chem., 74 (1976) 37.
12 M. Hepel and T. Hepel, J. Electroanal. Chem., 81 (1977) 161.
13 A. Etienne, Ph.D. Thesis, University of British Columbia, Vancouver, 1969.
14 M. Koebel, N. Ibl and A. M. Frei, Electrochim. Acta, 19 (1974) 287.
15 E. P. Medvedeva, Z. B. Rozhdestvenskaya and A. K. Kulikovskii, Izv. Acad. Nauk Kazakh. SSR, Ser. Khim., 26 (1976), No. 4., 80.
16 Orion Research, Inc., Cupric Ion Electrode Instruction Manual, Form IM 94-29/1721, 1971.
17 G. B. Oglesby, W. C. Duer and F. J. Millero, Anal. Chem., 49 (1977) 877.
18 D. J. Crombie, G. J. Moody and J. D. R. Thomas, Talanta, 21 (1974) 1094.
19 D. Midgley, Anal. Chim. Acta, 87 (1976) 19.
20 R. Jasiński, I. Trachtenberg and D. Andrychuk, Anal. Chem., 46 (1974) 364.
21 R. G. Bates, Determination of pH, National Bureau of Standards, J. Wiley, New York, 1964.
22 J. N. Butler, Ionic Equilibrium, Reading, Massachusetts, 1964.
23 J. Bjerrum and L. H. Skibsted, Acta. Chem. Scand., A 31 (1977) 673.
24 V. G. Levich, Physicochemical Hydrodynamics, Prentice Hall, NY, 1962.
25 A. E. Martell and L. G. Sillen, Stability Constants, Chem. Soc., Special Publ. No. 17, The Chem. Soc., London, 1962.
26 T. Hepel, M. Hepel and M. Leszko, Analyst, 102 (1977) 132.
27 S. Venkatachalam and R. Mallikarjunan, Trans. Inst. Min. Metall., Sec. C, 79 (1970) 181.

Analytica Chimica Acta, 123 (1981) 161—173

CHLORIDE INTERFERENCE WITH NON-STOICHIOMETRIC COPPER SULPHIDE COPPER(II)-SELECTIVE ELECTRODES
Part 2. Exact Determination of the Chloride Interference Region

TADEUSZ HEPEL

Institute of Chemistry, Jagiellonian University, 30—060 Kraków (Poland)

(Received 7th February 1980)

SUMMARY

A general equation for calculating the limit of the ligand interference region with the non-stoichiometric copper sulphide single-crystal electrode is described. The critical ligand concentration can be computed for a preselected maximal error in copper(II) ion determinations. The effect of the composition of the electrode material is discussed. The experimental results for the chloride interference show good agreement with theoretical predictions.

Much attention has been paid to the examination and use of different types of copper-selective electrodes [1]. Most investigations have been done with Ag_2S/CuS or Ag_2S/Cu_2S mixtures or the non-stoichiometric phases $Ag_{2-x}Cu_xS$, but interesting results have also been obtained for copper sulphide single-crystal electrodes [1—4]. The selectivity of the copper(II)-selective electrodes is similar for the different types of electrodes. Not only do mercury and silver ions poison the electrode, but some other ions [5] and concentrated oxidizing acids [6] interfere with the electrode operation. Chloride ion interference has been studied extensively [1] as an important factor in practical applications of the electrodes. The chloride interference has been attributed to the formation of a silver chloride film at the electrode surface, but Crombie et al. [7] showed that chloride interference occurs even at low concentrations where silver chloride would not precipitate. The reactions occurring at a non-stoichiometric copper sulphide single-crystal electrode in concentrated chloride solutions were discussed in Part 1 [1], and mechanisms of chloride interference were proposed. In this paper, a general equation describing the ligand interference region in terms of the error in copper(II) determination is discussed with regard to chloride solutions.

THEORY

The mechanism for the chloride interference, proposed in Part 1 [1] for the non-stoichiometric copper sulphide electrode in concentrated chloride solutions, is based on the assumption that the reactions

$$CuCl_p^{2-p} + (q - p)Cl^- + e^- = CuCl_q^{1-q} \quad (1a)$$

$$CuCl_p^{2-p} + CuS(n - s) + 2e^- = Cu_2S(n - s) + pCl^-, \quad (1b)$$

at the electrode surface involve anodic oxidation of the electrode material

$$Cu_2S(n - s) + qCl^- - e^- = CuS(n - s) + CuCl_q^{1-q} \quad (2)$$

the overall corrosion reaction being

$$CuCl_p^{2-p} + (2q - p)Cl^- + Cu_2S(n - s) = CuS(n - s) + 2CuCl_q^{1-q} \quad (3)$$

The values of the coefficients p and q depend on the free chloride ion activity in the solution. Of course, the general reaction (3) could occur chemically, but reaction (2) would not then be the potential-determining reaction (see Part 1 [1]). Reaction (3) indicates that chlorocopper(I) complexes form at the electrode surface until the equilibrium of this reaction is attained. The greater the chloride ion activity in the solution, the greater the conversion of copper(II) to copper(I) at the attained equilibrium. Because reaction (3) is fast, the equilibrium is easily attained at the electrode surface; therefore, with some assumptions concerning the degree of conversion of Cu(II) to Cu(I) at the electrode surface, it is possible to determine the critical chloride concentration at which chloride interferes with the electrode operation. It should be emphasized that this method of determining the chloride interference region neglects the effect of kinetic parameters and is thermodynamic in nature.

Simplified treatment

If it is assumed that the accuracy required for the measurement of copper(II) ion activity is ±15%, then if 15% of copper(II) ions vanish during the course of reaction (3), the actual concentration of copper(I) ions will be

$$C_I = 0.353\, C_{II} = 0.3\, C_{II}^{in} \quad (4)$$

where C_{II}^{in} is the initial copper(II) concentration. If the ligand numbers are assumed to be p = 0 and q = 2, selected on the basis of Figs. 1 and 2, then from the general expression for the metastable equilibrium constant $K_{p,q}^0$ of reaction (3)

$$\log K_{p,q}^0 = 2 \log [CuCl_q^{1-q}] - \log [CuCl_p^{2-p}] - (2q - p) \log [Cl^-] + \log \{[CuS(n - s)]/[Cu_2S(n - s)]\} \quad (5)$$

we obtain the equation

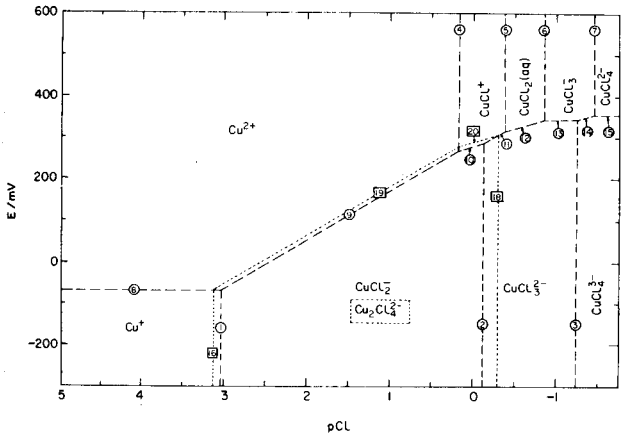

Fig. 1. The ionic equilibria diagram for the system copper—hydrochloric acid—aqueous sodium perchlorate solution at 25°C and an ionic strength (μ) of 5 M. The potential is referred to the Ag/AgCl electrode in 0.1 M chloride solution at μ = 5 M. Lines are plotted for equal concentrations of the given species. Lines 16, 18—20 (and the domain of relative predominance of the complex $Cu_2Cl_4^{2-}$) concern the condition $[Cu_2Cl_4^{2-}]$ = 0.333 M with the concentrations of other species as involved in eqns. (16) and (18—20) in Table 5, see Appendix. pCl is taken here in terms of concentration.

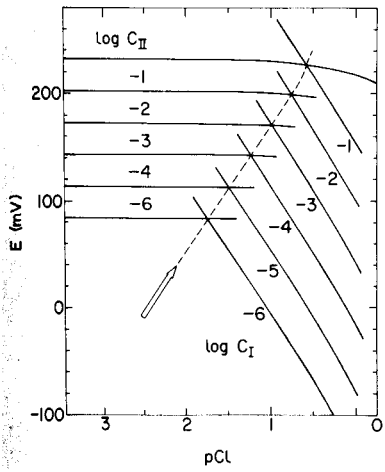

Fig. 2. The potential—pCl diagram for the non-stoichiometric copper sulphide electrode with β = 0.052. Solid curves correspond to the constant total Cu(II) or Cu(I) concentration. The dashed line corresponds to eqn. (27) for ϵ_0 = —33% and $C_{II}^{in} = 1.5\ C_{II}$. Conditions as for Fig. 1.

$$\log K^{0}_{2,0} = 2 \log [CuCl_2^-] - \log [Cu^{2+}] - 4 \log [Cl^-] + \log \{[CuS(n-s)]/[Cu_2S(n-s)]\} \quad (6)$$

or

$$\log K^{f'}_{n-s} = 2 \log [CuCl_2^-] - \log [Cu^{2+}] - 4 \log [Cl^-] \quad (7)$$

where the new equilibrium constant $K^{f'}_{n-s}$ written for a given composition of the electrode material ($Cu_{2-x}S$) contains the activities of the solid phase components (cf. [1, 8]):

$$K^{f'}_{n-s} = K^0(\beta^I_{1,2})^2 [Cu_2S(n-s)] [CuS(n-s)]^{-1} (f_2/f_+^2) \quad (8)$$

where $\beta^I_{1,2}$ is the conditional stability constant for the complex $CuCl_2^-$; the constant K^0 relates to the condition p = q = 0 (eqn. 5) and is 1.80×10^{-13} M [8]; f_i relates to single ion activity coefficients.

Rearrangement of eqn. (7) and substitution of the respective terms resulting from eqn. (4) for the actual concentrations of Cu(II) and Cu(I) ions gives

$$4 \log [Cl^-] - \log [Cu^{2+}]^{in} = -\log K^{f'}_{n-s} - 0.975 \quad (9)$$

This equilibrium equation is valid when the concentrations of the copper complexes other than $Cu^{2+}(aq)$ and $CuCl_2^-$ can be neglected. On the basis of eqn. (9), the region of chloride ion interference with the non-stoichiometric copper sulphide electrode operation may be determined from

$$4 \log [Cl^-] - \log [Cu^{2+}]^{in} \geqslant -0.351 - \log (f_{2+}/f_+^2) + \log [CuS(n-s)]/Cu_2S(n-s)] \quad (10)$$

In this relation, the value 0.238 M^{-2} was used for the metastable equilibrium constant $K_0(\beta^I_{1,2})^2$. This value was calculated on the basis of thermodynamic data given by the National Bureau of Standards [9]. Pure crystals of CuS (covellite) and Cu_2S (copper sulphide) were taken as the standard states for the non-stoichiometric solid-phase components, CuS(n − s) and Cu_2S(n − s) [9]. The value of $\beta^I_{1,2}$ was taken from Ahrland and Tagesson [10] for an ionic strength of 5 M ($NaClO_4$). Only a slightly different value was given by Latimer [11]. The simplified relation (10) shows that the solid-phase composition is an important factor in determining the critical chloride concentration. Ion-sensing materials with a greater activity of the CuS(n − s) component are less sensitive to chloride ions.

General relationship

In this section, the actual total concentrations of copper(I) and copper(II) species in the solution are represented by means of the expressions $C_I = [Cu^+]\alpha_I$ and $C_{II} = [Cu^{2+}]\alpha_{II}$, where $\alpha_k = 1 + \sum_{q,L} \beta^k_{1,q} [L]^q$. Here $[L]$ is the free ligand concentration and β is the concentration stability constant for the particular copper complexes $Cu(L)_q$; signs are omitted and only mono-

nuclear complexes are considered. When these expressions are introduced into the equation for the equilibrium constant

$$\log K^0 = 2 \log [Cu^+] - \log [Cu^{2+}] + \log \beta \quad (11)$$

for the reaction $Cu^{2+} + Cu_2S(n-s) = 2Cu^+ + CuS(n-s)$, then

$$\log K^{0,f}_{n-s} = 2 \log C_I - \log C_{II} - \log (\alpha_I^2/\alpha_{II}) \quad (12)$$

where $K^{0,f}_{n-s} = (K^0/\beta)\ (f_{2+}/f_+^2)$ and $\beta = [CuS(n-s)]/[Cu_2S(n-s)]$. If it is assumed that the determination error ϵ defined in molar percent

$$\epsilon = (C_{II} - C^{in}_{II})\ (C^{in}_{II})^{-1} \times 100 \quad (13)$$

should be $\leqslant \epsilon_0$, the actual total concentrations at equilibrium may be expressed by the relations (note that errors are negative)

$$C_I \leqslant -2 \times 10^{-2}\ \epsilon_0\ C^{in}_{II} \quad \text{and} \quad C_{II} \geqslant (100 + \epsilon_0)\ 10^{-2}\ C^{in}_{II} \quad (14)$$

Insertion of expressions (14) into eqn. (12) gives the limiting equation

$$\log (\alpha_I^2/\alpha_{II}) - \log C^{in}_{II} = -\log K^{0,f}_{n-s} - \log (100\ \epsilon_0^{-2} + \epsilon_0^{-1}) - 1.398 \quad (15)$$

Equation (15) describes the metastable equilibrium of the non-stoichiometric copper sulphide—aqueous solution system, written in terms of the actual free ligand concentration, the initial copper(II) concentration, the degree of copper(II) conversion (ϵ_0) and ionic strength ($K^{0,f}_{n-s}$ and β values). The region of the ligand interference with the electrode operation may be described then by the general relationship

$$\log \lambda - \log C^{in}_{II} \geqslant -\log K^{0,f}_{n-s} - \log (100\ \epsilon_0^{-2} + \epsilon_0^{-1}) - 1.398 \quad (16)$$

$$\text{or } \log \lambda - \log C^{in}_{II} \geqslant +11.35 + \log \beta + \log (f_+^2/f_{2+}) - \log (100\ \epsilon_0^{-2} + \epsilon_0^{-1}) \quad (17)$$

where $\lambda = \alpha_I^2/\alpha_{II}$. The ratio f_+^2/f_{2+} can be calculated by dividing the thermodynamic equilibrium constant K^0_{Cu} of the reaction: $Cu^{2+} + Cu^0 = 2Cu^+$, by the conditional equilibrium constant $K^{0,f}_{Cu}$ (of the same reaction) determined at the given strength. Many experimental values of $K^{0,f}_{Cu}$ for different media have been reported [12, 13]. The value of K^0_{Cu} calculated from the generally accepted thermodynamic functions [9, 14] is 6.11×10^{-7} M at 25°C.

Determination of the critical ligand concentration irrespective of the composition of the electrode material

The general equation (eqn. 15) determining the limits of the ligand interference region shows that the electrode material is an important factor which must be considered in practical applications. An equation of the form (15) or (9) may be easily compared with those given earlier [5, 7] (see below). The necessary value of β for a given electrode material may be determined as described previously [4, 8]. However, an equation independent of the electrode composition would be more convenient for practical analysis. Such an equation can be derived as follows. Under metastable equilibrium conditions, equilibria of the redox reactions

$$Cu^{II}(L)_p + (q - p)L + e^- = Cu^{I}(L)_q \quad (18)$$

are also attained. The Nernst equation

$$E = E^0_{2/1} + (RT/F) \ln (C_{II}/C_I) + (RT/F) \ln [(\alpha_I/\alpha_{II})(f_{2+}/f_+)] \quad (19)$$

is then fulfilled. If one of the chlorocopper(I) complexes, $Cu^{I}(L)_q$, or analogously a $Cu_{II}(L)_p$ complex is predominant in a certain range of ligand concentration, eqn. (19) may be rearranged to

$$[L] = [(C_I/C_{II})]^{1/(q-p)} W[(f_+/f_{2+})(\beta_{II,1p}/\beta_{I,1q})]^{1/(q-p)} \times \exp \{(E - E^0_{2/1})F/[(q - p)RT]\} \quad (20)$$

or using eqn. (13),

$$[L] = \phi W \exp \{(E - E^{0,f}_{II/I})F/[(q - p)RT]\} \quad (21)$$

where $\phi = [-2\epsilon_0/(100 + \epsilon_0)]^{1/(q-p)}$ and

$$E^{0,f}_{II/I} = E^0_{2/1} + (RT/F) \ln (f_{2+}/f_+) + (RT/F) \ln (\beta_{I,1q}/\beta_{II,1p}) \quad (22)$$

The correction function W defined by

$$W^{q-p} = (\alpha_{II}/\alpha_I)(\beta_{I,1q}/\beta_{II,1p})[L]^{q-p} \quad (23)$$

is equal to 1 when the remaining complexes of copper(I) and copper(II) can be neglected.

For the chloride ligand and the conditions p = 0 and q = 2, eqn. (21) takes the form

$$[Cl^-] = [-2\epsilon_0(100 + \epsilon_0)^{-1}]^{1/2} W \exp\{(E - E^{0'}_f)F(2RT)^{-1}\} \quad (24)$$

where $E^{0'}_f$ is for reaction 1a with p = 0 and q = 2, and contains the stability constant $\beta^I_{1,2}$ and the activity coefficients f_+ and f_{2+}: $E^{0'}_f$ = 289.4 mV vs. E(Ag/AgCl, 0.1 M Cl^-) at μ = 5 M.

To calculate the critical chloride concentration as a first approximation, only the value of the electrode potential actually measured and the required value of the relative error ϵ_0 are needed. The value of $[Cl^-]_{crit}$ may be also determined from the diagram in Fig. 3 plotted for p = 0 and q = 2 (i.e. for W = 1 in eqn. 24) or from the diagram in Fig. 4, where the correction function W, and another function, Z (see below) are taken into account. The slopes ϕ of the particular curves in Figs. 3 and 4, and the potential differences ΔE: $\Delta E = E([Cl^-] = 0) - E([Cl^-]_{crit})$ are given in Table 1.

Ligand interference when binuclear complexes are formed

If binuclear complexes of copper(I) or copper(II) are formed, the total concentration of copper(I), or analogously that of copper(II), in solution can be expressed by

$$C_I = [Cu^+](\alpha_I + \alpha'_I[Cu^+]) \quad (25)$$

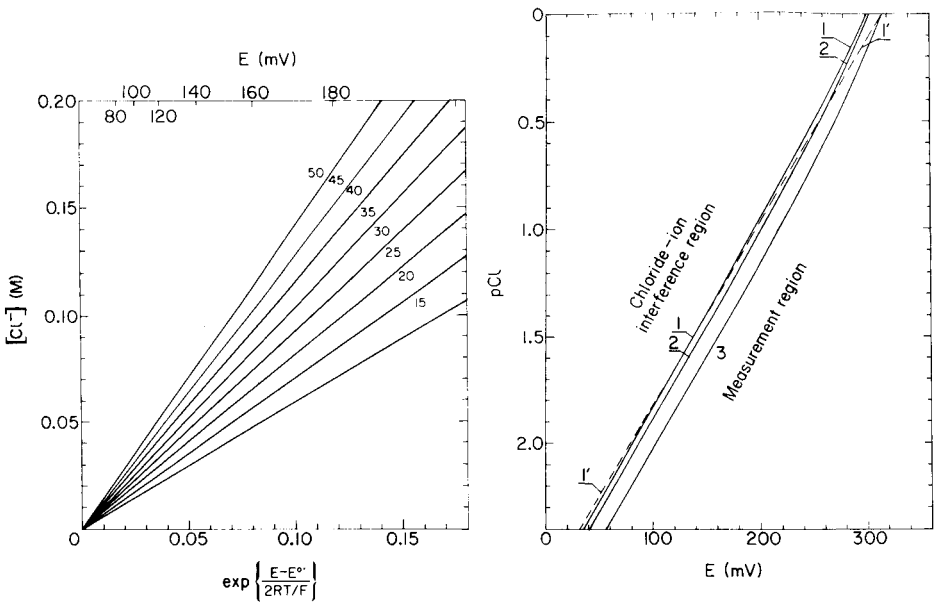

Fig. 3. The dependence of the critical chloride concentration on the electrode potential measured, plotted for various values of required error ϵ_0 (given as a percentage on each line, on the basis of eqn. (24) for $W = 1$ (25°C, $\mu = 5$ M).

Fig. 4. The exact relation (see eqn. 27 for the chloride ligand) between the critical pCl and the electrode potential (curves 1—3) for different C_{II}^{in} values: (1) $\leqslant 10^{-2}$ M; (2) 10^{-1} M; (3) 1 M. Curve 1′ is plotted for $W = 1$ and $Z = 1$. All the curves correspond to a preset error of $\epsilon_0 = -15\%$; $\mu = 5$ M, 25°C. The diagram may be used for any copper sulphide electrode.

TABLE 1

Values of the e.m.f. changes ΔE and the parameters ϕ and ω corresponding to a preset error ϵ_0 of the copper(II) determination in the chloride interference region using the copper sulphide single-crystal electrode at 25°C

ϵ_0(%)	ΔE(mV)	ϕ[a]	ω[b]	ϵ_0(%)	ΔE(mV)	ϕ[a]	ω[b]
−5	−0.66	0.3244	−0.5798	−30	−4.58	0.9258	+1.1091
−10	−1.35	0.4714	+0.0458	−35	−5.53	1.0377	+1.2753
−15	−2.09	0.5941	+0.4228	−40	−6.56	1.1547	+1.4260
−20	−2.87	0.7071	+0.6989	−45	−7.68	1.2792	+1.5661
−25	−3.70	0.8165	+0.9208	−50	−8.90	1.4142	+1.6989

[a]From eqns. (21), (24) and (27). [b]From eqns. (15—17); $\omega = -\log (100\,\epsilon_0^{-2} + \epsilon_0^{-1})$.

where $\alpha'_I = 2\sum_{L,q'} \beta^I_{2,q'}[L]^{q'}$ and α_I is given by the expression $1 + \sum_{q,L} \beta^I_{1,q}[L]^q$. In this case, instead of eqn. (19), we obtain, after some algebra

$$E = E^0_{2/1} + (RT/F)\ln(C_{II}/C_I) + (RT/F)\ln[(\alpha_I/\alpha_{II})(f_{2+}/f_+)] +$$

$$(RT/F)\ln\{[1 + (1 + 4\alpha'_I\alpha_I^{-2}C_I)^{1/2}]/[1 + (1 + 4\alpha'_{II}\alpha_{II}^{-2}C_{II})^{1/2}]\} \quad (26)$$

If again one of the mononuclear complexes of copper(I), $Cu^I L_q$, and one of the complexes of copper(II), $Cu^{II}L_p$, predominate in a certain range of ligand concentration, then analogously to the method used in deriving eqn. (21), it is possible to achieve the enlarged equation

$$[L] = \phi WZ \exp[(E - E^{0,f}_{II/I})F(q - p)^{-1}(RT)^{-1}] \quad (27)$$

$$\text{where } Z = \left\{\frac{1 + [1 + 4(1 + 10^{-2}\epsilon_0)\alpha'_{II}\alpha_{II}^{-2}C^{in}_{II}]^{1/2}}{1 + [1 - 0.08\epsilon_0\alpha'_I\alpha_I^{-2}C^{in}_{II}]^{1/2}}\right\}^{1/(q-p)} \quad (28)$$

At low values of α' and C^{in}_{II} and high values of α, the function Z approximates to 1.

Returning to the chloro complexes of copper: $\alpha'_{II} = 0$, $\alpha'_I = 2\beta^I_{2,4}[Cl^-]^4$ and

$$Z = 2^{1/2}/[1 + (1 - 0.08\,\epsilon_0\alpha'_I\alpha_I^{-2}C^{in}_{II})^{1/2}]^{1/2} \quad (29)$$

The value of Z differs from unity at initial copper(II) concentrations greater than 10^{-3} M. The effect of the value C^{in}_{II} on the critical chloride concentration for a preset error $\epsilon_0 = -15\%$ is presented in Fig. 4

EXPERIMENTAL

The measurements were done with copper sulphide single-crystal electrodes synthesized in this laboratory [15]. Solutions were prepared from triply distilled water and analytical-grade reagents purified by recrystallization. The equipment was similar to that used earlier [15]. In all measurements, the cell was

Cu | Ag, AgCl(s) |

| 0.1 M NaCl, 10^{-3} M $HClO_4$, 4.899 M $NaClO_4$ |

| 10^{-3} M $HClO_4$, 4.999 M $NaClO_4$ |

| 10^{-3} M $HClO_4$, x M $Cu(ClO_4)_2$, (4.999 − 3x) M $NaClO_4$ |

| $Cu_{2-x}S$ | Au | Cu

The e.m.f. values were recorded after lengthy equilibration of the solutions with the finely powdered copper sulphide obtained by crushing the molten mineral $Cu_{2-x}S$ (i.e., the same material as used for the electrode preparation). Equilibrium was achieved after 1—20 h, depending on the copper concentration. Argon, purified from traces of oxygen in the usual way, was passed through the measurement vessel before, and during, the experiments.

Masking agents (e.g., for iron) were not added to the solutions.

RESULTS AND DISCUSSION

The experimental results obtained are presented in Figs. 5 and 6. As can be seen, the experimental points are in good agreement with the theoretical predictions, both in relation to the value of ϵ, and the slope ($\partial \log [Cl^-]_{crit} / \partial \log C_{II}^{in}$). The small deviations from eqn. (9) are due to the fact that the existence of complexes of copper(I) (other than $CuCl_2^-$) has been neglected, to the effect of liquid junction potentials, and to some difficulties with the precise determination of $[Cl^-]_{crit}$ from the experimental curves 1—3 (Fig. 5) and from the data for other values of C_{II}^{in}, in constructing the plot in Fig. 6. In Fig. 6, the dependence of the critical chloride concentration on the initial copper(II) concentration is presented for the preset relative error ϵ_0 of −15%. The potential difference ΔE is −2.09 mV for this case. The dependence of the critical chloride concentration on the electrode potential measured (irrespective of the phase composition of the electrode material) is presented in Table 2 for $C_{II}^{in} \leqslant 10^{-3}$ M ($Z = 1$), and in Table 3 for $C_{II}^{in} > 10^{-3}$ M. Tables 3 and 4 and Figs. 4 and 5 show that the simplified relations (9) and (24) with $W = 1$ are useful for approximate determination of the chloride interference region. The most reliable values of the stability constants given recently by Bjerrum and Skibsted [16] for chlorocopper(II) complexes and by Ahrland et al. [10, 12] for chlorocopper(I) complexes (see Table 4) were used in calculating the values of λ, W and Z.

It is interesting to compare the derived eqns. (10) or (17) with the experimental results obtained for the mixed Cu_xS/Ag_2S electrode. For the Orion

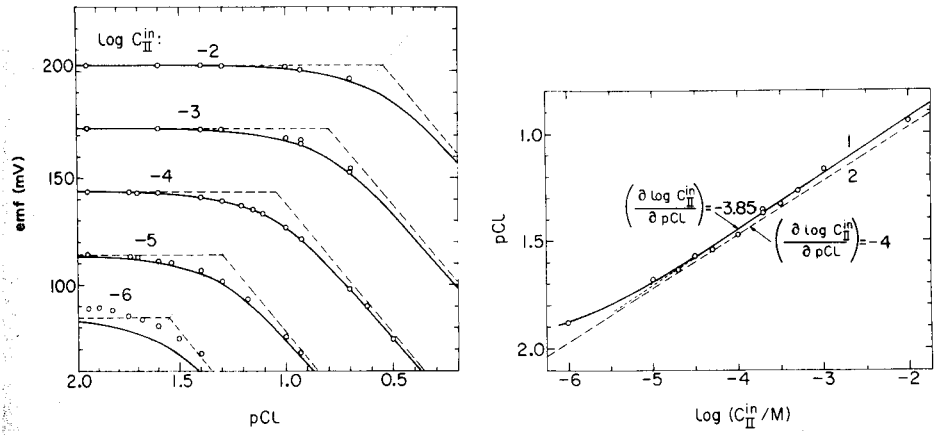

Fig. 5. The e.m.f.—pCl diagram for various initial copper(II) concentrations ($C_I^{in} = 0$): (o) experimental points; (——) theoretical for $W = 1$, $Z = 1$ and $\beta = 0.052$. 25°C; $\mu = 5$ M ($NaClO_4$).

Fig. 6. Comparison of the experimental results (curve 1) obtained for the non-stoichiometric copper sulphide single-crystal electrode with $\beta = 0.052$ at 25°C and $\mu = 5$ M ($NaClO_4$), and the theoretical results from eqn. (9) (curve 2).

TABLE 2

Dependence of the critical chloride concentration on the electrode potential measured for the preset error ϵ_0 in Cu(II) determination of −15% at 25°C and μ = 5 M ($NaClO_4$)

ΔE(mV)	$[Cl^-]_{crit}$(M)	W	log λ	E(mV)[a]	ΔE(mV)	$[Cl^-]_{crit}$(M)	W	log λ	E(m
−2.09	4×10^{-3}	0.928	+2.654	+36.2	−2.09	0.08	1.026	7.732	185
	6×10^{-3}	0.957	3.307	55.5		0.1	1.034	8.119	196
	8×10^{-3}	0.970	3.784	69.6		0.2	1.071	9.322	229
	0.01	0.978	4.158	80.6		0.4	1.140	10.527	262
	0.02	0.996	5.339	115.4		0.6	1.206	11.232	280
	0.04	1.009	6.532	150.3		0.8	1.271	11.732	292
	0.06	1.018	7.233	170.6		1.0	1.355	12.120	301

[a]Vs. Ag/AgCl/0.1 M Cl^- at μ = 5 M ($NaClO_4$).

TABLE 3

The effect of the initial concentration of copper(II) on the value of the critical electrode potential E_{crit} (calculated for ϵ_0 = −15%) at various chloride concentrations[a] for 25°C and μ = 5 M ($NaClO_4$)

$[Cl^-]$ (M)	C_{II}^{in} = 0.1 M		$C_{II}^{in} = 10^{-2}$ M		$C_{II}^{in} = 10^{-3}$ M	
	Z	E_{crit}[b]	Z	E_{crit}[b]	Z	E_{crit}[b]
4×10^{-3}	0.898	+41.8	0.986	+37.0	0.999	+36.3
6×10^{-3}	0.889	61.6	0.984	56.4	0.998	55.6
8×10^{-2}	0.885	75.8	0.983	70.4	0.998	69.7
1×10^{-2}	0.883	87.0	0.983	81.5	0.998	80.7
2×10^{-2}	0.880	121.9	0.982	116.3	0.998	115.5
4×10^{-2}	0.880	156.8	0.982	151.2	0.998	150.4
6×10^{-2}	0.882	177.1	0.983	171.6	0.998	170.7
8×10^{-2}	0.884	191.4	0.983	185.9	0.998	185.1
0.1	0.886	202.3	0.984	197.0	0.998	196.2
0.2	0.897	235.6	0.986	230.7	0.998	230.0
0.4	0.914	267.0	0.989	262.9	0.999	262.4
0.6	0.928	284.1	0.991	280.7	0.999	280.3
0.8	0.939	295.6	0.993	292.7	0.999	292.4
1	0.948	304.0	0.994	301.6	0.999	301.3

[a]If the electrode potential measured at the given values of C_{II}^{in} and $[Cl^-]$ is lower than that given in the Table, the error ϵ is greater than 15%. [b]mV vs. Ag/AgCl/0.1 M Cl^- at μ = 5 M ($NaClO_4$).

TABLE 4

The values of the conditional stability constant for chlorocopper complexes at 25°C and ionic strength 5 M ($NaClO_4$)

	$\beta_{1,1}$	$\beta_{1,2}$	$\beta_{1,3}$	$\beta_{1,4}$	$\beta_{2,4}$	$K_{Cu}^{0,f}$ [a]	Ref.
Cu(I)	$\leqslant 5 \times 10^{2}$ [b]	1.14×10^{6}	0.87×10^{6}	$< 5 \times 10^{4}$ [b]	8.8×10^{12}	–	[10, 12]
						1.22×10^{-6}	[12]
Cu(II)	1.5	0.63	8.8×10^{-2}	3.2×10^{-3}	—	—	[16]

[a] For $Cu^{2+} + Cu^{0} = 2\,Cu^{+}$. [b] The maximal value of $\beta_{1,q}$ was taken in calculations.

94–29 copper(II)-selective electrode Crombie et al. [7] found the following experimental relation

$$2.8 \log [Cl^-] - \log C_{II}^{in} > -2.7 \qquad (30)$$

Here, the coefficient 2.8 is less than that resulting from eqns. (9) and (10), but the signs of the particular terms in eqns. (9), (10) and (30) are identical. Estimation of the value of the right side of eqn. (9) for this case shows good agreement between expression (30) and the present predictions. In contrast, the limiting equation for the chloride interference given by Ross [5] is of the form

$$2 \log [Cl^-] + \log [Cu^{2+}]^{in} \geqslant -5.80 \qquad (31)$$

which is obviously from eqn. (30). Because eqn. (31) was derived on the assumption of formation of a superficial silver chloride phase

$$Cu^{2+} + 2\,Cl^- + Ag_2S = 2\,AgCl + CuS$$

it seems that two different mechanisms of chloride interference may be considered for mixed copper sulphide/silver sulphide electrodes. This problem will be evaluated in later papers.

The author is indebted to Professor M. Leszko for his kind interest in this work.

APPENDIX

The diagram of ionic equilibria for the system copper–hydrochloric acid–aqueous sodium perchlorate solutions presented in Fig. 1 was calculated on the basis of recent data (see Table 4). The formal standard electrode potential for the reaction $Cu^{2+} + 2e^- = Cu^0$ at $\mu = 5$ M was taken from Ahrland and Rawsthorne [12]: $E^{0,f} = 0.3000$ V vs. Ag/AgCl/0.1 M Cl^- at $\mu = 5$ M. The liquid junction potentials in the cell used here and in the cell used by Ahrland and Rawsthorne were assumed to be negligible.

The reaction equations and the equilibrium equations are listed in Table 5.

TABLE 5

Reaction and equilibrium equations used in this work

Reactions of Cu(I)

(1) $CuCl_2^- = Cu^+ + 2Cl^-$; $pCl = 3.03 + 0.5 \log \{[Cu^+]/[CuCl_2^-]\}$
(2) $CuCl_3^{2-} = CuCl_2^- + Cl^-$; $pCl = -0.12 + \log \{[CuCl_2^-]/[CuCl_3^{2-}]\}$
(3) $CuCl_4^{3-} = CuCl_3^{2-} + Cl^-$; $pCl = -1.24 + \log \{[CuCl_3^{2-}]/[CuCl_4^{3-}]\}$

Reactions of Cu(II)

(4) $CuCl^+ = Cu^{2+} + Cl^-$; $pCl = 0.176 + \log \{[Cu^{2+}]/[CuCl^+]\}$
(5) $CuCl_2(aq) = CuCl^+ + Cl^-$; $pCl = -0.38 + \log \{[CuCl^+]/[CuCl_2]\}$
(6) $CuCl_3^- = CuCl_2(aq) + Cl^-$; $pCl = -0.85 + \log \{[CuCl_2]/[CuCl_3^-]\}$
(7) $CuCl_4^{2-} = CuCl_3^- + Cl^-$; $pCl = -1.45 + \log \{[CuCl_3^-]/[CuCl_4^{2-}]\}$

Redox reactions

(8) $Cu^{2+} + e^- = Cu^+$; $E = -0.0687 + 0.5916 \log \{[Cu^{2+}]/[Cu^+]\}$
(9) $Cu^{2+} + 2Cl^- + e^- = CuCl_2^-$; $E = 0.2894 + 0.05916 \log \{[Cu^{2+}]/[CuCl_2^-]\} - 11832\ pCl$
(10) $CuCl^+ + Cl^- + e^- = CuCl_2^-$; $E = 0.2790 + 0.05916 \log \{[CuCl^+]/[CuCl_2^-]\} - 0.05916\ pCl$
(11) $CuCl^+ + 2Cl^- + e^- = CuCl_3^{2-}$; $E = 0.2719 + 0.05916 \log \{[CuCl^+]/[CuCl_3^{2-}]\} - 0.11832\ pCl$
(12) $CuCl_2(aq) + Cl^- + e^- = CuCl_3^{2-}$; $E = 0.2942 + 0.05916 \log \{[CuCl_2]/[CuCl_3^{2-}]\} - 0.05916\ pCl$
(13) $CuCl_3^- + e^- = CuCl_3^{2-}$; $E = 0.3446 + 0.05916 \log \{[CuCl_3^-]/[CuCl_3^{2-}]\}$
(14) $CuCl_3^- + Cl^- + e^- = CuCl_4^{3-}$; $E = 0.2714 + 0.05916 \log \{[CuCl_3^-]/[CuCl_4^{3-}]\} - 0.05916\ pCl$
(15) $CuCl_4^{2-} + e^- = CuCl_4^{3-}$; $E = 0.3568 + 0.05916 \log \{[CuCl_4^{2-}]/[CuCl_4^{3-}]\}$

Reactions of binuclear complex $Cu_2Cl_4^{2-}$

(16) $Cu_2Cl_4^{2-} = 2Cu^+ + 4Cl^-$; $pCl = 3.24 + 0.25 \log \{[Cu^+]^2/[Cu_2Cl_4^{2-}]\}$
(17) $2CuCl_2^- = Cu_2Cl_4^{2-}$; $\log \{[Cu_2Cl_4^{2-}]/[CuCl_2^-]^2\} = 0.829$
(18) $Cu_2Cl_4^{2-} + 2Cl^- = 2CuCl_3^{2-}$; $pCl = -0.53 + 0.5 \log \{[Cu_2Cl_4^{2-}]/[CuCl_3^{2-}]^2\}$
(19) $2Cu^{2+} + 4Cl^- + 2e^- = Cu_2Cl_4^{2-}$; $E = 0.3139 + 0.02958 \log \{[Cu^{2+}]^2/[Cu_2Cl_4^{2-}]\} - 0.11832\ pCl$
(20) $2CuCl^+ + 2Cl^- + 2e^- = Cu_2Cl_4^{2-}$; $E = 0.3035 + 0.02958 \log \{[CuCl^+]^2/[Cu_2Cl_4^{2-}]\} - 0.05916\ pCl$

REFERENCES

1 T. Hepel, Anal. Chim. Acta, 123 (1981) 151. (Part 1) and references therein.
2 A. Hulanicki, M. Trojanowicz and M. Cichy, Talanta, 23 (1976) 47.
3 J. Vesely, Collect. Czech. Chem. Commun., 36 (1971) 3364.
4 T. Hepel and M. Hepel, Electrochim. Acta, 22 (1977) 295.
5 J. W. Ross, in R. A. Durst (Ed.), Ion Selective Electrodes, NBS Spec. Publ. 314, U.S. Government Printing Office, Washington, DC, 1969; Orion Research Inc., Cupric Ion Electrode Model 94-29, Instruction Manual, 1971.
6 D. Midgley, Anal. Chim. Acta, 87 (1976) 19.
7 D. J. Crombie, G. J. Moody and J. D. R. Thomas, Talanta, 21 (1974) 1094.
8 T. Hepel, M. Hepel and M. Leszko, Analyst (London), 102 (1977) 132.
9 F. D. Rossini, D. D. Wagman, W. H. Evans, S. Levin and I. Jaffe, Natl. Bur. Standards Circular No. 500, U.S. Dept. of Commerce, U.S. Government Printing Office, Washington, 1952.
10 S. Ahrland and B. Tagesson, Acta Chem. Scand., A31 (1977) 615.
11 W. M. Latimer, Oxidation Potentials, Prentice Hall, New York, 1952.
12 S. Ahrland and J. Rawsthorne, Acta Chem. Scand., 24 (1970) 157.
13 J. Małyszko, PhD Thesis, Siedlce, Poland, 1978.
14 M. Pourbaix (Ed.), Atlas of Electrochemical Equilibria in Aqueous Solutions, Pergamon, Oxford, 1966.
15 M. Hepel, J. Electroanal. Chem., 74 (1976) 37.
16 J. Bjerrum and L. H. Skibsted, Acta Chem. Scand., A31 (1977) 673.

Analytica Chimica Acta, 123 (1981) 175—186

THE SOLVENT EXTRACTION OF FLURAZEPAM AND ITS MAJOR METABOLITES AND THEIR DETERMINATION BY POLAROGRAPHY

W. FRANKLIN SMYTH*

Department of Chemistry, University College Cork, Cork (Republic of Ireland)

J. A. GROVES

Health and Safety Executive, Brunell House, Cardiff (Gt. Britain)

(Received 23rd July 1980)

SUMMARY

The solvent extraction of flurazepam and its major metabolites from aqueous solutions of varying pH has been studied at concentrations encountered in body fluids following therapeutic dosage. Distribution ratios have been calculated over the pH range 0—14 and for the solvents, ethyl acetate, diethyl ether, cyclohexane and petroleum ether (40—60°C). Based on this study, a solvent extraction scheme is evaluated for the recovery of such concentrations of these compounds in mixtures, with final polarographic determinations. Recoveries exceeding 95% were found; the method is specific for the determination of flurazepam and its acetic acid metabolite in mixtures. The total concentration of the remaining metabolites, i.e. the hydroxyethyl-, *N*-1-desalkyl-, and *N*-1-desalkyl-3-hydroxy metabolites can be estimated after solvent extraction and differential pulse polarography in alkaline solutions.

Flurazepam (Dalmane; I) exhibits anticonvulsant, muscle-relaxant and taming properties in animals and has induced unique hypnotic effects in humans [1]. Its metabolism in dogs, beagles, rhesus monkeys and humans has been studied and the metabolites (II)—(VIII) have been identified. The major human metabolite was (IV) with measurable amounts of (V) which further metabolised to (VII) in urine. Minor quantities of (II) and (III) were detected in human urine. These structures are given in Fig. 1. Radio-labelling, spectrophotofluorimetric [2], spectrophotometric [2], electron-capture gas chromatographic [3] and differential pulse polarographic [3, 4] techniques have been used to confirm this metabolic route. Recently, forensic cases involving this drug have appeared in connection with driving accidents [5].

To date, there has been no systematic study of the solvent extraction of flurazepam and its metabolites. Although these molecules are structurally quite similar, they contain distinctly different functional groups, e.g., aliphatic amine groups in (I), (II) and (III), carboxylic acid group in (VI), and ionisable N—H groups in (V) and (VII) [6]. It would therefore be expected, considering the acid/base nature of these functional groups, that pH would influence the efficiency of liquid—liquid distribution of these

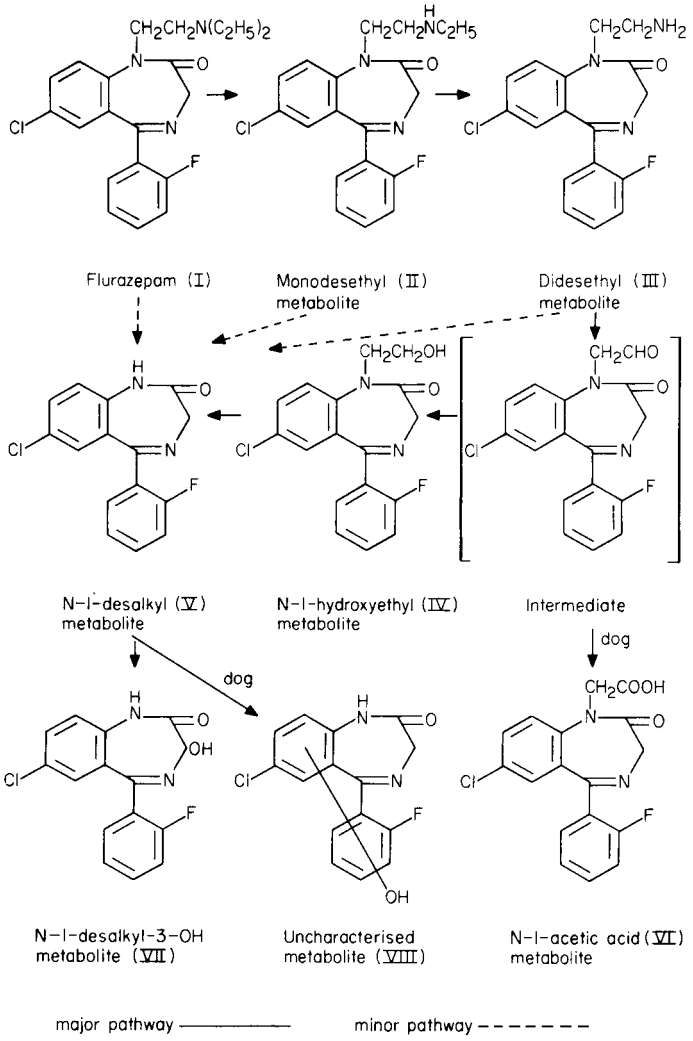

Fig. 1. Postulated pathways of flurazepam metabolism in man and dog.

molecules, in addition to other factors such as polarity of the organic solvent, etc. Such a study, aimed at improving the selectivity of the solvent extraction of mixtures of these molecules, is necessary prior to their polarographic determination since such 7-fluoro-1,4-benzodiazepines are polarographically reduced at similar potentials over a wide pH range [7]. An analytical method based on a solvent extraction scheme with final polarographic measurements is evaluated in this paper for such mixtures at the molar concentrations encountered in body fluids following therapeutic dosage.

EXPERIMENTAL

Reagents

The investigations were carried out on the following five compounds: flurazepam (I), *N*-1-hydroxyethylflurazepam (IV), flurazepam-*N*-1-acetic acid (VI), *N*-1-desalkylflurazepam (V) and *N*-1-desalkyl-3-hydroxyflurazepam (VII). Stock solutions were prepared in analytical-grade methanol at concentrations of about 10^{-3} M. These were stable for at least 2 weeks without taking any special storage precautions. Britton—Robinson buffers were used (pH 1.8—12.0) in conjunction with hydrochloric acid and sodium hydroxide to extend the pH range on either side for the extraction investigations. The ionic strength of these Britton—Robinson buffers did not remain constant over the entire pH range but the variation was small. At the lower end of the scale, the ionic strength was about 0.07 and approximately 0.15 at pH 12.0. Reagent-grade ethyl acetate, diethyl ether, cyclohexane and petroleum ether (40—60°C) were used in the extraction study, and the first two were selected in the final scheme for recovery and determination of flurazepam and its major metabolites.

A formic acid/sodium formate buffer of pH 4.0 was employed for much of the analytical polarography because its background response at low current settings was superior to that of the Britton—Robinson buffer at this pH. The formate solution was prepared by diluting 146 ml of 1 M formic acid (38.5 ml of 98—100% formic acid per l) and 100 ml of 1 M NaOH to 1 l. The resulting solution had a pH of 4 and an ionic strength of 0.1.

Apparatus

Two commercially available polarographs were used during this study: the Davis differential cathode ray polarograph A1660 and the PAR 174 Polarographic Analyser. The cathode ray polarograph was operated in the single cell mode and the limiting current was measured following the recording of the cathode ray trace on u.v.-sensitive paper with an ultra-violet oscillograph recorder series M1300 (Southern Instruments). Both normal and derivative polarograms were recorded. The PAR 174 Analyser was operated in the normal d.c. and sampled d.p.p. modes with 3-electrode operation. A Bryans—Southern X—t chart recorder, model 27000 with 10 V full scale deflection was linked to the Analyser. Typical settings in the sampled d.c. mode were scan rate 1 mV s^{-1}, scan range 3 V, modulation amplitude 50 mV, low pass filter 0.3 s, droptime 1 s.

The polarographic cell developed for routine work was based on a 10-ml quickfit flask (pear shape) and was suitable for solution volumes of 0.5—10 ml, the optimum being about 2 ml. The platinum wire counter electrode was sealed into the glass of the vessel as were the inlet tubes for passing gas into and over the sample solution. The Radiometer K401 calomel electrode used as the reference was inserted into a B10 socket adjacent to the B14 socket which housed the d.m.e. This reference electrode could be easily

removed for washing between the recording of the polarograms. Several of these cells were manufactured so that samples could be deaerated while one was being subjected to polarography.

Determination of the variation of distribution ratio D with pH

The solvent extractions were done at intervals of two pH units. In the pH range 2—12, Britton—Robinson buffers were used to maintain the pH of the aqueous phase. Hydrochloric acid was used at pH 0 and sodium hydroxide at pH 14.

The organic and aqueous phases were equilibrated in 30-ml stoppered centrifuge tubes. The insides of these tubes were coated with a 2% solution of dimethyldichlorosilane in carbon tetrachloride. This produced a water-repellent layer which prevented any appreciable adsorption of the drug and its metabolites onto the glass. It also changed the shape of the aqueous—organic interface from concave to convex. This facilitated the almost total removal of the organic upper phase with a dropping pipette.

Some organic solvents, especially the more polar ones, are miscible with water to some extent. In order to prevent this property leading to erroneous values of the distribution ratio, all solvents were presaturated with the relevant buffer solution before the extraction, simply by shaking the aqueous buffered phase with the solvent in a separating funnel. The two saturated phases were drawn off and employed in the solvent extraction studies. In this way, errors from volume changes on mixing were avoided.

Stock solutions of each compound were prepared at 10^{-3} M in methanol. A 0.05-ml aliquot of this solution was pipetted into a 25-ml volumetric flask and made up to volume with the relevant presaturated organic solvent to result in a concentration of 2×10^{-6} M. An aliquot (10 ml) of this solution was placed in a 30-ml centrifuge tube and 10 ml of the presaturated buffer solution added. The tube was stoppered, a drop of distilled water being placed on the stopper to aid proper sealing, and the contents were agitated for 10 min on a rotary shaker. The solutions were centrifuged and 5 ml of the organic (upper) phase was withdrawn and evaporated in a round-bottomed flask under nitrogen on a water bath at about 40°C. The residue remaining after removal of the solvent was dissolved in 5 ml of formic acid/sodium formate buffer, pH 4, and the concentration of the electroactive species in this solution was determined with the Davis A1660 cathode-ray polarograph. The percentage recovery was calculated by reference to the polarogram of a standard solution.

The above procedure was adopted rather than the apparently simpler process of polarographing each aqueous layer after solvent extraction for three reasons: organic solvents dissolved in the aqueous phase cause distortion of the polarographic waves; the instability of these compounds in highly acidic and alkaline media would have interfered with the determination of the distribution ratios; the wave heights of the drug and its metabolites do not remain exactly constant across the entire pH range. This would have necessitated the preparation of a standard solution at each pH.

Testing the recovery of compounds from aqueous solutions using the solvent extraction scheme (Fig. 2)

The method of establishing the recovery was by the construction of internal and external recovery curves and by testing the reproducibility of replicate assays. Compound (VI) is taken as an example. Into each of four 30-ml stoppered centrifuge tubes was pipetted 10 ml of Britton—Robinson buffer pH 9. By means of an Agla micrometer syringe, 0.1 ml of a stock 10 μg ml^{-1} solution of (VI) was added to the first tube, 0.06 ml to the second tube and 0.03 ml to the third tube. The fourth tube was used as a blank.

The contents of each tube were extracted with two 8-ml portions of ethyl acetate by shaking for 10 min each time on a rotary shaker. After each equilibration, the organic layer was discarded. The pH of the aqueous phase was adjusted to 3 by the dropwise addition of about 0.5 ml of 1 M hydrochloric acid until the pH was around 3 (indicator papers). A portion (2 ml) of the concentrated Britton—Robinson solution was added to the aqueous solution to maintain the pH at 3. This solution was then extracted with two 12-ml portions of diethyl ether. The ethereal fractions were evaporated to dryness under nitrogen in a 50-ml round-bottomed flask on a water bath at about 40°C. The residues were dissolved in 2 ml of formate buffer pH 4 and the polarogram was recorded. (The formate buffer contained 0.002% Triton X-100, which helped to wash the residue from the bottom of the flask after evaporation and so aided dissolution of the sample.) The results provided the internal standard recovery and were plotted as polarographic current versus concentration. The slope of this curve was compared with the slope of the corresponding external standard curve prepared by evaporating 0.1-, 0.06- and 0.03-ml aliquots of 10 μg ml^{-1} solution, dissolving the residues in 2 ml of formate buffer and recording the polarograms. This provided the polarographic response which would be obtained if 100% extraction had been achieved.

The results were checked by performing replicate extractions on known additions of the stock solution containing 10 μg ml^{-1} (VI) to 10 ml of Britton—Robinson buffer pH 9 and repeating the above procedure.

A PAR 174 Analyser was used in these recovery experiments with the following settings: initial potential —0.55 V; scan rate 1 mV s^{-1} potential scan 3.0 V; low pass filter 0.3 s; chart speed 1 min cm^{-1}; droptime 1 s; differential pulse mode; current range 0.5, 0.2 μA; modulation amplitude 50 mV.

Polarographic determination of a mixture of compounds (IV), (V) and (VII)

Mixtures of all 3 compounds were prepared by pipetting 0.1-ml aliquots of each metabolite solution (containing 10 μg ml^{-1}) into a round-bottomed flask and evaporating off the methanol under nitrogen. A 2 M NaOH solution was serially diluted to produce concentrations of 1 M, 0.5 M and 0.1 M NaOH. The residues containing the mixtures of all three metabolites were taken up into 2 ml of the alkaline solutions and the polarograms were recorded in

turn. The blank was also recorded. Settings on the PAR 174 were as described immediately above except that a current range of 1 μA was employed and the low pass filter was increased to 1 s. The initial potential was set at -1.0 V.

RESULTS AND DISCUSSION

The extraction results are presented in Table 1 as values of the distribution ratio D for compounds (I), (IV), (V), (VI) and (VII) between the organic phases, ethyl acetate, diethyl ether, cyclohexane or petroleum ether and aqueous phases of varying pH. Equal volumes of organic and aqueous layers were used and only one extraction step employed. The five compounds display a wide range of extractability in the four solvents considered. To a first

TABLE 1

Values of the distribution ratio, D, evaluated from % extraction = 100 $D/(D + 1)$ for the distribution of compounds (I), (IV), (V), (VI) and (VII) between equal volumes of various organic solvents and aqueous phases of varying pH

Compound	pH of aqueous phase				
	0	2	4	9	14
Ethyl acetate					
(I)	0	0.02	0.33	$\sim 10^3$	9.0
(IV)	0.43	17.0	$\sim 10^3$	$\sim 10^3$	$\sim 10^3$
(V)	0.82	$\sim 10^3$	$\sim 10^3$	$\sim 10^3$	19
(VI)	11.5	$\sim 10^3$	11.5	0	0.05
(VII)	$\sim 10^3$	$\sim 10^3$	$\sim 10^3$	$\sim 10^3$	$\sim 10^3$
Diethyl ether					
(I)	0	0	0.11	$\sim 10^3$	1.9
(IV)	0.11	9.0	32	$\sim 10^3$	$\sim 10^3$
(V)	0.25	32	$\sim 10^3$	$\sim 10^3$	1.5
(VI)	0.66	24.0	$\sim 10^3$	0.02	0.11
(VII)	1.5	$\sim 10^3$	$\sim 10^3$	9.0	0.06
Cyclohexane					
(I)	0	0.02	0.03	9.0	4.0
(IV)	0	0.05	0.23	0.25	0.43
(V)	0	0.09	0.43	0.66	0
(VI)	0	0.05	0.11	0.11	0.11
(VII)	0.05	0.05	0.05	0.05	0
Petroleum ether (40—60°C)					
(I)	0	0.02	0.03	6.9	32.0
(IV)	0	0.05	0.11	0.14	0.14
(V)	0	0.14	0.37	0.37	0
(VI)	0	0	0	0	0
(VII)	0	0.02	0.02	0.02	0

approximation, these results should be explicable in terms of the acid—base properties of the molecules.

The overall recovery of the compounds with ethyl acetate and diethyl ether is greater than that with cyclohexane and petroleum ether. The affinity of the drug and its metabolites for the more polar solvents indicates the polar nature of the molecules. The order of polarity in the series of five compounds can be obtained from the extraction results from cyclohexane. In the simple case, the least polar compound would extract the most into a non-polar solvent and the most polar would extract the least. Thus, at pH 7.4, the pH of human blood, the order of descending polarity is *N*-1-desalkyl-3-hydroxy > *N*-1-acetic acid > *N*-1-hydroxyethyl > *N*-1-desalkyl > flurazepam. As will be seen presently, flurazepam is a special case but nevertheless, the series is in accordance with the general theory that the metabolites are usually more polar than the parent drug.

All five compounds show decreased extractability into the organic solvent below pH 2. This is almost certainly attributable to the protonation of the nitrogen in the azomethine group resulting in a non-extractable charged species. Such pK_a values are in the range 1.07—2.57 [6].

The ionisation of the *N*-1 proton in the *N*-1-desalkyl and *N*-1-desalkyl-3-hydroxy metabolites (compounds V and VII) shows up as a decrease in the percentage extraction into the organic phase above pH 12. A decrease in extraction of the *N*-1-desalkyl-3-hydroxy metabolite is observed around pH 6 with diethyl ether. This is some 5.3 units less than its upper pK_a value corresponding to ionisation of its *N*-1 proton [6]. Ethers are known to associate with hydroxyl groups so this could be due to the breakdown of such an association between the metabolite and the ether. The pK_a of the 3-hydroxy group has been shown to be about 5.5 [7] which corresponds closely to the pH at which a change in the extraction behaviour of this metabolite into ether is observed.

The *N*-1-hydroxyethyl metabolite has only one pK_a value in the pH range 0—14 and remains essentially wholly extractable into diethyl ether and ethyl acetate above pH 3.

The acetic acid compound (VI) is not extracted appreciably into either cyclohexane or petroleum ether. Above pH 4, it exhibits a marked fall in extractability when either ethyl acetate or diethyl ether is used as the solvent. This arises from the ionisation of the acetic acid substituent to produce an ionic form which is not extractable. The extraction data indicate that the pK_a of this ionisation is about 5, which is close to the pK_a value of acetic acid (4.75).

Flurazepam appears to present something of an anomaly. The nitrogen atom in the substituent at position 1 would be expected to be protonated below approximately pH 11. Table 1 shows that despite this, extraction into the organic phase still occurs in the pH range 7—11 with an efficiency of 80—100% with all four solvents. At a pH below 7, the extractability of this compound begins to fall sharply until at pH 5, only 50% recovery is

achieved. This falls almost to zero at pH 2. Since these changes occur at pH values far removed from any of the pK_a values of flurazepam it is probable that some kind of ion-pair formation/breakdown is responsible. The pK_a value of around 5 for this process again suggests some involvement of an acetic acid moiety. Thus, it is possible that the protonated amine function forms ion-pairs with the acetate present in Britton—Robinson buffer solution. Above pH 5, acetate ions can pair with the amine, forming extractable species. Below this pH, acetic acid is not appreciably ionised so the required anion is not available for ion-pair formation, resulting in a decrease in the extractability of the drug.

Above pH 10—11, the tertiary amine in flurazepam is no longer protonated so ion-pair formation again ceases. Results in Table 1 indicate that the free amine does not extract as readily as the ion-pair. It is only with petroleum ether as solvent that an increase in recovery is recorded as the pH of the aqueous phase is increased above 10.

In order to assess the applicability of these results to the separation of mixtures of these compounds, it is necessary to consider the mixtures of the metabolites which are likely to be encountered in the body fluids after therapeutic dosage. De Silva et al. [3] state that in the assay of blood after oral ingestion of Dalmane, only the quantification of flurazepam, *N*-1-desalkylflurazepam, *N*-1-desalkyl-3-hydroxyflurazepam and *N*-1-hydroxyethylflurazepam are of significance. In urine, the major metabolites are monodesethyl- and didesethyl-flurazepam, *N*-1-hydroxyethylflurazepam and the *N*-1-acetic acid metabolite. Bearing in mind that the mono- and didesethyl metabolites were not available at the time of this study, the following treatment will be restricted to the blood assay case. Some comment on the urinary metabolite determination will however be possible.

The solvent extraction scheme

On the basis of the information in Table 1, the extraction scheme shown in Fig. 2 was devised as a possible means of separating some of the compounds from each other. An initial extraction of the mixture at pH 9 with ethyl acetate results in the recovery of all except the acetic acid metabolite which remains in the aqueous phase. This remaining compound can be extracted into diethyl ether on adjusting the aqueous phase to pH 3. The ethyl acetate solution obtained from the first extraction stage is evaporated to dryness in a centrifuge tube. The residue is taken up in 10 ml of pH 2 buffer solution and extracted with diethyl ether. This results in the back-extraction of flurazepam into the aqueous phase whilst the three other compounds remain in the ether layer. The aqueous layer is adjusted to pH 9 and again equilibrated with diethyl ether to recover the flurazepam. Some degree of hydrolysis might be expected while the flurazepam is in acidic solution at pH 2. This does not, however, affect the recovery since in a solution of pH 9, a reversible back-reaction occurs and any hydrolysed drug is reformed.

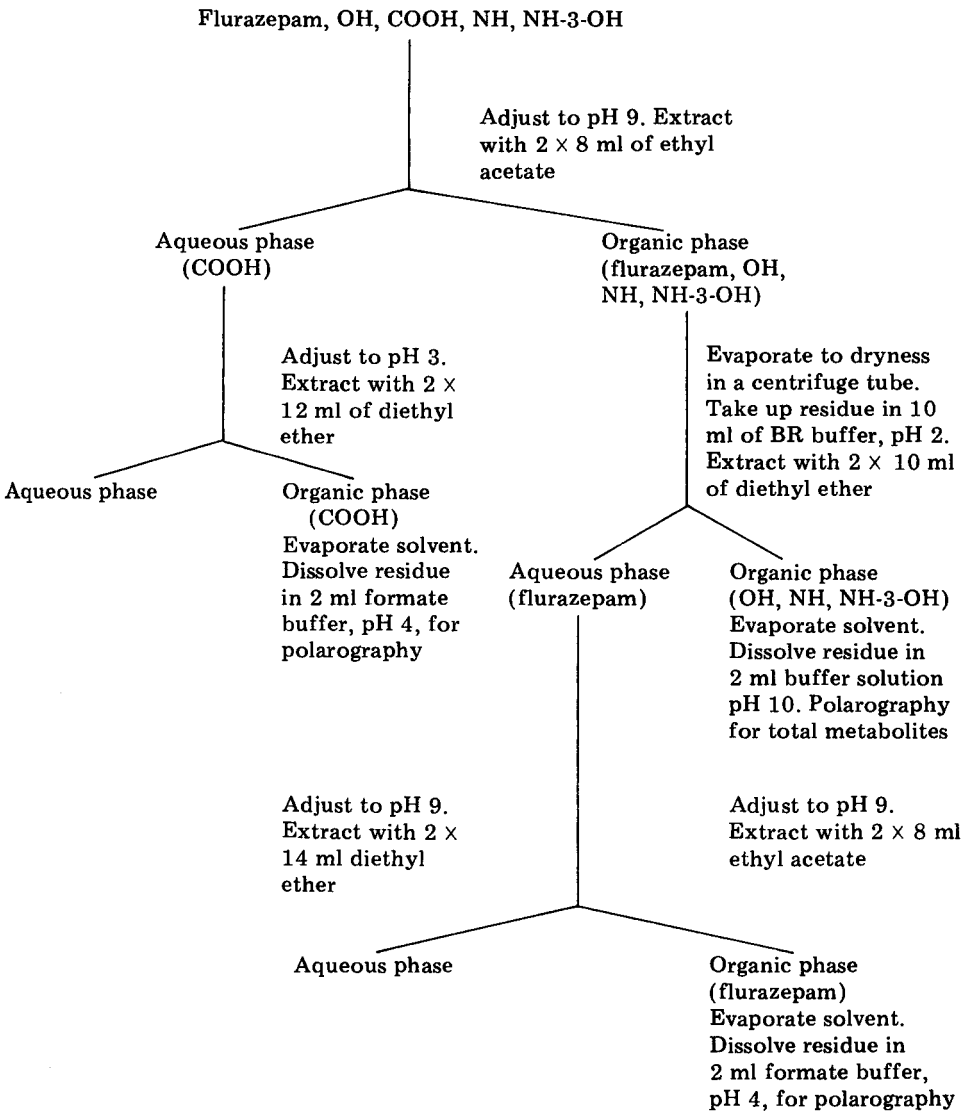

Fig. 2. Solvent extraction scheme for the recovery of flurazepam and its metabolites. OH = *N*-1-hydroxyethyl metabolite (IV); COOH = *N*-1-acetic acid metabolite (VI); NH = *N*-1-desalkyl metabolite (V); NH-3-OH = *N*-1-desalkyl-3-hydroxy metabolite (VII).

The initial extraction stage into ethyl acetate from aqueous solution at pH 9 could be replaced by an extraction with diethyl ether. This does not affect the percentage recovery and greatly speeds up any solvent evaporation stages. Diethyl ether has the added advantage that it tends to result in cleaner extracts, i.e., there is generally less co-extractable material.

Recovery of compounds (VI) and (I) from solvent extraction scheme (Fig. 2)

Comparison of the slopes of the internal standard recovery curves indicated a recovery of metabolite (VI) of 98.6% over the concentration range considered. The reproducibility of the assay is indicated by the results in Table 2. The concentrations refer to the volume of 2 ml used for the polarographic determination. The concentrations in the "added" row therefore assume an initial volume of biological fluid of 2 ml. Expressing the results as standard deviations from the mean, the recovery at the 501 ng ml^{-1} level was 493 ± 7 ng ml^{-1} or 98.4 ± 1.4%. At the 201 ng ml^{-1} level, the results were 198 ± 3 ng ml^{-1} or 98.5 ± 1.5%. Thus after two extraction stages, a recovery of about 98.5% may be expected.

The comparison of the slopes of internal and external standard recovery curves for flurazepam (I) indicated an average recovery of 97.1%. The reproducibility of the assay is shown by the results in Table 3. The mean recovery and standard deviation at each level was 469 ± 7 ng ml^{-1} or 97.1 ± 1.5% and 186 ± 3 ng ml^{-1} or 96.7 ± 1.6%, i.e. the average recovery in the concentration range studied is about 97%. This is marginally lower than the recovery of the acetic acid metabolite, but it must be remembered that the extraction of flurazepam (I) involves three stages.

Polarographic determination of mixtures of N-1-desalkyl, N-1-desalkyl-3-hydroxy and N-1-hydroxyethyl flurazepam (compounds V, VII and IV)

The acetic acid metabolite (VI) and flurazepam (I) can be isolated from the other metabolites for polarographic determination (Fig. 2). The three remaining compounds (IV, V, VII) cannot be separated from each other by the solvent extraction scheme used. Polarographic determination of all three metabolites simultaneously was considered as an alternative.

Plots of $E_{1/2}$ vs. pH for each of these compounds showed that, in acidic or neutral solution, the half-wave potentials of these compounds are all very similar and would not allow resolution of the polarographic waves from each

TABLE 2

Replicate extractions of the acetic acid metabolite (VI) (concentration in ng ml^{-1})

Concn. added	501	501	501	501	501	501	501	201	201	201
Concn. found	492	483	492	486	505	497	494	201	198	196
% recovery	98.2	96.4	98.2	97.0	101	99.2	98.6	100	98.5	97.5

TABLE 3

Replicate extractions of flurazepam (I) (concentrations in ng ml^{-1})

Concn. added	483	483	483	193	193	193
Concn. found	460	473	473	190	184	183
% recovery	95.2	97.9	97.9	98.4	95.3	94.8

compound in a mixture. In more alkaline solutions, however, greater differences in the potentials begin to appear [7]. This is exemplified in Table 4 which shows the $E_{1/2}$ value for each compound in the interval pH 9—14. At pH 13, the 3-hydroxy metabolite (VII) is well resolved from the other two compounds, but the latter two are still too close to allow complete separation of the waves for accurate quantification. At pH 14, the difference between the half-wave potentials of the *N*-desalkyl and *N*-hydroxyethyl metabolites has increased to 100 mV which should be sufficient to allow recording of the polarograms without appreciable overlap. The 3-hydroxy compound now appears at even more negative potentials, well removed from the other two compounds.

However, although it appears that the simultaneous determination of all three metabolites should be possible at pH 14, this is not the medium of choice as far as sensitivity is concerned [7]. The polarographic current from *N*-hydroxyethyl and the 3-hydroxy metabolites is acceptable but that of the *N*-desalkyl compound is much reduced compared with the values at lower pH. Despite this, the possibilities of the method were further investigated. The differential pulse polarograms obtained are shown in Fig. 3. The results were found to be in accord with the predictions from Table 4. At pH 13, the 3-hydroxy metabolite exhibits a measurable peak whilst the two remaining compounds are indistinguishable. In 0.5 M sodium hydroxide, these

TABLE 4

$E_{1/2}$ values of compounds (IV), (V) and (VII) at different pH (V vs. s.c.e.)

pH	9	10	11	12	13	14
$E_{1/2}$ (IV)	−1.028	−1.066	−1.106	−1.145	−1.177	−1.193
$E_{1/2}$ (V)	−1.018	−1.060	−1.108	−1.151	−1.224	−1.292
$E_{1/2}$ (VII)	−1.023	−1.066	−1.092	−1.135 } −1.390 }	−1.502	−1.576

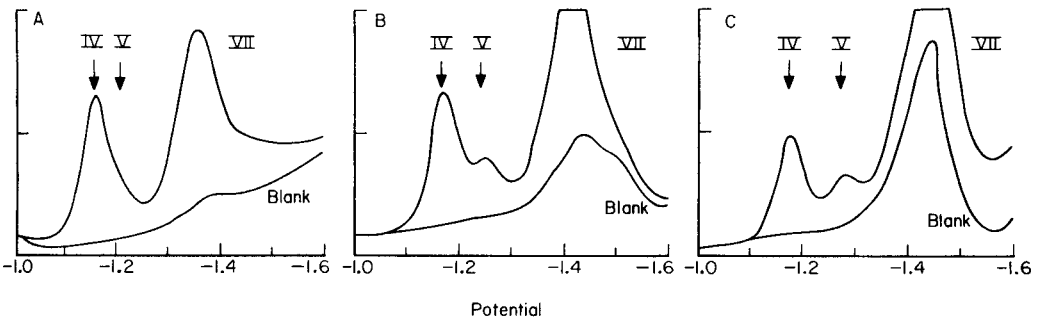

Fig. 3. Differential pulse polarograms of a mixture of compounds (IV), (V) and (VII) at different alkalinities. (A) 0.1 M NaOH; (B) 0.5 M NaOH; (C) 1.0 M NaOH. In all cases, full scale deflection is 0.1 μA and potentials are in V vs. s.c.e.

two metabolites are just resolved but the 3-hydroxy metabolite (VII) sits on a large interfering peak in the supporting electrolyte which makes measurement difficult. The resolution of the two compounds is complete in 1 M sodium hydroxide but the electrolyte interference then makes quantification of compound VII impossible. The addition of EDTA to the sodium hydroxide solution, in an attempt to remove the interfering peak, did not improve the situation. It became evident that in such a mixture the 3-hydroxy metabolite could only be determined in 0.1 M sodium hydroxide while the simultaneous assay of the other two compounds required 1 M sodium hydroxide. The method would be quite insensitive for the *N*-desalkyl molecule.

It is evident that background interferences from the sodium hydroxide solutions is one of the main limiting factors in this proposed method. Experience has shown that in the extraction of drugs from blood and urine, a general deterioration of the background polarographic current takes place owing to the large quantities of co-extractable material. It is therefore likely that the polarograms of these metabolites in sodium hydroxide after extraction from body fluids would display a high degree of interference. Add to this the masking peak already present in the sodium hydroxide solution and the practicability of such determinations without extensive clean-up procedures becomes somewhat improbable.

An estimate of the concentration of the *N*-hydroxyethyl metabolite (IV) might be possible in 1 M sodium hydroxide but it is unlikely that the other two compounds could be determined. An alternative might be to dissolve the residue containing the three compounds in a Britton—Robinson buffer solution of pH 10. Table 4 shows that at this pH, the three metabolites have very similar half-wave reduction potentials. Thus, a more or less composite wave from all three compounds would be obtained which would allow a rough estimate of total metabolites, exclusive of the acetic acid metabolite.

These results have demonstrated how polarography can be applied to the estimation of flurazepam and its metabolites in biological fluids. Although the acetic acid metabolite can be determined separately, the method is probably best suited to the estimation of total metabolites. Some of these results have been used in the formulation of a polarographic method for the determination of flurazepam and its major metabolites in animal blood [4].

REFERENCES

1 L. O. Randall, W. Schallek, C. L. Scheckel, P. L. Stefko, R. F. Banziger, W. Pool and R. A. Moe, Arch. Int. Pharmacodyn. Ther., 178 (1969) 216.
2 J. A. F. de Silva and M. Strojny, J. Pharm. Sci., 60 (1971) 1303.
3 J. A. F. de Silva, C. V. Puglisi, M. A. Brooks and M. R. Hackman, J. Chromatogr., 99 (1974) 461.
4 J. M. Clifford, M. R. Smyth and W. Franklin Smyth, Fresenius Z. Anal. Chem., 272 (1974) 198.
5 A. Clatworthy, Forensic Police Laboratories, Lambeth, London, private communication.
6 J. A. Groves and W. Franklin Smyth, Spectrochim. Acta, 35A (1979) 603.
7 J. A. Groves and W. Franklin Smyth, Ph.D thesis, University of London, 1976.

Analytica Chimica Acta, 123 (1981) 187—199

CONVOLUTION VOLTAMMETRY OF METAL COMPLEXES

J. J. TOMAN, R. M. CORN and S. D. BROWN*

Department of Chemistry, University of California, Berkeley, CA 94720 (U.S.A)

and

Materials and Molecular Research Division, Lawrence Berkeley Laboratory, 1 Cyclotron Road, Berkeley, CA 94720 (U.S.A.)

(Received 2nd June 1980)

SUMMARY

The application of convolution potential voltammetry to questions of metal complexation is described. Theoretical relations are derived to show that the stability constants may be directly related to the shift in the peak potential of the semiderivative wave, provided the complexes are labile. Equations are also given for inert and quasi-labile complexes. Stability constants for the $PbCl_x$ and $CdCl_x$ systems are reported, illustrating the use of convolution techniques with linear scan voltammetry and with linear scan anodic stripping voltammetry. Advantages of convolution techniques are discussed.

The current interest in trace metal speciation has led to renewed efforts at obtaining precise stability constants for metal complexes, including those of possible environmental significance. Electroanalytical methods, particularly those at a stationary electrode such as the hanging mercury drop electrode (h.m.d.e.), have been used in the bulk of these studies (e.g., [1]).

One problem in using the h.m.d.e. for metal speciation studies is the shape of the current peak produced — a relatively broad, asymmetric waveform even in the reversible case. Identification of the peak potential can be difficult in the best of conditions, and may be impossible when several electroactive species are present, because of peak overlap [2]. Because the major source of error in a determination of metal complex stability constants has been shown to be the measurement of peak potentials [3], the precision of the results can be significantly affected.

A second problem inherent in the use of an electrochemical method to determine stability constants is the treatment of the lability of the metal complex(es) present in the solution [4, 5]. Theoretical analysis of this problem is made difficult by the lack of a simple, closed form expression for linear potential scan voltammetry, the simplest waveform to treat both instrumentally and mathematically.

This paper reports the application of convolution voltammetry to studies of metal speciation at the hanging mercury drop electrode. Both linear scan

voltammetry and linear scan anodic stripping voltammetry were examined using numerical convolution techniques coupled with computer-controlled instrumentation. To demonstrate the applicability of the method, the stability constants for the cadmium and lead chloride systems were determined.

THEORY

Linear scan voltammetry (l.s.v.)

Previous workers [6, 7] have outlined the use of convolution integrals of the current with $t^{-1/2}$, either by use of RC ladder circuits [8, 9] or by digitization of waveforms and subsequent numerical processing of scans on large computers [10]. In this work, the convolution was performed immediately after the potential scan, so that it is more convenient to convolute the current with the potential. The semi-integral, $m(E)$, is defined as

$$m(E) = \pi^{-1/2} \int_{E_i}^{E} i(\gamma)\,(E - \gamma)^{-1/2}\,\mathrm{d}\gamma \tag{1}$$

and the semiderivative, $e(E)$, as: $e(E) = \delta m(E)/\delta E$, where E is the potential applied to the electrode, E_i is the initial potential of the experiment, and i is the current as a function of the potential. The expression for $m(E)$ is effectively equivalent to the semi-integral used by Savéant [6, 10], Oldham [7, 8] and co-workers, while the expression for $e(E)$ is equivalent to the semiderivative used by Goto and Ishii [9]; since the scan is linear, these expressions differ from those of previous workers only by $\nu^{1/2}$, the root of the scan rate.

When these definitions, and the approach of Goto and Oldham [11] for the usual electrode reaction where no complexes are present ($Ox + ne^- = Red$), are used, the surface concentrations for the oxidized and reduced species are, respectively

$$C_o(E) = C_o^* - (nFA\nu^{1/2}D_o^{1/2})^{-1}\, m(E) \tag{2}$$

$$C_R(E) = (nFA\nu^{1/2}D_R^{1/2})^{-1}\, m(E) \tag{3}$$

where n is the number of electrons transferred, A is the surface area of the electrode, F is Faraday's constant, D_o and D_R are the diffusion constants of the chemical species, and C_o^* is the concentration of oxidized species in the bulk solution. For a reversible reaction, the expression obtained for the shape of the wave is

$$E = E_{1/2}^R + \frac{RT}{nF} \ln\left[(m^* - m(E))/m(E)\right] \tag{4}$$

where $E_{1/2}^R = E^0 + RT(nF)^{-1} \ln(D_o\, D_R^{-1})^{1/2}$, $m^* = (D_o\,\nu)^{1/2}\, nFAC_o^*$, and E^0 is the standard electrode potential; these equations are analogous to the expressions obtained by Goto and Oldham [11].

The shape of the semidifferential wave, obtained by differentiation of eqn. (4) is

$$e(E) = [n^2F^2Av^{1/2}C_o^* (4RT)^{-1} D_o^{1/2}] \operatorname{sech}^2 [nF(2RT)^{-1} (E - E_{1/2}^R)] \quad (5)$$

Note that it is centered at $E_{1/2}^R$, and is a symmetric peak.

For the case of one complex, assumed to be electroinactive, the reaction

$$MX_L^{(n-Lp)^+} \underset{k_f}{\overset{k_b}{\rightleftharpoons}} M^{n+} + L\,X^{p-} \overset{ne^-}{\rightleftharpoons} M^0 \quad (6)$$

may be written, where M is the metal, X is the ligand and $MX_L^{(n-Lp)^+}$ is the complex. The equilibrium constants are defined as $K = k_f/k_b = 1/\beta_L[X]^L$, where β_L is the stability constant of the complex, and k_f and k_b are the forward and backward exchange rate constants of the ligand, respectively. For large excesses of ligand, the reaction may be considered pseudo-first-order, since K is nearly constant. This is identical to the case of a first-order chemical reaction preceding the electrochemical reaction, first examined by Savéant and Vianello [12]. By recasting their treatment in terms of convolution integrals, defining M^{n+} as ox, and M^0 as red, the following equations are obtained

$$C_o(E) = C_o^* - (\pi D_o v)^{-1/2} (nFA)^{-1} \int_{E_i}^{E} \{((K)/(1+K)) + (\exp[-k(E-\gamma)])/$$

$$(1+K)\}\, i(\gamma)d\gamma \times (E-\gamma)^{-1/2} \quad (7)$$

and

$$C_R(E) = (nFAv^{1/2}D_R{}^{1/2})^{-1}\, m(E) \quad (8)$$

where $k = (k_f + k_b)/v$. These equations contain the effects of complex lability upon the shape and position of the semi-integral wave.

Examination of eqn. (7) leads to three cases:

Case 1, Inert complexes. For inert complexes, the exchange rate is slow, and k approaches zero. Then eqn. (7) reduces to

$$C_o(E) = C_o^* - (nFAv^{1/2}D_o^{1/2})^{-1}\, m(E) \quad (9)$$

which, upon substitution into the Nernst equation, gives an unshifted wave of height proportional to the concentration of the uncomplexed metal, because of the speed of the electrochemical measurement relative to the kinetics of ligand exchange.

Case 2, Labile complexes. For rapid exchange rates, k approaches infinity, and eqn. (7) reduces to

$$C_{ox}(E) = [K/(1+K)]\,[C_{tot}^* - (nFAD_{ox}^{1/2}\, v^{1/2})^{-1}\, m(E)] \quad (10)$$

where C_{tot}^* is the total analytical concentration of metal in solution. Substitution of eqns. (8) and (10) into the Nernst equation yields a wave of height proportional to C_{tot}^*, shifted from the wave observed for a "free" metal ion

$$E = E_{1/2}^R + RT(nF)^{-1} \ln [(m^* - m(E))/(m(E))^{-1}] + RT(nF)^{-1} \ln (1 + K^{-1}) \quad (11)$$

so that, using the half-wave point on the semi-integral, or at the peak maximum on the semiderivative wave

$$\Delta E_{1/2} = E_{1/2,\,\text{free}} - E_{1/2,\,\text{complexed}} = RT(nF)^{-1} \ln (1 + \beta_L[X]^L) \qquad (12)$$

Equation (12) reduces to the Lingane equation [13] for cases where $\beta_L[X]^L \gg 1$.

For the labile case, one may calculate the concentration of the complex at the electrode surface, and show that, in fact

$$[MX_L^{(n-p)^+}][M^{n+}]^{-1} = K \qquad (13)$$

Thus, the species are always in equilibrium.

The above treatment can be extended to N labile complexes in equilibrium at the electrode surface. By similar arguments

$$\Delta E_{1/2} = RT(nF)^{-1} \ln F_o(X) \qquad (14)$$

where $F_o(X)$ is defined by: $F_o(X) = 1 + \beta_1[X] + \beta_2[X]^2 + \beta_3[X]^3 + \cdots$. This expression is identical to that found by DeFord and Hume for an analogous situation in classical polarography, where the diffusion layer is renewed [14].

Case 3, Quasi-lability. Here k is finite, and dependent upon the scan rate. One can often fit both k and K to the results of a number of runs, analogously to the method used by Carney [15] for nitroloacetic acid complexes of Cd and Pb, or one can use the scan rate dependence of k to force the reaction into either the labile or inert regimes.

These three cases are analogous to those proposed by Davison, using reaction layer theory [4], and by Van Leeuwen [5]. Use of convolution potential voltammetry allows a simple test of the kinetic control of the process in the shape of the semi-integral and semidifferential waves, and their variation with scan rate. Labile complexes will show "normal" semi-integral and semidifferential waves, shifted from the "free"-ion position, while inert complexes will not shift, but will decrease in height. Quasi-labile complexes will show a broadening of the semiderivative peak into a waveform somewhat similar to that of a normal l.s.v. wave; this effect will be more pronounced with increasing scan rate.

Anodic stripping voltammetry using linear scans (a.s.v.)

The same equations for linear scan voltammetry apply to linear scan a.s.v. anodic stripping voltammetry provided that the boundary conditions governing reactant transport remain valid. The problem then reduces to a pseudo-first-order chemical reaction (complexation) following the electrode process. For the equations to apply to a.s.v., the boundary conditions that must be met are that : (i) the initial potential of the scan must be well below the half-wave potential for oxidation; (ii) the concentration of reduced species must be homogeneous within the mercury drop; (iii) the concentration of oxidized species in solution must be small compared to the con-

centration of reduced metal in the drop; and (iv) the concentration of ligand in the system must be greatly in excess of that of the metal ion.

For many speciation studies involving a.s.v., these conditions can be met, and one may judge the lability of the complex by its response to scan rate, as well as determine its stability constant by the methods developed here for l.s.v. For labile complexes, the DeFord—Hume relation applies to convolution a.s.v.

A difficulty arises, however, in a.s.v. studies involving very small amounts of strongly complexing ligand, in that the reaction is no longer pseudo-first-order in metal ion. For quasi-labile systems, this effect complicates the treatment.

EXPERIMENTAL

Reagents

For the l.s.v. runs, reagent-grade $NaClO_4$, $Cd(NO_3)_2$, Na_2EDTA, and NaCl were used as received. The pH of the solutions was adjusted with reagent-grade perchloric acid. Solutions for a.s.v. study were prepared by electrolysing filtered solutions of reagent-grade $NaClO_4$ and NaCl at −1.5 V (vs. s.c.e.) over a mercury pool cathode for three days under argon. These solutions were stored in thoroughly pre-leached teflon bottles. Water for the runs was taken from a leached all-vitreous silica still and stored in pre-leached 5-l linear polyethylene containers. No electrochemically active impurities were observed when 5 ml each of the purified NaCl and $NaClO_4$ solutions were added to 25 ml of the water, plated at the h.m.d.e. for 20 min at −1.00 V (vs. s.c.e.), and subsequently stripped. The lead nitrate used was reagent grade, added just before the a.s.v. scans with an Eppendorf pipette utilizing pre-leached tips. The pH for the a.s.v. runs was adjusted with ultrapure perchloric acid (Ventron).

Equipment and electrodes

The cell used for all runs was the standard Princeton Applied Research (PAR) polarographic cell and cell holder, thermostatted to 20.0°C. The cell was thoroughly leached between runs for the a.s.v. experiments, using Transistar-grade nitric acid (Mallinckrodt). The working electrode was a PAR 9323 h.m.d.e., containing triply-distilled mercury, precleaned by passage through a pinhole. The reference electrode was an Ag/AgCl electrode with a 1.0 M $NaClO_4$/0.1 M NaCl bridge solution; the potential of this electrode was observed to be +40 mV vs. s.c.e., for the l.s.v. experiment, and +44 mV for the a.s.v. experiment. The counter electrode was a length of heavy-gauge platinum wire. Solutions were degassed with purified argon before scans were taken, using a PAR gas inlet tube, with only teflon tubing contacting the solution. Magnetic stirring was used for the a.s.v. runs.

A conventional three-electrode potentiostat (PAR 173) was used, along with a linear scan generator (PAR 175). These were controlled by Digital

Equipment Corporation MINC-11B computer with data acquisition via a 25-kHz, 12-bit analog-to-digital converter coupled to a PAR 179 current-to-voltage converter. The LSI-11/2 processor used has 30K words of usable memory as well as two double-density floppy disk units for data and program storage. Computer control of the scans was achieved by coupling the PAR 175 to the 16-bit digital output module of the MINC system. A programmable clock was used for all timing, and a 12-bit digital-to-analog converter was used to control plating potentials for the a.s.v. runs.

Computer programs

Control of the l.s.v. and a.s.v. experiments was performed by MACRO-11 assembly language subroutines linked to a FORTRAN driver. Data were stored on disks for processing, which consisted of digital filtering using the fast Fourier transform [16] and semi-integration by a FORTRAN program employing the method of Huber [17], as given by Nicholson and Olmstead [18]. The FORTRAN program then numerically differentiated the semi-integral wave to produce the semiderivative wave. Potential shift vs. ligand concentration curves were analyzed by using a polynomial regression routine supplied by Digital Equipment Corporation; this routine was previously checked by us with known data and found to behave properly. Species distributions were calculated from our results using MINEQL [19].

Procedure

For the complexation with l.s.v. studies, solutions of NaCl were made up to an ionic strength of 0.99 ± 0.01 with $NaClO_4$, and cadmium nitrate was added to make the final solutions 1.2×10^{-4} M in Cd^{2+}. The pH was adjusted with perchloric acid to 5.00, and the solution was degassed. Ten l.s.v. scans were taken from −0.400 to −0.900 V (vs. Ag/AgCl), averaged, and digitally filtered. The filtered scans were then semi-integrated and differentiated to yield the semiderivative scan. It was observed that the order of filtering and semi-integration made no difference in the value obtained for the half-wave potential which was obtained via a parabolic interpolation routine. Studies of the peak shape of the CdEDTA wave were done with a solution containing 10^{-4} M Cd^{2+} and 10^{-2} M Na_2EDTA, adjusted to pH 4.0 with perchloric acid. The scan rate was varied, and the data taken as before.

The a.s.v. studies of metal complexation used purified solutions of NaCl and $NaClO_4$, of total ionic strength 2.22 ± 0.3, to which enough lead nitrate was added to give a final Pb^{2+} concentration of 4.4×10^{-7} M (insuring that the K_{so} (1.0×10^{-5}) for lead chloride would not be exceeded) and the pH adjusted to 4.00. The solutions were degassed, then stirred for 15 s at a potential of −0.131 V (vs. Ag/AgCl) to establish a reproducible flux. The potential was changed to −1.000 V and held for 600 s; 6 s before the end of the plating period, stirring was halted. The potential was changed to the rest potential of −0.800 V vs. s.c.e., where it was held for 15 s to insure a homogeneous amalgam. Stripping then took place at a rate of 1.00 V s^{-1},

and the resultant voltammogram was recorded, after which the potential was held at −0.135 V for 60 s to remove all remaining lead from the drop. The potential was then changed to the rest potential and held there for 15 s, and a second stripping voltammogram was performed and recorded. Both this background scan and the a.s.v. scan were stored on disk. Subsequent processing began with the numerical subtraction, point by point, of the background scan from the a.s.v. scan to remove capacitative and other background currents [19]. The rest of the processing took place as in the l.s.v. scans.

The precision in obtaining half-wave potentials was observed to be about 0.3 mV; in changing plating times from 60 s to 600 s during some preliminary studies for the a.s.v. runs, the shift (ca. 0.3 mV) of peak potential with the logarithm of the plating time could be distinguished, as predicted by pseudo-polarographic theory [20, 21].

RESULTS AND DISCUSSION

Scan rates

A sample l.s.v. scan and the resulting semiderivative are shown in Fig. 1. For these scans, 512 data points were taken, with the maximum available scan rate (100 V s^{-1}) being limited by the interrupt latency time of the LSI 11/2 microcomputer and the throughput of the analog-to-digital converter; higher scan rates are possible at the cost of lowering the resolution of voltage. A.s.v. scan rates were limited to below 20 V s^{-1} to obtain reproducible background-subtracted waves. Figure 2 shows the a.s.v. and background scans, and also illustrates the resulting semiderivative. Removal of the larger background currents in a.s.v. is necessary to obtain well-shaped semiderivatives at moderate scan rates.

Effects due to the sphericity of the electrode have been observed by

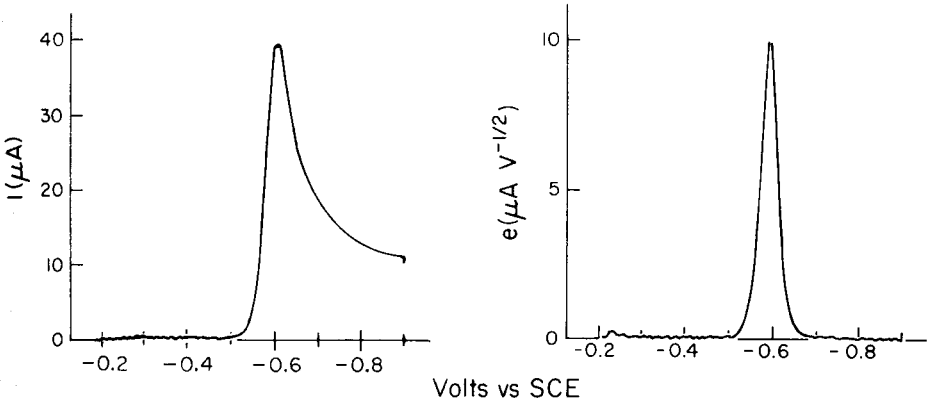

Fig. 1. Linear scan voltammetry wave for cadmium and its resulting semiderivative wave. Supporting electrolyte is 1 M KNO_3.

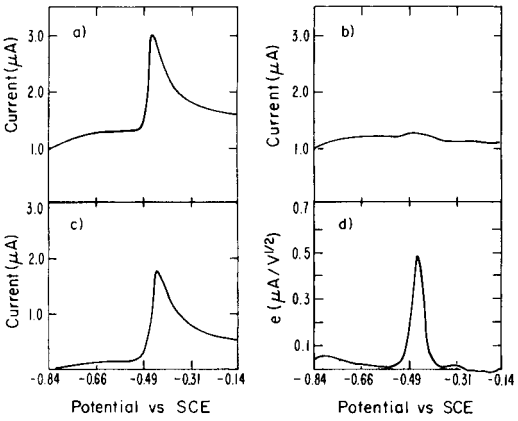

Fig. 2. Numerical generation of semiderivative wave in anodic stripping voltammetry. (a) A.s.v.; (b) background scan; (c) background-subtracted wave; (d) resulting semiderivative wave.

others in convolution potential voltammetry [6]. Because the scan rates used here are relatively fast, relatively small effects on the semi-integral caused by electrode sphericity may be expected, with these effects being most prominent well after the $E^{R}_{1/2}$ value [6]. The main effect will be a slight altering of the baseline past the peak in the semidifferential scan. A series of experiments were performed on the same solution, using different drop sizes, ranging from 0.27 to 0.57 mm in radius. No shift in the potential of the peak maximum of the semidifferential peak was observed. The data have therefore not been corrected for sphericity. The effects of uncompensated resistance were minimized by careful location of the reference electrode adjacent to the working electrode.

Peak shapes

The reversible, 2-electron semidifferential waveform is predicted to have a peak width (at half-height) of 45.4 mV [22]. In the studies of cadmium and lead, widths of 45.6 mV for cadmium and 45.5 mV for lead were observed, indicating a good degree of reversibility. Analysis of the raw l.s.v. and a.s.v. scans also indicated both systems to be reversible at the scan rates used for the complexation studies. Both the cadmium and lead systems in chloride were observed to be labile, in that the semiderivative peak shape and width was invariant to scan rate, as shown in Fig. 3. The cadmium—EDTA system, however, was observed to be quasi-labile in that the shape of the semiderivative peak was strongly dependent upon the scan rate, as predicted by eqns. (7) and (8). This dependence is illustrated in Fig. 4. For scan rates below 200 mV s^{-1}, symmetric semiderivative waves were obtained for the system, indicating that the complex is somewhat labile. Studies of this complex have shown that the rate constant for dissociation of CdEDTA is 10.8 s^{-1} [23].

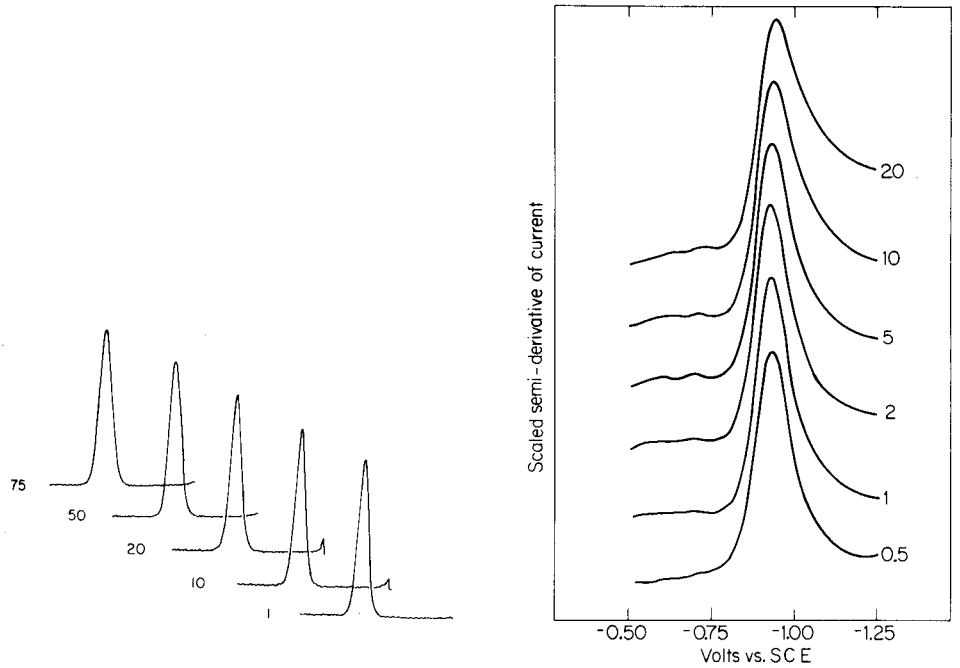

Fig. 3. Peak-shape dependence of the semiderivative wave for cadmium in chloride on scan rate. The numbers on the waves represent scan rate in V s^{-1}.

Fig. 4. Peak-shape dependence of the semiderivative wave for cadmium in EDTA on scan rate. The numbers on the waves represent scan rate in V s^{-1}.

It should be noted that the ability to scan rapidly is a distinct advantage of the numerical generation of semi-integral and semi-differential waves. The RC ladder network of Oldham [8] can be expected to induce distortions at higher scan rates via time constant effects. For studies of the kinetics of complex dissociation by convolution voltammetry, these effects are particularly damaging, since any evaluation of kinetics will involve a fit of the peak widths to scan rate.

Stability constants

Tables 1 and 2 list the data observed for the $CdCl_x^{2-x}$ and $PbCl_x^{2-x}$ systems, respectively. From these data, a fit of the calculated DeFord–Hume F_1 function to a second-degree polynomial in $[Cl^-]$ for cadmium and a second-degree polynomial in $[Cl^-]$ for lead. Polynomials used were weighted with simple $1/F_o$ functions as described by Momoki et al. [24] and Varga [25], but unweighted fits were also attempted. Other models were investigated, but rejected because they either gave negative stability constants or gave constants with considerably larger errors (and correspondingly poorer fit parameters) than those reported here. The stability constants produced by these

TABLE 1

Potential shifts and DeFord—Hume functions for cadmium in chloride[a]

$[Cl^-]$ (M)	E_p(V)[b]	$\Delta E_{1/2}$(mV)	F_0	F_1	F_2	F_3
0	−0.6175	0	—	—	—	—
0.107	−0.6375	−18.2	4.23	30.3	28.0	—
0.191	−0.6429	−25.4	7.47	34.0	35.3	—
0.301	−0.6504	−32.9	13.5	41.9	48.4	—
0.398	−0.6547	−37.2	19.0	45.4	45.6	42.8
0.481	−0.6588	−41.3	26.3	52.7	52.8	50.4
0.588	−0.6625	−45.0	35.3	58.4	53.0	41.6
0.703	−0.6665	−49.0	48.4	67.5	57.3	40.9
0.783	−0.6699	−52.4	63.4	79.7	67.0	49.1
0.995	−0.6758	−58.3	101	100.7	53.9	45.5

[a]pH 5.01 ± 0.05; I = 0.99 ± 0.01 M; sensitivity 10 μA/full scale; scan rate 1.0 V s^{-1}, drop radius 0.61 mm; T = 20.0 ± 0.9°C. [b]Potential relative to the Ag/AgCl electrode.

TABLE 2

Potential shifts and DeFord—Hume functions for lead in chloride[a]

$[Cl^-]$ (M)	E_p(V)[a]	$\Delta E_{1/2}$(mV)	F_0	F_1	F_2	F_3
0	−0.4156	—	—	—	—	—
0.207	−0.4338	−18.2	4.23	15.6	15.7	—
0.464	−0.4484	−32.8	13.4	26.8	31.2	35.2
0.691	−0.4568	−41.2	26.1	36.4	34.8	35.2
0.895	−0.4651	−49.5	50.4	55.2	48.0	41.9
1.13	−0.4717	−56.1	84.9	73.8	54.0	38.3
1.60	−0.4828	−67.2	11.6	127	71.8	38.3
1.85	−0.4880	−72.4	206	167	83.6	39.2
2.04	−0.4907	−75.6	309	195	89.3	38.6
2.26	−0.4949	−79.3	533	235	98.7	39.0

[a]pH 3.99 ± 0.06; I = 2.22 ± 0.04 M; sensitivity 1.0 μA/full scale; drop radius 0.58 mm, scan rate 1.0 V s^{-1}; T = 20.0 ± 0.5° C. [b]Potential is relative to the Ag/AgCl electrode.

fits are reported in Tables 3 and 4. These results have not been corrected for ionic strength effects because no good literature data on mixed NaCl—$NaClO_4$ electrolytes could be found. Other work on these systems is compared with the present results in Tables 3 and 4; agreement is quite good. Figure 5 shows the calculated distribution of species in the two systems with chloride.

The agreement of values obtained using rapid-scan convolution potential voltammetry with slower, more tedious techniques is encouraging. The advantage of being able to obtain peak shifts through examination of peak maxima and to avoid the use of thin-film electrodes, while still retaining

TABLE 3

Stability constants for cadmium chloride complexes

Method	Temp.	Medium	Log β_n	Ref.
Differential pulse polarography	25	$NaClO_4$ (1 M)	β_1 1.34 β_2 1.75 β_3 1.49	26
Potentiometry	25	$NaClO_4$ (1 M)	β_1 1.33 β_2 1.69 β_3 1.53	26
Polarography	25	$NaClO_4$ (1 M)	β_1 1.35 β_2 1.7 β_3 1.5	27
Polarography	25	$NaClO_4$ (0.76 M)	β_1 1.46 β_2 1.83 β_3 1.96	27
Convolution potential voltammetry	20	$NaClO_4$ (1 M)	β_1 1.44 ± .08 β_2 1.46 ± .05 β_3 1.66 ± .03	This work[a]

[a]Multiple regression coefficient = 0.996.

TABLE 4

Stability constants for lead chloride complexes

Method	Temp.	Medium	Log β_n	Ref.
Potentiometry	25	3 M ($NaClO_4$)	β_1 1.05 β_2 1.51 β_3 1.83	28
Potentiometry	25	3 M ($NaClO_4$)	β_1 1.16 β_2 1.7 β_3 1.97 β_4 0.7	28
Cyclic voltammetry	23	0.7 M (KNO_3)	β_1 0.96	29
Polarography	25	3 M	β_1 1.17 ± .03 β_2 1.7 ± .1 β_3 1.4 ± .2 β_4 1.2 ± .2	27
Convolution potential voltammetry	20	2.22 M ($NaClO_4$)	β_1 1.09 ± .18 β_2 1.02 ± .10 β_3 1.59 ± .01	This work[a]

[a]Multiple regression coefficient = 0.999.

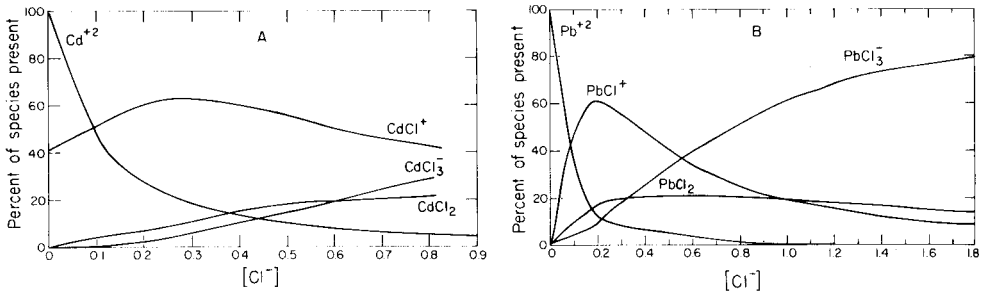

Fig. 5. Species distribution of cadmium (A) and lead (B) in chloride media as a function of chloride concentration. pH 5.00, K_{so} ($PbCl_2$) = 1.0 × 10^{-5}, I = 1.00 for Cd^{2+}, I = 2.22 for Pb^{2+}.

fairly narrow peaks makes the technique quite attractive for studies involving multi-metal systems, or where the thin-film electrode is easily fouled [4]. Further, since no RC circuitry is used, no distortions are introduced into the scan, allowing kinetic information to be obtained in quasi-labile systems.

We are pleased to recognize the assistance of C. M. Phillips, who calculated the distribution of species, and of N. Edelstein, who provided access to the potentiostat. This research was supported by the Office of Nuclear Waste Isolation and by the Division of Chemical Sciences under Contract No. W-7405-Eng-48, both affiliated with the U.S. Department of Energy.

REFERENCES

1 H. Bilinski, R. Huston and W. Stumm, Anal. Chim. Acta, 84 (1976) 157.
2 T. M. Florence, J. Electroanal. Chem., 27 (1970) 273.
3 L. N. Klatt and R. L. Rouseff, Anal. Chem., 42 (1970) 1234.
4 W. Davison, J. Electroanal. Chem., 87 (1978) 395.
5 H. P. van Leeuwen, J. Electroanal. Chem., 99 (1979) 93.
6 J. C. Imbeaux and J. M. Savéant, J. Electroanal. Chem., 44 (1973) 169.
7 M. Grenness and K. B. Oldham, Anal. Chem., 44 (1972) 1121.
8 K. B. Oldham, Anal. Chem., 45 (1973) 39.
9 M. Goto and D. Ishii, J. Electroanal. Chem., 61 (1975) 361.
10 J. M. Savéant and D. Tessier, J. Electroanal. Chem., 77 (1977) 225.
11 M. Goto and K. B. Oldham, Anal. Chem., 45 (1973) 2043.
12 J. M. Savéant and E. Vianello, Electrochim. Acta, 8 (1963) 905.
13 J. J. Lingane, Chem. Rev., 29 (1941) 1.
14 D. D. DeFord and D. N. Hume, J. Am. Chem. Soc., 73 (1951) 5321.
15 J. H. Carney, Anal. Chem., 47 (1975) 2267.
16 J. W. Hayes, D. E. Glover, D. E. Smith and M. W. Overton, Anal. Chem., 45 (1973) 277.
17 A. Huber, Monatsh. Math. Phys. 47 (1939) 240,
18 R. S. Nicholson and M. C. Olmstead, in J. S. Matlson, H. B. Mark and H. C. McDonald (Eds.), Electrochemistry, M. Dekker, New York, 1972.
19 S. D. Brown and B. R. Kowalski, Anal. Chim. Acta, 107 (1979) 13.
20 M. S. Shuman and J. L. Cromer, Anal. Chem., 51 (1979) 1546.
21 S. D. Brown and B. R. Kowalski, Anal. Chem., 51 (1979) 2133.
22 P. Dalrymple-Alford, M. Goto and K. B. Oldham, J. Electroanal. Chem., 85 (1977) 1.

23 N. Tanaka, R. Tamamushi and M. Kodana, Z. Phys. Chem., N. F., 14 (1958) 141.
24 K. Momoki, H. Sato and H. Ogawa, Anal. Chem., 39 (1967) 1072.
25 L. P. Varga, Anal. Chem., 41 (1969) 323.
26 G. A. Heath and G. Hefter, J. Electroanal. Chem., 84 (1977) 295.
27 R. M. Smith and A. E. Martell, Critical Stability Constants, Vol. 4, Plenum Press, New York, 1976.
28 L. Sillén and A. E. Martell, Special Publication No. 25, Supplement No. 1, part I, The Chemical Society, London, 1971.
29 L. M. Petrie and R. W. Baier, Anal. Chem., 50 (1978) 351.

Analytica Chimica Acta, 123 (1981) 201–212

THE DETERMINATION OF TRACES OF THIOCYANATE AND COPPER(II) IONS BY CATHODIC STRIPPING VOLTAMMETRY

RENATA BILEWICZ and ZENON KUBLIK*

Department of Chemistry, University of Warsaw, 02093, Pasteura 1, Warsaw (Poland)

(Received 29th July 1980)

SUMMARY

Cathodic stripping methods are described for the determination of traces of thiocyanate ions down to 2×10^{-8} mol l^{-1} and Cu(II) ions down to 1×10^{-8} mol l^{-1}. The method involves electrolytic accumulation of copper(I) thiocyanate on the surface of a hanging mercury drop electrode followed by stripping of the deposit during the cathodic scan. For the determination of thiocyanate, a copper amalgam electrode can be used. Examples of application of the method for the determination of traces of thiocyanate in common salts, in saliva and urine as well as for the determination of copper(II) ions in tap water are described.

There is a lack of simple and sensitive methods for the determination of traces of thiocyanate ions in real sample solutions. Potentiometric determinations with a thiocyanate-selective electrode suffer from inadequate detection limits (about 10^{-5} mol l^{-1}) and cannot be used if bromide and iodide ions are present in solution even in very small amounts [1]. Nota [2] tried to use a cyanide-selective electrode for the determination of thiocyanate, but the method required the chemical conversion of thiocyanate to cyanide and could not be used in the presence of the numerous metal cations. The polarographic [3] and voltammetric [4] methods proposed for the determination of thiocyanate ions have low sensitivity. Parubotchaya et al. [5] tried to determine traces of thiocyanate by cathodic stripping voltammetry at a silver electrode. The detection limit attained by these authors is 2×10^{-6} mol l^{-1} but the procedure is cumbersome because of the formation of two cathodic stripping peaks corresponding to AgSCN reduction.

Recently, it has been shown that solid copper(I) thiocyanate is easily accumulated on the surface of a mercury electrode [6]. The present work describes the exploitation of this effect for the determination of traces of thiocyanate and copper(II) ions by cathodic stripping voltammetry at a hanging mercury drop electrode (HMDE). In the literature there is only one report [7] on the exploitation of copper(I) thiocyanate accumulation on the mercury surface for the determination of small amounts of copper(II); in that work, however, copper(II) was determined in organic solvents by the anodic not the cathodic stripping technique.

EXPERIMENTAL

The voltammetric curves were recorded with a Radelkis OH-102 polarograph using a conventional three-electrode cell. The reference electrode was a saturated calomel electrode and all the potentials given here are referred to this electrode. The counter electrode consisted of a platinum foil. The indicating electrode was a HMDE made as described by Kemula and Kublik [8]; the surface area of the hanging drop was 0.024 cm^2. Most of the work was done with electrodes filled with pure mercury but some experiments were done with an electrode filled with copper amalgam, which was prepared by dissolving an appropriate amount of copper in mercury. The concentration of copper in the amalgam was determined on the basis of the Ševčik–Randles equation from the height of the copper dissolution peak recorded in a solution 0.1 mol l^{-1} $NaClO_4$.

The solutions were prepared from reagent-grade chemicals and triply distilled water. In some cases the thiocyanate supporting electrolyte was purified electrolytically at a large mercury cathode with a surface area of about 20 cm^2. The potential of the large cathode was held at −1.0 V by means of a potentiostat (ZE-21; Chemipan, Warszawa). The solutions were deoxygenated with argon prior to recording of the voltammetric curves. All experiments were done in a cell with a water jacket, the water being thermostatted at 20 ± 0.2°C. In the stripping experiments, the deposition step was done while the solution was stirred with a magnetic stirrer.

RESULTS

Preliminary experiments

Figure 1 presents the cyclic and stripping curves obtained in perchloric acid supporting electrolyte containing a low concentration of thiocyanate ions and a very low concentration of copper(II) ions. As curve 2 shows, addition of thiocyanate to the perchloric acid solution leads to the appearance of the nearly reversible system of peaks a_1/c_1 corresponding to the formation and reduction of the thiocyanate complexes of mercury(II). Pre-electrolysis done in stirred solution at a potential of +0.3 V, i.e. at the limiting portion of peak a_1, had no essential influence on the height of the cathodic peak, which means that in the anodic process only soluble species are formed. This finding is in agreement with the polarographic data given in the literature [9, 10].

The cyclic curve 3 obtained after addition of a small amount of copper(II) ions does not exhibit any significant changes but on the stripping curves obtained after pre-electrolysis at 0.0 V, the additional peaks c_2 and a_2 appear; these are due to reduction and oxidation of solid copper(I) thiocyanate accumulated on the electrode surface during the pre-electrolysis step. As curve 4 shows, in the presence of a slightly higher copper(II) concentration, peaks c_2 and a_2 also appear during the cyclic run. In this case, precon-

centration at the potential 0.0 V leads to an increase in the height of peaks a_2 and c_2. Peak c_2 is well developed whereas peak a_2 has a complicated shape. In hydrochloric acid supporting electrolyte (curve 5), the dissolution potential of mercury is more negative than the potentials of peaks c_1, a_1 and a_2, but the well developed peak c_2 again appears on the cathodic portion of the curve.

Exploitation of the stripping peaks of CuSCN for the determination of traces of copper(II)

Figure 2 shows the influence of variations in the concentration of thiocyanate ions on the cathodic and anodic stripping peaks of copper(I) thiocyanate as well as on the anodic stripping peak a_3 corresponding to the dissolution of copper amalgam. In very dilute thiocyanate solution, all the peaks shown on curves 1, 1′ and 1″ are poorly developed. In addition, the anodic stripping peak a_2 merges significantly with the final rise of the anodic current. With increase of the thiocyanate ion concentration the shapes of stripping peaks c_2 and a_3 improve whereas the overlap of peak a_2

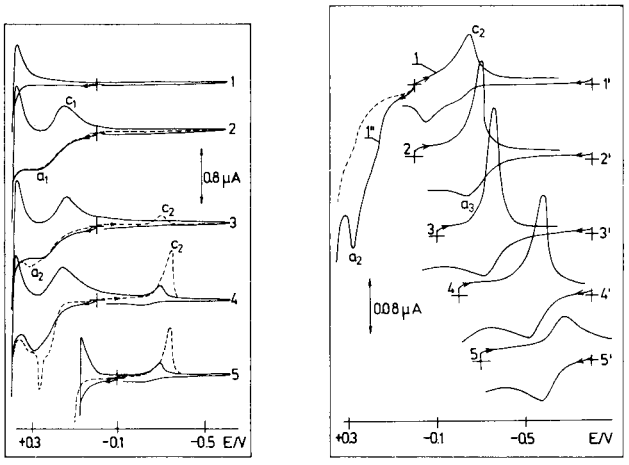

Fig. 1. Cyclic and stripping voltammetric curves obtained in the presence of SCN^- and Cu^{2+} ions. The solutions contained: (1) 0.01 mol l^{-1} $HClO_4$; (2) 0.01 mol l^{-1} $HClO_4$ + 1 × 10^{-4} mol l^{-1} NaSCN; (3) as (2) + 5 × 10^{-7} mol l^{-1} Cu(II); (4) as (2) + 5 × 10^{-6} mol l^{-1} Cu(II); (5) 0.01 mol l^{-1} HCl + 1 × 10^{-4} mol l^{-1} NaSCN + 5 × 10^{-6} mol l^{-1} Cu(II). The dashed lines are the curves recorded separately towards the negative and positive potential from the preconcentrating potential. Preconcentration for 1 min in stirred solution at the potentials: (2—4) 0.0 V; (5) —0.1 V. Voltage scan rate 1.5 V min^{-1}.

Fig. 2. Stripping voltammetric curves obtained after 6-min pre-electrolysis in stirred solution at the potentials: (1′—5′) —0.8 V; (1,1″ and 2) 0.0 V; (3) —0.1 V; (4) —0.2 V; (5) —0.3 V. The solutions contained 0.1 mol l^{-1} $NaClO_4$ (pH 3) and 2 × 10^{-7} mol l^{-1} Cu(II) with increasing thiocyanate concentrations: (1,1′, 1″) 5 × 10^{-6}; (2, 2′) 5 × 10^{-5}; (3, 3′) 1 × 10^{-3}; (4, 4′) 1 × 10^{-1}; (5, 5′) 1 mol l^{-1}. The dashed line is the blank test for the curve 1″. Voltage scan rate 1.5 V min^{-1}.

with the final rise of the anodic current is more severe. In solutions containing more than 1×10^{-3} mol l^{-1} thiocyanate this peak disappears completely. It is evident that in aqueous solutions the anodic stripping peak a_2 is not applicable for the determination of copper, although it has been utilized by Zakharova and Chernova [7] for the stripping determination of copper in organic solvents. In comparison to the poorly shaped anodic stripping peak a_2, the cathodic peak c_2 is very well defined. Over a wide range of thiocyanate concentration (5×10^{-4}—0.1 mol l^{-1}) the shape of this peak varies only slightly. For the same deposition time, peak c_2 is about three times higher than the anodic stripping peak a_3 in which copper amalgam is oxidized in one-electron step to copper(I) thiocyanate.

Figure 3 shows the cathodic (c_2) and anodic (a_3) stripping peaks obtained after the same deposition time for increasing concentrations of copper(II). In the investigated range of concentrations, the cathodic peak is significantly better developed than the anodic peak, which exhibits severe tailing particularly at low concentrations of copper(II). The blank test obtained

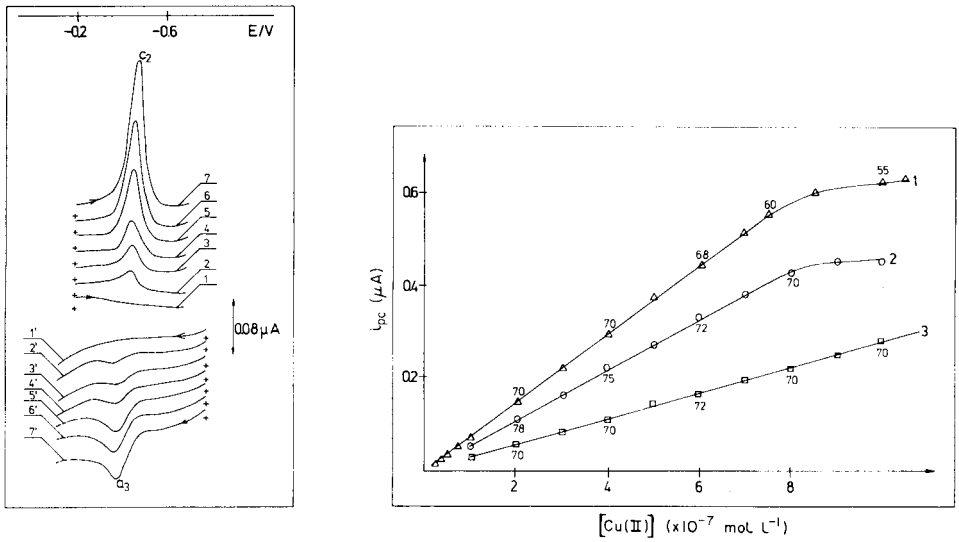

Fig. 3. Cathodic (1—7) and anodic (1′—7′) stripping curves obtained after 10-min preelectrolysis in stirred solution at the potentials: (1—7) —0.2 V; (1′—7′) —0.8 V. The solutions contained 0.1 mol l^{-1} $HClO_4$, 1×10^{-2} mol l^{-1} Na SCN and increasing concentrations of Cu(II): (1, 1′) blank tests in prepurified supporting electrolytes; (2, 2′) blank tests in unpurified supporting electrolyte; (3, 3′) 5×10^{-8}; (4, 4′) 7×10^{-8}; (5, 5′) 1.4×10^{-7}; (6, 6′) 1.9×10^{-7}; (7, 7′) 2.9×10^{-7} mol l^{-1}. Voltage scan rate 1.5 V min^{-1}.

Fig. 4. Dependence of the height of the cathodic stripping peak on the concentration of Cu(II) in solution. The supporting electrolytes contained: (1 and 3) 1×10^{-2} mol l^{-1} NaSCN; (2) 0.01 mol l^{-1} $HClO_4$ and 5×10^{-5} mol l^{-1} NaSCN. Deposition potential —0.1 V. Deposition time: (1, 2) 10 min; (3) 3 min. Voltage scan rate 1.5 V min^{-1}. Numbers near the experimental points give the $b_{1/2}$ values in mV.

after a 10-min deposition time for the electrolytically prepurified supporting electrolyte (curves 1 and 1′), is zero, and under such conditions the detection limit estimated for copper(II) on the basis of peak c_2 is 1×10^{-8} mol l^{-1}. When the supporting electrolyte was not purified (curves 2 and 2′), the inherent copper(II) concentration was close to $3—4 \times 10^{-8}$ mol l^{-1} and the detection limit was therefore worse.

Figure 4 shows the dependence of i_p^{c2} on the copper(II) concentration under conditions where the thiocyanate concentration significantly exceeds the concentration of copper(II). For a 10-min deposition time, the dependence of i_p^{c2} on copper(II) concentration is linear in the range 1×10^{-8}—7×10^{-7} mol l^{-1}.

For copper(II) concentrations greater than 9×10^{-7} mol l^{-1}, the peak height attains a constant value, and simultaneously a new cathodic peak appears at a more negative potential. The problem of occurrence of the additional peak on the cathodic stripping curves obtained for copper(II) in thiocyanate solutions has been discussed in detail [6]. The quantity of electricity involved in the formation of peak c_2 at its limiting height is close to 60 μC cm^{-2} which corresponds to monomolecular coverage by CuSCN [6]. The i_p^c—[Cu(II)] plot obtained for a significantly lower concentration of thiocyanate ions has a smaller slope (curve 2) but the horizontal portion of this plot is attained again at the same concentration of copper(II). Moreover, the same quantity of electricity was involved in the formation of peaks with limiting height of both thiocyanate concentrations. Such behaviour is caused primarily by the change of the shape. With a decrease of thiocyanate concentration the peak width increases and the peak height decreases.

With the increase in thiocyanate concentration, the changes in the height of the cathodic stripping peak become smaller. Variations in thiocyanate concentration between 5×10^{-4} and 1×10^{-2} mol l^{-1} had no significant influence on the height of peak c_2. Careful maintenance of a constant thiocyanate concentration is, therefore unnecessary in obtaining reproducible results for copper(II). Constant pH is also unnecessary; so long as the pH is in the range 1—4, the shape and height of the cathodic stripping peak remain unaltered.

For shorter deposition times (t_d), the slope of the plot i_p^c—[Cu(II)] is smaller (curve 3) and under these conditions the plot extends to higher copper(II) concentrations. In solutions with sufficiently low copper(II) concentration, the i_p^c—t_d plot was linear up to times as high as 25 min, but at longer deposition times there was deviation from linearity. This deviation was not caused by coverage of the electrode by a monolayer of the deposit, but was likely due to poisoning the electrode surface by surface-active agents present unintentionally.

An attempt to decrease the detection limit by addition of some ethanol to the solution proved to be unsuccessful. In 50% water—ethanol solution the shape and height of the cathodic stripping peak remained unchanged. The presence of ethanol has also no beneficial effect on the shape of the anodic stripping peak a_2.

Exploitation of the cathodic stripping peak of CuSCN for thiocyanate determinations

As shown in Fig. 1, only soluble species are formed during anodic polarization of the HMDE in thiocyanate solutions. Thus there is no chance of determining thiocyanate by cathodic stripping voltammetry on the basis of the formation of slightly soluble mercury thiocyanate compounds. However, as was shown in the previous section, thiocyanate ions in the presence of copper(II) ions give a well developed cathodic stripping peak at the HMDE. This reaction was therefore examined for the determination of traces of thiocyanate. In these experiments, copper(I) species were generated at the mercury surface either by reduction of copper(II) ions or by oxidation of copper amalgam introduced into the HMDE reservoir.

In the previous section, it was shown that with a sufficient excess of thiocyanate ions the height of the cathodic stripping peak did not depend on changes in thiocyanate concentration but only on the concentration of copper(II). It was impossible to reverse the situation by using a sufficient excess of copper(II) ions to make the height of the stripping peak independent of copper(II) concentration, because copper(II) species are electroactive in the potential range where the cathodic stripping peak occurs. During the determination of thiocyanate by the method proposed, the concentration of copper(II) must therefore be fairly low and must be kept constant in each series of experiments. Some i_p^c—$[SCN^-]$ plots obtained with different copper(II) concentrations are given in Fig. 5. It is evident that at each copper(II) concentration, the i_p^c—$[SCN^-]$ relationship is initially linear but at higher thiocyanate concentrations the peaks obtained at different copper(II) concentrations have the same constant height, presumably when the electrode surface becomes covered by a monolayer of CuSCN. The quantity of electricity involved in the formation of the peaks with limiting height was again close to 60 $\mu C\ cm^{-2}$. The lower the copper(II) concentration, the greater the range of thiocyanate concentration giving a linear dependence (curve 1). However, under such conditions the cathodic stripping peak is lower and broader. The width of the peak at half height is about 70 mV, whereas at higher copper(II) concentrations (curves 2 and 3) the peak is sharper and its width at half height attains about 55 mV. The blank test obtained for a 3-min deposition time was zero, and the detection limit was then 4×10^{-8} mol l^{-1}.

Figure 6 shows the shapes and heights of the cathodic stripping peaks obtained for increasing concentrations of thiocyanate ion when a copper amalgam was used in the electrode reservoir. The residual currents obtained are lower and more regular than those obtained for solutions containing copper(II) ions. When the copper amalgam electrode is used, it is easier to measure the small stripping peaks, but the peak height is more dependent on the deposition potential. The detection limit obtained with copper amalgam electrode containing 3.4×10^{-3} mol l^{-1} copper was 2×10^{-8} mol l^{-1}.

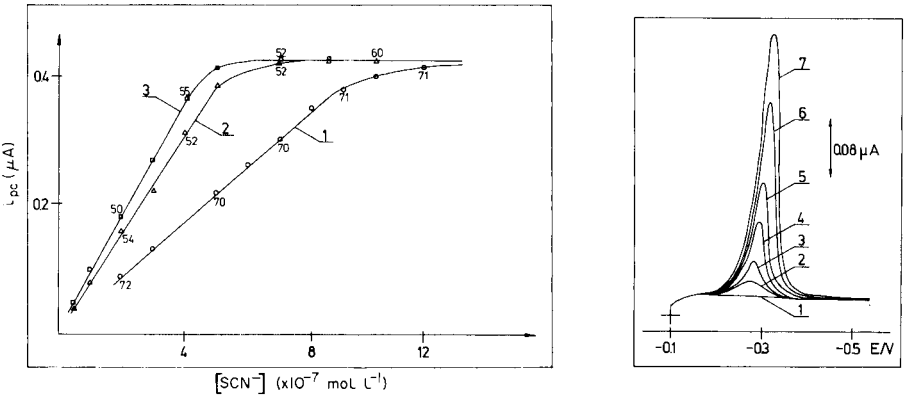

Fig. 5. Dependence of the height of the cathodic stripping peak on the thiocyanate concentration. The solutions contained 0.1 mol l^{-1} $NaClO_4$ (pH 2) and (1) 5 × 10^{-6}; (2) 1 × 10^{-5}; (3) 5 × 10^{-5} mol l^{-1} copper(II). 3-min deposition at −0.1 V. Voltage scan rate 1.5 V min^{-1}. Numbers near the experimental points give $b_{1/2}$ values in mV.

Fig. 6. Cathodic stripping curves obtained with HMDE filled with 3.4 × 10^{-3} mol l^{-1} copper amalgam. The solutions contained 0.1 mol l^{-1} $NaClO_4$ (pH 2) and increasing thiocyanate concentrations: (1) 0; (2) 5 × 10^{-8}; (3) 1 × 10^{-7}; (4) 2 × 10^{-7}; (5) 3 × 10^{-7}; (6) 5 × 10^{-7}; (7) 6.5 × 10^{-7} mol l^{-1}. 3-min deposition at −0.1 V. Voltage scan rate 1.5 V min^{-1}.

Interferences

Interferences encountered during the cathodic stripping determination of thiocyanate and copper(II) ions may be classified in three groups. First, interferences are caused by competition between the formation of CuSCN deposit and the formation of other stable compounds of Cu^{2+} or SCN^- ions. Thus, during the determination of thiocyanate the presence of iron(III) may be harmful. For instance, the height of the cathodic stripping peak obtained for 2 × 10^{-7} mol l^{-1} thiocyanate in a solution containing 1 × 10^{-5} mol l^{-1} copper(II) and 0.1 mol l^{-1} $HClO_4$ decreased by 10% when the concentration of iron(III) exceeded 5 × 10^{-6} mol l^{-1}. During the determination of copper(II), i.e. with high concentrations of thiocyanate (0.1 mol l^{-1}), the cathodic stripping peak decreased by 10% when the concentration of iron(III) exceeded 1 × 10^{-3} mol l^{-1}. However, the harmful action of iron(III) may be easily removed by addition of fluoride.

Hydrogen sulfide and hydrocyanic acid interfere in the determination of copper(II), but not in the determination of thiocyanate provided that deaeration is done in acidified solution (pH 1) and copper(II) is added only after deaeration. In a strongly acidic solution, HCN and H_2S are expelled during the deaeration.

The second type of interferences results from peak overlapping or from mixed deposit formation. Additional cathodic stripping peaks may be formed in the presence of chloride, bromide and iodide ions or selenous acid. A comparison of the cathodic stripping peaks obtained for these interfering

substances is shown in Fig. 7. Obviously, the possibility of the formation of Hg_2Cl_2, Hg_2Br_2 and Hg_2I_2 deposits depends not only on the concentration of the interfering substance but also on the electrode potential used for pre-electrolysis. The more negative the potential of the deposition step, the less interfering deposits will be formed at the electrode surface. Accordingly, the procedure proposed for the determination of copper(II) is less susceptible to interferences of this type than the procedure for thiocyanate. In the presence of interfering substances, 0.1 mol l^{-1} NaSCN should be used for the determination of copper(II) with the deposition at —0.35 V. Under such conditions, a 10% decrease of peak c_2 was observed in the presence of 1×10^{-4}, 1×10^{-2}, $> 1 \times 10^{-1}$, and 3×10^{-5} mol l^{-1} concentrations of I^-, Br^-, Cl^- and H_2SeO_3, respectively.

For the determination of 5×10^{-7} mol l^{-1} thiocyanate in the presence of 1×10^{-5} mol l^{-1} copper(II) with deposition at —0.1 V, a 10% decrease of the height of peak c_2 was caused by 5×10^{-7}, 1×10^{-4}, 5×10^{-3} and 2×10^{-5} mol l^{-1} concentrations of I^-, Br^-, Cl^- ions and selenous acid, respectively. Neutral salts such as sodium perchlorate, nitrate or sulfate added at a concentration of 0.1 mol l^{-1} did not affect the cathodic stripping peak height. In the presence of 2 mol l^{-1} $NaClO_4$ or $NaNO_3$, 1 mol l^{-1} Na_2SO_4 or 0.5 mol l^{-1} NaCl, the cathodic stripping peaks decreased by 1.4, 5.0, 13.5 and 85%, respectively.

A third type of interference was encountered during the determination of certain sulfur-containing compounds [11, 12]. This is caused by chemical reactions between sulfur-containing compounds and mercury. The effect can lead to unexpected enhancement of the cathodic stripping peak when the electrode is held for some time in a solution without applied voltage,

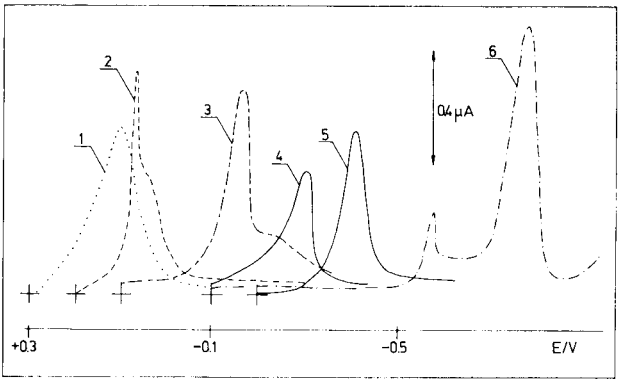

Fig. 7. Comparison of the location of the cathodic stripping peaks obtained after 2-min accumulation in 0.1 mol l^{-1} $HClO_4$ solutions containing (1) 3×10^{-5} mol l^{-1} chloride; (2) 4×10^{-6} mol l^{-1} bromide; (3) 8×10^{-7} mol l^{-1} iodide; (4) 5×10^{-7} mol l^{-1} thiocyanate and 1×10^{-5} mol l^{-1} Cu(II); (5) 2×10^{-6} mol l^{-1} Cu(II) and 1×10^{-2} mol l^{-1} thiocyanate; (6) 2×10^{-6} mol l^{-1} Se(IV). Deposition potentials: (1) +0.3; (2) +0.2; (3) +0.1; (4) —0.1; (5) —0.2; (6) —0.1 V. Voltage scan rate 1.5 V min^{-1}.

or to losses of the analyte when some mercury is present at the bottom of the cell. This effect was observed earlier [6] in solutions containing moderate concentrations of thiocyanate and copper(II), but it did not occur under the conditions used in the present work for the determination of traces of thiocyanate. There was, however, a slight interference in the determination of traces of copper(II) in the presence of a large excess of thiocyanate. The matter was dealt with simply by always using fresh mercury drops.

Practical applications

The utility of the developed methods was tested by determining thiocyanate in diverse samples: salt solutions, saliva and urine. Copper(II) was determined in tap water. For the determination of thiocyanate in salts, the solutions contained 0.1 mol l^{-1} perchloric acid, 1×10^{-5} mol l^{-1} copper(II), 1×10^{-4} mol l^{-1} sodium fluoride and appropriate amounts of the investigated salt. The results obtained are presented in Table 1. The data obtained for samples spiked with thiocyanate showed good recoveries at lower (about 0.1 mol l^{-1}) concentrations of the added salts, which means that calibration curve 2 in Fig. 5 could be used. At higher concentrations of the added salt, recoveries calculated on the basis of this calibration curve were poor, and so a standard addition method had to be used. The results given in Table 1 show that in solutions prepared from reagent-grade salts (about 0.1 mol l^{-1}), thiocyanate was not detected, i.e., less than 4×10^{-8} mol l^{-1} was present. Technical-grade ammonium sulfate solution (0.1 mol l^{-1}) contained 6×10^{-8} mol l^{-1} thiocyanate. Thiocyanate could not be detected even in 1 mol l^{-1} solutions of analytical-grade ammonium sulfate or ammonium nitrate. In order to check the precision of the method, replicate determinations were done on the technical-grade ammonium sulfate solution under the conditions outlined in Table 1. The average of six results was 5.9×10^{-8} mol l^{-1} thio-

TABLE 1

Determination of thiocyanate in different salts
(Solutions contained 0.01 mol l^{-1} $HClO_4$, 1×10^{-5} mol l^{-1} Cu(II) and 1×10^{-4} mol l^{-1} NaF; 3-min deposition in stirred solution at −0.1 V; voltage scan rate 1.5 V min^{-1})

Salt[a]	Grade[b]	Thiocyanate ($\times 10^{-7}$ mol l^{-1})			Recovery of spike (%)
		Found	Added	Total found	
$(NH_4)_2SO_4$	AR	0	1.0	0.95	95
		0	2.0	2.10	105
NH_4NO_3	AR	0	1.0	1.08	108
		0	2.0	1.96	98
$(NH_4)_2SO_4$	TG	0.59	1.0	1.57	98
		0.59	2.0	2.47	94

[a]Sample solutions were 0.1 mol l^{-1} in all cases. [b]Analytical reagent (AR) or technical grade (TG).

cyanate with a relative standard deviation of 7.8%; the average recovery of 1×10^{-7} mol l^{-1} thiocyanate spikes was 99% (range 90—110%).

To check whether the developed method could be applied to the determination of thiocyanate in more complex media some experiments were done with urine and saliva. Several cathodic stripping curves obtained in the presence of urine are presented in Fig. 8. Comparison of curves 1 and 2 shows that the addition of 1% urine to the electrolyte leads to a marked enhancement of the background current. After addition of copper(II) ions, a distinct peak corresponding to CuSCN reduction appears though it is slightly broader than the peak obtained in pure solution. Application of a multiple standard addition procedure to solutions containing 1% urine showed that the i_p^c—[SCN^-] plot was linear; the slope of this plot was, however, smaller than the slope of curve 2 in Fig. 5. The height of the CuSCN stripping peak obtained in the presence of 1% urine was proportional to the deposition time. The concentrations of thiocyanate ions found in two different samples of urine were 2.5×10^{-5} and 9×10^{-6} mol l^{-1}; these values are consistent with literature data [13].

Tests on saliva showed that the thiocyanate concentration was significantly higher than that found in urine. Therefore, to work in the linear portion of the calibration graph, it was necessary to dilute the saliva 10000-fold. The cathodic stripping peaks obtained under these conditions for CuSCN reduction did not differ from the curves obtained in pure thiocyanate solutions. For determinations of thiocyanate in 0.01% saliva, calibration curve 2 (Fig. 5) could be used. The concentration of thiocyanate found in saliva was 2×10^{-3} mol l^{-1}, which is consistent with data given in the literature [14].

The application of anodic stripping voltammetry to the determination of traces of copper(II) in water, particularly in water with a significant content of chloride, encounters difficulties because the copper stripping peak lies close to the final rise of the anodic current. To eliminate this disadvantage, Mann and Deutscher [15] proposed an anodic stripping determination of copper in the presence of thiocyanate. It seems that better resolution of

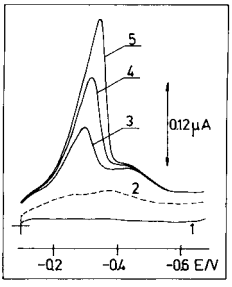

Fig. 8. Cathodic stripping curves obtained for diluted urine. The solutions contained: (1) 0.1 mol l^{-1} $HClO_4$; (2) as (1) + 1% of urine; (3) as (2) + 1×10^{-5} mol l^{-1} Cu(II); (4) as (3) + 3×10^{-7} mol l^{-1} SCN^-; (5) as (3) + 3×10^{-7} mol l^{-1} SCN^- 3-min deposition at —0.1 V. Voltage scan rate 1.5 V min^{-1}.

the copper peak from the final rise of the anodic current can be attained by applying the cathodic stripping technique.

Tap water from Warsaw was analysed without pretreatment apart from the addition of 0.1 mol l^{-1} perchloric acid, 1×10^{-2} mol l^{-1} sodium thiocyanate and 1×10^{-4} mol l^{-1} sodium fluoride. The concentrations of copper(II) ions were determined on the basis of the calibration curve given in Fig. 4. The data obtained are presented in Table 2. Reagent purity is a major limiting factor in the analysis of samples with still lower concentrations of copper(II). The storage of the acidified sample led to a small decrease of copper(II) concentration.

DISCUSSION

Two variations of cathodic stripping voltammetry can be used successfully for the determination of traces of thiocyanate. In the first variation, copper(II) ions are added in excess to the test solutions and the CuSCN deposit is formed on the electrode surface by cathodic reduction of copper(II) to copper(I) ions. Brainina [16] classified a procedure of this type as cathodic stripping voltammetry for variable valence ions. In the second variation, a copper amalgam electrode is used instead of pure mercury electrode, and copper(I) ions are formed in the vicinity of the electrode by anodic oxidation of the copper amalgam. This appears to be the first description of a cathodic stripping procedure with an amalgam electrode.

At lower concentrations of copper(II) and thiocyanate ions, the detection limits seem to be controlled by the solubility product of CuSCN. For example, the detection limits for thiocyanate in solutions containing 1×10^{-6} and 1×10^{-5} mol l^{-1} copper(II) were 3.2×10^{-7} and 4×10^{-8} mol l^{-1}, respectively.

TABLE 2

Determination of copper(II) in tap water[a]
(Deposition for 10 min at −0.1 V in stirred solution; voltage scan rate 1.5 V min^{-1})

Sample	Copper(II) conc. ($\times 10^{-7}$ mol l^{-1})			Recovery of spike (%)
	Found	Added	Total found	
Blank test	0.29	1.0	1.31	102
Taken just after tap opening	4.52	1.0	5.53	101
Taken 10 min after tap opening	1.86	1.0	2.89	102
,,	,,	,,	2.60[b]	—
Taken 1 h after tap opening	1.11	1.0	2.09	98

[a]The results are averages from 3 experiments. [b]Determined after storage for 24 h.

The pK_{so} values calculated on the basis of these data are 12.5 and 12.4, respectively; the pK_{so} value given by Ringbom [17] is 12.7 and by Smith and Martell [18] 13.4. However, when the concentration of copper(II) exceeded 1×10^{-5} mol l^{-1}, the solubility products calculated on the basis of detection limits began to decrease.

The detection limit achieved for thiocyanate, i.e. 2×10^{-8} mol l^{-1}, is lower than the detection limits achieved in cathodic stripping voltammetry for ions such as Cl^-, Br^-, I^- and S^{2-} [16, 19]. The detection limit is also significantly lower than the limits suggested for other methods of thiocyanate determination [1—4]. The proposed method is highly selective. Interferences caused by chloride and bromide ions may be easily overcome by applying an appropriate deposition potential. From the common cationic contaminants, only iron(III) can interfere, and this effect is easily removed by the addition of fluoride ions.

The cathodic stripping procedure proposed here for the determination of copper(II) ions is not as sensitive as the anodic stripping procedure at the HMDE but the cathodic stripping method has an essential advantage in its higher selectivity.

REFERENCES

1 F. Oehme and L. Dolzalova, Fresenius Z. Anal. Chem., 251 (1970) 1.
2 G. Nota, Anal. Chem., 47 (1975) 763.
3 R. A. Plowman and I. R. Wilson, Analyst, 85 (1960) 222.
4 M. M. Nicholson, Anal. Chem., 31 (1959) 128.
5 K. S. Parubotchaya, V. V. Pnev and M. S. Zakharov, Zh. Anal. Khim., 33 (1978) 1800.
6 R. Bilewicz, Z. Stojek and Z. Kublik, J. Electroanal. Chem., in press.
7 E. A. Zakharova and L. A. Chernova, Zh. Anal. Khim., 29 (1974) 881.
8 W. Kemula and Z. Kublik, Anal. Chim. Acta, 18 (1958) 104.
9 I. M. Kolthoff and C. S. Miller, J. Am. Chem. Soc., 63 (1941) 1405.
10 C. J. Nyman and G. S. Alberts, Anal. Chem., 32 (1960) 207.
11 I. E. Davidson and W. F. Smyth, Anal. Chem., 49 (1977) 1195.
12 T. M. Florence, J. Electroanal. Chem., 97 (1979) 219.
13 H. B. Elkins, The Chemistry of Industrial Toxicology, J. Wiley, New York, 1959.
14 C. Long (Ed.), Biochemists' Handbook, Spon, London, 1961.
15 A. W. Mann and R. L. Deutscher, Analyst, 101 (1976) 652.
16 Kh. Z. Brainina, Talanta, 18 (1971) 513.
17 A. Ringbom, Complexation in Analytical Chemistry, Interscience, New York, 1963.
18 R. M. Smith and A. E, Martell, Critical Stability Constants, Vol. IV, Inorganic Complexes, Plenum Press, New York, 1976.
19 W. Kemula, Z. Kublik and J. Taraszewska, in N. D. Cheronis (Ed.), Proc. Intern. Symp. Microchem. Techn., Interscience., New York, 1963, p. 865.

Analytica Chimica Acta, 123 (1981) 213–220

THE ANALYSIS OF ALIQUAT-336 BY GAS CHROMATOGRAPHY

GEAT LEAN LEE, R. W. CATTRALL*, HAYATI DAUD and J. F. SMITH

Department of Inorganic and Analytical Chemistry and Physical Chemistry, La Trobe University, Bundoora, Victoria 3083 (Australia)

I. C. HAMILTON

Department of Chemistry, Footscray, Institute of Technology, Footscray, Victoria 3011 (Australia)

(Received 20th August 1980)

SUMMARY

The determination of the quaternary ammonium components of Aliquat-336 by gas chromatography using tetraheptylammonium chloride as an internal standard is described. The method relies on the fact that long-chain quaternary ammonium salts undergo thermal decomposition at high injection port temperatures to form tertiary amines. The major component in Aliquat-336 is methyldioctyldecylammonium chloride with up to four other quaternary ammonium compounds being present. Aliquat-336 also contains 1-octanol and 1-decanol and some water.

The use of Aliquat-336 in solvent extraction and ion-selective electrode studies is well known. Aliquat-336 ($R_3CH_3N^+Cl^-$) is a commercial reagent manufactured by General Mills Chemicals, Inc. (now Henkel Corporation) and is obtained as a straw-colored viscous liquid. In many publications it is simply referred to as tricaprylylmethylammonium chloride and has been assumed by most workers to consist of a mixture of C_8 and C_{10} carbon chains, with the C_8 chain compound methyltrioctylammonium chloride predominating.

Hartman et al. [1] in a recent study of some chloride-sensitive ion-selective electrodes synthesized certain components of Aliquat-336 with a view to determining which was most suitable for the preparation of PVC-based membranes. However, this work was done without a knowledge of the true composition of Aliquat-336. It is, of course, useful to attempt to correlate the behaviour of Aliquat-336 in both solvent extraction systems and ion-selective electrode studies with the behaviours of the pure components. Such correlations can, however, be made only if the true composition of Aliquat-336 is known. It is also useful to have some knowledge of the variation in composition of different batches of Aliquat-336, particularly if variations in performance are observed.

In this paper, a gas chromatographic procedure is reported for the analysis of different batches of Aliquat-336 to obtain the percentages of the individual

quaternary ammonium chloride components in the material. In addition, other minor components, viz. 1-octanol and 1-decanol, in Aliquat-336 are determined by gas chromatography, and water by the Karl Fischer method.

EXPERIMENTAL

Chemicals

Aliquat-336 was obtained from General Mills Chemicals, Inc. Tetraheptylammonium chloride (Eastman Kodak), tri-n-octylamine, tri-n-decylamine (both Aldrich Chemical Co. Ltd.), 1-octanol and 1-decanol (both Polyscience Corporation) were used as received.

Methyltrioctylammonium chloride (MTOACl) and methyltridecylammonium chloride (MTDACl) were prepared as follows. Methyl iodide (May and Baker) was reacted with the appropriate tertiary amine in absolute ethanol in the mole ratio of 2:1. The mixture was stirred in a closed vessel for 3—5 days until the yellow solution turned dark brown. The ethanol was removed at 60—80°C under reduced pressure, and a brown oily product (occasionally a brown solid) was obtained. The quaternary ammonium iodide was purified by dissolving the brown product in anhydrous diethyl ether with warming, after which the solution was cooled to room temperature and a few drops of ethanol were added. The solution was then cooled in an ice bath, and slow crystallization allowed to proceed. Slow crystallization was essential otherwise an oil was obtained. The product was filtered under suction, washed with cold anhydrous diethyl ether and dried overnight at room temperature. Further recrystallizations were carried out to obtain a white, flaky solid (yield 90%).

The salts were analysed for iodide potentiometrically by dissolving the solid in aqueous ethanol and titrating with silver nitrate solution. (Found, 25.6% I; calculated for $C_{25}H_{54}NI$(MTOAI), 25.6% I. Found, 21.9% I; calculated for $C_{31}H_{66}NI$(MTDAI), 21.9% I.)

The iodide salts were unstable and rapidly became yellow and so were immediately converted to the chlorides by stirring a solution in anhydrous ethanol with an excess of freshly precipitated silver chloride which had been dried overnight at 110°C. The mixture was stirred for at least 3 days until the yellow solution of the iodide became colorless and silver iodide formed. The solution was filtered, and the filtrate purified by passing through an acid-washed alumina column using ethanol as the eluent. Ammoniacal silver nitrate was used to test the solvent for iodide. The ethanol was removed under reduced pressure on a water bath at 60—80°C, leaving a whitish waxy solid which was dried overnight in vacuo (yield 70%).

Both chloride salts were obtained as white solids which were very hygroscopic, particularly methyltrioctylammonium chloride, which became waxy immediately on exposure to air. After prolonged exposure to the air both salts became oily. Chloride determinations (potentiometrically as before) suggested that the waxy solids are the monohydrates and the oils are the

dihydrates. (Found, 74.5% C, 13.7% H, 3.0% N, 7.3% Cl; calculated for $C_{31}H_{66}NCl$(MTDACl), 76.2% C, 13.5% H, 2.9% N, 7.3% Cl. Found, 71.4% C, 13.0% H, 3.15% N, 8.23% Cl; calculated for $C_{25}H_{54}NCl \cdot H_2O$ (MTOACl·H_2O), 71.2% C, 13.3% H, 3.3% N, 8.4% Cl.) Because of the extremely hygroscopic nature of methyltrioctylammonium chloride, the analysis was carried out on the waxy solid.

Instruments

A Perkin-Elmer Model F11 gas chromatograph with flame ionization detection (temperature 270—275°C) was used for the gas chromatographic study. For qualitative work, the linear programmer was set to cover the range of 50—260°C at 25°C min^{-1}. For quantitative measurements of the quaternary components, this was adjusted to 165—260°C at 18°C min^{-1}, and for the alcohols to 60—110°C at 4°C min^{-1}. The injection port temperature was 260°C. The nitrogen flow rate was 30 cm^3 min^{-1} for the quaternary components and 10—12 cm^3 min^{-1} for the alcohols. A glass column was used (length 1 m, o.d. 4 mm, i.d. 3 mm), which was packed with 2.5% OV101 on GasChrom Q (100—120 mesh). Integration measurements were carried out using a LDC Model 301 integrator.

Gas chromatography—mass spectrometry studies were carried out using a JEOL model JMS D100 g.c.—m.s. system.

RESULTS AND DISCUSSION

Paatero [2] who used infrared spectrometry, gas chromatography and mass spectrometry has reported that Aliquat-336 has the approximate composition, 2—5% methyltridecylammonium chloride, 20—25% methyloctyldidecylammonium chloride, 35—40% methyldioctyldecylammonium chloride, 25—30% methyltrioctylammonium chloride, 6—9% methylhexyldioctylammonium chloride, 4—5% n-octanol, 2—3% n-decanol and about 3% water. In carrying out the gas chromatography of Aliquat-336, Paatero made use of the fact that long-chain quaternary ammonium salts undergo thermal decomposition at high injection port temperatures to form tertiary amines. Identification by mass spectrometry of the amines formed, together with the knowledge of how quaternary ammonium salts containing one methyl group undergo thermal decomposition, enabled Paatero to identify these five quaternary ammonium components in Aliquat-336. Paatero also calculated approximate amounts of the quaternary ammonium chlorides in Aliquat-336, using a statistical approach which relates the amounts of the various tertiary amines formed in the gas chromatography to factors such as the tendency to split off particularly alkyl groups and the number of common alkyl groups present in the quaternary ammonium chloride. Because of the assumptions made in this approach, the amounts calculated may be subject to considerable error.

To overcome this difficulty, in the gas chromatographic method used here, a pure quaternary ammonium chloride (tetraheptylammonium chloride) was employed as an internal standard. The procedure relies on the assumption that under standard conditions, the ratio of the decomposition products will be constant and can be measured by determination of peak areas in the gas chromatograms.

The gas chromatograms of two separate samples of Aliquat-336 are shown in Fig. 1. The peaks in the chromatograms were identified by g.c.—m.s. and are listed in Table 1 along with the retention times relative to trioctylamine. The two chromatograms are almost identical except for the presence of methylhexyloctylamine in sample (b) (peak 4a) and the reversal of the relative heights of peaks 1 and 2. The retention time of trioctylamine was verified separately by obtaining the gas chromatogram of the pure tertiary amine.

Aliquat-336 was analysed quantitatively in the following way. A standard curve (Fig. 2) was constructed by using mixtures containing various weight ratios of methyltrioctylammonium chloride and tetraheptylammonium chloride: the gas chromatograms of the mixtures were obtained, and the peak area ratios of trioctylamine to triheptylamine were plotted against the weight ratios of the quaternary ammonium chlorides.

Aliquat-336 was then analysed by adding a weighed amount of tetraheptylammonium chloride to a weighed amount of Aliquat-336 and measuring the peak area ratio of the trioctylamine to triheptylamine in the gas chromatogram. The weight ratio of methyltrioctylammonium chloride to tetraheptylammonium chloride was then obtained from the standard curve enabling the percentage by weight to be calculated for methyltrioctylammonium chloride in the Aliquat-336 sample. The percentages by weight of the other quaternary ammonium components of Aliquat-336 were determined from

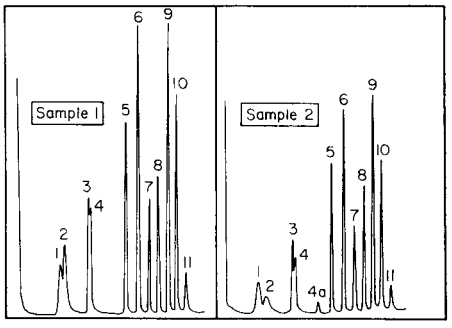

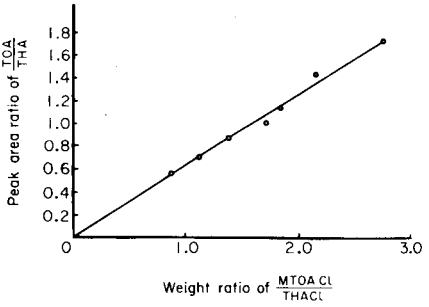

Fig. 1. Gas chromatograms of two samples (1 and 2) of Aliquat-336 obtained at different times from the supplier (refer to Table 1).

Fig. 2. Standard curve for the determination of the percentage of methyltrioctylammonium chloride in Aliquat-336.

TABLE 1

Identification and origin of peaks in gas chromatograms

Peak	Product	Relative retention time	Parent quaternary ammonium compound[a]
1	1-Octylchloride	0.34	
2	1-Octanol	0.36	
3	1-Decylchloride	0.53	
4	1-Decanol	0.54	
4a	Methylhexyloctylamine	0.69	Methylhexyldioctylammonium chloride
5	Methyldioctylamine	0.78	Methyldioctyldecylammonium chloride Methyltrioctylammonium chloride Methylhexyldioctylammonium chloride
6	Methyloctyldecylamine	0.87	Methyloctyldidecylammonium chloride Methyldioctyldecylammonium chloride
7	Methyldidecylamine	0.94	Methyltridecylammonium chloride Methyloctyldidecylammonium chloride
8	Trioctylamine	1.0	Methyltrioctylammonium chloride
9	Dioctyldecylamine	1.07	Methyldioctyldecylammonium chloride
10	Octyldidecylamine	1.13	Methyloctyldidecylammonium chloride
11	Tridecylamine	1.18	Methyltridecylammonium chloride

[a]From Paatero [2].

the peak areas of the other tertiary amines relative to the trioctylamine peak area. The assumption is, of course, made that the detector response is similar for each of the tertiary amines. The results obtained for the two batches of Aliquat-336 are given in Table 2.

In addition, sample 2 showed the presence of a small amount of methylhexyldioctylammonium chloride which could not be estimated quantitatively. This is indicated by the presence of the small peak (4a) in the gas chromatogram of sample 2 which was confirmed by g.c.—m.s. to be methylhexyloctylamine. The other decomposition product of the parent quaternary ammonium compound, hexyldioctylamine, is located in the front portion of the methyldidecylamine peak (peak 7) and cannot be separated but its presence was revealed in the mass spectra obtained during the elution of this peak.

It is interesting to compare these results obtained by using the internal standardization procedure with the statistical approach of Paatero [2]. The present results support the preferential splitting off of the methyl group compared to the longer carbon chain, but the decomposition pattern of the quaternary ammonium compounds does not fit the simple probability approach associated with the number of carbons and length of the alkyl chains postulated by Paatero. For example, Paatero argued that since methyldioctylamine can come from methyltrioctylammonium chloride and from methyldioctyldecylammonium chloride, the probability of its arising from the former compared to the latter is 3:1 simply on the basis of bond

TABLE 2

Percentages of quaternary ammonium chlorides in Aliquat-336

Compound	% By weight	
	Sample 1	Sample 2
Methyltrioctylammonium chloride	14.4 ± 1.1[a]	19.6 ± 0.5
Methyldioctyldecylammonium chloride	32.5 ± 3.1	34.2 ± 1.4
Methyloctyldidecylammonium chloride	24.4 ± 2.3	22.7 ± 1.0
Methyltridecylammonium chloride	6.5 ± 0.9	5.2 ± 0.3
Total quaternary ammonium chloride	77.7 ± 7.4	81.4 ± 3.2

[a]Errors calculated from 3σ associated with the peak area determination.

breakage. However, there is another factor to be considered, arising from the tendency for the shorter chain to be removed in preference to the longer one. Thus Paatero assumed that the tendency to split off an eight carbon chain compared to a ten carbon chain is 10:8. Using these probabilities, he concluded that methyldioctylamine should arise from methyltrioctylammonium chloride and methyldioctyldecylammonium chloride in the ratio of 30:8. Expressed as a percentage, 78.9% of the methyldioctylamine should come from methyltrioctylammonium chloride and 21.1% from methyldioctylammonium chloride. The present results do not support this. For pure methyltrioctylammonium chloride, the gas chromatogram showed the ratio of the peak areas of methyldioctylamine to trioctylamine to be 0.84:1.00. In Aliquat-336 sample 1, the ratio was 1.46:1.00, which indicates that 42.5% of the methyldioctylamine arose from methyldioctyldecylammonium chloride.

A similar discrepancy occurs for methyldidecylamine. According to Paatero, 70.6% of this tertiary amine should arise from methyltridecylammonium chloride and 29.4% from methyloctyldidecylammonium chloride. In the work described here, the gas chromatogram for pure methyltridecylammonium chloride showed a peak area ratio for tridecylamine to methyldidecylamine of 1.00:0.81. In Aliquat sample 1, the ratio was 1.00:2.65, indicating that 69.4% of the methyldidecylamine arose from methyloctyldidecylammonium chloride.

To confirm the validity of these results, a known mixture of methyltrioctylammonium chloride, methyltridecylammonium chloride and tetraheptylammonium chloride was analysed by the above procedure. The results (Table 3) demonstrate the reliability of the method.

A comparison of the present results with those of Paatero shows that the component present in Aliquat-336 in the highest amounts is methyldioctyldecylammonium chloride in all cases. However, somewhat lower amounts of methyltrioctylammonium chloride and methylhexyldioctylammonium chloride and slightly higher amounts of methyltridecylammonium chloride were observed in the present work. Small differences between the two samples

TABLE 3

Analysis of a mixture of methyltrioctylammonium chloride, methyltridecylammonium chloride and tetraheptylammonium chloride

Compound	% By weight	
	Expected	Found
Methyltrioctylammonium chloride	51.5	52.6
Methyltridecylammonium chloride	12.1	13.9

of Aliquat-336 studied were also observed here. The procedure based on internal standardization is believed to provide a reliable method for the determination of the quaternary ammonium components of Aliquat-336.

The 1-octanol and 1-decanol in the Aliquat-336 samples were also determined by gas chromatography. The only variations in the experimental technique were the temperature program and the nitrogen flow rate (see Experimental). The standard addition technique used for these determinations consisted of comparing the peak area ratio of alcohol (i.e. 1-octanol or 1-decanol) to alkylchloride (i.e. 1-octylchloride or 1-decylchloride) for a weighed amount of Aliquat-336 with the ratio obtained for a similar amount of Aliquat-336 to which known amounts of pure 1-octanol and 1-decanol were added. The normal calculation procedure for the standard addition method was carried out assuming a linear relationship between peak area and amount of component. The results are shown in Table 4; the percentages of water found in each Aliquat-336 sample are also shown.

The apparent molecular weights of both samples of Aliquat-336 were determined in terms of the total chloride content by potentiometric titration with standard silver nitrate solution and were found to be 514.6 for sample 1 and 507.8 for sample 2. Comparison of these values with the ranges calculated based on the percentages of the individual quaternary ammonium components present after taking into account the errors suggests a small overestimate of the chloride in both samples.

This can be accounted for in sample 2 by the presence of the small amount of methylhexyldioctylammonium chloride which could not be determined quantitatively. In addition, as Paatero [2] pointed out, Aliquat-

TABLE 4

Percentages of 1-octanol and 1-decanol in Aliquat-336

Alcohol	% By weight	
	Sample 1	Sample 2
1-Octanol	4.4 ± 0.9	2.6 ± 0.8
1-Decanol	3.7 ± 0.8	4.6 ± 0.8
Water	3.0 ± 0.1	5.4 ± 0.1

336, according to the manufacturer, may contain small amounts of NaCl (maximum 0.5%).

We are grateful for the award of a La Trobe University postgraduate scholarship to G. L. L. and for the award of a Colombo Plan Sponsored Fellowship to H. D.

REFERENCES

1 K. Hartman, S. Luterotti, H. F. Osswald, M. Oehme, P. C. Meier, D. Ammann and W. Simon, Mikrochimica Acta, II (1978) 235.
2 Paatero, J., Acta Acad. Abo. Ser. B., 34(1) (1972) 19.

Analytica Chimica Acta, 123 (1981) 221–228

ZONE-SAMPLING PROCESSES IN FLOW INJECTION ANALYSIS

B. F. REIS, A. O. JACINTHO, J. MORTATTI, F. J. KRUG, E. A. G. ZAGATTO, H. BERGAMIN F°* and L. C. R. PESSENDA

Centro de Energia Nuclear na Agricultura, Universidade de São Paulo, 13400 Piracicaba, S. Paulo (Brasil)

(Received 15th July 1980)

SUMMARY

In flow injection analysis, it is possible to select a small portion of a dispersed zone and inject it into another carrier stream. The potentialities of such zone-sampling processes are discussed, and the main factors involved are investigated by spectrophotometric measurements. The usefulness of zone sampling in routine work is demonstrated in the atomic absorption spectrometry of potassium in plant digests. The simple system, which provides automatic dilution, allows analysis of 120 samples per hour, although the required sample dispersion factor was 0.0076; the results agreed with those obtained by conventional a.a.s. after hundredfold manual sample dilution.

The theory of dispersion in flow injection analysis is far from exact and complete, but an experienced worker understands it qualitatively and can control dispersion for the development of new flow injection procedures. The uniqueness of a dispersion pattern under defined constant flow parameters [1] is now well established, and measurements of peak heights [2] or peak widths [3], exploitation of peak profiles [4], and achievement of complete overlap between two or more peaks (merging zones) [5–8] have been employed to provide methods with good analytical characteristics.

As the dispersion pattern is reproducible for a given system, zone-sampling processes become possible in flow injection analysis. In this new variation, the species of interest is injected into an initial carrier stream, creating a well defined zone [9] which undergoes continuous dispersion and possibly chemical reactions, while it is directed towards a second injection port. Only a selected portion of this zone is introduced into a second carrier stream, and is then processed while being transported towards a flow-through detector. For this process, precise timing control is essential.

This paper introduces this expansion of the flow injection concept: potentialities of the approach are discussed for model systems, and applications to real analytical systems are described.

Theory

The zone-sampling process in flow injection analysis utilises the introduction of well-defined aliquots of a processed zone into a second carrier

stream. The flow system is, therefore, composed of at least two almost independent parts (Fig. 1), each of which behaves as a single flow injection system. Each part follows all the flow injection rules.

The species of interest, usually the sample (S), is injected into the first carrier stream (C_S) and, after a time interval Δt, an aliquot ΔS of the dispersed zone (Z) is taken from point a and introduced into the second carrier stream (C'_S). A second zone is then established, processed and measured in a flow-through detector (D) before going to waste (W). It must be emphasized that in Fig. 1, R_C and R'_C represent the entire flow injection manifold, which is often constituted of single coils.

Of the various factors related to the zone-sampling process, only Δt and ΔS are discussed here, because other factors such as pumping rates, initial injected volumes, coil lengths, dead volumes in the analytical path, etc., have the same influence as in usual flow injection systems. Further investigation of these factors is beyond the scope of this paper. The main effect of Δt is to select the portion of the first dispersed zone to be trapped. Of course, the value of Δt is strongly dependent on the pumping rate of C_S and the size of R_C. The value ΔS defines the quantity sampled from the zone Z and has a marked influence on the dispersion inside R'_C.

The zone-sampling process can be used in conjunction with any configuration or approach already proposed for flow injection methods. Some advantages of the proposed technique are outlined in the following paragraphs.

Controlled dispersion. Sampling a small portion of a dispersed zone and injecting it into a second carrier stream is more efficient in achieving a high degree of dispersion than the use of very small injected volumes, long coils or even more complex systems. The injection of very small volumes is not

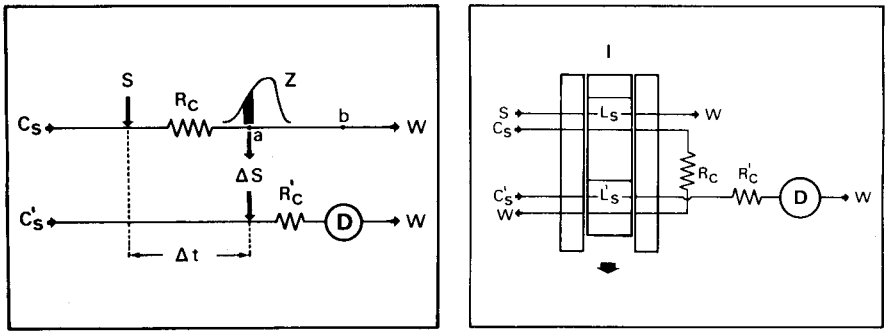

Fig. 1. Schematic representation of the zone-sampling process. Symbols are explained in the text.

Fig. 2. Flow diagram of the systems used. S is the sample (sample aspiration rate, 3.4 ml min^{-1}). L_S is the first sample loop (30 cm) and L'_S is the second loop, which defines the ΔS value. C_S and C'_S are the carrier streams, pumped at 7.8 ml min^{-1} and R_C (500 cm) and R'_C (200 cm) are the reaction coils. I represents the injector commutator, D is the flow-through detector and W denotes waste. For details see text.

recommended for obvious practical reasons. Long coils should be avoided, because as the reaction coil length increases, troubles arise from increase in hydrodynamic pressure and decrease in analytical speed.

Simultaneous determinations. A fraction of the sample zone Z is taken from point *a* (Fig. 1), introduced into C'_S and analysed for one chemical species. The remainder of the sample zone is directed towards *b* for the determination of other chemical species; *b* represents the partial flow diagram for this determination. This approach is particularly useful when the required sample dispersions are very different for two different determinations.

Calibration graph with one standard. As the value Δt selects the portion of the entire dispersed zone to be sampled, and since each portion of the zone corresponds to a different concentration, a calibration graph with only one standard can be obtained by employing suitable Δt values. After calibration, Δt is fixed and the samples are analysed. Finally, other Δt values may also be employed in the analysis of those samples originally outside the analytical range.

Detailed study of dispersion. Scans using different Δt values enable the entire dispersed zone to be transferred stepwise to the second carrier stream, allowing detector D to build an image of the sample zone at point *a* (see Fig. 3). In this situation, a detailed study of the sample zone in the vicinity of point *a* can be performed. When ΔS is small enough, this system can be considered as a point sampler, permitting a detailed study of the boundary of the sample zone and the carrier stream. The general shape of the first sample zone is maintained regardless of the dimensions of C'_S and R'_C, the dead volume of detector D and its response time.

EXPERIMENTAL

Instrumentation

The peristaltic pump and all components of the manifold were the same as used in earlier work [7]. The injector commutator, similar to those already described [2, 7, 8, 10] consisted of two 2:3:2 commutation sections [8] and was operated by two solenoids (SERMAR, 0.6 Kgf closed, 10 W) electronically controlled. The electronic circuit was similar to that already described [10], but the time resistors connected to pin 7 of integrated circuits 2 and 4 were variable resistors, to permit continuous variation of the injection and Δt times.

The flow diagram of the systems used is shown in Fig. 2, with the injector commutator (I) in the sampling position. The species of interest (*S*) is aspirated to fill the first loop (L_S), which defines exactly the volume to be injected. The excess is discarded (W). After the injector commutator has been switched to the injection position, the volume selected is introduced into the first carrier stream (C_S) and the second loop (L'_S) is placed in the same path. The injected species provides a well defined zone which under-

goes dispersion in coil R'_C, being directed towards the second loop and then to waste (W). Next, switching of the injector commutator back to the initial position causes the portion of the dispersed zone inside L'_S to be introduced into the second carrier stream (C'_S) and the second cycle starts. In coil R'_C the final chemical processes occur before measurement in the flow-through detector (D).

Procedures

The zone-sampling process in flow injection analysis was first studied for a model system where a dye solution (0.1% w/v eriochrome cyanine R, pH 2.90) was employed to simulate the sample. Both carrier streams consisted of a buffer solution (0.05 M potassium hydrogenphthalate plus 0.025 M hydrochloric acid, pH 2.90) which, being of the same acidity as the injected species, avoided changes in the molar absorptivity of the dye caused by pH variations. The system in Fig. 2 was used, the detector being a Beckman model 25 spectrophotometer connected to a Beckman 24/25 ACC recorder, and equipped with a Hellma type 178 flow-cell (inner volume 80 μl; optical path 10 mm). The wavelength was set at 535 nm and the sampling time, unless otherwise stated, was 10 s.

The effect of Δt was studied by varying the resting time of the injector commutator in the injection position. Δt values of 12, 13, 14, ... 30 s were employed and all measurements were performed in triplicate. The effect of ΔS was studied by employing loops (L'_S) of 7.5, 15, 30 and 60 cm, which correspond to injected volumes of 38, 75, 150 and 300 μl, respectively. This experiment was performed using four different Δt values, as specified later.

For each situation, total dispersion was evaluated as the ratio between the absorbances corresponding to maximum peak height and to the undispersed dye solution, expressed as $\%C_0$. The original absorbance of the eriochrome cyanine R solution, which corresponds to its initial concentration C_0, was obtained after replacement of C'_S (Fig. 2) by a diluted dye solution (one part of the cyanine solution plus nine parts of the buffer solution) and waiting for the steady-state situation; the corresponding absorbance was then multiplied by ten. The dispersion inside R'_C was calculated after replacement of C_S by the diluted dye solution; in this situation, the entire system can be regarded as a normal flow injection system and the dispersion can also be evaluated in terms of $\%C_0$. Once the total dispersion and also the partial dispersion inside R'_C are known, it is possible to determine the dispersion caused by the zone-sampling process, since the total dispersion is the product of both partial dispersions. The concept of dispersion number as proposed by Růžička and Hansen [9] does not hold in this situation, because it takes into account only the absorbance measured at the top of the peak, while the zone-sampling process utilises other portions of the dispersed zone as well.

The feasibility of the zone-sampling process in real analysis was verified in the atomic absorption spectrometry of potassium in plant digests. A

Perkin-Elmer model 306 atomic absorption spectrometer equipped with a single-element hollow-cathode lamp was used with a Radiometer REC61 recorder with a REA112 high-sensitivity unit. The Perkin-Elmer standard procedures for maximum sensitivity with the air—acetylene flame were followed, and a damping factor of 1.3 s was set. Interfacing with the flow injection system, and the preparation of samples and standards, were the same as described elsewhere [6]. The system in Fig. 2 was employed: the sampling time was 8 s, Δt was 24 s, ΔS was 15 cm, and both carrier streams were distilled—deionized water.

RESULTS AND DISCUSSION

Studies with eriochrome cyanine R

The distribution of the dispersed zone around point *a* (Fig. 1), obtained after a Δt scan, is shown in Fig. 3. The interval between peaks increases with Δt because this interval, which determines the sampling rate for each situation, is the sum of the constant sampling time plus Δt. For peak heights corresponding to Δt values of 15, 18, 25 and 30 s, relative standard deviations of 2.67%, 0.56%, 0.71% and 2.79%, respectively, were calculated after ten measurements. The sampling precision is worst in the front portion of the dispersed zone (Δt = 15 s) because the concentration gradient is higher and

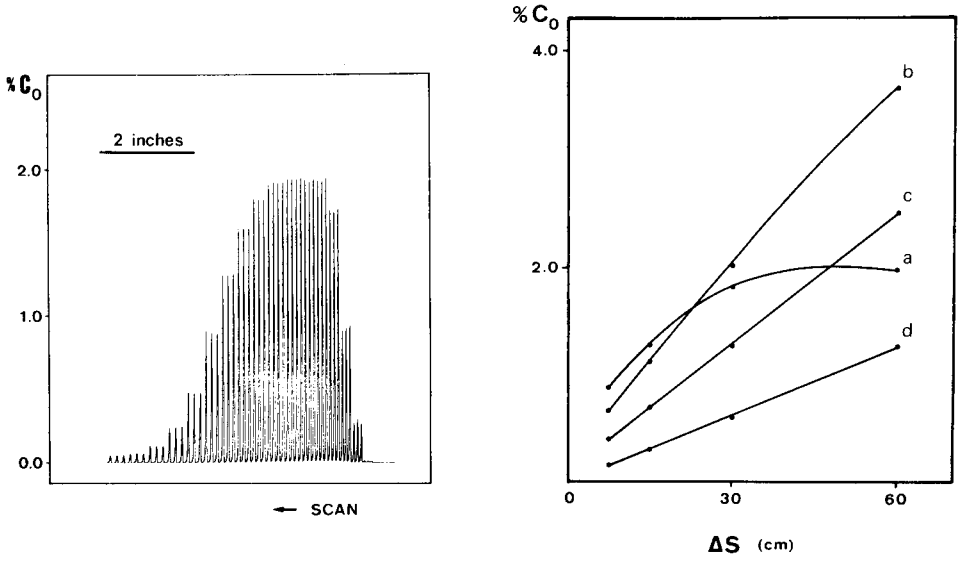

Fig. 3. Effect of Δt value. From left to right, triplicate measurements correspond to a ΔS value of 30 cm and Δt values of 30, 29, 28, ... 13s. C_0 corresponds to the concentration of the undispersed sample. Paper speed, 0.2 in. min^{-1}.

Fig. 4. Effect of ΔS value. Curves a, b, c and d correspond to Δt values of 15, 18, 24 and 26s, respectively. C_0 is referred to in Fig. 3.

the available time for mixing (Δt) is shorter. Therefore, sampling within the front portion of a dispersed zone is not recommended for analytical purposes. As the precisions related to Δt values of 18 s (top of the peak) and 25 s (first portions of the tail) are similar, any portion of the dispersed zone except its front can be sampled. It must be emphasized that, in order to determine the relative standard deviation of the measurements corresponding to Δt value of 30 s, a tenfold expansion in the scale of the recorder was necessary. The decrease in reproducibility in this situation is probably due to a decrease in the signal-to-noise ratio and not to the zone-sampling process.

There is an almost linear relationship between the dispersion factor and ΔS (Fig. 4). Three main factors affect this linearity as ΔS increases: the saturation volume, the partial filling of loop L_S' and the finite size of the dispersed zone Z. The saturation volume effect is well known in flow injection analysis [1, 8]: as the injected volume increases dispersion decreases, but near the saturation volume dispersion reaches a minimum which corresponds to the undispersed sample. Partial filling of L_S' occurs when Δt is inadequate for complete loop filling: this is the main reason for the experimentally observed bending of the curves in Fig. 4. Finally, as the dispersed zone Z has a finite size, ΔS cannot be increased at will.

In the model system, total dispersions near 0.1% were easily attained (Figs. 3 and 4) with a small decrease in analytical speed, although the calculated factor for dispersion inside R_C' was only 0.2. Measurement precision was good even under conditions of partial loop filling. This shows that, as timing is always reproducible in flow injection procedures, processes involving either partial loop filling or partial injection are feasible. Finally, it should be possible to achieve a higher degree of dispersion in the model system by lowering ΔS and choosing longer Δt values. Other parameters, including the initial injected volume, could also be modified to enhance dispersion; details of such modifications would depend on the particular chemistry selected for the analytical procedure.

Routine determination of potassium in plant materials

When the zone-sampling process is applied to real analysis, a rather simple and stable system results. An experiment to demonstrate the long-term stability of the system for the atomic absorption spectrometry of potassium indicated that negligible changes occurred in the calibration curve after 4 h. Figure 5 shows that about 120 samples per hour can be analysed with good precision, despite the high degree of dispersion involved (dispersion factor 0.76%). Table 1 indicates the good agreement between results obtained with the proposed method and with a conventional a.a.s. procedure [11] requiring manual sample dilution prior to the measurements.

Partial support of this project by CNPq (Conselho Nacional de Desenvolvimento Científico e Tecnológico) is greatly appreciated. The authors thank Peter B. Vose for his assistance during preparation of the manuscript.

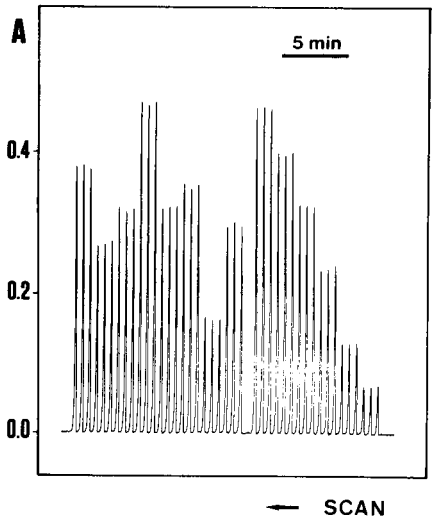

Fig. 5. Routine run for potassium determinations in plant material by atomic absorption spectrometry. From right to left, six standards (50, 100, 200, 300, 400 and 500 ppm K) followed by eight plant digests. All measurements in triplicate.

TABLE 1

Comparative results obtained in the potassium atomic absorption spectrometry of leaves from *Coffea arabica* L. with the proposed method and with a conventional a.a.s. procedure [11]

Sample	K in dried material (%)		Sample	K in dried material (%)	
	Proposed method	A.a.s.		Proposed method	A.a.s.
1	2.63	2.62	5	5.05	5.02
2	1.35	1.38	6	3.03	2.95
3	3.37	3.34	7	2.32	2.33
4	3.03	2.90	8	3.75	3.63

REFERENCES

1 J. R. Růžička and E. H. Hansen, Anal. Chim. Acta, 114 (1980) 19.
2 E. A. G. Zagatto, A. O. Jacintho, J. Mortatti and H. Bergamin F°, Anal. Chim. Acta, 120 (1980) 405.
3 J. R. Růžička, E. H. Hansen and H. Mosbaek, Anal. Chim. Acta, 92 (1977) 235.
4 D. Betteridge and B. Fields, Anal. Chem., 50 (1978) 832.
5 H. Bergamin F°, E. A. G. Zagatto, F. J. Krug and B. F. Reis, Anal. Chim. Acta, 101 (1978) 17.
6 E. A. G. Zagatto, F. J. Krug, H. Bergamin F°, S. S. Jørgensen and B. F. Reis, Anal. Chim. Acta, 104 (1979) 279.
7 B. F. Reis, H. Bergamin F°, E. A. G. Zagatto and F. J. Krug, Anal. Chim. Acta, 107 (1979) 309.

8 B. F. Reis, E. A. G. Zagatto, A. O. Jacintho, F. J. Krug and H. Bergamin F°, Anal. Chim. Acta, 119 (1980) 305.
9 J. R. Růžička and E. H. Hansen, Anal. Chim. Acta, 99 (1978) 37.
10 H. Bergamin F°, B. F. Reis, A. O. Jacintho and E. A. G. Zagatto, Anal. Chim. Acta, 117 (1980) 81.
11 Analytical Methods for Atomic Absorption Spectrophotometry, Perkin-Elmer, Norwalk, CT, 1973, pp. 1–15.

Analytica Chimica Acta, 123 (1981) 229—237

DISPERSION IN OPEN TUBES AND TUBES PACKED WITH LARGE GLASS BEADS
The Single Bead String Reactor†

J. M. REIJN, W. E. VAN DER LINDEN*[a] and H. POPPE

Laboratory for Analytical Chemistry, University of Amsterdam, Nieuwe Achtergracht 166, 1018 WV Amsterdam (The Netherlands)

(Received 1st September 1980)

SUMMARY

A semi-quantitative description of the dispersion process in open tubes is presented for conditions prevailing in flow injection analysis. It is shown that uncoupling the two functions of the tube (i.e., mixing and creating a residence time) can be accomplished by making use of a simple mixing device followed by a tube packed with glass beads of relatively large diameter (up to 70% of the i.d. of the tube): this gives a single bead string reactor (s.b.s.r.). With a flow injection system consisting of such an s.b.s.r., longer residence times can be obtained without loss of peak height or loss of sampling frequency.

When a well-defined sample zone is injected into a moving stream, progressive spreading of the sample zone takes place. The simplicity with which this dispersion process can be manipulated by changing flow conditions such as flow velocity, tube diameter, etc., and the remarkable reproducibility of this dispersion process, once the conditions have been fixed, are important factors that have contributed to the success of flow injection analysis (f.i.a.).

Růžička and Hansen [1, 2] classify dispersion as limited, medium and large. Each of these three categories has its own type of applications. Thus, limited dispersion is desirable if the original composition of the sample is to be measured and chemical reactions are not required. In such cases, the flow injection system serves merely as a means of reproducible supply of sample to the detector. Any dispersion has to be considered as a negative effect because broadening of the sample zone will lower the possible sampling frequency and mixing with the carrier stream will lead to dilution and consequently a decrease of the signal to be measured. In contrast, if a chemical reaction is necessary, so that mixing with one or more reagents has to occur, a situation of so-called medium dispersion has to be adopted. The appropriate degree of dispersion must be a compromise based on consideration of the following aspects: (i) the degree of mixing wanted; (ii) the degree of

†This paper was presented at the conference SAC 80 in Lancaster in July 1980.

[a]Present address: Department of Chemical Technology, Technical University, Enschede, The Netherlands.

completeness to which the reaction has to proceed; (iii) the sampling interval that can be accepted.

Unfortunately, these aspects are not mutually independent in open tubes. Because the dispersion process in open tubes is not a very effective way of mixing, a certain length of tube is always necessary even if the reaction proceeds very quickly. This sets an upper limit to the sampling frequency. When slow reactions must be used and long tubes are necessary to create a sufficiently long residence time, dispersion leads to a considerable loss of sensitivity and also to a loss of sampling frequency. In practice, flow injection systems in open tubes are therefore limited to reactions that need residence times of about 20 s or less. From the two examples given, it must be clear that the optimization of f.i.a. can be facilitated if the two functions of the tube, i.e. mixing and creating a residence time, are distinguished. Accordingly, a system should have the following characteristics: (i) an adequate direct micro-mixing of sample and reagents in the carrier stream followed by (ii) a tube with very low dispersion so that the length of tube, and thus the residence time, can be chosen on the basis of the reaction time required without a substantial loss of height of the signal and/or loss of sampling frequency; (iii) the device must remain simple and cheap which means that the flow resistance must be kept as low as possible so that the system can be operated with simple peristaltic pumps. It will be shown that the "single bead string reactor" (s.b.s.r.) meets these latter two requirements to a considerable extent.

In order to explain why the presence of such a string of glass beads in the tube leads to a decrease of the dispersion, it is necessary to discuss briefly the dispersion process in straight open tubes.

THEORY

Under normal f.i.a. conditions, Poiseuille flow must be considered. This means that at the wall the velocity of the stream tends to zero whereas in the centre the velocity is twice the average velocity $\langle v \rangle$. For each line of the stream, the velocity, v, is expressed by the parabolic equation

$$v = 2 \langle v \rangle \{1 - r^2/R^2\} \quad (1)$$

in which r is the distance from the centre of the tube and R is the radius of the tube.

When the sample is injected as a slug, initially each volume element containing sample molecules will be carried along at the velocity corresponding to the respective line in the stream. If there were no diffusion, the sample would be distributed along the tube as indicated in the lower part of Fig. 1. If diffusion has to be taken into account, the situation that will arise will correspond to that shown schematically in the upper part of Fig. 1. This drawing represents one volume element of the slug which is transported at

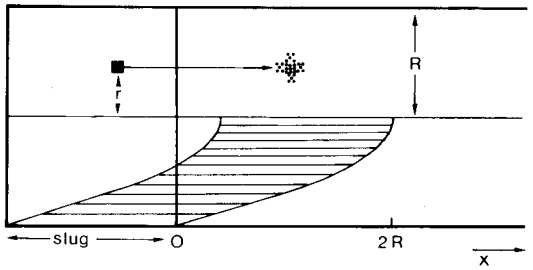

Fig. 1. Distribution of a sample injected as a slug after convective transport in a tube under conditions of Poiseuille flow. Lower part: without diffusion. Upper part: with diffusion; only one volume element is drawn.

the particular velocity of that line in the stream, the content of this volume element becoming distributed partly over neighbouring volume elements. The redistribution procedure that will be adopted in the calculations in this paper, is based on the model introduced by Golay and Atwoods [3]. In the present model, this redistribution is performed in such a way that a certain percentage is retained and half of the remaining part is transferred to the volume element ahead and the other part to the volume element behind. After this procedure has been completed for all volume elements in the slug, the same redistribution is performed in the direction perpendicular to the flow direction. This whole procedure completes one cycle. The next cycle starts with transport of all volume elements according to the respective lines in the stream and so on. The distance covered by convection and the percentage to be redistributed over neighbouring volume elements depend on the choice of the iteration time which in turn should be related to the ratio R^2/D, where D is the diffusion constant of the relevant component (see Appendix). Sample distributions after one to three consecutive cycles are shown in Fig. 2.

Because most detectors will sense an average concentration in the tube perpendicular to the flow direction, it is important to calculate the mean concentration in each slice of the tube, for this mean distribution curve will determine the shape of the signal. These mean distribution curves after one to five iterations are shown in Fig. 3. Initially, the front of the sample zone is not seriously affected, but it is interesting to note that after three iterations a bump begins to form at the rear, the concentration being much larger than the concentration to be expected on the basis of pure convection. This can be explained by the fact that sample molecules diffuse from the wall and are caught up in the more central lines of the stream which are of higher velocity. Golay and Atwoods [3] have shown that when the number of iterations is increased, the distribution curve will tend to a Gaussian shape. This will be the situation when most of the sample molecules have had enough time to be subject to several lines in the stream, causing an averaging of the velocity with which each molecule is transported through the tube.

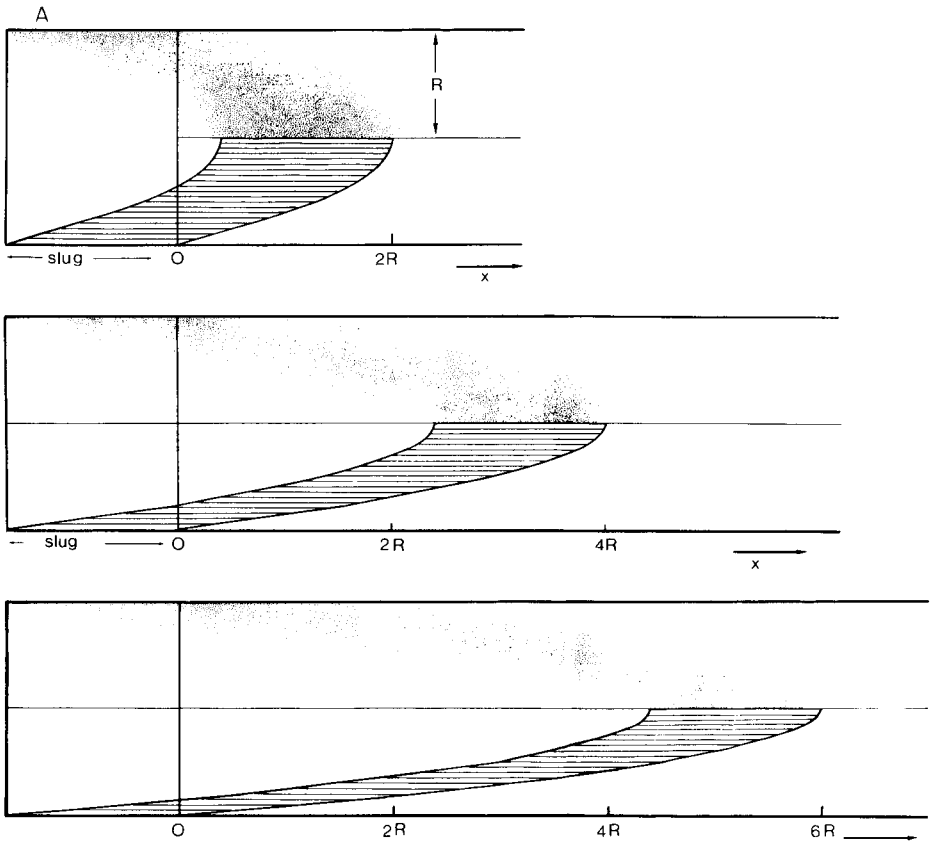

Fig. 2. Distribution of sample at consecutive times. I.d. of the tube 0.6 mm; flow rate 0.045 ml min^{-1}; diffusion coefficient 2×10^{-9} m^2 s^{-1}. Lower parts: without diffusion. Upper parts: with diffusion. (A) After 0.113 s; (B) after 0.226 s; (C) after 0.339 s.

According to Taylor [4], this will be the case if the following inequality holds true: $t \gg (1/3.8)^2 \ (R^2/D)$, where t is the residence time. Other authors [5, 6] have derived more strict criteria: $t \geqslant 1/2 \ R^2/D$ or even $t \geqslant (1/1.25) \ (R^2/D)$. The latter criterion is in close agreement with the one that can be calculated from the results of the computer simulation performed by Golay and Atwoods [3].

It is important to emphasize that, although in the end the mean concentration distribution curve in the tube, and accordingly the elution curve, tend to an almost Gaussian shape, this does not mean that the radial distribution is homogeneous. There will always be more sample molecules in the centre that are ahead of the zone where the mean concentration has its maximum, and more sample molecules at the wall that are behind that zone. Thus, the parabolic shape of the boundaries of the sample zone will become more diffuse but in principle remain unimpaired.

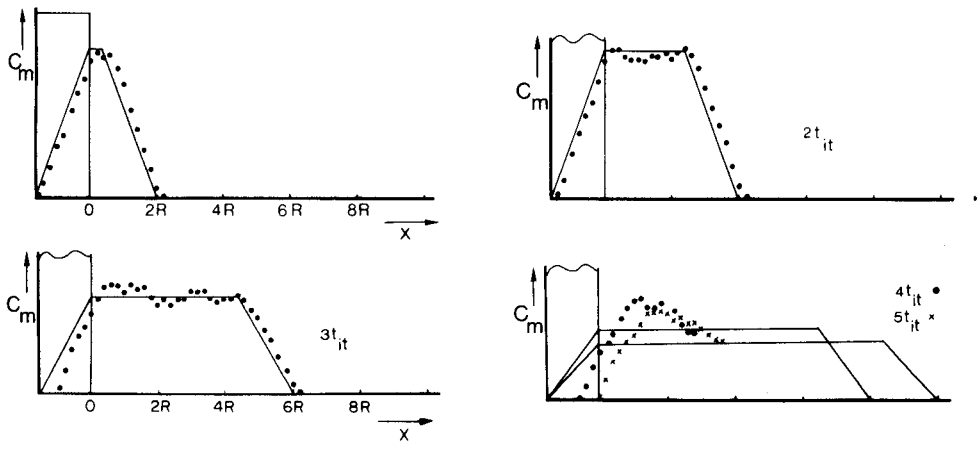

Fig. 3. Mean distribution curve of the sample in the tube after one to five iterations. Time for one iteration, 0.113 s; i.d. of tube 0.6 mm; flow rate 0.045 ml min^{-1}. Without diffusion (——); with diffusion (•). In the calculations, $R = 3 \times 10^{-4}$ m, $\langle v \rangle = 0.27 \times 10^{-2}$ ms^{-1}, $D = 2 \times 10^{-9}$ m^2 s^{-1}, and $t_{it} = 0.113$ s.

From the semi-quantitative picture of the dispersion process presented above, in which the non-uniform velocity distribution is the prime cause of dispersion and in which radial transport by diffusion tends to offset the different velocities at which individual sample molecules are transported, it is evident that dispersion can be reduced by preventing the development of the parabolic velocity profile and/or by increasing radial transport.

Two possibilities have been suggested: (i) coiling of the tube, and (ii) making use of a packed bed [7, 8]. Coiling does indeed yield some reduction of the dispersion because of the so-called secondary flow, but only to a limited extent. Packed bed reactors offer better prospects in this respect, but they have the disadvantage of a much larger flow resistance. This places much more stringent demands on the pressure capability of the pump, the injection valve and the connections of the various parts of the flow injection system.

It is shown here that filling of the tube with relatively large glass beads adequately decreases peak spreading while the flow resistance remains low. Typical ratios of tube diameter to glass bead diameter range from 1:1.2 to 1:1.6. Another advantage of the use of large glass beads is that no complicated packing techniques are required to obtain regularly packed reactors.

EXPERIMENTAL

To illustrate the differences between open straight or coiled tubes and the s.b.s.r., the determination of chloride based on the spectrophotometric measurement of iron(III) thiocyanate [9] was chosen. For comparison,

some experiments were also done with 10^{-3} M and 5×10^{-4} M potassium permanganate solutions. The flow injection system consisted of a Gilson Minipuls 2 pump, polyethylene tubes of 0.6 mm i.d., and a home-made flow-through cell (path length 1 cm; volume about 20 μl). Injections were done with a teflon rotary valve (Rheodyne, type 50). In order to obtain injection volumes as small as 30 μl, it was necessary to line the tubes connected to the valve ports, with tubing of smaller diameter. The glass beads used has a mean diameter of approximately 0.4 mm. Dry packing was preferable; a Finn pipet tip was used as the filling funnel. When correctly packed, the glass beads exhibited a regular zigzag pattern. Y-piece connectors were made from drilled perspex blocks.

RESULTS AND DISCUSSION

Figure 4(A) shows the single elution curves obtained when a large volume (125 μl) of potassium permanganate solution was directly injected into a carrier stream of pure water. If little or no dispersion had occurred, a block-shaped elution curve would have appeared. Apparently, neither the open tubes nor the s.b.s.r. can prevent dispersion, but peak spreading is less with the s.b.s.r. Under exactly the same conditions, chloride samples were in-

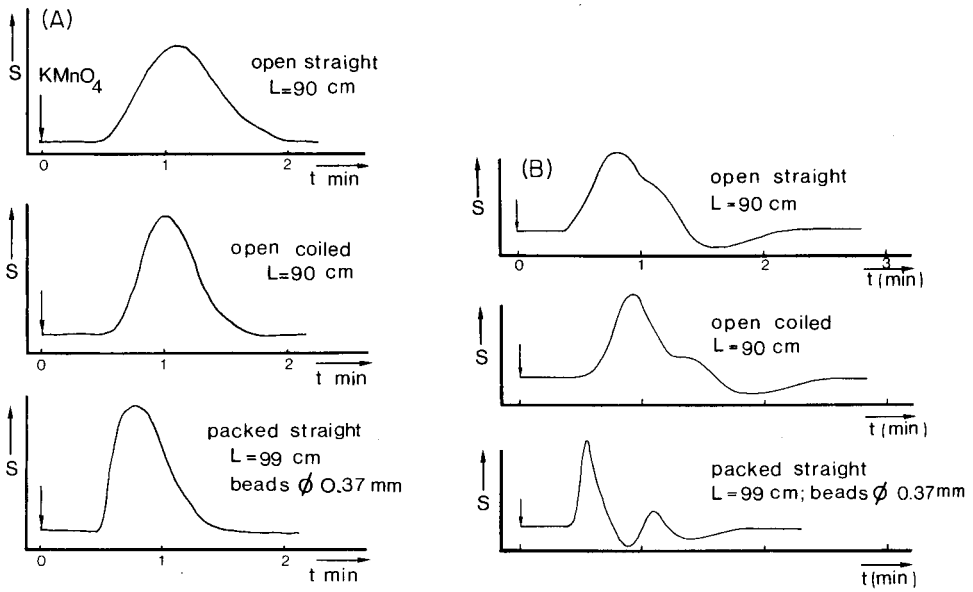

Fig. 4. (A) Elution curves after injections of 125 μl of $KMnO_4$ solution directly into a carrier stream of pure water for open straight and coiled tubes, and for the s.b.s.r.; i.d. of tube 0.6 mm; diameter of glass beads in the s.b.s.r. ca. 0.37 mm. (B) Analogous elution curves after injections of 125 μl of 5×10^{-4} M chloride solution into a carrier stream of $Hg(SCN)_2$ and Fe^{3+}.

jected into a carrier stream containing the mercury(II) thiocyanate–iron(III) reagent (Fig. 4B). That dispersion is not synonymous with adequate mixing is shown by the distortion of the peak in the open straight tube. A homogeneous mixing of sample and reagent in the dispersed sample zone would have given the same peak shape as in the case of permanganate. (The fact that the absorbance dips below the baseline is due to the slight colouring of the reagent solution whereas the injected sample itself is colourless; changes in the manifold used would readily have overcome this problem [9].) If dispersion is small, sample molecules will meet reagent molecules only at the boundaries of the large sample zone and the middle of the zone will remain colourless. This picture is illustrated best with the s.b.s.r. The somewhat more distinct shoulder in the case of the coiled tubes illustrates its intermediate position with respect to dispersion.

When the analysis is based on a chemical reaction, a low-dispersion tube has to be preceded by a micro-scale mixing device. Several types were tested, ranging from a Y-piece connected to a short tube filled with glass beads as suggested by Huber et al. [10], to the mixing devices used by Frei et al. [11]. A home-made mixing device was also tested; this consisted of a sealed tube inserted in the tube containing the carrier stream; small holes which functioned like nozzles were made in the sealed end of the tube. Since no significant differences were observed, when used in combination with the s.b.s.r., the Y-piece device was used throughout further experiments. In that case, the short tube filled with glass beads could be omitted as a part of the mixing device; its role was taken over by the first part of the s.b.s.r.

An example of the improvement which can be attained with the s.b.s.r. in comparison with the open tube is presented in Fig. 5. Figure 5(A) shows the single peak as well as a sequence of peaks at an injection interval of 20 s in an open tube of 96-cm length (i.d. 0.6 mm) at a flow rate of 1 ml min^{-1}. Figure 5(B) shows the picture for the s.b.s.r. In order to obtain the same residence time when the flow rate was maintained at 1 ml min^{-1}, the length of the s.b.s.r. had to be about 2 m. The other conditions were kept the same. As can be seen, a much smaller dispersion and a larger signal are observed with the s.b.s.r.

The s.b.s.r. was shown to provide constant peak height even when the residence time was increased by a factor of five simply by decreasing the flow rate. This is in contrast to straight open or coiled open tubes where under the same conditions a marked, continuous decrease of the peak height was observed as the flow rate was decreased.

It is interesting that with an s.b.s.r. about 2-m long the sampling frequency can be increased to such an extent that the line can contain up to three to four samples at a time without significant overlap.

In conclusion, it appears that the large dispersion observed macroscopically in open tubes contributes relatively little to the effective micro-mixing of sample and reagent solution. Single bead string reactors show less dispersion and, at the same time, enhanced micro-mixing. A more detailed study of the s.b.s.r. is in progress.

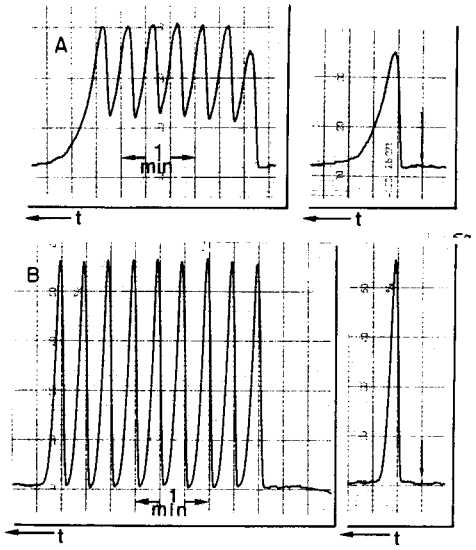

Fig. 5. Elution curves after injection of 30-μl samples of a 5×10^{-4} M chloride solution into a water stream subsequently mixed with the reagent stream. Flow rate 1 ml min^{-1}; injection interval 20 s; volume injected 30 μl. (A) Open tube, length 96 cm; (B) s.b.s.r., length 192 cm.

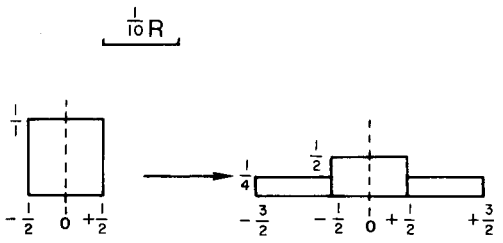

Fig. 6. Dispersion scheme.

The authors are greatly indebted to Mr. R. Oostervink for his experimental contributions.

APPENDIX

For a distribution function that meets the requirement $\int_{-\infty}^{+\infty} E(\theta)d\theta = 1$, the kth statistical moment around the mean, m, is defined by $\mu'_k = \int_{-\infty}^{+\infty} (\theta - m)^k E(\theta)d\theta$. The second moment ($k = 2$) is normally called the variance, σ^2. When this formula is applied to the dispersion scheme presented in Fig. 6, then the change in variance is $\Delta\sigma^2 = 1/2\,(X)^2$. In the example given in Fig. 2, $X = R/10$. Thus $\Delta\sigma^2 = R^2/200$.

The change in variance is related to the diffusion by $\Delta\sigma^2 = 2Dt$. Thus $t =$

$\Delta\sigma^2/2D = R^2/400\ D$. When $R = 0.3 \times 10^{-3}\ m$ and $D = 2 \times 10^{-9}\ m^2\ s^{-1}$, this leads to $t = 0.1125$ s. In this period of time the sample front has travelled a distance $2R$ by means of convection, so that $2\ \langle v \rangle = 2R/t \rightarrow \langle v \rangle = 0.266 \times 10^{-2}\ m\ s^{-1}$.

REFERENCES

1 J. Růžička and E. H. Hansen, Anal. Chim. Acta, 99 (1978) 37.
2 J. Růžička and E. H. Hansen, Anal. Chim. Acta, 114 (1980) 21.
3 M. J. E. Golay and J. G. Atwoods, J. Chromatogr., 186 (1979) 353.
4 G. Taylor, Proc. R. Soc. London, Ser. A, 219 (1953) 186.
5 M. J. Lighthill, J. Inst. Math. Its Appl., 2 (1966) 97.
6 V. Ananthakrishnan, W. N. Gill and A. J. Barduhn, AIChE J., 11 (1965) 1063.
7 R. Tijssen, Anal. Chim. Acta, 114 (1980) 71.
8 J. H. M. van der Berg, R. S. Deelder and H. G. M. Egberink, Anal. Chim. Acta, 114 (1980) 91.
9 J. Růžička, J. W. B. Stewart and E. A. G. Zagatto, Anal. Chim. Acta, 81 (1976) 387.
10 J. F. K. Huber, K. M. Jonker and H. Poppe, Anal. Chem., 52 (1980) 2.
11 R. W. Frei, L. Michel and W. Santi, J. Chromatogr., 126 (1976) 665.

Analytica Chimica Acta, 123 (1981) 239—246

"STAT" METHODS IN CONTINUOUS FLOW ANALYSIS
Determination of Copper, Iron, Iodide and Hydrochloric Acid

HERBERT WEISZ* and GÜNTER FRITZ

Lehrstuhl für Analytische Chemie, Chemisches Laboratorium der Universität, Freiburg i.Br. (Federal Republic of Germany)

(Received 4th August 1980)

SUMMARY

A continuous flow "stat" method is described in which a certain arbitrarily imposed state in the flowing stream is automatically maintained by regulating the rate of flow of one of the components. The electronic system is regulated by measuring a physical phenomenon in the flowing solution. The method is illustrated by the examples of a continuous flow absorptiostat [$Fe(III)/S_2O_3^{2-}/Cu(II)$] for determinations of copper(II) (1—10 $\mu g\ ml^{-1}$), iron(III) (25—250 or 12.5—125 $\mu g\ ml^{-1}$), as well as for determination of iodide (12.8—128 $\mu g\ ml^{-1}$). A continuous flow conductostat [HCl/NaOH] for determination of 1—2.5 × 10^{-4} M HCl is also described. This analytical technique is intended for automatic continuous monitoring of sample streams.

One of the kinetic methods of analysis is based on the measurement of that process which is necessary to keep a certain phenomenon of a system at a preset value. In these so-called "stat" methods [1—7], a certain state is arbitrarily imposed and maintained during the course of reaction by either addition of a reagent or removal of a reaction product. The speed of this necessary addition (or removal) provides a measure of the concentration of the substances to be determined.

The combination of stat methods with continuous flow analysis offers realistic possibilities for determinations in flowing systems. In this context, continuous flow analysis means that the continuously changing concentration of a sample in an unsegmented stream is measured, by using one, or several likewise unsegmented streams of reagent solution. In this procedure, no individual samples will be determined, but a stream of a solution can be monitored continuously without interruption.

In a stream of a solution, a given state can be maintained by varying the pumping rate of one component, while the flow rates of the others are kept constant. For this purpose, the quantity of the observed phenomenon (e.g., absorption, conductivity) is measured and compared with the preset value. As long as both values are identical, the rate of addition (pumping rate) is not varied. As soon as they differ, due to the change of concentration of the sample, the rate of addition of one reactant (or sample) is enhanced or

decreased, depending on the direction and magnitude of the difference. In order to change the addition rate, a different command voltage is given to the peristaltic pump which delivers the component to be varied. This regulation works until the observed phenomenon has reached the preset value again. The command voltage given to the peristaltic pump provides a measure of the necessary pumping rate, and consequently a measure of the concentration of the sample to be determined. This command voltage is recorded versus time.

Any phenomenon can be used in this control system, e.g., absorbance, potential or conductivity. In this way the concentration of either a product or a reactant or the ratio of concentrations of product and reactant in the streaming solution can be kept constant. Similar regulatory systems have been described [8—10] for the titration of individual and continuously changing samples.

Continuous flow stat methods, as described in the present paper, can be applied for any kinetic measurement, even where no sudden change in a physical phenomenon takes place. Here, a continuous flow absorptiostat using both catalyzed and uncatalyzed reactions will be illustrated by the examples of determinations of iron, copper and iodide. Then the principle of a continuous flow conductostat will be demonstrated by the example of an acid—base reaction.

DETERMINATIONS IN A CONTINUOUS FLOW ABSORPTIOSTAT

Iron(III) is reduced rather slowly by thiosulphate but this reaction is catalyzed by copper(II) ions [11]. With potassium thiocyanate the change of the iron(III) concentration can be followed optically. The copper catalyst as well as the iron reactant can be determined in this way.

The apparatus used for the continuous determinations is shown in Fig. 1, and the circuit diagram of the control system in Fig. 2. The same apparatus is used for the determination of iron and copper. The procedure may be illustrated on the example of the determination of copper as catalyst. The flow streams of reactant 1 (iron thiocyanate) and reactant 2 (thiosulphate) are pumped separately (Fig. 1, R1/R2; 2 mm i.d. tubing) into the mixing chamber (MC). The copper(II) catalyst is likewise pumped into the mixing chamber (R3; 1 mm i.d. tubing). The debubbling opening serves to prevent any gas bubbles, produced during the mixing, from entering the cuvette. After mixing, the solution flows into the vertical cuvette (C; glass tube, 150 mm long, 1.4 mm i.d.). Light from the light pipe enters the cuvette at the lower end, passes through the solution, and reaches the photodetector (Siemens BPX 79). The voltage produced in this detector is transferred to the control system and recorded versus time on one channel of the two-channel recorder (Metrawatt Servogor 2s; see PV, Fig. 3). The command voltage (depending on the catalyst concentration and transferred from the control system to the peristaltic pump) is recorded on the other channel

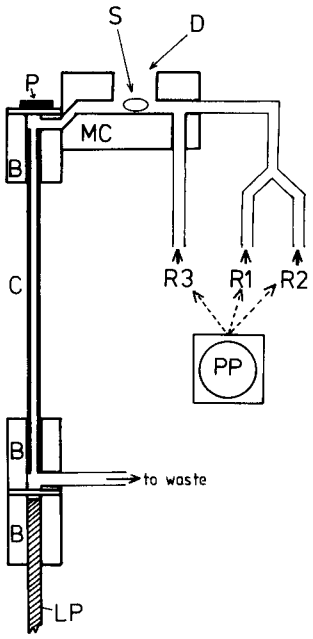

Fig. 1. Continuous flow absorptiostat. (B) Plexiglas blocks; (C) vertical glass cuvette; (D) debubbling opening; (LP) fiber glass light pipe leading the light from the light source (Schott KL 150B, 15 V, 150 W) to the optical cell; (MC) mixing chamber (length 5.5 cm, 0.5 cm i.d., volume 1.08 ml); (P) photodetector (Siemens BPX 79); (PP) regulated peristaltic pump (Ismatec IP4), delivering the solution to one of the three channels (R1, R2, R3); (R1, R2, R3) channels for the three different solutions; (S) magnetic stirrer. The unregulated peristaltic pump (Ismatec MP-GE) for the remaining two channels is not shown.

(CV, Fig. 3). This command voltage is converted by motor M, which is mechanically coupled to the 10-turn potentiometer controlling the pumping rate of the peristaltic pump.

The absorption corresponding to the solution with the lowest catalyst concentration (1 μg Cu ml^{-1}), and so added at the highest pumping rate, was chosen as the preset value. The command voltage proportional to this highest pumping rate, recorded on the two-channel recorder, served as baseline for the determination of the other samples (BL, Fig. 3). If the concentration of the sample increases, the system decreases the pumping rate. The distance D between the trace of the new command voltage (a horizontal line) and the baseline is the measure for the concentration of the catalyst. These distances, corresponding to known standard concentrations of the catalyst, plotted versus the various standard concentrations, provide the standard graph for evaluating the results.

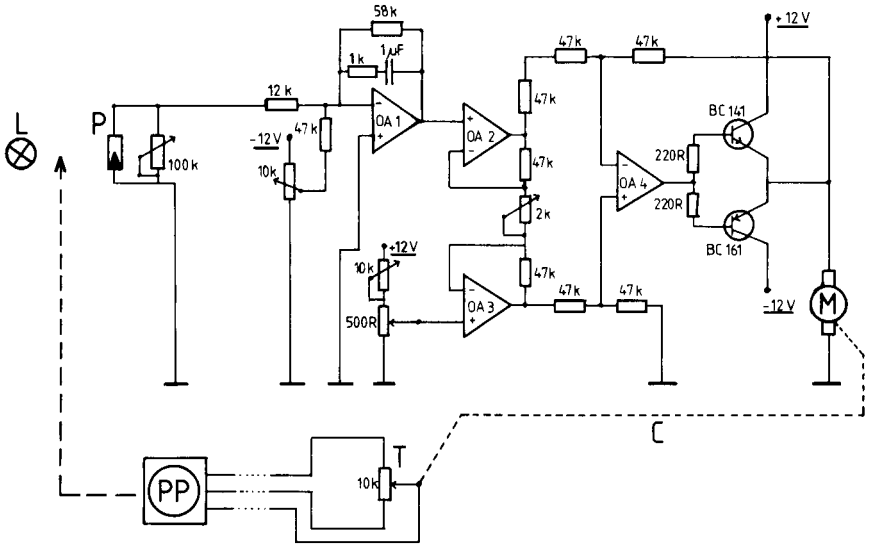

Fig. 2. Circuit diagram of regulation system. (C) Mechanical coupling; (L) lamp; (M) motor, mechanically coupled to a 10-turn potentiometer (T); (OA 1-4) operational amplifier type 741; (P) photodetector; (PP) regulated peristaltic pump.

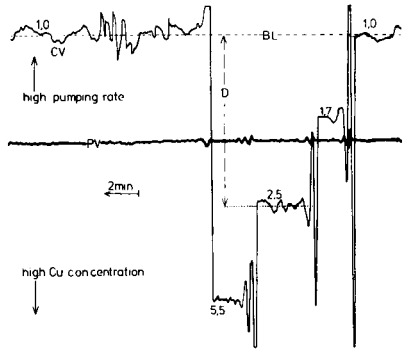

Fig. 3. Recorder graph for the copper determination in the continuous flow absorptiostat. (BL) Baseline; (CV) command voltage; (D) distances evaluated; (PV) voltage produced in the photodetector. The numbers on the traces represent the copper concentrations in $\mu g\ ml^{-1}$.

Determinination of copper(II)

The lowest pumping rate, obviously corresponding to the highest catalyst concentration (10 μg Cu ml^{-1}) was 0.2 ml min^{-1}, whereas the highest pumping rate was about 2.2 ml min^{-1}. The flow rate of the iron(III) solution was 8.8 ml min^{-1} ; that of the thiosulphate solution was about 2.2 ml min^{-1}. To simulate the continuous variation of the concentration of a sample stream, a mixing chamber was used. The continuously pumped new samples caused a slow change of concentration in the chamber.

The solutions used were 0.064 M sodium thiosulphate pentahydrate (15.8 g l^{-1}), an iron thiocyanate solution (250 mg Fe as $FeCl_3$, 3 ml of 11 M HCl and 10 ml of 1 M KSCN diluted to 1 l), and a copper sulphate solution (1—10 μg Cu ml^{-1}).

The standard graph is shown in Fig. 4. Table 1 gives some results for copper determinations. The time necessary to reach the preset state again for each new sample depends of course on the difference of the successive sample concentrations. It never exceeded about 10 min.

Determination of iron(III)

In the same reaction, the iron(III) reactant can be determined instead of the copper(II) catalyst. In this case, it was advisable to regulate the pumping rate of the iron(III) sample stream (R1, Fig. 1) and to keep the two other streams constant. Obviously the catalyst concentration had to be kept constant (5 μg Cu ml^{-1}); its flow rate was 3.3 ml min^{-1} (R3, Fig. 1). The flow rate of the reactant solution (0.1 M $Na_2S_2O_3$, 0.1 M KSCN) was 9 ml min^{-1}. The concentration range of the iron samples was 25—250 μg Fe ml^{-1}. The flow rate of the sample solution varied between 0.15 and 1.9 ml min^{-1}. The standard graph for the determination of iron is similar to that shown in Fig. 4. Table 1 gives some results for iron determinations. As can be seen, the determination of a reactant (Fe) is less sensitive than that of the catalyst (Cu), as would be expected.

In the same apparatus, iron can also be determined simply by adding thiocyanate and measuring the absorbance of the red iron thiocyanate complexes

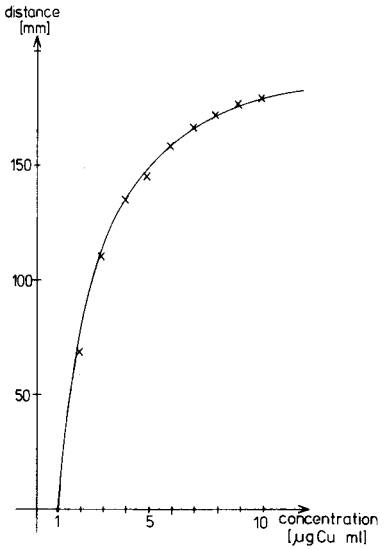

Fig. 4. Standard graph for the determination of copper.

TABLE 1

Determination of copper(II), iron(III) or iodide in a continuous flow absorptiostat[a] (All results are given as $\mu g\ ml^{-1}$)

Determination of copper(II)										
Taken	5.9	8.4	10.0	4.0	2.0	3.0	7.4	1.0	6.4	1.5
Found	6.4	8.6	9.4	4.2	1.8	3.1	8.6	1.1	6.2	1.7
Diff.	+0.5	+0.2	−0.6	+0.2	−0.2	+0.1	+1.2	+0.1	−0.2	+0.2
Determination of iron(III) by the kinetic method										
Taken	200	42	142	38	126	34	223	70	223	110
Found	170	49	140	43	123	35	213	83	240	93
Diff.	−30	+7	−2	+5	−3	+1	−10	+13	+17	−17
Determination of iron(III) by the direct method										
Taken	114	115	58	50	84	87	44	110	124	112
Found	112	116	59	60	80	76	48	110	106	125
Diff.	−2	+1	+1	+10	−4	−11	+4	0	−18	+13
Determination of iodide										
Taken	68.1	79.0	128.5	19.3	16.7	122.0	97.6	25.7	38.5	51.4
Found	66.8	78.3	128.5	15.4	18.0	125.9	97.6	25.7	38.5	51.4
Diff.	−1.3	−0.7	0	−3.9	+1.3	+3.9	0	0	0	0

[a]Concentrations were selected randomly to represent real analyses.

formed. The iron sample solution flow (R1) was regulated by the system in the range 0.19—1.5 ml min^{-1}. The reagent stream (R2) (0.05 M KSCN) was kept constant at 14 ml min^{-1}. The third stream R3 was obviously not used in this case. Iron could thus be determined within the range 12.5—125 μg Fe ml^{-1}. Although this was not a kinetic determination, the standard graph was nevertheless similar to that shown in Fig. 4. Typical results are again given in Table 1.

Determination of iodide

In the same apparatus, iodide was also determined by a non-kinetic method. The concentration of the iodine formed by the oxidation with cerium(IV) was measured. Cerium sulphate (0.01 M) in sulphuric acid (0.005 M) was pumped at a rate of 3.2 ml min^{-1} (R1), and starch solution (aqueous 1%) at a rate of 1 ml min^{-1} (R3). The flow rate of the sample solution, containing 12.8—128 $\mu g\ I^-\ ml^{-1}$, varied between 0.325 and 1.48 ml min^{-1}, depending on the sample concentration. The standard graph was similar to that shown in Fig. 4. Table 1 shows some results of iodide determinations.

DETERMINATION OF HYDROCHLORIC ACID IN A CONTINUOUS FLOW CONDUCTOSTAT

As an alternative indicating method for the continuous flow stat, conductivity was utilized to regulate the flow rate of one of the components. To measure the conductivity in a flowing stream, two plates (0.9 × 1.5 cm) of stainless steel were inserted 3 mm apart in a plexiglas tube (11 cm long, 12 mm i.d.) and an alternating current was imposed by a conductometer. The voltage between the two plates changed, depending on the conductivity of the flowing solution, and was rectified by a bridge rectifier circuit before introduction into the circuit shown in Fig. 2, regulating the flow rate of one of the components.

In the example of an acid—base reaction, conductivity measurements certainly cannot distinguish whether high conductivity is caused by an excess of acid or of base. To overcome this difficulty, one of the two components had to be present in excess. In the determination of hydrochloric acid (1×10^{-4}—2.5×10^{-4} M), sodium hydroxide solution (10^{-3} M) was therefore added in excess. In contrast to the examples described above, the pumping rate of the reagent (NaOH) was regulated; the flow rate of the sample solution was kept constant at 7.3 ml min^{-1}. The pumping rate of the sodium hydroxide solution varied between 0.4 and 7.2 ml min^{-1}.

The baseline was indicated (as in Fig. 3) by the pumping rate of the sodium hydroxide solution for the highest hydrochloric acid concentration; lower acid concentrations obviously needed a lower flow rate. The difference was a measure of the concentration of the hydrochloric acid. It should be emphasized that this is certainly not a titration to an equivalence point. The standard graph was similar to that shown in Fig. 4. Table 2 gives some results for the determination of hydrochloric acid. In this case, the range of determination is rather narrow.

DISCUSSION

The continuous flow stat method is certainly not intended for the analysis of single samples, but rather for monitoring sample streams within certain limits of concentration. It is obvious that by altering the conditions (pumping rate, concentrations, pH, etc.), the possible range of the determinations can be extended. All the experiments described here were done without thermo-

TABLE 2

Determination of hydrochloric acid in a continuous flow conductostat

Taken ($\times 10^{-4}$ M)	1.0	1.4	1.8	2.2	1.5	1.1	1.4	2.0
Found ($\times 10^{-4}$ M)	1.1	1.45	1.8	2.4	1.6	1.25	1.3	2.35
Diff. ($\times 10^{-4}$ M)	+0.1	+0.05	0	+0.2	+0.1	+0.15	−0.1	+0.35

statting. When better reproducibility is desired, the temperature parameter should also be controlled.

Other physical phenomena such as luminescence, potential, etc., could most likely also be used to regulate the flow rate in analogous methods.

We are very grateful to Dr. M. Kowalski (Universität Freiburg, Institut für Makromolekulare Chemie) for his help in the construction of the electronic regulation system.

REFERENCES

1 H. V. Malmstadt and E. H. Piepmeier, Anal. Chem., 37 (1965) 34.
2 H. Weisz, D. Klockow and H. Ludwig, Talanta, 16 (1969) 921.
3 S. Pantel and H. Weisz, Anal. Chim. Acta, 70 (1974) 391.
4 S. Pantel and H. Weisz, Anal. Chim. Acta, 74 (1975) 275.
5 H. Weisz and K. Rothmeier, Anal. Chim. Acta, 75 (1975) 119.
6 D. Klockow, G. Karenovics and W. Meiners, Anal. Chim. Acta, 100 (1979) 485.
7 S. Pantel and H. Weisz, Anal. Chim. Acta, 109 (1979) 351.
8 M. M. Nicholson, Anal. Chem., 33 (1961) 1328.
9 W. J. Blaedel and R. H. Laessig, Anal. Chem., 36 (1964) 1617.
10 R. E. Adams and P. W. Carr, Anal. Chem., 50 (1978) 944.
11 A. C. Oudemans, Fresenius Z. Anal. Chem., 6 (1867) 129.

Analytica Chimica Acta, 123 (1981) 247–253

DETERMINATION OF FREE CHLORINE IN WATER BY CHEMILUMINESCENCE REACTION WITH HYDROGEN PEROXIDE

D. F. MARINO and J. D. INGLE, JR.*

Department of Chemistry, Oregon State University, Corvallis, OR 97331 (U.S.A.)

(Received 10th July 1980)

SUMMARY

The analytical utility of the hydrogen peroxide—hypochlorite singlet oxygen chemiluminescence reaction for the determination of hypochlorite in water is investigated. Effects of pH and hydrogen peroxide concentration are discussed and interference data for over 35 species in the absence and presence of hypochlorite are provided. The limit of detection is 4 $\mu g\ l^{-1}$ with a usable non-linear calibration curve up to about 200 $\mu g\ l^{-1}$. The new method is shown to be relatively free from interferences and to give results for tap water comparable to a standard colorimetric method based on a reaction with N, N-diethyl-*p*-phenylenediamine.

Several accepted titrimetric, colorimetric, potentiometric and amperometric techniques exist for the determination of free chlorine (HOCl, OCl^-, Cl_2) in water, but none possesses a detection limit below 10 $\mu g\ l^{-1}$ [1]. Recently a highly sensitive chemiluminescence technique involving reaction with luminol has been reported [2]. Although the luminol method possesses a detection limit about two orders of magnitude lower than the standard hypochlorite methods, it is subject to about the same degree of interference from monochloramine. Because of the much greater disinfecting power of free chlorine, a technique with better selectivity for free chlorine is needed.

That the H_2O_2—OCl^- singlet oxygen reaction produces chemiluminescence was discovered by Mallet [3] and reconfirmed by Seliger [4]. The process has since been investigated in terms of its spectral, chemical, and mechanistic characteristics [5—11]. A proposed mechanism [5] is

$$H_2O_2 + OCl^- \xrightarrow{k_1} H_2O_2 + OOCl^- \quad (1)$$

$$2\,OOCl^- \xrightarrow{k_2} 2Cl^- + 2O_2(^1\Delta_g) \quad (2)$$

$$2O_2(^1\Delta_g) \xrightarrow{k_3} 2O_2(^3\Sigma_g^-) + h\nu \quad (3)$$

where production of the chloroperoxy ion is rate-limiting ($k_1 = 2.8 \times 10^3$ l mol^{-1} s^{-1}). Two molecules of singlet oxygen ($O_2(^1\Delta_g)$) formed in step 2 react together and either excited O_2 ($^1\Sigma_g^+$) is produced which emits at 762 nm

or a two-molecule, one-photon process occurs giving luminescence at 633 and 703 nm [5, 11]. Emission at other wavelengths has also been noted [11].

To date, however, investigation of the analytical utility of this reaction has been neglected. Since previous work in this laboratory on the determination of hypochlorite in water with luminol proved encouraging, it was decided to evaluate the analytical utility of the H_2O_2—hypochlorite system. The result is a new procedure for free chlorine determination in water with a detection limit better than any non-chemiluminescence method and negligible interference from chloramine.

EXPERIMENTAL

All chemiluminescence measurements were obtained with a discrete sampling photometer system reported earlier [12], and with the modifications and instrumental conditions similar to those previously described [13]. All solutions were prepared with deionized water from a Millipore Milli-Q system fed by distilled water. Hydrogen peroxide (30%, Baker reagent) was used without further purification in spite of its high trace metal content [14, 15] in an effort to simplify the procedure. Solutions of H_2O_2 were prepared at pH 4.0 for maximum stability. Standard dilute solutions of hypochlorite, chlorine dioxide and chloramine were prepared at pH 4.0, as it had been determined that dilute solutions of hypochlorite were most stable at this pH [2]. Sources and standardization techniques for these species were also as previously described [2]. The pH of the reaction mixture was controlled with 0.5 M borate buffers, adjusted with nitric acid or potassium hydroxide. All other solutions (e.g. potential interferences) were prepared as previously described [2, 13].

The general procedure consisted of the addition of 0.5 ml of buffer and 1.0 ml of hypochlorite sample to the sample cell with Eppendorf pipets followed by injection of 0.5 ml of H_2O_2 solution with an automatic syringe and measurement of the resulting peak height. About 120 samples per hour can be run once solutions are ready. In the time interval between addition of the buffer solution to the hypochlorite sample and injection of the H_2O_2 solution, some hypochlorite decomposition can occur (see above). Variability in this time interval can lead to imprecision. However, worse precision was obtained when a premixed H_2O_2—buffer solution was injected into a pH 4 hypochlorite sample because of the instability of H_2O_2 at higher pH. Because of the above, the imprecision is about twice as large as with the luminol method for hypochlorite where the luminol reagent is premixed with buffer such that the hypochlorite sample is kept at pH 4 until the reaction is initiated by injection of this mixture.

A colorimetric determination of hypochlorite with N,N-diethyl-*p*-phenylenediamine (DPD) was carried out with a prepackaged kit (Hatch Chemical 10470) as previously described [2]. Determination of hypochlorite in tap

water samples was conducted in such a manner as to minimize the period between colorimetric and chemiluminescence determinations (<3 min) in order to avoid hypochlorite decomposition in the sample between determinations. Colorimetric determinations were run on samples without dilution, while for chemiluminescence determinations, samples were run after a 1:10 dilution at pH 4.0.

The detection limit (c_l) for any species is defined as the concentration yielding an analytical signal equal to twice the standard deviation of the blank and the interference level (c_l^*) of a species is defined as the concentration of the species required to produce a change in the hypochlorite signal at the hypochlorite detection limit equal to twice the standard deviation in the blank [16]. This is evaluated by testing solutions containing the potential interferent plus hypochlorite at ten times the detection limit of hypochlorite (40 $\mu g\ l^{-1}$ in this case).

Because the H_2O_2—hypochlorite reaction produces light in the red portion of the spectrum (ca. 633 and 703 nm), a wavelength region in which the 1P28 photomultiplier tube (p.m.t.) is not very sensitive [17], a RCA 4840 red-sensitive p.m.t. was tried. The latter yielded an increase in signal intensity about three-fold compared to the former but with an increase in dark noise by a factor of about 10. Thus, because the 1P28 p.m.t. yielded a detection limit four times lower than the 4840 p.m.t., the 1P28 tube was used for all work.

RESULTS AND DISCUSSION

Parameter dependencies

The pH of the H_2O_2—hypochlorite reaction mixture was varied with 0.05 M borate and hydrogen-carbonate buffers of several different values in order to maximize both the signal and signal to background ratio. Figure 1 illustrates the results obtained. Signals in all plots are reported as photoanodic currents. It can be seen that borate buffers give somewhat greater signals than carbonate buffers. In addition, a slight blank signal (ca. 0.15 nA) occurs at all pH values with the carbonate buffers, but is absent with the borate buffers. Since pH 8.0 represents a reasonable maximum on the borate buffer curve, this value was chosen for both the buffer and reaction mixture pH.

With the pH of the reaction mixture fixed at 8.0, the H_2O_2 concentration was varied to maximize the signal. Figure 2 illustrates the results of this study. Note that the signal rises rapidly as the H_2O_2 concentration varies from 10^{-4} to about 5×10^{-3} M H_2O_2 (cell concentration), after which a plateau is reached and little gain is achieved in further increasing the H_2O_2 concentration. To avoid working on the "knee" of this curve, a value of 5×10^{-2} M H_2O_2 (0.02 M pre-cell concentration) was chosen.

With the above reagent conditions, rapid (ca. 2 s) peaks of the type shown in Fig. 3 resulted and the calibration curve shown in Fig. 4 was obtained.

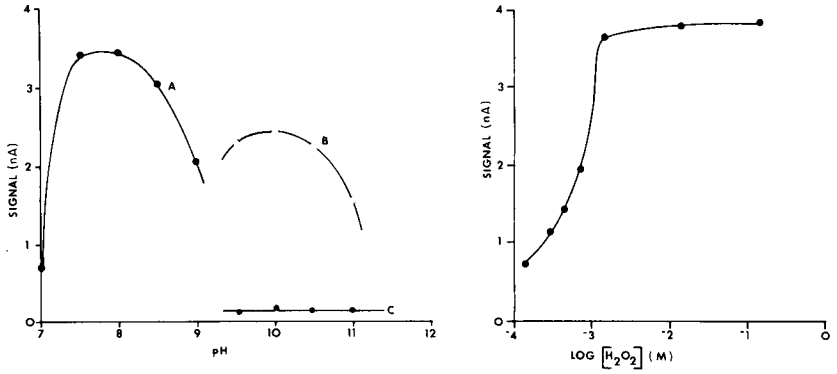

Fig. 1. Effect of pH on chemiluminescence response. [Buffer] = 0.05 M, [OCl^-] = 25 $\mu g\ l^{-1}$, [H_2O_2] = 0.5 M. (A) OCl^- signal with borate buffer; (B) OCl^- signal with carbonate buffer; (C) Blank signal with carbonate buffer.

Fig. 2. Effect of H_2O_2 concentration on chemiluminescence response. pH = 8.0, [OCl^-] = 25 $\mu g\ l^{-1}$.

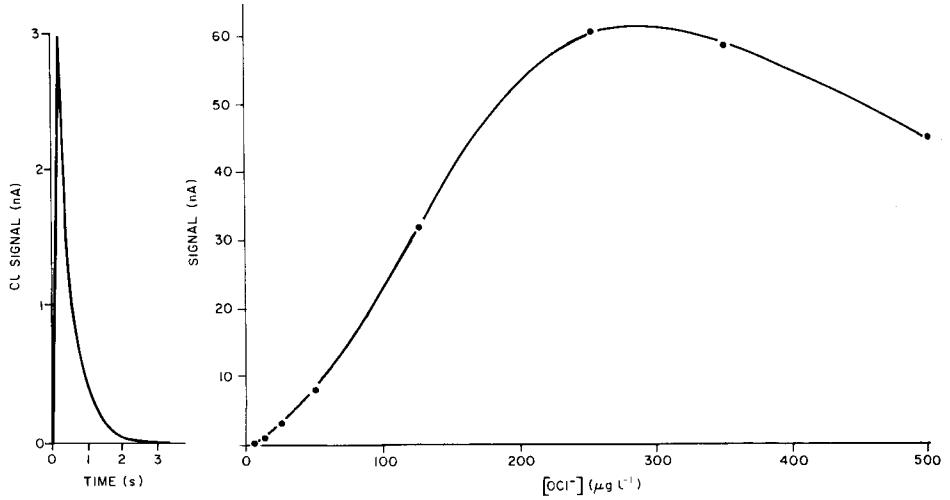

Fig. 3. Typical OCl^-—H_2O_2 peak shape. [OCl^-] = 25 $\mu g\ l^{-1}$, [H_2O_2] = 0.05 M, pH = 8.0.

Fig. 4. Dependence of chemiluminescence response on OCl^- concentration. pH = 8.0, [H_2O_2] = 0.05 M.

The calibration curve is non-linear but usable up to about 200 $\mu g\ l^{-1}$ if unknowns are closely bracketed by standards. A log—log plot of signal versus concentration is linear up to about 100 $\mu g\ OCl^-\ l^{-1}$ with a slope of 1.4. The detection limit of 4 $\mu g\ l^{-1}$ is lower than that of any standard non-chemiluminescence method. The reason for the decline in signal with in-

creasing concentration above about 250 $\mu g\ l^{-1}$ is not immediately explainable. It was confirmed that neither hypochlorite or H_2O_2 absorb in the wavelength region of chemiluminescence. Also the molar ratio of H_2O_2 to give hypochlorite is greater than 1000 so that the reaction does not appear to be limited by the H_2O_2 concentration.

There is no blank reaction so that the detection limit is imposed by dark current noise from the p.m.t. detector. The RSD is typically 2% at the 100 μg $OCl^-\ l^{-1}$ level. While the reproducibility is not as good as that of the luminol method (about 1%), it is to be expected as a consequence of buffer decomposition of the sample prior to initiation of the reaction as previously discussed.

The dependence of intensity on $[OCl^-]^{1.4}$ below 100 $\mu g\ l^{-1}$ is interesting. As discussed in the introduction, the production of O_2 ($^1\Delta_g$) is first order in $[OCl^-]$. However, the resulting deactivation and emission of O_2 ($^1\Delta_g$) is proposed to be dependent on reaction between two O_2 ($^1\Delta_g$) molecules which would yield a second-order dependence if rate limiting. The non-integral order may indicate that both the production of O_2 ($^1\Delta_g$) and its deactivation are rate-limiting.

Interference studies

Table 1 lists calibration slopes, detection limits, and interference levels for various species. Of the listed species, none occurs in sufficient concentration in typical natural waters to cause interference, provided a 1:10 dilution of the sample is performed. Since free residual hypochlorite exists at typical levels of 0.4—1 mg l^{-1} in treated water, this dilution is required in any event to insure working on the optimum portion of the hypochlorite calibration curve (Fig. 4). Alternatively, a 0.1 ml rather than 1.0 ml sample size could be employed instead of dilution.

Note particularly that monochloramine would have to be present in the original sample at concentrations exceeding 170 mg l^{-1} in order to interfere, a very high concentration for this species. Thus the chemiluminescence method based on reaction with H_2O_2 is over 4000 times more sensitive to hypochlorite than NH_2Cl and much less subject to chloramine interference compared to other methods including the chemiluminescence method based on reaction with luminol. For many species, $c_I^* < c_I$ and the interference effect is depressive (negative sensitivity). These species probably cause interference by decomposing some of the hypochlorite. Reaction with these species in real samples is, of course, not a problem, as one is measuring the residual hypochlorite after such reactions have occurred. Interference levels for sulfide, ammonium and monochloramine were unobtainable because of reaction with the hypochlorite present in the sample cell, a condition evidenced by relative standard deviations of about 50—75% between runs.

The species listed in Table 1 that most likely could cause interference is ClO_2, but it is used very rarely in water chlorination owing to the problems associated with on-site generation of this toxic, highly explosive gas [1].

TABLE 1

Interferences in the hypochlorite—H_2O_2 chemiluminescence system[a]

Species	Sensitivity[b] (nA mg^{-1} l)	Detection limit (mg l^{-1})	Sensitivity[c] (nA mg^{-1} l)	Interference level (mg l^{-1})
Mg(II)	—	>100	—0.019	2.0
Ca(II)	0.046	1.0	0.0092	4.5
Fe(III)	—	>100	1.1	0.22
Fe(II)	—	>100	-2.0×10^{-3}	25
Ba(II)	0.0046	10	0.16	0.30
K(I)	6.9×10^{-5}	580	1.7×10^{-4}	229
Cs(I)	—	>100	—0.0022	20
Pb(II)	—	>100	0.053	0.75
Ag(I)	—	>100	—0.0064	6.0
Cd(II)	—	>100	—0.0042	10
Co(II)	0.0018	22	—0.035	0.11
Cu(II)	—	>100	—0.016	2.7
Ga(III)	—	>100	—2.7	0.15
Rb(I)	—	>100	—0.047	0.85
F^-	—	>1000	-5.5×10^{-4}	72
Br^-	—	>1000	0.01	4.0
I^-	—	>1000	-5.4×10^{-4}	0.09
NH_4^+	—	>100	—	—
S^{2-}	—	>100	—	—
MnO_4^-	0.013	4.0	0.0038	10
NH_2Cl	0.0033	17	—	—
ClO_2	490	0.000080	—	—

[a]Species with c_l and c_l^* > 100 mg l^{-1}: Cr(III), Cr(VI), Mn(II), SO_4^{2-}, CO_3^{2-}, PO_4^{3-}, Ni(II), Zn(II), Sr(II), Al(III), Ti(IV). Species with c_l and c_l^* > 1000 mg l^{-1}: Na(I), Cl^-, NO_3^-. [b]Slope of calibration curve of Cl signal vs. [interferent] in absence of OCl^-. [c]Slope of enhancement of depressive curve, Δ Cl signal of 40 μg OCl^- l^{-1} vs. Δ [interferent].

As previously mentioned [2], ClO_2 appears to be a universal interferent in hypochlorite determinations [1], although Isaacson and Wettermark have developed a method involving luminol in a flow system based on different chemiluminescence decay times to distinguish between hypochlorite and ClO_2 [18].

Determination of hypochlorite in tap water

The applicability of the proposed method for determination of hypochlorite in water was demonstrated by a comparison of results obtained with the chemiluminescence and colorimetric procedures. The two methods yielded results for 0.60—0.74 mg l^{-1} concentrations of hypochlorite that differed by an average of 1.3%. The relative standard deviation of the chemiluminescence procedure was 2% and about a factor of 2.5 lower than the colorimetric method.

Acknowledgement is made to the NSF (grants CHE 7616711 and CHE 7921292) for partial support of this research.

REFERENCES

1 APHA-AWWA-WPCF, Standard Methods for the Examination of Water and Wastewater; 14th edn., 1975, pp. 309—49.
2 D. F. Marino and J. D. Ingle, Jr., Anal. Chem., in press.
3 L. Mallet, Acad. Sci., Paris, 185 (1927) 352.
4 H. Seliger, Anal. Biochem., 1 (1960) 60.
5 B. Z. Shakhashiri and L. G. Williams, J. Chem. Educ., 53 (1976) 358.
6 H. H. Seliger, J. Chem. Phys, 40 (1964) 3133.
7 A. U. Khan and M. Kasha, J. Chem. Phys. 39 (1963) 2105.
8 S. J. Arnold, E. A. Ogryzlo and H. Witzke, J. Chem. Phys., 40 (1964) 1769.
9 A. U. Khan and M. Kasha, J. Am. Chem. Soc., 88 (1966) 1574.
10 R. E. Connick, J. Am. Chem. Soc., 69 (1947) 1509.
11 A. U. Khan and M. Kasha, J. Am. Chem. Soc., 92 (1970) 3293.
12 S. Hoyt and J. D. Ingle, Jr., Anal. Chim. Acta, 87 (1976) 163.
13 L. A. Montano and J. D. Ingle, Jr., Anal. Chem., 51 (1979) 926.
14 J. W. Mitchell, Anal. Chem., 50 (1978) 195.
15 Fisher Chemical Index 71C, Fisher Scientific Company, Pittsburgh, PA.
16 D. F. Marino and J. D. Ingle, Jr., Anal. Chem., in press.
17 RCA-1P28/V/ Data Sheet, RCA Corp.
18 U. Isaacson and G. Wettermark, Anal. Lett., A11 (1978) 13.

Analytica Chimica Acta, 123 (1981) 255–261

CORRECTION OF QUENCHING ERRORS IN ANALYTICAL FLUORIMETRY THROUGH USE OF TIME RESOLUTION

GARY M. HIEFTJE*

Department of Chemistry, Indiana University, Bloomington, IN 47405 (U.S.A.)

GILBERT R. HAUGEN

Department of Chemistry, Lawrence Livermore Laboratory, Livermore, CA 94550 (U.S.A.)

(Received 22nd July 1980)

SUMMARY

Varying concentrations of quenching agents can cause serious errors in analytical fluorimetry. The origin of these errors is an unexpected change in the quantum efficiency for the observed luminescence. It is known that quantum efficiency can be expressed as the ratio of an observed luminescence decay time to the decay time which would be observed in the absence of quenchers. Because this latter quantity is a constant for any particular fluorophore, quantum efficiency variations can be compensated through measurement of the decay time. For such measurements, the time-correlated single photon technique was employed and measured luminescence values were taken both from averaged photon count rates and from integrated fluorescence decay plots. Division of these values by measured luminescence lifetimes produced values which were independent of quencher concentration. Systems studied were quinine bisulfate quenched with chloride ion and 1-pyrenebutyric acid quenched by iodide.

Compared with other photometric methods, fluorimetry provides some of the lowest detection limits for many species of clinical, environmental, or forensic interest. However, fluorimetric measurements, unlike absorption methods, can suffer interferences from foreign species which quench excited analyte molecules. Although a number of mechanisms for such quenching action exist, they produce the same result: a reduced quantum efficiency and a consequent loss in fluorescence intensity. Because the concentration of the quenching agent is ordinarily unknown, correction for quenching is difficult; consequently, strong measures are taken to exclude quenchers from the analytical medium or to control their concentration carefully.

In the present paper, an alternative approach to overcoming quenching errors is explored. In this approach, quantum efficiency is indirectly measured by monitoring luminescence lifetime; correction for quenching then involves division of the measured fluorescence intensity by the observed lifetime.

Fundamentally, the new approach is straightforward. It is well known that the fluorescence intensity (F) from the sample is related to sample concentration (c) through the quantum efficiency (Φ) and a proportionality constant K

$$F = K\Phi c \tag{1}$$

In turn, quantum efficiency is the ratio of the intrinsic decay rate of an excited state (k_F) to the sum of the decay rates of all processes which depopulate the state (Σk)

$$\Phi = k_F(\sum k)^{-1} \tag{2}$$

The denominator in eqn. (2) is the reciprocal of the decay time for the sample under examination (τ_m), whereas the numerator is a reciprocal of the intrinsic lifetime of the fluorophore (τ_F)

$$\Phi = \tau_m \tau_F^{-1} \tag{3}$$

Combining eqns. (1) and (3) yields

$$F\tau_m^{-1} = k'c \tag{4}$$

where k' contains both K from eqn. (1) and τ_F.

From eqn. (4), it should be possible to obtain a quantity which is independent of sample quantum efficiency by dividing a measured fluorescence signal (F) by the measured luminescence lifetime (τ_m). In the present investigation, these measurements were carried out for two different fluorophore/quencher combinations using a time-correlated single photon technique for measurement of both luminescence lifetimes and fluorescence intensities. Although the precision of the resulting corrected values was limited to approximately 4% by errors in the lifetime measurement procedure, it was found possible to correct for quenching effects in samples whose fluorescence had been quenched by 95%. Although the procedure does not overcome errors caused by all kinds of quenching processes, it is expected to be important in situations involving diffusional quenching and changes in intersystem crossing rates.

EXPERIMENTAL

Two different instrumental configurations were employed for both the measurement of fluorescence intensities and luminescence decay curves. The first configuration (system 1) is similar to those available in many laboratories and reveals the practicability of the new approach. The second arrangement (system 2) is new in design and shows how all measurements for quenching-corrected fluorimetry can be made with a single instrument. These configurations are described separately.

System 1

For the lifetime measurements, a commercial time-correlated single photon fluorimeter (ORTEC model 9200), modified for high data acquisition rates [1], was employed. The pulsed excitation source was run in air at 20 psig at a frequency of 25 kHz. For excitation wavelength selection, an interference filter peaked at 334 nm and having a bandwidth of 11 nm was

used; emission was selected by a cutoff filter (Corning 0-52). The photomultiplier (RCA 8850) was uncooled and operated at a voltage of 2700 V.

Fluorescence intensities were measured using a computer-compatible system described previously [2]. An excitation wavelength of 340 nm and emission wavelengths of 375 and 395 nm were employed. Analog data collection was accomplished by chopping of the exciting radiation (4 kHz) and measurement with a tuned lock-in amplifier. A 4-pole Bessel active filter with a bandwidth of 0.2 Hz smoothed the output of the lock-in amplifier. A photomultiplier with S-20 photocathode surface (Hamamatsu 65TUVP) was operated at 2060 V.

System 1 was utilized for examining the correction of 1-pyrenebutyric acid quenched by potassium iodide [3].

System 2

A second instrumental system was employed in an attempt to extract all necessary data for corrected luminescence measurements from a single device. Unfortunately, such capability does not exist in conventional time-correlated single photon instruments because of large fluctuations in source intensity. Attempts were made to overcome this limitation through counting of lamp pulses during the elapsed measurement interval and integrating the resulting luminescence decay curve. However, precision of these measurements was far poorer than could be obtained from a conventional luminescence spectrometer.

To overcome these difficulties, the high-pressure air-discharge lamp was replaced by a more stable source consisting of a synchronously pumped, cavity-dumped, frequency-doubled dye laser. The laser was a commercial unit (models 171, 375, and 344, Spectra Physics, Mountain View, CA) operated with rhodamine 6-G as the dye. A pump wavelength of 514.5 nm and dye emission wavelength of 617 nm were utilized, resulting in an excitation pulse train at 308.5 nm. The frequency doubling crystal (Cleveland Crystal Co.) was potassium dihydrogenphosphate. This arrangement resulted in a primary beam having a power of approximately 17 mW and consisting of a train of 20 ps pulses at a frequency of 0.8 MHz. These primary pulses are calculated to have a peak power of approximately 1 kW and result in the production of frequency-doubled pulses of approximately 2-W peak power.

To serve as a trigger for the time-to-amplitude converter (TAC) of the correlation fluorimeter, a PIN photodiode registered the arrival of a fraction of the primary beam pulses. The primary and doubled beams were separated using a simple prism arrangement. The only other change from system 1 was the use of a different cut-off filter (Schott KV389) for separating the fluorescence radiation from background. A similar arrangement has been described previously [1].

With this stable pulsed source, it became possible to measure fluorescence intensity directly from recorded decay curves. Two approaches for this

measurement were examined. The first approach involved measuring the average anode pulse rate from the photomultiplier detector over a 10-s time period. The second approach utilized the integral of the processed luminescence decay curve as an indication of fluorescence intensity. This integral was readily obtained and could be directly read out from the commercial multichannel pulse-height analyzer employed in these studies.

The second system was employed to study the quenching of quinine bisulfate by chloride ion.

Reagents and chemicals

Both quenching systems have been discussed in some detail in the literature and solutions were prepared in accordance with instructions in that publication [3].

Stock solutions of 1-pyrenebutyric acid were prepared in 0.01 M potassium hydroxide and combined with varying amounts of iodide ion (as KI) in Tris buffer solutions (pH 8.0). Potassium iodide was stabilized by the addition of sodium thiosulfate. Solutions were made to have a range of lifetimes between 18 and 115 ns, the latter solution being totally unquenched. No attempt was made to exclude oxygen from the sample solution, since the technique should also correct for intersystem crossing rates induced by the presence of dissolved oxygen.

Quinine bisulfate solutions were prepared in 0.05 M sulfuric acid and were combined with varying amounts of chloride ion (added as NaCl) to yield a group of solutions having expected lifetimes between 1.5 and 18.9 ns.

RESULTS AND DISCUSSION

In general, results were similar for the studies on 1-pyrenebutyric acid and those on quinine bisulfate. However, instrumental system 2 seemed to perform better than system 1 and was employed for all subsequent investigations. Consequently, results obtained with this more elegant (but more complex) arrangement are emphasized here.

It was verified initially that quenching in both systems occurred by diffusion-controlled processes. Stern—Volmer plots for quinine bisulfate are shown in Fig. 1, which summarizes the results for both the anode pulse rate (curve A) and pulse-height spectrum integral (curve B) methods of monitoring fluorescence intensity. Examination of these curves indicates the slightly better precision of the latter approach, an unsurprising result in view of the larger number of data points utilized by the technique.

The influence of quencher (chloride ion) concentration on quinine bisulfate luminescence intensity is shown in Fig. 2; parts A and B again correspond to the different methods for monitoring fluorescence intensity. The lower curve in each figure reflects the drastic change in fluorescence which would be noted if no correction were made. In contrast, the upper, nearly flat line shows the improvement which is obtained by dividing the measured

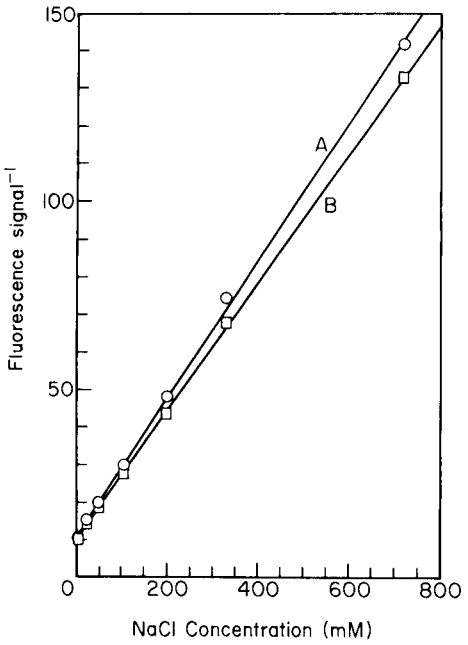

Fig. 1. Stern—Volmer plots for the quenching of quinine bisulfate by chloride ion. (A) Fluorescence intensity monitored through average anode pulse rate; (B) fluorescence intensity obtained by integration of luminescence decay curve (pulse-height spectrum).

fluorescence intensity for each sample by its measured luminescence lifetime. All curves are least-squares fits to recorded data. For the lifetime-corrected values, relative standard deviations of 5.9% and 4.0% were obtained for, respectively, the anode pulse rate and pulse height integral techniques for monitoring fluorescence intensity. Essentially all this error can be ascribed to uncertainties in the measurement of luminescence decay times.

One of the limitations in the time-correlated single photon technique for the measurement of luminescence lifetimes is that data acquisition times are long, being limited by the need to avoid pulse pile-up in the detection system. Although there are ways to minimize this limitation [1, 4], there is often a tendency to push data collection limits to improve acquisition time. Consequently, it was decided to examine the influence of unusually high anode pulse rates on the ability to correct for quantum efficiency changes.

The results of these investigations are shown in Fig. 3. Although the Stern—Volmer plots were linear for both methods of monitoring fluorescence intensity, even at high anode pulse rates, errors in measuring accurate luminescence lifetimes increased dramatically. At high anode pulse rates, fluorescence decay curves appear skewed toward shorter times; unless anode rates are matched exactly for samples having different degrees of quenching, decay curves yield erroneous lifetime values. Moreover, anode pulse overlap would result in a loss of integrated counts in the pulse-height spectrum and

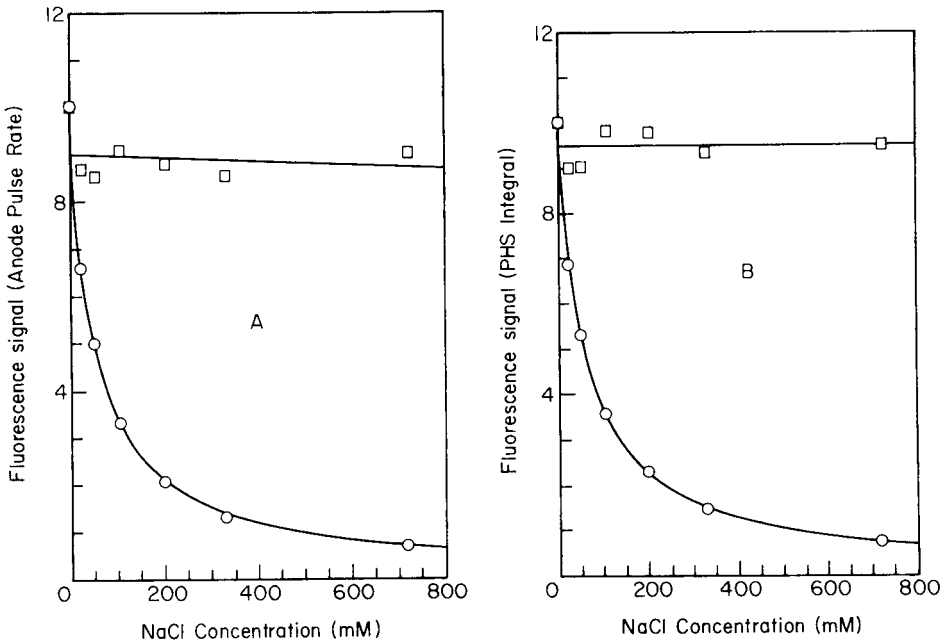

Fig. 2. Correction of measured fluorescence by ratioing with observed luminescence lifetime. Bottom curve in each figure is directly monitored fluorescence; upper plot shows the corrected values. (A) anode pulse rate is used to indicate fluorescence intensity; (B) integral of pulse-height spectrum is used to indicate fluorescence intensity.

in the measurement of anode pulse rate, thereby yielding incorrect values for fluorescence intensity. In the present experiment, anode pulse rates were measured with a high-frequency counter, so that error in those values was minimized. In contrast, the pulse-height spectrum integral was obtained directly from the time-correlated single photon counting apparatus, which had a relatively long dead-time. Consequently, data scatter in the corrected values obtained with this latter technique was much greater (relative standard deviation = 7.9%, Fig. 3B).

In summary, it has been shown that errors ordinarily caused by quantum efficiency variations in analytical fluorimetry can be overcome through use of time resolution. To perform the correction, one need only monitor simultaneously or consecutively the fluorescence intensity and luminescence lifetime for each sample and use the ratio to determine the concentration independently of collisional quenching processes. Conveniently, both intensity and lifetime can be monitored using the time-correlated single photon technique, if a source having stable pulse amplitudes is employed. However, for conventional instruments, it will be necessary to utilize an independent method for monitoring fluorescence signals.

In this correction procedure, as in most others using the time-correlated method, errors in measured lifetimes arise if fluorescence photons are

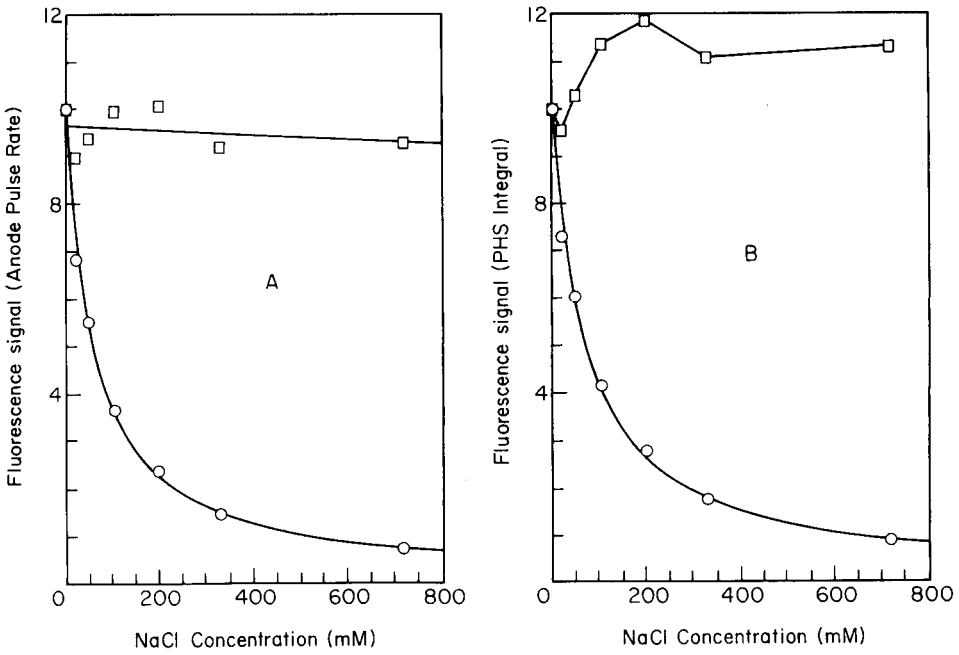

Fig. 3. Effect of high frequency of detected fluorescence photons on validity of quenching correction method. All parameters similar to those in Fig. 2.

detected at excessively high frequencies. These errors have greatest effect in the present measurements if fluorescence intensity is monitored through use of the pulse-height spectrum integral; their effect is minimized if the anode pulse rate is measured directly.

The authors thank Esther E. Vogelstein for helpful comments and suggestions made during the preparation of this manuscript. One of the authors (GMH) acknowledges the support, in part, by the Office of Naval Research and by the National Institutes of Health through grant PHS GM 24473. The other author (GRH) acknowledges the support of the U.S. Energy Research and Development Administration under contract W-7405-ENG-L18.

REFERENCES

1 G. R. Haugen, B. W. Wallin and F. E. Lytle, Rev. Sci. Instrum., 50 (1979) 65.
2 G. R. Haugen, B. A. Rabi and L. P. Rigdon, Chem. Instrum., 6(3) (1975) 205.
3 R. F. Chen, Anal. Biochem., 57 (1974) 593.
4 D. W. Peterson and J. M. Hayes, in D. M. Hercules, G. M. Hieftje, L. R. Snyder, and M. A. Evenson (Eds.), Contemporary Topics in Analytical and Clinical Chemistry, Vol. 3, Plenum Press, New York, 1978, Ch. 5.

Analytica Chimica Acta, 123 (1981) 263—270

SPECTROPHOTOMETRIC DETERMINATION OF SILICATE IN NATURAL WATERS BY FORMATION OF α-MOLYBDOSILICIC ACID AND REDUCTION WITH A TIN(IV)—ASCORBIC ACID—OXALIC ACID MIXTURE

J. DAVID SMITH* and PETER J. MILNE

Marine Chemistry Laboratory, School of Chemistry, University of Melbourne, Parkville, Victoria 3052 (Australia)

(Received 21st June 1980)

SUMMARY

Reaction of dissolved silicate with molybdate at pH 3.8—4.8 in acetate buffer yields only the α-molybdosilicic acid. Treatment of this acid with a solution containing tin(IV) chloride, ascorbic acid and oxalic acid rapidly gives the blue reduced acid without reducing the excess of molybdate reagent. In the recommended procedure, Beer's Law is followed at 740 nm over the range 0—2000 μg Si l^{-1} with a coefficient of variation of 0.34% at 400 μg Si l^{-1} and 0.52% at 40 μg Si l^{-1}. The sensitivity of the method is not affected by ionic strength.

Accurate measurement of dissolved silicate is a fundamental requirement in some biological, geochemical and marine studies. In many cases the ionic strength of the sample solutions varies over a wide range, and this is especially so for estuarine waters. In previous work, the analytical methods used to measure dissolved silicate have been subject to variation of sensitivity with ionic strength. The method of Mullin and Riley [1] and the modified procedure of Strickland and Parsons [2] include the use of an empirical formula to correct for salinity of the sample. The magnitude of the difference in sensitivity of the method for the same concentration of silicate in fresh water and sea water is about 8% [2, 3]. Thus the determination of dissolved silicate by these methods entails two measurements, i.e., of the salinity and the silicate.

Spectrophotometric methods for the determination of dissolved silicate in natural waters are usually based on formation of a yellow heteropoly acid with molybdenum and reduction of the product to the more intense blue form. The variety of conditions [1—16] that have been used to achieve the two steps of the reaction, reflects both the interest in the determination of silicic acid and the complex chemistry of its reaction with molybdate [17, 18].

The existence of α- and β-forms of molybdosilicic acid was demonstrated by Strickland [19]. These acids have different absorption spectra, and quantitative procedures have been based on the use of empirically specified

conditions intended to produce one form only, or a mixture of the α- and β-forms in a reproducible ratio. Mullin and Riley [1] used conditions for the formation of molybdosilicic acid similar to those previously used by Armstrong [4], and which according to Strickland [19] would give the β-acid. Grasshoff [10] re-examined the conditions for formation of the α- and β-molybdosilicic acids, and found that above pH 3.5 the α-acid predominated. The β-acid, formed at lower pH, changed spontaneously to the α-acid at a rate increasing with pH and ionic strength of the solution. Grasshoff [10] used analytical conditions where the α-acid was formed in a solution held at pH 3—4 by added monochloroacetic acid. A reaction time of 6 h was allowed for formation of the molybdosilicic acid, and a further 8 h for reduction after addition of metol. Becker [20], cited by Grasshoff [10], suggested that even after reduction the β-acid was unstable, re-oxidizing slowly into the stable reduced α-acid.

The effect of having a mixture of α- and β-acids was recognized by Fanning and Pilson [13] who studied the "salt factor" for a modification of the method of Mullin and Riley [1], and measured its variations with time of reaction of silicate and the molybdate reagent. Fanning and Pilson varied the ratio of hydrogen ion to molybdate, as this was the factor reported by Strickland [19] to determine whether α- or β-molybdosilicic acid was formed. It is now known, because of the more recent work of Truesdale and Smith [14], that Strickland's results can be misinterpreted, and consequently Fanning and Pilson were not producing pure α- and β-molybdosilicic acids.

Formation of the β-acid free from the α-form apparently cannot be achieved under conditions suitable for an analytical procedure. Use of a mixture of the α- and β-acids, the ratio of which will vary with ionic strength even when other factors are strictly controlled, is inherently unsatisfactory.

The α-acid can be produced free of the β-form, and Kato [16] developed a method of silicate determination based on production of the α-molybdosilicic acid at pH 4.2, but did not extend this work to a study of salt effects, or increase the sensitivity by reducing the yellow compound to the blue form.

In the work described here, the conditions shown by Truesdale and Smith [14] and Kato [16] to form the α-molybdosilicic acid were used and a reduction step was added to give an analytical method for silicate that is free of salt effect, rapid in execution, and highly sensitive.

EXPERIMENTAL

Apparatus

A Pye-Unicam SP500B spectrophotometer was used with glass cells of 10 mm or 100 mm path length for single wavelength determinations. The wavelength setting of the instrument was checked by using a didymium filter. Absorption spectra were scanned with a Varian 635 spectrophotometer and displayed on a Houston Instrument Omnigraphic X-Y recorder. This

equipment was also used to monitor changes in absorbance with time. A Radiometer model pHM62 pH meter with combination pH electrode was used and calibrated against Merck Titrisol buffer solutions.

Reagents

All chemicals were of analytical-reagent grade. Solutions were made up using water that had been distilled, deionised, and redistilled, and were stored in polyethylene bottles.

Standard silicate solution. (500 mg Si l^{-1}). Fuse 1.0694 g of ground pure silica with 5 g of sodium carbonate in a gold—platinum crucible. Dissolve the melt in water and make to 1 l. This solution was stable for many months, and a blank determination showed the sodium carbonate to be free of silicate.

Acetate buffer. Dissolve 20 g of anhydrous sodium acetate in water, add 58 ml of acetic acid (d. 1.049) and dilute to 500 ml with water.

Molybdate. Dissolve 4.4 g of ammonium molybdate in 100 ml of water.

Combined reductant solution. Prepare a tin(IV)—ascorbic acid solution as follows: to 4 ml of anhydrous tin(IV) chloride in a dry 50-ml volumetric flask, add 40 ml of distilled water with caution (HCl fumes are evolved), followed by 2 g of ascorbic acid, and dilute to 50 ml with water. (Stored under refrigeration, this solution is stable for at least two days.) Add 10 ml of this tin(IV)—ascorbic acid solution to 40 ml of a freshly filtered solution containing 17 g of oxalic acid dihydrate in 200 ml of water. Prepare the combined solution daily.

Recommended procedure

Pipette 25 ml of the sample solution into a clean dry polyethylene bottle. Add 3 ml of acetate buffer solution and 5 ml of the molybdate reagent. After 15 min add 5 ml of the combined reductant solution. After a further 20 min to allow for colour development, measure the absorbance of the solution at 740 nm against distilled water. The colour is stable for at least 24 h. Measure a blank value for the reagents added to 25 ml of distilled water, and prepare a calibration graph using appropriate dilutions of the standard silicate solution to cover the range 0—2000 μg Si l^{-1}. For samples containing more than 2000 μg Si l^{-1}, take a smaller aliquot and dilute to 25 ml with water before adding the buffer solution.

DEVELOPMENT OF THE METHOD

Formation of α-molybdosilicic acid

The α-acid is formed at pH 3.8—4.8 [15]. In the experiments reported here, 25 ml of diluted standard silicate solution containing 400 μg Si l^{-1} was placed in a polyethylene bottle with 3 ml of acetate buffer, and 5 ml of molybdate reagent added. The solution was allowed to stand for 10 min for complete formation of the α-acid. The absorption spectrum of the α-acid (Fig. 1) shows that any procedure based on the unreduced α-acid would be

unsatisfactory because of high reagent blank and low sensitivity. These restrictions prevail under analytical conditions, as the blank is due to the excess of molybdate that must be present for the rapid formation of the α-molybdosilicic acid. A procedure for production of a reduced α-molybdosilicic acid was sought to overcome these problems.

Reduction with tin(II)

In early work Strickland [19] showed that α-molybdosilicic acid would be reduced by tin(II); an analytical procedure for the determination of low levels of silicate in sea water was developed by Armstrong [4]. Mullin and Riley [1] used tin(II) in an analytical method of high sensitivity, but found that the product was unstable, and they preferred to use the slower acting metol—sulphite reducing agent. Reduction of the α-molybdosilicic acid using the faster acting and potentially more convenient tin(II) was re-examined here. To prevent reduction of excess of molybdate by the tin(II), it was necessary to acidify the test solution, and addition of 5 ml of 50% (v/v) sulphuric acid/water was found to be effective. To prevent interference by phosphate and arsenate, which also form heteropoly acids, oxalic acid was added, and 4 ml of an 8.5% (w/v) oxalic acid solution was found to be adequate. The sulphuric acid and oxalic acid solutions were added after the α-molybdosilicic acid formation, but before addition of the reductant.

Solutions of the acidified α-molybdosilicate acid were treated with various amounts of tin(II), added as a solution of $SnCl_2$ in dilute hydrochloric acid. The spectrum of the tin(II)-reduced α-acid (Fig. 2, curve A) showed the optimum wavelength for analytical sensitivity to be 740 nm. The absorbance of test solutions treated with different amounts of tin(II) increased up to a level equivalent to 1 ml of 0.06 M tin(II); above this level no further increase in sensitivity occurred. The absorbance of the solution containing the tin(II)-

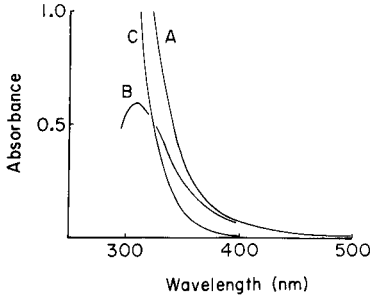

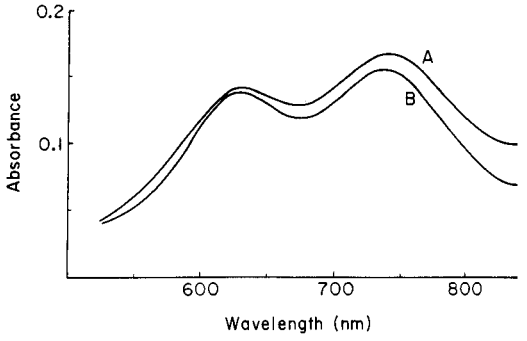

Fig. 1. Absorption spectra of α-molybdosilicic acid solutions (2000 μg Si l^{-1}) before reduction: (A) α-molybdosilicic acid solution vs. water; (B) α-molybdosilicic acid solution vs. reagent blank; (C) reagent blank vs. water.

Fig. 2. Absorption spectra of solutions of α-molybdosilicic acid (400 μg Si l^{-1}) after reduction: (A) reduction by tin(II); (B) reduction by tin(IV)—ascorbic acid.

reduced α-molybdosilicic acid changed slowly with time. The change was shown to be due in part to changes in the absorbance of the excess of molybdate reagent. When formation of the α-molybdosilicic acid was prevented (by adding sulphuric acid to the silicate solution before addition of molybdate), the absorbance of the "blank" solution changed with time in the same way. These results showed that tin(II) was not a suitable reductant for this analytical use, even when the pure α-form of the molybdosilicic acid was used. Other reductants were therefore studied.

Reduction with tin(IV)—ascorbic acid

Andersson [8] reported that a solution containing tin(II), tin(IV) and ascorbic acid, in the presence of sufficient perchloric acid, reduced the yellow molybdosilicic acid to give a stable blue colour. The preparation of the reductant solution as described by Andersson is elaborate, with optimum amounts of tin(IV), tin(II) and ascorbic acid given as ranges, not as precise values. In the present tests, separate solutions of tin(II) chloride, tin(IV) chloride, ascorbic acid and perchloric acid were added to the α-molybdosilicic acid solutions in various proportions, to investigate the use of this reductant system further. When the final concentrations were similar to those reported by Andersson for his combined reductant, a stable blue colour was obtained. Combination of tin(II), tin(IV), and ascorbic acid into one reductant solution was also effective. In these tests, it was observed that: (1) reduction to give a blue colour occurred even when tin(II) was omitted; and (2) in solutions containing oxalic acid, selective reduction of the α-molybdosilicic acid and not the molybdate reagent occurred, even when perchloric acid was omitted entirely (Table 1). This selective reduction, with consequently low blank, occurred under conditions of relatively low acidity, compared with those in previous reports [1—16, 19]. The pH of the final solution was found to be 1.5 as a result of the combined effect of the added $SnCl_4$, ascorbic acid and oxalic acid solutions. Eckert [6] described the reduction of β-molybdosilicic acid with a mixture of tin(II) oxalate and formic acid, but this required strong acid conditions to avoid reduction of excess of molybdate.

TABLE 1

The effects of oxalic and perchloric acids on the reduction of α-molybdosilicic acid by tin(II)—ascorbic acid. (Absorbance readings are given.)

$HClO_4$ added (ml)	With oxalic acid		Without oxalic acid	
	Blank	400 μg Si l^{-1}	Blank	400 μg Si l^{-1}
0	0.004	0.168	[a]	[a]
1	0.008	0.178	[a]	[a]
3	0.008	0.179	[a]	[a]
5	0.010	0.175	0.007	0.070

[a]Gelatinous white precipitate formed.

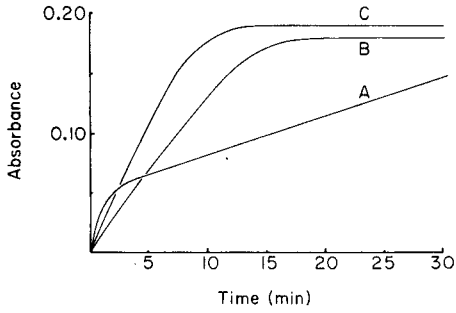

Fig. 3. Effects of different amounts of tin(IV) and ascorbic acid in the reducing solution on rate of colour development at 740 nm: (A) 1 ml $SnCl_4$ + 2 g ascorbic acid; (B) 4 ml $SnCl_4$ + 2 g ascorbic acid; (C) 8 ml $SnCl_4$ + 2 g ascorbic acid.

Rate of colour development

Solutions containing α-molybdosilicic acid were prepared by mixing 25 ml of diluted silicate standard (400 μg Si l^{-1}), 3 ml of acetate buffer, 5 ml of molybdate reagent, and adding 4 ml of oxalic acid solution. The rate of colour development after addition of 5-ml aliquots of differing reducing solutions is shown in Fig. 3. A reducing solution containing 4 ml of tin(IV) chloride and 2 g of ascorbic acid made up to 50 ml with water gave full colour development in 15 min, and the colour was then stable for at least 24 h. Doubling the concentration gave only slightly faster colour development and higher sensitivity. A reducing solution combining the tin(IV) chloride—ascorbic acid mixture and the oxalic acid gave results identical to those obtained with the separate solutions.

The absorption spectrum of the tin(IV)—ascorbic acid-reduced α-molybdosilicic acid is very similar to that of the tin(II)-reduced α-acid (Fig. 2), with the optimum analytical wavelength remaining at 740 nm.

Reagent blank

Reduction of the α-molybdosilicic acid with tin(IV)—ascorbic acid mixture gave a low blank because there was no reduction of the excess of molybdate. The "blank" obtained by reversing the order of addition of the reducing solution and the molybdate, was less than 0.002 absorbance units for a

TABLE 2

Absorbances given by different concentrations of dissolved silicate added to distilled water and to sea water of salinity 35.4‰

Silicate added (μg Si l^{-1})	Absorbance increment from added silicate	
	Distilled water	Sea water
40	0.016_5	0.016_5
400	0.163	0.161
1000	0.407	0.407

100-mm light path at 740 nm. Silicate contamination of the ammonium molybdate reagent although low, was found to be the major contributor to the reagent blank.

PERFORMANCE OF THE METHOD

Beer's law and precision

When the recommended procedure was used and absorbances were measured in 10-mm cells at 740 nm, Beer's Law was followed over the range 0—2000 μg Si l^{-1} in both distilled water and sea water (Table 2). Five replicate determinations of a solution containing 400 μg Si l^{-1} gave a mean absorbance of 0.164 with a coefficient of variation of 0.34%. At the 40 μg Si l^{-1} level, with 100-mm cells, the coefficient of variation was 0.52%.

Interferences and salt effects

Potentially interfering species are phosphorus and arsenic anions that form heteropolymolybdates. Changes in the absorbance of solutions containing 40 μg Si l^{-1} in the presence of 50-fold amounts of phosphate, arsenate and arsenite are listed in Table 3. The results indicate that at levels commonly found in natural waters interference from phosphate and arsenate will be negligible.

Determination of silicate after standard additions of silicate to distilled water and to sea water showed the sensitivity to be identical in both solutions (Table 2).

Application to estuarine waters

Silicate concentrations in sea water vary over a wide range. In surface waters, the content may be as low as 10 μg Si l^{-1}, but in deep water it may reach up to 5000 μg Si l^{-1} [21]. The recommended method has been applied in a study of dissolved silicate in the Yarra River estuary, and some results are given in Table 4. The linearity of the salinity—silicate relationship, and the agreement of the amounts of silicate with the levels reported by others [22] support the accuracy of the method.

TABLE 3

Influence of phosphate, arsenate and arsenite on the determination of dissolved silicate at the 40 μg Si l^{-1} level

Anion	Concentration added	% Change in absorbance
Phosphate	2000 μg P l^{-1}	+9.4
Arsenate	2000 μg As l^{-1}	+3.2
Arsenite	2000 μg As l^{-1}	0.0

TABLE 4

Salinity and dissolved silicate concentrations (μg Si l^{-1}) in waters of the Yarra River estuary (December 1976)

Salinity (‰)	0.4	3.5	6.9	14.7	17.4	21.8	28.2	32.4	33.1
Si (μg l^{-1})	3660	3370	3085	2290	1920	1400	840	320	295

REFERENCES

1 J. B. Mullin and J. P. Riley, Anal. Chim. Acta, 12 (1955) 162.
2 J. D. H. Strickland and T. R. Parsons, A Practical Handbook of Sea Water Analysis, Bull. Fish. Res. Bd., Canada, No. 167 (1968) 65.
3 G. S. Bien, Anal. Chem., 30 (1958) 1525.
4 F. A. J. Armstrong, J. Marine Biol. Assoc. U.K., 30 (1951) 149.
5 A. Ringbom, P. E. Ahlers and S. Siitonen, Anal. Chim. Acta, 20 (1958) 78.
6 G. Eckert, Fresenius Z. Anal. Chem., 161 (1958) 421.
7 G. J. S. Govett, Anal. Chim. Acta, 25 (1961) 69.
8 L. H. Andersson, Ark. Kemi, 19 (1962) 223.
9 I. R. Morrison and A. L. Wilson, Analyst, 88 (1963) 88, 100, 446.
10 K. Grasshoff, Deep-Sea Res., 11 (1964) 597.
11 H. E. Garrett and A. J. Walker, Analyst, 89 (1964) 642.
12 P. S. Liss and C. P. Spencer, J. Marine Biol. Assoc. U.K., 49 (1969) 589.
13 K. A. Fanning and M. E. Q. Pilson, Anal. Chem., 45 (1973) 136.
14 V. W. Truesdale and C. J. Smith, Analyst, 100 (1975) 203.
15 V. W. Truesdale and C. J. Smith, Analyst, 101 (1976) 19.
16 K. Kato, Anal. Chim. Acta, 82 (1976) 401.
17 G. P. Haight and D. R. Boston, J. Less-Common Metals, 36 (1974) 95.
18 J. P. Launay, R. Massart, and P. Souchay, J. Less-Common Metals, 36 (1974) 139.
19 J. D. H. Strickland, J. Am. Chem. Soc., 74 (1952) 862, 868, 872.
20 W. Becker, Dissertation, Würzburg, 1962.
21 J. P. Riley and R. Chester, Introduction to Marine Chemistry, Academic Press, London, 1971, p. 177.
22 P. S. Liss, in J. D. Burton and P. S. Liss (Eds.), Estuarine Chemistry, Academic Press, Ch. 4, London, 1976.

Analytica Chimica Acta, 123 (1981) 271—277

FLOTATION—SPECTROPHOTOMETRIC DETERMINATION OF OSMIUM WITH THIOCYANATE AND METHYLENE BLUE

Z. MARCZENKO* and J. UŚCIŃSKA

Department of Analytical Chemistry, Technical University, Warsaw (Poland)

(Received 28th July 1980)

SUMMARY

A sensitive flotation—spectrophotometric method, based on the ion associate formed by the anionic thiocyanate complex of osmium with the basic dye methylene blue (MB) is described. The ion associate precipitates when the aqueous solution is shaken with toluene, and the separated and washed compound is dissolved in acetone. The molar absorptivity is 2.2×10^5 l mol^{-1} cm^{-1} at 655 nm. Beer's law is obeyed. The molar ratio of Os:SCN:MB in the separated and washed ion associate is 1:6:3. Ruthenium reacts similarly. The method is applied to the determination of traces of osmium in crucible platinum after separation of osmium by distillation as tetroxide.

With the growing demands of trace analysis, the role of sensitive spectrophotometric methods increases [1]. This group of methods includes procedures based on the ion associates formed with basic dyes by suitable anionic complexes of the elements to be determined [2]. Ion associates with a molar ratio of 1:1 are generally soluble in non-polar solvents and are used in extraction—spectrophotometric methods. Ion associates of more complex structure may precipitate at the phase boundary or on the walls of the separatory funnel when the aqueous phase is shaken with some organic solvents. This provides the basis of flotation-spectrophotometric methods. The sparingly soluble ion associate, separated from both liquid phases, is dissolved in a polar solvent and the absorbance of the solution obtained is measured. Since in this case the number of molecules of the basic dye per atom of the element to be determined is higher than one, these methods exhibit very high sensitivity.

Sensitive flotation—spectrophotometric methods for the determination of rhodium and platinum based on malachite green and crystal violet have been described previously [3, 4]. The purpose of the present work was to develop a similar method for osmium on the basis of its anionic thiocyanate complex and a suitable basic dye. Thiocyanate complexes of osmium and ruthenium have been applied to the extractive separation and spectrophotometric determination of these metals [5]. The molar absorptivities in these methods were not high, amounting to 1.71×10^4 (620 nm) and 5.5×10^3 l mol^{-1} cm^{-1} (570 nm), respectively.

EXPERIMENTAL

Reagents

Osmium standard solution (1 mg Os ml^{-1}). Weigh a glass ampoule containing ca. 0.5 g OsO_4, score it with a file, and then crush it carefully in a beaker containing 100 ml of water. Collect the glass fragments, wash them carefully, dry and weigh. The amount of osmium tetroxide used is found from the difference in the weights of the original ampoule and the glass fragments. Dilute the solution with water to obtain a concentration of 1 mg Os ml^{-1}, and store it in a dark glass bottle with a ground-glass stopper. Working solutions are obtained by diluting the stock solution with water.

According to Alimarin et al. [6], OsO_4 solutions in water are more stable than in acids. Osmium tetroxide volatilizes more rapidly from acidic solutions than from neutral ones.

Methylene blue (MB; Merck). A 10^{-3} M solution (ca. 0.032%) was used.

Apparatus

A SPEKOL spectrocolorimeter and a SPECORD u.v.—visible spectrophotometer were used with 1-cm cells. The pH meter was an ELPO N-512 model.

Procedure

Add 5 ml of aqueous 5% (w/v) ammonium thiocyanate solution to the examined solution containing not more than 20 μg of osmium (in any oxidation state) and adjust the pH of the solution to 2—3 with diluted sulphuric acid or ammonia. Dilute the solution to 20 ml with water and heat on a boiling water bath for about 15 min. Allow the solution to cool to room temperature and transfer it to a 100-ml separatory funnel. Add 1 ml of the methylene blue solution and 5 ml of toluene and shake for about 30 s. Carefully remove the aqueous phase, and then wash the toluene phase and the separated precipitate, by shaking with three portions of water for about 15 s each time. Carefully decant the toluene, and dissolve the ion associate in acetone. Transfer the solution to a 25-ml volumetric flask and dilute to the mark with acetone. Measure the absorbance of the solution at 655 nm against a reagent blank prepared in the same way.

RESULTS AND DISCUSSION

Preliminary studies were aimed at finding a basic dye which at suitable acidity forms an extractable or floatable ion associate with the anionic thiocyanate complex of osmium. The following 13 basic dyes were examined: crystal violet, malachite green, brilliant green, methyl green, Victoria blue B and Victoria blue 4R (triarylmethane dyes), rhodamine B and rhodamine 6G (xanthene dyes), Nile blue A, Meldola blue and Capri blue (oxazine dyes), methylene blue (thiazine dye) and safranine T (phenazine dye). The tests

were carried out at various acidities (from pH ca. 3 to 3 M sulphuric acid) and at a 20—30-fold molar excess of the dye with respect to osmium. The amount of osmium in these experiments was 12 μg. The aqueous solutions were shaken with benzene, toluene, carbon tetrachloride, chloroform or diisopropyl ether.

Carbon tetrachloride and chloroform extract the ion associates formed by thiocyanate ion and basic dyes. In the case of benzene, toluene, and diisopropyl ether, flotation of the associates of the thiocyanato—osmium complex takes place; the compound precipitates at the phase boundary and on the walls of the separatory funnel. At the same time sparingly soluble associates of the thiocyanate ion with basic dyes precipitate. In some cases, the associate of thiocyanate ion with the dye can readily be separated from the associate of the thiocyanato—osmium complex with the dye by washing with water; in this way the blank value is low. The systems methylene blue—toluene and Capri blue—diisopropyl ether lead to sensitive flotation—spectrophotometric methods for the determination of osmium. In the case of rhodamine B and diisopropyl ether, the method is highly sensitive but not precise; the final absorbance depends on the acidity of the aqueous phase during flotation. In these experiments, the absorbances of acetone solutions of the separated and washed ion associates were measured.

The osmium—thiocyanate—MB system

In slightly acidic medium (H_2SO_4 or HCl), osmium forms an anionic complex with thiocyanate ions, which then reacts with methylene blue to form an ion associate. The ion associate separates at the phase boundary on shaking with toluene. The associate is then dissolved in acetone and the absorbance of the solution is measured. It was found that the absorbance (for the same amount of osmium) depends on the concentration of thiocyanate ions and on the acidity, as well as on the time and temperature of heating of the osmium solution with thiocyanate. The anionic osmium complex that exhibits the highest stable absorbance is obtained when the solution, after addition of thiocyanate, is heated on a boiling water bath for at least 10 min, at a thiocyanate concentration higher than 0.15 M and in the pH range 1.5—3.5. In more acidic solutions, the reproducibility of the results is worse. For quantitative separation of osmium from the aqueous phase in the form of the sparingly soluble associate, at least a 15-fold molar excess of methylene blue (with respect to osmium) is necessary. Further increase in the concentration of the dye in the solution has no effect on the final results, but the blank value increases. These relations are shown in Fig. 1.

Toluene and benzene are equally good as flotation solvents. Toluene was chosen because it is less toxic. With both these solvents, shaking with the aqueous phase caused the sparingly soluble associate to precipitate on the walls of the separatory funnel. When diisopropyl ether was used for flotation, the final results were similar, but the solvent was less convenient in use:

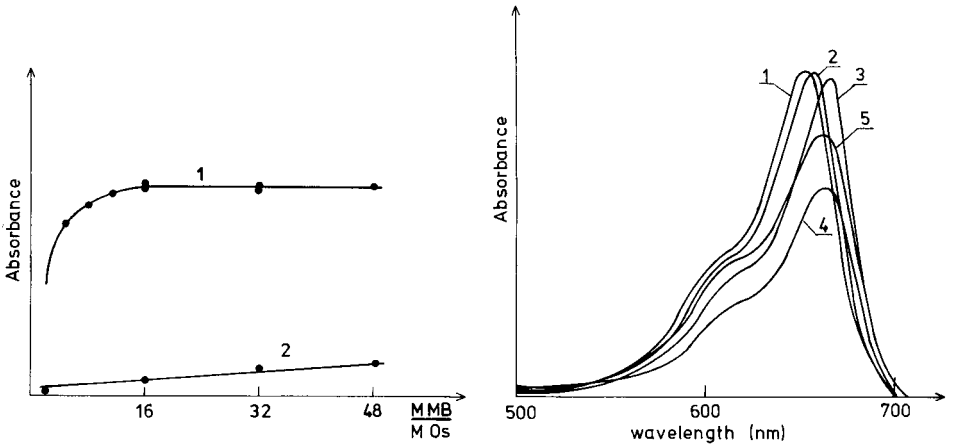

Fig. 1. Dependence of the absorbance of the acetone solution of the ion associate on the excess of methylene blue (flotation with toluene). (1) Absorbance of the solutions measured against the blank; (2) absorbance of the blank measured against water.

Fig. 2. Absorption spectra of the methylene blue from the ion associate dissolved in: (1) methanol; (2) acetone; (3) dimethylformamide directly after dissolution; (4) dimethylformamide after 1 h. (5) Spectrum of the methylene blue in water. The concentration of MB was the same in all cases.

after shaking, the precipitate collected mainly at the phase boundary, which made it difficult to remove without losses of the ion associate. The ratio of the phase volumes has no effect on the flotation efficiency. Separation of osmium from the aqueous phase is quantitative after shaking with toluene for at least 20 s.

The associate of thiocyanate ion with methylene blue precipitates together with the associate of the thiocyanate complex of osmium. On washing with water the osmium-free precipitate decomposes and the dye passes to the aqueous phase. The excess of the dye can be quantitatively removed by shaking the precipitate and toluene with three portions of water; the blank value does not exceed 0.05.

For dissolution of the separated and washed precipitate, the following solvents were examined: ethanol, methanol, acetone, and dimethylformamide. In practice, it is difficult to dissolve the precipitate completely in ethanol. The precipitate can be completely dissolved in methanol and acetone by a short shaking. Dissolution in dimethylformamide takes place immediately. Of the above solvents, acetone was chosen because in the case of many preparations of dimethylformamide the colour intensity rapidly decreased with time (Fig. 2), whereas the colour of the acetone solution was stable with time. As can be seen in Fig. 2, solutions of methylene blue in various solvents show small differences in the position of the maximum wavelength. The spectra of methylene blue are known to be different in water and in ethanol [7].

Analytical characteristics and interferences

On the basis of these studies, a standard curve for determining osmium with thiocyanate and methylene blue was prepared. Beer's law is obeyed up to a concentration of 0.8 μg Os ml^{-1}. The molar absorptivity (ϵ) is 2.2×10^5 l mol^{-1} cm^{-1} (specific absorptivity $a = \epsilon$/at. mass $\times$ 1000 = 1.16) at 655 nm.

The precision and accuracy of the method were evaluated by analysis of solutions containing known amounts of osmium. The results are presented in Table 1.

Metals that form anionic thiocyanate complexes can interfere with this determination of osmium. The method becomes highly selective when the determination of osmium is preceded by a distillation of OsO_4 from solutions containing oxidizing agents such as hydrogen peroxide or nitric acid. When some stronger oxidizing agents are used (e.g. perchloric acid, potassium permanganate), ruthenium also distils as RuO_4 [8, 9].

The experiments carried out showed that ruthenium forms with thiocyanate ions and methylene blue a compound similar to that of osmium and can also be determined by a flotation–spectrophotometric method under conditions similar to those for osmium (see Procedure). Microgram amounts of osmium and ruthenium can be determined by means of the proposed method after extractive separation of these metals as their thiocyanate complexes [5].

Sulphate, chloride and nitrate up to a concentration of 2 M do not interfere with the determination of osmium. Perchlorate interferes because perchlorate and methylene blue form an ion pair which is floated simultaneously with that of osmium, and is not readily soluble in water.

The molar ratio of osmium to methylene blue in the separated ion associate, according to the results obtained by the method of isomolar series, is 1:3 (Fig. 3). This result was confirmed by absorbance measurements of acetone solutions of the ion associate with a known amount of osmium and of acetone solutions of the dye, the molar amount of the dye being three times higher than that of osmium in the first solution. The absorbances in both the cases were practically equal.

The number of thiocyanate ions corresponding to one osmium atom in the separated precipitate was found to be six. The separated precipitate of the ion associate was oxidized by means of concentrated hydrochloric

TABLE 1

Precision of the results for the determination of osmium with thiocyanate and methylene blue (n = 6)

Osmium added (μg)	Osmium found (μg)	s (μg)	s_r (%)	Confidence limits (probability level 0.95)
4.00	4.06	0.09	2.3	4.06 ± 0.10
8.00	8.08	0.16	2.0	8.08 ± 0.17
16.00	15.91	0.28	1.8	15.91 ± 0.30

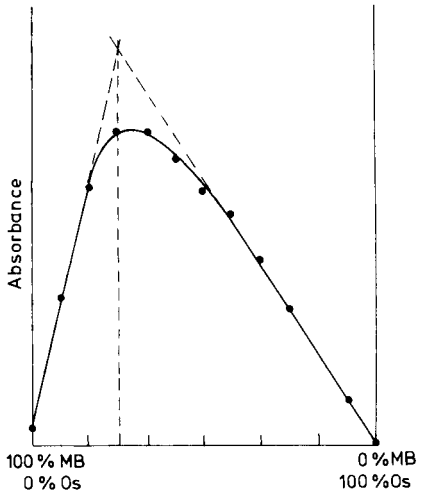

Fig. 3. Determination of the ratio of osmium to methylene blue in the ion associate by the isomolar series method.

and nitric acids (1 + 1). The sulphur of the thiocyanate ions and the sulphur contained in the three molecules of methylene blue were thereby oxidized to sulphate. This sulphate was then determined spectrophotometrically by means of the well-known methylene blue method based on reaction of sulphide with *p*-aminodimethylaniline in the presence of iron(III) [10]. On the basis of these experiments, the number of sulphur atoms corresponding to one osmium atom was found to be 9.4 (range 9.1—9.8; n = 4). The difference between the values obtained and the expected value (9) can be ascribed to the fact that the separated ion associate retains some thiocyanate as well as dye. The ion associate that forms the basis of the proposed flotation—spectrophotometric method for the determination of osmium therefore corresponds to the formula: $[MB^+]_3[Os(SCN)_6^{3-}]$.

Determination of traces of osmium in platinum

The proposed method was applied to the determination of trace impurities of osmium in crucible platinum. The metal was dissolved in aqua regia in a closed system, the evolving osmium tetroxide and the gaseous products of the reaction of concentrated hydrochloric and nitric acids being absorbed in a receiver containing water after passing through the condenser. The solution obtained was diluted with water and osmium was distilled off as OsO_4 into a receiver containing thiocyanate solution (acidified to pH 2—3). Osmium was then determined according to the above procedure. Under the conditions described, any ruthenium present in the sample is not converted to volatile RuO_4.

The results presented in Table 2 for the sample of platinum itself and with additions of osmium indicate the good accuracy of the proposed method.

TABLE 2

Results of determination of osmium in platinum sample

Sample weight (g)	Osmium added (μg)	Osmium found (μg)	Os content in platinum[a] ($\times 10^{-4}$%)
0.52		2.2	4.3
0.48		2.1	4.4
0.69		3.0	4.4
1.01		4.5	4.5
1.03		3.9	3.8
0.53	4.0	6.5	4.7
0.77	4.0	7.2	4.2
1.00	4.0	8.0	4.0

[a]Statistical data: $\bar{x} = 4.29 \times 10^{-4}$%; $s = 2.8 \times 10^{-5}$%; $s_r = 6.5$%; $\mu_{0,95} = (4.29 \times 10^{-4} \pm 0.23 \times 10^{-4})$%.

REFERENCES

1 Z. Marczenko, Crit. Rev. Anal. Chem., 9 (1980), in press.
2 Z. Marczenko, Mikrochim. Acta, (1977II) 651.
3 Z. Marczenko and E. Kowalczyk, Anal. Chim. Acta, 108 (1979) 261.
4 Z. Marczenko and J. Maruszak, Chem. Anal. (Warsaw), 24 (1979) 341.
5 Z. Marczenko and M. Balcerzak, Anal. Chim. Acta, 109 (1979) 123.
6 I. P. Alimarin, V. P. Khvostova and G. I. Kadyrova, Zh. Anal. Khim., 30 (1975) 2007.
7 L. Michaelis and S. Granick, J. Am. Chem. Soc., 67 (1945) 1212.
8 F. E. Beamish and J. C. van Loon, Analytical Chemistry of the Noble Metals, Pergamon, Oxford, 1972.
9 Z. Marczenko and M. Balcerzak, Chem. Anal. (Warsaw), 24 (1979) 867.
10 Z. Marczenko, Spectrophotometric Determination of Elements, Ellis Horwood, Chichester, 1976, p. 506.

Analytica Chimica Acta, 123 (1981) 279—287

SPECTROPHOTOMETRIC DETERMINATION OF IRON(III) WITH CHROME AZUROL S OR ERIOCHROME CYANINE R AND SOME CATIONIC SURFACTANTS

Z. MARCZENKO* and H. KAŁOWSKA

Department of Analytical Chemistry, Technical University, Warsaw (Poland)

(Received 19th May 1980)

SUMMARY

Sensitive spectrophotometric methods for the determination of iron(III), based on ternary complexes with a triphenylmethane reagent, chrome azurol S (CAS) or eriochrome cyanine R (ECR), and cetyltrimethylammonium (CTA) or cetylpyridinium (CP) ions, are described. For the system Fe—CAS—CTA, the molar absorptivity is 1.35×10^5 l mol^{-1} cm^{-1} at 645 nm; for Fe—ECR—CTA it is 1.28×10^5 l mol^{-1} cm^{-1} at 635 nm. Maximum absorbance is attained (at about pH 4) when the molar ratio (to iron) or CAS or ECR is about 20 and that of CTA or CP is 60—80. Citrate, tartrate, oxalate and EDTA interfere. Interference by metals (e.g. Be, Al, Ga, In, Sc, Zr, Th) can be eliminated by preliminary extraction of iron(III) as thiocyanate complex. The method was successfully applied to determining traces of iron in analytical-grade sodium hydroxide.

The sensitivity of spectrophotometric methods for the determination of many cations with some triphenylmethane reagents is significantly increased in the presence of long-chain cationic surfactants, e.g. cetyltrimethylammonium (CTA) or cetylpyridinium (CP) ions [1, 2]. Ternary complexes involving CTA or CP exhibit much higher absorbance than the corresponding binary complexes; in addition, considerable bathochromic effects can be observed.

Previous papers have been devoted to the determination of beryllium [3], gallium [4] and indium [5] by means of chrome azurol S or eriochrome cyanine R and CTA. The present paper is concerned with the development of sensitive methods for the determination of iron with the above-mentioned chromophoric reagents and CTA or CP. The systems iron—chrome azurol S—CTA [6, 7] and iron—eriochrome cyanine R—CTA [8] have been studied by other workers. The mechanism of the formation of ternary complexes of some metals with triphenylmethane reagents and long-chain quaternary bases has been discussed [9—11].

EXPERIMENTAL

Reagents and apparatus

Iron(III) standard solution (1 mg Fe ml^{-1}). Dissolve 8.6350 g of iron(III) ammonium sulphate, $FeNH_4(SO_4)_2 \cdot 12H_2O$, in water with addition of 5 ml of concentrated sulphuric acid and dilute the solution with 0.01 M H_2SO_4 to 1 l. Prepare working solutions by suitable dilution with 0.01 M HCl.

Chrome azurol S (CAS), 5×10^{-4} M solution. Dissolve 67.4 mg of CAS in water and dilute with water to 250 ml. Purify the reagent by reprecipitation from about 1.5 M HCl.

Eriochrome cyanine R (ECR), 5×10^{-4} M solution. Dissolve 58.8 mg of ECR in water and dilute with water to 250 ml. Purify the reagent by reprecipitation from about 1.5 M HCl.

Cetyltrimethylammonium bromide (CTA) or cetylpyridinium chloride (CP), 4×10^{-3} M solution. Dissolve 0.3645 g of CTA (Hopkins and William) or 0.3580 g of CP (Loba) in water and dilute to 250 ml.

Acetate buffer (pH 4.3). Add 225 ml of 0.1 M sodium acetate solution to 250 ml of 0.1 M acetic acid and dilute with water to 500 ml.

A Specord u.v.—visible recording spectrophotometer and a VSU-2P spectrophotometer were used with 1-cm cells.

Recommended procedures for the determination of iron

Add 7 ml of the chrome azurol S or eriochrome cyanine R solution and 3 ml of the CTA solution to the sample solution (pH 1—2) containing not more than 10 μg Fe. Adjust the pH to pH ca. 4 with ammonia solution and add 5 ml of the acetate buffer. Transfer the solution to a 25-ml volumetric flask, fill with water to the mark and mix. For the CAS system, measure the absorbance of the solution after 15 min at 645 nm against a blank. For the ECR system, measure the absorbance of the solution at 610 nm against a blank.

RESULTS AND DISCUSSION

Iron(III) ions form coloured complexes with chelating triphenylmethane reagents, which are advantageously used in spectrophotometric determinations of this metal [12]. Molar absorptivities in these methods do not exceed 3×10^4 l mol^{-1} cm^{-1}. In a preliminary study, tests were made to establish if additions of cationic surfactants (CTA or CP) to systems containing iron(III) and chrome azurol S, eriochrome cyanine R, xylenol orange and pyrocatechol violet resulted in increased absorbance. Only in the case of the first two chromophoric reagents did the presence of cetyltrimethylammonium or cetylpyridinium ions result in a significant increase of absorbance compared to the binary systems.

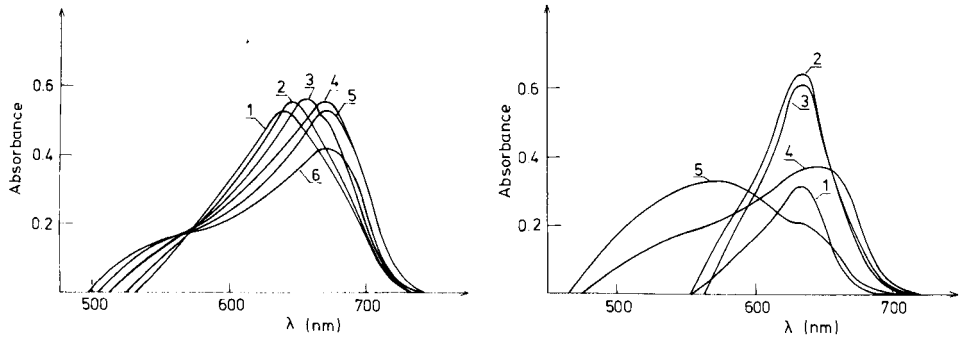

Fig. 1. Dependence of the absorption spectra on pH in the system Fe—CAS—CTA (5×10^{-6} M Fe^{3+}, 5×10^{-5} M CAS, 4×10^{-4} M CTA against reagent blank). pH values: (1) 2.4; (2) 3.5; (3) 4.7; (4) 5.5; (5) 6.4; (6) 7.5.

Fig. 2. Dependence of the absorption spectra on pH on the system Fe—CAS—CP (5×10^{-6} M Fe^{3+} 1×10^{-4} M CAS, 4×10^{-4} M CP against reagent blank). pH values: (1) 2.1; (2) 2.9; (3) 3.9; (4) 6.1; (5) 8.2.

Ternary system: iron(III)—CAS—CTA (CP)

In the presence of CTA or CP ions, iron(III) forms ternary complexes; the absorption spectra change with pH (Figs. 1 and 2). The optimum values of pH for the formation of the Fe—CAS—CTA complex are 3.7 ± 0.9 at 645 nm 5.0 ± 0.4 at 660 nm and 6.0 ± 0.4 at 675 nm. In the Fe—CAS—CP system, the maximum absorbance is obtained at 635 nm in the pH range 2.9 ± 0.2.

The absorbance of the Fe—CAS—CTA and Fe—CAS—CP complexes is considerably affected by the concentration of chrome azurol S. Depending on the concentration of the chromophoric reagent the complexes obtained show various maximum wavelengths. The variations in the absorption curves for the Fe—CAS—CTA and Fe—CAS—CP systems with changes in the concentration of chrome azurol S are shown in Fig. 3. At a chrome azurol S

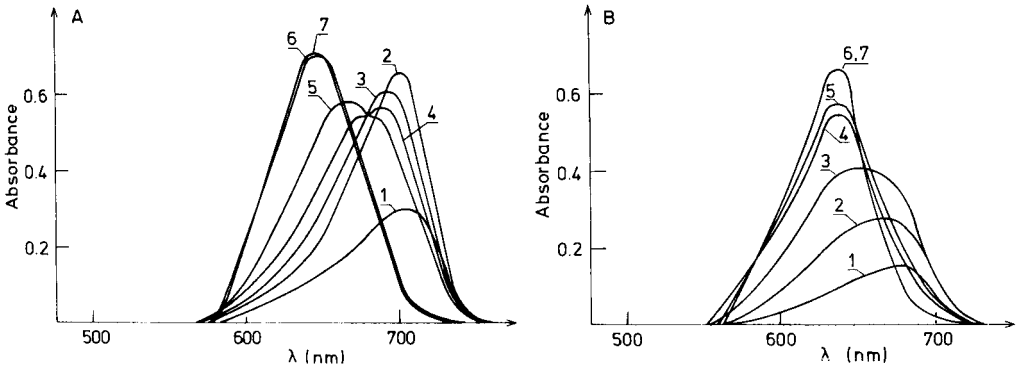

Fig. 3. Absorption spectra in (A) the Fe—CAS—CTA system and (B) the Fe—CAS—CP system, for various concentrations of CAS (5×10^{-6} M Fe^{3+}, 4×10^{-4} M CTA, pH 4.3 (for A) and pH 3.0 (for B), against reagent blank). CAS concentration (M) (1) 5×10^{-6}; (2) 1×10^{-5}; (3) 2×10^{-5}; (4) 4×10^{-5}; (5) 5×10^{-5}; (6) 1×10^{-4}; (7) 1.5×10^{-4}.

molarity twice the iron molarity the Fe—CAS—CTA and Fe—CAS—CP complexes have their maximum wavelengths at ca. 700 nm and 680 nm, respectively. As the concentration of chrome azurol S increases, there is a hypsochromic shift. In both systems (CTA and CP), maximum absorbance of the ternary complexes is obtained when the molar ratio of chrome azurol S to iron is not less than 20:1 at 645 nm and 635 nm, respectively, for CTA and CP.

The variations in the absorption spectra in the Fe—CAS—CTA system with change in CTA concentration are shown in Fig. 4. In the case of the CP complex, the changes in the absorption spectra are similar. The maximum absorbance of the Fe—CAS—CTA and Fe—CAS—CP complexes is obtained when the molar ratio of CTA or CP to iron is in the range 60—100:1. When the molar ratio of CTA or CP to iron is 6—30:1, precipitation occurs, even in the blanks. At high CTA and CP concentrations (above 100-fold excess), a decrease in the absorbance is observed.

In work devoted to similar ternary systems [1] the complexes have been reported to contain relatively low numbers of CTA or CP ions (e.g., 2, 4, 6) per metal atom. From Fig. 4, however, it appears that the Fe—CAS—CTA complex of analytical importance, i.e. the complex which exhibits maximum and stable absorbance, must contain in its structure a considerably higher number of CTA molecules than the complexes which exhibit significantly lower absorbance, at slightly different maximum wavelengths, formed in the systems containing low concentrations of cationic surfactants. According to the suggestions of Savvin et al. [10] and Martynov et al. [11], the ternary complexes formed at suitable CTA or CP concentrations do not contain single CTA or CP ions but their micelles. The decrease in absorbance at very high concentrations of CTA or CP can be ascribed to the fact that the chelating groups of the chromophoric reagents are partially blocked by the quaternary base.

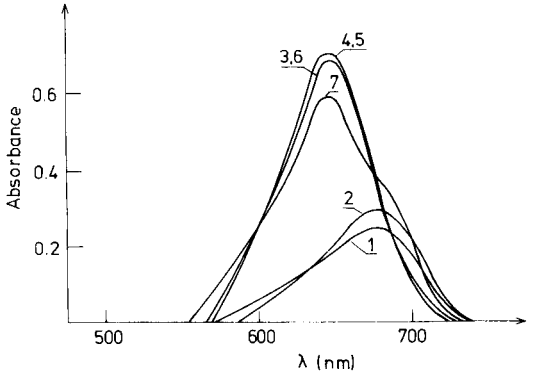

Fig. 4. Absorption spectra in the Fe—CAS—CTA system for various CTA concentrations (5×10^{-6} M Fe^{3+}, 1×10^{-4} M CAS, pH 4.3, against reagent blank). CTA concentration (M): (1) 1×10^{-5}; (2) 2×10^{-5}; (3) 2×10^{-4}; (4) 3×10^{-4}; (5) 4×10^{-4}; (6) 5×10^{-4}; (7) 7.5×10^{-4}.

The maximum absorbance of the Fe—CAS—CTA and Fe—CAS—CP complexes at pH 4.3 is obtained after 15 min; it then remains stable for 24 h, at least. At pH 6, the time necessary to attain maximum absorbance is about 2 h. Attainment of equilibrium can be accelerated by heating the complexes (40—80°C). The absorbance is constant for ionic strengths of 0.1—1.0 (adjusted with sodium chloride). In order to maintain constant pH in the system Fe—CAS—CTA acetate buffer is used. In the case of the Fe—CAS—CP solutions, which are adjusted to pH ca. 3 with ammonia solution, addition of acetate buffer is not necessary. Acetate ions have no effect on the absorbance of Fe—CAS—CP complex.

Numerous metals (Be, Al, Ga, In, Sc, rare earths, Cr(III), Zr, U(VI), Th, V) which yield coloured compounds with chrome azurol S interfere with the determination of iron(III) with chrome azurol S and CTA or CP. EDTA, oxalate, tartrate and citrate also interfere. Thiocyanate does not interfere at low concentrations but at higher concentrations precipitation takes place.

Under the conditions of the recommended procedure, iron(II) does not react with CAS and CTA (CP) to form coloured compounds. Nevertheless, the colour reaction proceeds slowly as a result of oxidation of Fe(II) to Fe(III). This happens even in the presence of hydroxylamine or pyrosulphite, but not in the presence of ascorbic acid, iron remaining in the lower oxidation state in the latter case.

The methods for the determination of iron with CAS and CTA (or CP) become highly selective if the determination of iron is preceded by extractive separation of iron as its thiocyanate complex [12].

The molar ratio of iron to chrome azurol S in the ternary complexes with CTA or CP, as determined by the method of isomolar series, is 1:2. It can be supposed that in the presence of a large excess of the chromophoric reagent (see Fig. 3) complexes containing more than two CAS per iron atom are also formed.

The coloured solution, obtained as described in the recommended procedure, was shaken with organic solvents (chloroform, 1,2-dichloroethane, methyl isobutyl ketone (MIBK), and butyl or amyl alcohol. The ion associate of chrome azurol S and CTA (CP) slowly passes into the organic phase until the aqueous solution becomes decolorized. This indicates that after the excess of chrome azurol S has been extracted (as an ion associate with CTA or CP) the ternary complex decomposes. Benzene and carbon tetrachloride do not extract the associate of CAS with CTA (CP).

The application of CTA or CP makes it possible to increase considerably the sensitivity of the spectrophotometric determinations of iron with chrome azurol S, as has been shown previously for CTA [6, 7]. The absorption spectra of chrome azurol S, of its binary complex with iron(III) ions and of the ternary complexes Fe—CAS—CTA and Fe—CAS—CP are shown in Fig. 5. A very large increase of absorbance takes place, but the bathochromic effect characteristic of similar ternary complexes with other metals [3—5] does not occur.

The standard curve for the system Fe—CAS—CTA shows a negative

deviation from Beer's law. The mean molar absorptivity (ϵ) amounts to 1.35×10^5 l mol^{-1} cm^{-1} at 645 nm (specific absorptivity $a = \epsilon$/at. wt $\times$ 1000 = 2.42). The standard curve for the system Fe—CAS—CP obeys Beer's law in the concentration range 0.1—0.4 μg ml^{-1}. The molar absorptivity amounts to 1.28×10^5 l mol^{-1} cm^{-1} at 635 nm while in the binary Fe—CAS system under the optimum conditions (pH 6.4) it amounts to only 4.3×10^4 at 650 nm.

Ternary system: iron(III)—ECR—CTA (CP)

In the pH range 2—10, ternary complexes of iron(III) with eriochrome cyanine R and CTA (or CP) are formed. The wavelength of maximum absorbance of these complexes lies at 610 nm for solutions of pH 3—6. At higher pH values λ_{max} is shifted towards longer wavelengths (Fig. 6). The pH values optimal for the formation of the Fe—ECR—CTA and the Fe—ECR—CP complexes are 4.5 ± 0.5 and 3.5 ± 0.6, respectively. The absorbance and the position of λ_{max} of the complexes Fe—ECR—CTA and Fe—ECR—CP depend on the concentration of eriochrome cyanine R. This dependence in the Fe—ECR—CTA system is shown in Fig. 7. In the case of cetylpyridinium ions, the changes in the absorption spectra are similar. Maximum and stable absorbance (at 610 nm) is obtained when a 20-fold molar amount of eriochrome cyanine R with respect to iron is present.

In order to obtain maximum absorbance of the Fe—ECR—CTA and Fe—ECR—CP complexes, at least a 50-fold molar excess of CTA or CP ions is necessary. The development of the absorption spectra in the Fe—ECR—

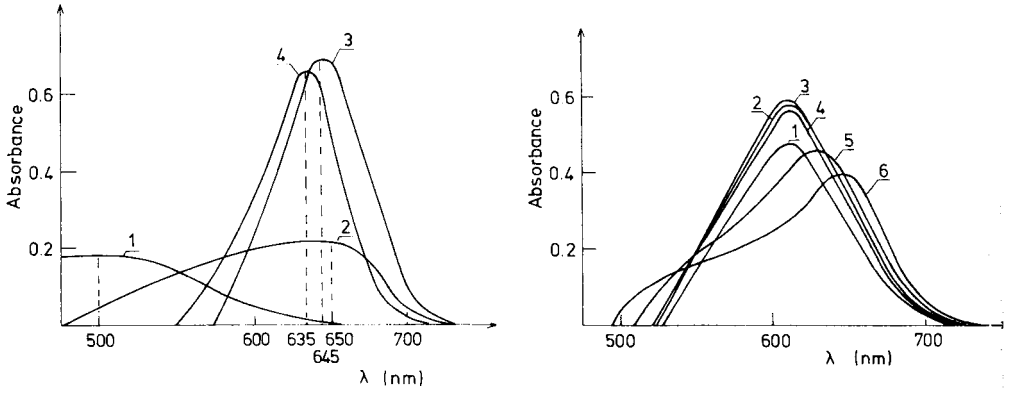

Fig. 5. Absorption spectra of: (1) CAS (1×10^{-5} M CAS, pH 4.3) against water; (2) Fe—CAS complex (5×10^{-6} M Fe^{3+}, 1×10^{-4} M CAS, pH 6.4) against reagent blank; (3) Fe—CAS—CTA complex (5×10^{-6} M Fe^{3+}, 1×10^{-4} M CAS, 4×10^{-4} M. CTA, pH 4.3) against reagent blank; (4) Fe—CAS—CP complex (5×10^{-6} M Fe^{3+}, 1×10^{-4} M CAS, 4×10^{-4} M CP, pH 3.0) against reagent blank.

Fig. 6. Dependence of the absorption spectra on pH in the Fe—ECR—CTA system (5×10^{-6} M Fe^{3+}, 5×10^{-5} M ECR, 4×10^{-4} M CTA against reagent blank). pH values: (1) 3.0; (2) 3.9; (3) 5.1; (4) 6.0; (5) 6.9; (6) 8.2.

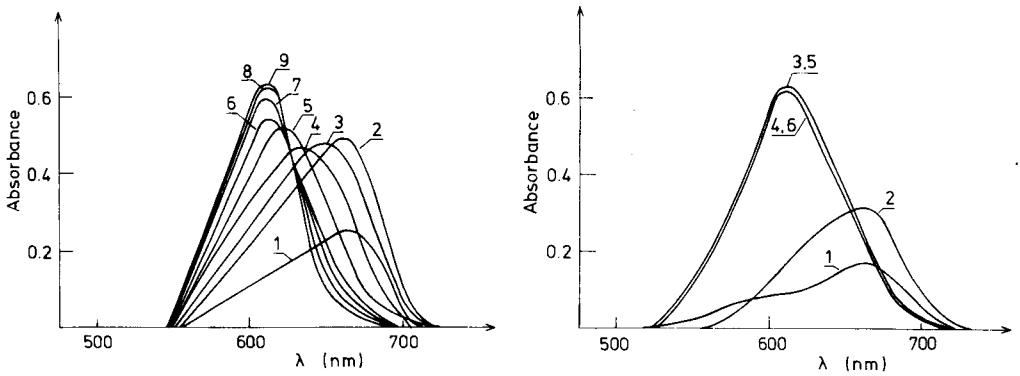

Fig. 7. Absorption spectra in the Fe—ECR—CTA system for various concentrations of ECR (5×10^{-6} M Fe^{3+}, 4×10^{-4} M CTA, pH 4.3, against reagent blank). ECR concentration (M): (1) 5×10^{-6}; (2) 1×10^{-5}; (3) 1.5×10^{-5}; (4) 2×10^{-5}; (5) 3×10^{-5}; (6) 4×10^{-5}; (7) 5×10^{-5}; (8) 1×10^{-4}; (9) 1.5×10^{-4}.

Fig. 8. Absorption spectra in the Fe—ECR—CTA system for various CTA concentrations (5×10^{-6} M Fe^{3+}, 1×10^{-4} M ECR, pH 4.3, against reagent blank). CTA concentration (M): (1) 1×10^{-5}; (2) 2×10^{-5}; (3) 2.5×10^{-4}; (4) 5×10^{-4}; (5) 1×10^{-3}; (6) 1.5×10^{-3}.

CTA system with change in CTA concentration is shown in Fig. 8. The position of the maximum wavelength of the ternary complexes formed depends also on the concentration of CTA ions. At a 10—40-fold excess of CTA (or CP), there is turbidity of the solution followed by precipitation, as in the case of the system with chrome azurol S.

Maximum absorbance of the complexes Fe—ECR—CTA and Fe—ECR—CP is obtained immediately after mixing the reagents; the absorbance is stable for at least 3 h. The pH is adjusted by means of acetate buffer. The effects of foreign opms on the colour reaction of ECR and CTA (or CP) are similar to those in the chrome azurol S systems. Iron(II) again behaves similarly. Ionic strength again does not influence the absorbance.

The molar ratio of eriochrome cyanine R in the ternary system, as determined by the method of isomolar series, is 1:2. It can be supposed that, in the presence of a high excess of the chromophoric reagent, complexes are formed that contain more ECR molecules per iron atom.

Extraction studies of the Fe—ECR—CTA (CP) system gave results similar to those described for the analogous chrome azurol S system. In the case of eriochrome cyanine R, the coloured ion associate passes into the organic phase more rapidly.

It can be seen from the absorption spectra shown in Fig. 9 that there is a large increase in sensitivity of the method based on the ternary system ($\epsilon = 1.27 \times 10^5$ l mol^{-1} cm^{-1}) compared to the binary system ($\epsilon = 3.3 \times 10^4$). The course of curve 3 (Fig. 9) is identical for CTA and CP ions. In contrast to the system with chrome azurol S, a bathochromic effect is

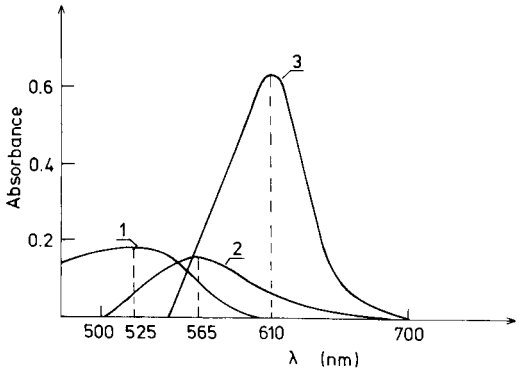

Fig. 9. Absorption spectra of: (1) ECR (1×10^{-5} M ECR, pH 4.3) against water; (2) Fe—ECR complex (5×10^{-6} M Fe^{3+}, 1×10^{-4} M ECR, pH 6.4) against reagent blank; (3) Fe—ECR—CTA complex (5×10^{-6} M Fe^{3+}, 1×10^{-4} M ECR, 4×10^{-4} M CTA, pH 4.3) against reagent blank.

observed. The system based on the ternary complex obeys Beer's law up to a concentration of 0.3 μg Fe ml^{-1}.

Determination of iron in analytical-grade sodium hydroxide

The developed method, based on the Fe—ECR—CTA ternary complex, was applied to the determination of traces of iron in sodium hydroxide (p.a.; POCh, Gliwice). Attempts were made to separate traces of iron from the sample by precipitation as $Fe(OH)_3$ on filter paper pulp, but the separation was not quantitative. Poor separation of iron was achieved even when some iron was added to the sample prior to separation.

Satisfactory results were obtained in the following way. The sample was dissolved in water in a quartz vessel. The solution was acidified with hydrochloric acid (high-purity) and heated. After the solution had been cooled and adjusted to pH 1 with ammonia, ammonium thiocyanate was added and iron was extracted with two portions of MIBK. The solvent was then evaporated,

TABLE 1

Determination of traces of iron in analytical-grade sodium hydroxide

Sample weight (g)	Iron			R.s.d. (%)	Recovery (%)
	Added (μg)	Found			
		(μg)	(%)		
1.0	—	5.5[a]	5.5×10^{-4}	6.4	
0.5	—	2.9[b]	5.8×10^{-4}	9.5	
0.5	3.0	5.9[b]		4.7	102

[a]Mean of 4 determinations. [b]Mean of 6 determinations.

the residue mineralized with concentrated sulphuric and nitric acids, and iron determined by the recommended procedure for the ECR system. The results of the determination of iron in samples of the sodium hydroxide examined, and in samples to which known amounts of iron had been added, are shown in Table 1. Quantitative recovery of iron indicates the good accuracy of the method.

REFERENCES

1 V. N. Tikhonov, Zh. Anal. Khim., 32 (1977) 1435.
2 Z. Marczenko, Crit. Rev. Anal. Chem., 9 (1980), in press.
3 Z. Marczenko and H. Kałowska, Chem. Anal. (Warsaw), 22 (1977) 935; Microchem. J., 23 (1978) 71.
4 Z. Marczenko and H. Kałowska, Mikrochim. Acta, II (1979) 507.
5 Z. Marczenko and H. Kałowska, Chem. Anal. (Warsaw), 25 (1980) 555.
6 Y. Shijo and T. Takeuchi, Bunseki Kagaku, 17 (1968) 1519.
7 Y. Nakamura, H. Nagai, D. Kubota and S. Himeno, Bunseki Kagaku, 22 (1973) 1156.
8 Y. Shijo and T. Takeuchi, Bunseki Kagaku, 20 (1971) 980.
9 R. K. Chernova, Zh. Anal. Khim., 32 (1977) 1477.
10 S. B. Savvin, R. K. Chernova, V. V. Belousova, L. K. Sukhova and S. N. Shtykov, Zh. Anal. Khim., 33 (1978) 1473.
11 A. P. Martynov, V. P. Novak and B. E. Reznik, Ukr. Khim. Zh., 44 (1978) 203.
12 Z. Marczenko, Spectrophotometric Determination of Elements, Ellis Horwood, Chichester, 1976.

Analytica Chimica Acta, 123 (1981) 289—296

EXTRACTION—SPECTROPHOTOMETRIC DETERMINATION OF TRACES OF CADMIUM WITH 4-(2-PYRIDYLAZO)RESORCINOL AND A LONG-CHAIN QUATERNARY AMMONIUM SALT

D. NONOVA* and S. PAVLOVA

Department of Analytical Chemistry, University of Sofia, 1126 Sofia (Bulgaria)

(Received 2nd June 1980)

SUMMARY

A simple and highly sensitive extraction—spectrophotometric determination of cadmium is described. The ion-associate formed between the cadmium—PAR anionic chelate and cetyldimethylbenzylammonium chloride (CDBA) is extracted with chloroform at pH 10. The absorption maximum of the extracted species occurs at 505 nm, the molar absorptivity being $(9.82 \pm 0.30) \times 10^4$ l mol^{-1} cm^{-1}. The optimal concentration range for measurements is 0.2—1.0 μg Cd ml^{-1}; Beer's law is obeyed. The composition of the ion-associate is estimated to be $CdPAR_2 \cdot 2CDBA$. The conditional extraction constant is $\log K'_{ex} \approx 8$. The stability constant of the cadmium—PAR chelate in aqueous solution is $\log \beta_2 = 17.5 \pm 0.3$. Extraction with N-benzoyl-N-phenylhydroxylamine is used to avoid several interferences. Moderate amounts of zinc are masked with sodium hydroxide.

The determination of trace amounts of cadmium has recently received considerable attention owing to the toxicity of the element and the problems of environmental pollution. At present, the most commonly used spectrophotometric method for cadmium determination is that with dithizone. Drapkina et al. [1] suggested 6-bromobenzthiazol-(2-azo-1′)-2′-naphthol as a sensitive and selective reagent for cadmium [ϵ (600 nm) = $(5.76 \pm 0.06) \times 10^4$], extracting the cadmium complex with xylene at pH 13.5. Various masking agents were necessary to eliminate interferences in the analysis of some high-purity salts. Recently, Shibata et al. [2] proposed 2-[2-(5-bromopyridyl)azo]-5-dimethylaminophenol as the most sensitive reagent for cadmium ($\epsilon = 1.41 \times 10^5$); this method copes with interferences by means of a preliminary extraction of cadmium with dithizone in strongly alkaline solution, but very little zinc could be tolerated. A selective isolation of cadmium by extraction from fission products and after neutron activation has been suggested [3].

Analytical applications of 4-(2-pyridylazo)resorcinol (PAR) chelate—quaternary ammonium cation systems have been extensively investigated because their sensitivity can be readily increased by simple extraction [4—11]. In the present paper, an analogous study of the extraction of the cadmium—PAR complex is described.

EXPERIMENTAL

Apparatus and reagents

A Unicam model SP1800 double-beam ultraviolet spectrophotometer equipped with 10-mm stoppered quartz cells, a SPECORD UV-VIS recording spectrophotometer, and a precise pH-meter LPU-01 were used.

For the standard cadmium solutions, a cadmium perchlorate stock solution containing 1000 μg Cd ml^{-1} was diluted to prepare a working solution containing 1 μg Cd ml^{-1}. 4-(2-Pyridylazo)resorcinol was purified by recrystallization from ethanol; its purity was checked by spectrophotometric titration with copper(II) [12]. Diverse metal ion solutions (10^{-2} M) were prepared from analytical reagent-grade substances and standardized complexim etrically [13].

A nominal 10^{-2} M solution of cetyldimethylbenzylammonium chloride (CDBA) was standardized by Volhard's method: 15.00 ml of CDBA solution was mixed with 5.00 ml of 0.0990 M standard silver nitrate solution and the excess of silver ion was back-titrated with ammonium thiocyanate solution using iron(III) ammonium sulphate as indicator. From the mean of three titrations, the actual concentration of CDBA was 0.954×10^{-2} M. More dilute solutions were prepared as required.

Borate buffer solutions (0.05 M) were prepared [14].

The chloroform and all other chemicals were of analytical reagent grade. The water was twice-distilled.

Preliminary studies in aqueous solutions

Several authors have studied the reaction between cadmium and PAR in aqueous solution [15, 16]. Kitano and Ueda [17] have discussed the analytical aspects of this reaction and found the composition of the complex in alkaline medium to be Cd:PAR = 1:2. Some contradictions in the literature data made it necessary to conduct a detailed spectrophotometric study in aqueous solutions.

The absorption spectra (Fig. 1) and the absorbance—pH curve (Fig. 2) show considerable changes over the pH range 6—10.5 as a result of the complex formation. The single isosbestic point (Fig. 1) and the S-shaped curve obtained in this study confirm the formation of only one kind of absorbing species in alkaline solutions. Curves 1 and 2 (Fig. 1) are presumably due to the partial precipitation of the neutral species $Cd(HL)_2$ formed below pH 6. In this pH range, PAR exists as the ionic form HL^-. The steep part of the S-shaped curve over the pH range 8.14—9.76 was used for calculations. The number of protons, n, released during the complexation in equimolar solution was determined by using the equation [10] :$\log \beta_2' = \log K_{eq} + n$ pH. The conditional stability constants β_2' were calculated and plotted against the corresponding pH values. The plot gave a straight line with a slope $n = 1.9$, i.e. two protons split off; thus in the pH range studied the reaction is $Cd^{2+} + 2HL^- \rightleftharpoons CdL_2^{2-} + 2H^+$.

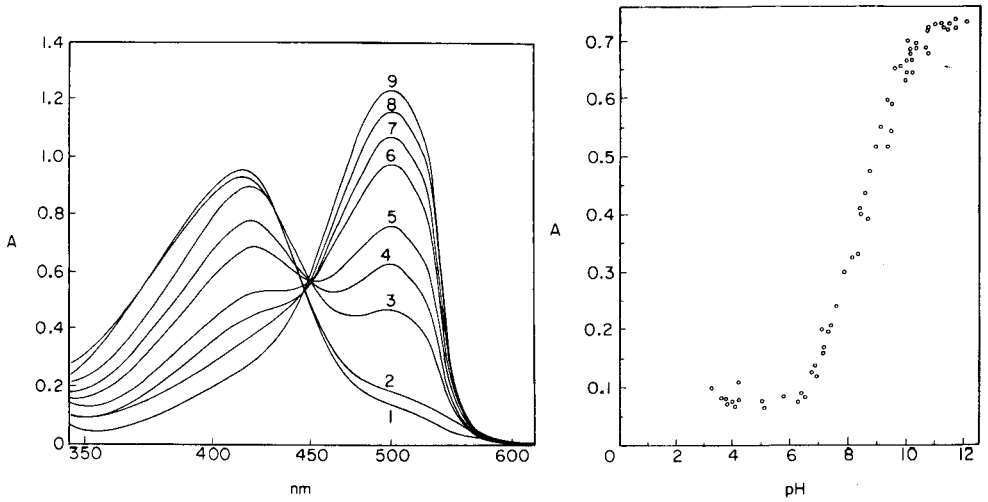

Fig. 1. Absorption spectra of the cadmium—PAR complex at various pH values. Solutions contained 0.83×10^{-5} M Cd^{2+} and 1.66×10^{-5} M PAR (μ = 0.1, $NaNO_3$); 20-mm cells; vs. water. pH values: (1) 5.85; (2) 5.89; (3) 7.70; (4) 7.98; (5) 8.12; (6) 8.66; (7) 9.10; (8) 9.80; (9) 10.83.

Fig. 2. Absorbance—pH dependence of the cadmium—PAR complex for solutions containing 0.80×10^{-5} M Cd^{2+} and 1.58×10^{-5} M PAR (μ = 0.1, 495 nm, vs. water).

These results indicate that the cadmium—PAR complex bears two negative charges in aqueous solution; this was further confirmed by determining the composition of the ion-associate extracted in the presence of the quaternary ammonium salt (see below). The stability constant of the cadmium—PAR complex was estimated to be $\log \beta_2' = 17.5 \pm 0.3$. The molar absorptivity calculated from 10 experiments was $(9.08 \pm 0.08) \times 10^4$ l mol^{-1} cm^{-1} at pH 10.5—12.0 and 495 nm (compared to 8.4×10^4 recorded earlier [17]).

Extraction—spectrophotometric procedure

Pipette into a 100-ml separatory funnel an aliquot of the sample solution containing up to 5 μg of cadmium. Add 5 ml of borate buffer solution pH 10, 1.0 ml of aqueous 4×10^{-4} M PAR solution (0.01%), 2 ml of 4×10^{-4} M CDBA and dilute with water to 20 ml. Add an exactly measured 5.00-ml portion of chloroform and shake vigorously for about 1 min. Allow the layers to separate and run the reddish-purple organic extract into a 10-mm cell supplied with a stopper. If necessary, add a small amount of anhydrous sodium sulphate crystals to remove water droplets. Measure the absorbance at 505 nm vs. a reagent blank as reference solution; it should be noted that the excess of PAR is also extracted.

Procedure for preliminary separation of interferences

Pipette a sample aliquot containing up to 5 μg of cadmium and the interfering metal ions into a 100-ml separatory funnel. Add 5 ml of borate buffer solution pH 9.2 and extract with 5 ml of 0.01 M N-benzoyl-N-phenylhydroxylamine solution in chloroform for 30 s. Allow the layers to separate and discard the organic extract. Complete the determination of cadmium in the aqueous phase as described above.

RESULTS AND DISCUSSION

Absorption spectra

Absorption spectra of the extracted species at various pH are similar to those in Fig. 1. In order to prove the favourable influence of the quaternary ammonium salt on the optical characteristics of the system, the absorption spectra of cadmium—PAR complex and PAR in water as well as their ion-associates in chloroform were recorded. As shown in Fig. 3, extraction with the quaternary salt produces a bathochromic shift for the metal complex of 10 nm and a hypsochromic shift of 15 nm for PAR. The maximum wavelengths are 505 nm for the Cd—PAR—CDBA ion-associate and 400 nm for the PAR—CDBA ion-associate, compared with 495 nm and 415 nm, respectively, for the complex and free PAR in water. The contrast factor in the spectrophotometric reaction is thus improved.

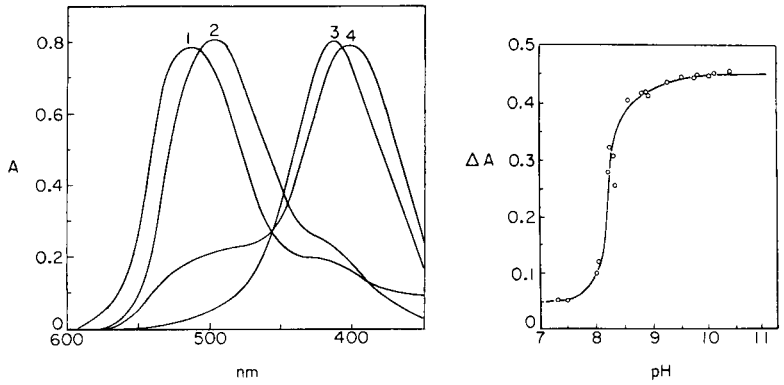

Fig. 3. Absorption spectra of the cadmium—PAR complex and free PAR in water and chloroform respectively. (1) Cd—PAR—CDBA in $CHCl_3$, 8.1×10^{-6} M; (2) Cd—PAR in water, 8.9×10^{-6} M; (3) PAR in water, 1.7×10^{-5} M; (4) PAR—CDBA in $CHCl_3$, 1.1×10^{-5} M.

Fig. 4. Absorbance—pH dependence of the Cd—PAR—CDBA ion-associate in the pH range 7.32—10.36. Solutions contained 5.36×10^{-6} M Cd^{2+}, 4.8×10^{-5} M PAR, 4×10^{-4} M CDBA; 505 nm; reagent blank.

Effect of pH and reagent concentrations

The effect of pH on the extraction of cadmium—PAR complex with CDBA and chloroform can be seen from Fig. 4. The absorbance depends greatly on pH, but is constant above pH 9.5 (against pH 10.5 in aqueous solution).

The effect of varying the PAR concentration on the absorbance of the ion-associate at 505 nm was examined. The absorbance of the organic phase increased rapidly on addition of the reagent up to a Cd:PAR mole ratio of 1:2; above this value, the colour intensity depended only slightly on the reagent concentration. These data confirmed that the composition of the cadmium—PAR complex in the organic phase is 1:2, i.e., the same as in aqueous solutions. In analytical applications 1 ml of 4×10^{-4} M PAR was used.

The extraction depended strongly on the excess of cationic surfactant, which affected the rate at which the two phases separated and remained clear. A very large excess of CDBA produced a stable emulsion on shaking so that the phases did not separate. Complete extraction and satisfactory phase separation was possible with 2-ml portions of 4×10^{-4}—10^{-3} M CDBA solutions.

Stability, Beer's law, sensitivity and precision

The effect of time on the colour formation was examined by the recommended procedure for 2.2 μg Cd ml^{-1} solutions. The intense colour appeared immediately after shaking and attained a constant and maximum value with no change in the absorbance during 15—20 min. Thereafter the absorbance decreased very slowly.

Beer's law was found to be valid up to an absorbance of 0.859; this corresponds to a range of 0.2—1.0 μg Cd ml^{-1}. The conditional molar absorptivity was found to be $(9.82 \pm 0.30) \times 10^4$ l mol^{-1} cm^{-1}, evaluated from seven results for the extraction procedure. The Sandell sensitivity was 0.0011 μg Cd cm^{-2} at 505 nm, which classifies the colour reaction studied as one of the most sensitive available for cadmium. The method compares favourably with the dithizone method ($\epsilon = 8.8 \times 10^4$ at 520 nm [18]).

Composition of the Cd—PAR—CDBA complex

By the molar ratio and continuous variation methods, the composition of the extracted species was determined to be Cd:PAR:CDBA = 1:2:2. The Cd:PAR and Cd:CDBA molar ratios in the ternary system were also examined by the equilibrium-shift method. The two plots had slopes of about 2, i.e., the ratio of Cd:PAR:CDBA is 1:2:2. The plots clearly indicated that the anionic cadmium—PAR chelate couples with two molecules of CDBA, thus neutralizing the two negative charges. These results allow the conclusion that the extraction proceeds by an ion-association mechanism.

$$CdL_2^{2-} + 2Q^+ \rightleftharpoons (CdL_2^{2-} \cdot 2Q^+)_{aq} \rightleftharpoons (CdL_2^{2-} \cdot 2Q^+)_{org}$$

TABLE 1

Conditional extraction constants for the cadmium—PAR—CDBA system

Reagent added	Constant concn. (M)	Slope	Intercept on the abscissa	log K'_{ex}
CDBA	4.8×10^{-5} (PAR)	1.8	−4.24	7.6
PAR	0.8×10^{-4} (CDBA)	1.8	−4.94	8.9

where Q^+ denotes CDBA. The intercepts of the figures plotted were used to calculate the order of the conditional extraction constant given in Table 1. The high value of K'_{ex} confirms the quantitative extraction of the ion-associate.

Interference studies

Synthetic mixtures were prepared with some cations commonly found with cadmium. The interference of the foreign ions was eliminated by extraction of their chelates with N-benzoyl-N-phenylhydroxylamine (BPHA) into chloroform, making use of the slight extractability of cadmium under these conditions [19]. Depending on the nature of the metal ion, the extraction can be carried out from an acidic or alkaline solution. In this study, extraction from alkaline media was examined.

The behaviour of cadmium itself in the recommended BPHA extraction (see Experimental) was studied. The results showed that BPHA had little effect on the cadmium determination. When standards containing 5 μg of cadmium were tested, the mean absorbance measured was 0.880 without the BPHA extraction, and 0.861 after the BPHA extraction. Thus, with appropriate calibration, the preliminary BPHA separation could be used to avoid several interferences.

The results in Table 2 show that BPHA was successful in eliminating the interferences from zinc and copper when present in ratios (Cd:Me) of 1:3; the tolerable ratios were 1:2 for cobalt and 1:500 for tin, whereas aluminium, manganese, nickel and bismuth still interfered very seriously (iron is extracted in acidic medium [19]). This method of eliminating interferences has the advantage that cadmium remains in the aqueous solution. In this respect, it compares very favourably with the troublesome dithizone method of cadmium separation. Moreover, the metal—BPHA chelates formed are not intensely coloured.

Effect of zinc. As electronic homologues, zinc and cadmium are usually present together at various ratios in samples. Since zinc interferes with the determination of cadmium by the proposed method, its effect was carefully studied. Preliminary investigations were carried out with reagents which might be useful for masking zinc when present in more than 3-fold amounts. Sodium hydroxide proved to be the best masking agent for zinc; hence this

TABLE 2

Effect of foreign ions on the determination of 5 μg of cadmium after BPHA extraction ($V_{aq}/V_{org} = 6$)[a]

Ion	Amount added (μg)	Cd found (μg)	Error (μg)	Ion	Amount added (μg)	Cd found (μg)	Error (μg)
Zn(II)	6.5	5.0	±0.0	Mn(II)	5.5	7.20	+2.20
	13	5.16	+0.16	Ni(II)	5.9	6.10	+1.10
	16	5.35	+0.35	Bi(III)	5	6.22	+1.22
Al(III)	1	5.37	+0.37	Cu(II)	5	5.06	+0.06
	5	8.89	+3.89		10	5.20	+0.20
Sn(IV)	5	4.98	−0.02		15	5.17	+0.17
	10	5.0	±0.0		20	5.52	+0.52
	20	5.03	+0.03	Co(II)	5.9	5.0	±0.0
	100	5.06	+0.06		10	5.11	+0.11
	500	5.11	+0.11		15	6.10	+1.10
	1000	5.23	+0.23				

[a]A change of more than ±0.020 units in the absorbance was regarded as indicating interference.

TABLE 3

Effect of zinc on the determination of cadmium (5 μg) using 1 M sodium hydroxide as masking agent ($V_{aq}/V_{org} = 4$)

1 M NaOH added (ml)	1	3	4	5	4	4	4	4	4	4
Zn added (μg)	6.5	6.5	6.5	6.5	15	30	50	460	800	1000
Abs.[a]	0.880	0.720	0.675	0.680	0.670	0.695	0.695	0.675	0.650	0.655

[a]Absorbance at 505 nm. Correct absorbance for 5 μg Cd under these conditions was 0.680.

reagent was studied in detail. The results obtained (Table 3) showed that the addition of at least 4 ml of 1 M sodium hydroxide solution to the aqueous phase is necessary for masking up to 200-fold amounts of zinc (0.2 M alkaline solution). Because of the formation of cadmium—hydroxide complexes under these conditions, the sensitivity of the reaction is, however, lowered, the molar absorptivity then being 7.5×10^4 l mol^{-1} cm^{-1}.

The most difficult problem with the zinc interference arises when zinc is the basic component of the sample to be analyzed. Thus when zinc powder (p.a. certified, Merck) containing 0.05% of cadmium was examined, a preliminary extraction of cadmium with dithizone was found to be essential. Yet the PAR—CDBA method compares favourably with other methods in

most cases because it does not need a preliminary extraction with dithizone except for metallic zinc samples. Further work is in progress to extend the scope of the applicability of the method.

REFERENCES

1 D. A. Drapkina, V. G. Brudz, K. A. Smirnova and N. I. Doroshina, Zh. Anal. Khim., 17 (1962) 940.
2 S. Shibata, E. Kamata and R. Nakashima, Anal. Chim. Acta, 82 (1976) 169.
3 S. Bajo and A. Wyttenbach, Anal. Chem., 49 (1977) 158.
4 T. Yotsuyanagi, Y. Takeda, R. Yamashita and K. Aomura, Anal. Chim. Acta, 67 (1973) 297.
5 T. Yotsuyanagi, R. Yamashita and K. Aomura, Fresenius Z. Anal. Chem., 253 (1971) 301.
6 M. Nishimura, K. Matsunaga, T. Kudo and F. Obara, Anal. Chim. Acta, 65 (1973) 466.
7 T. Yotsuyanagi, H. Hoshino and K. Aomura, Anal. Chim. Acta, 71 (1974) 349.
8 H. Hoshino, T. Yotsuyanagi and K. Aomura, Anal. Chim. Acta, 83 (1976) 317.
9 T. Yotsuyanagi, R. Yamashita, H. Hoshino and K. Aomura, Anal. Chim. Acta, 82 (1976) 431.
10 D. Nonova, V. Nenov and N. Lihareva, Talanta, 23 (1976) 679.
11 E. Papp and J. Inczédy, Talanta, 27 (1980) 49.
12 T. Iwamoto, Bunseki Kagaku, 10 (1961) 189.
13 G. Schwarzenbach and H. Flaschka, Complexiметric Titrations, 2nd edn., Methuen, London, 1969.
14 I. M. Kolthoff, Acid—Base Indicators, MacMillan, New York, 1937.
15 M. Hniličková and L. Sommer, Collect. Czech. Chem. Commun., 26 (1961) 2189.
16 T. Iwamoto, Bull. Chem. Soc. Jpn., 34 (1961) 605.
17 M. Kitano and J. Ueda, Nippon Kagaku Zasshi, 91 (1970) 760.
18 G. Charlot, Chimie Analytique Quantitative, II, Masson et Cie, Paris, 1974, p. 365.
19 A. K. De, S. M. Khopkar and R. A. Chalmers, Solvent Extraction of Metals, Van Nostrand-Reinhold, London, 1970.

Analytica Chimica Acta, 123 (1981) 297--302

DETERMINATION OF BISMUTH OXIDE IN AND ON HIGH-PURITY BISMUTH

KEN MATSUMOTO

Department of Chemistry, Faculty of Science, Kanazawa University, 1-1 Marunouchi, Kanazawa, Ishikawa 920 (Japan)

(Received 7th July 1980)

SUMMARY

Bismuth is dissolved in mercury on shaking with ammonium nitrate solution in a nitrogen atmosphere; bismuth oxide is insoluble and so can be separated by flotation and dissolved in nitric acid for spectrophotometric determination as tetraiodobismuthate(III). The method is applied to various bismuth samples containing about 0.01% Bi_2O_3, the relative standard deviation being 7—11%.

The quality of bismuth is dependent on the levels of impurities found in the finished product. Among possible contaminants, oxide is most likely to affect the physical and mechanical properties of bismuth and is also most likely to be present as an impurity from trace oxides introduced during the casting and storage processes. The determination of bismuth oxide in pure bismuth is a difficult analytical problem, and until now, no solution has been reported. Several techniques for determination of oxygen in bismuth such as vacuum fusion [1, 2], and photon activation [3] have been proposed, but do not give direct results for bismuth oxide; moreover, these methods need much skill and expensive apparatus, and are often tedious. Therefore, a rapid, simple and direct method involving ordinary apparatus and reagents is required. The procedure described in this paper is the outcome of several years of practical experience with high-purity metals. It is based on the fact that bismuth metal is soluble in mercury, while bismuth oxide is insoluble in both bismuth amalgam and in pure mercury. The insoluble bismuth oxide is separated by flotation, and is determined spectrophotometrically. The method is similar in principle to those described recently for cadmium oxide in cadmium [4] and lead oxide in lead [5].

EXPERIMENTAL

Chemicals

A 1 M ammonium nitrate solution was prepared by dissolving 80 g of ammonium nitrate (extra pure) in water and diluting to 1 l. Mercury (guaranteed grade) was used after purification as follows. Mercury was passed through

an Ostwald mercury cleaning set filled with 0.1 M ammonium iron(III) sulfate solution and washed three times by shaking with water. It was further purified by washing with deoxygenated ammonium nitrate solution in a nitrogen atmosphere just before use.

Bismuth oxide (Bi_2O_3) was a powder of 99.9% purity (Kishida Chemical Reagents Co. Ltd.). The following bismuth samples were used: bismuth granules (99.999% and 99.99%, both from Kishida Chemical Co. Ltd.) and bismuth pellets (99.9%; Mitsuwa Chemical Reagents Ltd.).

Nitrogen (99.9%) was used after deoxygenation by passage through an alkaline pyrogallol solution, followed by a vanadium(II) solution kept over zinc amalgam. All other chemicals (analytical-reagent grade) were used as received. A standard solution of bismuth was prepared by diluting a 1000 ppm solution made by dissolving bismuth metal in (1 + 2) nitric acid. All chemicals used in the spectrophotometric procedure were identical to those recommended earlier [6, 7].

Apparatus

A Hitachi 239 digital spectrophotometer was used for the final determination of bismuth.

The dissolution reaction was carried out in a separatory funnel with a long stem as shown in Fig. 1. It was designed so as to leave as little mercury as possible in the funnel and also to float bismuth oxide on the surface of the mercury. By using a polyethylene chimney placed above the top of the funnel and by providing an adequate pure nitrogen supply, the funnel can be enclosed and isolated from the air.

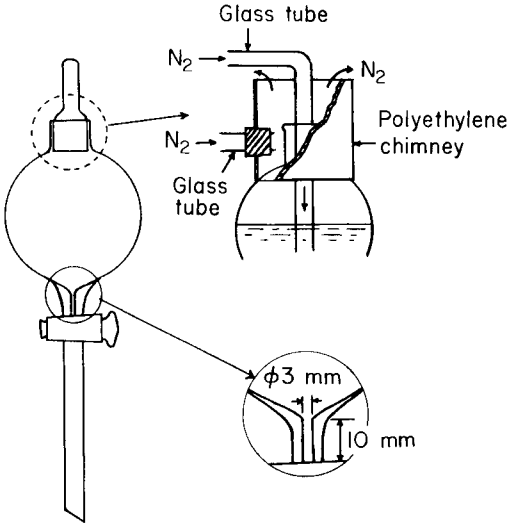

Fig. 1. Apparatus for dissolution and deoxygenation.

Recommended procedure

The following procedure was adopted on the basis of the detailed study described below. A 25-ml portion of 1 M ammonium nitrate solution was added to the 100-ml separatory funnel, and nitrogen was passed through for 5 min (700 ml min^{-1}) to remove air from the vessel and from the aqueous solution. Then 5 ml of mercury was added, followed by a sample of bismuth metal in a nitrogen atmosphere. The funnel was stoppered and immediately shaken vigorously for 5 min. The metal dissolved in the mercury while the bismuth oxide remained as a residue floating on the surface of the mercury. The contents were permitted to stand for at least 2 min. The mercury was separated through the stem of the funnel, and only ca. 0.06 ml of mercury with the bismuth oxide was left in the funnel. The residual bismuth amalgam in the funnel was diluted by addition of 3.5 ml of pure mercury, shaking was continued for 3 min, bismuth oxide again floated on the surface of mercury on standing, and the mercury was removed from the funnel as before. Dilution of the residual mercury was carried out again as above with careful exclusion of oxygen, and most of the mercury was removed. To the residue in the funnel, 25 ml of 4 M nitric acid was added, and the oxide was dissolved by shaking for 5 min. A 20-ml portion of the solution was pipetted into a 25-ml volumetric flask, 2 ml of 20% (w/w) sodium hypophosphite solution and 1 ml of 10% (w/w) potassium iodide solution were added, and the solution was diluted to the mark with water. Its absorbance was measured at 450 nm in 1-cm cells against a blank solution prepared in the same way. The bismuth concentration was determined from a calibration graph obtained by treating aqueous bismuth standard solutions as in the above spectrophotometric procedure.

RESULTS AND DISCUSSION

Dissolution of bismuth oxide and metal

In order to determine the concentration of nitric acid and the shaking time required to dissolve bismuth oxide, accurately weighed portions of pure bismuth oxide were added to 50-ml stoppered centrifuge tubes containing 25 ml of ammonium nitrate solution or nitric acid, and the contents were shaken for 0—5 min. After centrifuging, suitable aliquots were titrated with 0.01 M EDTA solution (or 0.001 M EDTA solution) to a xylenol orange end-point. The results are shown in Table 1, from which it may be concluded that the bismuth oxide was insoluble in 1 M ammonium nitrate solution but completely dissolved in 2 M nitric acid by shaking for 2 min.

After high-purity bismuth metal had been washed successively with 2 M nitric acid and water, it was shaken with 25 ml of 1 M ammonium nitrate solution for 5 min and the dissolved bismuth was measured by the spectrophotometric method described above. The results showed that bismuth metal was insoluble in 1 M ammonium nitrate solution.

TABLE 1

Effect of concentration of nitric acid and shaking time on dissolution of bismuth oxide

Bi_2O_3 taken (mg)	HNO_3 (M)	Shaking time (min)	Bi_2O_3 found (mg)	Recovery (%)
9.19	(1 M NH_4NO_3)	5	0	0
15.32	(1 M NH_4NO_3)	5	0	0
8.95	0.05	5	5.60	62.6
11.42	0.1	5	8.27	72.4
8.89	0.2	5	7.71	86.7
8.65	0.6	5	8.09	93.5
10.88	1.0	5	10.78	99.1
11.27	2.0	5	11.27	100.0
11.60	6.0	5	11.60	100.0
10.68	2.0	0	1.40	13.1
11.05	2.0	1	10.07	91.1
10.62	2.0	2	10.62	100.0
9.20	2.0	4	9.20	100.0
9.28	2.0	5	9.28	100.0
1.83	2.0	5	1.83	100.0
25.37	2.0	5	25.34	99.9
51.49	2.0	5	51.49	100.0

Effect of oxygen in solution

Bismuth amalgam reacts even with traces of oxygen in the aqueous solution to give bismuth oxide; any bismuth oxide thus formed will give a positive error. To identify this effect, experiments were carried out with 5 ml of 0.7% (w/w) bismuth amalgam and 25 ml of ammonium nitrate solution containing various amounts of oxygen, according to the recommended procedure. A large amount of bismuth (650 μg Bi ml^{-1}) was dissolved by working in an air atmosphere. When nitrogen was passed for more than 4 min only a slight amount of bismuth was dissolved (0.30 μg Bi ml^{-1}). This was a constant value, which may be caused by the traces of oxygen that could not be removed from aqueous solution by passing nitrogen.

Although various reductants (sodium tetrahydroborate, ascorbic acid, etc.) were added during the process of deoxygenation by passing nitrogen as previously described [5], no consistent deoxygenation could be achieved with these reagents.

Effect of mercury exchange and blanks

When bismuth oxide is dissolved in nitric acid, any bismuth dissolved from the amalgam will give a positive error. Therefore, any residual amalgam must be diluted with pure mercury until the error from this source is eliminated. Experiments were carried out with 3.5 ml of mercury. Pure mercury was successfully added by use of another separatory funnel, the stem of

which was filled with deoxygenated ammonium nitrate solution to prevent contact with air. After two dilutions, as described in the procedure, the concentration of bismuth in the amalgam was decreased to 1/3500 of its initial 0.7% (w/w) concentration and the bismuth dissolved in the nitric acid became constant at 0.30 μg Bi ml^{-1}, as described above. This value gives rise to a small but significant positive error in the analytical results. Consequently, the analytical results must be corrected by subtracting a blank corresponding to this value. To establish such a blank correction, experiments were done with various concentrations of bismuth amalgam. As shown in Table 2, the results were independent of the concentration of amalgam used. The blank value also varied little with the size of the separatory funnel (Table 2).

Accuracy and applicability

The results obtained by the proposed method for synthetic mixtures prepared from bismuth oxide and bismuth amalgam were satisfactory. As shown in Table 3, the added bismuth oxide can be determined without loss, which indicates that the method is suitable for the determination of bismuth oxide in bismuth metal.

The method was applied to the determination of bismuth oxide in bismuth metal of various forms. The results are given in Table 4. The method is simple, fast, precise and apparently accurate even when quite small samples are used.

The author thanks Professor T. Kiba for valuable discussions and encouragement, and Mr. M. Asai for invaluable assistance during this work.

TABLE 2

Variation of blank value with dissolution vessel and amalgam concentration

Separatory funnel (ml)	Bi conc. range in amalgam (%, w/w)	Range of blank (μg Bi ml^{-1})	No. of detns.	Mean blank (μg Bi ml^{-1})
100	0.2—0.7	0.25—0.35	7	0.30
50	0.15—0.45	0.23—0.29	5	0.28

TABLE 3

Determination of known quantities of bismuth oxide added to bismuth amalgam

Taken (mg)	2.49	4.74	7.65	9.10	15.17	55.27
Found (mg)	2.49	4.72	7.64	9.10	15.17	54.94
Recovery (%)	100.0	99.6	99.9	100.0	100.0	99.4

TABLE 4

Determination of bismuth oxide in bismuth metals

Sample	Mass taken (mg)	Mean Bi_2O_3 content (%)	Standard deviation (%)	No. of detns.	Coefficient of variation (%)
Granules (99.999%)	164—428	0.0082	0.00056	7	6.8
Granules (99.99%)	131—521	0.017	0.0018	9	11
Pellets (99.9%)	213—298	0.011	0.0012	5	11

REFERENCES

1 E. S. Funston and S. A. Reed, Anal. Chem., 23 (1951) 190.
2 C. B. Griffith and M. W. Mallet, J. Am. Chem. Soc., 75 (1953) 1832.
3 W. D. Mackintosh and R. E. Jervis, Nat. Bur. Stand. (U.S.), Spec. Publ., 312 (1969) 835.
4 T. Kiba, K. Matsumoto and G. Shimizu, Bunseki Kagaku, 24 (1975) 116.
5 K. Matsumoto, Analyst, in press.
6 Muki Oyo Hisyoku Bunseki, Vol. 1, Kyoritsu Shuppan, Tokyo, 1973, p. 343.
7 N. H. Furman (Ed.), Standard Methods of Chemical Analysis, Vol. I, 6th edn., Van Nostrand, New York, 1962, p. 201.

Analytica Chimica Acta, 123 (1981) 303—308

OPTIMIZATION OF CALCULATIONS FOR THE PREPARATION OF STANDARD SOLUTIONS

D. TODOROVSKY*, K. KOSTADINOV and R. DJINGOVA

Radiochemical Laboratory, Faculty of Chemistry, University of Sofia, 1126 — Sofia (Bulgaria)

(Received 10th April 1980)

SUMMARY

The calculations necessary in the preparation of a large number of solutions used as standards, are time-consuming and tedious. The scheme proposed significantly shortens the time and makes the work more routine. The equations used are derived from well-known stoichiometric expressions and mathematical representations of some necessary restrictions. The scheme has advantages when many solutions must be prepared for any analytical method.

Many relative analytical methods require preparation of standard solutions with various and usually low concentrations of the elements. Although in recent years commercially available standard reference materials (produced by N.B.S., U.S.G.S., I.A.E.A., etc.) have been applied increasingly, the preparation of artificial standards is unavoidable and the problems of their preparation are still a topic of discussion [1, 2].

When a solution with a given concentration must be prepared, the calculations are absolutely simple and well known, but when it becomes necessary, as in modern neutron activation (n.a.a.) methods, to perform such calculations for 30—40 elements, the work becomes time-consuming and tedious. Yet the real complications arise when some limitations of principle or practical aspects have to be considered. Such considerations may involve for example, the necessity of ensuring reasonable stability during storage over a period of time, minimal total error, use of the smallest possible amounts of very pure, expensive reagents, etc. If such restrictions are largely ignored, the subsequent work may suffer from various shortcomings.

The present paper represents an attempt to simplify, and make more routine, the calculation part of this common analytical work. The equations used are derived from simple stoichiometric expressions and mathematical representations of some necessary restrictions and only the final results are given. The symbols used in the subsequent reactions are listed in Table 1.

TABLE 1

Symbols used

A	Atomic mass of the element
M	Molecular mass of the initial compound containing the element
N	Number of atoms of the element in one molecule of the compound
C	Expected concentration of the element in the analysed sample (g g^{-1}). This is conveniently denoted as $C = q \times 10^x$ where $10 < q \leqslant 1$ and $x = -1, -2, \ldots$
a	Mass of the analysed sample (g)
H	Minimal concentration of the element in the initial solution (g cm^{-3})
b	Minimal amount (g) of the compound necessary to ensure an error from weighing less than an accepted error
G	Necessary amount (g) of the compound that has to be weighed
V_i	Volume (cm^3) of the solutions (or the flasks in which the solutions are prepared). For convenience, it is assumed that $V_i = 10n_i$ where $n_i = 1, 2.5, 5, 10, 25, 50, 100$ or 200
l_i	Aliquot from solution i taken to prepare solution $i + 1$ (cm^3)
l_f	Aliquot taken from the final solution of the element to prepare the complex standard (cm^3)
w	Mass of the element in the final standard (g)
z	The portion of the amount contained in l_f and transferred to the final standard: $z = l' l''/v v'$
v	Volume of the complex standard solution (cm^3)
l'	Aliquot (cm^3) of the complex solution used in the analysis (e.g., subjected to irradiation in the case of n.a.a.)
v'	Volume (cm^3) of the flask in which the irradiated aliquot l' is diluted (dissolved)
l''	Aliquot taken from the volume v' for the preparation of the final standard (cm^3)
r	This index is used to indicate the real volumes and masses, which obviously may differ from the calculated ones.

THE GENERAL PROBLEM

The general problem is to prepare an artificial standard (i.e., a solution with a known concentration of the element, prepared by the experimenter [2]) for a multicomponent analysis. In the case of instrumental n.a.a., for example, such a standard would be prepared by the following procedure: (1) preparation of solutions of the elements with the required concentrations; (2) preparation of the complex standard solution (i.e. the solution containing all the elements of interest in known concentrations [1] by mixing aliquots, l_f, from every solution in a flask of volume v; (3) irradiation of an aliquot l' from this solution together with the analysed sample; (4) dilution of the irradiated aliquot to volume v' and transference of an aliquot l'' from it to a suitable matrix for the preparation of the final standard sample (i.e., the standard which is to be used in the measurement, and is here equivalent to a multicomponent standard).

The question of the chemical compatibility of the elements is not considered in this paper here. Mathematically the procedure (items 3, 4) may be characterized by a coefficient z (see Table 1). Obviously when no dilution is needed after irradiation, $z = l'/v$, and in the case when no complex standard is prepared, $z = 1$.

The restrictions that must be imposed in the preparation of standard solutions from different points of view can be listed as follows. (a) The amount of every element in the final standard should be as near as possible to its content in the sample. (b) Only commercially availiable laboratory equipment must be required. (c) The minimal concentration, H, of the initial solution, prepared after dissolution of an element or its compound, must ensure reasonable storage stability. Obviously, if more concentrated solutions are needed, the initial concentration will be higher than that. (d) The total error in the mass of the element in the standard must be minimal or at least should not exceed some value accepted on the basis of defined considerations. For this purpose, the following points are important. First, the minimal amount, b, of the compound must be chosen so as to ensure an acceptable error from weighing. Secondly, it is necessary to prescribe a suitable selection of the aliquots taken from the solutions and of the necessary pipettes. Thirdly, the number of dilutions should be minimal; this not only decreases the error but saves working time. (e) The restrictions mentioned under (d) mean that a minimal amount $G \geqslant b$ of the compound should be used. This is also one of the factors ensuring lower analytical costs.

OPTIMIZATION OF THE CALCULATIONS

Initial parameters

It is obvious that the values of A, M, C, H, a, b, z, $m = AN$ and $l_{f,min}$ must be known, accepted or calculated from considerations of the analysis actually required; in general, it is convenient to calculate the ratio M/m. The lower limit of l_f, $l_{f,min}$, is defined by the maximal permissible error from pipetting. For example, when pipettes of 0.1 or 0.2 cm^3 are available, $l_{f,min} = 0.1$ is an acceptable value.

Calculations

Criteria for the determination of the number of dilutions. If $C = q10^x \geqslant Hzl_{f,min}/a$, the desired solution may be prepared directly, i.e. after dissolution of the weighed amount of the element or compound.

If $C = q10^x \geqslant (Hzl_{f,min}/a)(q10^{-2}/n_{2,max})$, the solution is prepared after one dilution of the initial solution.

If $C = q10^x \geqslant (Hzl_{f,min}/a)(q10^{-4}/n_{2,max}n_{3,max})$, the solution is prepared after two dilutions.

Direct preparation of the solution (without dilutions). The volume of the solution is calculated from the expression $V_1 = 10n_1$, where n_1 should take the minimal value from the permissible values that satisfy the expression

$$CM/m \geqslant bzl_{f,min}/10n_1a \qquad (1)$$

Determination of the aliquot l_f, involves the following conditions : if $n > 1$, then $l_f = l_{f,min}$, and if $n = 1$, then l_f must satisfy the condition CM/m

$\geqslant bzl_f/10a$. In the latter case, the lower limit of l_f is fixed by the preset value of $l_{f,min}$. The upper limit depends on the method used for the preparation of the standard and on the preset permissible error from pipetting.

The desired amount, G of the element (or its compound) which has to be weighed and dissolved may be calculated from the equation

$$G = aH(M/m)(10n_1/l_f z) \tag{2}$$

The real amount w_r of the element in the final standard can be determined from

$$w_r = G_r l_{f,r} z_r / 10 n_1 M/m \tag{3}$$

Indirect preparation of the solution. The volume of the initial solution ($i = 1$) is calculated by using the same principle as for the direct preparation but the condition that has to be satisfied by n_1 is

$$M/m \geqslant b/10Hn_1 \tag{4}$$

The aliquots taken from solution i to prepare the solution $i + 1$, are $l_1 = q \times 10^{-1}$ cm^3 and $l_2 = 10^{-1}$ cm^3.

The amount G is calculated from $G = H\ 10n_1\ M/m$. The volumes of the subsequent more diluted solutions and the aliquots, l_f, for the preparation of the complex standard solution are calculated from the equations

$$n_2/l_f = Hz/a10^{x+2} \tag{5}$$

and

$$n_2 n_3/l_f = Hz/a10^{x+4} \tag{6}$$

for one and two dilutions, respectively. In the determination of l_f, the above-mentioned restrictions on its limits must be considered.

The real amount of the element in the standard is calculated, for one dilution, from

$$w_r = G_r l_{f,r} z_r l_{1,r} / (10^2 n_1 n_2 M/m) \tag{7}$$

and, for two dilutions, from

$$w_r = G_r l_{f,r} z_r l_{1,r} l_{2,r} / (10^3 n_1 n_2 n_3 M/m) \tag{8}$$

APPLICATION OF THE CALCULATIONS

The application of the proposed scheme for calculation is advantageous when a large number of solutions is needed for any multicomponent analysis. In such a case it is convenient to draw up a table similar to Table 2. Once made, such a table permits a very quick determination of all values necessary for the preparation of the solutions. The table is compiled in the following way. First, the values of the initial parameters $b,H,a,z,l_{f,min}$ are chosen. Then the criteria stated for the determination of the number of dilutions are used

TABLE 2

Working table for calculation of standard solutions
(Initial parameters: $b = 5 \times 10^{-2}$ g; $z = 4 \times 10^{-3}$; $H = 10^{-3}$ g cm^{-3}; $l_{f,min} = 10^{-1}$ cm^3; $a = 10^{-1}$ g)

Method for preparation		$C = q \times 10^x$ ($10 > q \geq 1$, $x = -1, -2, \ldots$)		n_1	l_1 (cm^3)	n_2	l_2 (cm^3)	n_3	l_f (cm^3)	G (g)
1		2	3	4	5	6	7	8	9	10
Direct		$\geq 4 \times 10^{-6}$	$CM/m \geq 2 \times 10^{-4}$						1.00	2.5×10^2 CM/m
			$2 \times 10^{-4} > CM/m \geq 1 \times 10^{-4}$						0.50	5×10^2 CM/m
			$1 \times 10^{-4} > CM/m \geq 2 \times 10^{-5}$	1	—	—	—	—	0.10	2.5×10^3 CM/m
			$2 \times 10^{-5} > CM/m \geq 8.\times 10^{-6}$	2.5					0.10	6.25×10^3 CM/m
			$8 \times 10^{-6} > CM/m \geq 4 \times 10^{-6}$	5					0.10	1.25×10^4 CM/m
Indirect	One dilution (i = 1)	$(4 \div 9.99)$ 10^{-6}	$M/m \geq 5$	1	$q \times 10^{-1}$	1	—	—	2.50	10^{-2} M/m
		$q \times 10^{-7}$				1			0.25	
		$q \times 10^{-8}$	----------			10			0.25	----------
		$q \times 10^{-9}$				100			0.25	
	Two dilutions (i = 2)	$q \times 10^{-10}$	$5 > M/m \geq 2$	2.5		10		10	2.50	2.5×10^{-2} M/m
		$q \times 10^{-11}$	----------			10		10	0 25	----------
		$q \times 10^{-12}$				10	10^{-1}	100	0.25	
		$q \times 10^{-13}$	$2 > M/m \geq 1$	5		100		100	0.25	5×10^{-2} M/m
		$q \times 10^{-14}$				200		200	0.10	

to establish the concentration intervals within which the required solution may be prepared directly or with dilutions. The intervals in which the solutions can be prepared with dilutions are divided into subintervals as shown in Table 2. Secondly, eqns. (1) and (4) are used, by inserting the values 1, 2.5, ... for n_1, to establish criteria for the determination of the volume V_1. Next, the value of l_f for direct preparation of the solutions is calculated according to the conditions, $l_f = l_{f,\min}$ for $n > 1$ and $CM/m \geqslant bzl_f/10a$ for $n = 1$. If l_f is always kept equal to $l_{f,\min}$, the preparation of solutions with higher concentrations will be difficult. That is why it is more convenient to give sensible values to l_f and to obtain the concentration subintervals in which these values may be used from the expression $CM/m \geqslant bzl_f/10a$. Thus the concentration subintervals at $n_1 = 1$ are shown in Table 2, column 3. There the value of l_f (0.5 and 1 cm^3) is chosen only for convenience sake. Fourthly, eqns. (5) and (6) are applied in each concentration subinterval in which they are valid, to calculate the volumes of the subsequent more diluted solutions and of the aliquots to be used for the preparation of the complex standard. Then the values of l_i are calculated from $l_1 = q \times 10^{-1}$ cm^3 and $l_2 = 10^{-1}$ cm^3. Finally, the amount G is calculated from eqn. (2) and from $G = H10n_1M/m$, after the optimal values have been replaced by the real values.

Conclusions

The scheme proposed for the calculation of standard solutions significantly shortens the time necessary for the usual calculations, makes the work more routine and minimizes the total error. Although it is based on an example in the neutron activation field, it is applicable to any analysis where many solutions with various concentrations of the elements are needed. The scheme demonstrates its advantages clearly when a large number of solutions has to be prepared.

REFERENCES

1 D. De Soete, R. Gijbels and J. Hoste, Neutron Activation Analysis, Wiley—Interscience, London, 1972, p. 283.
2 Z. Řanda, M. Vobecký, J. Kuncir and J. Benada, J. Radioanal. Chem., 46 (1978) 95.

Analytica Chimica Acta, 123 (1981) 309—313

Short Communication

CHELATING ION-EXCHANGERS CONTAINING N-SUBSTITUTED HYDROXYLAMINE FUNCTIONAL GROUPS
Part 6. Sorption And Separation Of Gold And Silver By A Polyhydroxamic Acid

F. VERNON* and WAN MD. ZIN

The Ramage Laboratories, Department of Chemistry and Applied Chemistry, University of Salford, Salford M5 4WT, Lancs. (Gt. Britain)

(Received 11th July 1980)

Summary. The sorption and desorption characteristics of gold and silver on a polyhydroxamic acid chelating resin are described. Gold is quantitatively sorbed from 0.5 M nitric acid or neutral solutions, and readily eluted with 0.5% (w/v) potassium cyanide solution. Silver is removed from 0.05 M nitric acid or neutral solutions, and can be eluted with the cyanide solution or with 0.5 M nitric acid. Gold can be quantitatively separated from copper, iron and silver; gold and silver are sorbed from dilute cyanide solutions. Tests with river water and other eluting systems are reported.

Earlier papers in this series have described the preparation of a polyhydroxamic acid ion exchanger [1] and its application to the separations of several transition metal species [2]. Sorption and desorption of gold and silver by this exchanger and the separation of these species from each other and from other metals are reported here.

The recovery of gold from cyanide solution by means of zinc metal is an established procedure in the gold mining industry, but this simple and cheap process has its limitations. For instance, in the processing of very low-grade ores where the concentrations of other impurities are high, an ion-exchange concentration and purification step is thought to be more profitable. The use of anion-exchange resins entails sorption of gold from chloride solutions [3]; both weak base [4] and strong base exchangers [5] have been utilized for gold recovery from cyanide solutions. Cyanide complexes of other metals were sorbed along with the gold and separation was by selective elution. Anion exchange has also been used for the removal of silver from thiosulphate solutions [6, 7], whilst the porous polyacrylate Amberlite XAD-7 resin removes gold selectively from acid leach liquors [8].

Few chelating or complexing resins demonstrate selectivity towards gold and silver. The resin described by Bayer [9], with a glyoxal bis(-2-mercaptoanil) functionality, is probably the most widely used resin for analytical preconcentration of gold from dilute solution. Fritz [10] has reported that a resin containing a thioglycolate functional group demonstrated high selectivity for gold, silver, mercury and bismuth, whilst chelating resins containing

2-mercaptobenzimidazole or rhodamine groupings have also shown selectivity towards gold and silver [11]. The commercially available Srafion NMRR, a polyisothiuronium chelating resin, gives quantitative removal of gold from acidic solutions [12] in addition to its high capacity for platinum metals. The polyamidoxime Duolite CS-346, is said to form a very stable complex with gold [13] although full sorption/desorption studies have apparently not been reported. As amidoximes are rapidly broken down in acidic solution, being hydrolysed to hydroxamic acids, and the polyhydroxamic acid exchanger is both cheap and simple to prepare, its use for preconcentration and separation of gold and silver has been investigated.

Experimental

Polyhydroxamic acid resin. The method of preparation described earlier [1] was modified to give improved resin properties. A microbead, macroporous, acrylonitrile—ethyl acrylate copolymer cross-linked with 5% divinylbenzene was prepared by suspension polymerization. The product was converted by a single-step hydrolysis—oximation to a polyhydroxamic acid by treatment with hydroxylamine in the presence of sodium hydroxide. After reaction, the product was washed with methanol, then repeatedly with 2 M hydrochloric acid, and finally with deionized water until chloride-free.

A glass column (0.9 cm i.d.) was packed to a height of 15 cm with the resin for most of the work. A slightly larger column (1.1 cm i.d. and 15 cm resin height) was used in tests of the recovery of gold added to surface water.

Procedures. The capacity—pH contours were obtained by batch equilibration of 0.5 g of resin with metal solutions overnight. Timed equilibrations with copper(II) solutions were used to obtain the $t_{1/2}$ of the resin. All quantitative measurements of metals were done with an IL-351 atomic absorption spectrometer.

Results

Table 1 gives the resin properties; copper(II) at pH 4 was used to assess both total capacity and the kinetics of sorption. The capacity is high and for a chelating exchanger the rate of uptake is comparatively fast, 50% of the available sites being occupied by copper(II) in 8 min. Figure 1 shows the pH contours of the exchanger for the metals studied and suggests the possibility

TABLE 1

Properties of the macroporous bead polyhydroxamic acid resin

Bead size	50—100 mesh fraction
Cross-linking (%)	5
Water regain (g g^{-1})	2.1
Total capacity (mmol g^{-1})	3.0 for Cu (pH 4); 4.0 for Au (pH 1); 1.2 for Ag (pH 1)
$t_{1/2}$	8 min for Cu at pH 4

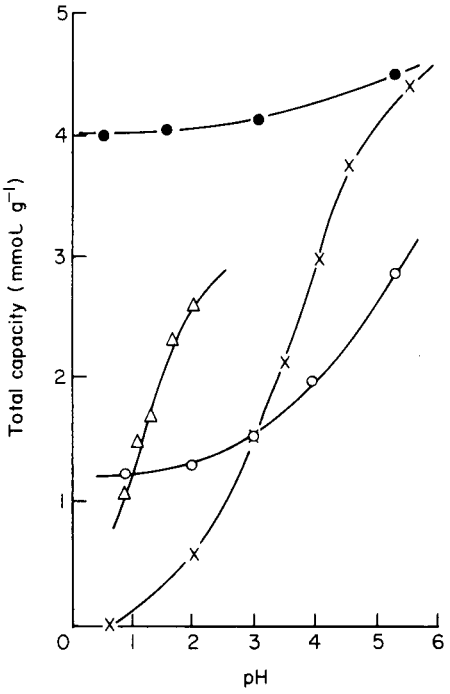

Fig. 1. Total capacity vs. pH contours for gold (•), silver (○), copper (×), and iron (△) on the polyhydroxamic acid resin.

of preferential sorption of gold and silver over copper and iron below pH 1. A separation of gold from silver around pH 0 is also indicated. The high capacity for gold, 4.0 mmol g^{-1}, means that at saturation there will be 788 mg of gold associated with each g of dry resin. At this loading, burning of the resin to recover gold would be economic, but an effective elution system for gold is available (see below).

Sorption and desorption characteristics of gold and silver. Gold(III) chloride (40 μg Au ml^{-1}) in various aqueous media was applied to columns which had been preconditioned with 0.5 M hydrochloric acid and then washed with water until chloride-free. Elution rates were varied between 0.5 ml and 3.5 ml min^{-1}. Sorption of gold was quantitative from all the media tested (Table 2). Sorption from solutions containing cyanide was studied for possible application to cyanide wastes; uptake was complete even when the cyanide was present in tenfold excess. When the resin was preconditioned by 0.5 M nitric acid and water washing, sorption of silver(I) (40 μg ml^{-1}) was incomplete from a 0.5 M nitric acid medium but complete from 0.05 M nitric acid, as well as from water and cyanide solution (50 μg ml^{-1}) (Table 2).

The gold is very strongly bound to the resin, and elution with 4 M hydrochloric acid in water gave poor gold recoveries (Table 3). Various hydro-

TABLE 2

Sorption of gold(III) and silver(I) from 40 $\mu g\ ml^{-1}$ solutions in various media

Solution	Metal in effluent (mg)	% Sorption	Solution	Metal in effluent (mg)	% So
Gold(III)			*Silver(I)*		
0.5 M HCl	0	100	0.5 M HNO_3	0.46	89
Water, pH 6.5	0	100	0.05 M NHO_3	0.02	99
1% NaCl, pH 6.5	0	100	Water, pH 6.5	0	100
KCN (50 $\mu g\ CN^-\ ml^{-1}$)	0	100	KCN (50 $\mu g\ CN^-\ ml^{-1}$)	0	100
KCN (500 $\mu g\ CN^-\ ml^{-1}$)	0	100			

chloric acid/ethanol eluants were investigated. The best system proved to be 0.1 M hydrochloric acid in ethanol (99%); 100 ml removed 93% of gold from the column and obviously further washing would yield quantitative recoveries. However, the best eluant was found to be a 0.5% (w/v) solution of potassium cyanide which quickly and quantitatively desorbed the gold.

As gold may be quantitatively sorbed from 0.5 M acid, desorption of silver by 0.5 M nitric acid was studied. Desorption of silver was, however, slow (Table 3). Again, desorption of silver by 0.5% (w/v) potassium cyanide was rapid and quantitative (Table 3).

Separation of gold from iron, copper or silver. Solutions containing 4 mg of gold and 50 mg of copper in 0.5 M hydrochloric acid were applied to the column and eluted at 3.5 ml min^{-1}. When the column was washed with 100 ml of 0.5 M hydrochloric acid, copper was recovered almost completely (99%) in the total volume eluted. The column was then washed with water, and the sorbed gold was quantitatively eluted with 0.5% (w/v) potassium cyanide.

The above procedure was repeated using a solution initially containing 5 mg of iron(III) and 4 mg of gold. Iron recovery was only 95%, but when the column was washed with 100 ml of 2 M hydrochloric acid, iron was removed quantitatively (100%). Subsequent elution with cyanide gave quantitative gold recovery.

TABLE 3

Elution of gold(III) and silver(I) from the column by aqueous and ethanolic eluants

Eluant	Volume needed (ml)	Recovery (%)	Eluant	Volume needed (ml)	Recover (%)
Gold(III)			*Silver(I)*		
4 M HCl (aq.)	100	19	0.5 M HNO_3	100	64
1 M HCl (90% EtOH)	55	50		200	77
	100	84		400	92
0.1 M HCl (99% EtOH)	100	93	0.5% KCN	100	100
0.05 M HCl (99% EtOH)	100	40			
0.5% KCN (aq.)	100	100			

In testing the effectiveness of the gold/silver separation, the two ions could not be applied simultaneously to the column because the gold was present as the chloride. Consequently, 4 mg of gold(III) in neutral solution was applied to the column which was then washed until chloride-free. A solution containing 8 mg of silver(I) was then applied and the column was washed with deionized water. Most (98%) of the original silver was eluted with 500 ml of 0.5 M nitric acid and, after the column had been washed with water, quantitative gold recovery was achieved with the cyanide eluant.

Recovery of gold added to surface water. A sample (1 l) of river water (R. Irwell sampled at Salford) was filtered and 1 mg of gold(III) was added to it; the pH of the sample was 7.1. This solution was passed through a column of the resin (1.1 cm diameter, 15 cm high) at a rate of 1 ml min^{-1}; the resin was preconditioned with 0.5 M hydrochloric acid and then washed chloride-free. The column was washed with 2 bed volumes of deionized water, and the gold was eluted by 100 ml of 0.5% (w/v) potassium cyanide; the column was then washed with 100 ml of deionized water. Quantitative recovery of the gold in the total eluate was achieved.

Conclusions

Gold(III) is sorbed more strongly than silver(I) by the polyhydroxamic acid resin, so that these ions can be separated by selective elution of silver with 0.5 M nitric acid. Both gold(III) and silver(I) can be separated from copper and iron. Desorption of gold is a problem when acid eluants are used, although it is possible with ethanol/hydrochloric acid mixtures. Both gold and silver are rapidly eluted from the resin by 0.5% (w/v) potassium cyanide solution.

This resin should find applications in analytical work for the removal of these species from waters, and for hydrometallurgical and electroplating solutions where gold and silver recoveries from dilute cyanide solutions are required.

REFERENCES

1 F. Vernon and H. Eccles, Anal. Chim. Acta, 82 (1976) 369.
2 F. Vernon and H. Eccles, Anal. Chim. Acta, 83 (1976) 187.
3 S. Sussman, F. C. Nachod and W. Wood, Ind. Eng. Chem., 37 (1945) 618.
4 F. H. Burstall, P. J. Forrest, N. F. Kember and R. A. Wells, Ind. Eng. Chem., 45 (1953) 1648.
5 F. H. Burstall and R. A. Wells, S.C.I. Symp. on Ion Exchange, London, April, 1954.
6 M. L. Schreiber, J. Soc. Motion Pict. Eng., 74 (1965) 505.
7 F. Nelson, K. A. Kraus and J. S. Gilbert, 31st Purdue Ind. Waste Conf., Lafayette, IN, May, 1976.
8 R. I. Edwards, A. K. Haines and W. A. M. Te Riele, S.C.I. Symp., The Theory and Practice of Ion Exchange, Cambridge, 1976.
9 E. Bayer, Angew. Chem., Int. Ed., 3 (1964) 325.
10 J. S. Fritz, Pure Appl. Chem., 49 (1977) 1547.
11 E. Blasius and B. Brozio, in H. A. Flaschka and A. J. Barnard (Eds.), Chelates in Analytical Chemistry, Vol. 1, M. Dekker, NY, 1967.
12 T. E. Green and S. L. Law, U.S. Bur. Mines, Rep. Invest., Rep. 7358, 1970.
13 Diamond Shamrock Chemical Co., Duolite CS-346 Technical Sheet, 1972.

Analytica Chimica Acta, 123 (1981) 315—317

Short Communication

DETERMINATION OF SELENIUM IN WATER SAMPLES BY MOLECULAR EMISSION CAVITY ANALYSIS AFTER COPRECIPITATION

TH. A. KOUIMTZIS, M. C. SOFONIOU and I. N. PAPADOYANNIS

Laboratory of Analytical Chemistry, University of Thessaloniki, Thessaloniki (Greece)

(Received 28th July 1980)

Summary. Selenium (0.2—5 ppb) is coprecipitated with hydrated iron(III) oxide, dissolved in acid, reprecipitated as the element and determined by molecular emission cavity analysis. For a 250-ml water sample, the detection limit is 0.2 ppb. For >5 ppb selenium there is no need for coprecipitation.

In recent years, considerable attention has been focussed on the physiological role of selenium as a trace element. Various authorities have presented evidence that selenium is an essential nutrient [1]. Total daily intake of selenium has been estimated at 60—150 μg from food. As an antioxidant, selenium has been reported to reduce cancer rates. Selenium is, however, a cumulative toxic substance that can be a serious health hazard when present in food, air or water supplies in excessive amounts. Because of this, the presence of even minute amounts of this element in water is of serious concern. Present regulations require that the selenium concentration in drinking water never exceeds 10 ppb. Selenium occurs in sea water as selenite ions (SeO_3^{2-}) at an average concentration of 0.2 ppb. Selenium(IV) is the thermodynamically most probable state of the element under normal aerobic conditions.

Various methods have been developed for the determination of trace selenium in water samples. Hydride generation followed by flame [2, 3] or electrothermal [4, 5] atomic absorption provides the best sensitivity, with reported detection limits around 1—2 ppb. Belcher et al. [6, 7] have proposed methods for determining selenium based on molecular emission cavity analysis (m.e.c.a.). In the present communication, this technique has been used to determine selenium in water samples. Selenium is first coprecipitated with hydrated iron(III) oxide. The precipitate is dissolved in hydrochloric acid, selenium is reduced to the element, filtered off and determined by m.e.c.a. For a 250-ml sample, the detection limit is 0.2 ppb.

Experimental

Reagents. A standard selenium solution (1000 ppm) was prepared by dissolving exactly 1 g of selenium powder in 5 ml of concentrated nitric acid, and diluting to 1 l with distilled water. All other reagents used were of analytical grade.

Apparatus. Emissions were measured by a Unicam SP90 atomic absorption spectrometer, modified to accommodate a sample holder assembly for the cavity. The cavity was the hexagonal aperture at the end of a 3-cm long mild steel screw into which the piece of filter paper with selenium deposit was placed. A Unicam emission burner head (2-cm o.d.) was used. The location of the cavity in the flame and flame conditions which gave maximum intensity were as established previously [6].

Procedure. Transfer 100—250 ml of water sample, containing 0—5 ppb of selenium, to a 500-ml cylinder. Add 20 ml of 2 M sodium acetate solution followed by 1 ml of 0.1 M iron(III) chloride solution. After 12 h, filter the hydrated iron(III) oxide precipitate on a No. 4 Gooch crucible. Dissolve the precipitate in 10 ml of 8 M hydrochloric acid, and add 0.5 ml of 5% hydroxylamine solution, or bubble sulphur dioxide for 15 min. Heat at 70°C for 3—5 min. Filter the hot suspension through a glass-fibre filter disc (2—3 mm diameter; Whatman GF/C), which quantitatively retains the selenium, supported on an asbestos sheet disc in a Millipore filtration apparatus. Wash the selenium precipitate with a few ml of 8 M hydrochloric acid followed by hot water. Dry the filter disc and transfer it to the cavity so that it fits the contour of the cavity, with the selenium deposit towards the aperture [6]. Place the cavity in the flame, and measure the maximal emission intensity at 411 nm. Determine the amount of selenium present by referring to a calibration graph prepared by measuring the emission of known amounts of selenium taken through the reduction and filtration procedure.

If the concentration of selenium in the samples is >5 ppb, then there is no need for coprecipitation. Take 1—15 ml of water sample and mix with concentrated hydrochloric acid so that the acidity exceeds 6 M. Then add hydroxylamine solution or bubble sulphur dioxide and continue as described above.

Results and discussion

Hydrated iron(III) oxide is an efficient coprecipitating agent for selenium. Chau and Riley [8] found that it carries down 97.0 ± 0.8% of the selenium (as selenite) present in 2 l of sea water after 48 h of coprecipitation. Their procedure, modified slightly, has been used in the present work for coprecipitation of less than 5 ppb of selenium. It should be emphasized that selenium must be in the selenite form prior to coprecipitation.

The coprecipitate is easily dissolved in hydrochloric acid and reduction of selenium to the element is done either by adding hydroxylamine or bubbling sulphur dioxide. Both selenite and selenate are reduced to the elements. The presence of large amounts of iron has no effect on this reduction. The collection of the elemental selenium on a small glass-fibre filter disc must be done carefully. For this purpose the filtration should be done by applying vacuum. Organic selenium compounds, if present, may first be decomposed by digestion with potassium permanganate in hot acid solution. The selenate formed may then be reduced to elemental selenium as described above.

TABLE 1

Determination of selenium in spiked water samples

Sample	Sample volume (ml)	Se present (ppb)	Se found[a] (ppb)
Spiked distilled water	250	1.0	0.9 ± 0.1
	250	2.0	1.9 ± 0.1
	250	5.0	5.0 ± 0.2
	10	10.0	9.8 ± 0.2
	10	15.0[c]	14.4 ± 0.4
Spiked sea water[b]	250	1.0	0.9 ± 0.2
	250	2.0	2.0 ± 0.2
	250	5.0	4.8 ± 0.3
	10	10.0	9.9 ± 0.2
	10	15.0[c]	14.1 ± 0.5

[a]Mean of 5 determinations ± standard deviation. [b]Selenium in sea-water samples from Thessaloniki Gulf was 0.5 ppb. [c]Spiked with selenate and organoselenium compounds.

The 2σ detection limit for 250-ml samples is 0.2 ppb of selenium. The precision of the method was evaluated with spiked distilled water and sea-water samples. Replicate analyses were carried out at various ppb selenium levels. The results of five determinations at each level are summarized in Table 1.

REFERENCES

1 E. J. Calabrese, Pollutants and High-Risk Groups, Wiley—Interscience, New York, 1978, pp. 102, 114.
2 M. Lansford, E. McPherson and M. Fishman, At. Absorpt. Newsl., 13 (1974) 103.
3 F. Schmidt, J. Royer and S. Muir, Anal. Lett., 8(2) (1975) 123.
4 E. Henn, Anal. Chem., 47 (1975) 428.
5 G. Kunselman and E. Huff. At. Absorpt. Newsl., 15 (1976) 29.
6 R. Belcher, T. Kouimtzis and A. Townshend, Anal. Chim. Acta, 68 (1974) 297.
7 R. Belcher, S. L. Bogdanski, E. Henden and A. Townshend, Anal. Chim. Acta, 113 (1980) 13.
8 Y. Chau and J. Riley, Anal. Chim. Acta, 33 (1965) 36.

Analytica Chimica Acta, 123 (1981) 319—324

Short Communication

CHARACTERISTICS OF THE BACKGROUND EMISSION SPECTRUM FROM A MINIATURE INDUCTIVELY-COUPLED PLASMA

R. N. SAVAGE and G. M. HIEFTJE*

Indiana University, Department of Chemistry, Bloomington, IN 47405 (U.S.A.)

(Received 20th March 1980)

Summary. The spectral characteristics of the background radiation emitted by a miniature inductively-coupled plasma (i.c.p.) are carefully examined and methods for reducing undesirable features discussed. The complex nature of the background emission spectrum for the mini-i.c.p. indicates that careful line selection criteria and background correction procedures should be employed. Extending the torch coolant tube to the bottom of the region being observed in the plasma proved to be the most effective method for reducing undesirable spectral band features. Acute changes in background emission levels with r.f. power and nebulizer gas flow rates emphasize the need for careful control of these parameters to achieve high precision. Comparison between mini-i.c.p. and conventional i.c.p. spectra reveals the basic similarity of the two sources.

In a recent publication [1], a modified i.c.p. torch was described which was one-third smaller than a conventional unit. This new torch sustains a high-temperature plasma at low radio-frequency power levels (i.e., <1.0 kW) and consumes less than 8 l min^{-1} of argon, resulting in significant savings for the user in both initial equipment price and operating costs. Significantly, a mini-i.c.p. operating at these reduced levels demonstrated the same high sensitivity, broad linear operating range, and simultaneous multi-element capabilities associated with conventional i.c.p. sources. However, in addition to the emission from the atoms of interest, the plasma also radiates its own background. The purpose of the present communication is to evaluate the spectral characteristics of this background emission.

Radiation emitted by the mini-plasma has been recorded using a high-resolution scanning monochromator; the influence on this spectrum of several experimental parameters (i.e., coolant tube length, r.f. power and coolant and nebulizer gas flow rates) has been evaluated.

Background emission spectra from conventional i.c.p. sources have been examined by others [2—8] and their importance was recently discussed by Horlick [9]. Comparison between these conventional i.c.p. spectra and those of the mini-i.c.p. reveals the basic similarity of the two sources.

*Present address: Instrumentation Laboratory, Inc., Wilmington, MA 01887, U.S.A.

Experimental

The experimental system and general operating procedures were the same here as previously described [1], except for the optical system which was altered slightly for spatial emission profiling studies underway in this laboratory. Typical operating conditions are outlined in Table 1.

Modified optical design. Radiation emitted from the tail flame of the mini-plasma was collected by a 6-in. (15.2 cm) spherically concave front-surface mirror (f = 40.5 cm, Al—MgF_2/2000 coating, Oriel Corp., Stamford, CT) held in place by a gimbal mount (Model 760, Newport Research Corp., Fountain Valley, CA). The mirror imaged the plasma at a point 34.7 cm from the entrance slit of a 1-m monochromator (Model HR1000, I.S.A., Inc., Metuchen, NJ, employing a 120 × 140 mm holographic grating with 2400 grooves mm^{-1} and having a reciprocal linear dispersion of 0.39 nm mm^{-1}). This image was then refocused by a plano-convex lens (f = 7.5 cm, diameter = 2.5 cm, fused silica, Melles Griot, Irvine, CA) onto the monochromator entrance slit, to yield a system magnification factor of 0.625. Accordingly, slit dimensions given in Table 1 resulted in a 8-mm high by 80-μm wide observation region, centered 15 mm above the plasma load coil.

Reagents

Stock solutions were prepared as suggested by Dean and Rains [10], using reagent-grade salts and acids; analyte solutions were prepared by suitable dilution.

Results and discussion

Spectral features in mini-i.c.p. background emission. Figure 1 illustrates a typical mini-i.c.p. background emission spectrum, taken while a solution containing 100 μg Mn ml^{-1} and 10 μg Ca ml^{-1} was being nebulized. A high-resolution scan such as this illustrates that the spectral background consists of three kinds of features, namely continuum, line spectra, and band spectra.

The continuum background (i.e., non-zero baseline) has been attributed mainly to bremsstrahlung radiation [5]. (Note that the spectrum in Fig. 1 has not been corrected for the wavelength-dependent response of the optical

TABLE 1

Operating conditions for background scans

R.f. power 1.0 kW (Forward power output from r.f. generator)
Gas flows (l min^{-1}) coolant, 7.9; plasma, 0.3; nebulizer, 0.97, 1.0 mm (i.d.) capillary injection tube in torch (cf. Fig. 2 in [1])
Monochromator[a] slit width, 50 μm; slit height, 5 mm; scan rate, 15 nm min^{-1}.
Picoammeter scale 10 × 10^{-9} A.
Recorder 1 in. min^{-1}.
Solution delivery rate 0.8 ml min^{-1}. By peristaltic pump.

[a]Entrance slit = exit slit.

system and detector.) As detailed later, the magnitude of the continuum can change with experimental conditions, emphasizing the need for careful background-correction procedures. In general, the intensity of the continuum was low as long as the viewing zone was restricted to the plasma tail flame and did not overlap with the core [5] of the plasma.

Superimposed on the continuum were narrow spectral lines and broad-band features. The most prominent lines were those of the support gas, argon. The intensities of the 415.8-nm and 420.1-nm lines (excitation energies of approximately 14.7 eV, each) indicate the high excitation capabilities of the plasma and suggest a high density of argon metastable species [4]. Some of the more interesting lines were those of hydrogen which appear very broad. Most of the Balmer series can be seen, but by far the most intense feature in this group was the H_β line at 486.1 nm. The close proximity of the 397.0-nm H line to the 396.9-nm Ca II line could result in significant interference. The carbon line at 247.9 nm was assumed to arise from a still-unidentified impurity in the argon support gas.

The most troublesome spectral features in the mini-i.c.p. background were the molecular emission bands, originating from species such as NO, NH and OH. Presumably, nitrogen-containing molecules formed when air was entrained into the plasma tail flame. The NO_γ system present in the 200—275-nm region could easily interfere with the 257.6-nm Mn II and other analyte lines (e.g., Zn, Cd or P). The NH band at 336.0 nm was also very prominent. Bands near 360 nm, 390 nm and 420 nm which degrade to the blue and the one at 610 nm degrading to the red were believed to arise from CN, although those at 360 nm and 390 nm might have originated from N^2 and N^{2+}, respectively [7]. Because an aqueous solvent was used, strong OH bands at 306.4 nm and 281.1 nm were generated, which could interfere with elemental lines of Al, Be, Bi, Cu, Mg, Si, and V. Background spectra similar to Fig. 1 were also obtained from a conventional i.c.p. operating in this laboratory, emphasizing the similarity of the sources.

Effect of coolant tube length on plasma background. The spectrum shown in Fig. 1 was taken from a mini-plasma sustained by a torch whose coolant tube extended 18 mm beyond the end of its plasma tube (cf. Fig. 2 in [1]). When the coolant tube was shortened to only 14 mm above the plasma tube, the background changed dramatically. In particular, the continuum level decreased to one-third that in Fig. 1, and the Ar and H line intensities dropped. Conversely, all the band emission levels rose in intensity. The NH, NO and CN bands increased sharply while OH rose only slightly. In addition, C_2 and CH bands appeared. These findings agree with Truitt and Robinson [4] who reported that conventional-size torches with shorter coolant tubes sustained plasmas whose background spectra were richer in band features.

The reasons for these changes in background emission become evident when one carefully observes the size and location of the plasmas formed by the two torches. When a shorter coolant tube was employed, the optical

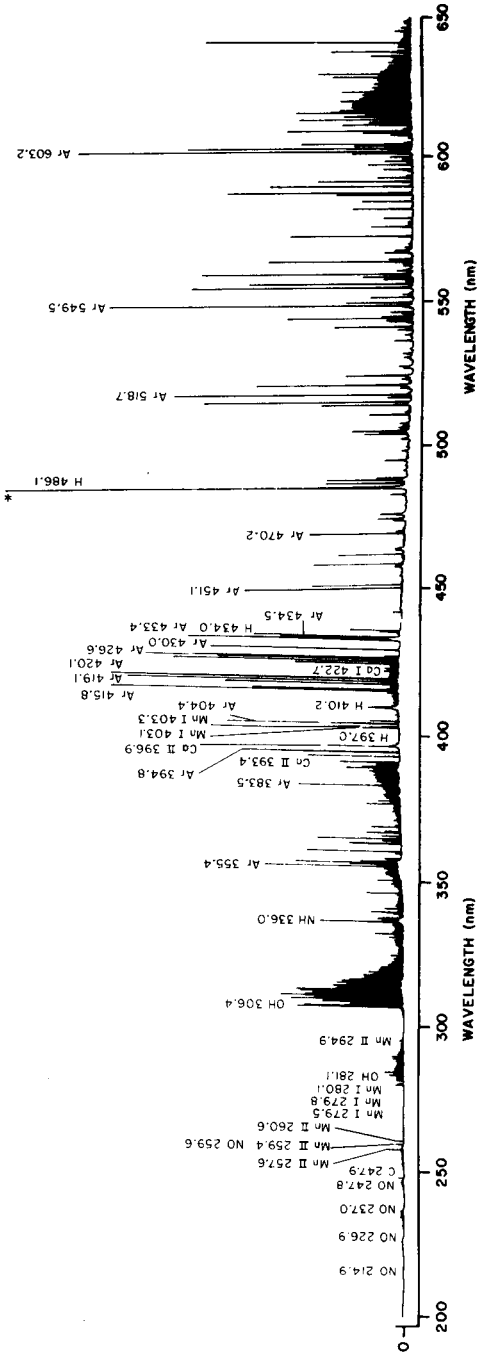

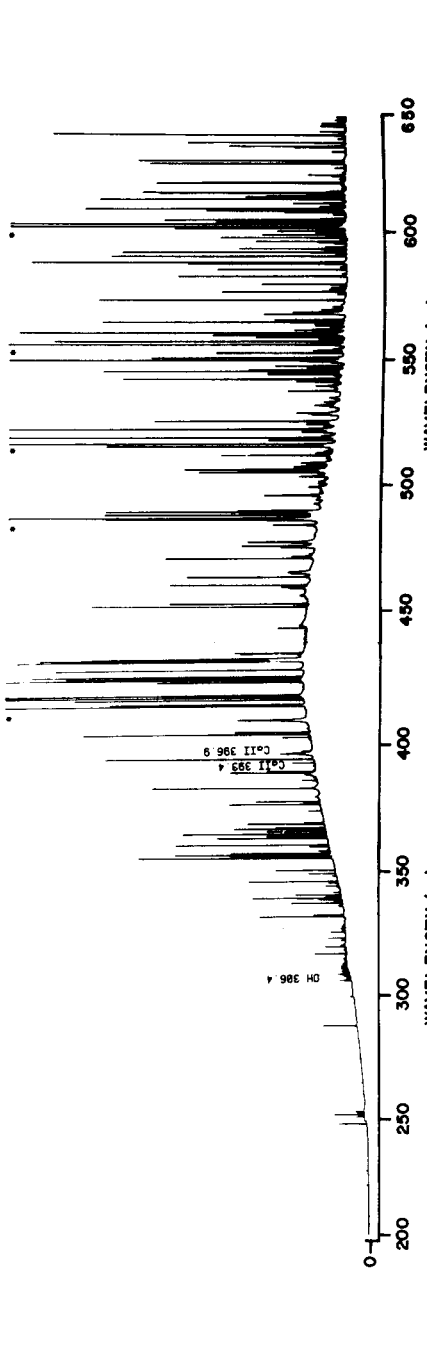

Fig. 1. Typical mini-i.c.p. background spectrum. Asterisk denotes off-scale reading; 18-mm long coolant tube (see text for explanation).

Fig. 2. Background emission from a plasma torch having an extended coolant tube (vertical scale same as Fig. 1). Asterisk denotes off-scale reading; 6-cm long coolant tube.

system viewed a region slightly above the plasma core. In contrast, the longer torch sustained an extended plasma whose core partially fell into the monochromator viewing region. Consequently, when a longer torch was employed, a hotter region in the plasma was viewed, resulting in increased continuum and line intensities and decreased molecular formation. In addition, the longer coolant tube reduced air entrainment into the plasma, thereby lowering further the intensity of nitrogen-containing bands. Because band spectra often cause the most troublesome interferences, it seems advisable to employ torches with longer coolant tubes.

Extending this line of reasoning, it would seem appropriate to elongate the coolant tube to encompass the entire observation region. Figure 2 shows the spectrum generated by a plasma with a torch that contained a coolant tube which extended 6 cm above its plasma tube. Compared to Fig. 1, the spectrum in Fig. 2 (same intensity scale) has a much more intense continuum and is richer in narrow lines. However, band spectra have almost completely disappeared; only a weak OH band at 306.4 nm remains. The Ca and Mn lines appear weaker than in Fig. 1 because a solution containing only 1 μg ml^{-1} of each element was introduced. It is surprising that the Ca II 393.4-nm line is less intense than the Ca II 396.9-nm line; possibly a different excitation mechanism prevails in this type of plasma than in those operated conventionally.

The unusual features in the spectrum of Fig. 2 can be related to the radically different plasma sustained by the extended torch. The core of the plasma (although diluted) extends the full length of the coolant tube (i.e. 6 cm) with a tail flame protruding approximately 5 cm beyond the end of the torch. Because the observation zone is fixed, the spectrum in Fig. 2 originates from the core of the plasma itself where higher temperatures produce more intense continuum and line spectra and enhanced molecular decomposition. In addition, atmospheric gases are completely excluded from the plasma.

An extended plasma of this nature possesses several intriguing attributes, including freedom from molecular emission and enhanced stability. Moreover, it was possible to sustain the extended mini-plasma (under the gas flow and sample introduction conditions given in Table 1) with as little as 400 W of r.f. power. However, even at these lower power levels, the extended quartz coolant tube fogged up quickly (i.e., within two hours of operation), causing a decrease in analyte emission intensity. Consequently, it seems prudent to extend the coolant tube only to the bottom of the observation zone but not beyond it.

Effect of r.f. power and gas flow rates on background emission. Radio-frequency power level has a profound effect on mini-i.c.p. background spectra. As r.f. power was increased, all background features intensified accordingly, demonstrating the necessity for accurate control of r.f. power during determinations. Importantly, the 396.9-nm and 393.4-nm Ca II lines each increased in intensity only 20% when the r.f. was increased from 1.0 kW to 1.5 kW, while

the background level rose over 300%. Therefore, better signal-to-background ratios (and correspondingly, lower detection limits) can be obtained at low powers; similar conclusions were reached by Boumans and de Boer [11] for a conventional plasma.

Increasing the coolant gas flow rate from 7.9 to 9.8 l min^{-1}, caused band intensities to decrease slightly while continuum and line intensities rose. These changes result from both a reduction in air entrainment at the higher flow and also a growth in the plasma core size. In general, these changes were small and little reduction in plasma background seemed to be gained by increasing the coolant gas flow rate.

Nebulizer gas flow also influenced the background; most features decreased in intensity when the nebulizer flow was raised from 0.97 to 1.30 l min^{-1}, presumably because of reduced temperatures in the plasma tail flame [12]. In contrast, the OH band was observed to intensify as aerosol flow rate was raised, probably because of the larger quantities of aerosol being delivered to the plasma. Obviously, precise control of the nebulizer flow is imperative if maximum precision is to be achieved.

This work is taken in part from the thesis of R. N. Savage. The work was supported in part by the National Science Foundation through grants CHE 76-10896 and 77-22152 and by the Office of Naval Research.

REFERENCES

1 R. N. Savage and G. M. Hieftje, Anal. Chem., 51 (1979) 408.
2 C. D. West and D. N. Hume, Anal. Chem., 36 (1964) 412.
3 R. H. Wendt and V. A. Fassel, Anal. Chem., 38 (1966) 337.
4 D. Truitt and J. W. Robinson, Anal. Chim. Acta, 49 (1970) 401.
5 G. F. Kirkbright and A. F. Ward, Talanta, 21 (1974) 1145.
6 J. M. Mermet, Spectrochim. Acta, Part B, 30 (1975) 383.
7 M. H. Abdallah and J. M. Mermet, J. Quant. Spectrosc. Radiat. Transfer, 19 (1978) 83.
8 V. A. Fassel, Science, 202 (1978) 183.
9 G. Horlick, Ind. Res. Dev., 20 (1978) 70.
10 J. A. Dean and T. C. Rains, Flame Emission and Atomic Absorption Spectrometry, Vol. 2, M. Dekker, New York, 1971, Ch. 13.
11 P. W. J. M. Boumans and F. J. de Boer, Spectrochim. Acta, Part B, 32 (1977) 365.
12 D. J. Kalnicky, V. A. Fassel and R. N. Knisely, Appl. Spectrosc., 31 (1977) 137.

Analytica Chimica Acta, 123 (1981) 325—328

Short Communication

RAPID DETERMINATION OF MOLYBDENUM IN BOTANICAL MATERIAL BY ELECTROTHERMAL ATOMIC ABSORPTION SPECTROMETRY

DENNIS R. NEUMAN* and FRANK F. MUNSHOWER

Reclamation Research Group, Montana Agricultural Experiment Station, Montana State University, Bozeman, MT 59717 (U.S.A.)

(Received 7th July 1980)

Summary. Low levels of molybdenum in plant samples are determined by simple digestion in nitric acid followed by electrothermal spectrometry. Sensitivity is enhanced by nitric acid whereas chloride, sulfuric acid, and perchloric acid have inhibiting effects. Recovery of molybdate added to plant samples averaged 94.3%, with a relative standard deviation of 10% for 0.50 μg Mo g^{-1} of plant material. Large numbers of samples can be screened for molybdenum content without tedious organic extractions or long dry ashing processes.

The determination of trace amounts of molydenum in plant samples has gained considerable attention [1—5]. The potential of molybdenosis in cattle and sheep in the western United States [6—8], coupled with the return of stripmined land to forage production have placed added emphasis on determinations of molybdenum in plants grown in revegetated areas.

Determination of molybdenum is commonly done by the thiocyanate method [9, 10]. This procedure requires complete destruction of the sample and suffers interferences from other metal cyanate complexes, particularly iron and copper. The use of flame atomic absorption has gained some attention; however, the relatively poor analytical sensitivity dictates the use of organic extraction to concentrate the analyte and there have been reports of interferences [11—14]. These factors generally preclude the use of flame atomization for determination of molybdenum in botanical materials. Atomic absorption using a graphite atomizer has been successful in the determination of molybdenum in ashed plant samples [15]. This communication describes a procedure that uses furnace atomic absorption to quantify the molybdenum content of acid hydrolyzed plant material. The study includes a discussion of effects of chloride [16], perchloric acid [17], and nitric acid [18] on molybdenum sensitivity.

Experimental

A Varian-Techtron model AA6 atomic absorption spectrophotometer and model 90 carbon rod atomizer were used for the flameless determination of molybdenum. A spectral band pass of 0.5 nm was used to isolate the wavelength of 313.3 nm and peak height absorbance signals were displayed on a

Varian A-25 recorder set at 2 mV range. The carbon rod atomizer parameters (temperature/time) for the dry, ash and atomize cycles were 90°C/30 s, 700°C/30 s and 2750°C/3 s, respectively. Glassware used in the determination was rinsed before use with dilute nitric acid.

Dried plant tissues were ground with a stainless steel Willey mill to pass a 40-mesh screen and a 2.000-g sample was placed in a 250-ml Erlenmeyer flask where a modification of hot acid hydrolysis [19] was used to destroy the organic material. After addition of 20 ml of 7 M HNO_3 (Baker Ultrex), the mixture was heated to a gentle boil for 20 min, cooled, and filtered into a 100-ml volumetric flask using Whatman No. 42 paper. The solution was diluted to volume with distilled, deionized water, and 5-μl aliquots were added to the carbon rod atomizer with a pipet for molybdenum determination.

Standards containing 0, 10, 20, 30, 40 and 50 ng Mo ml^{-1}, prepared from an ammonium molybdate solution containing 1000 mg Mo l^{-1}, were treated identically as the samples.

Results and discussion

The ash temperature of 700°C was adequate to remove the sample matrix and preheat the atomizer tube prior to the atomization cycle. The lifetime of the pyrolytically coated atomizer tubes was reduced to approximately sixty firings owing to the high atomization temperature and acid content of the samples. Background absorbance during the atomization state was below the noise level for both plant samples and molybdenum standards.

The effects of different acid matrices and the addition of chloride on the absorbance of molybdenum were investigated. Solutions of 200 ng Mo ml^{-1} were prepared in 1.4 M HNO_3, 1.8 M H_2SO_4, 0.6 M $HClO_4$ and in an aqueous matrix. Potassium chloride, $CaCl_2$, and NaCl were added to each solution at five levels from 0 to 2000 μg Cl ml^{-1}. In the aqueous solution the absorbance value of 200 ng Mo ml^{-1} was 0.272 ± 0.013. A pronounced enhancement of the molybdenum absorbance signal was exhibited by the 1.4 M HNO_3 matrix (0.405 ± 0.019), while 1.8 M H_2SO_4 reduced the absorbance on molybdenum to 0.200 ± 0.008. Perchloric acid was not fully removed during the ash cycle and considerable "smoke" evolved during atomization. Automatic background correction was inadequate to separate the molybdenum signal from this matrix. All three chloride salts added to aqueous matrix depressed the sensitivity of molybdenum. At a chloride concentration of 500 μg ml^{-1}. potassium chloride reduced the absorbance by 3%, NaCl by 6% and $CaCl_2$ by 4%. Inhibition of the absorbance signals increased with increasing added interferent. At the 2000 μg ml^{-1} added chloride level, the absorbance value was reduced 18, 26 and 28% by KCl, NaCl and $CaCl_2$, respectively. Added chloride exhibited no effect on the absorbance of molybdenum in the 1.4 M HNO_3 or 1.8 M H_2SO_4 matrices.

Enhancement of the absorbance of 200 ng Mo ml^{-1} Mo by nitric acid showed a small increase in absorbance at 0.07 M HNO_3 relative to the aqueous

matrix with increasing absorbances up to a 51% enhancement at 1.4 M HNO_3. The use of 2.8 M HNO_3 rapidly degraded the atomizer tube with resultant loss of reproducibility.

To ascertain the effectiveness of the nitric acid hydrolysis in extracting metals from the plant material, the copper content of fourteen plant samples was determined by a traditional dry ashing and flame atomic absorption method. The results were compared to copper determined by acid hydrolysis—furnace atomization. The averages and standard deviations were 5.5 ± 1.2 μg Cu g^{-1} and 5.6 ± 1.4 μg Cu g^{-1}, respectively. The geometric mean for both procedures was 3.3 μg Cu g^{-1}. These data show good agreement between the two methods. Simpson and Blay [19] obtained excellent extractions of Ca, Fe, Cu, Zn and Sn using hot hydrochloric acid hydrolysis of food samples.

Standard additions of molybdenum to hydrolyzed National Bureau of Standards, Standard Reference Material, Orchard Leaves were carried out to evaluate linearity in the matrix and to compare results with the 1.4 M HNO_3 matrix. The Orchard Leaves were spiked at 0.5, 1.5 and 2.5 μg Mo g^{-1} prior to digestion and determinations were made in triplicate.

Figure 1 shows the standard curve, prepared in 1.4 M HNO_3 and the multiple additions curve, with their linear regression equations. The standard error of the estimate was 0.007 for both regressions. The molybdenum content of the Orchard Leaves determined by multiple additions was 0.39 ± 0.03 μg Mo g^{-1} and a value of 0.36 ± 0.04 μg Mo g^{-1} was calculated using molybdenum standards. Recovery of added molybdenum averaged 94.3%.

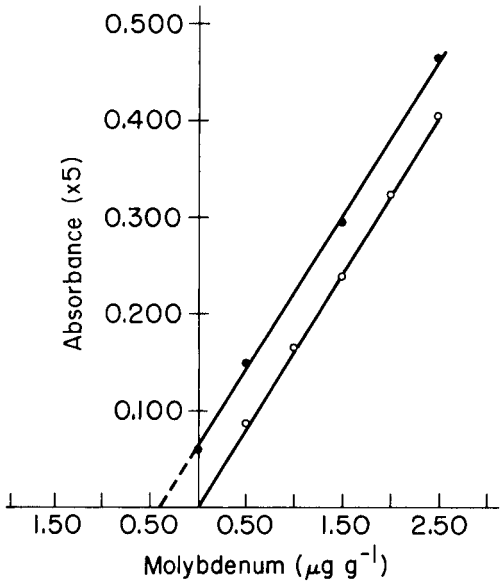

Fig. 1. Calibration curves for molybdenum. Scale expansion (5×). (•) Standard additions curve, Abs (5×) = (0.160 ± 0.005) μg Mo g^{-1} + (0.062 ± 0.004); (○) Standard curve (1.4 M HNO_3), Abs (5×) = (0.166 ± 0.004) μg Mo g^{-1} + (0.005 ± 0.000).

The relative standard deviation for determinations of Mo in Orchard Leaves during a one year period was 10.4% at a level of 0.39 ± 0.04 μg Mo g^{-1} (N = 42). The certified value of molybdenum in Orchard Leaves is 0.3 ± 0.1 μg Mo g^{-1}.

This procedure was compared to another method which employed an acid digestion, complexing the molybdenum with 8-hydroxyquinoline, and extraction with chloroform [20], followed by atomic absorption measurement. Molybdenum was determined in six alfalfa samples, two sweetclover samples, and NBS Orchard Leaves. The levels ranged from 0.33 to 13.4 μg Mo g^{-1}. Linear regression of the data indicated a slope of 1.031 ± 0.043, intercept of −0.003 ± 0.002, standard error of the estimate of 0.586, and a coefficient of correlation of 0.988. The sweetclover sample solutions were diluted by a factor of 5 with 1.4 M HNO_3 to bring them within the concentration range of the analytical standards. The alfalfa levels of molybdenum agree well with those values reported by Kubota [21].

The author expresses appreciation to Dr. Lynn Hageman of the Montana Department of Agriculture for his determination of molybdenum in plant samples using the acid digestion, extraction technique. This work was supported in part by the Peabody Coal Company and the Montana Power Company.

REFERENCES

1 W. H. Parker and T. H. Rose, Vet. Rec., 67 (1955) 276.
2 J. K. Miller, B. R. Moss, M. C. Bell and N. N. Sneed, J. Anim. Sci., 34 (1972) 846.
3 W. R. Chappell and K. K. Petersen (Eds.), Molybdenum in the Environment, Vol. 2, M. Dekker, New York, 1977, p. 375.
4 W. J. Clawson, A. L. Lesperance, V. R. Bohman and D. C. Layhee, J. Anim. Sci., 34 (1972) 516.
5 B. J. Alloway, J. Agric. Sci., 80 (1973) 521.
6 J. A. Erdman, R. J. Ebens and A. A. Case, J. Range Manage., 31 (1978) 34.
7 J. Kubota, J. Range Manage., 28 (1975) 252.
8 J. Kubota, V. A. Lazar, L. N. Langan and K. C. Beeson, Soil Sci. Soc. Am., Proc., 25 (1961) 227.
9 W. Horwitz (Ed.), Official Methods of Analysis, Assoc. Off. Anal. Chem., 12th edn., Washington, DC, 1975, p. 42.
10 E. B. Sandell, Colorimetric Determination of Traces of Metals, Wiley—Interscience, New York, 1959, p. 644.
11 T. V. Ramakrishna, P. W. West and J. W. Robinson, Anal. Chim. Acta, 44 (1969) 437.
12 J. C. VanLoon, At. Absorpt. Newsl., 11 (1972) 3.
13 C. L. McIsaac, Eng. Min. J., 170 (1969) 155.
14 P. Sutcliffe, Analyst, 101 (1976) 949.
15 S. Henning and T. L. Jackson, At. Absorpt. Newsl., 12 (1973) 100.
16 T. Nakahara and C. L. Chakrabarti, Anal. Chim. Acta, 104 (1979) 99.
17 K. Julshamn, At. Absorpt. Newsl., 16 (1977) 149.
18 J. F. Alder and D. A. Hickman, At. Absorpt. Newsl., 16 (1977) 110.
19 G. R. Simpson and R. A. Blay, Food Trade Rev., Aug. (1966) 35.
20 S. R. Koirtyohann and M. Hamilton, The Determination of Molybdenum in Fertilizers, Associate Referee Report to 84th Annual Meeting of AOAC, October 1970.
21 J. Kubota, in W. R. Chappell and K. K. Petersen (Eds.), Molybdenum in the Environment, Vol. 2, M. Dekker, New York, 1977, p. 569.

Analytica Chimica Acta, 123 (1981) 329—333

Short Communication

THE DETERMINATION OF CHLORIDE BY MICROWAVE HELIUM PLASMA EMISSION SPECTROMETRY USING A HYDROGEN CHLORIDE GENERATION TECHNIQUE

J. F. ALDER*, QINHAN JIN** and R. D. SNOOK

Chemistry Department, Imperial College, London SW7 2AY (Gt. Britain)

(Received 1st August 1980)

Summary. Hydrogen chloride is generated from aqueous solution from a concentrated sulphuric acid—potassium sulphate mixture and is passed into a microwave-induced atmospheric pressure helium plasma. Measurement at the Cl-(II) 479.5-nm line gives a linear calibration graph over the range 6 ng (detection limit) to 50 μg of chloride. Other halides, and arsenic, do not interfere, but Te and Hg depress the emission.

In a recent paper [1], a method was reported for the determination of chloride in aqueous solutions by means of a chlorine generation procedure and microwave-induced argon plasma. Another approach is to use a helium plasma supported in a flat TM_{010} cavity at atmospheric pressure, similar to that used by Beenakker [2], and a hydrogen chloride generation method. Beenakker used this cavity and plasma as an element-selective detector for gas chromatography and report improved detection limits for the halogens compared to those obtained with an argon plasma [2]. Beenakker et al. also used the plasma for the determination of metals in solution, but results for chlorine were not reported [3, 4].

Experimental and optimization

Reagents and equipment. The monochromator, microwave generator and recorder have been described previously [1]. The microwave cavity (EMS, Wantage, Berks) similar to that used by Beenakker [2] was mounted so that the helium plasma discharge, contained in a 6.2 mm o.d. by 1.1 mm i.d. fused-silica tube could be viewed axially by the monochromator.

The generating vessel was a 25-ml conical flask with a septum sealed side-arm, to permit introduction of the analyte sample, and was mounted on a stirrer/hot plate. The generated hydrogen chloride was swept through a 20-ml desiccator vessel containing 5 ml of 98% sulphuric acid and into the helium discharge. All reagents were of analytical grade and the helium of high-purity grade (B.O.C., Ltd.).

**On leave from Department of Chemistry, Jilin University, Changchun, People's Republic of China.

Preliminary test. Hydrogen chloride can be generated on a micro-scale from aqueous solutions of chloride by using sulphuric acid. The hydrogen chloride formed can be readily swept out of solution and thus provides an easy means of separating chloride in a form readily amenable to determination by microwave plasma emission. A small amount of water vapour is carried over in the generation process and would perturb the helium plasma so a 98% sulphuric acid trap is placed in the line to desiccate the gas mixture.

Various experiments were carried out using aqueous analyte solutions of sodium chloride in order to optimize the analytical conditions. Poor results were obtained if 98% sulphuric acid was used as the generation medium because too much water vapour was produced to be readily trapped in the desiccant. A concentration of 95% (w/v) sulphuric acid (3 ml H_2O: 97 ml of 98% H_2SO_4) was found to be the highest concentration to give good results. The addition of anhydrous potassium sulphate to the 95% sulphuric acid improves the generation efficiency, possibly by reducing the solubility of hydrogen chloride in the acid mixture: 0.2—0.3 g of K_2SO_4 in 7.5 ml of acid increased the sensitivity by ca. 30%.

Recommended procedure. Potassium sulphate (0.3 g) was dissolved in 7.5 ml of 95% sulphuric acid just prior to the analysis for use as the generation solution. Raising the temperature of the solution, with vigorous stirring, gave improved sensitivity (Fig. 1); 90°C was chosen for normal operation. The effect of decreasing the helium flow rate was to increase the chloride emission intensity, the limit being the cessation of hydrogen chloride transfer into the plasma. The recommended flow rate is 50 ml min^{-1} (Fig. 2). A 50-μl sample aliquot was used; up to 15 injections could be made into the same generating solution without loss of sensitivity (see below). The optimal operating conditions are summarized in Table 1.

Results and discussion

Spectral line and calibration plot. In the method based on the generation of chlorine and its excitation in an argon microwave-induced plasma [1] the

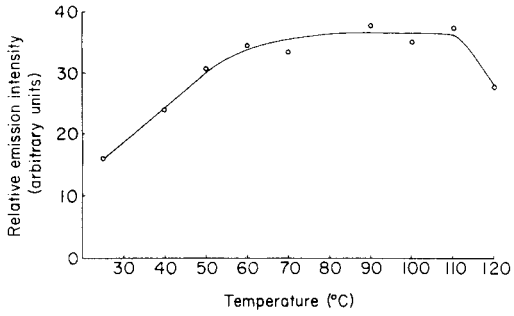

Fig. 1. The effect of the generating solution temperature on the analytical signal.

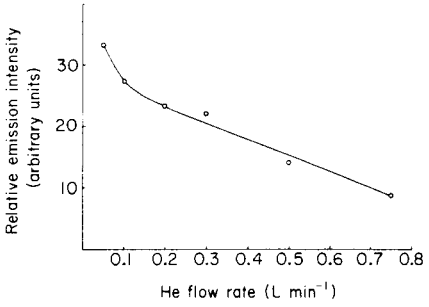

Fig. 2. The effect of helium flow rate on the analytical signal.

TABLE 1

Optimal operating conditions for determination of chloride

Generator forward power	110 W	Temperature of generating solution	90°C
reflected power	18 W	Sample solution volume	50 μl
Photomultiplier e.h.t.	1100 V	Entrance slit width	30 μm
Helium flow-rate	50 ml min^{-1}	Entrance slit height	2 mm
Generating cell volume	25 ml	Exit slit width	30 μm
Generating solution volume	7.5 ml	Wavelength [Cl(II)]	479.5 nm

most sensitive emission was found to be from the 257.6 nm Cl_2 band. In the present study, however, emission from the Cl(II) 479.5-nm line was found to give the best analytical response.

Under optimal operating conditions (Table 1), the plot of log(peak height) vs. log([Cl] added) was rectilinear with a slope of 1 over the range 6 ng—50 μg. The detection limit, defined as that weight of chlorine required to produce a signal twice the standard deviation of the blank, was 6 ng of Cl as NaCl in 50 μl of solution.

The generating ability of the sulphuric acid/potassium sulphate solution decreased only slightly with addition of small volumes of aqueous samples, and up to 1 ml could be added without any change in sensitivity. Above this amount, the peak responses broadened.

Interferences. The effect of a range of elements on the determination of chloride was measured (Table 2). It can be seen that only tellurium and mercury significantly affect the sensitivity. The effect of tellurium is unusual. The addition of 250 ng of chloride to the generating cell in pure aqueous solution yielded a signal of 30 arbitrary units which was reduced to 19 when tellurium was present in 200-fold excess. Subsequent addition of pure 5 ppm chloride solution to the resulting solution in the generation cell, contaminated with tellurium, also gave a signal of 19. The mechanism of this interference is unknown but its effect can be overcome by standard additions of chloride to tellurium-contaminated solutions. There was no trace of any tellurium lines in the spectrum from the plasma under these conditions, thus ruling out the possibility of a volatile tellurium compound being formed and influencing the plasma.

The depressive effect of mercury was studied in more detail. When totally clean glassware and plasma silica tube were employed, emission at the mercury 253.6-nm line was undetectable. When mercury vapour was passed into the plasma (in order to line up the monochromator), the silica tube and plastic connector became contaminated with mercury, and emission at the mercury line remained quite noticeable for a long period. When 250 ng of chloride as the sodium salt was added to the generating solution under these circumstances the emission at the Hg 253.6-nm line increased by a factor of 2.5, whereas a water blank did not affect the signal. Later injections of sodium chloride gave a decreased enhancement because the hydrogen chloride

TABLE 2

Effect of potential interfering elements on the signal obtained for 0.1 μg of chlorine

Element	Salt added	Ratio element/Cl (w/w)	Change in signal[a] (%)	Element	Salt added	Ratio element/Cl (w/w)	Change in signal[a] (%)
F	NaF	200	0	As	Na_3AsO_4	500	−5
Br	NaBr	100	+8	Te	$Te(NO_3)_2$	500	−34
I	KI	200	−3	Hg	$Hg(NO_3)_2$	1000	−90

[a]Mean of three replicates; r.s.d. of signal from 100 ng Cl = 9%.

transported the residual mercury into the plasma. When the experiment was repeated with 250 ng of chloride as sodium chloride and 125 μg of mercury as mercury(II) nitrate in the generating cell, the mercury signal only increased by about 15%. This suggests that the hydrogen chloride is being retained earlier in the system. It seems likely that the mechanism of this interference involves reaction of the hydrogen chloride generated in the reaction vessel with mercury vapour formed either by reduction of the mercury(II) nitrate with sulphuric acid or disproportionation of a mercury(I) salt which may be formed.

Experiments showed that when 125 μg of mercury(II) nitrate was added to the generating cell containing 95% sulphuric acid/potassium sulphate at 90°C, a signal appeared at the Hg 253.6-nm line. This was small when the sulphuric acid desiccator was in the line and larger when it was removed. Examination of the physical constants of mercury salts excludes the possibility of their carry-over and it seems very likely that mercury vapour is the responsible species. It was also observed that the plasma tube became contaminated with mercury during experiments on its interference effects. There is some evidence in the literature that this reduction may occur [5].

The reaction of mercury vapour with hydrogen chloride is known in carbon furnace atomic absorption studies and has been exploited to stabilize mercury [6]. It seems likely that the mercury chloride species formed is trapped in the sulphuric acid desiccator and hence accounts for the depressive interference. What is more interesting is that the signal at the mercury 253.6-nm line when 250 ng of sodium chloride is put into the generating cell and a plasma tube contaminated with mercury is used, is about twenty times that at the Cl-(II) 479.5-nm line. It seems possible, therefore, that this may provide a more sensitive indirect method for chloride.

Conclusion. This method provides a simple and rapid method for the determination of chloride in aqueous solutions and complements the method described previously [1]. The possible exploitation of the effect noticed with mercury is being investigated. It is probable that with suitable sample pretreatment the method could easily be extended to the determination of chloride in biological and petroleum matrices.

We are grateful to the Royal Society of London for a grant for the purchase of the monochromator and to EDT Research for the loan of the microwave cavity.

REFERENCES

1 J. F. Alder, Q. Jin and R. D. Snook, Anal. Chim. Acta, 120 (1980) 147.
2 C. I. M. Beenakker, Spectrochim. Acta, 31B (1976) 483; 33B (1978) 53.
3 C. I. M. Beenakker and P. W. J. M. Boumans, Spectrochim. Acta, 32B (1977) 173.
4 C. I. M. Beenakker, B. Bosman and P. W. J. M. Boumans, Spectrochim. Acta, 33B (1978) 373.
5 E. de Barry Barnett and C. L. Wilson, Inorganic Chemistry, Longmans, London, 1953, pp. 241—244.
6 J. F. Alder and D. A. Hickman, At. Absorpt. Newsl., 16 (1977) 110.

Analytica Chimica Acta, 123 (1981) 335—338

Short Communication

DETERMINATION OF COPPER BY ANODIC STRIPPING VOLTAMMETRY: ANOMALOUS BEHAVIOR IN SEA WATER

REBECCA J. SIEBERT and DAVID N. HUME*

Department of Chemistry, Massachusetts Institute of Technology, Cambridge, MA 02139 (U.S.A.)

(Received 27th May 1980)

Summary. Repeated cycles of plating and stripping using a mercury-coated graphite electrode in raw sea water show increasing negative errors for copper while lead and cadmium are unaffected. This phenomenon, which is not observed in acidified sea water, is attributed to formation of electroinactive Cu(I) species on the electrode.

In the course of a study of the effect of surface-active agents on the determination of heavy metals in sea water by anodic stripping voltammetry, it was noted that copper frequently showed anomalous behavior. When raw (pH 8.4) sea-water samples with or without surface-active agents present were repeatedly plated and stripped using a pre-formed mercury-coated graphite electrode, peak heights and potentials were stable and reproducible for cadmium and lead but changed markedly for copper (Fig. 1). After half a dozen cycles of plating and stripping, the peak potential might have shifted up to 50 mV in the cathodic direction and the peak height or area decreased by as much as 75%. A similar phenomenon observed by Branica et al. [1] with co-deposited mercury films was attributed to limited solubility of copper in mercury, but this observation could not account for our observations and therefore the present investigation was undertaken.

Experimental

Voltammetric measurements were made using a Princeton Applied Research model 174A Polarographic Analyzer coupled with an x-y recorder. Plating was done while stirring at potentials between −0.85 and −1.00 V (SCE) with plating times between 1.5 and 5 min, followed by a 30—45-s rest period. Stripping was done with an anodic scan at 5 mV s^{-1} to −0.10 V and the voltammogram recorded in the differential pulse mode with pulse amplitude 10 mV and a 0.5-s period. The electrode was held at −0.10 V between determinations and during sample additions.

Most of the work was done using an Environmental Science Associates (ESA; Bedford, MA) cell tower and electrode assembly (model 310). The electrode consists of a tube of crystalline pyrolytic graphite (9.35 mm i.d., 31.75 mm long) covered with an impermeable polymeric coating, except for the active inner surface which was plated fresh daily with mercury to

a density of about 6×10^{-7} mol cm^{-2}. In use, the electrode is stationary and the sample is circulated through it by a graphite stirring propeller attached to a constant speed motor. Cell volumes were 5 or 25 ml. Similar results were obtained with a conventional mercury-coated wax-impregnated graphite electrode [2].

Sargasso sea water, known to be low in both trace metals and dissolved organic carbon, was used as the standard background electrolyte, which for most of the experiments was made about 10^{-8} M in cadmium and copper and 5×10^{-9} M in lead. Mercury coatings were applied by electrolyzing sea water which was 5×10^{-3} M in mercury(II) chloride at pH 2.

Results

The following ten sets of experiments were performed to identify the relevant variables and explain the effects.

Repeated cycles of plating and stripping in the same sample gave increasingly smaller copper peaks with little or no change in cadmium or lead as shown in Fig. 1. The absence of cadmium and lead did not affect the copper behavior; hence the electrode itself is not generally deactivated and the effect is peculiar to copper.

Addition of more copper solution to a sample which had been cycled until the copper peak had been largely suppressed immediately resulted in a peak size normal for the amount of copper just added, but which diminished

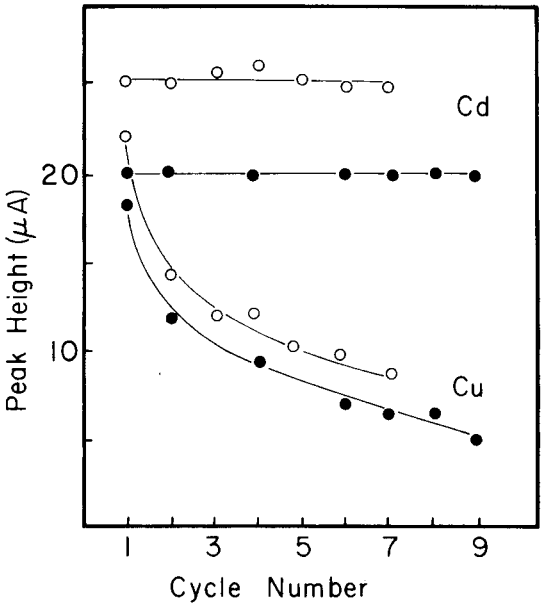

Fig. 1. Peak height as a function of repeated plating—stripping cycles for pH 8.4 sea-water samples made approximately 10^{-8} M in cadmium and copper. Filled and open circles represent runs on two different electrodes.

again on further cycling. This indicates that it is not deactivation of the electrode, but of the copper in the sample that is taking place.

The decrease in the height of the copper peak was the same whether the plating was done at −0.6 V or at −1.0 V. At −0.6 V there is no possibility of plating zinc in this medium, therefore formation of a copper–zinc intermetallic compound cannot be the explanation.

Replacement of the silver chloride reference electrode with a calomel electrode had no effect. The interfering effect of silver on copper which has sometimes been observed [3] is not present.

A background electrolyte of 0.5 M sodium chloride at pH 7.0 showed the same behavior as raw sea water, but in 0.5 M potassium nitrate at pH 7, the copper peak did not decrease on cycling. Chloride ion is therefore an important factor.

Sea water acidified to pH 3.0 with hydrochloric acid gave a higher copper peak and showed no decrease in copper peak height on cycling. A raw sea-water sample plated and stripped until the peak height had diminished substantially did, if acidified, give a peak height normal for acidic solutions on plating and stripping. Both pH and chloride are important factors.

A raw sea-water sample was cycled until the copper peak had decreased about 75%. It was then plated for the usual length of time and, without changing the potential or breaking the circuit, the sample was replaced with acid sea water having the same copper concentration as the original raw sea water. On stripping, the peak current was substantially greater than would have been expected from a single cycle in acidified sea water. Evidently stripping rather than plating is gradually inhibited in raw sea water.

An acidified sea-water sample was cycled several times showing a reproducible peak height for copper. It was then plated and, without changing the potential or breaking the circuit, the sample was replaced with raw sea water. The first stripping peak was the same as it had been in the acidified sample, but on repeated cycling, the peak size decreased in the manner characteristic of raw sea-water samples.

The drastic drop in peak height on cycling was characteristic of small (5 ml) samples. With large (25—50 ml) samples, the decrease was much less, of the order of 10—15%. With the large surface area and high plating efficiency of the electrode used, the copper concentration cannot be assumed constant during a plating cycle. For small sample volumes, a significant fraction of the total is deposited on the electrode during each cycle.

A raw sea-water sample was placed in the cell and held with constant stirring at a potential slightly anodic to the copper stripping peak (−50 to −200 mV) for a period of time equivalent to several plating–stripping cycles. A plating–stripping cycle was then performed, and the initial peak height showed essentially the same decrease as would have been found if plating–stripping cycles had been going on during the holding period.

Discussion

It is known from polarographic studies that at potentials between −50 and −200 mV vs. SCE, Cu(II) ions in approximately 0.5 M chloride medium are reduced to Cu(I), predominantly as the $CuCl_2^-$ ion [4]. At more negative potentials, the reduction proceeds to copper metal at mercury electrodes. Similarly, a copper amalgam held at potentials more positive than about −200 mV in such a chloride medium is oxidized to $CuCl_2^-$. If, in a neutral or slightly alkaline chloride medium, the Cu(I) ions form an insoluble or highly adsorbable species which is relatively electro-inactive and adheres to the electrode surface, the observed behavior becomes understandable. A fraction of the Cu(I) generated in each cycle, or in the holding time equivalent to a cycle, is deposited on the electrode in a less reactive form, decreasing the peak height. Acidification of the depleted sample dissolves the deposit and subsequent cycles are normal. If the acidification is done at the end of a plating cycle with the electrode still at the plating potential, the Cu(I) released at the electrode surface in relatively high concentration could be plated immediately, giving a higher than normal peak when stripped. Although no basic copper(I) chloride compound with the required characteristics seems to have been described in the literature, the postulation of such a compound appears to be the only simple explanation of the observed behavior.

From a practical standpoint, it is well to avoid the determination of copper in raw sea water whenever possible. Acidification of the sea water is also desirable to prevent loss of copper by adsorption on container walls or suspended matter, and to increase sensitivity. If determination of copper in raw sea water is attempted, large sample volumes, short plating times, and the method of known additions should be used.

This work was supported in part by the National Oceanic and Atmospheric Administration through the M.I.T. Sea Grant Program.

REFERENCES

1 M. Branica, L. Sipos, S. Bubic, and S. Kozar, in P. D. LaFleur (Ed.), Accuracy in Trace Analysis, N.B.S. Special Publication 422, U.S. Dept. of Commerce, Washington, DC, 1976, pp. 917—928.
2 T. R. Gilbert and D. N. Hume, Anal. Chim. Acta, 65 (1973) 461.
3 W. R. Seitz, Ph.D. Thesis, Massachusetts Institute of Technology, 1970.
4 J. J. Lingane, Ind. Eng. Chem., Anal. Ed., 15 (1943) 583.

Analytica Chimica Acta, 123 (1981) 339—340

Short Communication

A SIMPLE FLOW CELL FOR QUANTITATIVE ELECTRON SPIN RESONANCE MEASUREMENTS ON AQUEOUS SOLUTIONS

WARREN G. BRYSON

Hugh Adam Cancer Biology Research Unit, Department of Surgery, University of Otago, P.O. Box 913, Dunedin (New Zealand)

BARRIE M. PEAKE*

Department of Chemistry, University of Otago, P.O. Box 56, Dunedin (New Zealand)

(Received 30th July 1980)

Summary. The flow cell decreases the time required to change samples to 1 min, and a typical relative standard deviation of measurement is improved from about 0.3% to 0.1%.

Electron spin resonance (e.s.r.) spectroscopy has been successfully applied to the determination of several paramagnetic transition metal ions in aqueous solutions [1]. The technique had the disadvantage that changing samples is time-consuming because of the necessity to remove the e.s.r. cell from the microwave cavity. This step requires detuning the spectrometer, releasing the locking device springs on the cell holders, removing the cell, manual rinsing and filling of the cell with the new sample, replacement and realignment of the cell in the microwave electric field and retuning the cavity. This procedure required up to 5 min per sample. Small errors in repositioning each sample decreased the precision of analysis. To alleviate both these problems, a flow cell which allows changing of samples without removing the cell was developed. Although flow cells for e.s.r. work have been described before [2], this note is the first to report the use of such a cell for analytical e.s.r. applications.

Experimental

A Varian E-4 e.s.r. spectrometer with a single TE_{102} cavity was used for all measurements. A standard Suprasil cell (Scanco S812 flat cell) was modified for use as a flow cell as shown in Fig. 1. A silicone rubber outlet tube (a) connected the cell to a variable-speed peristaltic pump. A glass stopper with a glass tube attachment (b) connected the outlet tube (c) to a section of silicone rubber (d) inserted into the cell. This arrangement reduced void volume, which allowed faster rinsing of the sample cell with smaller volumes of sample. The outer and inner diameters of the silicone rubber tubing were chosen to provide watertight seals with the quartz outlet tube (c) and the stopper attachment tube (b). Samples were drawn into the cell through the polythene tube (g).

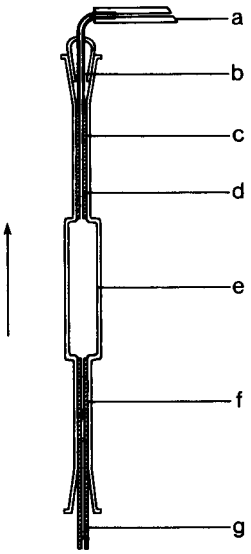

Fig. 1. Flow cell for quantitative e.s.r. measurements on aqueous samples.

Flow characteristics of the cell were determined by pumping through a strongly coloured solution such as 0.01 mol dm^{-3} potassium permanganate; 0.5 cm^3 of solution was required to fill the cell chamber (e) and inlet tube (g) completely, while 1.9 cm^3 of distilled water effectively rinsed the permanganate from the cell.

To change samples, the microwave power was reduced to 25 dB. The new sample was pumped through to rinse and load the cell. The microwave power was then reset and if the sample had different dielectric properties, the cavity tuning iris was used to readjust the detector current to 300 μA. The pump was turned off so that the sample solution was static in the cell, and the new e.s.r. spectrum was recorded.

Results

This cell was used for a wide range of measurements reported previously [1]. Its use decreased the average time for changing samples to no more than 1 min at a flow rate of 4 cm^3 min^{-1}. At the same time the precision of analysis was better than that obtained using standard sample changing procedures and is now limited solely by instrumental factors. For example, for the determination of 1×10^{-3} mol dm^{-3} chromium(III), the relative standard deviation (12 determinations) was 0.1%.

REFERENCES

1 W. G. Bryson, D. P. Hubbard, B. M. Peake and J. Simpson. Anal. Chim. Acta, 116 (1980) 353 and preceding papers.

2 See, for example, J. R. Bolton, D. C. Borg and H. M. Swartz, in H. M. Swartz, J. R. Bolton and D. C. Borg (Eds.), Biological Applications of Electron Spin Resonance, Wiley–Interscience, New York, 1972, p. 111.

Analytica Chimica Acta, 123 (1981) 341—345

Short Communication

POTENTIOMETRIC DETERMINATION OF SOME COMMON ALKALOIDS WITH A PICRATE-SELECTIVE ELECTRODE

E. P. DIAMANDIS and T. P. HADJIIOANNOU*

Laboratory of Analytical Chemistry, University of Athens, Athens (Greece)

(Received 9th July 1980)

Summary. Potentiometric methods are described for the determination of alkaloids, based on the formation of insoluble alkaloid picrate salts, using a picrate ion-selective indicating electrode. Micro-amounts of strychnine, papaverine, quinine and cocaine were determined by direct potentiometry and titrimetrically, using Gran plots, with average errors of about 4% and 2%, respectively. The method was successfully applied to pharmaceutical preparations.

The commonest procedure for the determination of alkaloids in pharmaceutical preparations includes precipitation by making the solution alkaline with ammonia, extraction with chloroform, evaporation to dryness, and weighing the residue. Such methods are fairly accurate but demand toxic reagents and are time-consuming. Alkaloids are also determined by spectrofluorimetry [1] and differential pulse polarography [2].

In this communication, potentiometric methods are described for the determination of several alkaloids with picrate ions, either by direct potentiometry or by potentiometric titration, using as indicator electrode the recently described picrate ion-selective electrode [3—5]. The method is based on the formation of insoluble alkaloid picrates. Both versions are sensitive, rapid, fairly accurate and simple, and were employed successfully for the determination of papaverine and quinine in pharmaceutical preparations. The method, properly modified, can be used for the determination of many alkaloids.

Experimental

Instrumentation. The electrodes, the reaction cell and the recording system were the same as previously reported [3].

Reagents. All solutions were prepared with deionized twice-distilled water and reagent-grade substances, except where stated.

Standard picrate solutions were prepared by neutralizing suitable picric acid solutions with sodium hydroxide to the appropriate pH value. All picrate solutions were stored in amber bottles. The picric acid used (Merck 99.8%) was standardized against standard sodium hydroxide solution.

Solutions of strychnine sulfate, papaverine hydrochloride, quinine hydrochloride, and cocaine hydrochloride (0.0100 M) were prepared by dissolving pure (Merck) substances in water. More dilute standard solutions were prepared by dilution.

Method 1. (For the direct potentiometric determination of alkaloids with sodium picrate.) Pipet into the reaction cell a 10.00-ml aliquot of the sample and 10.00 ml of standard sodium picrate solution. Start the stirrer, and after the potential has stabilized to ±0.1 mV (ca. 7 min) record the millivoltmeter reading (E_2). Repeat the procedure replacing the sample with 10.00 ml of water (E_1).

For strychnine samples in the ranges 2.00×10^{-4}—2.00×10^{-3} M and 4.00×10^{-3}—2.00×10^{-2} M, the sodium picrate solutions used were 3.00×10^{-3} and 3.00×10^{-2} M, respectively, at pH 5.8. For papaverine samples in the ranges 2.00×10^{-4}—1.00×10^{-3} M and 1.00×10^{-3}—1.00×10^{-2} M, the sodium picrate solutions used were 1.50×10^{-3} and 1.50×10^{-2} M, respectively, at pH 3.5. For quinine and cocaine samples in the range 1.00×10^{-3}—1.00×10^{-2} M, a 1.50×10^{-2} M sodium picrate solution at pH 6.0 was used.

After the completion of the reaction, the free picrate concentration, [P], is calculated from $[P] = [P]_0$ antilog $(\Delta E/S)$, where $[P]_0$ is the initial picrate concentration, $\Delta E = E_2 - E_1$, and S is the slope of the potential vs. log [P] curve.

Method 2. (For the titrimetric determination of alkaloids with sodium picrate, using a Gran plot.) Pipet into the reaction cell a 15.00-ml aliquot of the sample, start the stirrer and titrate with a standard sodium picrate solution. Reach the region of the equivalence point with 3 or 4 large increments of titrant, and then take 5—6 additional values of the cell potential vs. titrant volume in the range 10—100% beyond the equivalence volume.

Calculate the factor $F = (V_0 + V)10^{E/S}$, where V_0 is the initial volume, V is the volume of titrant added, and E is the cell potential [6]. The plot F vs. ml of titrant added is linear with the x-intercept at the equivalence volume. The line is calculated by a least-squares fit.

Clean the reaction cell and the reference electrode with acetone and the picrate electrode with water, and wipe with soft paper after each measurement.

Results and discussion

The optimum pH for each alkaloid was calculated from $pH \leqslant 12 - pK_b$, where K_b is the dissociation constant of the alkaloid. At this pH value the alkaloid is nearly 100% in the cationic form (protonated).

Determinations on aqueous alkaloid solutions of known concentrations by direct potentiometry gave the results shown in Table 1. The average recovery of strychnine was about 97%; similar results were obtained with a phosphate buffer of pH 5.8. The average recovery of papaverine was 99%; similar results were obtained with a phthalate buffer of pH 3.5. For papaverine solutions in the range 1×10^{-4}—2×10^{-4} M no precipitate was visible in the reaction cell, although ΔE values were obtained. The average recovery of quinine was 96%. The large negative error in the first (20 μmol) quinine sample is due to the solubility of the picrate salt. The positive errors in the determination of cocaine are due to the response of the picrate electrode to

TABLE 1

Results for aqueous solutions of alkaloids by direct potentiometry

Alkaloid	Picrate (μmol)	Alkaloid (μmol)		Error (%)
		Taken	Found[a]	
Strychnine sulfate,	30.0	4.00	3.88	−3
$2C_{21}H_{22}N_2O_2 \cdot H_2SO_4 \cdot 5H_2O$,	30.0	8.00	8.16	+2
M.w. 856.96	30.0	20.0	19.0	−5
	300	40.0	38.0	−5
	300	140	134	−4
	300	200	198	−1
Papaverine hydrochloride,	15.0	2.00	1.98	−1
$C_{20}H_{21}NO_4 \cdot HCl$,	15.0	4.00	3.92	−2
M.w. 375.9	15.0	10.0	9.6	−4
	150	40.0	39.2	−2
	150	70.0	70.7	+1
	150	100	101	+1
Quinine hydrochloride,	150	20.0	17.2	−14
$C_{20}H_{24}N_2O_2 \cdot HCl \cdot 2H_2O$,	150	40.0	37.2	−7
M.w. 396.9	150	70.0	72.1	+3
	150	100	101	+1
Cocaine hydrochloride,	150	20.0	22.6	+13
$C_{17}H_{21}NO_4 \cdot HCl$,	150	40.0	42.0	+5
M.w. 339.81	150	70.0	71.4	+2
	150	100	102	+2

[a]Single measurements.

the protonated form of cocaine. The picrate electrode exhibits near-Nernstian response to various quaternary ammonium compounds [7]. This was also true for most of the cations of the alkaloids tested.

In semi-automatic potentiometric titrations with liquid-membrane ion-selective electrodes, there is usually a blank. For better accuracy, an alternative is to carry out the titration manually and treat the results by Gran's method [8, 9]. Gran plots were used here to establish the equivalence point for two reasons: (a) before the equivalence point, the reaction is not fast enough so that obtaining a full titration curve is time-consuming; (b) in dilute solutions, the break at the end-point is too shallow for successful calculations of the end-point. Figure 1 shows typical titration curves for strychnine and the corresponding Gran plots.

Titrimetric determinations on aqueous alkaloid solutions of known concentrations gave the results shown in Table 2. The relative standard deviations were 0.30 and 0.34% for 1.07×10^{-2} and 1.07×10^{-3} M strychnine solutions, and 0.32 and 1.5% for 5.33×10^{-3} M papaverine and quinine solutions, respectively (n = 5).

Applications. The proposed methods were applied to the determination of papaverine and quinine in two pharmaceutical preparations. Thirty papaverine hydrochloride tablets (Knoll) and ten quinine hydrochloride tablets

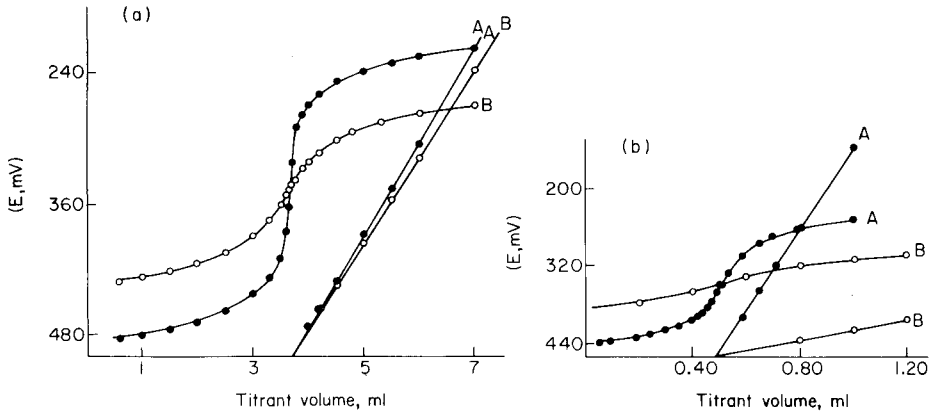

Fig. 1. Titration curves for the titration of 15 ml of strychnine sulfate with sodium picrate and the corresponding Gran plots. In (a): (A) 2 × 10^{-2} M strychnine sulfate with 8 × 10^{-2} M sodium picrate; (B) 2 × 10^{-3} M strychnine sulfate with 8 × 10^{-3} M sodium picrate; for curve B, factor F in the y-axis was multiplied by 10. In (b): (A) 2.67 × 10^{-3} M strychnine sulfate with 8 × 10^{-2} M sodium picrate; (B) 2.67 × 10^{-4} M strychnine sulfate with 8 × 10^{-3} M sodium picrate.

(Boehringer—Mannheim) were powdered and extracted with 400 ml of water. After filtering, the volume was adjusted to 500.0 ml in a volumetric flask. The samples were analyzed by a standard [10] and the proposed potentiometric methods. The results are summarized in Table 3.

TABLE 2

Titrimetric potentiometric determination of alkaloids with sodium picrate

Alkaloid	Concentration range (M)	Picrate[a] (M)	Alkaloid (μmol)		
			Taken	Found[b]	
Strychnine sulfate	2.67 × 10^{-4}—2.00 × 10^{-3}	8.00 × 10^{-3}	4.00	3.92	−2
			16.0	15.6	−2
			30.0	29.2	−2
	2.67 × 10^{-3}—2.00 × 10^{-2}	8.00 × 10^{-2}	40.0	39.2	−2
			160	154	−3
			300	294	−2
Papaverine hydrochloride	1.33 × 10^{-3}—1.00 × 10^{-2}	4.00 × 10^{-2}	20.0	19.9	−0
			80.0	80.8	+1
			150	151	+0
Quinine hydrochloride	1.33 × 10^{-3}—1.00 × 10^{-2}	4.00 × 10^{-2}	20.0	18.0	−10
			80.0	79.3	−0
			150	151	+0
Cocaine hydrochloride	2.67 × 10^{-3}—2.00 × 10^{-2}	8.00 × 10^{-2}	40.0	41.7	+4
			80.0	82.2	+2
			140	140	−
			300	298	−0

[a]The pH of the sodium picrate solution was about 6 for the titration of strychnine, quinine and cocaine, and 3.5 for the titration of papaverine. [b]Single measurements.

TABLE 3

Comparison of results by the potentiometric and gravimetric methods for the determination of papaverine and quinine in pharmaceutical preparations

Pharmaceutical preparation	Alkaloid (μmol)[a]		
	Standard method	Direct potentiometry	Titrimetric method
Papaverine hydrochloride tablets	756 (35)	707 (12)	640 (10)
Quinine hydrochloride tablets	729 (95)	788 (6)	783 (17)

[a]The numbers in parentheses are the differences between two measurements.

In conclusion, the proposed potentiometric methods are faster and simpler than the standard methods. They can also be applied to other alkaloids which give insoluble picrate salts. Efforts to determine atropine, codeine and morphine were unsuccessful because of the great solubility of their picrate salts. The K_{so} of the atropine picrate salt was calculated to be 1.5×10^{-5} at 26°C.

The authors thank the Hellenic Committee for Narcotics, Ministry of Social Services, for providing the alkaloids and M. A. Koupparis for valuable suggestions.

REFERENCES

1 N. V. Rama Rao and S. N. Tandon, Anal. Lett., 11 (1978) 477.
2 G. Sontag and G. Kainz, Mikrochim. Acta(Wien), (1977II) 425.
3 T. P. Hadjiioannou and E. P. Diamandis, Anal. Chim. Acta, 94 (1977) 443.
4 E. P. Diamandis and T. P. Hadjiioannou, Mikrochim. Acta (Wien), (1977II) 255.
5 E. P. Diamandis, M. A. Koupparis and T. P. Hadjiioannou, Microchem. J., 22 (1977) 498.
6 D. Midgley and K. Torrance, Potentiometric Water Analysis, J. Wiley, New York, 1978.
7 E. P. Diamandis and T. P. Hadjiioannou, Mikrochim. Acta (Wien), in press.
8 G. Gran, Analyst, 77 (1952) 661.
9 W. Selig, Microchem. J., 22 (1977) 1.
10 The Dispensatory of the United States of America, 1950 edn., H. Lippincott.

Analytica Chimica Acta, 123 (1981) 347—349

Short Communication

SPECTROPHOTOMETRIC DETERMINATION OF CHLORIDE IN PLANTS

CELSO A. FESSEL GRANER* and JOÃO BAPTISTA PAULUCCI

Departamento de Química Analítica, Instituto de Química, UNESP, Caixa Postal 174, 14800-Araraquara, São Paulo (Brasil)

(Received 24th June 1980)

Summary. This indirect spectrophotometric determination of chloride in plants is based on displacement of thiocyanate from mercury(II) thiocyanate. Thiocyanate is extracted into nitrobenzene as tris(1,10-phenanthroline)iron(II) thiocyanate for measurement at 516 nm. Accuracy and precision are similar to those of the Volhard method but only about 2—200 mg samples are needed.

A spectrophotometric method for the determination of thiocyanate by using extraction of tris(1,10-phenanthroline)iron(II) thiocyanate into nitrobenzene was proposed by Yamamoto et al. [1]. The method was extended to the determination of chloride [2] by utilizing the exchange reaction between mercury(II) thiocyanate and chloride to release thiocyanate [3], and was applied for determining chlorides in fluvial waters [2]. The remarkable color stability of the organic extract coupled with the high sensitivity and selectivity associated with the procedure makes it very suitable for the analysis of biological materials in which chloride occurs in low concentrations (e.g., in plants). Conventional titrimetric procedures for chloride in such materials [4, 5] are not always adequate or even feasible. The present communication deals with the determination of chloride in plants by applying the tris(1,10-phenanthroline)iron(II) thiocyanate method [2].

Experimental

Materials and equipment. The samples consisted of leaves of five different kinds of plants dried and ground by the usual method [4]. A Varian-Techtron spectrophotometer model 635, and an Orion Research model 701 pH meter were used for the absorbance and pH measurements, respectively.

Reagents. Mercury(II) thiocyanate solution (1.00×10^{-3} M) prepared by dissolving 0.3168 g of the salt in about 900 ml of warm deionized water, cooled and diluted to 1 l with water; the mercury(II) thiocyanate was prepared from stoichiometric quantities of mercury(II) nitrate and potassium thiocyanate [6]. Potassium dihydrogenphosphate (0.25 M) was adjusted to pH 2.5 with sulphuric acid. Tris(1,10-phenanthroline)iron(II) solution (1.00×10^{-2} M) was prepared by dissolving 0.3922 g of iron(II) ammonium sulphate hexahydrate and 0.5947 g of 1,10-phenanthroline monohydrate in 5×10^{-3} M sulphuric acid and diluting to 100 ml with the same acid; a 6.00×10^{-4} M solution was prepared by dilution with water as required.

Titrimetric determination of chloride. For comparison, Volhard's method [4, 5] was used, with nitrobenzene to isolate the silver chloride.

Indirect spectrophotometric determination. For the standard curve, 5 ml of the dihydrogenphosphate solution, 5 ml of the mercury(II) thiocyanate solution, 2—10 ml of 2.00×10^{-4} M sodium chloride solution and 5 ml of a 6.00×10^{-4} M tris(1,10-phenanthroline)iron(II) solution were transferred to a series of separatory funnels. After dilution to 25 ml with water, each solution was shaken vigorously with 10 ml of nitrobenzene for 1 min. The organic phase was percolated, through hydrophilic cotton in the funnel stem, into 10-mm optical cells for measurement at 516 nm against a reagent blank extract.

Plant samples (0.1—1 g) were ashed at 500°C and, after cooling, dissolved in 50 ml of 5×10^{-3} M sulphuric acid. The procedure was then the same as that described for the standard curve, except that the standard chloride solution was replaced by 1—10 ml of the plant extract.

Results and discussion

The residual water in the organic phase was removed simply by percolating the extract through hydrophilic cotton in the funnel stem, instead of treating with anhydrous sodium sulphate, as recommended earlier [2]. The relationship between absorbance and chloride concentration in aqueous solution was linear for the range specified, which confirms the validity of this simplification. Typically, the linear relationship corresponded to the expression: $\mu g\ Cl^-/25$ ml aqueous phase = $(A + 0.015) \times 122$, with a linear correlation coefficient of 0.997 ($N = 6$).

The percentages of chloride in samples of foliar tissues of different plants were estimated by the proposed method and by Volhard's procedure. The results, compared in Table 1, show that the methods give very similar results. However, there is a great difference in their sensitivity, and the proposed method is particularly valuable for determinations of low chloride contents. The conventional titrimetric procedure [4, 5] requires at least 25 g of citrus

TABLE 1

Determination of chloride in foliar tissue samples of different plants

Sample	Chloride content (%)			
	Volhard's method		Proposed method	
	Average[a]	R.s.d. (%)	Average[a]	R.s.d. (%)
Citrus tree	$(1.58 \pm 0.06) \times 10^{-2}$	4.4	$(1.63 \pm 0.04) \times 10^{-2}$	2.6
Coffee tree	$(1.83 \pm 0.04) \times 10^{-1}$	2.4	$(1.83 \pm 0.05) \times 10^{-1}$	2.9
Corn plant	$(3.20 \pm 0.06) \times 10^{-1}$	2.2	$(3.17 \pm 0.05) \times 10^{-1}$	1.7
Banana tree	$(6.25 \pm 0.02) \times 10^{-1}$	0.4	$(6.28 \mp 0.06) \times 10^{-1}$	1.1
Wild chicory	(2.57 ± 0.01)	0.4	(2.59 ± 0.03)	1.4

[a]Average of three determinations with standard deviation.

leaves for ashing, whereas the proposed method needs only 1 g of sample for ashing and only a fifth of the solution is actually used.

The authors thank the "Fundação de Ensino e Tecnologia de Alfenas, MG", for supplying the samples. J.B.P. thanks the "Fundação de Amparo à Pesquisa do Estado de São Paulo" for the award of a Junior Research Fellowship.

REFERENCES

1 Y. Yamamoto, T. Tarumoto and Y. Hanamoto, Bull. Chem. Soc. Jpn., 42 (1969) 268.
2 Y. Yamamoto, T. Kumamaru, A. Tatehata and N. Yamada, Anal. Chim. Acta, 50 (1970) 433.
3 I. Iwasaki, S. Utsumi and T. Osawa, Bull. Chem. Soc. Jpn., 25 (1952) 226.
4 W. Horwitz (Ed.), Official Methods of Analysis of the Association of Official Analytical Chemists, AOAC, Washington, DC, 1975, p. 34.
5 R. A. Catani, F. R. P. Morais and H. Bergamin F°, An. Esc. Super. Agric. "Luiz de Queiroz", 26 (1969) 93.
6 F. Wagenknecht and R. Juza, in G. Brauer (Ed.), Handbook of Preparative Inorganic Chemistry, Zinc, Cadmium, Mercury, Academic, New York, 1965, p. 1067.

Analytica Chimica Acta, 123 (1981) 351—354

Short Communication

DETERMINATION OF SULFUR DIOXIDE IN SOLUTIONS BY PYRIDINIUM BROMIDE PERBROMIDE AND TITRIMETRIC AND FLOW INJECTION PROCEDURES

T. R. WILLIAMS*, S. W. McELVANY and E. C. IGHODALO

Department of Chemistry, The College of Wooster, Wooster, OH 44691, (U.S.A.)

(Received 7th February 1980)

Summary. Sulfur dioxide can be determined by its reaction with pyridinium bromide perbromide using photometric titrations and flow injection procedures. Both methods are useful down to 30 ppm, and are unaffected by ammonia or nitrogen dioxide. Both mercury(II) and EDTA interfere under some circumstances.

Many methods are available for the determination of sulfur dioxide, but most have interferences. The most notable is the West—Gaeke method [1], which is suitable for monitoring sulfur dioxide down to 0.005 ppm in air (20 ppm in solution) [1], and in the presence of nitrogen dioxide after addition of sulfamic acid [2]. Although Scaringelli et al. [3] improved the sensitivity and reproducibility of the method, there has been debate concerning ammonia interference in the West—Gaeke method [4, 5].

In an attempt to develop a simple interference-free determination of sulfur dioxide, the reaction of sulfur dioxide with pyridinium bromide perbromide, PBPB, was explored. This reagent has been used to determine unsaturated compounds such as aromatic amines, phenols and ethers [6, 7]. The reagent oxidizes sulfur dioxide to sulphate with the concomitant reduction of bromine and loss of absorbance in the near-ultraviolet and visible regions.

Both titrimetric and flow injection techniques have been evaluated for SO_2 determinations. Ammonia and nitrogen dioxide cause no adverse effects. Under certain conditions, EDTA and mercury(II) ion may interfere.

Experimental

Titration apparatus. All photometric titrations were done on a Bausch and Lomb Spectronic 20 spectrophotometer. The titration cell was as designed by Rehm et al. [8]. A 10-ml buret was used.

Solutions were mixed using a magnetic stirrer.

Flow injection apparatus. The apparatus represented in Fig. 1 is similar to that described by Růžička and Hansen [9]. A Zeromax Sigmamotor peristaltic pump, with a variable pumping rate, was employed. The sulfur dioxide sample and reagent were mixed in a 0.3-m mixing coil, connected to a flow-through cuvette (Sargent-Welch S-75741) with a 1.00-cm path length and

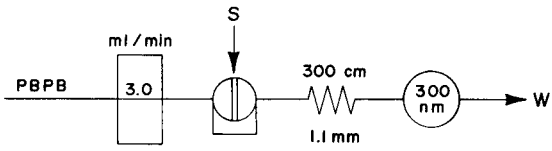

Fig. 1. Flow diagram for the spectrophotometric determination of SO_2. S, point of sample injection; W, waste; tube length in cm; tube internal diameter in mm.

a volume of 1.5 ml. Spectrophotometric measurements were made on a Beckman DU spectrophotometer equipped with a Gilford attachment (model 222) and a Bio-Rad Model 1310 strip chart recorder.

Reagents. Pyridinium bromide perbromide (Arapahoe Chemical Co., Boulder, CO) was used without further purification. For titrations, a 0.05 M solution was prepared in 10% methanol—90% glacial acetic acid (v/v), and standardized by spectrophotometric titrations against primary-standard arsenic trioxide. For flow injection work, a 5.67×10^{-5} M solution of PBPB was prepared by dilution of the stock solution with methanol. A stock solution (0.4 M of sulfur dioxide was prepared by bubbling anhydrous sulfur dioxide (Union Carbide Corp.), into a desired volume of deionized water, and standardized by titration [10]. Samples were prepared by dilution of the sulfur dioxide stock solution in deionized water for the titration procedure, and in methanol for flow injection determinations. Solutions of ammonia and nitrogen dioxide for the interference studies were prepared by adding the liquified gases to methanol. Concentrations of the solutions were determined from the weight changes of the methanol solutions.

Titration procedure. After setting the wavelength to 425 nm, a 10-ml aliquot of a sulfur dioxide sample was added to 50 ml of methanol, and the spectrophotometer reading was adjusted to zero. The solution was titrated with the 0.0500 M PBPB solution with three or four readings being made on each side of the equivalence point. The end-point was determined from the intersection of two straight lines formed by the flat baseline prior to the end-point and the increasing absorbance after the end-point.

Flow injection procedure. The 5.67×10^{-5} M solution of PBPB was pumped at a flow rate of 3 ml min^{-1} and the wavelength (between 290 and 300 nm) was selected for maximum sensitivity. After stabilization of the baseline, a 0.1-ml sample of sulfur dioxide solution was injected from a 1.0 ml plastic syringe and peak heights were measured. The sulfur dioxide concentration was established from a calibration graph obtained with standard solutions taken through the above procedure. Addition of ammonia, nitrogen dioxide, and EDTA to the flowing PBPB solution caused no change in absorbance.

Results

Results for titrations of sulfur dioxide with PBPB with and without ammonia and nitrogen dioxide are given in Table 1. Results for the flow injection determinations are given in Table 2.

TABLE 1

Titration of SO_2 with PBPB in the absence and presence of NH_3 and NO_2

SO_2 taken (M)	NH_3 added (M)	NO_2 added (M)	SO_2 found (M)	Recovery and 95% confidence limits[a] (%)
2.15×10^{-1}	0	0	2.10×10^{-1}	97.7 ± 1.28
2.19×10^{-3}	0	0	2.19×10^{-3}	100 ± 1.14
1.34×10^{-4}	0	0	1.33×10^{-4}	99.3 ± 1.78
4.33×10^{-5}	0	0	3.36×10^{-5}	77.6 ± 16.9
1.96×10^{-1}	0.434	0	1.95×10^{-1}	99.5 ± 2.94
3.13×10^{-2}	2.00×10^{-2}	0	2.92×10^{-2}	95.4 ± 2.35
4.96×10^{-3}	6.73×10^{-3}	0	4.96×10^{-3}	100 ± 0.44
1.31×10^{-1}	0	0.103	1.37×10^{-1}	105 ± 0.45
1.50×10^{-3}	0	0.121	1.51×10^{-3}	101 ± 0.32

[a]Based on 5 determinations.

The addition of large quantities of mercury(II) ion to the sulfur dioxide solution caused the formation of a precipitate which was presumed to be $HgSO_2 \cdot HgSO_4$. The presence of EDTA in the sulfur dioxide solution has different effects depending upon concentration. At 10^{-3} M SO_2, only 56.3% of the SO_2 is recovered when 4×10^{-4} M EDTA is present. At 1.12×10^{-4} M SO_2, 95.9% recovery was observed when 4×10^{-4} M EDTA is present. Determinations at lower concentrations of SO_2 gave results within ± 4% of expected values.

Discussion

Although the results for the titration procedure suggest that it is possible to titrate sulfur dioxide down to the 30 ppm level, the procedure is time-consuming. Near the end-point, the absorbance readings stabilize slowly so that individual titrations may require as much as 20 min at low concentrations. These titrations, however, are simple to perform and are reproducible. The absence of significant interferences from ammonia, nitrogen dioxide,

TABLE 2

Calibration results for SO_2 by flow injection method

Concentration SO_2 (mM)	Peak height[a] (cm ± 1 s.d.)
0.446	5.07 ± 0.03
0.892	6.65 ± 0.16
1.34	8.01 ± 0.22
1.78	8.70 ± 0.12
2.23	10.78 ± 0.32

[a]Average of 5 determinations.

and EDTA makes this procedure attractive as a possible alternative to the West—Gaeke method.

A simple flow injection procedure was studied in an attempt to reduce the time of individual determinations. While the results indicate that detection limits are higher than in the titration procedure, the speed and reliability make the technique attractive for routine determinations because it would be possible to process 100 samples per hour. A flow-through cell of smaller volume and a more pulse-free pump should also extend the range of concentrations that could be determined by this procedure. A major advantage of the flow injection method is that the concentration of PBPB does not need to be known accurately. Under normal conditions, PBPB decomposes slowly and while this does not present a problem with the flow injection determinations, it requires daily standardization for the titration method.

The authors acknowledge the support of the Chemistry Alumni Fund of The College of Wooster and Kevin Quinn's work in checking some of the experimental results.

REFERENCES

1 P. W. West and G. C. Gaeke, Anal. Chem., 28 (1956) 1816.
2 P. W. West and F. Ordoreza, Anal. Chem., 34 (1962) 1324.
3 F. P. Scaringelli, B. E. Saltzman and S. A. Frey, Anal. Chem., 39 (1967) 1709.
4 K. A. Rehme and F. P. Scaringelli, Anal. Chem., 47 (1975) 2474.
5 G. Balica, Rev. Chim., 21 (1970) 682.
6 T. R. Williams, J. Krudener and J. McFarland, Anal. Chim. Acta, 30 (1964) 155.
7 T. R. Williams and S. Wakeham, Anal. Chim. Acta, 52 (1970) 152.
8 C. Rehm, J. I. Bodin, K. A. Conners and T. Higuchi, Anal. Chem., 31 (1959) 483.
9 J. Růžička and E. H. Hansen, Anal. Chim. Acta, 87 (1976) 353.
10 L. Greenburg and M. B. Jacobs, Ind. Eng. Chem., 48 (1956) 1517.

Analytica Chimica Acta, 123 (1981) 355—357

Short Communication

AN EXTRACTION—SPECTROPHOTOMETRIC METHOD FOR THE DETERMINATION OF NON-IONIC SURFACTANTS

P. T. CRISP†, J. M. ECKERT*, N. A. GIBSON and I. J. WEBSTER

Department of Inorganic Chemistry, University of Sydney, Sydney, N.S.W. 2006 (Australia)

(Received 12th August 1980)

Summary. The surfactant is extracted into 1,2-dichlorobenzene as a neutral adduct with potassium tetrathiocyanatozincate(II), and zinc(II) in the extract is determined spectrophotometrically after addition of 1-(2-pyridylazo)-2-naphthol and triethanolamine. With a 150-ml water sample, the limit of detection is 15 $\mu g\ l^{-1}$ (as Triton X-100). The method requires only one extraction and is applicable, without modification, to fresh, estuarine and sea-water samples.

The extraction of surfactant molecules into 1,2-dichlorobenzene as a neutral adduct with potassium tetrathiocyanatozincate(II) is the basis of a simple and selective method for the determination of non-ionic surfactants [1]. The determination described earlier [1] was completed by flame a.a.s. for zinc in an acid back-extract. Reported now is a spectrophotometric version of the method.

Experimental

Standard reference non-ionic surfactant solution. The reference non-ionic surfactant used was Triton X-100 (Merck gas chromatography grade of polyethyleneglycol-mono-[*p*-(1,1,3,3-tetramethylbutyl)phenyl] ether, having an average of approximately 10 ethoxy units per molecule). A stock solution was prepared containing 1500 mg Triton X-100 l^{-1}, and diluted further as required.

Zinc—thiocyanate reagent. Dissolve 116 g of zinc sulphate heptahydrate, 312 g of potassium thiocyanate and 40 g of potassium acetate in hot water and dilute to 2 l with water. Extract with three 50-ml quantities of 1,2-dichlorobenzene before use.

PAN reagent. Dissolve 0.25 g of 1-(2-pyridylazo)-2-naphthol (PAN, Merck) in absolute ethanol. Add 15.0 g (12.5 ml) of triethanolamine (Merck) and dilute to 1 l with absolute ethanol. If care is taken to prevent evaporation, this reagent is stable for at least two months.

†Present address: Department of Chemistry, The University of Wollongong, Wollongong, N.S.W. 2500, Australia.

1,2-Dichlorobenzene. Pass the commercial solvent through a 20-cm column of activated alumina. Used solvent may be recycled by fractional distillation; the distillate is washed with water, dried over anhydrous calcium chloride and passed through the alumina column.

A Varian-Techtron model 635 spectrophotometer was used.

Recommended procedure. Place a suitable volume of the water for analysis in a 500-ml separating funnel fitted with a teflon stopcock, and, if necessary, adjust the pH to 6—8. Any volume of water up to 150 ml may be sampled but it should contain not more than 500 μg of non-ionic surfactant. Adjust the volume to about 150 ml with water and add 50.0 ml of zinc—thiocyanate reagent and 20.0 ml of 1,2-dichlorobenzene. Shake the funnel for 5 min and allow to stand until the phases separate.

Run about 13 ml of the organic phase into a dry 15-ml graduated centrifuge tube. Cover the top of the tube with a 5-cm square of aluminium foil and centrifuge at room temperature and 2500 rpm for 30 min. Pipette a 10.0-ml aliquot of the clarified extract into a small glass-stoppered flask. It is important to avoid contamination of the pipetted organic extract with aqueous phase, which is rich in zinc. Take care, therefore, that no drops of the aqueous phase pass into the centrifuge tube and that only clarified extract is sampled by pipette after centrifugation.

Add 1.0 ml of PAN reagent to the extract aliquot, shake the flask to mix well and allow to stand for at least 10 min. Measure the absorbance of this solution at 560 nm with a 10:1 1,2-dichlorobenzene—ethanol solution in the reference cell. The colour developed by the PAN reagent is stable for at least 24 h.

Carry out a blank determination with 150 ml of distilled water. The blank absorbance should not be more than 0.015. Calculate the surfactant concentration in the water sample by comparison with standards.

Results and discussion

PAN is a useful spectrophotometric reagent for a number of metals, including zinc [2]. In published determinations of zinc with PAN, however, the metal is present as zinc(II) in water, from which it is extracted into an organic solvent as an intensely coloured neutral zinc—PAN complex. In the present work, the zinc(II) has already been extracted into an organic solvent, as the potassium tetrathiocyanatozincate(II)—surfactant adduct, and addition of PAN by itself to the extract was found to produce little colour.

This difficulty was resolved by inclusion of an organic base (triethanolamine) in the PAN reagent. In the presence of triethanolamine, zinc(II) forms a bis complex with PAN ($\epsilon_{max} = 6.0 \times 10^4$ l mol^{-1} cm^{-1} at 560 nm in 1,2-dichlorobenzene—ethanol solution). The base promotes formation of the complex by deprotonating PAN.

Calibration. In the range 0—500 μg, the amount of non-ionic surfactant present (y μg, as Triton X-100) could be calculated from the measured absor-

TABLE 1

Recovery of Triton X-100 from water and sea water in the presence of LAS[a]

Triton X-100 added (mg l^{-1})	Triton X-100 found[b] (mg l^{-1})		Triton X-100 added (mg l^{-1})	Triton X-100 found[b] (mg l^{-1})	
	In water	In sea water		In water	In sea water
In presence of 5 mg LAS l^{-1}			In presence of 1 mg LAS l^{-1}		
0	0.06	0.06	0	0.02	0.02
0.10	0.15	0.15	0.10	0.14	0.13
1.00	1.11	1.14	1.00	1.12	1.14
2.00	2.06	2.04	2.00	2.13	2.16

[a]150-ml water and sea-water samples were used. [b]Mean of duplicate determinations.

bance (x), obtained with 1-cm cells and corrected for the blank, by means of the equation $y = 435.4x$.

Precision and limit of detection. The precision of the proposed method is essentially the same as given earlier [1] for the a.a.s. version. The limit of detection, taken as the amount of surfactant which gave an absorbance equal to twice the standard deviation of a set of at least 10 absorbance readings at or near blank level, was found to be 2 μg, as Triton X-100 (corresponding to a concentration of about 15 $\mu g\ l^{-1}$ for a sample volume of 150 ml).

Interferences. The pattern of interferences is similar to that for the a.a.s. method [1]. Of the common inorganic ions, only sulphide, iron(III) and aluminium(III) interfere at the concentrations likely to be found in contaminated waters. There is, however, no interference from sulphide up to 10 mg l^{-1} if the water is treated with 1 ml of 3% hydrogen peroxide solution, shaken and allowed to stand for at least 15 min before the addition of the zinc—thiocyanate reagent. Interference from up to 100 mg l^{-1} of iron(III) or aluminium(III) is suppressed by addition of EDTA [1].

Recovery data for Triton X-100 from water and sea water containing anionic surfactants, as linear alkylbenzene sulphonates (LAS), are given in Table 1. The proposed method, in common with the a.a.s. version, is well-suited to marine and estuarine analysis and is not seriously affected by anionic surfactants; the presence of up to 5 mg LAS l^{-1} introduces an error of no more than 0.16 mg l^{-1} (as Triton X-100) in the apparent non-ionic surfactant concentration.

REFERENCES

1 P. T. Crisp, J. M. Eckert and N. A. Gibson, Anal. Chim. Acta, 104 (1979) 93.
2 See, e.g., Z. Marczenko, Spectrophotometric Determination of Elements, Ellis Horwood, Chichester, 1976.

ANALYTICA CHIMICA ACTA, Vol. 123 (1981)

AUTHOR INDEX

(continued from inside of cover)

Short Communications

(continued from back cover)

(continued on facing page)

Printed in The Netherlands.

CONTENTS

(continued on inside page of cover)